DEPARTAMENT DE QUIMICA ANALÍTICA

DESARROLLO DE MÉTODOS DE CARACTERIZACIÓN Y AUTENTIFICACIÓN DE ACEITES DE OLIVA Y DE OTROS ACEITES VEGETALES.

MARÍA JESÚS LERMA GARCÍA

UNIVERSITAT DE VALÈNCIA
Servei de Publicacions
2011

Aquesta Tesi Doctoral va ser presentada a València el dia 21 de gener de 2011 davant un tribunal format per:

- Dr. Alejandro Cifuentes Gallego
- Dra. Alessandra Bendini
- Dra. Emma Chiavaro
- Dra. Mª Desamparados Salvador Moyá
- Dr. José Vicente Gimeno Adelantado

Va ser dirigida per:
Dr. Guillermo Ramis Ramos
Dr. Ernesto Francisco Simó Alfonso

Dipòsit legal: V-4128-2011
I.S.B.N.: 978-84-370-8079-6
Edita: Universitat de València
Servei de Publicacions
C/ Arts Gràfiques, 13 baix
46010 València
Spain
Telèfon:(0034)963864115

VNIVERSITAT DE VALÈNCIA

FACULTAT DE QUÍMICA

DEPARTAMENT DE QUÍMICA ANALÍTICA

DESARROLLO DE MÉTODOS DE CARACTERIZACIÓN Y AUTENTIFICACIÓN DE ACEITES DE OLIVA Y DE OTROS ACEITES VEGETALES

Memoria para alcanzar el grado de Doctor (Doctorado Europeo) presentada por:

María Jesús Lerma García

Directores:
Dr. Guillermo Ramis Ramos
Dr. Ernesto Fco. Simó Alfonso

Valencia, 2010

VNIVERSITAT DE VALÈNCIA

D. Guillermo Ramis Ramos, catedrático del Departamento de Química Analítica de la Universidad de Valencia y D. Ernesto Fco. Simó Alfonso, profesor titular del mismo departamento,

Certifican

Que la presente memoria, que lleva por título *Desarrollo de métodos de caracterización y autentificación de aceites de oliva y de otros aceites vegetales* constituye la Tesis Doctoral de Dña. María Jesús Lerma García.

Asimismo, certifican haber dirigido y supervisado tanto los distintos aspectos del trabajo, como su redacción.

Burjassot, Septiembre de 2010

Guillermo Ramis Ramos Ernesto Fco. Simó Alfonso

Esta tesis se ha realizado gracias a una beca de Formación
de Personal Investigador de la Generalitat Valenciana

A mi familia

AGRADECIMIENTOS

La realización de esta Tesis Doctoral no habría sido posible sin la ayuda y el apoyo de un gran número de personas:

En primer lugar, quisiera agradecer a mis Directores, el Dr. Guillermo Ramis Ramos y el Dr. Ernesto Fco. Simó Alfonso, por su ayuda y dedicación. Su confianza, su apoyo y sobre todo su paciencia durante todos estos años han sido fundamentales para mi formación como investigadora y para mi crecimiento como persona. De verdad, muchas gracias por todo.

A si mismo, quisiera dar las gracias al Dr. José Manuel Herrero Martínez, por su contribución al desarrollo de mi trabajo y por haber estado siempre dispuesto a ayudarme y a apoyarme cuando lo he necesitado.

También quisiera agradecer a todos aquellos que, de un modo u otro, hicieron posible mi estancia en la Universidad de Sevilla, especialmente a la Dra. María Teresa Morales Millán, al igual que a todos aquellos que hicieron posible mi estancia en el "Dipartimento di Scienze degli Alimenti" de la Universidad de Bolonia. Agradecer al Dr. Giovanni Lercker por dejarme trabajar en su grupo de investigación, y especialmente a la Dra. Alessandra Bendini y al Dr. Lorenzo Cerretani (grazie Lollo per la sempre tua disponibilità i per il tuo sostegno).

Por otro lado, agradecer también a mis compañeros del Laboratorio 10, con los que he compartido incontables horas de trabajo, además de muy buenos momentos: Amparo, Enrique, Laura, María N., Roberto, Victoria, Virginia, "los niños" Isabel, Aarón y María V., y como no a Miriam (Mari Miri, moltes gràcies per estar sempre ahi, sobretot quant les coses es compliquen i m'entren els agobios. Tot açò haguera sigut molt més difícil sense la teua ajuda).

También agradecer a mis amigos “fuera del laboratorio”, a los de siempre (Isa, Ana, Majo, Bea, Teresa, Eva, Miguel, David, Mara, Mari Toñi, Rus), y a los que encontré fuera de casa (Eugenia, Noelia, Martita, Mayra, Nune), por su amistad y por saber escucharme y aguantarme.

Como no, agradecer también a mi familia: mis tíos y primos, mi abuela, y mi hermano, por demostrar siempre tanto interés en mi trabajo y por estar ahí, y en especial a mis padres, por estar siempre a mi lado y por apoyarme en los momentos difíciles, sin vuestros consejos y vuestra ayuda esta tesis no habría sido posible.

Y por último, a mi marido Eloy, por su paciencia, su amor y su comprensión durante todo este tiempo: gracias por estar siempre a mi lado y por apoyarme en todas y cada una de mis decisiones aún cuando no te eran favorables. Gracias por estar ahí.

A todos vosotros, y a los que aunque no haya nombrado han sido partícipes de que todo haya llegado a buen fin, GRACIAS.

ABREVIATURAS

3,4-DHPAA	Ácido 3,4-dihidroxifenil acético; *3,4-dihydroxyphenyl acetic acid*
3,4-DHPEA	3,4-Dihidroxifenil etanol; *3,4-dihydroxyphenyl etanol*
α-T-AcO	Acetato de α-tocoferol; *α-tocopherol acetate*
ACN	Acetonitrilo; *acetonitrile*
AcPIN	1-Acetoxipinoresinol; *1-acetoxypinoresinol*
AIBN	α,α'-Azobisisobutironitrilo; *α,α'-azobisisobutyronitrile*
Ala	Alanina; alanine
ANN	Red neuronal artificial; *artificial neural network*
APCI	Ionización química a presión atmosférica; *atmospheric pressure chemical ionization*
API	Apigenina; *apigenin*
APPI	Fotoionización a presión atmosférica; *atmospheric pressure photoionization*
Arg	Arginina; *arginine*
Asn	Asparagina; *asparagine*
Asp	Ácido aspártico; *aspartic acid*
ATR	Reflectancia total atenuada; *attenuated total reflectance*
BDDA	Diacrilato de 1,3-butanodiol; *1,3-butanediol diacrylate*
BHT	Butilhidroxitolueno; *butylated hydroxytoluene*
CE	Electroforesis capilar; *capillary electrophoresis*
CEC	Electrocromatografía capilar; *capillary electrochromatography*
Cys	Cisteína; *cysteine*

CZE	Electroforesis capilar zonal; *capillary zone electrophoresis*
DAD	Detector de fila de diodos; *diode array detector*
DEA	Forma decarboximetilada del ácido elenólico; *decarboxymethylated form of elenolic acid*
DLA	Aglucona del decarboximetil ligustrósido; *decarboxymethyl ligstroside aglycon*
DOA	Aglucona de la decarboximetil oleuropeína; *decarboxymethyl oleuropein aglycon*
EA	Ácido elenólico; *elenolic acid*
EC	Comunidad europea; *European community*
EDMA	Dimetacrilato de etilenglicol; *ethylene dimethacrylate*
EEC	Comunidad económica europea; E*uropean economic community*
EIC	Cromatograma de ion extraído; *extracted ion chromatogram*
ELSD	Detector evaporativo de dispersion de luz; *evaporative light scattering detector*
EOF	Flujo electroosmótico; *electroosmotic flow*
ESI	Ionización por electronebulización; *electrospray ionization*
EtOH	Etanol; *ethanol*
EVOO	Aceite de oliva virgen extra; *extra virgin olive oil*
FID	Detector fotométrico de llama; *flame ionization detector*
FTIR	Infrarrojo con transformada de Fourier; *Fourier transform infrared*
GC	Cromatografía de gases; *gas chromatography*
Gln	Glutamina; *glutamine*
Glu	Ácido glutámico; *glutamic acid*
Gly	Glicina; *glycine*

HCl	Ácido clorhídrico; *hydrochloric acid*
His	Histidina; *histidine*
HPLC	Cromatografía líquida de alta resolución; *high performance liquid chromatography*
HYTY	Hidroxitirosol; *hydroxytyrosol*
ID	Diámetro interno; *internal diameter*
Ile	Isoleucina; *isoleucine*
IOC	Consejo oleícola internacional; *international olive council*
IR	Infrarroja; *infrared*
KOH	Hidróxido potásico; *potassium hydroxide*
LAg	Aglucona del ligustrósido; *ligstroside aglycon*
LA	Acrilato de laurilo; *lauryl acrylate*
LC	Cromatografía líquida; *liquid chromatography*
LDA	Análisis discriminante lineal; *linear discriminant analysis*
Leu	Leucina; *leucine*
LMA	Metacrilato de laurilo; *lauryl methacrylate*
LOD	Límite de detección; *limit of detection*
LOQ	Límite de cuantificación; *limit of quantification*
LPO	Peróxido de laurilo; *lauroyl peroxide*
LUT	Luteolína; *luteolin*
LVOO	Aceite de oliva virgen lampante; *lampante virgin olive oil*
Lys	Lisina; *lysine*
MeOH	Metanol; *methanol*
Met	Metionina; *methionine*
META	Cloruro de [2-(metacriloiloxi)etil] trimetilamonio; *[2-(methacryloyloxy)ethyl]trimethyl ammonium chloride*
MLP	Perceptrón multicapa; *multilayer perceptron*

MLR	Regresión lineal multiple; *multiple linear regression*
MOS	Semiconductor de óxido metálico; *metal oxide semiconductor*
MOSFET	Semiconductor de óxido metálico - transistor de efecto de campo; *metal oxide semiconductor field effect transistor*
MS	Espectrometría de masas; *mass spectrometry*
MW	Masa molecular; *molecular weight*
m/z	Relación masa-carga; *mass-charge ratio*
NAC	N-acetil-cisteína; *N-acetyl-cysteine*
NaCl	Cloruro sódico; *sodium chloride*
NaOH	Hidróxido sódico; *sodium hydroxide*
NMR	Resonancia magnética nuclear; *nuclear magnetic resonance*
NP	Fase normal; *normal phase*
OA	Aglucona de la oleuropeína; *oleuropein aglycon*
ODMA	Metacrilato de octadecilo; *octadecyl methacrylate*
OFA	Ácido graso oxidado; *oxidized fatty acid*
OLEA	Organización italiana de catadores de aceite de oliva; *italian organization of olive oil tasters*
OPA	*o*-Ftaldialdehído; *o-phthaldialdehyde*
OPO	Aceite de orujo de oliva; *olive pomace oil*
OSI	Instrumento de estabilidad oxidative; *oxidative stability instrument*
OxDEA	Forma oxidada del ácido decarboximetil elenólico; *oxidized form of decarboxymethyl elenolic acid*
OxDLA	Forma oxidada de la aglucona del decarboximetil ligustrósido; *oxidized form of decarboxymethyl ligstroside aglycon*

OxDOA	Forma oxidada de la aglucona de la decarboximetil oleuropeína; *oxidized form of decarboxymethyl oleuropein aglycon*
OxEA	Forma oxidada del ácido elenólico; *oxidized form of elenolic acid*
OxLAg	Forma oxidada de la aglucona del ligustrósido; *oxidized form of ligstroside aglycon*
OxOA	Forma oxidada de la aglucona de la oleuropeína; *oxidized form of oleuropein aglycon*
PCR	Regresión de componentes principales; *Principal component regression*
Phe	Fenilalanina; *phenylalanine*
PDO	Denominación de origen protegida; *protected designation of origin*
PLSR	Regresión de mínimos cuadrados parciales; *partial least squares regression*
Pro	Prolina; *proline*
QCM	Microbalanza de cristal de cuarzo; *quartz crystal microbalance*
r	Coeficiente de regresión lineal; *linear regression coefficient*
ROPO	Aceite de orujo de oliva refinado; *refined olive pomace oil*
RP	Fase reversa o inversa; *reverse phase*
RSD	Desviación estándar relativa; *relative standard deviation*
SAW	Onda acústica superficial; *surface acoustic wave*
sccm	Centímetros cúbicos estándares por minuto; *standard cubic centimetres per min*

SEM	Microscopía electrónica de barrido; *scanning electron microscope*
Ser	Serina; *serine*
SIR	Monitorización del ion seleccionado; *selected ion recording*
T	Tocoferol; *tocopherol*
T_3	Tocotrienol; *tocotrienol*
THF	Tetrahidrofurano; *tetrahydrofurane*
Thr	Treonina; threonine
TIC	Cromatograma de iones totales; *total ion chromatogram*
TLC	Cromatografía en capa fina; *thin layer chromatography*
t_R	Tiempo de retención; *retention time*
Tris	Tris(hidroximetil)aminoetano; *Tris(hydroxymethyl)amino ethane*
Trp	Triptófano; *tryptophan*
TY	Tirosol; *tyrosol*
Tyr	Tirosina; *tyrosine*
UPLC	Cromatografía líquida ultra rápida; *ultra performance liquid chromatography*
Val	Valina; *valine*
VOO	Aceite de oliva virgen; *virgin olive oil*

ÍNDICE

CAPÍTULO 1

INTRODUCCIÓN

1.1. Aceites comestibles

1.1.1. Introducción

Los aceites comestibles son principalmente aceites vegetales que han sido sometidos a varios procesos para eliminar constituyentes no deseados. Con el objeto de adecuarlos al consumo humano, la mayor parte de los aceites comestibles son sometidos a procesos de refinación (neutralización, decoloración y desodorización). El aceite de oliva virgen, que es un zumo natural obtenido por prensado, es el único aceite que se puede consumir sin refinar.

Los aceites vegetales se diferencian de las grasas animales, la mantequilla y el aceite de pescado en que tienen pocos componentes ácidos y una composición triglicerídica más simple. Los aceites vegetales comestibles tienen composiciones relativamente sencillas, aunque considerablemente variables de un aceite a otro, por lo que presentan un amplio rango de propiedades físicas y químicas (Rossell, 1991). Para la mayor parte de los usos, la idoneidad de un aceite depende tanto de su calidad como de su composición química. Para determinar la pureza de un aceite, además de la composición de ácidos grasos, se pueden usar el análisis de los ácidos grasos en la posición 2 de la molécula de los triacilgliceroles, el análisis de las especies moleculares de los triacilgliceroles, y la determinación de Ts, esteroles y otros constituyentes de la fracción del insaponificable del aceite.

1.1.2. Constituyentes de los aceites comestibles

Los constituyentes de los aceites comestibles se pueden agrupar en los pertenecientes a la fracción saponificable, tales como los triacilgliceroles, los ácidos grasos libres y los fosfátidos, o en aquellos pertenecientes a la fracción

insaponificable, como los hidrocarburos y los alcoholes grasos, entre otros. La fracción insaponificable representa, en general, el 0,5 – 1,5% de los aceites.

1.1.2.1. Fracción saponificable

La fracción saponificable constituye el 98,5 – 99,5% del peso de los aceites, estando formada mayoritariamente por triacilgliceroles (o triglicéridos) y ácidos grasos libres, así como por otros derivados de los ácidos grasos como mono- y di-acilgliceroles, fosfolípidos, ceras y ésteres de esteroles.

Triacilgliceroles. Estos compuestos constituyen el 98 – 99% de los aceites. Son ésteres provenientes de la unión del trialcohol glicerina (1,2,3-propanotriol) con ácidos grasos. El ácido graso en la posición central o posición 2 de la molécula de glicerol es casi siempre insaturado. Esta posición es ocupada por un ácido graso saturado únicamente cuando la concentración total de ácidos grasos saturados en el aceite es muy alta. Los triacilgliceroles mayoritarios en el aceite de oliva son POO (18,4%), SOO (5,1%), POL (5,9%), OOO (43,5%), OOL (6,8%) (P, ácido palmítico; O, ácido oleico; S, ácido esteárico; L: ácido linoleico) (Fedeli, 1977).

Mono- y di-acilgliceroles. Aparte de contener triglicéridos, los aceites también contienen glicéridos parciales, como los mono- y los di-acilgliceroles, que comprenden un 0,2% y un 1,3% sobre los ácidos grasos totales, respectivamente. La presencia de estos compuestos es debida, en parte, a una biosíntesis incompleta, pero principalmente a hidrólisis del aceite. Cuando los di-acilgliceroles están presentes, el aceite de oliva es de baja calidad (Mariani, 1985), por lo que su determinación se puede usar para evaluar su calidad.

Ácidos grasos libres. Su proporción en los aceites depende del grado de hidrólisis de los triglicéridos, variando su composición según la variedad botánica del aceite, o para aceites de oliva, según la variedad genética, las

condiciones climáticas, madurez del fruto y el origen geográfico del olivar (Aparicio, 1994; Boskou, 2002; D'Imperio, 2007; Stefanoudaki, 1999; Torres, 2006). Los ácidos grasos mayoritarios en el aceite de oliva son palmítico (7,5 – 20%), esteárico (0,5 – 5%), palmitoleico (0,3 – 3,5%), oleico (55 – 85%), linoleico (7,5 – 20%) y linolénico (0,0 – 1,5%), si bien, también se pueden encontrar los ácidos mirístico, margárico y araquídico a nivel de trazas.

Fosfolípidos. Se encuentran en pequeñas cantidades en aceites de oliva recién producidos (40 – 135 mg/kg) (Tiscornia, 1982), siendo su concentración menor conforme el aceite va envejeciendo. Entre los fosfolípidos encontrados en el aceite de oliva cabe mencionar la fosfatidilcolina, la fosfatidiletanolamina, el fosfatidilinositol y la fosfatidilserina (Alter, 1982; Boskou, 2002).

Ceras. Estos compuestos se producen mediante esterificación de los alcoholes grasos con los ácidos grasos libres presentes en el aceite. Las principales ceras de los aceites de oliva son de número de carbono elevado y par, en concreto, ésteres entre 36 y 46 átomos de carbono, siendo su contenido muy bajo, no superando los 35 mg/100 g (Boskou, 2002).

Ésteres de esteroles. Estos compuestos son combinaciones de los ácidos grasos con los diferentes tipos de esteroles, de los que se hablará a continuación.

1.1.2.2. Fracción insaponificable

La fracción insaponificable de los aceites comestibles está constituida por diversos compuestos que no están químicamente relacionados con los ácidos grasos: hidrocarburos, alcoholes grasos, esteroles libres, ya sean esteroles comunes, 4α-metil-esteroles, 4,4-dimetil-esteroles o alcoholes triterpénicos y dialcoholes triterpénicos, además de Ts y T_3s, pigmentos, diversos compuestos volátiles y aromáticos, compuestos fenólicos y proteínas.

Hidrocarburos. El escualeno, precursor bioquímico de los esteroles, es un importante hidrocarburo presente en los aceites de oliva vírgenes y refinados. El aceite de oliva contiene la mayor cantidad de escualeno (2500 – 9250 μg/g) en comparación con las cantidades encontradas en otros aceites comestibles (16 – 370 μg/g) (Gutfinger, 1974). En el aceite de oliva también se encuentran otros hidrocarburos, tales como los *n*-alcanos de 14 a 30 átomos de carbono, algunos *n*-alquenos e hidrocarburos terpénicos, como el α-farneseno. La concentración de estos hidrocarburos es de aproximadamente 150 – 200 μg/g (Lanzon, 1994). El β-caroteno, que por su estructura química podría incluirse en la familia de hidrocarburos terpénicos, se comenta, debido a sus propiedades, en el apartado dedicado a pigmentos.

Alcoholes grasos. Estos compuestos, aunque minoritarios, son constituyentes importantes de los aceites comestibles, y en el caso del aceite de oliva, pueden ser utilizados para diferenciar los distintos tipos de aceite (Reglamento (EEC) Nº 2568/91). Los alcoholes grasos pueden ser lineales (alifáticos) o triterpénicos (ver el apartado dedicado a esteroles). También dentro de esta fracción alcohólica se encuentran los alcoholes diterpénicos o diterpenoides acíclicos.

Los alcoholes alifáticos son compuestos de estructura lineal. Por otro lado, son precursores de la formación de ceras. Así, un alto contenido de alcoholes puede traer como consecuencia que el contenido de ceras aumente a lo largo del tiempo. Los principales alcoholes lineales presentes en el aceite de oliva, cuya concentración no suele ser mayor de 35 mg/100 g de aceite, son el docosanol (C22), el tetracosanol (C24), el hexacosanol (C26) y el octacosanol (C28). Otros alcoholes con número de átomos de carbono impar, presentes a nivel de trazas, son el tricosanol (C23), el pentacosanol (C25) y el heptacosanol (C27).

El aceite de oliva contiene también dos alcoholes diterpénicos importantes: el fitol (que se encuentra en una concentración comprendida entre 120 – 180 mg/kg, y que proviene posiblemente de la clorofila) y el geranilgeraniol (Paganuzzi, 1979).

Esteroles. Existen cuatro tipos de esteroles en los aceites vegetales: los esteroles comunes o 4α-desmetilesteroles, los 4α-metil-esteroles, los 4,4-dimetil-esteroles o alcoholes triterpénicos, y los dialcoholes triterpénicos.

Los 4α-desmetilesteroles son los esteroles más abundantes en los aceites, siendo su contenido en el aceite de oliva de 100 – 200 mg/100 g. Los principales esteroles en el aceite de oliva son el β-sitosterol (75 – 90%), el Δ^5-avenasterol (5 – 36%) y el campesterol (aproximadamente un 3% de la fracción total de esteroles). Otros esteroles presentes, aunque a nivel de trazas, son el colesterol, el campestanol, el estigmasterol, el Δ^7-campesterol, el clerosterol, el sitostanol, el $\Delta^{5,24}$-estigmastadienol, el Δ^7-estigmasterol y el Δ^7-avenasterol (Boskou, 2002).

Los 4α-metil-esteroles, intermedios de la biosíntesis de los esteroles, se encuentran siempre presentes en pequeñas cantidades en los aceites. Su concentración es de aproximadamente 20 – 70 mg/100 g (Boskou 1996). Los más abundantes en el aceite de oliva son el obtusifoliol, el cicloeucalenol, el gramisterol y el citrostadienol.

Por otro lado, los principales alcoholes triterpénicos presentes en el aceite de oliva, cuyo contenido oscila entre 100 – 150 mg/100 g de aceite (Kiosseoglou, 1987), son la α- y β-amirina, el cicloartenol, el butirospermol, el 24-metilen-cicloartanol, el taraxerol, el dammaradienol y el 24-metilen-24-dihidroparkeol (Boskou, 2002; Kiritsakis, 2003; Paganuzzi, 1982).

Los dos principales dialcoholes triterpénicos son el eritrodiol y el uvaol. El contenido total de eritrodiol más uvaol en el aceite de oliva varía desde 1 a 20 mg/100 g, pudiéndose obtener valores de hasta 280 mg/100 g en aceite β-residual (Boskou, 2002; Mariani, 1987).

Ts y T_3s. Son los constituyentes de la vitamina E. Ambas series de compuestos contribuyen a la estabilidad de los aceites protegiéndolos de la oxidación (Blekas, 1995; Manzi, 1998; Psomiadou, 1998), previenen la peroxidación lipídica en membranas biológicas (Panfili, 2003; Solomon, 1998) y tienen un papel biológico beneficioso como antioxidantes (Mateos, 2005). Mientras que los Ts se encuentran en todos los aceites, los T_3s se encuentran sobre todo en aceite de palma (Choo, 1996) y en aceites obtenidos a partir de cereales. Las concentraciones relativas de los diversos componentes de los Ts y T_3s varían según el tipo de aceite, siendo el α-T el más abundante en el aceite de oliva, representando un 95% del total de Ts (Gimeno, 2000A; Tasioula-Margari, 2001). El otro 5% lo constituyen principalmente los isómeros β- y γ-T.

Pigmentos. Los principales pigmentos presentes en los aceites comestibles son los carotenoides (Serani, 1992). Los principales carotenoides presentes en el aceite de oliva son el β-caroteno y la luteína, encontrándose también, aunque a nivel de trazas, la violaxantina, la neoxantina y sus isómeros (Boskou, 2002). El contenido total de pigmentos va desde 1 a 20 mg/kg, aunque normalmente no es mayor de 10 mg/kg. Por otro lado, el aceite de oliva también posee clorofilas, que son las responsables del color verde del aceite. Su contenido varía entre 10 y 30 mg/kg. La principal clorofila presente en el aceite embotellado es la feofitina "a", aunque se ha demostrado la presencia de clorofilas "a" y "b", y de feofitina "b" en aceites frescos (Minguez-Mosquera, 1990).

Compuestos volátiles y aromáticos. Son los responsables del aroma y del sabor del aceite de oliva virgen, esto es, de las características que lo distinguen de otros aceites comestibles. Se han identificado más de cien componentes directamente relacionados con el aroma y sabor, encontrándose entre ellos hidrocarburos, alcoholes, aldehídos, ésteres, derivados fenólicos, terpenos y derivados del furano (Boskou, 1996; Morales, 1999 y 2003; Reiners, 1998). Los más importantes constituyentes del aroma del aceite de oliva son los aldehídos con 6 carbonos y los alcoholes que se forman en el fruto a partir de ácidos grasos poliinsaturados.

Compuestos fenólicos. Estos compuestos, más comúnmente denominados polifenoles, son constituyentes minoritarios del aceite de oliva. El potencial antioxidante de estos compuestos ha despertado gran interés, tanto por su efecto quimio-protector en seres humanos (Bendini, 2007; Caponio, 1999; Vissers, 2001), como por ser uno de los factores más importantes en lo que a estabilidad oxidativa de los aceites se refiere (Caponio, 1999; Tsimidou, 1998; Tura, 2007; Velasco, 2002). La actividad antioxidante de los componentes del aceite de oliva virgen se ha relacionado con la protección frente a importantes enfermedades crónicas y degenerativas, tales como las enfermedades coronarias, las enfermedades de envejecimiento neuro-degenerativo y tumores localizados en diversas zonas del organismo humano (Franceschi, 1999; Hodge, 2004). Por otra parte, los polifenoles también contribuyen a las propiedades organolépticas de los aceites de oliva vírgenes (Servili, 2002), y más concretamente son los responsables de características tales como el amargor y la astrigencia (Gutiérrez-Rosales, 1992 y 2003; Tsimidou, 1998).

Los compuestos fenólicos pueden ser agrupados principalmente en las siguientes categorías (Harborne, 1989):

- Fenoles simples, como el TY, el HYTY, el ácido *p*-hidroxifenilacético y el ácido homovanílico.

-Ácidos fenólicos, con la estructura básica C6-C1 (ácidos benzoicos), tales como el ácido gálico, el gentísico, el benzoico, el vanílico, el protocateuico, el *p*-hidroxibenzoico y el siríngico, o los ácidos de estructura básica C6-C3 (ácidos cinámicos), como el ácido cafeico, el *p*-cumárico, el *o*-cumárico, el ferúlico, el cinámico y el sinápico.

- Alcoholes fenólicos, como el 3,4-DHPEA, la forma glucósida del 3,4-DHPEA y el acetato de 2-(4-hidroxifenil)etil.

- Secoiridoides tales como la oleuropeína, el ligustrósido, la OA, la LAg, la aglucona de la deacetoxi-oleuropeína, la aglucona del deacetoxi-ligustrósido, la forma dialdehídica de la oleuropeína, la forma dialdehídica del ligustrósido, la forma deacetoxi-dialdehídica de la oleuropeína y la forma deacetoxi-dialdehídica del ligustrósido.

- Flavonoides, como la API, la LUT y la taxifolina.

- Lignanos, tales como el AcPIN, el pinoresinol y el 1-hidroxipinoresinol.

Proteínas. Por último, se ha descrito la presencia de proteínas en los aceites vegetales (Hidalgo, 2001A, 2001B y 2002). El contenido total de proteínas varía ampliamente dependiendo del tipo de aceite y de su método de extracción (Hidalgo, 2006). Por otro lado, se ha demostrado que existen diferencias significativas en el contenido proteico en aceites de oliva, dependiendo del cultivo y del grado de madurez del fruto (Zamora, 2001).

1.1.3. Métodos de análisis de los principales constituyentes de los aceites comestibles

1.1.3.1. Determinación de triacilgliceroles

Se han utilizado diversas técnicas de LC para el análisis de triacilgliceroles en aceites vegetales, tales como la TLC (Christie, 1992) y la RP-HPLC (Carelli, 1993; Cunha, 2006A; Holčapek, 2005; Parcerisa, 1995). En RP-HPLC se han utilizado columnas cargadas con iones plata, ya que su presencia en la fase estacionaria favorece la retención selectiva de compuestos insaturados (Macher, 2001). Por otro lado, se han conseguido selectividades y capacidades de pico muy elevadas mediante cromatografía bidimensional completa (*comprehensive*), combinando una columna C18 con una segunda columna con carga de iones plata (Dugo, 2006; Robison, 1985; van der Klift, 2008). También se ha utilizado la GC capilar de alta temperatura (Aparicio, 2000; Carelli, 1993). De entre todas estas técnicas, la RP-HPLC es la metodología más empleada. El método oficial de análisis implica el uso de un detector de índice de refracción (Parcerisa, 1995), aunque debido a que éste no es compatible con el uso de elución en gradiente (deseable para reducir tiempos de análisis y para mejorar la resolución cromatográfica), también se han utilizado otros detectores tales como el UV a bajas longitudes de onda (Carelli, 1993; Holčapek, 2005; Van der Klift, 2008), el ELSD (Holčapek, 2005; Macher, 2001; Perona, 2001; Van der Klift, 2008) o la MS (Holčapek, 2005; Van der Klift 2008).

1.1.3.2. Determinación de ácidos grasos

El análisis de los ácidos grasos libres se lleva a cabo habitualmente mediante GC-FID, siendo éste además su método oficial de análisis (Hajimahmoodia, 2005; Reglamento (EEC) Nº 2568/91, anexo X; Sakouhia,

2008). A su vez, se han desarrollado otros métodos analíticos que hacen uso de la HPLC (Kotani, 2002), la CEC (Dermaux, 1999) o la NMR (Sacchi, 1997).

1.1.3.3. Determinación de alcoholes

Los alcoholes alifáticos y triterpénicos presentes en los aceites vegetales se han determinado habitualmente mediante GC-FID (Abou Hadeed, 1990; Azadmard-Damirchi, 2005; Benitez-Sánchez, 2003; Lazzez, 2008; Ntsourankoua, 1994; Ranalli, 2002; Rivera del Álamo, 2004; Sindhu-Kanya, 2007) o GC-MS (Abou Hadeed, 1990; Azadmard-Damirchi, 2005; Cunha, 2006B; Ntsourankoua, 1994; Sindhu-Kanya, 2007). Tan sólo en algunos trabajos se ha descrito el uso de la HPLC previa derivatización de los alcoholes con cloruro de 3,5-dinitrobenzoilo (Cortesi, 1987).

1.1.3.4. Determinación de esteroles

El análisis de esteroles se lleva a cabo habitualmente mediante GC-FID (Cercaci, 2007; Galeano, 2005; Parcerisa, 2000; Ranalli, 2002; Rivera del Álamo, 2004) o GC-MS (Cercaci 2007; Cunha, 2006B; Parcerisa, 2000; Thanh, 2006; Medvedovici, 1997), previa extracción de la fracción de los esteroles mediante TLC seguida de derivatización, tal como indica el método oficial (Reglamento (EEC) Nº 2568/91, anexo V). La mayor desventaja del uso de la GC es el empleo de columnas térmicamente estables, y la necesidad de derivatización previa. Por ello, más recientemente, se han descrito métodos alternativos basados en el uso de HPLC-MS (Cañabate-Díaz, 2007; Martínez-Vidal, 2007; Segura-Carretero, 2008) y CEC (Abidi, 2004).

1.1.3.5. Determinación de Ts y T_3s

El análisis de Ts y T_3s se ha llevado a cabo principalmente mediante GC (Melchert, 2002) y HPLC, usándose para ello diversos detectores (Abidi, 2000; Cunha, 2006C; Gruszka, 2007). Se ha utilizado tanto la NP-HPLC, que es capaz de separar los isómeros β y γ (Abidi, 2000), como la RP-HPLC, que ofrece una mayor estabilidad de la columna, mayor reproducibilidad de los tiempos de retención, y tiempos de análisis más cortos (Abidi, 2000; Gimeno, 2000B). Por otro lado, los Ts también se han determinado mediante espectroscopia FTIR (Silva, 2009), espectrometría de fluorescencia con barrido sincrónico (Sikorska, 2005), o mediante CEC con columnas particuladas (Aturki, 2005).

1.1.3.6. Determinación de compuestos volátiles

Han sido numerosos los esfuerzos hechos en el desarrollo de métodos instrumentales para determinar los componentes responsables del sabor y del aroma del aceite de oliva, que eliminen la subjetividad y otras desventajas de la evaluación sensorial mediante paneles de cata. Tradicionalmente, los compuestos volátiles se han determinado mediante GC-MS (Baccouri, 2008; Guth, 1993; Tateo, 1993). Posteriormente, se propuso otra metodología para la determinación de volátiles basada en el uso de matrices de sensores (nariz electrónica), que evalúan las percepciones básicas producidas por el aceite (Aparicio, 1995; Tena, 2007). En algunos casos, los resultados obtenidos mediante la nariz electrónica se han comparado con los proporcionados por un panel de cata (Camurati, 2006). A su vez, se han aplicado métodos combinados de GC y de olfatometría con matrices de sensores (Cimato, 2006; García-Gónzalez, 2010; López-Feria, 2008; Morales, 1994; Tena, 2007).

1.1.3.7. Determinación de compuestos fenólicos

Se han descrito muchos métodos analíticos para el análisis de compuestos fenólicos en el aceite de oliva. La técnica más utilizada ha sido la LC, acoplada un detector espectrofotométrico UV-Vis (Allalout, 2009; Baccouri, 2008; Bendini, 2003; Bonoli, 2004; Cerretani, 2006; Gutierrez-Rosales, 2003; Ocakoglu, 2009), electroquímico (Brenes, 2000), fluorimétrico (Cartoni, 2000; García, 2003) o por MS (Baccouri et al., 2008; Bendini, 2003; Bonoli, 2004; Carrasco-Pancorbo, 2007; Gutierrez-Rosales, 2003; Suárez, 2008). Otras técnicas, como la GC (Carrasco-Pancorbo, 2005; Liberatore, 2001; Ríos, 2005; Saitta, 2009) y la CE (Bendini, 2003; Bonoli, 2004; Carrasco-Pancorbo, 2004; 2006 y 2007B; Gómez-Caravaca, 2005), acopladas a su vez a diferentes detectores, han sido también ampliamente empleadas. Además, más recientemente, también se han utilizado los sensores voltamétricos (Rodríguez-Méndez, 2008) y la NMR de protón de alta resolución (Christophoridou, 2009).

1.1.3.8. Determinación de proteínas

Debido a la reciente descripción de las proteínas como componentes traza de los aceites vegetales, tan solo se ha descrito un único método para su determinación (Hidalgo 2001A). En dicho método se procede, en primer lugar, a la hidrólisis de las proteínas, seguida de derivatización de los aminoácidos obtenidos con dietil-etoximetilén-malonato, y posterior análisis de los derivados mediante HPLC-UV-Vis.

1.1.4. Detección de la adulteración

El EVOO es a menudo adulterado con otros aceites vegetales más baratos, como los aceites de maíz, cacahuete, girasol y soja (Kiritsakis, 1998), aunque la adulteración más frecuente se realiza con aceite de avellana, debido a la

dificultad que entraña su detección por la gran semejanza entre su composición química y la del aceite de oliva. A su vez, el EVOO también es adulterado con otros aceites de oliva de menor calidad, como el de orujo de oliva (Kiritsakis, 1998).

Para analizar y detectar la adulteración, se vienen aplicando varias pruebas físicas y químicas (Comisión del Codex Alimentarius, 1993; Fedeli 1977; Kiritsakis, 1991), así como diversos métodos cromatográficos (Fasciotti, 2010; Marcos Lorenzo, 2002; Maryam, 2009; Saba, 2005), espectroscópicos (Agiomyrgianaki, 2010; Fragaki, 2005; Fronimaki, 2002; Maryam, 2009; Poulli, 2006; Vlachos, 2006) y térmicos (Chiavaro, 2008; Maryam, 2009), entre otros.

Por otro lado, el análisis de la fracción completa del insaponificable suministra pruebas adicionales para detectar la adulteración y aumentar la fiabilidad de la diferenciación entre aceites vegetales de diferente origen botánico, o entre aceites de oliva de diferente calidad. Entre los constituyentes de la fracción insaponificable, la familia de los esteroles, cuya composición en los EVOOs es muy característica, proporciona excelentes trazadores de la adulteración, tanto para distinguir entre aceites vegetales de diferente origen botánico (Ballesteros, 1995; Cañabate-Diaz, 2007; Cercaci, 2003; Mariani, 2006), como para diferenciar aceites de oliva de distinta calidad (Martínez-Vidal, 2007; Philips, 2002), lo que explica que esta familia de compuestos haya sido muy utilizada en la autentificación de aceites.

1.2. Aceite de oliva

El aceite de oliva es el zumo oleoso de la aceituna. Cuando se obtiene por sistemas de elaboración adecuados, y procede de frutos frescos de buena calidad, sin defectos ni alteraciones y con la adecuada madurez, el aceite de oliva posee

excepcionales características de aspecto, aroma y sabor delicado, y es prácticamente el único entre los aceites que puede consumirse crudo, conservando íntegro su contenido en vitaminas, ácidos grasos esenciales y otros productos naturales de importancia dietética.

1.2.1. Calidades reglamentadas del aceite de oliva

Existen diferentes calidades reglamentadas de aceite de oliva, que se pueden clasificar en aceites de oliva virgen y aceites de orujo de oliva. Las características de los mismos, en el ámbito de la Unión Europea, se encuentran recogidas en el Reglamento (ECC) Nº 2568/91, modificado por el CE 796/2002.

1.2.1.1. Aceite de oliva virgen

El aceite de oliva virgen es el obtenido a partir del fruto del olivo únicamente por procedimientos mecánicos u otros métodos físicos, en condiciones, sobre todo térmicas, que no impliquen la alteración del mismo. Un aceite de oliva virgen no debe haber sufrido ningún tratamiento distinto del lavado, la decantación, el centrifugado y el filtrado. En la práctica, la totalidad de los aceites obtenidos en las almazaras se encuentran dentro de este grupo. No obstante, es obvio que es imposible obtener una calidad óptima en todos los casos. Por tanto, dentro del aceite virgen, se establecen a su vez una serie de categorías, atendiendo a sus características de acidez, puntuación organoléptica y ausencia de sabores defectuosos. Atendiendo a estos criterios, los aceites de oliva virgen se pueden clasificar en:

- *Aceite de oliva virgen extra o EVOO.* De acuerdo con su denominación debe considerarse como el mejor de los posibles aceites de oliva. Tiene unas características organolépticas que reproducen los olores y sabores de la aceituna. Es el zumo de la aceituna recolectada en su mejor momento de madurez y

procesada adecuadamente. Al no haber sido sometido a ningún proceso de refinado, tiene todos los compuestos de interés nutricional en su grado máximo. Su puntuación organoléptica (conjunto de aromas y sabor) debe de ser igual o superior a 6,5, y su acidez libre (porcentaje de ácido oleico) no puede superar los 0,8 g/100 g. Los EVOOs presentan multitud de matices, que dependen de una gran diversidad de factores que van desde la variedad de la aceituna a las condiciones de cultivo. De acuerdo a dichos factores, pueden obtenerse tipos diferenciados que se adapten a las demandas específicas de cada grupo de consumidores. Por ello, los EVOOs se podrían subdividir en al menos tres grandes grupos: aceites monovarietales, elaborados con una sola variedad de aceituna; coupages, elaborados en base a diversas variedades de aceituna con el fin de obtener siempre los mismos estándares de sabor y aroma; y aceites con PDO, elaborados en base a aceitunas procedentes de un área geográfica determinada, reconocida oficialmente.

- *Aceite de oliva virgen o VOO*. Es el aceite de oliva virgen que puede presentar ligeras alteraciones, bien sea en sus índices analíticos o en sus características sensoriales, pero siempre a pequeña escala. Estas alteraciones, sobre todo sensoriales, pueden ser prácticamente imperceptibles, pero deprecian la calidad en relación al EVOO. En este caso, la puntuación organoléptica debe de ser igual o superior a 5,5, y la acidez libre máxima de 2º (2 g de ácido oleico por cada 100 g de aceite).

- *Aceite de oliva virgen común*. Presenta alteraciones sensibles en sus parámetros físico-químicos, o en sus características sensoriales. Su puntuación organoléptica debe ser igual o superior o 3,5, y su acidez máxima de 3,3º. Se emplea como uno de los componentes de los llamados aceites de oliva (que se definen más adelante), siempre y cuando sus características organolépticas no estén sensiblemente alteradas, o para refinación, en caso de que lo estén.

- *Aceite de oliva virgen lampante o LVOO*. No se destina en ningún caso al consumo directo, y ha de someterse necesariamente a un proceso de refinación para hacerlo comestible. Su acidez libre es mayor de 3,3º, y su puntuación organoléptica menor de 3,5.

- *Aceite de oliva refinado.* Es el aceite resultante de la refinación de cualquiera de los dos anteriores. El aceite de oliva refinado debe tener una acidez libre no superior a 0,3º, y presentar unas características sensoriales prácticamente neutras (sin sabor ni olor), por lo que sirve de base para la elaboración de otros aceites de oliva.

1.2.1.2. Aceite de orujo de oliva crudo

Del residuo sólido de las almazaras, y mediante extracción con disolventes orgánicos, se obtiene el denominado aceite de orujo, que no es directamente apto para el consumo humano, por lo que ha de someterse necesariamente a refinación. Su comercialización se realiza, como se explica más adelante, mezclándolo con aceite de oliva virgen.

1.2.1.3. Otros aceites de oliva envasados

- *Aceite de oliva*. Es otro de los productos que se encuentran envasados en el mercado. Tiene aún una posición predominante en el mercado, aunque lentamente va cediendo cuota a favor del VOO y el EVOO. Se obtiene mezclando proporciones diversas de VOO o aceite de oliva virgen común con aceite de oliva refinado. Su acidez máxima es del 1º.

- *Aceite de orujo de oliva u OPO.* Es el obtenido mediante la mezcla de VOO con aceite de orujo refinado o ROPO.

1.2.2. Valoración sensorial de los aceites de oliva vírgenes

Aparte de los análisis químicos de los aceites de oliva virgen, el análisis sensorial es de gran importancia, tal y como se deduce del apartado anterior, debido a que es indicativo de la calidad de los aceites.

El análisis sensorial se aprovecha de la capacidad de los sentidos para reaccionar ante estímulos químicos, físicos y fisicoquímicos. Los cinco sentidos permiten evaluar las siguientes propiedades sensoriales:

- Apariencia, color y forma mediante la vista.
- Consistencia y características relacionadas (fluidez, viscosidad, dureza, fibrosidad, crujiente, flexibilidad) mediante el tacto y el oído.
- Aroma mediante el olfato.
- Sensaciones gustativas mediante el gusto.
- Sabor mediante una combinación de olfato, gusto y tacto.

1.2.2.1. Métodos de evaluación de las características sensoriales

Se han desarrollado diversas series de pruebas sensoriales con el fin de evaluar las diferencias, semejanzas, la calidad, la cantidad de las características sensoriales, las preferencias o aceptación de un producto y las habilidades de los sujetos (Institute of food technologists, 1981). Estas pruebas se pueden clasificar en pruebas discriminatorias, descriptivas o afectivas. Las pruebas discriminatorias (que son las que se usarán en esta tesis) se resumen en la **Tabla 1.1**.

Tabla 1.1. Pruebas discriminatorias en el análisis sensorial.

Prueba	Descripción breve
Comparación de pares	Se presentan dos muestras codificadas. El juez tiene que indicar las diferencias entre ellas
Dúo - trío	Tres muestras, dos idénticas y una diferente. Una de las muestras idénticas se pone como referencia y el juez identifica la muestra que coincide con la de referencia
Triángulo	Tres muestras, dos idénticas y una diferente. El juez debe indicar cual es diferente
Clasificación	El juez debe ordenar una serie de muestras según la intensidad de cierto atributo
Umbral	Se presenta una serie de muestras con una concentración descendente de un estímulo. El juez debe indicar para cada muestra si detecta el estímulo

1.2.2.2. Evaluación de la calidad sensorial del aceite de oliva virgen (panel de cata)

El análisis descriptivo cuantitativo desarrollado por el IOC, más conocido como panel de cata (Reglamento (CE) Nº 796/2002), es el mejor método para evaluar las características sensoriales del aceite de oliva virgen. Al aplicar procedimientos estadísticos a los datos provenientes de los expertos se obtienen unos resultados con una fiabilidad similar, debido a sus niveles significativos, a la fiabilidad conseguida por otros métodos normalmente utilizados en otros campos científicos.

La metodología, incluida en las regulaciones de la Unión Europea desde 1991, determina como instrumento de medida a un grupo de personas, de 8 a 12, seleccionadas de una manera regulada y entrenadas convenientemente para identificar y medir la intensidad de las diferentes sensaciones positivas y negativas percibidas por sus sentidos. La elección de un grupo de personas permite promediar las diferencias que existen en los umbrales de algunos olores

dependiendo de las personas, probablemente relacionadas con factores genéticos, culturales y ambientales, y así el resultado final representa a todos los consumidores.

Para solucionar el problema derivado del hecho de que las percepciones acerca del olor varíen de una persona a otra, lo que está relacionado con las propias experiencias de cada sujeto, evitando en lo posible la subjetividad de los conceptos, los catadores deben usar el mismo vocabulario. Una parte de este vocabulario, común a todos los alimentos, es el denominado "vocabulario general", en el que se incluyen términos como aspecto, atributo, panel, percepción, sensibilidad, catador, respuesta, fatiga sensorial, estímulo, aroma, sabor, textura, etc. El "vocabulario específico" fue desarrollado por los expertos del IOC para el análisis del aceite de oliva virgen. Un resumen del mismo se encuentra en la **Tabla 1.2**.

Para minimizar al máximo los factores que pueden comprometer el análisis sensorial y para hacer los resultados lo más objetivos posible, se adoptaron también medidas sobre las instalaciones. Los criterios para seleccionar las condiciones ambientales se centraron en la comodidad del catador para que pueda concentrarse en el ensayo. Se establecieron el volumen (15 mL) y la temperatura de la muestra de aceite (28 ± 2 ºC), ya que la concentración de los compuestos químicos que brindan las diferentes sensaciones se relaciona con la cantidad y la temperatura del aceite. Por lo tanto, la metodología oficial incluye indicaciones precisas sobre los dispositivos para calentar el aceite. Además, se reguló la forma y las dimensiones de la copa para la prueba, ya que estos factores afectan a la concentración relativa de los aromas, así como el color del cristal. El color del aceite de oliva virgen puede proporcionar indicaciones acerca de su sabor, produciendo expectativas sobre su clase e interfiriendo en la evaluación de la intensidad del sabor. Para evitar que los catadores perciban el color del aceite

antes de evaluar su olor y sabor, así como para eliminar cualquier prejuicio y la formación de tendencias que pueden afectar a la objetividad, los catadores utilizan copas oscurecidas (azules o ambarinas) para catar el aceite.

La presentación de las muestras se hace al azar, para evitar el efecto memoria, y su número es normalmente bajo (se considera aceptable hasta 4 o 5 muestras por sesión) para eliminar la influencia de la fatiga.

Los catadores utilizan una hoja de perfil (**Fig. 1.1**) que contiene los defectos sensoriales que se pueden encontrar normalmente en los aceites de oliva virgen. Entre las percepciones positivas, en la hoja se evalúan sólo los atributos que caracterizan el sabor del aceite: frutado, amargo y picante. El frutado, la sensación evocadora de la aceituna convenientemente madura, se evalúa mediante la inhalación directa, mientras que el resto de sensaciones se perciben por vía retronasal, ya que por esta vía su identificación es más precisa, gracias a que el estímulo tarda más tiempo en desaparecer. Es adecuado adoptar una escala, que normalmente es sencilla de usar por parte de personas expertas e inexpertas, para poder cuantificar los diferentes estímulos y procesar los datos estadísticos. Se utiliza una escala lineal de 10 cm de longitud para medir la intensidad de las notas sensoriales definidas en el vocabulario específico. Los datos de intensidad proporcionados por los catadores, expresados en centímetros, se tratan estadísticamente.

Tabla 1.2. Vocabulario específico para aceite de oliva desarrollado por el IOC.

Atributos negativos	
Mohoso	Sabor característico del aceite obtenido de olivas almacenadas en pilas
Mohoso-húmedo	Sabor característico del aceite obtenido de olivas almacenadas en condiciones húmedas durante varios días
Sedimento fangoso	Sabor característico del aceite que ha estado en contacto con los sedimentos depositados en los tanques subterráneos y las tinajas
Avinado-avinagrado	Sabor característico de algunos aceites que recuerda al vino o al vinagre. Es debido a la fermentación de las aceitunas que hace que se forme ácido acético, acetato de etilo y etanol
Metálico	Sabor que recuerda al metal, y que es característico de los aceites que se obtienen en plantas de procesamiento nuevas, o de los aceites procesados al principio de la cosecha
Rancio	Sabor resultado de un proceso oxidativo al estar en contacto con el aire
Atributos positivos	
Frutado	Serie de sensaciones olfativas que dependen de la variedad de la oliva. Se perciben por medio de la nariz
Amargo	Sabor característico del aceite que se obtiene sobre todo de aceitunas verdes
Picante	Sensación característica de los aceites producidos al principio de la cosecha, principalmente con aceitunas sin madurar
Otros atributos negativos	
Quemado	Sabor característico de los aceites que son calentados excesivamente durante el proceso, especialmente cuando la pasta se mezcla térmicamente en condiciones inadecuadas
Heno-madera	Sabor característico de los aceites producidos con olivas que se han secado
Áspero	Sensación pastosa y densa que producen ciertos aceites
Greasy	Sabor que recuerda a aceite mineral, gasoil o grasa
Agua vegetal	Sabor adquirido por el aceite como resultado del contacto prolongado con jugos acuosos de origen vegetal
Salmuera	Sabor del aceite obtenido de aceitunas conservadas en salmuera
Terroso	Sabor del aceite obtenido de aceitunas que se han recolectado con tierra o fango y que no se han lavado
Sucio	Sabor del aceite obtenido de aceitunas que han sido atacadas por las larvas de la mosca de la aceituna (*Bactrocera oleae*)
Pepino	Sabor que se produce cuando el aceite se envasa herméticamente durante mucho tiempo, especialmente en latas, y que se atribuye a la formación de 2-6-nonadienal

Sin embargo, se puede hallar más información en la hoja de perfil adoptada con anterioridad por la ECC en el Reglamento Nº 2568/91 (ver **Fig. 1.2**), y que, pese a no ser la hoja de perfil vigente, se sigue utilizando ya que proporciona un perfil más completo, es decir, un análisis cualitativo (descriptivo) de la muestra. En esta hoja de perfil, se solicita a los catadores que identifiquen el tipo de frutado, y que reconozcan las presencia de ciertos atributos como hierba, hojas, manzana y otras frutas. Los catadores miden la intensidad de los diferentes atributos en una escala que va del cero al cinco y, además, estiman el grado total usando una escala de nueve puntos. En esta escala se otorga el nueve a los aceites con características sensoriales excepcionales y el uno a los productos con la peor calidad. La puntuación media indica la categoría, y de ahí que un aceite sea EVOO cuando su calificación total sea mayor o superior a 6,5, VOO cuando su calificación esté comprendida entre 5,5 y 6,5, común entre 3,5 y 5,5 y lampante cuando sea menor de 3,5.

1.2.3. Variedades genéticas

A lo largo de los últimos años, el consumo de EVOO ha aumentado considerablemente en relación al consumo de aceites de oliva de inferior calidad, lo que se ha atribuido a las excelentes características organolépticas y nutricionales del mismo. Por ello, cada vez se producen más EVOOs monovarietales con el fin de responder a la creciente demanda por parte del consumidor, dado que la composición química de los aceites, así como las características organolépticas de los mismos, varían en función de la variedad genética de la aceituna empleada en su elaboración (Baccouri, 2008B; Tura, 2007).

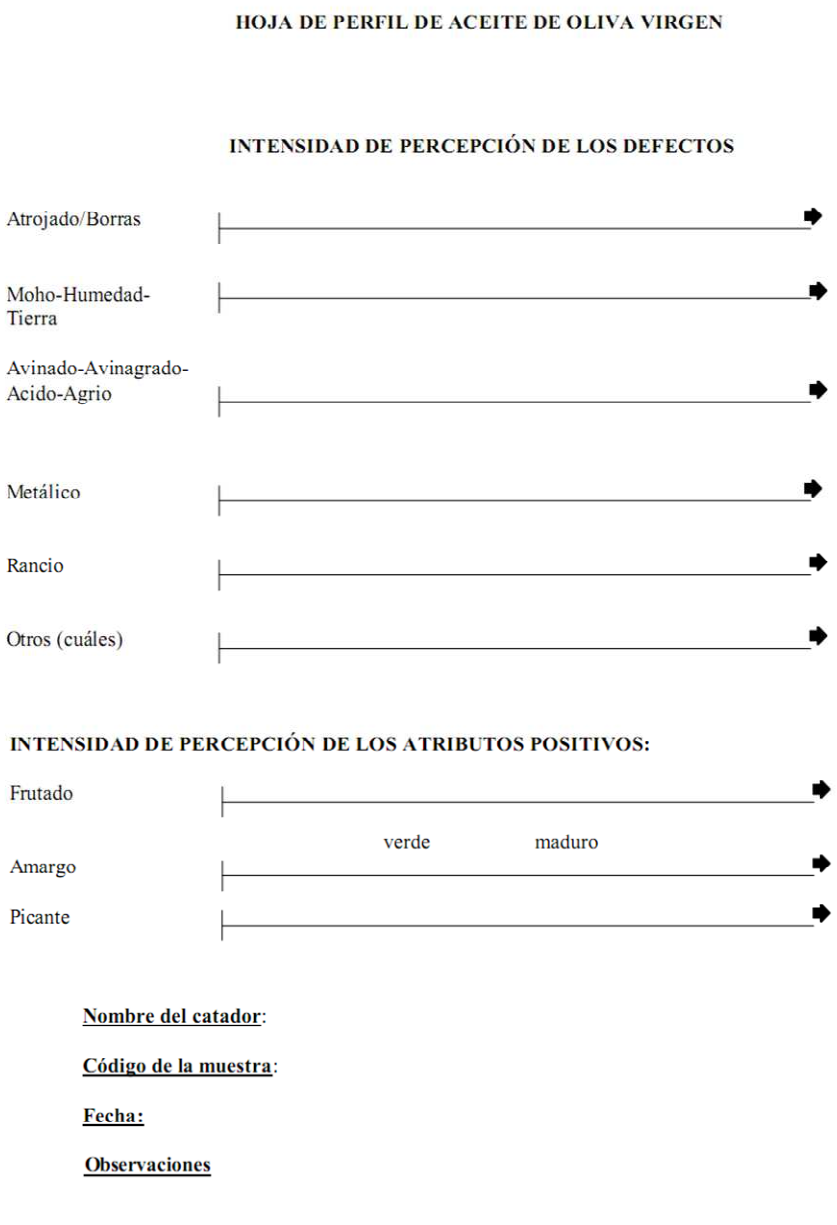
HOJA DE PERFIL DE ACEITE DE OLIVA VIRGEN

INTENSIDAD DE PERCEPCIÓN DE LOS DEFECTOS

Atrojado/Borras

Moho-Humedad-Tierra

Avinado-Avinagrado-Acido-Agrio

Metálico

Rancio

Otros (cuáles)

INTENSIDAD DE PERCEPCIÓN DE LOS ATRIBUTOS POSITIVOS:

Frutado

verde maduro

Amargo

Picante

Nombre del catador:

Código de la muestra:

Fecha:

Observaciones

Fig. 1.1. Ficha de cata de aceite de oliva virgen adoptada por el Reglamento (EC) Nº 640/2008, y vigente en la actualidad.

ACEITE DE OLIVA VIRGEN

HOJA DE PERFIL
NOTAS OLFATO-GUSTATIVAS-TÁCTILES

	(*)	1	2	3	4	5
Frutado de aceituna (madura y verde)						
Manzana						
Otra(s) fruta(s) madura(s)						
Verde (hojas, hierba)						
Amargo						
Picante						
Dulce						
Otro(s) atributo(s) tolerable(s) (especificar .....)						
Agrio/Avinado/Avinagrado/Ácido[1]						
Basto						
Metálico						
Moho/Humedad[1]						
Borras/Turbios[1]						
Atrojado						
Rancio						
Otro(s) atributo(s) intolerable(s) (especificar .....)						

[1] Táchese lo que no proceda.
* Percepción.
1 Casi imperceptible
2 Ligera
3 Media
4 Grande
5 Extrema

TABLA DE PUNTUACIONES

Defectos	Características	Evaluación global: Puntuación
Ninguno	Frutado de aceitunas Frutado de aceitunas y otros frutos frescos	9 8 7
Leves y casi imperceptibles	Frutado apagado de cualquier tipo	6
Perceptibles	Frutado algo defectuoso, olores y sabores anómalos	5
Notables, en el límite de aceptación	Claramente defectuoso, olores y sabores desagradables	4
Grandes y/o graves claramente perceptibles	Olores y sabores totalmente inadmisibles para el consumo	3 2 1

Observaciones: .....
.....
.....

Nombre del catador: .....

Clave de la muestra: .....

Fecha: .....

Fig. 1.2. Hoja de perfil para la cata de aceite de oliva virgen adoptada en el Reglamento (ECC) Nº 2568/91.

Existen muchos tipos y variedades de aceituna para la producción de aceite (Barranco, 2001). Actualmente, el mercado español está dominado principalmente por tres variedades que representan el 95% de los olivos: Arbequina, Hojiblanca y Picual, aunque el número de otras variedades también cultivadas en España es elevado y muy diverso, dependiendo de la región geográfica donde se ubique el cultivo. La variedad Picual o Marteña es la más importante y extendida, sobre todo en Andalucía, Castilla La Mancha y Extremadura. Su producción se aproxima al 50% del total de la aceituna de almazara española, y en torno al 20% de la producción mundial. La variedad Hojiblanca o Lucentina es la predominante en Málaga, muy abundante también en Sevilla y Córdoba. La variedad Arbequina se cultiva mayoritariamente en Lérida, Tarragona y Córdoba. Variedades cultivadas también en España son la Cornicabra, Lechín, Picuda y Verdial, entre otras.

Otras variedades genéticas de especial interés en el desarrollo de esta tesis son las cultivadas en la Comunidad Valenciana, entre las que cabe destacar la Serrana de Espadán y la Borriolenca (cultivadas principalmente en las provincias de Castellón y Valencia), y las variedades Farga y Canetera (cultivadas mayoritariamente en la provincia de Castellón).

1.2.4. Origen geográfico

Además de la variedad genética de las aceitunas, los EVOOs pueden mostrar características muy diversas en función del origen geográfico del cultivo (Cerretani, 2006). En España existen 32 PDOs (Ministerio de Medio Ambiente y Medio Rural y Marino (ed.): «Aceites de oliva virgen con denominación de origen»), cada una de ellas regida por sus propios estatutos, y establecidas con la finalidad de cuidar la calidad de los aceites por ellas producidos, marcando pautas de cultivo, recogida, elaboración, embotellado y etiquetado. Todas ellas están comprometidas con la calidad final del producto a través de rigurosos controles de calidad. En la **Fig. 1.3** se muestra la distribución geográfica de las distintas PDOs en España. Como se puede observar, la mayoría de ellas se concentran en Andalucía, que es la principal zona productora de aceite de oliva en el mundo.

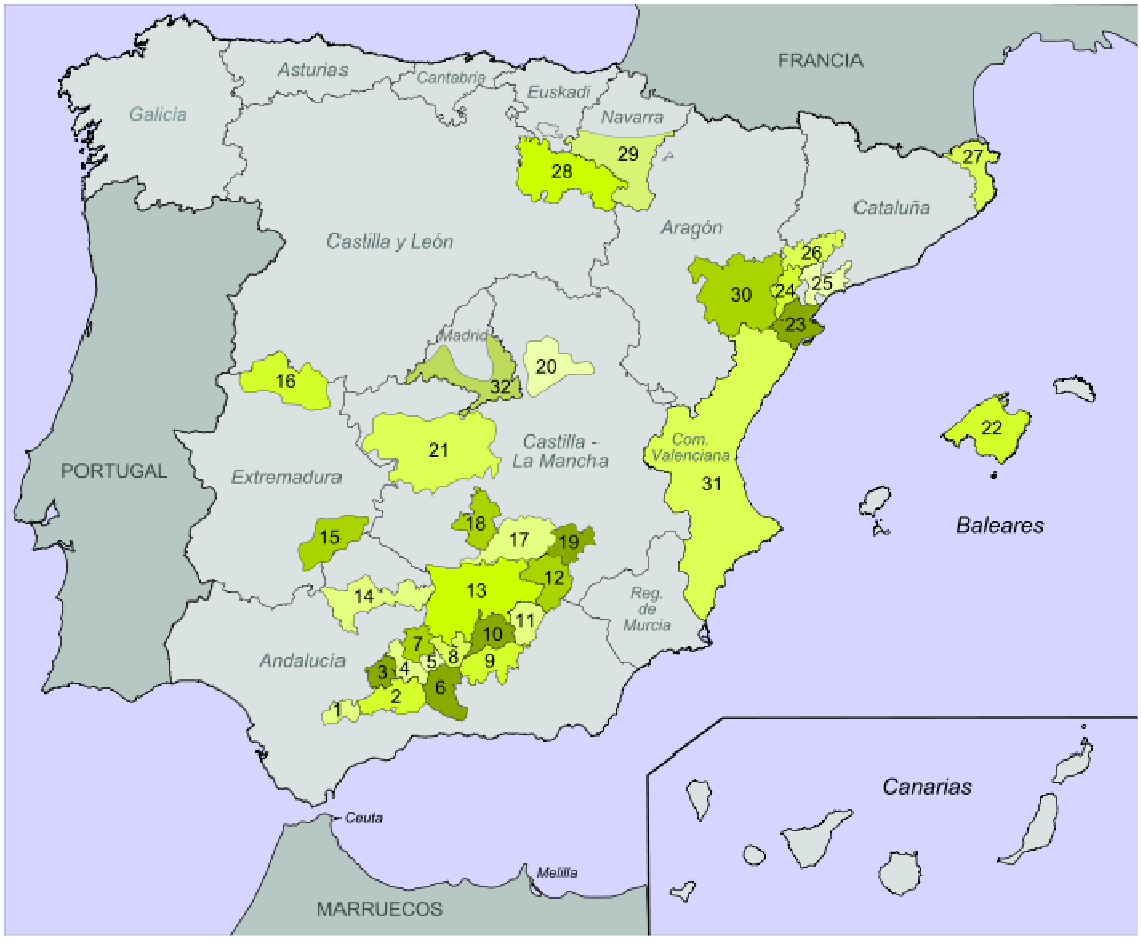

Fig. 1.3. Aceites de oliva virgen con PDO de España: 1. Sierra de Cádiz; 2. Antequera; 3. Estepa; 4. Lucena; 5. Priego de Córdoba; 6; Poniente de Granada; 7. Baena; 8. Jaén Sierra Sur; 9. Montes de Granada; 10. Sierra Mágina; 11. Sierra de Cazorla; 12. Sierra de Segura; 13. Campiñas de Jaén; 14. Montoro-Adamuz; 15. Monterrubio; 16. Gata-Hurdes; 17. Aceite Campo de Montiel; 18. Campo de Calatrava; 19. Aceite Montes de Alcaraz; 20. La Alcarria; 21. Montes de Toledo; 22. Aceite de Mallorca; 23. Baix Ebre-Montsià; 24. Oli de Terra Alta; 25. Siurana; 26. Les Garrigues; 27. Oli de l'Empordà; 28. Aceite de La Rioja; 29. Aceite de Navarra; 30. Aceite del Bajo Aragón; 31. Aceite de la Comunitat Valenciana; 32. Aceite de Madrid.

1.2.5. Compuestos procedentes de la oxidación del aceite de oliva

El aceite de oliva se caracteriza por una alta estabilidad oxidativa con respecto a otros aceites comestibles, lo que es debido a su composición en ácidos grasos, con altas concentraciones de ácido oleico y bajas de ácidos grasos poliinsaturados, así como también a la presencia de antioxidantes naturales como el α-T y diversos compuestos fenólicos (Tsimidou, 1992; Bendini, 2007). Sin embargo, el aceite de oliva es susceptible a oxidarse, como ocurre con los demás aceites comestibles. Los procesos de oxidación dependen de varios factores, siendo la presencia de oxígeno y de trazas metálicas, la temperatura y la luz (Al-Ismail, 1998 y 1999) algunas de las causas del deterioro del aceite. El deterioro oxidativo puede deberse a procesos de oxidación enzimáticos (que se dan cuando el aceite aún está en el fruto, o bien durante el proceso de extracción del mismo), o a procesos de oxidación químicos, como la fotooxidación (que se da cuando el aceite está expuesto a la luz), o la autooxidación (producida mayoritariamente durante el procesado o almacenamiento del aceite en contacto con oxígeno) (Bendini, 2009; Frankel, 1985).

La oxidación de los aceites conduce a la formación de hidroperóxidos, que son productos primarios muy inestables; a su vez, los hidroperóxidos se pueden descomponer o reaccionar con otras moléculas presentes en la matriz lipídica, dando lugar a toda una serie de productos secundarios, donde se incluyen centenares de compuestos con propiedades muy distintas, tales como compuestos volátiles, polímeros oxidados o moléculas con estructuras similares a sus respectivas moléculas de partida (como por ejemplo los OFAs) (Choe, 2006). Todos estos compuestos afectan negativamente al sabor y aroma de los aceites. Por ello, el estudio de la estabilidad oxidativa de los aceites es importante para determinar su calidad y tiempo de almacenaje (*shelf-life*) (Hamilton, 1994).

1.2.5.1. Evaluación de los productos primarios de la oxidación

Los ensayos analíticos normalmente usados para evaluar los productos primarios de la oxidación de un aceite son el índice de peróxidos y la medida de la absortividad de los dienos y trienos conjugados en el UV.

El valor del índice de peróxidos es aún, hoy en día, el parámetro más utilizado para medir el deterioro oxidativo de un aceite. Tradicionalmente, se establece mediante valoración iodométrica (método oficial, Reglamento (EEC Nº 2568/91), aunque se han desarrollado otros métodos que hacen uso de enzimas, HPLC y colorimetría. Sin embargo, y pese a la buena estimación que el índice de peróxidos proporciona sobre el estado oxidativo, su medida debe acompañarse de la determinación de otros parámetros, con el fin de tener un cuadro más completo de la evolución de la oxidación (Gordon, 2001). En la **Fig. 1.4** se observa que cuando se ha alcanzado el máximo valor del índice de peróxidos en la matriz, aparece una tendencia a su disminución, a la vez que aumenta proporcionalmente la velocidad de formación de los productos secundarios de la oxidación. Es por esto que la medida del índice de peróxidos no es suficiente para evaluar correctamente el estado oxidativo del aceite. Además, existen otros parámetros que pueden influenciar el valor del índice de peróxidos, como por ejemplo la temperatura, que produce la descomposición espontánea de los hidroperóxidos si es superior a 150 ºC (Gordon, 2001).

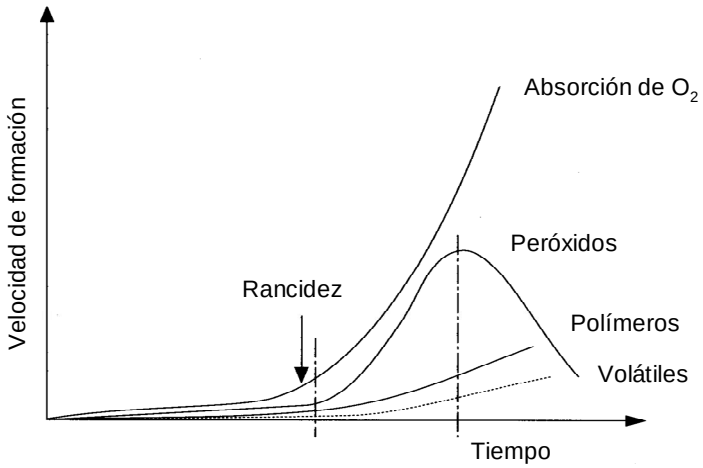

Fig. 1.4. Evolución de los principales productos de la oxidación lipídica (Lercker, 1997).

Por otro lado, durante la formación de radicales peróxidos e hidroperóxidos, tiene lugar un cambio en la posición de los dobles enlaces, que modifica su conjugación. El ensayo de dienos y trienos se basa en los cambios de conjugación que afectan a estas estructuras moleculares. Los dienos conjugados muestran una absorción a 232 nm y los trienos a 268 nm. Sin embargo, se forman también otros productos, derivados de los hidroperóxidos, que poseen una conjugación igual o similar, con lo cual pueden contribuir a la absorción, haciendo que la medida de los dienos y trienos conjugados sea menos específica que la del índice de peróxidos.

1.2.5.2. Evaluación de los productos secundarios de la oxidación

Se han propuesto diferentes métodos para establecer, junto con la evaluación de los productos primarios de la oxidación, un índice fiable que proporcione una idea real sobre el estado de oxidación de una matriz grasa (Farhoosh, 2009). Entre los índices propuestos, cabe destacar el de la p-anisidina, el de los compuestos reactivos frente al ácido tiobarbitúrico (Frankel, 1998), los

del hexanal, nonanal o su cociente (Frankel, 1998; Vichi, 2003), el de la medida del total de compuestos polares (Caponio, 2002; Melton, 1994), el del tiempo OSI, y más recientemente la determinación del contenido de OFAs mediante HPLC (Cortesi, 1991). Entre todos ellos, se comentan a continuación los métodos basados en el tiempo OSI y en la determinación de OFAs, que son los utilizados en esta tesis.

El OSI, es un instrumento que opera en condiciones estandarizadas de flujo de aire y de temperatura (90 – 110 ºC). Una de las ventajas de este instrumento es que, al trabajar en condiciones controladas, atenúa la termo-oxidación, lo que es importante para la evaluación de la cantidad de productos secundarios volátiles. El OSI hace pasar una corriente de aire purificado y caliente a través del aceite que se calienta a 90 – 110 ºC. El efluente de este aire se burbujea a través de un tubo que contiene agua desionizada. Este efluente, contiene ácidos orgánicos volátiles, como el fórmico (Jebe, 1993), así como otros compuestos volátiles formados durante la oxidación térmica del aceite, cuya disolución en agua da lugar a un aumento de la conductividad en la misma. Los resultados obtenidos, que se expresan como tiempo de inducción en horas, permiten una evaluación comparativa entre diferentes matrices lipídicas, si bien, su medida no se puede aplicar a estudios predictivos de la oxidación, ni para conocer a priori el tiempo de vida de un aceite. De hecho, las condiciones de estrés térmico, junto con el flujo de aire, aceleran la oxidación del aceite, por lo cual se promueven cinéticas de reacción entre el oxígeno y los ácidos grasos que difieren de aquellas que se producen en las condiciones normales de conservación del aceite.

Por otro lado, el uso de la HPLC, según un método puesto a punto por Cortesi y col. (1991), permite la identificación y la cuantificación de los principales productos secundarios de la oxidación de los ácidos grasos, tales

como hidroxiácidos y quetoácidos, previa derivatización de los mismos mediante una reacción de trans-esterificación. Analizando la matriz, se pueden comparar las cantidades generadas de estos productos, y establecer con ello la pauta seguida durante la evolución de la oxidación.

1.3. Técnicas analíticas

1.3.1. CEC

La CEC es una técnica analítica de separación en fase líquida que combina la elevada eficacia de la CZE con la alta selectividad y reproducibilidad proporcionadas por la HPLC. En CEC, la separación se lleva a cabo en columnas capilares rellenas total o parcialmente con una fase estacionaria. Como en CZE, el EOF a través de la columna es generado por un campo eléctrico. El EOF es un fenómeno interfacial que se genera debido a la presencia de cargas sobre la superficie del relleno de la columna. Por otro lado, es el responsable del bombeo en CEC y en otras técnicas de electroseparación. A su vez, da lugar a un perfil plano de velocidad de la fase móvil, a diferencia del perfil parabólico que se obtiene cuando el bombeo es por presión externa como en HPLC, lo que da lugar a picos con elevadas eficacias.

En CEC el mecanismo de separación es doble (Rathore, 1996). Por un lado, hay un mecanismo cromatográfico, ya que se produce un reparto de los solutos entre una fase móvil y una estacionaria. Por otro lado, los solutos iónicos también se separan mediante un mecanismo electroforético, esto es, en base a las diferencias de movilidad electroforética, por lo que la naturaleza del relleno de la columna determina el EOF e influye sobre la calidad de la separación.

1.3.1.1. Instrumentación en CEC

Un instrumento para CEC (ver el esquema de la **Fig. 1.5**) está constituido básicamente por una fuente de alto voltaje, un sistema para aportar disolvente y/o muestras hasta los viales de entrada y de salida de la columna, una columna capilar con una fase estacionaria en la cual se genera el EOF y tiene lugar la separación electrocromatográfica, un compartimento isotérmico para la columna y un sistema de detección capaz de registrar los perfiles de concentración de los analitos en el eluyente.

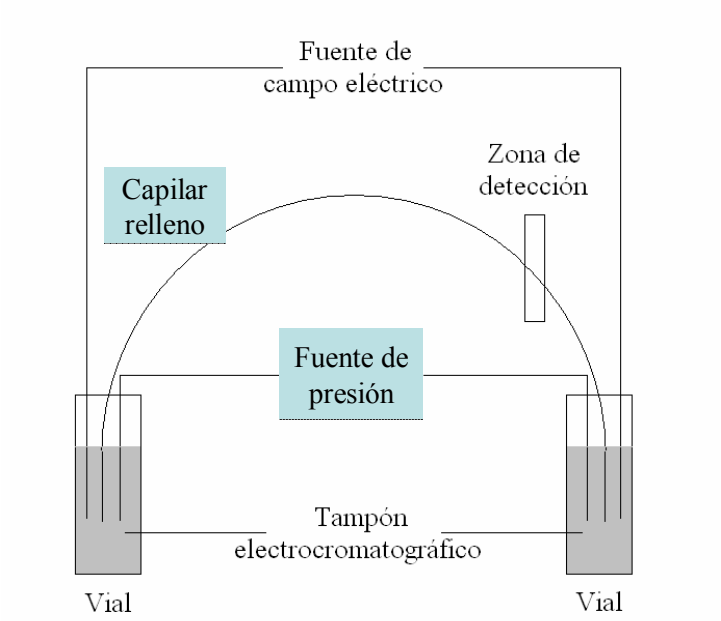

Fig. 1.5. Esquema de un instrumento de CEC.

La misma instrumentación utilizada en CE sirve para CEC, si bien, en este caso se debe de disponer de un sistema de presurización de los viales de entrada y salida. Esta presurización es necesaria para evitar la formación de burbujas, que podrían interrumpir la corriente. Las burbujas pueden originarse por diversas causas, ya sea por diferencias locales en la velocidad del EOF (Rathore, 1998), por diferencias locales en el campo eléctrico, por pérdida del gas atrapado en los poros de la fase estacionaria, o por gas formado electroquímicamente (Carney,

1999), por calentamiento (Knox, 1988; Tsuda, 1987), o en el caso de columnas empaquetadas, por la presencia de las fritas que mantienen la integridad estructural del relleno (Rebscher, 1994). La presurización se puede realizar en el vial de entrada o en el de salida, aunque generalmente se realiza en ambos viales, ya que así se asegura un flujo reproducible. Para presurizar los viales se usa un gas inerte, normalmente N_2, a unas presiones próximas a 10 bar.

La calidad de una técnica de separación se caracteriza por la eficacia, la selectividad, la sensibilidad y la reproducibilidad. Para obtener resultados reproducibles en CEC, es necesario el control de parámetros como la temperatura de la columna, el voltaje aplicado y la presión. En los equipos comerciales de CE, estos parámetros se controlan automáticamente, lo que da lugar a mejoras significativas de la reproducibilidad y seguridad de las separaciones.

La detección espectrofotométrica UV-Vis es la más utilizada en CEC (Choudhary, 2000; Rozing, 2001; Devowsky, 2002; Cahours, 2002), siendo posible trabajar en los modos de detección directo e indirecto. La detección se realiza en la misma columna, utilizando como celda de detección una pequeña sección de la misma, adyacente al relleno, y de la cual se ha retirado la capa protectora de polímero. Otras técnicas de detección también ampliamente utilizadas son la fluorescencia inducida por láser (Wall, 2002; Horstkötter, 2002; Liu, 2001), y más recientemente la MS (Shamsi, 2004; Klampfl, 2004; Barceló-Barrachina, 2004).

1.3.1.2. Columnas empleadas en CEC

Las columnas para CEC se preparan normalmente a partir de capilares de sílice fundida con diámetros internos comprendidos entre 100 y 200 μm. En base a las diferencias de soportes cromatográficos, se pueden distinguir tres tipos de columnas: las abiertas, las empaquetadas y las monolíticas.

Las columnas monolíticas, constituidas por un lecho continuo, poseen una estructura porosa que permite trabajar en HPLC con caudales elevados, y por tanto, obtener separaciones rápidas sin que ello conlleve un aumento excesivo de la presión necesaria para mantener el caudal, a diferencia de lo que sucede con las columnas particuladas. En CEC las columnas monolíticas constituyen igualmente una alternativa a las empaquetadas, con algunas interesantes ventajas. Así, dada su estructura continua, no es necesario el empleo de fritas en los extremos del lecho monolítico, ya que éste está anclado directamente sobre la pared del capilar mediante enlaces covalentes. Además, pueden prepararse *in situ*, por lo que la fabricación de lechos monolíticos es relativamente sencilla en comparación con las técnicas de empaquetado de partículas.

Las columnas monolíticas se pueden clasificar en dos categorías principales, de sílice y poliméricas. Las columnas de sílice se preparan usando la tecnología sol-gel. La estructura de un monolito de sílice muestra esqueletos interconexionados que crean una distribución determinada de poros.

Por otro lado, la preparación de las columnas monolíticas poliméricas se lleva a cabo fácilmente mediante el relleno de las columnas capilares con una mezcla de polimerización constituida por monómeros, un agente entrelazante (*cross-linker*), una mezcla porogénica de disolventes y un iniciador radicalario. La hidrofobicidad del monolito resultante se puede controlar seleccionando la naturaleza del monómero (Liao, 1996; Palm, 1997). El EOF se asegura mediante la presencia de monómeros derivados de los ácidos acrílico o sulfónico, o mediante sales de amonio cuaternario en la mezcla de polimerización (Ericson, 1999). La polimerización se inicia por medios térmicos, químicos o mediante radiación UV.

Para evitar cualquier desplazamiento del monolito a lo largo de la columna es necesario anclar el polímero a la pared interna del capilar. Para ello, antes de

introducir en el capilar la mezcla de polimerización, se silaniza la pared interna del mismo. Con este fin, en la mayor parte de los casos, se utiliza 3-(trimetoxisilil)propil metacrilato (*silano binding*).

Para construir monolitos se han utilizado diferentes tipos de polímeros, pudiendo distinguirse principalmente entre los derivados de acrilamida, poliestireno y ésteres de metacrilato o acrilato. En las primeras columnas monolíticas que fueron descritas se utilizó acrilamida y metacrilamida (Hjertén, 1989; Fujimoto, 1995; Hoegger, R. 2001). Estos polímeros se preparan por polimerización de acrilamida, metacrilamida o sus derivados en presencia de metilenbisacrilamida o piperazina diacrilamida como agentes entrelazante. Las columnas monolíticas basadas en poliestireno (Gusev, 1999; Petro, 1996) se obtienen por polimerización de estireno o sus derivados con divinilbenceno como agente entrelazante. Los monolitos basados en ésteres de metacrilato (Merthar, 2003; Zhang, 2003; Peters, 1998A y B) se preparan mediante polimerización de butilmetacrilato u otros ésteres derivados del metacrilato empleando etilenglicol dimetacrilato como agente entrelazante.

1.3.1.3. Polimerización de columnas monolíticas basadas en ésteres de metacrilato y acrilato

Las columnas monolíticas basadas en polimetacrilato son las más extendidas y mejor caracterizadas, habiendo sido ampliamente desarrolladas por Svec y col. (Peters, 1998A y B), quienes han descrito aplicaciones tanto en HPLC como en CEC. Los polímeros de metacrilato y acrilato poseen características mecánicas y químicas que les hacen altamente apropiados como fases estacionarias. Son estables en un amplio rango de valores de pH (2–12), a diferencia de las fases estacionarias basadas en sílice, que se degradan con gran

facilidad por encima de pH 9. Su síntesis es rápida y sencilla, pudiendo partir de monómeros de polaridades muy diversas.

La polimerización de los monolitos basados en ésteres de metacrilato y/o acrilato se realiza mediante una reacción radicalaria, iniciada generalmente por una temperatura elevada, por irradiación UV, o por agentes químicos a temperatura ambiente. Para la iniciación térmica de la polimerización se suele adicionar a la mezcla de monómeros AIBN (Peters, 1998A y B; Chirica, 2001), peróxido de benzoilo (Xie, 1997), u otros peróxidos (Cantó-Mirapeix, 2008).

Svec y col. (Peters, 1998A y B) han demostrado que las propiedades cromatográficas (eficacia, selectividad, permeabilidad, etc) de estos materiales pueden alterarse variando la composición de la mezcla de polimerización, lo que constituye una vía interesante, no sólo para el desarrollo y optimización de las separaciones cromatográficas, sino para sus aplicaciones de interés ambiental, bioquímico e industrial.

1.3.1.4. Caracterización de materiales monolíticos

Los materiales monolíticos se pueden caracterizar estudiando tanto sus propiedades morfológicas como electrocromatográficas (ver sección 1.3.3).

Existen numerosas técnicas que proporcionan información acerca de la influencia de diversos factores sobre las propiedades morfológicas de los materiales monolíticos.

Para el estudio de las propiedades morfológicas, existen numerosos métodos y herramientas analíticas que proporcionan información acerca de la influencia de diversos factores sobre la morfología de los materiales monolíticos. Entre ellas cabe citar la SEM (Baeuml, 2002), la porosimetría de intrusión de mercurio (Doneanu, 2002), la adsorción/desorción de nitrógeno evaluada mediante la ecuación de Brunauer-Emmet-Teller (Brunauer, 1938) y la

permeabilidad cromatográfica. Las columnas monolíticas utilizadas en esta tesis se han caracterizado principalmente mediante SEM, por lo que esta técnica se comenta más extensamente a continuación.

Mediante SEM se obtienen imágenes de la estructura de un material. Sobre la superficie del material se enfoca un haz de electrones. Este haz barre la superficie del material, produciendo principalmente la emisión de electrones secundarios de baja energía y electrones retrodispersados de mayor energía, recogiéndose ambos mediante los adecuados sistemas de detección (Aballe, 1996). La información obtenida varía según las características del detector empleado. Los electrones secundarios se forman en una delgada capa superficial, del orden de 5 a 10 nm de espesor. La señal está constituida en parte por electrones que emergen de la muestra con una energía inferior a 50 eV. El número de electrones de este tipo es suficientemente elevado como para establecer un buen contraste entre las estructuras que se quieren describir. Por otra parte, al tratarse de electrones de baja energía, pueden desviarse fácilmente de su trayectoria emergente inicial, y se puede obtener información de zonas que no están a la vista del detector. Esta particularidad es fundamental para otorgar a la señal la posibilidad de aportar una información tridimensional de la topografía de la muestra, siendo quizás la característica más conocida de esta técnica.

Por otro lado, la principal utilidad de la señal de electrones retrodispersados, compuesta por aquellos electrones que emergen de la muestra con una energía superior a 50 eV, reside en que su emisión depende fuertemente del número atómico de los elementos de la muestra. Por esta razón, dos zonas con distinta composición química se revelarán con distinta intensidad, aunque no exista ninguna diferencia de topografía entre ellas.

Para aplicar SEM la muestra a analizar debe estar seca. En caso contrario, la baja presión existente en el microscopio causaría la evaporación de los

componentes volátiles que saldrían despedidos violentamente, alterando la estructura de la muestra. Además, la superficie debe ser conductora, lo que se consigue recubriéndola con una película de un material conductor. Para ello, se utilizan técnicas de pulverización catódica a alto vacío. Por otro lado, la reducida estabilidad térmica de los polímeros limita el voltaje que puede aplicarse para obtener las imágenes.

1.3.2. LC

La cromatografía es un método físico de separación en el cual los componentes a separar se distribuyen entre dos fases: la fase estacionaria, que permanece fija, y la fase móvil, que se mueve en una dirección definida. Un sistema cromatográfico (ver **Fig. 1.6**) se compone al menos de un sistema de bombeo, un dispositivo para la introducción de la muestra o inyector, una columna y un detector, más el sistema adecuado de adquisición de datos y control.

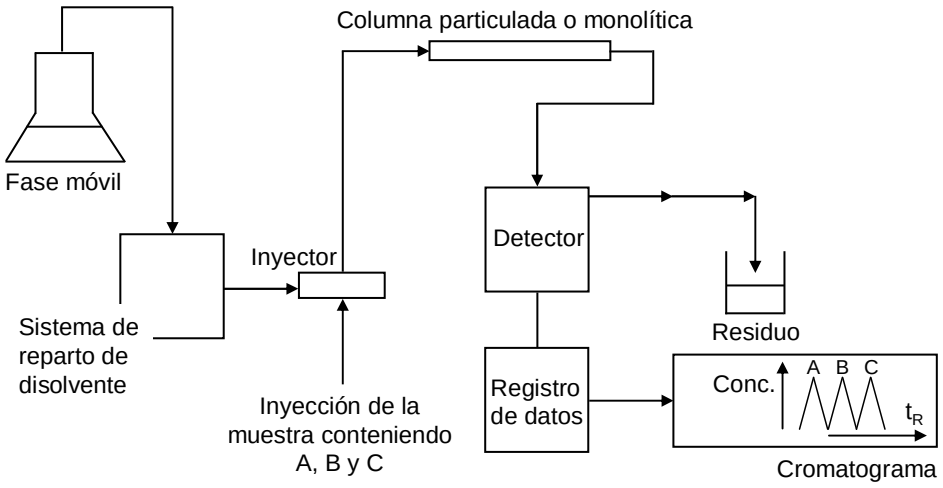

Fig. 1.6. Diagrama de bloques de los componentes de un cromatógrafo de líquidos.

Las bombas empleadas en LC pueden ser de dos tipos: bombas isocráticas o bombas de gradiente. Los módulos de bombas para gradiente generan, mediante su control programado, mezclas de composición variable. Según el tipo de bomba, las mezclas se preparan a baja o a alta presión, siendo distintas las características, ventajas y limitaciones de cada tipo.

Tanto en LC como en otras técnicas analíticas, la muestra se inserta en el flujo de corriente de la fase móvil a través de un bucle de inyección mediante una válvula de 6 vías y 2 posiciones, que puede ser manual o automática. El contenido del bucle se intercala entre el módulo de bombas y la entrada de la columna.

El tipo de columna a emplear dependerá del mecanismo de retención con el que se quiera trabajar. En base a esto, los tipos de LC más habituales son:

- Cromatografía de reparto: se utiliza una columna con una fase líquida enlazada. Dependiendo de las polaridades relativas de las fases móvil y estacionaria, se distinguen dos modalidades: RP, cuando la fase estacionaria es apolar y la fase móvil es polar, o bien NP, cuando la fase estacionaria es polar y la fase móvil es apolar.
- Cromatografía iónica: la fase estacionaria es un intercambiador catiónico o aniónico de tipo ácido fuerte, base fuerte, ácido débil o base débil.
- Cromatografía de exclusión molecular: como fase estacionaria se utilizan los poros de un sólido microporoso o de un gel.

Por otro lado, es importante desgasificar los disolventes para prevenir la formación de burbujas en el equipo. Para ello, los cromatógrafos líquidos suelen incluir un desgasificador en línea, antes del paso de la fase móvil por el módulo de bombas.

Las técnicas de detección más empleadas en LC son la espectrofotometría UV-Vis y la MS. Como detectores alternativos se utilizan los de índice de

refracción, así como diversos detectores evaporativos. Para aplicaciones específicas se usan los detectores amperométricos y fluorimétricos. Finalmente, la detección conductimétrica es habitual en cromatografía iónica. En espectrofotometría UV-Vis, la señal es proporcional a la concentración molar del soluto, cuya absortividad molar depende de la naturaleza del grupo o grupos absorbentes. Cuando los LODs no son lo suficientemente bajos, se utilizan técnicas de preconcentración, o se exalta la absortividad de los solutos aumentando su conjugación por derivatización. Los detectores obedecen a dos tipos de diseños: longitud de onda variable y fila o matriz de diodos. En los primeros, se selecciona una longitud de onda de medida fija, mientras que los segundos son capaces de barrer todo el rango del espectro UV-Vis varias veces por segundo. En este último caso, no existe monocromador, de modo que sobre la muestra incide radiación de todas las frecuencias. Después del paso del haz por la muestra, se dispersa la radiación transmitida, de modo que cada longitud de onda incide sobre un fotodiodo distinto.

En MS, el detector es un instrumento que proporciona información de alto nivel sobre las estructuras moleculares de los analitos, diferenciando entre grupos funcionales, elementos químicos e isótopos, separando los fragmentos en función de su relación *m/z*. Un detector de MS acoplado a un cromatógrafo puede diferenciar compuestos con características de retención muy similares, siendo posible identificarlos y/o cuantificarlos aunque sólo estén parcialmente resueltos, o incluso no resueltos en absoluto. En la sección 1.3.5 se explican más extensamente las características y tipos de espectrómetros de masas.

Más recientemente, se han introducido modalidades cromatográficas que implican miniaturización, bien en el tamaño de la columna o en el diámetro partícula. Entre las ventajas de estas técnicas de miniaturización, cabe citar la reducción de los tiempos de análisis, del consumo de reactivos, del volumen de

residuos generados y del tamaño de muestra. A su vez, se obtienen mejoras en la sensibilidad (los LODs son menores), mayores eficacias y tiempos de análisis más cortos.

Entre sus desventajas, hay que indicar las mayores exigencias instrumentales, como el uso micro-bombas, micro/nano-nebulizadores, miniaturizar conexiones, etc.

Atendiendo al diámetro de la columna, y a otras características relacionadas, se distingue entre micro-LC, LC capilar y nano-LC. En la siguiente tabla se muestran algunas de las características representativas de cada una de estas modalidades.

Tabla 1.3. Características representativas de las diversas técnicas de miniaturización.

Parámetro	LC clásica	Micro-LC	LC capilar	Nano-LC
Diámetro interno	4,6 mm	1 – 2,1 mm	0,1 – 1 mm	25 – 100 µm
Longitud	1,5 – 25 cm	1,5 – 20 cm	1,5 – 20 cm	1,5 – 20 cm
Diámetro partícula	1,8 – 5 µm	1,8 – 5 µm	1,8 – 5 µm	1,8 – 3 µm
Volumen inyección	5 – 100 µL	1 – 5 µL	0,03 – 0,3 µL	0,03 – 0,3 µL
Caudal típico	< 1 mL min^{-1}	10 – 100 µL min^{-1}	1 – 10 µL min^{-1}	0,1 – 1 µL min^{-1}

Por otro lado, existe otra modalidad cromatográfica, la UPLC, que trabaja con tamaños de partícula más pequeños y caudales más elevados que la cromatografía convencional con el fin de obtener mayor velocidad de análisis, capacidad de pico, resolución y sensibilidad.

1.3.3. Medida de parámetros cromatográficos

Para llevar a cabo una separación cromatográfica, el analista debe establecer si se puede separar adecuadamente al analito del resto de componentes de la muestra, y si la cantidad en que se halla es suficiente como para poderlo detectar y/o determinar. El tiempo que transcurre desde la inyección hasta la detección de un analito es su tiempo de retención o t_R. Por su parte, el factor de capacidad o retención relativa (k) expresa la retención neta en unidades de tiempo muerto, t_0, o tiempo que tarda en eluir un compuesto que no presenta retención:

$$k_i = \frac{t_{R,i} - t_0}{t_0} \quad (1)$$

donde $t_{R,i}$ es el tiempo de retención del analito i. El intervalo óptimo de valores de k se sitúa entre 1 y 5, si bien valores entre 0,2 y 20 son aceptables. Valores de k inferiores a 0,2 indican poca retención, preferencia excesiva del soluto por la fase móvil. Por el contrario, valores de k superiores a 20 indican una retención demasiado alta, producida por una preferencia excesiva del soluto por la fase estacionaria, lo que implica tiempos de análisis muy largos y en general picos anchos y de baja altura, difíciles de detectar y de medir con precisión, y por tanto, con LODs mayores de lo esperado.

La capacidad de un sistema cromatográfico para distinguir entre dos solutos se expresa mediante el factor de selectividad $\alpha_{i,j}$, que se calcula como el cociente entre las retenciones relativas de ambos solutos:

$$\alpha_{i,j} = \frac{k_j}{k_i} \quad (2)$$

siendo i y j dos picos adyacentes, e i es el compuesto menos retenido.

El grado de separación entre dos solutos se mide mediante la resolución, R:

$$R = \frac{t_{R,i} - t_{R,j}}{0{,}5(w_i + w_j)} \tag{3}$$

siendo w_i y w_j las anchuras de las bases de los picos de los compuestos *i* y *j*.

Por su parte, la eficacia describe el grado de ensanchamiento de bandas. Se obtiene una elevada eficacia cuando los picos se mantienen estrechos a pesar de haber permanecido mucho tiempo dentro del sistema. La eficacia global de un sistema se describe mediante el número de platos teóricos (*N*), y la eficacia por unidad de longitud por la altura equivalente a un plato teórico (*H*).

Para un soluto determinado, *N* puede calcularse a partir de las expresiones:

$$N = 16 \cdot \left(\frac{t_R}{w}\right)^2 \quad \text{y} \quad N = 5{,}54 \cdot \left(\frac{t_R}{w_{1/2}}\right)^2 \tag{4}$$

donde t_R es el tiempo de retención del soluto y *w* y $w_{1/2}$ son la anchura de la base del pico y su anchura a media altura, respectivamente. Por su parte, *H* se relaciona con *N* a través de la expresión:

$$N = \frac{L}{H} \tag{5}$$

donde L es la longitud de la columna.

La ecuación de Van Deemter describe las contribuciones a *H*, esto es, indica como los diversos factores de construcción y funcionamiento de la

columna influyen sobre la eficacia. Para el caso de columnas microparticuladas tanto en HPLC como en CEC, se tiene:

$$H = A + \frac{B}{\bar{u}} + C \cdot \bar{u} \qquad (6)$$

donde $\bar{u}$ es la velocidad lineal promedia de la fase móvil.

El término *A* de la ecuación de van Deemter se conoce como difusión de remolino o torbellino, y se debe a la distinta longitud de los caminos recorridos y a las distintas velocidades de los solutos en su avance por el lecho cromatográfico (ver **Fig. 1.7A**). Como las moléculas se mueven a distinta velocidad según sea la anchura del camino seguido, se produce un ensanchamiento de banda que es debido a la "tortuosidad" del lecho, y también a que la fase móvil que avanza por el centro de los "canales" se mueve más rápidamente que la que avanza pegada a las paredes. Esta contribución a *H* es función sólo de la geometría del relleno, esto es, no depende de $\bar{u}$.

El término *B* representa la difusión molecular longitudinal (en la dirección axial), que es debida al movimiento de los solutos a nivel molecular (**Fig. 1.7B**). Esta difusión es proporcional a la difusibilidad de los solutos y al tiempo de residencia de la muestra en la columna. Conforme aumenta el tiempo de permanencia, mayor es la difusión, y por tanto el término *B* sólo cobra importancia a velocidades de flujo bajas. Esta dependencia con el tiempo de permanencia se refleja en la proporcionalidad inversa de esta contribución repecto a $\bar{u}$.

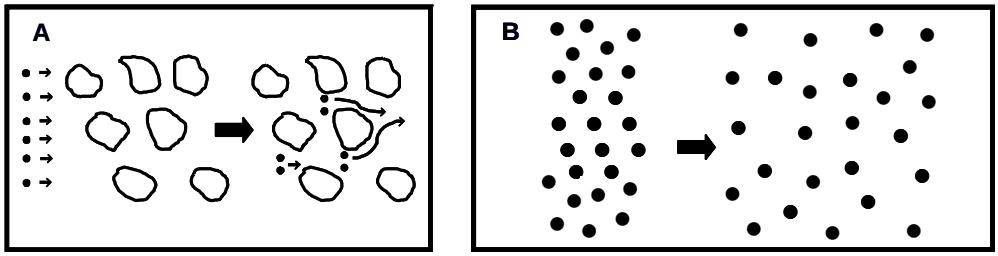

Fig. 1.7. A) Difusión de remolino y B) difusión molecular longitudinal.

El término *C* corresponde a la contribución combinada de la velocidad de las transferencias de masa entre las fases móvil y estacionaria (C_M y C_S). Este término es proporcional a $\bar{u}$ debido a la lentitud de las transferencias de masa del soluto entre ambas fases, de modo que la importancia del término *C* aumenta con la velocidad de la fase móvil al ser menor el tiempo de equilibrado entre ambas fases. La lentitud o retraso con la que se efectúan las transferencias de masa después de cada "etapa" de avance de la fase móvil origina un ensanchamiento de la zona ocupada por el soluto.

Los términos *A* y *C* de la ecuación de van Deemter indican que la eficacia de la columna puede mejorarse utilizando partículas de fase estacionaria más pequeñas, o también rellenos más uniformes. La forma de la curva de van Deemter proporciona información acerca de la calidad del empaquetado o relleno de la columna cromatográfica. Cuanto menores sean las contribuciones de los términos *A* y *C* mayor será el número de platos teóricos a una determinada velocidad de la fase móvil. En la **Fig. 1.8** se muestra una representación típica de esta ecuación.

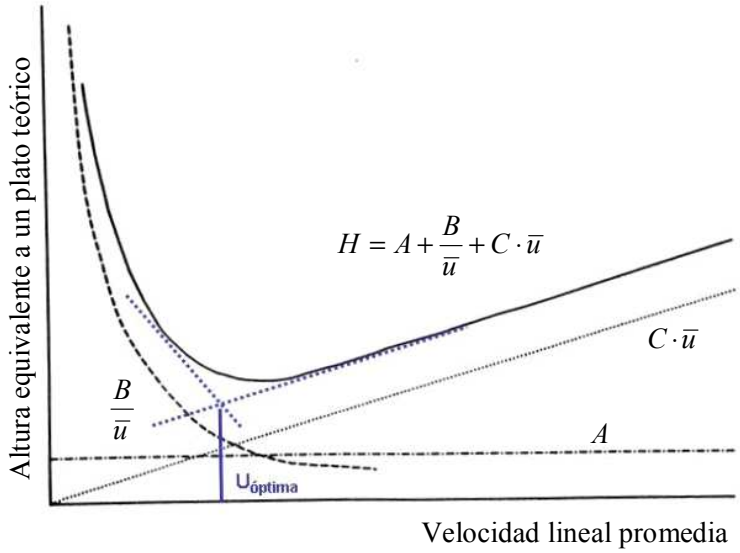

Fig. 1.8. Representación de H frente a $\overline{u}$ (curva de Van Deemter).

1.3.4. Espectroscopia IR

La región IR del espectro electromagnético se extiende entre el final de la zona del visible y el inicio de la región de las microondas, tal como se muestra en la **Fig. 1.9**.

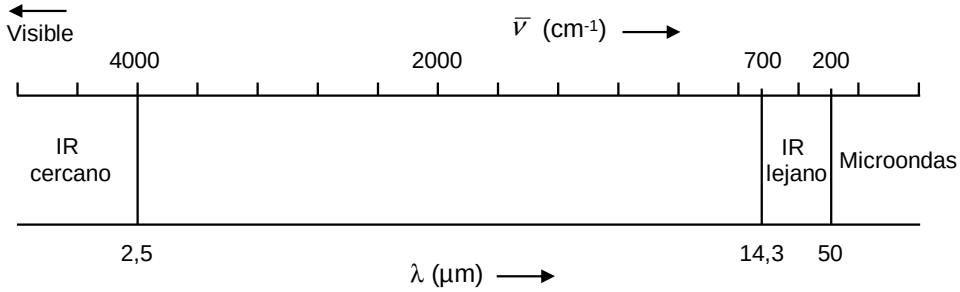

Fig. 1.9. Región IR del espectro electromagnético.

La sección de la extensa región IR que proporciona mayor cantidad de información estructural a nivel molecular es la que se extiende entre 4000 y 650 cm^{-1}. Esta región se denomina región IR media. El empleo del IR lejano (entre

650 y 200 cm^{-1}) se ha extendido considerablemente en las últimas décadas, sobre todo para el estudio de compuestos organometálicos e inorgánicos. La región IR cercana, entre 12500 y 4000 cm^{-1}, accesible a la óptica de cuarzo, y donde se presentan los armónicos de las transiciones del IR medio, se utiliza extensamente con fines clasificatorios y estudios de autenticidad de muestras, si bien es escasa su utilización con fines estructurales. Moléculas relativamente sencillas pueden dar lugar a espectros de absorción IR muy complejos. Puede decirse que el espectro IR caracteriza a una estructura molecular, dado que dos moléculas diferentes, a excepción de los isómeros ópticos, deben mostrar espectros IR diferentes. Esta propiedad ha sido utilizada ampliamente en la caracterización de compuestos orgánicos. La existencia de extensas bases de datos de espectros IR permite el uso de esta técnica acoplada a sistemas cromatográficos en la identificación y determinación rápida de componentes de mezclas orgánicas. Aunque el espectro IR caracteriza a cada compuesto, ciertas agrupaciones atómicas dan lugar siempre a bandas en determinados intervalos de frecuencias, que son relativamente independientes de la naturaleza del resto de la molécula. Estas bandas, características de grupos funcionales, permiten una amplia utilización de la espectroscopia IR en determinación estructural. La espectroscopia IR se puede aplicar con fines cuantitativos haciendo uso de la ley de Lambert-Beer. Esta ley se cumple si la anchura nominal de la radiación de excitación (monocromaticidad del haz) es mucho menor que la anchura de la banda de absorción. Esta relación es con frecuencia poco favorable en espectroscopia IR, donde las bandas de absorción son mucho más estrechas que en la zona UV-Vis. Pueden también presentarse problemas con la reproducibilidad de los espectros por las dificultades inherentes a la preparación de muestras para espectroscopia IR. No obstante, estas dificultades pueden

solventarse con un trabajo más cuidadoso que el usual en las determinaciones cuantitativas en UV-Vis.

1.3.4.1. Espectrofotómetros de IR

Los espectrofotómetros de IR se clasifican, de acuerdo con la técnica de medición utilizada, en dispersivos y FTIR. Los espectrofotómetros IR dispersivos fueron los primeros en desarrollarse, y funcionan mediante barrido de frecuencias. Los espectrofotómetros FTIR, basados en un barrido interferométrico, someten a la muestra a irradiación IR policromática. Los espectrofotómetros FTIR, que suministran la información en forma digitalizada, se han impuesto frente a los de tipo dispersivo en las últimas décadas por la rapidez, sensibilidad, resolución y relación señal/ruido alcanzables, siendo los utilizados en esta tesis.

1.3.4.2. Técnicas de reflexión en el IR

La espectroscopia IR puede ser utilizada para estudiar una amplia variedad de materiales. No obstante, en muchos casos, los tratamientos utilizados para la preparación de las muestras pueden resultar perjudiciales o simplemente impracticables, como por ejemplo cuando se intenta registrar espectros IR de sólidos que dispersan la radiación, tales como papel, polímeros de elevada masa molecular, gomas, etc. En estos casos las técnicas de reflexión constituyen una alternativa viable. Entre todas ellas, se comenta a continuación la técnica de ATR, que es la utilizada en esta tesis.

La técnica de ATR se basa en el hecho de que cuando la radiación electromagnética que se propaga a través de un medio ópticamente denso llega a una interfase con un medio de menor índice de refracción, y además el ángulo de incidencia es mayor que el ángulo crítico, la radiación no escapa del medio

denso, sino que es totalmente reflejada internamente. Sin embargo, debido a la naturaleza ondulatoria de la radiación electromagnética, la reflexión no ocurre directamente en la interfase de los dos medios; la radiación realmente sale del medio más denso y se extiende a lo largo de una distancia corta al otro lado de la interfase, en el seno del medio de bajo índice de refracción, antes de retornar. La profundidad con la cual la radiación penetra en el medio de bajo índice de refracción depende de la longitud de onda de la radiación. La distancia de penetración se puede calcular mediante la ecuación de Harrick:

$$d = \frac{\lambda_1}{2\pi n_1 \left[sen^2\theta_1 - (n_2 / n_1)^2 \right]^{1/2}} \qquad (7)$$

donde λ_1 es la longitud de onda de la radiación incidente, θ_1 es el ángulo de incidencia, n_1 es el índice de refracción de la muestra y n_2 es el índice de refracción del prisma o plato reflector.

Así pues, si un haz de radiación monocromática atraviesa un prisma de forma que el medio más denso está formado de algún material de elevado índice de refracción que trasmite la radiación IR, y el otro medio por una muestra, entonces la muestra absorberá algo de la radiación IR incidente. El registro de la radiación cuando finalmente sale del medio más denso suministra un espectro muy similar al espectro IR convencional. Así, cuando un haz de radiación monocromática atraviesa el prisma de forma que se refleje en su cara posterior, sobre la que se encuentra la muestra (**Fig. 1.10A**), dependiendo del ángulo de incidencia θ_1 del haz, y de la razón entre los índices de refracción del medio menos denso n_2 (muestra) al más denso n_1 (prisma), se pueden observar tres casos (**Fig. 1.10B**):

1.-Si sen $\theta_1 < n_2/n_1$ se producirá alguna reflexión, pero la mayor parte del haz será refractado, siendo el ángulo de refracción $\theta_2 > \theta_1$.

2.-Si sen $\theta_1 = n_2/n_1$ el ángulo de refracción $\theta_2 = 90º$ y la radiación se desplazará a lo largo de la interfase. En este caso θ_1 se denomina ángulo crítico, θ_c.

3.-Si sen $\theta_1 > n_2/n_1$ el ángulo de refracción θ_2 es imaginario y la radiación se refleja hacia el medio más denso. Esta situación corresponde a la reflexión total interna.

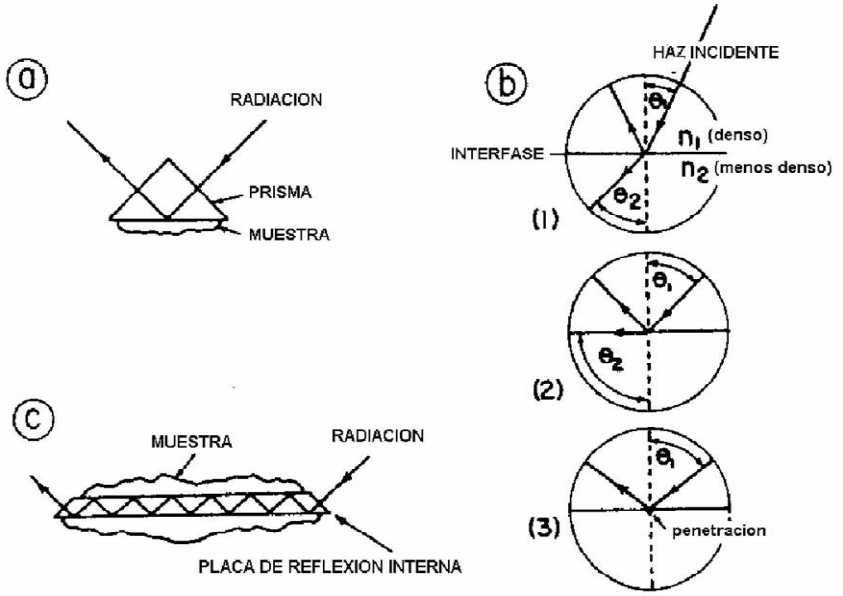

Fig. 1.10. Técnica de reflexión interna: a) Reflexión interna simple en un prisma; b) características de la reflexión en dependencia con el ángulo de incidencia; c) método de reflexión múltiple.

En los accesorios de ángulo fijo más modernos, el ángulo de incidencia es alrededor de unos 45º, y la profundidad de penetración es igual a una fracción de la longitud de onda de la radiación incidente, si bien su valor exacto depende de los índices de refracción de la muestra y del plato reflector.

A partir de fundamentos teóricos y de la experiencia práctica, se ha establecido que en la reflexión interna total se produce una onda evanescente de

igual frecuencia que la de la radiación reflejada, cuya amplitud decrece de forma logarítmica dentro del material menos denso más allá de la interfase. Esa onda evanescente es capaz de interactuar con el medio absorbente en la zona posterior a la interfase, originando una reducción o atenuación de la radiación reflejada total.

En esta técnica la muestra es presionada contra un prisma o placa de material óptico denso que trasmite la radiación IR, tal como se muestra en la **Fig. 1.10C**. La penetración controlada de la onda evanescente en la muestra hace que la radiación IR pueda ser selectivamente absorbida en la superficie de la muestra en contacto con el prisma o placa. El espectro de la radiación reflejada internamente es similar al espectro IR de absorción convencional de la muestra.

Para que ocurra un efecto ATR tiene que existir una gran diferencia entre los índices de refracción de la muestra y el medio. Dado que el índice de refracción de la mayoría de las sustancias orgánicas se encuentra entre 1 y 2, el del medio debe ser superior a 2. Un material muy utilizado es el KRS-5, cristal mixto de bromuro y yoduro de talio con índice de refracción 2,4. Otros materiales utilizados son el cloruro y el bromuro de plata, el germanio y el seleniuro de zinc. El germanio, que tiene un índice de refracción de 4,0, es utilizado para el registro de espectros de muestras con elevados índices de refracción, tales como el negro de humo. El seleniuro de zinc se utiliza esencialmente para muestras acuosas. Tanto el cristal de seleniuro de zinc como el de germanio son sumamente frágiles, por lo que el trabajo con ellos debe ser muy cuidadoso. Dado que en la técnica ATR la absorción es débil, pueden incrementarse las intensidades de las bandas mediante la reflexión múltiple (hasta 25 veces) tal y como se muestra en la **Fig. 1.10C**. La intensidad de las bandas depende además del área y la eficiencia del contacto entre la muestra y el reflector.

Los espectros obtenidos mediante la técnica de la ATR son muy similares a los espectros de transmisión comunes, aunque existen algunas diferencias significativas. Una de ellas es causada por la profundidad de penetración de la radiación en la muestra. Esta penetración es función de la longitud de onda, siendo la profundidad de penetración del haz evanescente a longitudes de onda cortas menor que a longitudes de onda más largas, como se muestra en la **Fig. 1.11**.

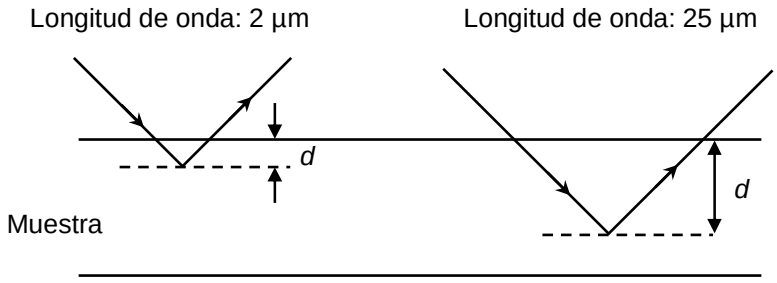

Fig. 1.11. Penetración de la onda evanescente en la muestra.

Así, cuando se compara un espectro de ATR con un espectro de transmisión, en la medida en que crece la longitud de onda de la radiación, se acentúan las intensidades de las bandas en el espectro de ATR respecto al espectro IR ordinario. También, debido a que la penetración del haz evanescente es función inversa de $[\text{sen}^2\theta_1 - (n_2/n_1)]^{1/2}$ y dado que el índice de refracción de la muestra n_2 fluctúa en las cercanías de las bandas de absorción, se pueden producir deformaciones de las bandas. Esta dificultad se minimiza trabajando con valores de θ_1 elevados y separados del ángulo crítico.

Por ello, la técnica de la ATR es de gran utilidad para el registro de espectros IR de muestras difíciles de tratar mediante otros métodos. La calidad del espectro obtenido puede ser influida por varios factores externos entre los cuales se destacan el efecto de la presión sobre el portamuestras, la textura de la superficie de la muestra y el índice de refracción de ésta.

1.3.5. MS

La MS es una técnica de aplicación general, capaz de suministrar información sobre la composición cualitativa y cuantitativa, tanto de analitos orgánicos como inorgánicos, en muestras complejas. Los espectros de masas se obtienen por conversión de los componentes de una muestra en sus respectivos iones en fase gas, que se separan en función de su relación *m/z*, siendo la señal analítica la abundancia o intensidad para cada valor *m/z*.

En la **Fig. 1.12** se muestra un esquema de los componentes principales de un espectrómetro de masas.

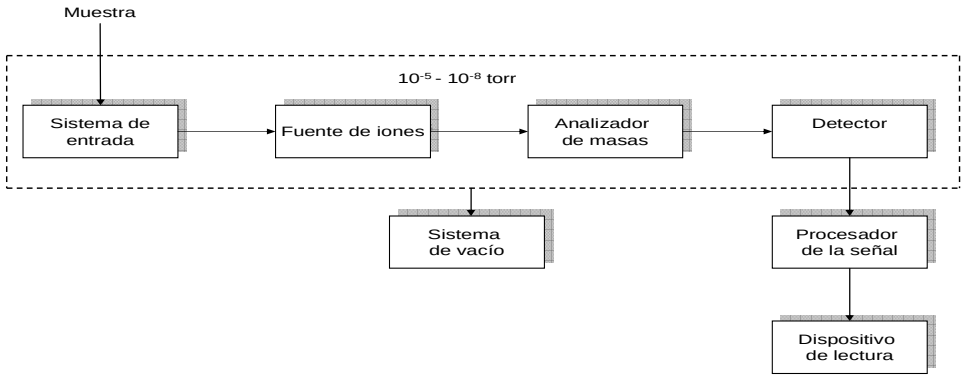

Fig. 1.12. Componentes de un espectrómetro de masas.

Como se ilustra en la figura, un espectrómetro de masas está formado en primer lugar por un sistema de entrada, que permite la introducción de una pequeña cantidad de muestra en el espectrómetro. El sistema de entrada elegido será diferente según se quieran introducir muestras sólidas, líquidas o gaseosas. La muestra se puede introducir de manera discreta mediante una jeringa o una sonda directa, o de forma continua mediante el acoplamiento con un sistema de inyección en flujo o mediante un sistema cromatográfico o electroforético.

Junto al sistema de entrada, la fuente de iones es la encargada de convertir los componentes de la muestra en iones por bombardeo con electrones, moléculas, fotones o por otros medios. En muchas ocasiones, como es el caso de los espectrómetros usados en esta tesis, el sistema de entrada y la fuente de iones están combinados en un único componente. Una vez producidos los iones, éstos pasan al analizador de masas, que es responsable de separar los diferentes fragmentos iónicos producidos en la fuente de iones en función de su relación *m/z*. Estos fragmentos llegarán al detector, que es el encargado de convertir el haz de iones en una señal eléctrica que es amplificada y registrada. Estos cuatro componentes se encuentran, generalmente, dentro de un sistema de vacío, a unas presiones de 10^{-7} – 10^{-10} atm, necesarias para evitar colisiones con el gas de fondo u otras moléculas. Solo en algunos casos, el vacío se aplica tan solo al analizador de masas y al detector. Por último, una vez registrada la señal analítica se procede a su posterior procesado y análisis, obteniéndose así un espectro de masas.

1.3.5.1. Fuentes de iones

Las fuentes de iones más utilizadas, sobretodo en el acoplamiento LC-MS, son la ESI, la APCI y la APPI, que son además las utilizadas en los estudios que se describen posteriormente.

En una fuente ESI (ver **Fig. 1.13**), la muestra en disolución se hace pasar a través de un capilar de nebulización junto a un flujo coaxial de N_2. A la salida del nebulizador se aplica un elevado potencial eléctrico que, junto a la corriente de N_2 hace que se cree un aerosol fino de partículas cargadas. El gas que circula a presión atmosférica en la cámara del spray transporta los iones hacia un tubo de vidrio capilar en dirección a la salida, en donde la presión se reduce a aprox 3 mbar mediante la bomba de vacío.

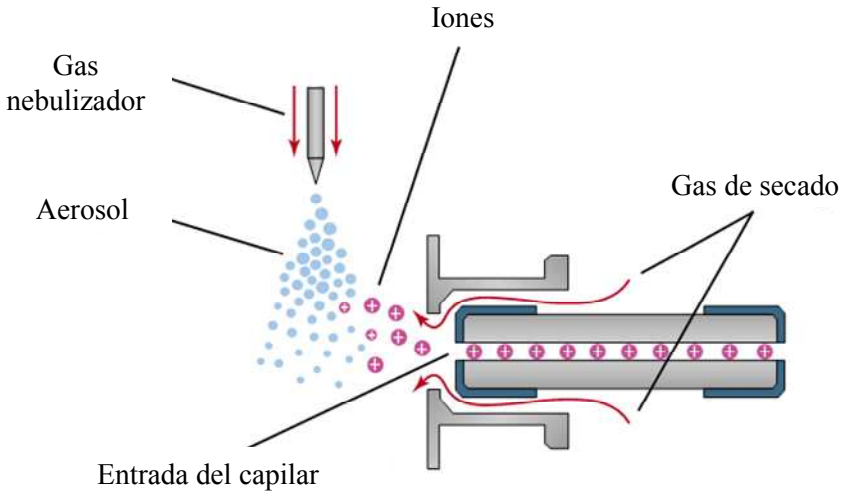

Fig. 1.13. Esquema de una fuente ESI.

La fuente APCI (ver **Fig. 1.14**), utiliza el calor proporcionado por un vaporizador, que trabaja normalmente a temperaturas de 250 – 400 ºC, y un flujo coaxial de N_2, para convertir la muestra en disolución en un aerosol fino. La evaporación da lugar a moléculas en fase gaseosa se ionizan con electrones acelerados que se producen en un electrodo mediante una descarga en corona. Este electrodo está formado por una aguja metálica a la que se le aplica un elevado potencial. Una vez creados los iones, estos pasan a través de un capilar de vidrio al analizador de masas.

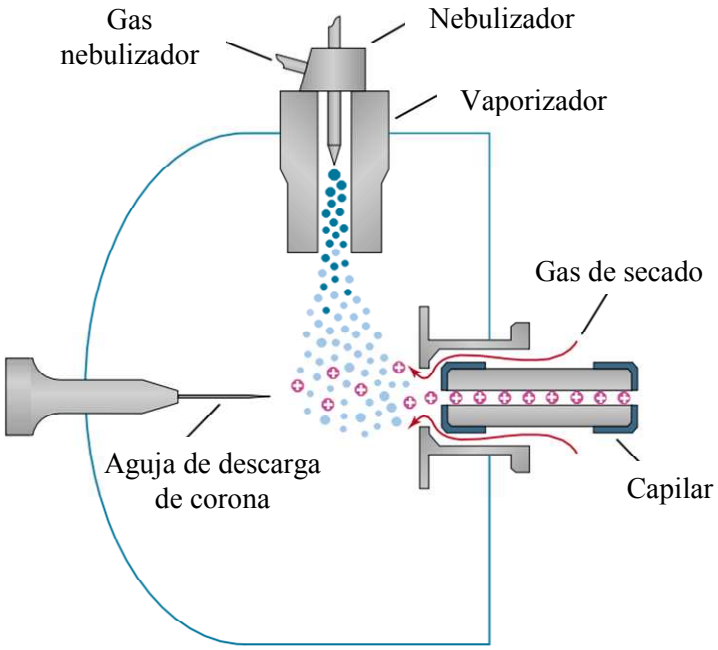

Fig. 1.14. Esquema de una fuente APCI.

En una fuente APPI (ver **Fig. 1.15**), al igual que en la APCI y a diferencia de la ESI, los procesos de nebulización e ionización se producen de modo independiente. Para que la interfaz funcione correctamente es necesario añadir a la fase móvil una cierta concentración de un disolvente que absorba la radiación UV (agente dopante), tal como por ejemplo un 1% de acetona.

En esta fuente, al igual que en la APCI, se utiliza el calor proporcionado por un vaporizador y un flujo coaxial de N_2 para convertir el eluato en un aerosol fino, que pasa por una zona intensamente iluminada por una lámpara de kripton. La radiación UV del kriptón ioniza al agente dopante, el cual a su vez ioniza los solutos, sin que su longitud de onda sea lo suficientemente corta como para ionizar a los disolventes habituales, como agua, MeOH y ACN. Finalmente, los iones producidos por los solutos son atraídos hacia el capilar y los de disolvente son rechazados.

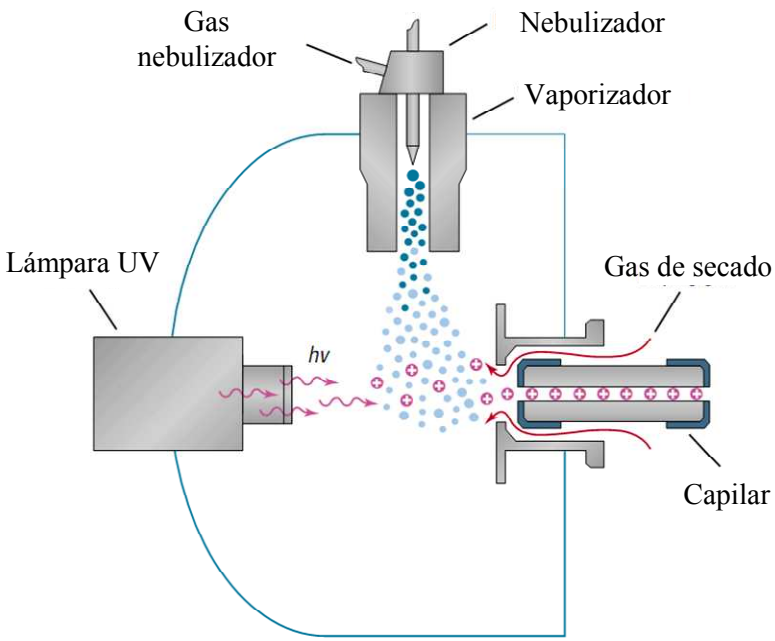

Fig. 1.15. Esquema de una fuente APPI.

1.3.5.2. Analizadores de masas

Los analizadores de masas más ampliamente utilizados en el mercado son el cuadrupolo (simple o triple), la trampa iónica y el tiempo de vuelo. A continuación se comentan los analizadores utilizados durante el desarrollo de los métodos propuestos en esta tesis.

Un analizador cuadrupolar o filtro de masas cuadrupolar está formado por cuatro barras paralelas a las que se aplica una corriente continua sobre la que se superpone un potencial de radiofrecuencia (ver **Fig. 1.16**). Los voltajes aplicados a las barras afectan a la trayectoria de los iones: aquellos con trayectoria estable (iones resonantes) pasan entre las barras experimentando oscilaciones de poca amplitud; por el contrario, los iones con trayectoria inestable (iones no resonantes) experimentan oscilaciones de amplitud creciente y colisionan con las barras. De este modo, un espectro de masas se conseguirá realizando un barrido de *m/z* variando la frecuencia del campo aplicado a las barras.

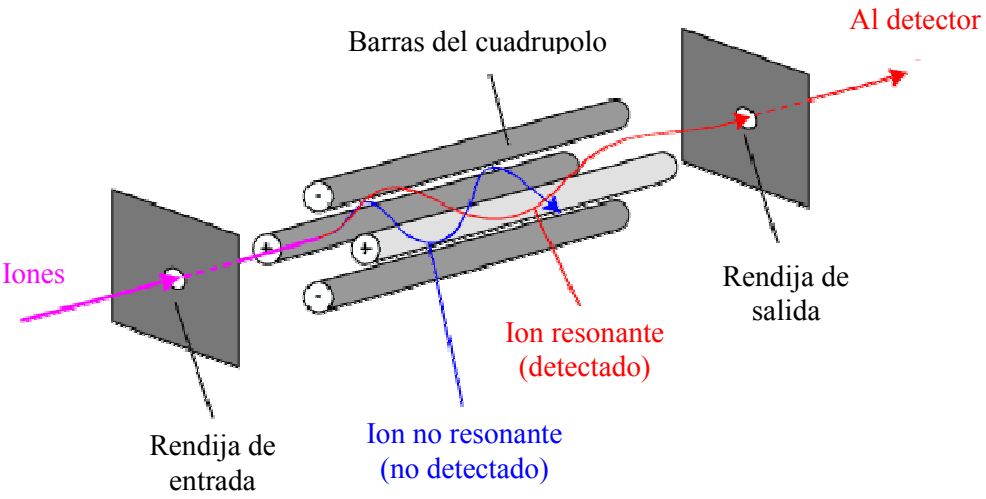

Fig. 1.16. Esquema de un analizador de masas cuadrupolar.

Por otro lado, un analizador de trampa iónica está formado por tres electrodos: el electrodo anular, el electrodo de entrada y el electrodo de salida. Estos tres electrodos forman una cavidad en la cual es posible almacenar y analizar iones, siguiendo el esquema de funcionamiento descrito en la **Fig. 1.17**.

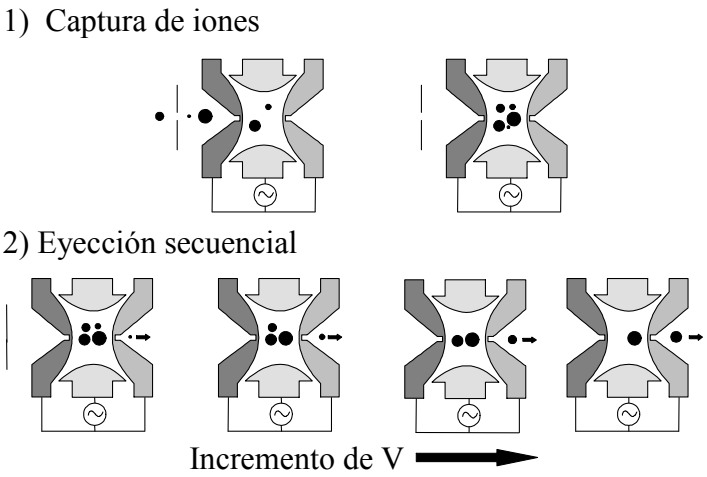

Fig. 1.17. Esquema de funcionamiento de una trampa de iones.

Los iones formados en la fuente entran en el analizador, donde se aplican diferentes voltajes, generando un campo eléctrico tridimensional en la cavidad de la trampa. Durante la etapa de almacenaje, este campo atrapa y concentra los iones en trayectorias de oscilación estables, dependiendo éstas del potencial y de la relación *m/z* de los iones. Durante la etapa de barrido o detección, los potenciales de los electrodos se alteran para provocar inestabilidad en las trayectorias de los iones y expulsarlos en la dirección axial. La expulsión o vaciado de la trampa se realiza en función de la relación *m/z* de los iones, dando lugar a un espectro de masas. Una de las características del cuadrupolo de trampa iónica es su capacidad para aislar un ion y fragmentarlo, obteniéndose así lo que se denomina "espectro de fragmentación" o espectro MS/MS o MS^2. La fragmentación se induce mediante colisión con átomos de helio, siendo posible controlar la energía de las colisiones regulando la velocidad de los iones en la trampa.

1.3.5.3. Resolución

La capacidad de un espectrómetro de masas para distinguir entre masas similares se expresa normalmente en términos de resolución, *R*, que se define como:

$$R = m/\Delta m \tag{8}$$

Siendo *m* la masa nominal del primer pico, e Δm la diferencia entre dos picos adyacentes que están resueltos o la anchura del primer pico a media altura.

La resolución que se necesita en un espectrómetro de masas depende en gran parte de su aplicación. Por ejemplo, para diferenciar entre iones de la misma

masa nominal pero con diferentes masas exactas, se necesitan equipos de elevada resolución.

1.3.6. Olfatometría electrónica

1.3.6.1. Antecedentes

Las primeras teorías relacionadas con el olfato artificial comenzaron a aparecer hacia 1920. Éstas se basaban en la posibilidad de detectar olores en disolucióna acuosa midiendo la carga eléctrica, pero no se llegó a fabricar ningún dispositivo basado en esa idea. El primer "olfato electrónico" experimental se desarrolló en la década de los 50 y consistía en un sensor electroquímico basado en un electrodo mecánico en contacto con la superficie de una barra saturada con un electrolito diluido. En esa misma época otros investigadores desarrollaron dispositivos similares basados en el uso de termistores recubiertos con distintos materiales. A mediados de la década de los 60 se propusieron detectores cuyo funcionamiento estaba basado en los cambios de conductividad o del potencial de contacto. Sin embargo, fue en 1982 (Dood, 1982) cuando se anunció el comienzo de una nueva tecnología: la olfatometría electrónica. Estos autores publicaron el diseño de una nariz electrónica basada en un conjunto de sensores reversibles y semi-selectivos con distintas propiedades químicas. La selectividad la consiguieron aplicando técnicas de reconocimiento de pautas a las respuestas obtenidas con dichos sensores.

En 1993, Gardner y Barlett (Gardner, 1993) definieron la nariz electrónica como un instrumento que consiste en un conjunto de sensores electroquímicos con especificidad parcial, asociado a un sistema de reconocimiento de pautas, capaz de reconocer olores simples o complejos. Si se compara con el sistema olfativo humano, éste también consta de un sistema de detección de olores

(receptores olfativos humanos) y un sistema de procesado de datos (el cerebro), que requiere un entrenamiento o aprendizaje y un almacenamiento en la memoria. De hecho, en ambos casos, el funcionamiento se basa en relacionar el aroma percibido con una respuesta que, una vez almacenada en la memoria, actuará de modelo en posteriores análisis. En el caso de la nariz electrónica, esa memoria consiste en bases de datos creadas a partir de muestras anteriormente analizadas por el instrumento e información externa que permita describir la calidad o identificar la muestra. De esta forma se "entrena" el sistema de reconocimiento para obtener buenas clasificaciones que permitan identificar el olor. Otra similitud con los sistemas biológicos es que el aroma percibido se procesa de forma global, sin identificar cada uno de los compuestos que lo constituyen, de forma que la clasificación se hace en base a la similitud aromática percibida al reconocer la pauta o el modelo de componentes de la muestra problema.

1.3.6.2. Componentes de la nariz electrónica

Una nariz electrónica consta de tres partes bien diferenciadas. En primer lugar es necesario un dispositivo de toma de muestra desde el que las sustancias a determinar se hagan llegar al conjunto de sensores. Los sensores actúan como receptores, dando como respuesta un cambio en sus propiedades físico-químicas al entrar en contacto con dichas sustancias. Por último, las técnicas quimiométricas son las encargadas de transformar en información analítica las respuestas de los sensores, proporcionando una huella digital del aroma medido.

Toma de muestra. El primer paso consiste en acondicionar la muestra por medio de métodos de extracción de compuestos volátiles que permitan el paso de la fracción volátil a analizar al conjunto de sensores. El sistema de muestreo está formado por una zona destinada a contener la muestra, un sistema de control y un

sistema de transporte del flujo generado a las cámaras que contienen los sensores. Se utilizan principalmente sistemas de muestreo basados en el principio del espacio de cabeza, ya sean dinámicos o estáticos.

Sensores. La diferencia fundamental entre los sistemas de olfato electrónico reside en la naturaleza de los sensores utilizados. El objetivo es encontrar conjuntos de sensores con perfiles de selectividad amplios que sean distintos pero a la vez se solapen para el rango de compuestos volátiles de interés. Este conjunto de sensores debe generar un modelo de reconocimiento de pautas capaz de diferenciar distintas muestras. Además, un sensor individual debe ser capaz de responder a un amplio rango de compuestos pero no ser demasiado específico en su respuesta. Las respuestas del conjunto de sensores a un compuesto específico deben ser tan independientes como sea posible (en un sentido estadístico), para reunir la máxima información posible sobre dicho compuesto.

Dependiendo del tipo de medidas en las que basen su respuesta estos sensores, se pueden clasificar como:

- Sensores de conductividad: Dentro de los sensores de conductividad, se encuentran los MOS, que están basados en cambios en la conductancia inducidos por la absorción o reacción de los gases en su superficie. Estos sensores están formados por el depósito de una fina capa porosa de óxidos metálicos dentro de una pieza cerámica calentada eléctricamente. Estos dispositivos están fabricados con SnO_2, ZnO, In_2O_3, WO_3, Fe_2O_3, Ga_2O_3 y TiO_2, y normalmente se encuentran barnizados con una fina capa de un metal catalítico como platino o paladio (ver **Fig. 1.18**). La absorción de oxígeno en la superficie se lleva a cabo capturando un electrón del material, por lo que dicho electrón deja de estar disponible para la conducción, de forma que ésta pasa a ser menor y la resistencia aumenta. Una vez que el sensor está estable bajo la atmósfera oxigenada, es capaz de alcanzar

una condición de equilibrio con el oxígeno absorbido en la superficie del material, obteniéndose así un valor característico de la resistencia que es lo que se conoce como línea base. Estos sensores son capaces de trabajar a altas temperaturas (200-400 ºC) y su sensibilidad es bastante alta (5-5000 ppm), sin embargo presentan importantes problemas de deriva y contaminación.

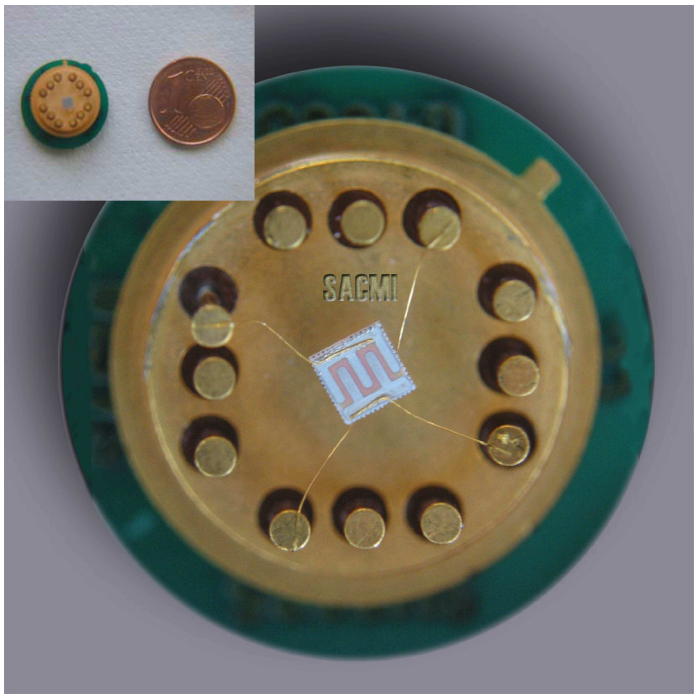

Fig. 1.18. Imagen de uno de los sensores MOS utilizado en este estudio.

- Polímeros conductores: Estos sensores de gas están basados en los cambios de resistencia en una fina película polimérica. Se han utilizado distintos tipos de polímeros basados en diferentes clases de monómeros: pirroles, anilinas, indoles, furanos. Al igual que los anteriores, la propiedad medida es el cambio de conductividad cuando las moléculas volátiles interactúan con los polímeros. Variaciones en la estructura o en los grupos funcionales incorporados en los polímeros, y el uso de distintos iones de recubrimiento, conducen a cambios en la selectividad y sensibilidad. El amplio rango de composiciones disponibles hace

que sean muy versátiles y que puedan responder a una amplia variedad de vapores orgánicos. Entre sus características, se encuentra el hecho de que pueden trabajar a temperatura ambiente, simplificando su construcción y reduciendo su consumo, tienen un tiempo de respuesta del orden de 10 s, son normalmente reversibles a temperatura ambiente y son de pequeño tamaño, si bien, son también sensibles a la humedad y a la luz, presentan deriva con el tiempo, son susceptibles a la contaminación y la respuesta es poco reproducible. A pesar de estas limitaciones, el hecho de su bajo coste, su versatilidad y su precisión hace que en la actualidad sean los más extendidos comercialmente.

- Sensores piezoeléctricos: Dentro de este tipo cabe destacar los sensores de QCM y los sensores de SAW. Los sensores de QCM miden la masa de absorción de las moléculas. El elemento activo es un cristal piezoeléctrico con una frecuencia de resonancia fundamental que está recubierto con una fina película de material absorbente, químicamente selectiva, que forma una membrana sensitiva. Cuando las moléculas se absorben en dicha membrana, aumenta la masa del sistema, y, por tanto, la frecuencia de resonancia disminuye, lo que es fácilmente medible. Entre las características de estos sensores destacan la alta sensibilidad, la linealidad de la respuesta, la alta reproducibilidad, la alta estabilidad a lo largo del tiempo, el pequeño tamaño, el trabajo a temperatura ambiente y el bajo consumo. Por otro lado, los sensores de SAW están fabricados formando electrodos interdirigidos en un sustrato piezoeléctrico como el cuarzo. Sobre su superficie se deposita una fina película cubierta de un material absorbente selectivo. Cuando se aplica un voltaje de radiofrecuencia se produce una onda acústica superficial (onda Rayleigh). La absorción de moléculas sobre la superficie aumenta su masa perturbando la onda y cambiando su frecuencia, midiéndose dicho cambio. El control de temperatura en estos sensores es imprescindible para reducir la deriva. La respuesta de ambos tipos de sensores,

QCM y SAW, puede alterarse utilizando absorbentes distintos en la composición de la membrana. Sin embargo, presentan ciertas diferencias entre ellos. Los sensores de SAW trabajan a frecuencias más elevadas (cientos de MHz) y tienen áreas muy pequeñas, por lo que tienen mayor sensibilidad y responden más rápido que los sensores QCM. A su vez, para medir cambios de masa del mismo orden, los sensores SAW dan lugar a mayores cambios de frecuencia que los obtenidos con los sensores QCM, lo que es debido a que tienen una mayor relación superfície/volumen. Esto hace que sean menos sensibles que los sensores QCM en algunos casos.

- Sensores basados en transistores de efecto de campo: Los sensores MOSFET consisten en un transistor cuya base está recubierta por un material aislante (un óxido) recubierto con un metal catalítico. La señal obtenida con estos sensores deriva del cambio de conductividad de la base debido a la polarización eléctrica cuando las moléculas reaccionan en la superficie catalítica. La sensibilidad y selectividad de los dispositivos se pueden optimizar variando el tipo y grosor del catalizador, y también haciéndolos trabajar a distinta temperatura. Estos sensores trabajan a temperaturas comprendidas entre 100 y 200 ºC. Los sensores MOSFET presentan problemas de deriva similares a los sensores de tipo MOS.

- Sensores ópticos: Los sensores ópticos se basan en el uso de fibras ópticas que modifican sus propiedades de absorbancia, reflectancia, fluorescencia o quimioluminiscencia en presencia de sustancias químicamente activas. Una de las ventajas de este tipo de sensores es que no son sensibles a interferencias electrónicas. Además, gracias a la disponibilidad de numerosos tintes y pigmentos que se utilizan en investigación biológica, estos sensores son baratos y fáciles de fabricar, aunque la complejidad del dispositivo de medida encarece el sistema. Otra desventaja de estos sensores es que tienen un tiempo de vida limitado ya que pierden color con el tiempo.

Técnicas quimiométricas. La interpretación de los datos a partir de variables múltiples, como las proporcionadas por matrices de sensores, requiere el uso de métodos de interpretación propios de la estadística multivariante. Las técnicas quimiométricas proporcionan un camino para presentar los datos de una forma comprensible diseñada para una necesidad específica: clasificación, cuantificación, etc.

Estas técnicas podrían clasificarse en dos grupos: técnicas para el pre-procesado de la señal y técnicas de reconocimiento de pautas.

El pre-procesado de señal se utiliza para tratar de compensar desviaciones de las señales de los sensores, comprimir datos y reducir posibles variaciones entre la medida de una muestra y la siguiente. Las técnicas aplicadas en estos casos incluyen:

- Manipulación de la línea base, que es una transformación basada en los valores iniciales de los sensores.
- Normalización de las respuestas. El escalado es capaz de reajustar los valores de las respuestas de los sensores para evitar que algunas variables tengan más peso que otras en el resultado obtenido. Por ejemplo, el autoescalado normaliza las dimensiones de cada muestra a media cero y desviación típica unidad. Los métodos de normalización son capaces de evitar variaciones experimentales y reducir los errores computacionales cuando se aplican técnicas de reconocimiento de pautas (Gardner, 1993).
- Selección de las zonas de la respuesta del sensor que proporcionan información discriminatoria sin eliminar la información esencial. Si se trabajara con todos los datos proporcionados por una matriz de sensores se obtendrían matrices de grandes dimensiones, por lo que es conveniente reducirlas para alcanzar así dimensiones razonables.

Muchos autores han utilizado diversos algoritmos para este fin (Hermle, 1999), aunque un equipo comercial normalmente utiliza un único dato por sensor (respuesta al alcanzar la estabilidad, respuesta máxima, etc.).

Por otro lado, las técnicas de reconocimiento de pautas buscan básicamente dos objetivos: el primero de ellos está relacionado con la reducción de los datos y el análisis de sus estructuras (reconocimiento de pautas no supervisado), mientras que el segundo se encarga de modelizar los datos (reconocimiento de pautas supervisado) por medio de regresiones o de modelos de clasificación. Más información sobre las técnicas de reconocimiento de pautas se puede encontrar en la sección 1.3.7 de la presente memoria.

1.3.7. Tratamientos estadísticos de datos

1.3.7.1. Análisis clasificatorio supervisado

En el análisis clasificatorio supervisado se construyen modelos capaces de pronosticar la pertenencia de un objeto a una categoría a partir de sus características. La matriz de datos contiene al menos una variable categórica, que indica la categoría a la que pertenece cada objeto y que constituye la respuesta o variable que se quiere predecir, y una o más variables de escala que describen otras tantas características de los objetos y que se utilizan como predictoras.

Para construir el modelo es necesario disponer de una muestra de objetos cuya categoría sea conocida y para los que también se conozcan los valores de las predictoras. La pertenencia de los objetos a las categorías puede ser supuesta, esto es, puede tratarse de una hipótesis a comprobar. La asignación de los objetos a las categorías debe ser exhaustiva (todos los objetos pertenecen a alguna categoría) y mutuamente exclusiva (ningún objeto pertenece a más de una

categoría). Estos objetos forman el conjunto de entrenamiento (*training set*), con el cual se construye el modelo de clasificación. Una vez construido, el modelo se utiliza para predecir la categoría de nuevos objetos a partir de la medida de las predictoras. La predicción sobre un conjunto de evaluación (*evaluation set*) permite validar el modelo, que luego se aplicará a predecir la categoría de las muestras problema.

Se utilizan diversos tipos de técnicas clasificatorias, tales como el análisis discriminante, que puede ser lineal (LDA) o cuadrático y la técnica de las ANN.

LDA. En LDA se utiliza un algoritmo que busca funciones o vectores discriminantes, esto es, combinaciones lineales de las variables manifiestas que maximizan la varianza entre categorías, a la vez que minimizan las varianzas intra-categorías. Para construir el modelo, es necesario asignar los objetos del conjunto de entrenamiento a una categoría dada. Para ello, se añade una variable categórica a la matriz de datos conteniendo tantas categorías como sean necesarias. El LDA estima los coeficientes a_1, a_2, …, a_m de la función discriminante lineal, f, que es capaz de predecir la pertenencia de los objetos a una u otra categoría:

$$f = a_1 x_1 + a_2 x_2 + ... + a_m x_m \tag{9}$$

Las funciones discriminantes se contruyen de una en una, buscando las direcciones del espacio que hacen máxima la expresión:

$$\lambda' = \frac{SC_D}{SC_I} \tag{10}$$

donde SC_D es la suma de cuadrados de las distancias euclídeas entre los objetos que pertenecen a distintas categorías en la dirección que indica la función

discriminante, y SC_I es la suma de los cuadrados de las distancias euclídeas entre los objetos que pertenecen a la misma categoría, también en la dirección de la función discriminante. A partir de *q* categorías se obtienen *q*-1 funciones discriminantes (aunque si el número de variables predictoras, *N*, es menor que *q*, se obtendrán *N*-1 funciones discriminantes). Las funciones discriminantes se obtienen en orden decreciente de su valor de λ', y manteniendo ortogonalidad entre ellas.

La función λ' no está acotada, por lo que varía ampliamente con el número de objetos y con la separación entre ellos. Por ello, en lugar de maximizar λ', se suele minimizar la lambda de Wilks, que se define como:

$$\lambda_W = \frac{1}{1+\lambda'} = \frac{SC_I}{SC_I + SC_D} \tag{11}$$

Esta función toma valores entre 0 y 1. Categorías con una separación nítida dan valores de λ_w próximos a 0, mientras que categorías ampliamente solapadas dan valores de λ_w cercanos a la unidad.

ANN. Una ANN es un procedimiento sistemático de procesado de datos, basado en la imitación del funcionamiento de los sistemas nerviosos biológicos, y que es capaz de predecir con precisión variables categóricas y de escala. Un ANN, al contrario que el LDA, no se basa en un modelo algebraico explícito, sino en un conjunto de unidades de activación, denominadas nodos, perceptrones o neuronas artificiales, que están conectadas entre sí en forma de red.

Una neurona artificial contiene dos algoritmos, uno de los cuales calcula la suma ponderada de los valores que le llegan por las conexiones de entrada, y el otro, denominado función de transferencia, genera una respuesta o salida que se comunica a otras neuronas. La red de neuronas es capaz de "aprender", lo que

realiza principalmente mediante el ajuste de los "pesos" de las conexiones entre neuronas, hasta que la red en su conjunto proporciona predicciones con la suficiente precisión.

En la **Fig. 1.19** se muestra el esquema de una red sencilla, con neuronas dispuestas en tres filas o capas, denominadas capa de entrada, capa oculta y capa de salida.

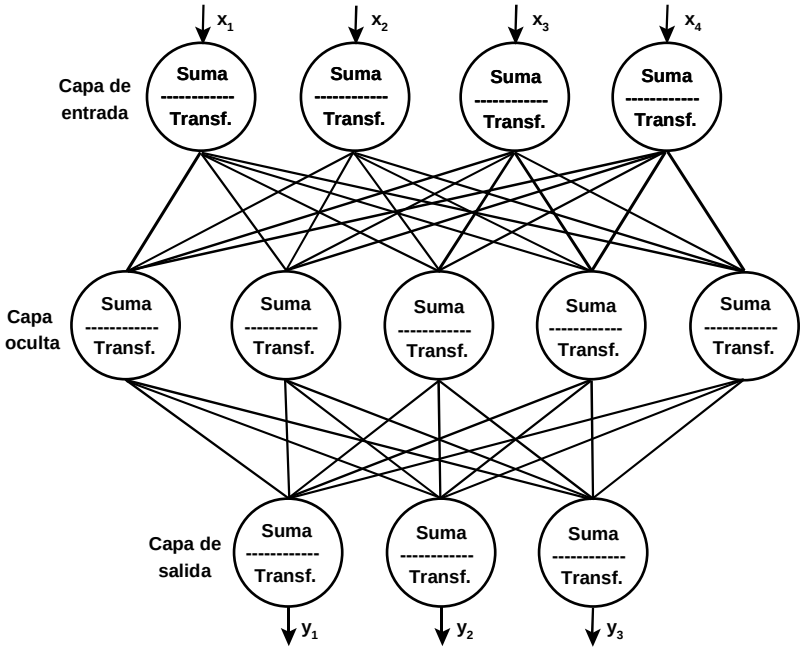

Fig. 1.19. Esquema de una red neuronal diseñada para predecir tres respuestas a partir de cuatro variables predictoras.

La capa de entrada tiene tantas entradas como variables manifiestas, generando tantas salidas como nodos hay en la capa de salida. La capa oculta suele tener una o dos neuronas más que la capa de entrada. Finalmente, la capa de salida tiene tantas neuronas como variables categóricas se quieran predecir.

Para que la red funcione correctamente es necesario someterla a una etapa de aprendizaje o entrenamiento. Cuando la red está entrenada, las neuronas de la capa de entrada se alimentan con los valores de las variables manifiestas para el

nuevo objeto. Los resultados de la capa de entrada se procesan de nuevo en la capa oculta, y los resultados generados por ésta se vuelven a procesar en la capa de salida. Los resultados de la capa de salida son las probabilidades de que el nuevo objeto pertenezca a cada una de las categorías para cada una de las variables categóricas.

En una neurona *k* cualquiera, la suma ponderada de las entradas se calcula del siguiente modo:

$$x_k^* = \sum_{j=1}^{m} w_{jk}(x_j + \theta_{jk}) \tag{12}$$

donde w_{jk} es el peso aplicado a la entrada, x_j, y θ_{jk} es el sesgo o desplazamiento del cero. La suma se utiliza para calcular la salida mediante la función de transferencia. Una función de transferencia habitual es:

$$s_k = \frac{1}{1+\exp\left(\frac{1-x_k^*}{\gamma_k}\right)} \tag{13}$$

donde γ_k es otro coeficiente denominado ganancia o factor de amplificación de la respuesta. El valor de s_k es la salida de la neurona *k*, que se alimenta a las entradas de la capa siguiente, salvo si se trata de la capa de salida, en cuyo caso, s_k es una de las respuestas buscadas.

Las redes neuronales "aprenden" la solución de un problema ajustando los pesos, sesgos y ganancias durante su etapa de entrenamiento.

1.3.7.2. La regresión lineal

La regresión lineal es un modelo explicativo con el que se pretende "explicar" el valor de P variables dependientes (variables respuesta) a partir de la información proporcionada por Q variables independientes (predictoras). Una vez definido el modelo, expresado en forma de ecuaciones algebraicas, la finalidad práctica será predecir futuros valores de las variables dependientes a partir de las independientes.

Modelos univariantes. El modelo más sencillo que puede postularse es el modelo de "regresión lineal simple", con una variable dependiente y una independiente, y que se reduce a:

$$y = b_0 + b_1 x + e \tag{14}$$

siendo $\hat{y} = b_0 + b_1 x$ la función lineal ajustada, donde b_0 y b_1 son los coeficientes de regresión muestrales.

Sin embargo, se pueden necesitar Q variables independientes para explicar los datos experimentales. En este caso el modelo responde a una regresión lineal múltiple o MLR, que se ajusta a una ecuación de primer grado con Q variables independientes:

$$y = b_0 + b_1 x_{i1} + b_2 x_{i2} + b_3 x_{i3} + \ldots + b_Q x_{iQ} + e_i = b_0 + \sum_{q=1}^{Q} b_q x_{iq} + e_i \tag{15}$$

que es la expresión general del modelo lineal univariante muestral, donde e_i es el error asociado a la i-ésima observación cuando se acepta el modelo, x_{iq} es la i-ésima observación de la variable independiente X_q, y b_0, b_1, …, b_Q son los Q+1 parámetros a determinar.

Modelos multivariantes. En estos modelos se suponen, en vez de una única variable dependiente, P variables dependientes (P > 1). Estos modelos no plantean mayores inconvenientes formales que la transformación de todos los vectores del modelo en matrices.

A continuación se describe el MLR, que será el modelo de regresión utilizado en esta tesis.

Una de las operaciones críticas de la MLR es la selección de variables predictoras que deben incluirse en el modelo. El modelo debe incluir una única variable predictora para representar cada una de las fuentes de varianza presentes en los datos que, siendo relevantes, estén además correlacionadas con la respuesta. Si no se tienen en cuenta todas las fuentes de varianza significativas que influyen sobre la respuesta, se obtienen modelos "subajustados", que se caracterizan por realizar predicciones afectadas de error sistemático. En el caso opuesto, el modelo tiene más parámetros que los estrictamente necesarios para representar todas las fuentes de varianza relevantes correlacionadas con la respuesta, y se dice que el modelo está "sobreajustado". Un modelo sobreajustado realiza predicciones afectadas de un excesivo error.

Un procedimiento simple de selección de variables consiste en incluir inicialmente en el modelo todas las variables que tengan cierta probabilidad de influir sobre la respuesta. Se obtienen los coeficientes de regresión y luego se elimina la variable asociada al más bajo. El proceso se repite hasta que todas las variables tienen valores no despreciables del coeficiente de regresión. Sin embargo, esta técnica debe de aplicarse con precaución, puesto que la presencia en el modelo de una variable correlacionada con otra también presente en el mismo reduce su coeficiente de regresión. Por ello, cuando existe un grupo de variables fuertemente correlacionadas, debe elegirse una única variable para representar al grupo.

Por otro lado, existen los procedimientos de selección conocidos como "hacia delante", "hacia atrás" y "por pasos sucesivos" (*stepwise*), que son mucho más rigurosos y racionales. Estos procedimientos suelen encontrarse programados en los paquetes estadísticos, y son de gran ayuda cuando se dispone de un gran número de variables, y cuando no es fácil asignar las variables a fuentes de varianza concretas. En los tres procedimientos las variables se introducen o se eliminan del modelo siguiendo un criterio de "entrada-salida". Así, en el procedimiento "hacia delante", se calculan las correlaciones lineales simples de todas las variables con la respuesta, y se elige como candidata la que presenta el mayor valor de r^2. La variable se introduce tan sólo si satisface el criterio de entrada, que es el siguiente ensayo *F*:

$$F = \frac{SC'_{\exp} - SC_{\exp}}{\frac{SC'_{res}}{n-p}} \qquad (16)$$

donde $SC'_{\exp}$ y $SC_{\exp}$ son las sumas de cuadrados de las varianzas explicadas por los modelos construidos incluyendo y excluyendo respectivamente la variable candidata, y SC'_{res} es la suma de cuadrados de la varianza residual del modelo construido incluyendo la variable candidata. La diferencia de sumas de cuadrados del numerador tiene sólo un grado de libertad, y es el aumento de varianza explicada por el hecho de incluir la variable estudiada. El ensayo *F* compara dicho aumento (numerador de la ecuación (16)) con la varianza residual del nuevo modelo (denominador), lo que permite decidir si es significativo para el nivel de confianza deseado. Si la primera variable ha entrado, se considera como siguiente candidata la variable que mayor correlación tiene con los residuos del modelo ya formado, esto es, la que está más correlacionada con la respuesta después de haber eliminado la varianza debida a la primera variable. La segunda

variable entra en el modelo si también satisface el criterio de entrada. El proceso continúa con una tercera candidata, y termina cuando ya no existen variables que tengan una correlación parcial con la respuesta significativamente distinta de cero, y que satisfagan además el criterio de entrada.

En el procedimiento "hacia atrás" se introducen en el modelo todas las variables, y se van eliminando de una en una. La primera candidata para ser eliminada es la variable que tiene la menor correlación con la respuesta, y se elimina si satisface el criterio *F* de salida, y así sucesivamente. El proceso termina cuando no existen en el modelo variables que satisfacen el criterio de salida.

Por último, en el procedimiento "por pasos sucesivos" las variables se introducen secuencialmente, igual que en el procedimiento "hacia delante". Sin embargo, después de la introducción de cada nueva variable, se considera la posible eliminación de alguna de las variables incluidas con anterioridad. La eliminación puede tener lugar si existe correlación entre la nueva variable y alguna de las anteriores.

Una vez obtenido el modelo, se debe de estimar la calidad del ajuste. Ésta puede estimarse en función del coeficiente de determinación múltiple, R^2, y también mediante la suma de cuadrados de los residuos. Sin embargo, si la suma de cuadrados se calcula exclusivamente considerando los objetos del conjunto de calibración, puede ofrecer una visión excesivamente optimista sobre la capacidad del modelo para predecir con exactitud objetos nuevos, no incluidos en dicho conjunto. Es por ello que se utilizan técnicas de validación cruzada, siendo la más habitual la del objeto excluido (*leave-one-out*), en la que el modelo se construye excluyendo previamente uno de los objetos, y luego se utiliza para predecirlo. Repitiendo el proceso para todos los objetos se obtienen *n* residuos, ($y_i - \hat{y}_i^*$), donde y_i es el valor esperado para el objeto *i* excluido, y $\hat{y}_i^*$ es el valor

predicho; el asterisco indica que el modelo utilizado para realizar la predicción ha sido construido excluyendo ese objeto. La capacidad predictiva se estima a partir de la suma de cuadrados de los residuos obtenidos para los objetos excluidos cada vez, o suma de cuadrados de los errores de predicción:

$$SC_{rp} = \sum (y_i - \hat{y}_i^*)^2 \qquad (17)$$

El mejor modelo es el que da un valor más bajo de estos parámetros y a la vez contiene el menor número posible de predictoras.

Otro modo de evaluar la capacidad predictiva de un modelo consiste en el empleo de un conjunto de evaluación, el cual permite determinar el porcentaje de objetos correctamente predichos.

1.3.7.3. PCR y PLSR

En MLR, los procedimientos "hacia delante", "hacia atrás" y "por pasos sucesivos" solucionan el problema de la selección de variables, pero dejan sin resolver el problema de la colinealidad. En el mejor de los casos, cada una de las predictoras incluidas en el modelo representa a una única fuente de varianza relevante correlacionada con la respuesta, sin embargo, dichas variables siguen estando parcialmente correlacionadas entre sí. Por otro lado, la selección implica desperdiciar mucha información útil, especialmente cuando se dispone de cromatogramas, espectros o, en general, de señales obtenidas mediante el barrido de alguna variable instrumental. El aprovechamiento de toda la información útil, sin complicar el modelo y sin deteriorar sus prestaciones, se consigue mediante la rotación propia. En MLR, tal y como se ha comentado, el modelo se obtiene utilizando directamente las variables manifiestas como predictoras. En cambio, en el método de PCR, se realiza primero la rotación propia del bloque X o matriz

objetos-predictoras, y luego se establece el modelo de MLR, utilizando una selección de los componentes principales como predictoras. Puesto que los componentes principales son combinaciones lineales de todas las variables manifiestas, este procedimiento las incluye en el modelo en su totalidad.

Sin embargo, los modelos obtenidos mediante PCR tienen una limitación importante, y es que los componentes principales interpretan y modelan la varianza contenida únicamente en el bloque X, y por tanto no tienen por qué estar correlacionados con las respuestas o variables que representan a las fuentes de varianza. Por ello, se introduce la regresión de mínimos cuadrados parciales o PLSR, que utiliza vectores que explican menos varianza que los componentes principales, pero a cambio están más correlacionados con las respuestas. Los componentes principales se obtienen en orden de máxima varianza explicada decreciente, por lo que no es posible aumentar su correlación con la respuesta sin perder varianza. Este razonamiento puede hacerse también a la inversa: si se combinan linealmente las variables del bloque X con el único criterio de obtener vectores correlacionados con las respuestas, es posible que los vectores resultantes expliquen poca varianza, y por tanto pueden estar dominados por varianzas aleatorias.

En PLSR se construyen vectores que establecen un compromiso razonable entre ambas situaciones extremas. Dichos vectores se suelen denominar "variables latentes". Éste término significa que el vector en cuestión ha sido optimizado desde el punto de vista de su utilización como variable predictora para predecir una respuesta única (método PLSR1 para regresión múltiple), o para predecir un pequeño grupo de respuestas simultáneamente (método PLSR2, para regresión multivariante).

Sin embargo, y pese a las ventajas que PCR y PLSR presentan con respecto a MLR, existe una desventaja, y es que, dado que las variables

predictoras en ambas son combinaciones lineales de las variables de partida, su aplicación obliga a la medida de todas estas variables, haciendo el trabajo experimental tedioso y largo cuando son muchas las variables a medir, implicando esta medida la intervención manual del experimentador, mientras que en un modelo MLR solo sería necesario medir las variables elegidas por el modelo.

CAPÍTULO 2

OBJETIVOS Y PLAN DE TRABAJO

2. Objetivos y plan de trabajo

Se propone el desarrollo de métodos rápidos y sensibles para la caracterización de aceites vegetales en función de su origen botánico, y más concretamente para la caracterización y autentificación de aceites de oliva en relación a su calidad, origen genético y geográfico. Para ello, se hará uso de aceites seleccionados considerando todos y cada uno de los factores anteriormente citados, así como posibles categorías dentro de cada factor.

En primer lugar, se establecerán métodos basados en la determinación del contenido de Ts y T_3s en aceites de distinto origen botánico. Para ello, se hará uso de técnicas como la CEC y la nano-LC. A su vez, el contenido de esteroles en aceites de distinto origen botánico se establecerá mediante UPLC y CEC. Para el análisis mediante CEC y nano-LC, se emplearán columnas de relleno (sílice porosa) y columnas monolíticas de metacrilato. Éstas últimas, que no son comerciales, se desarrollarán en nuestro laboratorio.

Por otro lado, la aplicación de diversas herramientas quimiométricas, como el LDA, permitirá el desarrollo de métodos de alta capacidad discriminante con el fin de clasificar a los aceites vegetales en función de su origen botánico. Para ello, se utilizarán los espectros de FTIR obtenidos al depositar los aceites directamente en el prisma de ATR, el perfil de la fracción alcohólica establecido mediante HPLC-MS, y los perfiles de aminoácidos y esteroles obtenidos bien por infusión directa en MS, o mediante HPLC, usándose tanto el UV como la MS como técnicas de detección.

Posteriormente, el trabajo se centrará en el estudio del aceite de oliva, para lo que, en primer lugar, se desarrollarán métodos capaces de evaluar su calidad. Para ello, se determinará el perfil de ácidos grasos libres mediante infusión

directa en MS. Los perfiles obtenidos se emplearán con el fin de clasificar las muestras de aceite de oliva en función de su calidad. Por otro lado, se desarrollará un método olfatométrico usando matrices de sensores MOS, para clasificar diversos aceites en función del umbral sensorial, establecido previamente por un panel de cata, de los defectos organolépticos típicos de los aceites de oliva, tales como avinado-avinagrado, rancio, mohoso, sedimento fangoso-borras y atrojado. A su vez, los datos obtenidos mediante la nariz electrónica se usarán para cuantificar el porcentaje de defecto presente en las muestras.

Por otro lado, y mediante la construcción de modelos de LDA, se desarrollarán diversos métodos capaces de clasificar a los EVOOs en función de su variedad genética. Para ello, se utilizarán los perfiles de ácidos grasos libres y compuestos fenólicos establecidos mediante MS por infusión directa, los perfiles de esteroles establecidos mediante HPLC-MS y UPLC-MS y los espectros de ATR-FTIR obtenidos al depositar los aceites directamente en el prisma del ATR. A su vez, se desarrollarán métodos con el fin de clasificar EVOOs en función de su origen geográfico, usándose para ello los perfiles de compuestos fenólicos establecidos mediante CEC.

Por último, se estudiarán los productos de oxidación del aceite de oliva, y se desarrollarán métodos para su evaluación. Por un lado, se estudiarán los cambios producidos durante el almacenamiento en dos alícuotas de una misma muestra de aceite de oliva, que diferirán en su contenido de compuestos fenólicos, ya que una de las alícuotas se habrá sometido a un proceso previo de extracción de los mismos. Ambas alícuotas se someterán a un proceso de envejecimiento acelerado durante 7 semanas, analizándose una porción de cada una de ellas una vez a la semana. Se estudiarán las diferencias obtenidas en los valores de acidez libre, absorbancia en el UV, índice de peróxidos, estabilidad

oxidativa, contenido en ácidos grasos y en Ts en función del contenido de fenoles en la muestra de partida, así como la evolución de estos valores con el tiempo de envejecimiento acelerado. A su vez, se estudiará la transformación experimentada por los compuestos fenólicos durante todo el proceso de oxidación mediante HPLC-MS. Estas mismas muestras serán también analizadas mediante infusión directa en el MS, y mediante una matriz de sensores MOS con el fin de poderlas clasificar en función de su estado oxidativo.

Por último, se construirán modelos de MLR con el fin de predecir el contenido de OFAs mediante el análisis de diversas muestras de aceite de oliva, bien mediante espectroscopia FTIR o mediante sensores MOS.

CAPÍTULO 3

MATERIALES Y MÉTODOS

3.1. Reactivos y materiales

3.1.1. Patrones

Se usaron los siguientes estándares: α-, γ-, δ-T y α-T-AcO (Sigma, St. Louis, MO, USA), eritrodiol (Fluka, Buchs, Suiza), β-sitosterol (mezcla de 75% de β-sitosterol y 10% de campesterol), ergosterol, stigmasterol (Acros Organics, Morris Plains, NJ, USA), colesterol (Aldrich, Milwaukee, WI, USA) y lanosterol (Maybridge Chemical Co., Cornwall, Reino Unido).

Por otro lado, se usaron los siguientes patrones de alcoholes lineales: 1-octadecanol (C18, Fluka), 1-hexadecanol (C16), 1-docosanol (C22), 1-tetracosanol (C24) y 1-hexacosanol (C26, Sigma), así como los siguientes aminoácidos: Ala, Asp, Cys, Glu, Gly, Gln, Leu, Val, Trp, Phe, Pro (Aldrich), Arg, Asn, His, Lys, Thr (Fluka), Met, Tyr (Merck, Darmstadt, Alemania), Ile (Guinama, Valencia, España) y Ser (Scharlau, Barcelona, España). Además, se empleó API, LUT, tricaproína, triheptadecanoína (Sigma) y 3,4-DHPAA (Fluka).

3.1.2. Disolventes

Se emplearon los siguientes disolventes de grado analítico: 1,4-butanodiol (Aldrich), acetona, EtOH, 1-propanol, 2-propanol, ACN, MeOH, THF, 1,4-dioxano anhidro, diclorometano (Scharlau), éter dietílico, cloroformo (J.T. Baker, Deventer, Países Bajos), iso-octano (Fluka) y *n*-hexano (Riedel-de-Haën, Seelze, Alemania).

3.1.3. Monómeros, agentes entrelazantes e iniciadores

Para la preparación de columnas monolíticas se emplearon los siguientes reactivos: LMA, ODMA, LA, EDMA, BDDA, META (75% en agua),

metacrilato de 3-(trimetoxisilil)propilo (*silano binding*), AIBN y LPO (Aldrich).

3.1.4. Otros reactivos

Anhídrido difénico (98%) (Aldrich)**,** Sylon HTP (mezcla 3:1:9 de hexametildisilazano, trimetilclorosilano y piridina, Supelco, Bellefonte, PA, USA)**,** BHT, Tris, urea (99,5%), yoduro potásico, OPA, NAC (Fluka), KOH (Probus, Barcelona), ácido bórico, HCl (37%), ácido acético (Panreac Química, Barcelona), NaOH, sulfato sódico anhidro, hidróxido amónico (Scharlau), NaCl (Carlo Erba, Milán, Italia), ácido cítrico, benzóxido sódico en alcohol bencílico, 2,7-diclorofluoresceína (Sigma), tiourea (Riedel-de-Haën), ácido fórmico, fenolftaleína, tiosulfato sódico y almidón (Merck).

El agua nanopura se obtuvo con un desionizador Barnstead (Sybron, Boston, MA, USA).

Se utilizaron también placas de vidrio para TLC, recubiertas de gel de sílice sin indicador de fluorescencia de 0,25 mm de espesor (Merck).

Para obtener columnas monolíticas se emplearon capilares de sílice fundida de 100 μm de ID y 375 μm de diámetro externo, con y sin recubrimiento externo transparente a la radiación UV (Polymicro Technologies, Phoenix, AZ, USA).

3.2. Muestras

Las muestras de aceites vegetales utilizadas en cada uno de los trabajos vienen especificadas en su correspondiente capítulo. Todas las muestras usadas son de origen botánico y geográfico, calidad y variedad genética garantizadas por los productores. En la mayoría de los casos, las muestras fueron adquiridas en supermercados de la zona o proporcionadas por los mismos productores y/o casas

comerciales, tales como Coosur (Vilches, Jaén, España), Borges (Tàrrega, Lleida, España), Grupo Hojiblanca (Antequera, Málaga, España), Intercoop Olival (Almassora, Castellón, España), Cooperativa de Altura (Altura, Castellón) y OLEA. Sólo en algunos casos, las olivas fueron recogidas directamente del campo, obteniéndose el aceite mediante un molino de aceite Oliomio 150 (Tem, Tavarnelle Val di Pesa, Florencia, Italia).

3.3. Preparación de muestras

3.3.1. Ts

La metodología de extracción de los Ts en los aceites se adaptó a partir de la bibliografía (Aturki, 2005). Para ello, 4 g de muestra se extraen dos veces con 10 mL de una disolución metanólica de BHT (0,1%), y una vez más con 10 mL de MeOH/2-propanol 80:20 (v/v). Los extractos se agitan durante 30 s y se centrifugan a 8000 *g* durante 10 min. Los extractos se combinan y se llevan a sequedad en un rotavapor a 40 ºC. El residuo se disuelve en 1 mL de MeOH y se almacena a -20 ºC en viales color topacio. En todos los casos, se realizaron 3 extractos de cada muestra. Posteriormente, estas disoluciones fueron diluidas con la fase móvil e inyectadas.

3.3.2. Esteroles y alcoholes

Los extractos de esteroles y alcoholes se obtuvieron siguiendo el procedimiento establecido por el Diario Oficial de las Comunidades Europeas (Reglamento (EEC) Nº 2568/91, anexos V y XIX). Dicho procedimiento consiste en la saponificación de 5 g de aceite diluido con 50 mL de una disolución etanólica de KOH 2 N. La saponificación se lleva a cabo calentando durante 20 min bajo reflujo. Tras finalizar la saponificación, se añaden 50 mL de agua

destilada. El contenido se transvasa a un embudo de decantación, donde se extrae 3 veces con éter dietílico (la primera extracción con 80 mL, las demás con 70 mL). Las tres fracciones etéreas se combinan en otro embudo de decantación, y se lava con agua destilada (50 mL cada vez) hasta que el agua de lavado presenta reacción neutra. Una vez eliminada el agua de lavado, la fracción etérea se seca con sulfato sódico anhidro y se filtra. Posteriormente los extractos se llevan a sequedad en un rotavapor. El residuo insaponificable resultante se disuelve en 2 mL de cloroformo, y se procede a la separación de cada una de las familias de compuestos presentes en el extracto mediante TLC, empleando como fase móvil una mezcla de *n*-hexano/éter dietílico 60:40 (v/v). Una vez llevada a cabo la separación cromatográfica, la placa se pulveriza ligera y uniformemente con 2,7-diclorofluoresceína. De las diversas bandas observadas en la **Fig. 3.1**, se transvasan con la ayuda de una espátula a otros recipientes por un lado la banda correspondiente a los esteroles, y por otro lado las bandas correspondientes a los alcoholes lineales y triterpénicos.

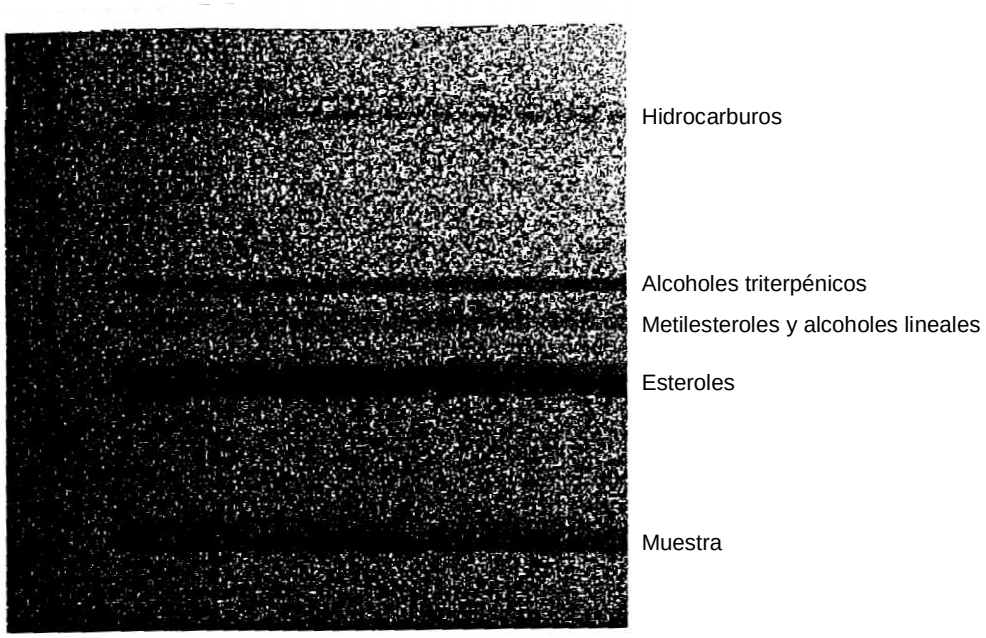

Fig. 3.1. Fracción insaponificable de un aceite purificada mediante TLC.

La banda de los esteroles se disuelve en 10 mL de éter dietílico y se filtra a través de un papel de filtro Whatman nº 1 (Whatman plc, Kent, Reino Unido) con la ayuda de un embudo Büchner. El filtrado se lleva a sequedad en un rotavapor. Cuando la muestra se analizó mediante CEC o mediante infusión directa en MS, el residuo se disolvió en 200 µL de 2-propanol (añadiéndose en el caso del análisis con MS un 1% de acetona), mientras que para la determinación de los esteroles mediante UPLC-MS y HPLC-MS se disolvió en 500 µL de 2-propanol. Las disoluciones se almacenaron en viales de color topacio a -20 ºC, para posteriormente ser diluidas con la fase móvil e inyectadas. Cuando las muestras fueron analizadas mediante GC, el residuo se derivatizó con 200 µL del reactivo de silanización (Sylon HTP) y se inyectó.

Por otro lado, las 2 bandas correspondientes a los alcoholes se juntan, se suspenden en 4 mL de THF y se introducen en un tubo de 15 mL provisto de tapón roscado, al que se ha añadido previamente 0,45 g de anhídrido difénico y 0,25 g de urea finamente molida. La reacción de esterificación que tiene lugar se ilustra en la **Fig. 3.2**. El tubo se agita y se mantiene durante 120 min en un baño termostático de aceite de silicona a 60 ºC. Una vez enfriado el tubo, se añaden 2 mL de una mezcla 2:1 de MeOH/agua, conteniendo esta última hidróxido amónico 0,1 M. La suspensión se sonica durante 15 min y posteriormente se filtra a través de un filtro de nylon de 0,45 µm (Albet, Barcelona). La disolución obtenida se almacena a -20 ºC.

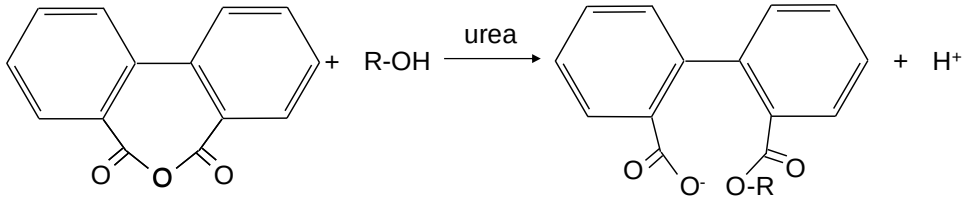

Fig. 3.2. Reacción de esterificación con anhídrido difénico.

3.3.3. Aminoácidos

El procedimiento de extracción de los aminoácidos se adaptó de la bibliografía (Hidalgo, 2001A). La precipitación de las proteínas se llevó a cabo partiendo de 40 g de aceite previamente mantenido a 18 ºC durante al menos 90 min, a los que se adicionan 98 mL de acetona a 4 ºC, manteniéndose la mezcla a 4 ºC durante 30 min más. Se filtra el conjunto a través de un filtro Whatman nº 1. Las proteínas precipitadas y retenidas en el papel se extraen en primer lugar con 5 mL de THF, y posteriormente con 5 mL de 1,4-dioxano. Ambos extractos se combinan en un tubo de ensayo y se lleva a sequedad empleando una corriente de nitrógeno. El residuo resultante se disuelve en 100 µL de HCl, y se hidroliza durante 24 h a 110 ºC (Gimeno-Adelantado, 2002; Peris-Vicente, 2005). Tras enfriar, y con el fin de disolver los aminoácidos, se añade un 1 mL de HCl 0,1 M y 1 mL de EtOH al tubo de ensayo que contiene las proteínas hidrolizadas. La infusión directa de los aminoácidos en el espectrómetro de masas se realiza utilizando esta mezcla, tras la filtración de dicha disolución a través de un filtro de nylon de 0,45 µm. Por otra parte, en la determinación de aminoácidos mediante HPLC-UV-Vis, esta mezcla se somete a un proceso de derivatización (ver **Fig. 3.3**).

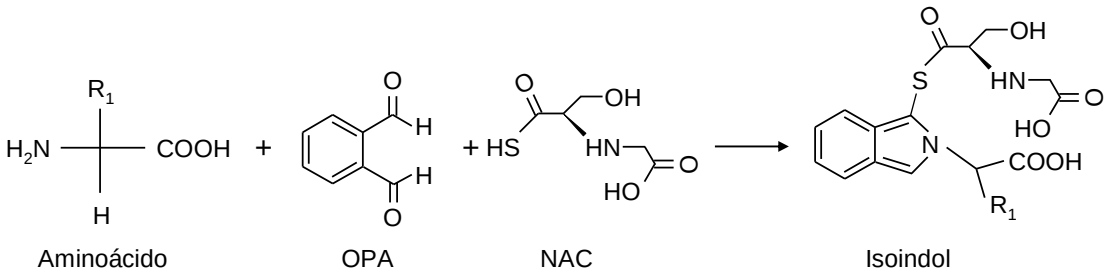

Fig. 3.3. Reacción de formación de isoindoles.

Para ello, 100 μL de la mezcla de aminoácidos se disuelven en 1 mL del reactivo derivatizante, que está compuesto por $1{,}25 \times 10^{-2}$ M OPA y $2{,}5 \times 10^{-2}$ M NAC tamponado con ácido-bórico-borato a pH 9,5 (Concha-Herrera, 2005), dando lugar a sus respectivos isoindoles. El reactivo derivatizante se protege de la luz con papel de aluminio, almacenándose a 4 ºC, y renovándose semanalmente.

3.3.4. Tratamiento de aceites para infusión directa en MS

Para la infusión directa en el espectrómetro de masas, tanto las muestras de aceites de oliva de diferente calidad como las de EVOOs de diferentes variedades genéticas, se prepararon pesando la cantidad adecuada de aceite, diluyéndola en una proporción 1:50 (v/v) con una mezcla 1-propanol/MeOH 85:15 (v/v) que contenía KOH 40 mM. Por otra parte, las muestras de EVOO previamente oxidadas se diluyeron en una proporción 1:4 (v/v) también con 1-propanol/MeOH 85:15 (v/v), alcalinizando en este caso con hidróxido amónico 40 mM.

3.3.5. Compuestos fenólicos

El procedimiento de extracción liquido-líquido utilizado para obtener la fracción fenólica de los aceites se adaptó del trabajo desarrollado por Carrasco-Pancorbo y col. (2004). En primer lugar, se toman 50 g de aceite y se diluyen con 50 mL de *n*-hexano, adicionándose, cuando fue necesario, 200 μL de 3,4-DHPAA (1000 mg L^{-1}) como patrón interno. La disolución resultante se extrae sucesivamente con 4 porciones de 20 mL de MeOH/agua (60:40, v/v). Una vez combinados los extractos, se lleva a sequedad en un rotavapor a 40 ºC. El residuo obtenido se disuelve con 1 mL de MeOH/agua (50:50, v/v) y se filtra a través de

un filtro de nylon de 0,45 μm. Posteriormente, esta fracción fenólica se diluye con la fase móvil y se inyecta.

3.3.6. Eliminación de compuestos fenólicos del EVOO

Para la eliminación de los compuestos fenólicos de los EVOOs se siguió el procedimiento descrito por Bonoli-Carbognin y col. (2008). En este procedimiento, se suspenden 35 g de muestra con 15 mL de una disolución de NaOH 0,5 M, y se centrifuga a 1000 *g* durante 5 min, retirándose la fase acuosa que contiene los compuestos fenólicos. El proceso global de eliminación se repite un total de 4 veces. La fracción lipídica se lava 2 veces con sendos volúmenes de 10 mL de HCl 0,5 M, y posteriormente se realizan 4 lavados de 15 mL cada uno con una disolución acuosa de NaCl saturada, centrifugándose también en este caso a 1000 *g* durante 5 min después de cada lavado. La fracción oleosa se seca con sulfato sódico anhidro y se filtra con succión a vacío, quedando finalmente el aceite exento de compuestos fenólicos.

3.3.7. Ácidos grasos

Para el análisis de ácidos grasos mediante GC-FID se siguió el procedimiento establecido por Bendini y col. (2006), en el que se obtienen los ésteres metílicos de los ácidos grasos al mezclar 0,05 g de aceite diluidos en 2 mL de *n*-hexano con 1 mL de una disolución metanólica de KOH 2 N.

3.3.8. OFAs

Para la obtención de los OFAs se siguió el procedimiento descrito en la bibliografía (Rovellini, 2004). Los OFAs, obtenidos tras la transesterificación del aceite con 1 M de benzóxido sódico en alcohol bencílico (ver **Fig. 3.4**), se determinaron mediante HPLC, empleándose tanto la espectroscopia UV-Vis

como la MS como técnicas de detección. Como patrones internos se usaron tricaproína y triheptadecanoína. Los resultados se expresan como porcentaje másico de OFA total, expresado como heptadecanoato de bencilo por 100 g de aceite. Por otra parte, el caproato de bencilo se usa como control interno del rendimiento de la reacción de derivatización.

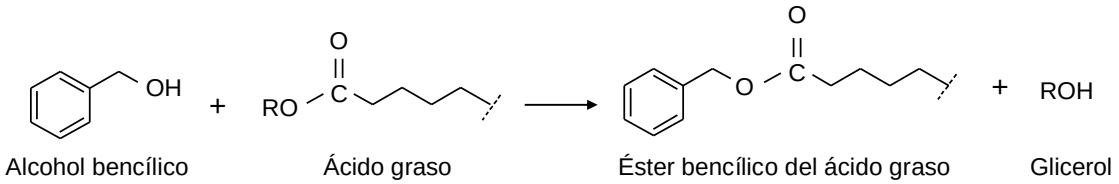

Fig. 3.4. Transesterificación de los ácidos grasos.

3.3.9. Otros parámetros analíticos

Se han hecho determinaciones del grado de acidez y del índice de peróxidos. También se llevó a cabo la medida espectrofotométrica en el UV del aceite, midiéndose la absorbancia a 232 y 270 nm ($k_{232,}$ k_{270}). Todos estos análisis se llevaron a cabo siguiendo los metódos descritos en el Diario de las Comunidades Europeas (Reglamento (EEC) Nº 2568/91, anexos II, III y IX, respectivamente).

3.4. Tratamiento de columnas

3.4.1. Acondicionado de columnas

Antes de rellenar las columnas con las disoluciones que contienen las mezclas para la síntesis de monolitos, se procede a modificar la superficie interna del capilar de sílice. Esta operación tiene como objeto favorecer el anclaje covalente del monolito a dicha superficie interna. Para ello se siguió el procedimiento descrito por Fréchet y col. (Peters, 1997):

Tras cortar 4 m de capilar se hicieron pasar sucesivamente, mediante la ayuda de una jeringa Hamilton conectada a una bomba de jeringa (kd Scientific, Holliston, MA, USA), las siguientes disoluciones a un caudal de 200 μL min^{-1} (salvo que se especifique lo contrario):

1. Acetona, hasta ver aparecer algunas gotas a la salida del capilar, para asegurar la limpieza de la pared interna.
2. Agua nanopura, hasta la eliminación completa de la acetona.
3. NaOH 0,2 M, hasta observar pH básico a la salida del capilar.
4. Agua nanopura, hasta eliminar el NaOH, para evitar cambios bruscos del pH al aplicar el siguiente tratamiento.
5. HCl 0,2 M, hasta observar pH ácido a la salida del capilar.
6. Agua nanopura, hasta pH neutro a la salida del capilar, para eliminar los restos de ácido.
7. EtOH hasta olor persistente, con el fin de eliminar el agua y evitar la hidrólisis del *silano-binding* que se adiciona en la siguiente etapa.
8. Disolución de *silano-binding* al 20% (m/v) en EtOH, acidulada con ácido acético hasta pH 5, a un caudal de 0,25 μL min^{-1} durante 60 min.
9. Acetona, para eliminar el exceso de *silano-binding*.

Se aplicó una corriente de nitrógeno para secar el capilar, dejándose en estas condiciones durante 24 h hasta completar la reacción de condensación de los grupos silanol con el *silano-binding*. Pasadas 24 h, se retiró la fuente de nitrógeno y se sellaron los extremos del capilar con sendos tapones, con el fin de evitar la hidrólisis de los enlaces siloxano.

3.4.2. Preparación de columnas monolíticas

Los monolitos se preparan mediante polimerización de mezclas de un monómero base (LMA, ODMA o LA), un agente entrelazantes (EDMA o

BDDA), un monoméro con carga para generación del EOF (META), y disolventes porogénicos, siendo los empleados en esta tesis doctoral el 1,4-butanodiol y el 1-propanol. Estas mezclas se preparan mediante la pesada de cada uno de sus componentes en una balanza analítica.

Las mezclas se polimerizan mediante el empleo de diversos activadores, usándose tanto la ionización térmica como la fotoionización. Los iniciadores empleados fueron AIBN y LPO, ambos al 1% respecto al total de monómeros. Antes de iniciar la polimerización, y con el fin de eliminar el oxígeno disuelto de las disoluciones, éstas se sonican durante 10 min y se purgan con nitrógeno durante 10 min más.

Los capilares, previamente pre-acondicionados, fueron cortados en trozos de 33,5 cm de longitud, rellenándose con las mezclas de polimerización un segmento de 8,5 o 25 cm de longitud. Una vez rellenos los segmentos, se sellan los extremos del capilar mediante tapones y se procede a la polimerización.

Finalmente, en el caso de la polimerización térmica, los capilares rellenos se introdujeron en una estufa a 70 ºC durante 24 h, mientras que en la fotopolimerización los capilares se sometieron a una irradiación de 0,9 J/cm^2 durante 10 min dentro de una cámara UV (ver sección 3.5.1 para sus especificaciones).

Una vez terminada la polimerización, se cortaron ligeramente los extremos de las columnas resultantes para liberar restos adheridos a los tapones, y garantizar la homogeneidad del relleno.

A continuación, las columnas se desobstruyeron con MeOH y la ayuda de una bomba de HPLC, eliminando tanto los disolventes porogénicos como los posibles monómeros sin reaccionar y oligómeros no incorporados a la estructura del monolito. Posteriormente, a las columnas polimerizadas térmicamente, se les practicó una ventana de detección en posición adyacente al material monolítico,

eliminando el recubrimiento externo del capilar con ayuda de una fuente de calor, mientras que en las columnas iniciadas con radiación UV no fue necesario practicar la ventana de detección, ya que su construcción requiere el uso de un capilar transparente a la radiación UV-Vis. A continuación, se cortaron las porciones de capilar necesarias para ajustar la posición de la ventana óptica a 8,5 cm de uno de los extremos, y también para que la longitud total del capilar fuera de 33,5 cm. Cortar un extremo también garantiza una sección transversal del monolito perpendicular al eje longitudinal del capilar en dicho extremo. Finalmente, antes de la inyección de estándares o muestras, se hace pasar fase móvil a través del capilar durante 30 min.

3.5. Instrumentación y condiciones de trabajo

3.5.1. CEC

Los ensayos de CEC se realizaron con un equipo de electroforesis capilar Agilent, modelo HP^{3D} (Agilent Technologies, Waldbronn, Alemania), dotado de un DAD, y de un sistema auxiliar capaz de suministrar hasta 10 bar de presión externa de nitrógeno sobre ambos extremos del capilar simultáneamente. La presurización del capilar es importante para evitar la aparición de burbujas que cortarían el paso de corriente eléctrica por el mismo. Para la adquisición de los datos se utilizó el software Chemstation (Rev. A.10.01, Agilent).

Con el fin de proceder a su acondicionado, la columna se colocó en el equipo de CEC y se equilibró con la fase móvil a 25 ºC, incrementándose el voltaje progresivamente en el rango de 5 a 25 kV, presurizando en todo momento ambos viales a 10 bares, hasta observar una señal analítica y una corriente estables. Esta etapa de equilibrado tuvo una duración de 45-60 min, dependiendo de las características de flujo de cada columna. Para los ensayos de CEC se

empleó, cuando fue necesario, una muestra de tiourea como marcador del EOF, además de los correspondientes estándares (Ts, esteroles o fenoles).

En la determinación de Ts, las separaciones se llevaron a cabo a +15 kV. Los patrones y las muestras se inyectaron electrocinéticamente, aplicando un voltaje de +20 kV durante 3 s. La detección se llevó a cabo a las longitudes de onda de 205 y 295 nm, empleándose como longitud de onda de referencia 450 ± 80 nm. Se utilizaron columnas monolíticas con una longitud de lecho de 8,5 cm.

Para la determinación de esteroles, las separaciones se llevaron a cabo a +20 kV. Los patrones y los extractos de las muestras se inyectaron electrocinéticamente, aplicando un voltaje de +10 kV durante 2 s. La detección se llevó a cabo a 210 nm (longitud de onda de referencia 450 ± 80 nm), usándose también en este caso columnas con 8,5 cm de lecho monolítico.

Por último, para la determinación de compuestos fenólicos las separaciones se llevaron a cabo a -10 kV, siendo los extractos fenólicos inyectados electrocinéticamente a -20 kV durante 3 s. La detección se llevó a cabo a 280 nm (longitud de onda de referencia, 450 ± 80 nm). En este caso, se utilizaron columnas monolíticas con una longitud total de lecho de 25 cm.

Para polimerizar las columnas por fotoionización, los capilares se introdujeron en una cámara UV (modelo CL1000) de UVP Inc. (Upland, CA, USA), equipada con 5 lámparas UV (5 × 8 W, 254 nm).

La morfología de los materiales monolíticos se estudió mediante el empleo de un microscopio electrónico de barrido Hitachi modelo S-4100 (Ibaraki, Japón), provisto de un sistema de captación de imágenes EMIP 3.0. Previamente, se metalizó la superficie de las columnas con un depósito de oro y paladio. Para ello, se utilizó un recubridor por pulverización BIORAD modelo SC-500 (Hemel Hempstead, Reino Unido).

3.5.2. Nano-LC

Los estudios empleando nano-LC se realizaron con un cromatógrafo líquido modelo 1200 Series (Agilent), dotado de un desgasificador, una nano-bomba y un DAD con una micro-celda de flujo. La columna se acopló directamente a un inyector de 10 nL equipado con una válvula pneumática (Valco, Schenkon, Suiza). La detección se llevó a cabo a 295 ± 16 nm (tomándose como longitud de onda de referencia 360 ± 100 nm). En todos los casos, se trabajó con un caudal de 0,5 μL min^{-1}. La separación de Ts se estudió con 2 columnas monolíticas diferentes, en concreto con una columna de sílice Chromolith CapRod RP-18 (150 × 0,1 mm, Merck) y con una columna de metacrilato de 20 cm desarrollada por nosotros en el laboratorio.

3.5.3. UPLC-MS

Los ensayos con UPLC se llevaron a cabo con un cromatógrafo líquido ultra rápido dotado de una bomba binaria (Waters, Mildford, MA, USA). La separación de los esteroles se llevó a cabo con una columna C18 (ACQUITY UPLC BEH, 50 × 2,1 mm, 1,7 μm, Waters). Las condiciones cromatográficas óptimas fueron las siguientes: volumen de inyección, 15 μL; temperatura de la columna, 10 ºC; caudal 0,8 mL min^{-1}. Como fase móvil se utilizaron mezclas ACN/agua conteniendo 0,01% de ácido acético. La elución se llevó a cabo mediante un gradiente lineal de 80 a 100% ACN durante 0,5 min, seguido de elución isocrática con 100% ACN durante 4,5 min más. Como sistema de detección se utilizó un espectrómetro de masas SQD (Waters) dotado de una fuente de ionización APCI, con la que se trabajó en modo ion positivo. Los datos se registraron en el modo SIR. Los parámetros óptimos de la fuente APCI, obtenidos automáticamente usando el software Waters Intellistar (Waters), fueron los siguientes: voltaje de la corona, 4 kV; temperatura de la fuente, 120

ºC; temperatura del gas de desolvatación, 400 ºC a un caudal de 750 L/h. Se utilizó nitrógeno como gas de desolvatación, que se obtuvo con un generador de nitrógeno Domnick Hunter (Gateshead, Reino Unido). El voltaje de cono óptimo para cada uno de los esteroles se obtuvo al inyectar 1 μg mL^{-1} de cada uno de los patrones, hasta que se obtuvieron las mejores condiciones instrumentales; el valor óptimo para todos los patrones fue de 30 V.

3.5.4. Espectroscopia FTIR

Para el análisis por espectroscopia FTIR de aceites vegetales de diferente origen botánico, se utilizó un espectrofotómetro FTIR Nicolet Nexus (Thermo Electron Corporation, Waltham, MA, USA). Las medidas se realizaron con una resolución de 4 cm^{-1} y un promedio de 32 barridos, midiéndose la absorbancia de los espectros desde 4000 a 500 cm^{-1}. Para ello, una pequeña cantidad de los aceites (≈ 2 μL) se depositó entre 2 discos de KBr, que se limpian entre muestras con *n*-hexano y acetona. El análisis de los datos se llevó a cabo usando el software EZ OMNIC 7.3 (Thermo Electron Corporation).

Por otra parte, para el análisis por espectroscopia FTIR de EVOOs de diferente variedad genética, se utilizó un espectrofotómetro Jasco 4100 tipo A (Jasco, Easton, MD, USA) dotado de un accesorio ATR (modelo PRO410-S, Jasco). La óptica IR de este accesorio incluye un cristal de reflexión de ZnSe. Las medidas se realizaron a temperatura ambiente con una resolución de 2 cm^{-1} y un promedio 15 barridos, midiéndose la absorbancia de los espectros desde 4000 a 600 cm^{-1}. De cada muestra, se depositan unos 20 μL en la superficie del cristal del ATR, midiéndose la absorbancia respecto a un blanco obtenido a partir de la celda sin muestra. Entre muestras, el cristal del ATR se limpió con un pañuelo de celulosa empapado de *n*-hexano, luego se limpió con acetona y posteriormente se secó. El análisis de los datos se llevó a cabo usando el software Spectra Manager

version 2.07.00 (Jasco).

Por último, para el análisis por espectroscopia FTIR de aceites de oliva previamente oxidados, se utilizó un espectrofotómetro FTIR Tensor 27^{TM} (Bruker Optics, Milán, Italia), dotado de un interferómetro Rocksolid^{TM}, y de un sistema de detección DigiTect^{TM} acoplado a un accesorio ATR (Specac Inc., Woodstock, GA, USA), que incluye un cristal de reflexión de ZnSe. Las medidas de la absorbancia se realizaron a temperatura ambiente con una resolución de 4 cm^{-1} y un promedio de 32 barridos, registrándose los espectros desde 4000 a 700 cm^{-1}. Para cada muestra, se depositan uniformemente 1 – 1,5 mL del aceite a lo largo de toda la superficie del cristal del ATR, obteniéndose también los espectros con respecto a un blanco. Entre una muestra y la siguiente, el cristal del ATR se limpió tal y como se ha especificado en el párrafo anterior. El análisis de los datos se llevó a cabo usando el software OPUS r. 6.0 (Bruker Optics).

3.5.5. Infusión directa en MS

Los estudios realizados para el análisis de muestras mediante MS por infusión directa se realizaron con un espectrómetro de masas provisto de un analizador de trampa iónica (serie HP 1100, Agilent), así como de las tres interfaces más habituales: ESI, APPI y APCI. La interfaz a utilizar se seleccionó dependiendo del analito a analizar. Para infundir las muestras en el espectrómetro, se utiliza una bomba de jeringa. El caudal de infusión empleado en todos los casos fue de 0,3 mL h^{-1} (5 μL min^{-1}). Entre muestra y muestra se realizó un lavado del sistema infusor, empleando en cada caso el disolvente usado para diluir la muestra. En todos los casos, se usó nitrógeno con una pureza superior al 99,5% como gas de nebulización y de secado (Gaslab NG LCMS 20 generator, Equcien, Madrid, España). La carga máxima de la trampa de iones fue

de 3×10^4 cuentas y el tiempo máximo de acumulación de 300 ms. En todos los casos, la señal se promedió durante 1 min.

En la determinación de esteroles, se utilizaron dos interfaces, ESI y APPI. Las condiciones de trabajo para la interfaz ESI fueron: presión del gas de nebulización, 15 psi; caudal del gas de secado, 12 L min^{-1} a 365 ºC; voltaje del capilar, -4,5 kV; voltajes de las máscaras (*skimmers*) 1 y 2, 25,9 V y 6,0 V, respectivamente, mientras que para la interfaz APPI fueron: presión del gas de nebulización, 15 psi; caudal del gas de secado, 12 L min^{-1} a 350 ºC; temperatura de vaporización, 275 ºC; voltaje del capilar, -4,4 kV; voltajes de las máscaras 1 y 2, 24,0 V y 7,4 V, respectivamente. Se registró el espectro en el rango de *m/z* 200-500 en modo ion positivo. El enfoque del espectrómetro se fijó a una relación *m/z* de 397 (ion $[M+H-H_2O]^+$del β-sitosterol).

Por otro lado, las condiciones de trabajo para el estudio del perfil de aminoácidos, para el que se usó una interfaz ESI, fueron: presión del gas de nebulización, 25 psi; caudal del gas de secado, 8 L min^{-1} a 250 ºC; voltaje del capilar, 3,5 kV; voltajes de las máscaras 1 y 2, -26,8 V y -6,0 V, respectivamente. Se registró el espectro en el rango de *m/z* 50-200 en modo ion positivo. El enfoque del espectrómetro se fijó a una relación *m/z* de 122 (ion $[M-H]^+$de la Cys).

Para el estudio del perfil de ácidos grasos de aceites de oliva de diferente calidad, así como para el estudio del perfil de ácidos grasos y compuestos fenólicos para EVOOs de diferentes variedades genéticas, las condiciones fueron las mismas que para el análisis de aminoácidos, excepto la temperatura y el caudal del gas de secado que fueron de 200 ºC y de 5 L min^{-1}, respectivamente. En este caso, el espectro se registró en el rango de *m/z* 100 - 800 en modo ion negativo, enfocándose el equipo a una *m/z* de 181 (ion $[M-H]^-$ del ácido oleico).

Para el estudio de muestras oxidadas de EVOO se utilizó una interfaz

APCI, siendo las condiciones de trabajo las siguientes: presión del gas de nebulización, 25 psi; caudal del gas de secado 5 L min^{-1} a 200 ºC; temperatura del vaporizador, 400 ºC; voltaje del capilar, 2,6 kV; voltajes de las máscaras 1 y 2, -41,5 V y -7,6 V, respectivamente. En este caso, el rango del espectro registrado también fue *m/z* 100-800 en modo ion negativo, fijándose el enfoque del espectrómetro a una *m/z* de 181 (ion $[M-H]^-$ del ácido oleico).

3.5.6. GC

Para la determinación de esteroles, se utilizó un cromatógrafo de gases, modelo HP-5890 dotado de un FID (Agilent). La separación se llevó a cabo mediante el empleo de una columna capilar HP-5 (30 m × 0,32 mm ID, 0,25 μm; J&W Scientific, Folsom, CA, USA). Las condiciones de trabajo, adaptadas del método oficial (Reglamento (EEC) Nº 2568/91, anexo V), fueron las siguientes: temperatura del horno, 263 ºC; razón de derivación, 1:10; temperatura del inyector, 290 ºC; temperatura del detector, 320 ºC y caudal del gas portador (hidrógeno), 30 mL min^{-1}.

Por otra parte, para la determinación de ácidos grasos, se utilizó un cromatógrafo de gases Clarus 500 (Perkin-Elmer, Waltham, MA, USA), también dotado de un FID. Para la separación de los analitos se utilizó una columna capilar de sílice fundida BPX70 (50 m × 0,22 mm ID, 0,25 μm) de SGE Forte (Palo Alto, CA, USA). Las condiciones de trabajo fueron las siguientes: rampa de temperatura, 140 ºC durante 5 min, luego 4 ºC min^{-1} hasta llegar a 240 ºC, manteniéndose esta temperatura durante 5 min más; temperatura del inyector, 250 ºC; temperatura del detector, 250 ºC y caudal del gas portador (helio), 0,8 mL min^{-1}.

3.5.7. HPLC-UV-Vis y HPLC-MS

Se ha utilizado un cromatógrafo líquido de la serie 1100 (Agilent), provisto de un desgasificador, una bomba cuaternaria, un compartimento termostatizador de columnas, un inyector automático y un DAD. En algunos casos, conjunta o alternativamente al DAD, también se utilizó como sistema de detección un espectrómetro de masas. En todos los casos, el tratamiento de los datos se llevó a cabo con el software ChemStation v.10.02 (Agilent).

Para el análisis de alcoholes, la separación se llevó a cabo en una columna C8 con un relleno de partículas de sílice de tipo núcleo fundido (Ascentis-Express, 150 × 4,6 mm ID, 2,7 μm, Supelco, Bellefonte, PA, USA). Las condiciones cromatográficas seleccionadas fueron las siguientes: volumen de inyección, 40 μL; temperatura de la columna, 25 ºC; caudal, 1 mL min^{-1}. Como fase móvil se utilizaron mezclas ACN/agua conteniendo 0,01% de ácido acético. La separación se llevó a cabo mediante elución isocrática con 90% ACN durante 25 min, seguida de un gradiente lineal de 90 a 100% ACN durante 10 min y de elución isocrática con 100% ACN durante 10 min más. La detección UV-Vis se realizó a 200 ± 10 nm, usándose como referencia la longitud de onda 360 ± 60 nm. En este trabajo, se utilizó también la MS como técnica de detección, para lo cual se hizo uso de un espectrómetro de masas de trampa iónica Agilent HP 1100, dotado de una interfaz ESI. Las condiciones de trabajo fueron las siguientes: presión del gas de nebulización, 35 psi; caudal del gas de secado, 7 L min^{-1} a 300 ºC; voltaje del capilar, 2,5 kV; voltajes de las máscaras 1 y 2, -41,0 V y -6,0 V, respectivamente. Se registró el espectro en el rango de *m/z* 300-800 en modo ion negativo. El enfoque del espectrómetro se fijó a una *m/z* de 605 (ion $[M-H]^-$ del hemiéster difénico del alcohol C26). Al igual que para los trabajos de infusión directa en MS, se usó nitrógeno como gas de nebulización y de secado,

siendo también la carga máxima de la trampa de iones de 3×10^4 cuentas, y el tiempo máximo de acumulación de 300 ms.

Para mejorar la sensibilidad en la detección de los iones $[M-H]^-$ de los hemiésteres en el espectrómetro de masas, se aumentó el pH del eluato antes de llegar al detector de masas. Para ello, se instaló una unión T entre el DAD y la interfaz ESI, haciéndose confluir el eluato procedente de la columna con una corriente de hidróxido amónico 0,01 M en agua a un caudal de 0,1 mL min^{-1}.

Para el análisis de aminoácidos, la separación se llevó a cabo en una columna C18 (Kromasil, 250 × 4 mm ID, 5 μm, Análisis Vínicos, Tomelloso, España). Las condiciones cromatográficas, adaptadas de la bibliografía (Beneito-Cambra, 2009; Concha-Herrera, 2005), fueron las siguientes: volumen de inyección, 20 μL; temperatura de la columna, 25 ºC; caudal, 1 mL min^{-1}. Como fase móvil se utilizaron mezclas ACN/agua conteniendo 5 mM de ácido cítrico, cuyo pH se ajustó a 6,5 mediante la adición de NaOH. La elución se llevó a cabo mediante un gradiente lineal de 5 a 30% ACN durante 30 min, seguido de otro gradiente lineal de 30 a 50% ACN en 5 min más. La detección UV-Vis se realizó a 335 ± 10 nm, usándose como referencia la longitud de onda 450 ± 30 nm.

Para la determinación de esteroles, la separación se llevó a cabo con una columna C18 (Atlantis, 100 × 3 mm ID, 3 μm, Waters). Las condiciones cromatográficas fueron las siguientes: volumen de inyección, 20 μL; temperatura de la columna, 25 ºC; caudal, 1 mL min^{-1}. Como fase móvil se utilizaron mezclas ACN/agua conteniendo 0,01% de ácido acético. La elución se llevó a cabo mediante un gradiente lineal de 90 a 100% ACN durante 10 min, seguido de elución isocrática con 100% ACN durante 2 min más. Como sistema de detección se utilizó un espectrómetro de masas con trampa iónica Agilent HP 1100, dotado de una interfaz APPI. Las condiciones de trabajo fueron las siguientes: presión del gas de nebulización, 15 psi; caudal del gas de secado, 12

L min^{-1} a 350 ºC; temperatura del vaporizador, 275 ºC; voltaje del capilar, -1,9 kV; voltajes de las máscaras 1 y 2, 25,9 V y 6,0 V, respectivamente. Se registró el espectro en el rango de *m/z* 200-500 en modo ion positivo. El enfoque del espectrómetro se fijó a una *m/z* de 397 (ion $[M+H-H_2O]^+$ del β-sitosterol). El resto de condiciones experimentales del espectrómetro de masas fueron iguales a las utilizadas para la determinación de alcoholes.

Para la determinación de OFAs, la separación se llevó a cabo con una columna C18 (Luna, 250 × 4,6 mm ID, 5 μm, Phenomenex, Torrance, CA, USA). Las condiciones cromatográficas, adaptadas del método oficial publicado por Norme Grassi e Derivati (Método NGD C-88, 2007), fueron las siguientes: volumen de inyección, 20 μL; temperatura de la columna, 25 ºC; caudal, 1 mL min^{-1}. Como fase móvil se utilizaron mezclas ACN/agua. La elución se llevó a cabo mediante un gradiente lineal de 60 a 100% ACN durante 50 min, seguido de elución isocrática con 100% ACN durante 20 min más. La detección UV-Vis se realizó a 255 ± 10 nm, usándose como referencia la longitud de onda 500 ± 50 nm. En este trabajo, se utilizó también la MS como técnica de detección, para lo cual se utilizó un analizador de masas de cuadrupolo simple HP 1100 Series de Agilent, dotado de una interfaz APCI. Las condiciones de trabajo fueron las siguientes: presión del gas de nebulización, 50 psi; caudal del gas de secado, 9 L min^{-1} a 350 ºC; temperatura del vaporizador, 300 ºC; voltaje del capilar, 3 kV; corriente de la corona, 4 μA; voltaje de fragmentación, 60 V. Se registró el espectro en el rango de *m/z* 300-500 en modo ion positivo.

Para la separación de compuestos fenólicos, se utilizó una columna C18 (Luna, 250 × 3 mm ID, 5 μm) con una precolumna C18, ambas de Phenomenex. En este caso, las condiciones cromatográficas fueron: volumen de inyección, 10 μL; temperatura de la columna, 25 ºC; caudal, 0,5 mL min^{-1}. Como fase móvil se utilizaron mezclas ACN/agua conteniendo 0,5% de ácido fórmico. La elución se

llevó a cabo siguiendo el gradiente descrito por Carrasco-Pancorbo y col (2007B). La detección UV-Vis se realizó a 240, 280 y 330 nm. En este trabajo, se utilizó también la MS como técnica de detección, para lo cual se dispuso de un analizador de masas de cuadrupolo simple (Agilent), dotado de una interfaz ESI. Las condiciones de trabajo fueron las siguientes: presión del gas de nebulización, 50 psi; caudal del gas de secado, 9 L min^{-1} a 350 ºC; voltaje del capilar, 3 kV. El espectro se registró en el rango de *m/z* 50-800 en modo ion positivo.

Para la determinación de Ts, se utilizó una columna Luna CN 100 A (150 × 4,6 mm ID, 5 μm, Phenomenex). En este caso, las condiciones cromatográficas fueron: volumen de inyección, 10 μL; temperatura de la columna, 25 ºC; caudal, 1 mL min^{-1}. La separación se llevó a cabo mediante eluación isocrática con *n*-hexano/diclorometano (95:5), realizándose la detección UV-Vis a 295 nm.

3.5.8. Nariz electrónica

Tanto para el análisis de muestras de aceites conteniendo los defectos sensoriales didácticos proporcionados por el IOC, como para el análisis de aceites de oliva previamente oxidados, se ha utilizado una nariz electrónica (EOS 507, Sacmi Imola S.C., Imola, Bolonia, Italia) dotada de un compartimento de 6 sensores MOS y un automuestrador (modelo HT500H) con carrusel para 10 muestras, que se conecta a un sistema que contiene carbón y sílice activa para eliminar la humedad ambiental. El sistema se completa con un ordenador portátil para la adquisición y análisis de los datos obtenidos. Los 6 sensores utilizados fueron: sensor 1 (SnO_2), sensor 2 (SnO_2 + SiO_2), sensores 3, 4 y 5 (SnO_2 catalizado con Au, Pt y Pd, respectivamente) y sensor 6 (WO_3). Durante el análisis, los sensores se mantienen en un rango de temperatura comprendido entre 350 – 450 ºC, mientras que las muestras se mantienen a una temperatura controlada de 37 ºC.

Las condiciones experimentales para el análisis de las muestras, fueron adaptadas de Camurati y col. (2006). En primer lugar, se pesan 15 g de aceite y se introducen en un vial de Pyrex de 100 mL con tapón provisto de silicona. La respuesta de los 6 sensores para una muestra de aceite de oliva se observa en la **Fig. 3.5**. Como podemos observar en la figura, la señal se puede dividir en 4 fases:

(A) Acondicionado, constituido por un periodo de 25 min durante el que se asegura una línea base constante.

(B) Pre-inyección, durante la cual las muestras se incuban a 37 ºC durante 7 min.

(C) Ciclo de medida, durante el cual, mediante una jeringa automática, se muestrean los compuestos volátiles recogidos en el espacio de cabeza del aceite. Estos compuestos son bombardeados hasta la superficie de los sensores durante 2 min, tiempo durante el cual se registra la señal proporcionada por cada uno de los sensores; en esta fase, los sensores son expuestos a un flujo constante de aire exento de humedad de 50 sccm, con el fin de obtener de nuevo la línea base.

(D) Recuperación, etapa compuesta por un periodo de 7 min necesaria para conseguir de nuevo las condiciones iniciales de los sensores.

Los datos obtenidos de la nariz electrónica se adquieren y se analizan con el paquete estadístico "Nose Pattern Editor" (Sacmi Imola S.C.). Este programa permite extraer los datos con diferentes algoritmos, tales como el "classical feature" o el "classical after feature".

En el algoritmo "classical feature", la respuesta extraída de cada uno de los sensores, X, se define como:

$$X = p_1 / p_0 \qquad (1)$$

donde p_0 es la resistencia inicial del sensor en contacto con el aire (ver **Fig. 3.5**) y p_1 es la resistencia del sensor en presencia de los compuestos volátiles bombeados desde el espacio de cabeza del aceite (que disminuye con respecto a p_0).

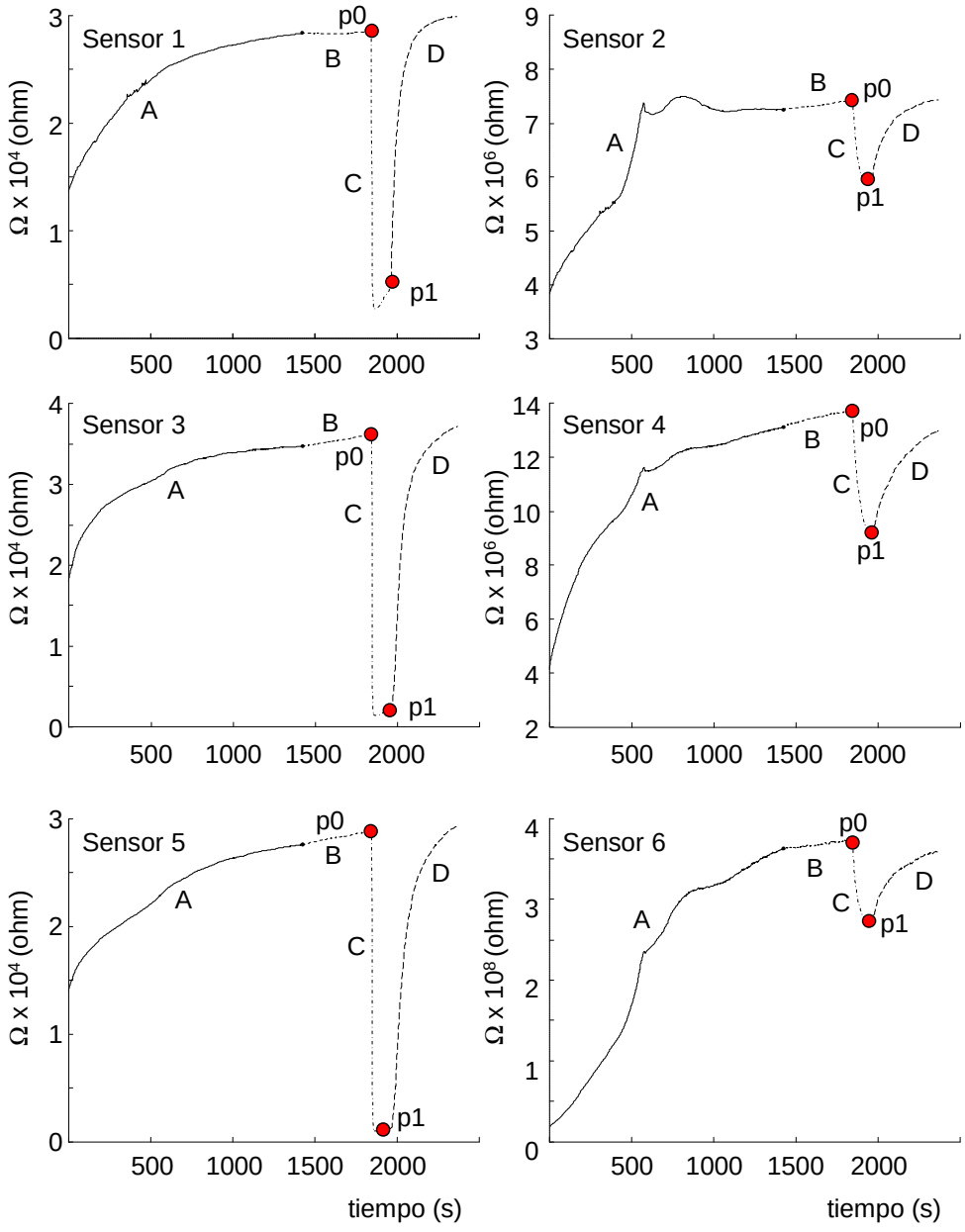

Fig. 3.5. Respuesta de los 6 sensores para una muestra de aceite de oliva obtenida con el algoritmo "classical feature": (A) acondicionado; (B) pre-inyección; (C) ciclo de medida; (D) recuperación.

Por otro lado, en el algoritmo "classical after feature", la respuesta extraída de cada uno de los sensores viene definida por:

$$X = p_1 / p_2 \tag{2}$$

donde p_1 es la resistencia del sensor en presencia de los compuestos volátiles bombeados desde el espacio de cabeza del aceite (ver **Fig. 3.6**) y p_2 es la resistencia del sensor después de la medida.

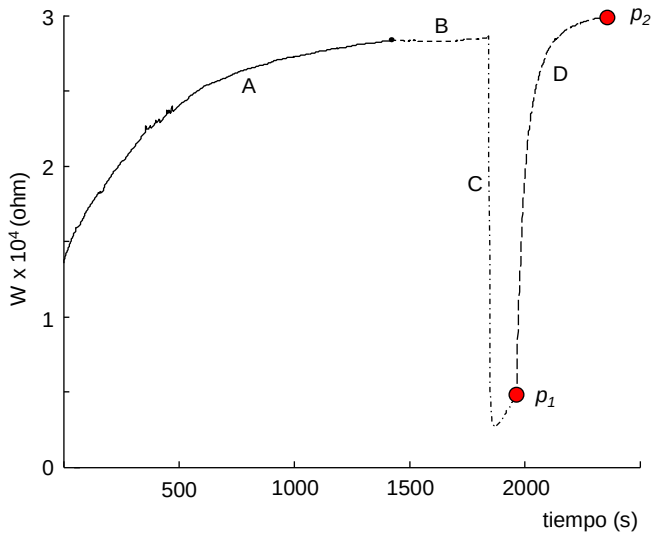

Fig. 3.6. Respuesta de uno de los sensores para una muestra de aceite de oliva extraída con el algoritmo "classical after feature": (A) acondicionado; (B) pre-inyección; (C) ciclo de medida; (D) recuperación.

3.5.9. OSI

Para el medir el estado de oxidación de los aceites de oliva, se utilizó un OSI de ocho canales (Omnion, Decatur, IL, USA). Tal y como se ha explicado en la sección 1.2.5.2, se hace pasar una corriente de aire purificado con un flujo de 120 mL min^{-1} a través de 5 g de aceite, que se calientan a 110 ºC. El efluente de este aire se burbujea a través de un tubo que contiene agua desionizada,

incrementando la conductividad del agua. Tal y como se ha indicado anteriormente, la estabilidad oxidativa viene expresada como tiempo de inducción en horas.

3.6. Análisis sensorial

El análisis sensorial se realizó según la normativa Europea publicada en el anexo XII del Reglamento (EEC) Nº 2568/91. Los análisis se llevaron a cabo por 10 catadores profesionales del panel de cata del Departamento de Ciencias de los Alimentos de la Universidad de Bolonia (reconocido por el Ministerio de la política agrícola, alimentaria y forestal de Italia el 20 de julio de 2006). Los catadores usaron una hoja de perfil (Cerretani, 2007) que contenía un listado con los defectos sensoriales que se pueden encontrar normalmente en los aceites de oliva virgen (avinado-avinagrado, atrojado, mohoso, sedimento fangoso-borras, rancio, otros), así como las siguientes percepciones positivas: frutado verde o maduro, hoja, hierba, alcachofa, tomate, almendra, manzana, otros). Los catadores cuantificaron sus percepciones tanto de los defectos como de las percepciones positivas en una escala que iba del 0 al 5. Posteriormente, se calculó la media, la mediana y la desviación estándar (Reglamento (EC) Nº 640/08) para cada uno de los atributos. Sólo cuando el valor de la desviación estándar fue menor del 20% se tomó como válido el análisis, repitiéndose cuando fue mayor del 20%.

Por otro lado, el panel de catadores también estableció el umbral sensorial de los diversos defectos (avinado-avinagrado, atrojado, mohoso, sedimento fangoso-borras, rancio). Para ello, se utilizaron los defectos didácticos proporcionados por el IOC. El jefe del panel prepara una serie de 12 a 15 muestras para cada uno de los defectos, haciendo diluciones sucesivas de los

defectos didácticos en aceite de girasol (aceite exento de defectos), hasta que el defecto ya no se percibe. Posteriormente, se realizan ocho ensayos de comparación entre estas muestras que contienen defecto y un blanco, con el fin de determinar el valor umbral de percepción de ese defecto. Después de cada ensayo, el catador debe de decir si a su juicio ambas muestras son iguales o no. Una vez realizadas todas las catas, el jefe del panel anota las respuestas correctas de los catadores para cada uno de los niveles de concentración y los expresa como un porcentaje. Se elabora un gráfico que representa las concentraciones (eje x) frente al porcentaje de respuestas correctas de los catadores (eje y), y mediante interpolación en la curva, se determina el valor umbral, que es la concentración a un porcentaje de acierto del 75%.

3.7. Tratamiento de variables para análisis estadístico

Debido a la variabilidad asociada al tratamiento de la muestra antes de su inyección y/o a otras posibles fuentes de varianza que pueden también afectar a las variables experimentales, éstas se sometieron a un proceso de normalización. Se probaron 2 procedimientos de normalización diferentes. En el procedimiento de normalización A, el valor de la variable original (área, intensidad de pico, etc) se dividió por la suma de los valores de todas las variables originales. En el procedimiento de normalización B, el valor de cada una de las variables originales se dividió por el valor de todas las demás variables originales para obtener así cocientes entre pares de variables, evitando en todos los casos duplicados. Así por ejemplo, para un espectro con 12 picos utilizados como variables, el valor de cada una de las 12 áreas se dividió por el valor de las 11 áreas restantes, obteniéndose en este caso un total de (12 x 11)/2 = 66 variables normalizadas.

Una vez obtenidas las variables normalizadas, y dependiendo del objetivo (clasificar, cuantificar, explorar) se aplicaron diversas técnicas estadísticas, tales como LDA, ANN, MLR y PLSR. El tratamiento de los datos se llevó a cabo mediante las herramientas programadas en Microsoft Excel y en los paquetes estadísticos SPSS (v. 12.0.1, SPSS Inc., Chicago, IL, USA), The Unscrambler (v. 7.6, CAMO Technologies Inc., Bergen, Noruega) y STATISTICA Neural Networks (v. 4.0, Statsoft Inc., Tulsa, USA). En todos los casos, los modelos construidos fueron validados por el método *leave-one-out*. Siempre que no se indique lo contrario, los modelos de LDA y MLR se construyeron mediante el modelo de selección de variables por pasos sucesivos, usándose los valores de probabilidad de F de entrada y F de salida de 0,05 y 0,1, respectivamente. En el caso del ANN, la red se construyó con 3 capas de nodos o perceptrones, entrenándose con un algoritmo de aprendizaje de retro-propagación. Por otro lado, en todos los modelos de regresión se realizó un análisis de los residuos, estudiándose la posible heterocedasticidad de los mismos.

CHAPTER 4

DEVELOPMENT OF METHODS FOR THE DETERMINATION OF TS, T_3S AND STEROLS IN VEGETABLE OILS

4.1. Determination of Ts by CEC using methacrylate monolithic columns

The aim of this study was to develop a CEC method for the determination of Ts and T_3s in edible oils using methacrylate ester-based monolithic columns. The potential of this method to evaluate olive oil adulteration with lower-cost oils of a different botanical origin was also investigated. For these purposes, the following vegetable oils were used: soybean, sunflower, grapeseed, EVOO (Coosur), hazelnut (Guinama), corn (Hacendado) and red palm (Blue Bay).

Stock solutions of 2000 μg mL^{-1} of the T standards described in section 3.1.1 were prepared in MeOH with 0.1% w/v BHT, and stored at -20ºC in amber vials. Working solutions were prepared daily by dilution of the stock solutions with the mobile phase. Thiourea was also added as EOF marker.

Methacrylate ester-based capillary monolithic columns were prepared from polymerization mixtures constituted by LMA, EDMA, 1,4-butanediol, 1-propanol and AIBN as thermal initiator. META was also added to generate the EOF.

4.1.1. Influence of pore size

Since the pore size and the surface area of the monoliths were highly dependent on the concentration of 1,4-butanediol in the polymerization mixture, different polymerization mixtures were prepared in order to examine the influence of pore size on the separation of Ts. For this purpose, the 1,4-butanediol/1-propanol ratio was modified, keeping the proportion of monomers to pore-forming solvents fixed at 40:60 wt%. The content of 1,4-butanediol in the polymerization mixture was varied from 10 to 25 wt%. Below this range (with less than 10 wt% 1,4-butanediol), small pore sizes (< 125 nm), clearly unsuitable

for any flow-through applications, were obtained, whereas with more than 25 wt% 1,4-butanediol, the components of the polymerization mixture were not completely dissolved.

Therefore, a monolith constructed using 10 wt% 1,4-butanediol was first used. The mobile phase composition used in these experiments was 95:5 (v/v) MeOH - 5 mM Tris at pH 8.0. As shown in **Fig. 4.1**, the monolithic column produced with 10 wt% 1,4-butanediol showed the highest resolution of the analytes; however, separation times were too long (> 35 min). With 12 wt% 1,4-butanediol, baseline separations of the successive T pairs were achieved within 19 min. With 15 wt% 1,4-butanediol, the α-T/α-T-AcO pair was poorly resolved. Monolithic columns prepared with 20 wt% or higher 1,4-butanediol contents were unable to resolve all the analyte pairs, even when the MeOH percentage in the mobile phase was reduced from 95% to 90% (data not shown).

When these phases were examined by SEM (**Fig. 4.2**), an increase of both the macropore size and the dimensions of the globules at increasing 1,4-butanediol percentages was observed. Thus, the best resolution was obtained with the lowest 1,4-butanediol content. This monolithic phase also showed the smallest pore size and the highest surface area. Then, the monolithic column obtained with 12 wt% 1,4-butanediol was selected as the best compromise between resolution and analysis time.

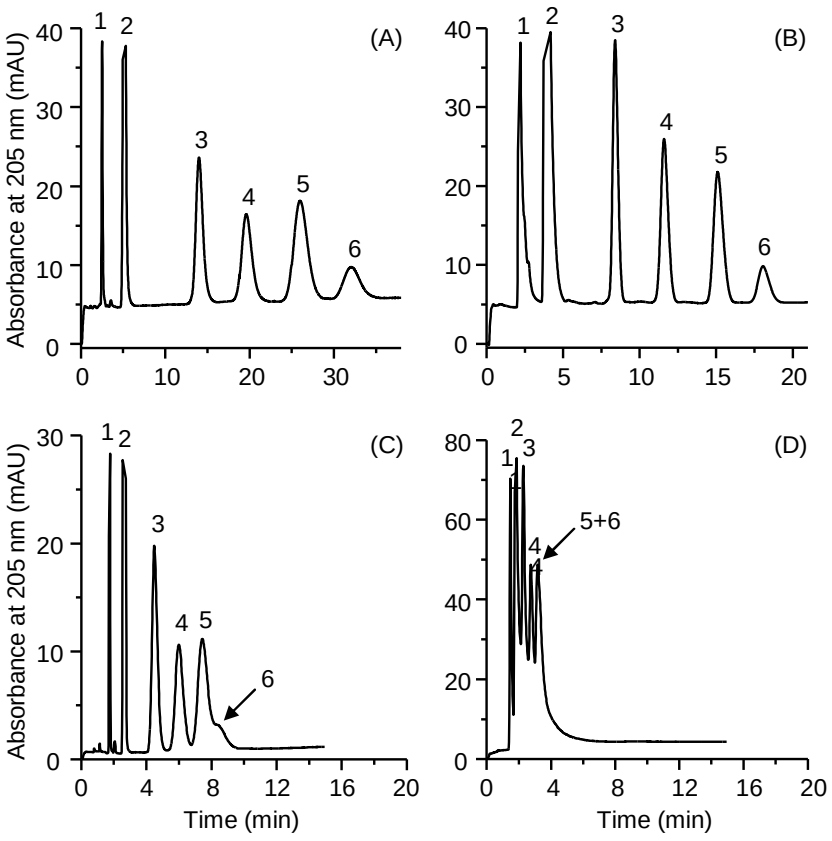

Fig. 4.1. Influence of the percentage of 1,4-butanediol in the polymerization mixture on the CEC separation of Ts: (A) 10, (B) 12, (C) 15 and (D) 20 wt% 1,4-butanediol. Working conditions: Mobile phase, 95:5 (v/v) MeOH - 5 mM Tris at pH 8.0; electrokinetic injection, 20 kV for 3 s; separation voltage, 15 kV. Peak identification: 1, thiourea; 2, BHT; 3, δ-T; 4, γ-T; 5, α-T and 6, α-T-AcO.

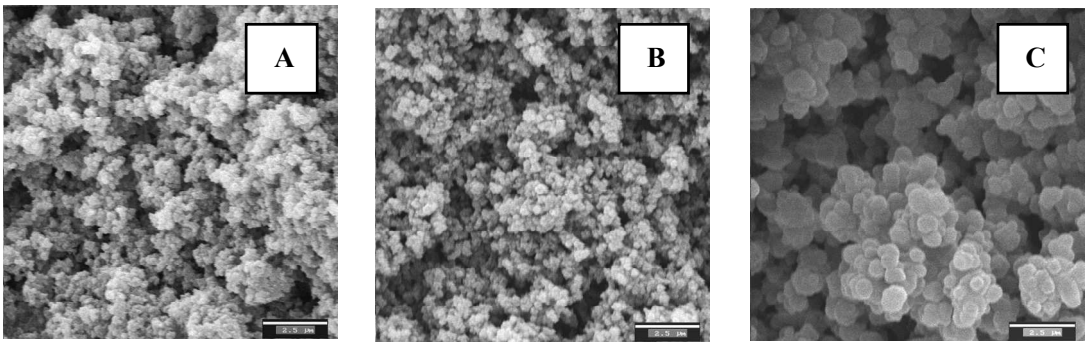

Fig. 4.2. SEM micrographs of the LMA monolithic materials prepared with (A) 10, (B) 12, and (C) 20 wt% 1,4-butanediol in the polymerization mixture, respectively. The bar lengths stand for 2.5 μm.

4.1.2. Influence of mobile phase composition

The influence of the MeOH concentration in the mobile phase was also studied. For this purpose, 90:10, 95:5 and 99:1 (v/v) mixtures of MeOH-aqueous buffer at pH 8 were tried. The results are shown in **Fig. 4.1B** and in **Fig. 4.3**. Resolution decreased when the concentration of MeOH increased; however, resolution of all the peak pairs was still higher than 1.5 with the 99:1 mixture, except for the α-T/α-T-AcO pair which gave R = 1.3. Efficiencies also increased, and analysis time largely decreased, when the MeOH content in the mobile phase increased from 90 to 99%. With 99:1, efficiencies within the 4200-65000 plates/m were obtained. This mobile phase was selected as the best compromise between resolution and analysis time (less than 10 min).

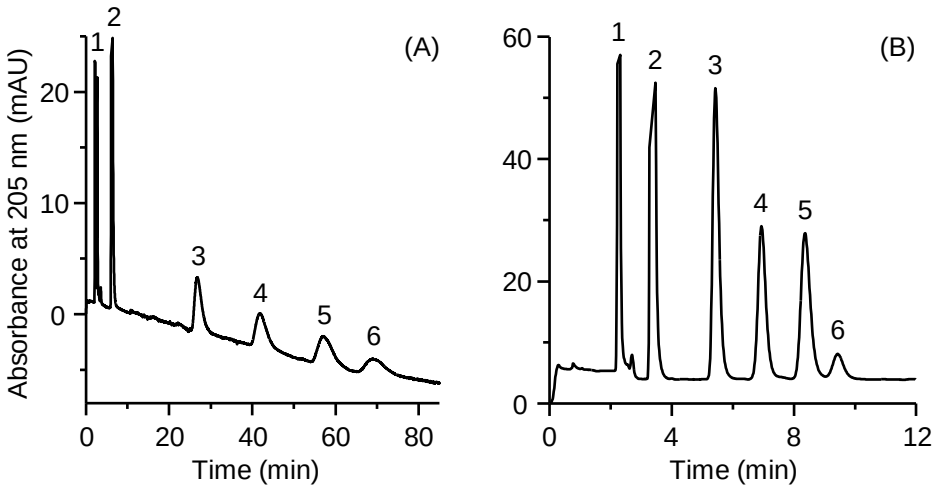

Fig. 4.3. Influence of the MeOH content in the mobile phase on the separation of Ts: (A) 90:10 and (B) 99:1 MeOH-aqueous buffer (5 mM Tris at pH 8). The monolithic capillary column was prepared with 12 wt% 1,4-butanediol in the polymerization mixture. Other experimental conditions as in **Fig. 4.1**.

4.1.3. Quantitation studies and application to real samples

Intra- and inter-day repeatabilities in the selected conditions were obtained by injecting a mixture containing 25 μg mL^{-1} of each T (**Table 4.1**). The mixture was injected eight times per day during three consecutive days. The column-to-column reproducibility was also tested by repeating the same number of injections on three monolithic columns, which were prepared with the same polymerization mixture. The reproducibility of EOF, retention times and peak areas are summarized in **Table 4.1**. As observed, the column-to-column reproducibilities of the retention times and peak areas were better than 4.5 and 5.6%, respectively. About 100 injections of the standard mixture and 60 injections of vegetable oil extracts were performed without the need of replacing the column, therefore, the stability of the columns was satisfactory.

External calibration curves were constructed by injecting six standard solutions of each solute within 5-100 μg mL^{-1} range, and measuring the peak areas. Straight lines with $r > 0.995$ were obtained. The LODs, calculated for a signal-to-noise ratio of 3, are also shown in **Table 4.1**.

The optimized method was applied to the determination of Ts in several oil samples (**Table 4.2**). α-T-AcO was not detected in any of the samples analyzed. Peak identification was performed by comparing the retention times and absorption spectra with those of the standards, and when necessary also by spiking the sample extracts with the standards. Additionally, standard addition calibration curves were obtained by adding increasing concentrations of the standards (up to 100 μg mL^{-1}) to the extracts. A minimum of four additions were performed. The curves were linear with $r > 0.992$, and in all cases the slope of calibration curve did not differ significantly from that obtained with the external calibration method. Therefore, no matrix effect was observed.

Table 4.1. Repeatability and column-to-column reproducibility of retention times and peak areas.

Compounds	Intra-day repeatability (n = 8) RSD, %		Inter-day repeatability (3 days) RSD, %		Column-to-column reproducibility (n = 3) RSD, %		LOD, μg mL^{-1}
	t_R	Peak area	t_R	Peak area	t_R	Peak area	
α-T	1.34	2.23	2.15	4.00	4.29	5.60	2.00
γ-T	1.19	1.76	1.92	3.30	3.64	5.20	1.80
δ-T	0.93	1.47	1.68	2.50	2.74	4.52	1.50
α-T-AcO	1.65	2.54	2.76	4.20	4.56	6.20	2.30
BHT	1.02	1.24	1.54	2.76	3.21	3.70	-
EOF	0.64	0.96	1.22	2.35	2.28	3.20	-

Table 4.2. Contents of Ts in vegetable oils (mg/100 g).

Oil	α-T	β-T + γ-T	δ-T
EVOO	12.2	1.12	ND [a]
Refined corn	31.2	128	7.1
Refined hazelnut	32.1	3.20	0.80
Refined sunflower	60.0	3.83	1.50
Crude red palm [b]	14.2	ND [a]	ND [a]
Refined grapeseed [b]	4.60	ND [a]	ND [a]
Refined soybean	23.1	162	80.4

[a] ND = Not detected.

[b] Quantitation performed with a mobile phase containing 93:7 MeOH-aqueous buffer (5 mM Tris, pH 8.0); the other results were obtained with 99:1 MeOH aqueous buffer.

Representative electrochromatograms of EVOO, corn and soybean oil extracts are shown in **Fig. 4.4**. As shown in this figure, different fingerprints of Ts were obtained according to the botanical origin of the oil. The monolithic

columns used in this work showed RP characteristics, being therefore unable to resolve the β-T and γ-T isomers. In this sense, these columns were not different from other RP-HPLC systems described in literature (Abidi, 1997 and 2000; Gimeno, 2000). Consequently, the sum of the concentrations of the two isomers is given in **Table 4.2**. The found concentrations of Ts were consistent with those reported for oils of the same botanical origins (Dionisi, 1995; Jee, 2002; Rovellini, 1997).

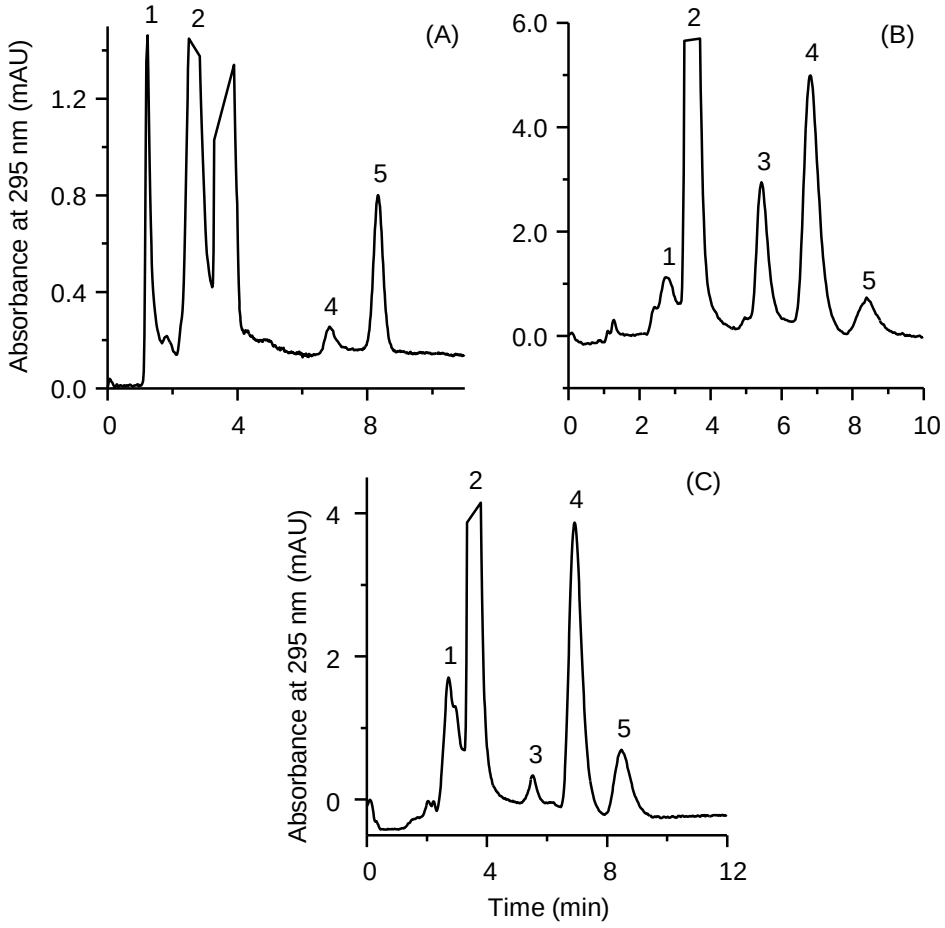

Fig. 4.4. Electrochromatograms of (A) EVOO, (B) soybean and (C) corn oils. Mobile phase: 99:1 MeOH-aqueous buffer (5 mM Tris, pH 8.0). Other conditions as in **Fig. 4.1**, except the peak labeled as 4 which accounts for the sum of the β–T and γ-T isomers.

Thus, α-T was the major T present in EVOO, while δ-T was not detected (**Table 4.2** and **Fig. 4.4A**). In soybean oil, large quantities of β-T + γ-T and δ-T

were observed (**Table 4.2** and **Fig. 4.4B**). Thus, these Ts can be used to detect the presence of soybean oil in adulterated EVOO (Dionisi, 1995). By injecting a series of mixtures of these two oils, and using the δ-T peak area as an adulteration marker, the presence of 10% soybean oil in EVOO was clearly evidenced. As also shown in **Table 4.2** and **Fig. 4.4C**, large quantities of β-T + γ-T and small amounts of α-T and δ-T were present in corn oil. Hazelnut and sunflower oils showed α-T concentrations higher than those of the others Ts; however, since α-T also predominates in EVOO, this T is not a good tracer for hazelnut and sunflower oils in EVOO.

Red palm and grapeseed oils constitute important sources of T_3s (Choo, 1996; Jee, 2002). Thus, these samples were analyzed to provide reference retention times and spectra for the identification of T_3s. Using the RP mode, T_3s eluted following the same order observed for the Ts (Abidi, 1999, 2001 and 2002). In addition, the double bonds of the side-chain of T_3s are not conjugated, thus, Ts and T_3s have closely similar UV spectra. These features were employed to assign the additional peaks observed with the grapeseed and palm oils to T_3s. Additionally, injections of these two oils, after spiking with the T standards, were performed.

Using a 99:1 MeOH-aqueous buffer mobile phase, the peaks of Ts and T_3s partially overlapped; however, an excellent resolution between the peaks of both series of compounds in these oil extracts was achieved by using a 93:7 MeOH-aqueous buffer mixture (data not shown). Since T_3s did not occur naturally in olive oil, their presence in a sample clearly indicate its adulteration with T_3s-rich oils, such as grapeseed or palm oils. An electrochromatogram of an EVOO spiked with 10% palm oil is shown in **Fig. 4.5**. Although the β-T_3 + γ-T_3 pair was not resolved, the presence of several T_3s was evidenced.

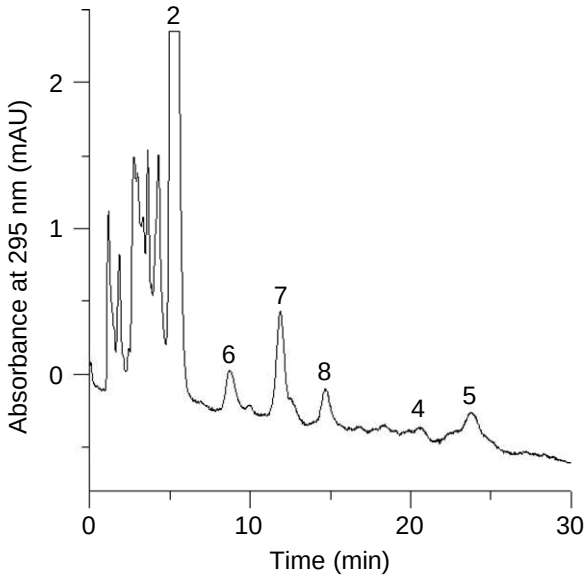

Fig. 4.5. Electrochromatogram of an EVOO containing 10% red palm oil. Peak identification: 6, δ-T_3; 7, β-T_3 + γ-T_3; 8, α-T_3. Mobile phase: 93:7 MeOH-aqueous buffer (5 mM Tris, pH 8.0). Other peaks and working conditions as in **Fig. 4.1**.

4.2. Determination of Ts and T_3s by nano-LC using a silica monolithic column

In this work, a procedure for the determination of Ts and T_3s in vegetable oils, using nano-LC with UV-Vis detection, was developed. For this purpose, a commercial C18 silica monolithic column was used. The vegetable oils employed in this study are specified in **Table 4.3**.

Stock solutions of *ca.* 1500 μg mL^{-1} of T standards were also prepared in MeOH with 0.1% BHT (w/v) and stored at -20 ºC in amber vials. Working solutions were prepared daily by dilution of the stock solutions with the mobile phase. As indicated in section 3.3.1, three extracts were performed for each sample, being each injected three times.

Table 4.3. Botanical origin, number of samples and brand of the oil samples used in this work.

Origin	No. of samples	Brand
Avocado	1	Guinama
	1	Marnys
Corn	1	Guinama
	1	Gloria
Extra virgin olive	1	Intercoop Olival[a]
	1	Tenuta Pennita[b]
Grapeseed	1	Guinama
	1	Coosur
Hazelnut	1	Guinama
	1	Percheron
Peanut	1	Guinama
	1	Maurel
Red Palm	2	Blue Bay
Soybean	1	Guinama
	1	Coosur

[a] Oil produced in Spain from Serrana cultivar.

[b] Oil produced in Italy from Brisighella cultivar.

4.2.1. Optimization of the separation conditions

In order to optimize T separation in terms of mobile phase composition, a test mixture composed of the α-, γ- and δ-T (*ca.* 300 μg mL^{-1}) standards was used. According to literature (Gruszka, 2007), an 89:10:1 ACN/MeOH/water mixture (v/v/v) containing 0.2% acetic acid was first tried as mobile phase. Isocratic elution mode with a flow rate of 0.5 μL min^{-1} was used. As observed in **Fig. 4.6A**, this mobile phase was unable to resolve all the analyte pairs. In order to improve resolution, water content was progressively increased from 1 to 21%, keeping constant the acetic acid percentage. As shown in **Fig. 4.6**, an increase of analysis time was observed when the water content increased.

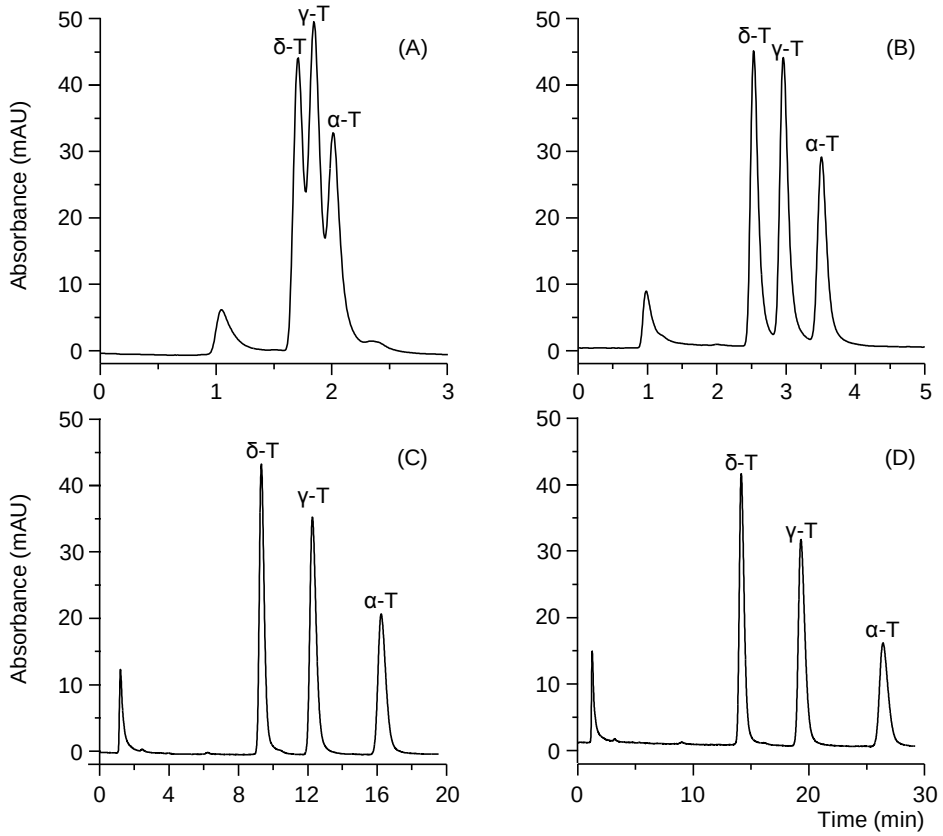

Fig. 4.6. Influence of water content in the mobile phase composition on the separation of T standards: (A) 89:10:1, (B) 84:9:7, (C) 75:8:17 and (D) 71:8:21 ACN/MeOH/water (v/v/v) with 0.2% acetic acid. Other conditions: flow rate, 0.5 μL min^{-1}; wavelength detection, 295 nm.

To evaluate the quality of T separation, efficiency and resolution values were calculated (see **Fig. 4.7**). As observed, both efficiency and resolution were highly dependent on the water content in the mobile phase. As shown in **Fig. 4.7A**, a progressive increase in the efficiency values of T peaks was observed when the water content was increased, reaching a maximum at 19% water. In all cases, theoretical plate values followed the order: α-T > γ-T > δ-T. On the other hand, resolution also improved when the water content increased, reaching a maximum at 17% (**Fig. 4.7B**). Therefore, a mobile phase containing 75:8:17 ACN/MeOH/water (v/v/v) was selected as the best compromise between efficiency, resolution and analysis time (*ca.* 18 min, see **Fig. 4.6C**).

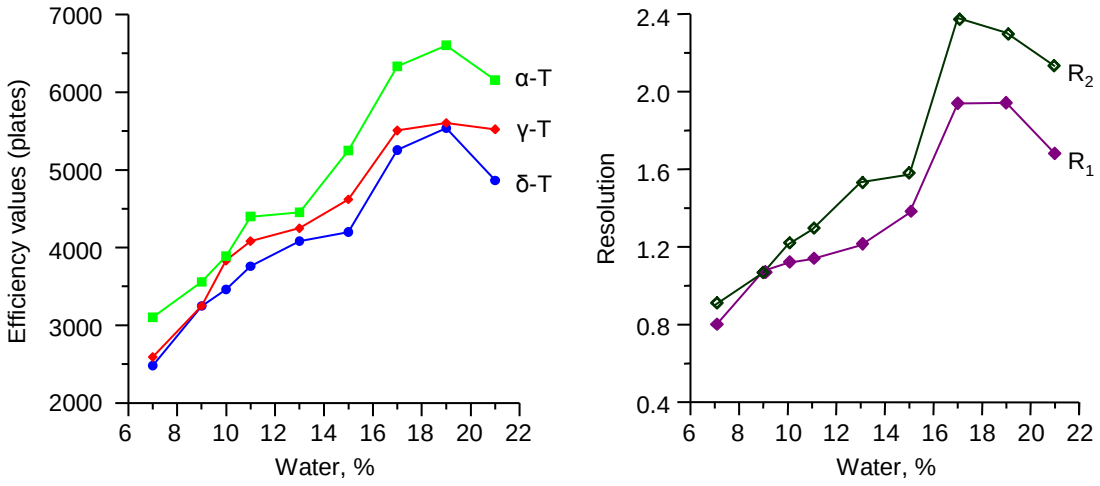

Fig. 4.7. (A) Efficiency and (B) resolution values of T pairs at several water contents in the mobile phase (R_1 = resolution between δ- and γ-T; R_2 = resolution between γ- and α-T).

4.2.2. Quantitation studies and application to real samples

External calibration curves were constructed by injecting six standard solutions in the range 5–500 μg mL^{-1} and measuring the peak areas. Each solution contained the three T standards. In all cases, an excellent linearity, with $r > 0.999$, was obtained. Other analytical figures of merit are shown in **Table 4.4**. The LODs and LOQs were estimated for a signal-to-noise ratio of 3 and 10, respectively. In all cases, these values were lower than others reported in literature (Lerma-García, 2007; Waseem, 2009). Calibration straight-lines with similar sensitivities were obtained for δ- and γ-T, being sensibility value lower for α-T than for δ- and γ-T. Therefore, a higher LOD was obtained for α-T with respect to the other two Ts. These results are in agreement with those reported in the literature (Fanali, 2004).

Table 4.4. Analytical figures of merit for the determination of Ts by nano-LC.

Analyte	Repeatability[a], RSD, %		LOD	LOQ	Relative
	area	t_R	($\mu g\ mL^{-1}$)	($\mu g\ mL^{-1}$)	sensitivity[b]
δ-T	2.8	0.1	0.07	0.2	1.81
γ-T	3	0.1	0.07	0.2	1.92
α-T	4.2	0.2	0.16	0.5	1.00

[a] For a T concentration of 50 $\mu g\ mL^{-1}$ (n = 30).

[b] As the ratio of the slopes of calibration curves of Ts (respect to α-T).

The optimized method was applied to the determination of Ts in several oil samples. Representative chromatograms of corn, grapeseed, hazelnut and soybean oil extracts are shown in **Fig. 4.8**. As indicated above, each extract was injected three times. In all cases, the RSD of the peak areas was below 2.3%. Different fingerprints of Ts were obtained according to the botanical origin of the oil. The monolithic column used in this study worked also in the RP mode, and as indicated in the previous section, separation of the β and γ isomers is not possible; then, the sum of the concentrations of these two isomers was used for quantification. The found concentrations of Ts, expressed as mg kg^{-1} oil, are reported in **Table 4.5**. These data are consistent with those previously reported for oils of the same botanical origins (Dionisi, 1995; Jee, 2002; Rovellini, 1997). As shown in **Table 4.5** and **Fig. 4.8A**, large quantities of β-T + γ-T and small amounts of α-T and δ-T were present in corn oil. Hazelnut oil showed α-T concentrations which were higher than those of the other Ts (**Table 4.5** and **Fig. 4.8C**). In soybean oil, large quantities of β-T + γ-T and δ-T were observed (**Table 4.5** and **Fig. 4.8D**). Thus, these Ts could be used to detect the presence of soybean oil in adulterated EVOO (Dionisi, 1995), whose major isomer was α-T

(**Table 4.5**).

As previously indicated in section 4.1.3, several vegetable oils are rich in T_3s; then, the T_3 concentration was also determined in these oils (see **Table 4.5**). Each T_3 was quantified using the calibration curve of its corresponding T. The found T_3 contents were also consistent with those reported in literature (Choo, 1996; Jee, 2002). Since T_3s did not occur naturally in olive oil, their presence in an olive oil sample clearly indicates its adulteration with T_3-rich oils.

Table 4.5. Contents of Ts and T_3s in vegetable oils (mg kg^{-1}).

Oil	δ-T	β-T + γ-T	α-T	δ-T_3	β-T_3 + γ-T_3	α-T_3
Avocado	12.2 – 23.9	6.3 – 67.6	34.2 – 55.1	0 – 7.9	0 – 9.3	0 – 5.3
Corn	11.1 – 22.3	125.0 – 237.0	51.7 – 82.6	4.8 – 7.1	4.6 – 7.3	2.3 – 12.4
EVOO	0 – 5.6	7.5 – 10.1	52.1 – 111.7	ND[a]	ND[a]	ND[a]
Grapeseed	6.0 – 10.2	6.3 – 17.2	5.8 – 54.8	0 – 8.2	10.3 – 31.0	2.1 – 12.3
Hazelnut	7.0 – 12.1	18.8 – 32.2	71.5 – 119.7	ND[a]	ND[a]	ND[a]
Peanut	6.9 – 31.3	36.7 – 74.1	42.6 – 44.5	ND[a]	ND[a]	ND[a]
Red palm	ND[a]	4.2 – 8.3	6.8 – 20.8	8.8 – 11.3	27.0 – 40.4	15.2 – 35.1
Soybean	66.9 – 87.8	95.4 – 177.1	17.4 – 52.6	ND[a]	ND[a]	ND[a]

[a] ND = Not detected.

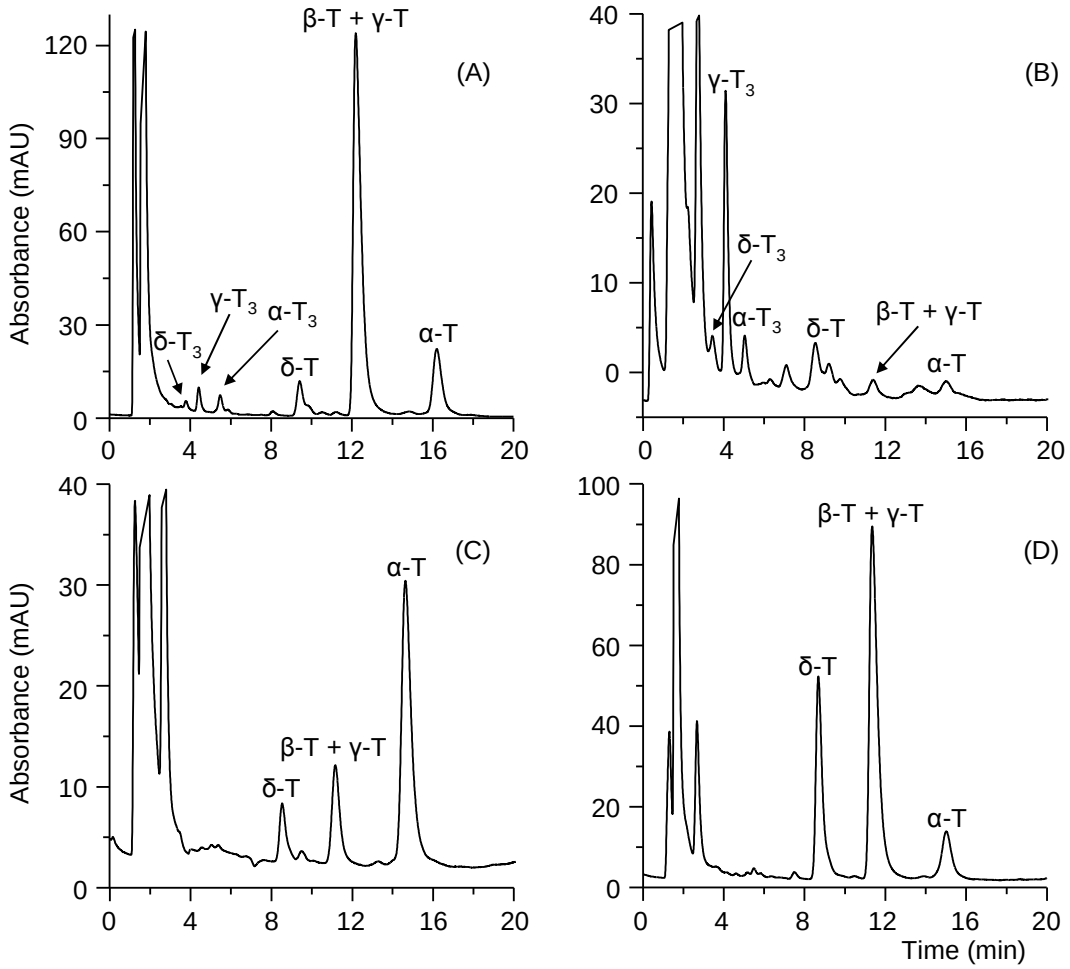

Fig. 4.8. Chromatograms of (A) corn, (B) grapeseed, (C) hazelnut and (D) soybean oil extracts. Mobile phase: 75:8:17 ACN/MeOH/water (v/v/v) with 0.2% acetic acid. Other experimental conditions as in **Fig. 4.6**.

4.3. Methacrylate monolithic columns for nano-LC determination of Ts and T_3s

In this work, a nano-LC-UV-Vis procedure to analyze Ts and T_3s in vegetable oils from different botanical origin using a methacrylate ester-based monolithic column has been developed. The vegetable oils employed in this study, which were the same used in section 4.2, are indicated in **Table 4.3**. As in this section, stock solutions of *ca.* 1500 μg mL^{-1} were prepared and used to

optimize T separation. Three extracts were performed for each sample, being each extract injected three times.

4.3.1. Influence of mobile phase composition

The initial conditions to prepare thermally initiated LMA-based monoliths were similar than those used in T separation by CEC (section 4.1); however, in this case, the total column length was 20 cm. The selected polymerization mixture composition contained 40 wt% monomers (59.8 wt% LMA, 40.2 wt% EDMA) and 60 wt% porogens (20 wt% 1,4-butanediol and 80 wt% 1-propanol) in the presence of AIBN as initiator. In this case, the positive charged monomer (META), which is usually introduced to provide EOF generation in CEC, was not added to the polymerization mixture. However, this monolith showed poor permeabilities, which was probably due to the absence of META, giving small globules and flow-through pores (see **Fig. 4.9A**).

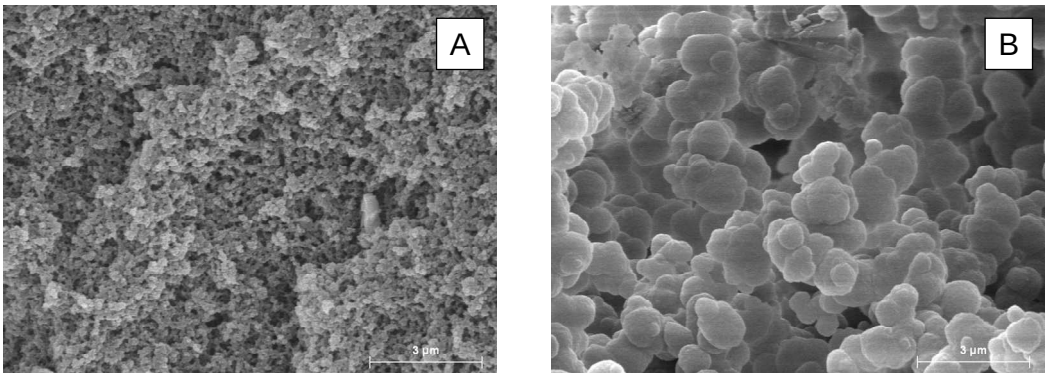

Fig. 4.9. SEM micrograph of the (A) thermally and (B) photo-polymerized LMA based monolithic columns prepared with 12 wt% 1,4-butanediol in the polymerization mixture. The bar lengths stand for 3 µm.

Several authors have demonstrated that the preparation of monolithic columns by UV irradiation show shorter polymerization times and higher permeabilities than those prepared by thermal initiation (Bernabé-Zafón, 2009; Yu, 2001). Then, the same polymerization mixture indicated above for thermal initiation, which was 40 wt% monomers (59.8 wt% LMA, 40.2 wt% EDMA) and 60 wt% porogens (20 wt% 1,4-butanediol and 80 wt% 1-propanol) in the presence of AIBN as initiator, was polymerized under UV irradiation. As it can be seen in **Fig. 4.9B**, the photo-polymerized column showed larger flow-through pores and globule sizes than that thermally polymerized (**Fig. 4.9A**).

Using the photo-polymerized column, and in order to optimize T separation, a test mixture containing the α-, γ- and δ-T (*ca.* 300 μg mL^{-1}) standards was used. First, different mixtures of ACN and water were tried as mobile phases. The efficiency and resolution values obtained at increasing water percentages are shown in **Fig. 4.10**. As observed in this figure, both efficiency and resolution were highly dependent on the water content in the mobile phase. As shown in **Fig. 4.10A**, a progressive increase in the efficiency values of Ts was observed when the water content increased, reaching a maximum at 24%, and decreasing at higher water percentages. On the other hand, resolution also improved when the water content increased (**Fig. 4.10B**). Based on these results, a mobile phase containing 76:24 ACN/water (v/v) was selected as the best compromise between efficiency, resolution and analysis time (*ca.* 23 min, see **Fig. 4.11A**). The retention order of the analytes (δ-, γ-, α-T) revealed that the RP mechanism (hydrophobic interaction with the stationary phase) predominated over other possible interactions. This behaviour agrees with other studies on Ts eluted with RP-HPLC-packed columns (Abidi, 2000; Gimeno, 2000).

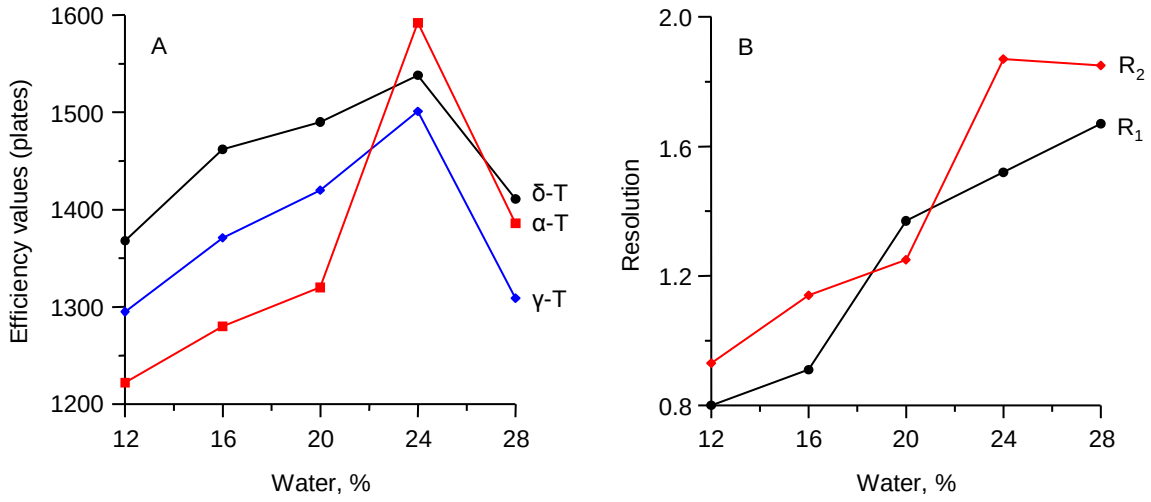

Fig. 4.10. (A) Efficiency and (B) resolution values of Ts at several water contents in the mobile phase (R_1 = resolution between δ- and γ-T; R_2 = resolution between γ- and α-T).

In order to improve T separation, several percentages of MeOH (from 2 to 10%) were added to the mobile phase keeping constant this optimal ACN/water ratio. The best results were obtained when 4% MeOH was added (see **Fig. 4.11B**), which showed better efficiencies, similar resolution and shorter analysis times than the mobile phase containing 76:24 ACN/water (v/v) (**Fig. 4.11A**). Then, a mobile phase containing 96% ACN/water (76:24) and 4% MeOH was selected as the best compromise between efficiency, resolution and analysis time (*ca.* 16 min).

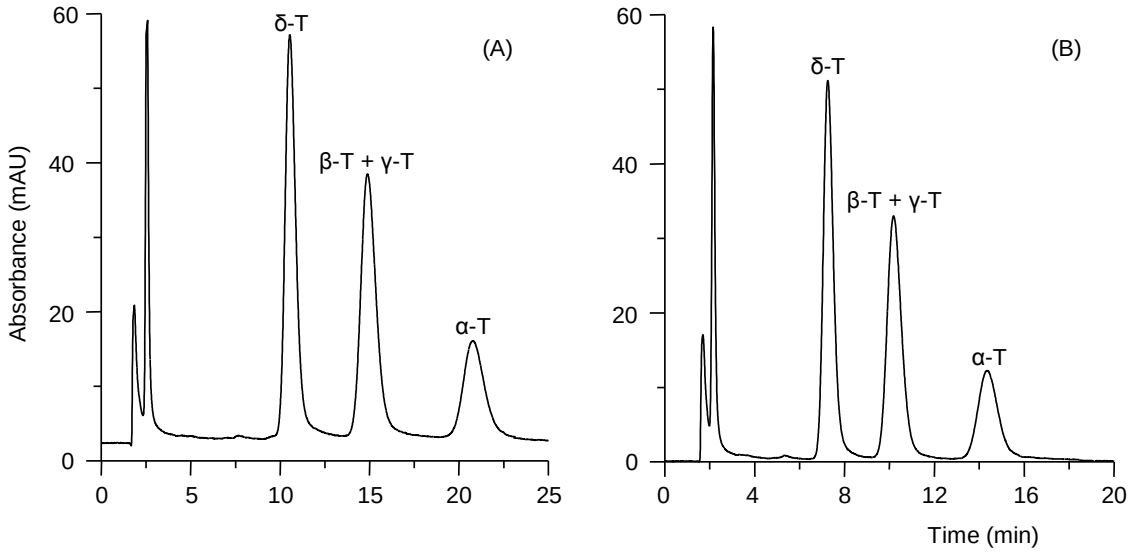

Fig. 4.11. Influence of MeOH content in the mobile phase composition on the separation of T standards: (A) 76:24% ACN/water and (B) 96% ACN/water mixture (76:24) and 4% MeOH. Chromatographic conditions: flow rate, 0.5 μL min^{-1}; wavelength detection, 295 nm.

4.3.2. Quantitation studies and application to real samples

Calibration curves were constructed under the proposed chromatographic conditions and as indicated in section 4.2.2. Straight-lines with $r > 0.998$ were obtained. The proposed method was also evaluated in terms of precision, linearity, LOD and LOQ. The values of these parameters, calculated as in section 4.2.2, are summarized in **Table 4.6**. The repeatability values for retention times and peak areas were in all cases below 0.15 and 3.1%, respectively. Similar sensitivities were obtained for δ- and γ-T, being this parameter lower for α-T. Then, a higher LOD was obtained for α-T with respect to the other two Ts. These results are in agreement with other reported data (Fanali, 2004) and with our previous studies.

Table 4.6. Analytical figures of merit for the proposed nano-LC method in the determination of Ts.

Analyte	Repeatability[a], RSD, %		LOD	LOQ	Relative
	Area	t_R	($\mu g\ mL^{-1}$)	($\mu g\ mL^{-1}$)	sensitivity[b]
δ-T	2.30	0.10	0.12	0.40	1.79
γ-T	2.80	0.10	0.14	0.40	1.88
α-T	3.10	0.15	0.26	0.70	1.00

[a] For a T concentration of 50 $\mu g\ mL^{-1}$ (n = 10).

[b] As the ratio of the slopes of calibration curves of Ts (respect to α-T).

The recommended method was applied to the determination of Ts in several oils with different botanical origins (**Table 4.7**). In general, the levels of Ts found in these samples were in good agreement with the data reported in edible oils (Dionisi, 1995; Jee, 2002). As mentioned above, the monolithic column used showed RP behavior; then, the sum of the concentrations of both isomers, β- and γ-Ts, was employed for quantification. Representative chromatograms of corn, hazelnut and soybean oil extracts are given in **Fig. 4.12**. As shown in **Table 4.7** and **Fig. 4.12A**, large quantities of β-T + γ-T and small amounts of α-T and δ-T were present in corn oil. Hazelnut oil showed α-T concentrations higher than those of the other Ts (**Table 4.7** and **Fig. 4.12B**). In soybean oil, large quantities of β-T + γ-T and δ-T were observed (**Table 4.7** and **Fig. 4.12C**). Thus, these Ts could be used to detect the presence of soybean oil in adulterated EVOO (Dionisi, 1995), in which the most abundant isomer was α-T (**Table 4.7**).

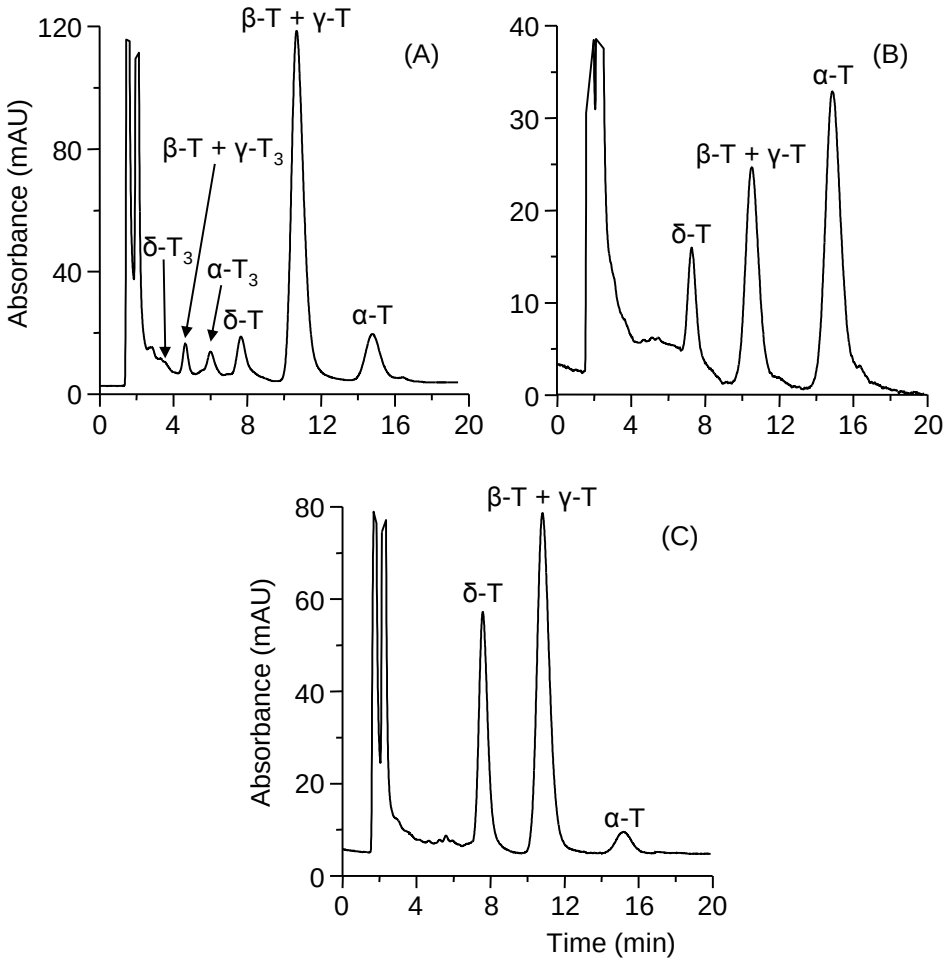

Fig. 4.12. Chromatograms of (A) corn, (B) hazelnut and (C) soybean oil extracts. Mobile phase: 96% ACN/water mixture (76:24) and 4% MeOH. Other working conditions as in **Fig. 4.11**.

As in sections 4.1.3 and 4.2.2, the presence of other peaks ascribed to T_3s, were also quantified (**Table 4.7**). As performed in section 4.2.2, T_3 concentrations were obtained using the calibration curve of the corresponding T. The contents found were consistent with those reported in literature (Jee, 2002; Watson, 2009).

Table 4.7. Contents of Ts and T_3s in vegetable oils (mg kg^{-1}).

Oil	δ-T	β-T + γ-T	α-T	δ-T_3	β-T_3 + γ-T_3	α-T_3
Avocado	11.6 – 25.9	7.8 – 64.1	27.1 – 52.7	0.5 – 6.9	ND[a] – 8.1	ND[a] – 6.9
Corn	10.0 – 21.1	120.7 – 228.3	53.1 – 86.2	3.9 – 8.5	3.9 – 6.7	3.2 – 14.2
EVOO	ND[a] – 4.5	8.0 – 9.9	50.0 – 120.5	ND[a]	ND[a]	ND[a]
Grapeseed	6.8 – 11.0	6.0 – 18.1	4.9 – 56.5	ND[a] – 9.1	11.9 – 33.1	2.8 – 11.9
Hazelnut	6.4 – 13.2	17.8 – 33.5	73.5 – 120.0	ND[a]	ND[a]	ND[a]
Peanut	5.9 – 32.3	33.3 – 72.4	41.6 – 45.8	ND[a]	ND[a]	ND[a]
Red palm	ND[a]	3.9 – 8.9	6.0 – 23.1	7.9 – 12.4	27.0 – 43.5	16.3 – 37.1
Soybean	65.4 – 89.7	94.7 – 179.1	16.9 – 55.1	ND[a]	ND[a]	ND[a]

[a] ND = Not detected (below the LOD value).

4.4. Determination of sterols by CEC using methacrylate monolithic columns

The aim of this study was to develop a fast CEC method to determine sterols in vegetable oils using methacrylate ester-based monolithic columns. The potential of this method to evaluate olive oil adulteration with sunflower and soybean oils was also studied. For these purposes, the following vegetable oils were employed: sunflower (Hacendado), EVOO (Carbonell), soybean (Biolasi), corn, peanut, grapeseed and hazelnut (Guinama).

Stock solutions (*ca.* 5 mM) of the following sterol standards (ergosterol, cholesterol, stigmasterol and β-sistosterol) were prepared in 2-propanol and kept at –20 ºC in amber vials until use. Working solutions were prepared daily by dilution of these stock solutions with the mobile phase.

4.4.1. Optimization of the separation conditions

For sterol separation, the optimal monolithic column obtained for the separation of Ts by CEC was first tried. The composition of the polymerization mixture was: 40 wt% of monomers (59.8 wt% of LMA, 39.9 wt% of EDMA and 0.3 wt% of META) and 60 wt% of porogens (80 wt% of 1-propanol and 20 wt% of 1,4-butanediol). A 1 wt% AIBN with respect to the monomers was also added.

To obtain an optimal mobile phase for sterol separation, ACN/THF/water ternary mixtures containing 5 mM Tris at pH 8.0 were first tried (Abidi, 2004). For this purpose, several volume fractions of THF in the 5-35% range, keeping a constant water percentage of 5%, were studied. With a mobile phase containing 35% THF, the co-elution of several sterol peaks was observed. By decreasing the THF percentage, peak resolution increased largely; however, with a 5% THF broad peaks were obtained. Then, a mobile phase containing 85:10:5 (v/v/v) ACN/THF/water gave the best resolution and efficiency values for all the sterol peaks in less than 10 min (see **Table 4.8** and **Fig. 4.13A**).

Table 4.8. Efficiency, resolution and *k*-values obtained with the two optimal mobile phases using an LMA-based monolithic column with 12 wt% 1,4-butanediol (column A3).

Solutes	ACN/THF/Tris (85:10:5)			ACN/2-propanol/Tris (85:10:5)		
	N (plates/m)	R[a]	*k*	N (plates/m)	R[a]	*k*
Ergosterol	28200	-	3.4	36300	-	2.2
Cholesterol	34700	3.4	4.8	46300	3.3	3.0
Stigmasterol	26000	1.5	5.7	28800	1.5	3.4
β-Sitosterol	34600	1.8	6.7	60900	2.0	4.1

[a] Resolution (R) was calculated between two adjacent peaks.

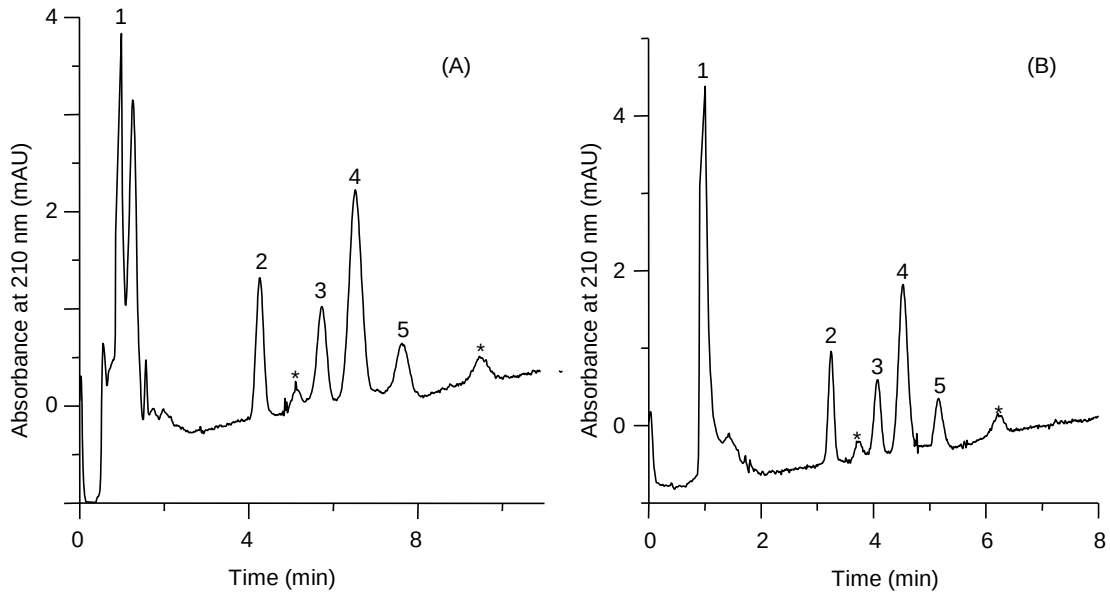

Fig. 4.13. Influence of the mobile phase composition on the separation of sterols: (A) 85:10:5 (v/v/v) ACN/THF/water and (B) 85:10:5 (v/v/v) ACN/2-propanol/water, both containing 5 mM Tris at pH 8.0. CEC conditions: LMA-based monolithic column prepared with 12 wt% 1,4-butanediol in the polymerization mixture (column A3) (Lerma-García, 2007); electrokinetic injection, 10 kV for 2 s; separation voltage, 20 kV. Peak identification: 1, thiourea; 2, ergosterol; 3, cholesterol; 4, stigmasterol; 5, β-sitosterol. Impurities were labeled with an asterisk.

A similar study, in which THF was substituted by 2-propanol in the mobile phase composition was carried out, since sterol are much more soluble in 2-propanol than in THF. The 2-propanol percentage in the mobile phase within the 5-35% range was also studied. The best results were obtained with a mobile phase constituted by 85:10:5 (v/v/v) ACN/2-propanol/water (see **Fig. 4.13B**). A comparison between efficiencies, *k*-values and peak pair resolutions obtained with the mobile phases containing either 10% THF or 10% 2-propanol is shown in **Table 4.8**. As observed, resolution between sterol peak pairs was similar with both mobile phases; however, better efficiencies and lower *k*-values were obtained for the mobile phase containing 2-propanol, which was selected for the studies that followed.

With the selected mobile phase, and keeping constant the proportion of monomers/porogens and monomers/crosslinker at 40:60 and 60:40 % (wt/wt), respectively, the effect of porogenic solvent composition on the monolith morphology and chromatographic performance was investigated (**Table 4.9**, columns A1-A4).

Table 4.9. Composition of the polymerization mixtures used for the preparation of LMA-based monolithic columns and their efficiency and retention values.

Column	Monomers/porogens, (%, wt/wt)	LMA/EDMA, (%, wt/wt)	1-Propanol/ 1,4-butanediol, (%, wt/wt)	$N_{\beta\text{-sitosterol}}$ (plates/m)	$k_{\beta\text{-sitosterol}}$
A1	40:60	60:40	86:14	NM[a]	NM[a]
A2	40:60	60:40	83:17	45200	6.2
A3	40:60	60:40	80:20	60900	4.1
A4	40:60	60:40	75:25	53600	3.9
A5	30:70	60:40	80:20	28200	2.9
A6	50:50	60:40	80:20	NM[a]	NM[a]
A7	40:60	70:30	80:20	58700	3.6
A8	40:60	50:50	80:20	NM[a]	NM[a]

[a] Not measured.

The content of 1,4-butanediol in the polymerization mixture was varied from 8 to 15 wt% (14 to 25 wt% for the porogenic solvents). With less than 10 wt% 1,4-butanediol (e.g. column A1), too small pore sizes (< 125 nm) (Lerma-García, 2007), clearly unsuitable for any flow-through applications, were obtained. In comparison to the use of 12 wt% 1,4-butanediol (column A3), a 10 wt% of this solvent (column A2) led to similar resolutions between the successive analyte peaks, but with lower efficiencies and longer analysis times (≈ 15 min). This increase in the retentivity of solutes was due to a strong decrease of

both the pore size of the monolith and the dimension of the globules, also implying an increase in the surface area, as observed for polymerization mixtures containing low 1,4-butanediol contents (Eeltink, 2005 and 2007). This behavior can be explained briefly as follows. In a mixture of porogenic solvents with small 1,4-butanediol content (low polarity), phase separation will occur late in the polymerization process, due to the relatively high solubility of the polymer in the solvent. At the time of phase separation, the system contains a large polymer concentration, which precipitates in the form of numerous nuclei. All these nuclei are allowed to grow for only a limited period of time before all the monomers are exhausted. Overall, the globules that are formed in such a system are small and, consequently, the voids between them (pores) are small as well. The result would be a polymer with high surface area, and consequently, more retentivity. The low efficiencies obtained at 10 wt% of 1,4-butanediol (column A2) could be explained by the double-layer overlap, as suggested by several authors (Eeltink, 2005; Peters, 1998A).

To check the possibility of achieving shorter analysis time while maintaining satisfactory resolution between analytes, monolithic columns prepared with 15 wt% 1,4-butanediol (column A4) were also examined. The analysis time was reduced to 5 min; however, cholesterol/stigmasterol peaks co-eluted. Then, a content of 12 wt% of butanediol (20 wt% in the porogenic solvent) was selected for further experiments.

The porogen weight fraction in the polymerization mixture has also some effect on the character of the monolithic structure (Eeltink, 2005; Peters, 1998A). In this way, this factor was investigated (**Table 4.9**, columns A3, A5 and A6). When the content of the porogenic solvent in the polymerization mixture reached 70 wt% (column A5), an overlapping between cholesterol/stigmasterol peaks was observed. This could be attributed to the large globule sizes formed in the

polymer network (Eeltink, 2005; Peters, 1998A). In contrast, when the content of the porogenic solvent was reduced to 50 wt% (column A6), the bed permeability was significantly reduced leading to blockage problems of columns. Then, a 40:60 % (wt:wt) monomer/porogen ratio was selected for the experiments that followed.

Next, the EDMA content in the monomer mixture was also studied (**Table 4.9**, columns A3, A7 and A8). When the weight content of porogenic solvent (80:20 (wt/wt) 1,4-butanediol/1-propanol) was kept constant at 60 wt%, and the weight content of EDMA in monomer mixture was decreased from 40 (column A3) to 30 wt% (column A7), the efficiency values were similar, but a partial overlapping between β-sitosterol and cholesterol was obtained. At 50 wt% EDMA (column A8), the permeability became so poor that it was impossible to flush the column due to the highly dense polymeric bed formed (Eeltink, 2005). At the sight of these results, column A3, which provided the best results in terms of efficiency, resolution and analysis time, was selected.

The influence of the nature of the alkyl methacrylate monomer was also investigated. Thus, the bulk monomer (LMA) was substituted by another one with a longer alkyl chain, such as ODMA. An optimization study of the composition of the polymerization mixture was also performed using this monomer. Thus, the 1,4-butanediol content in the polymerization mixture was examined in the 4-15 wt% range (7-25 wt% of the porogenic solvent mixture) (**Table 4.10**, columns B1-B5). With 4 wt% 1,4-butanediol (column B1), the permeability of the monolith was so poor that it was impossible to flush the column. Columns produced at 6 wt% of 1,4-butanediol (column B2) showed poor efficiencies and long analysis times. As commented above, this was attributed to the double-layer overlap. With 8 wt% (column B3), an efficiency of 42000 for β-sitosterol, and resolution values for all the consecutive peak pairs,

comprised between 1.2 and 2.9, were obtained. When 12 wt% (column B4) was tried, the resolution of sterols was similar to that obtained with 8 wt%, but an increase in efficiency, and a decrease in the analysis time, was obtained. Finally, a percentage of 15 wt% 1,4-butanediol (column B5) produced the co-elution of the cholesterol/stigmasterol peaks. Thus, a content of 12 wt% 1,4-butanediol in the polymerization mixture (column B4) was selected for further studies.

The porogen weight fraction in the polymerization mixture for ODMA monoliths was also studied (**Table 4.10**, columns B4, B6 and B7). When the porogen weight fraction was reduced from 60 to 50 wt% (columns B4 and B7, respectively), all solutes co-eluted as a single peak. When this fraction was increased up to 70 wt% (column B6), the column efficiency decreased from 46400 to 43800 plates/m for β-sitosterol, but the *k*-value increased from 4.6 to 6.2. Consequently, a porogen weight fraction of 60 wt% was selected for further studies.

Table 4.10. Composition of the polymerization mixtures used for the preparation of ODMA-based monolithic columns and their efficiency and retention values.

Column	Monomers/porogens, (%, wt/wt)	ODMA/EDMA, (%, wt/wt)	1-Propanol/ 1,4-butanediol, (%, wt/wt)	$N_{\beta\text{-sitosterol}}$ (plates/m)	$k_{\beta\text{-sitosterol}}$
B1	40:60	60:40	93:7	NM[a]	NM[a]
B2	40:60	60:40	90:10	26000	7.6
B3	40:60	60:40	86:14	42000	4.8
B4	40:60	60:40	80:20	46400	4.6
B5	40:60	60:40	75:25	36200	3.9
B6	30:70	60:40	80:20	43800	6.2
B7	50:50	60:40	80:20	NM[a]	NM[a]
B8	40:60	70:30	80:20	NM[a]	NM[a]
B9	40:60	50:50	80:20	34200	7.1

[a] Not measured.

Next, a change in the monomer/crosslinker ratio was done. The proportion of EDMA in the monomer mixture was varied from 30 to 50 wt% (**Table 4.10**, columns B4, B8 and B9). Using a 30 wt% EDMA (column B8), an overlapping of all solutes (in less than 2 min) was observed. However, a 50 wt% EDMA gave worse efficiency values (34200 plates/m for β-sitosterol) and longer retentions times (*ca*. 13 min) than those obtained with 40 wt% EDMA. Thus, a 40 wt% EDMA (column B4) was selected. An analysis of the sterol test mixture performed with this column is shown in **Fig. 4.14**.

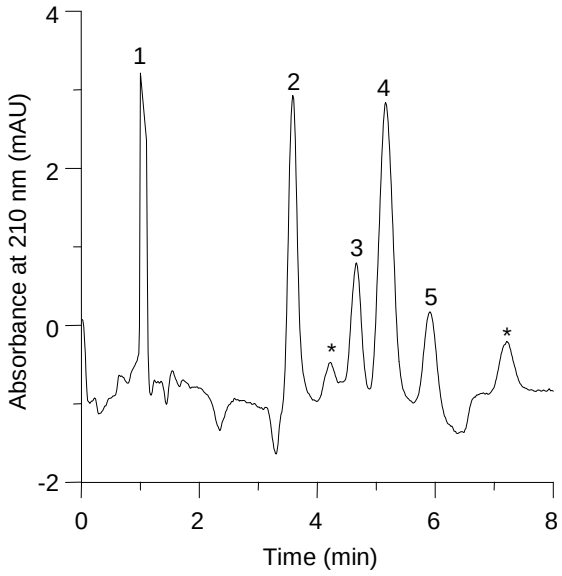

Fig. 4.14. Electrochromatogram obtained with an ODMA-based monolithic column prepared with 12 wt% 1,4-butanediol in the polymerization mixture (column B4). Mobile phase: 85:10:5 (v/v/v) ACN/2-propanol/water containing 5 mM Tris at pH 8.0. Peak identification and other experimental conditions as in **Fig. 4.13**.

As it can be observed, this ODMA-based column gave slightly longer retention times than those obtained with the optimum LMA-based column (**Fig 4.13B**), although a much larger increase in *k*-values could be expected, since the

ODMA alkyl chain is longer than that of LMA. This retention behavior could be explained taking into account that changes in the polymerization mixture (different bulk monomer) induce changes not only in the hydrophobicity of the monolith, but also in its structure. This was in agreement with previous reports (Delaunay-Bertoncini, 2004; Waguespack, 2005). As deduced from the SEM pictures (**Fig. 4.15**), both the ODMA- and LMA-based columns had voids and globules of similar sizes.

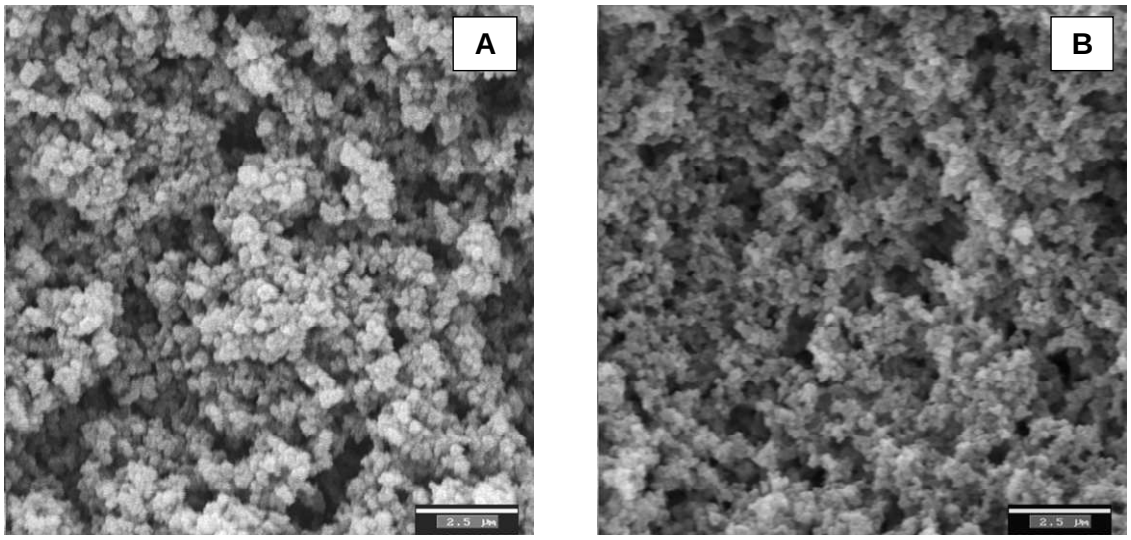

Fig. 4.15. SEM micrographs of the (a) LMA (column A3) and (b) ODMA (column B4) monolithic materials inside the capillary. The bar lengths stand for 2.5 μm.

Additionally, the peak efficiencies achieved with the ODMA-based column were lower (26000-46400) than those obtained with the LMA-based column (28800-60900 plates/m). Consequently, the monolithic column prepared with LMA containing 12 wt% 1,4-butanediol (column A3), was selected as the best compromise between resolution, efficiency and analysis time.

4.4.2. Quantitation studies and application to real samples

To estimate intra- and inter-day repeatabilities in the optimal conditions, a mixture containing 0.75 mM of each sterol was injected ten times per day during three consecutive days (**Table 4.11**). Series of ten injections on three different monolithic columns, prepared with the same polymerization mixture, were also performed to establish column-to-column reproducibility. The EOF reproducibility, retention times and peak areas are summarized in **Table 4.11**.

Table 4.11. Analytical figures of merit for the sterol standards.

Compounds	Intra-day rep. RSD, %		Inter-day rep. RSD, %		Column-to-column reprod. RSD, %		Sensitivities, mM^{-1}
	t_R	Peak area	t_R	Peak area	t_R	Peak area	
Ergosterol	0.12	2.62	2.15	4.40	3.81	5.20	31.3
Cholesterol	0.34	2.92	2.44	5.22	4.26	6.20	28.5
Stigmasterol	0.27	2.10	2.72	4.92	4.40	5.63	29.6
β-Sitosterol	0.11	2.84	2.91	4.74	3.73	5.44	31.5
EOF	0.43	1.92	1.52	3.52	3.10	4.92	-

In all cases, column-to-column RSD values for the retention times and peak areas were lower than 4.4 and 6.2 %, respectively. More than 80 injections of the mixture of standards and 50 injections of vegetable oil extracts were performed without the need of replacing the column; therefore, columns showed a satisfactory stability.

External calibration curves were constructed by injecting six standard solutions of each solute in the 0.125 - 5 mM range and by measuring the peak areas. Straight-lines with $r > 0.994$ were obtained. As it can be observed in **Table 4.11**, all the sterols gave closely similar sensitivities. The LODs, also calculated at a signal-to-noise ratio of 3, ranged from 0.025 to 0.037 mM^{-1} for stigmasterol

and ergosterol peaks, respectively.

The optimized method was applied to the analysis of oil samples. Representative electrochromatograms of EVOO, hazelnut and soybean oil extracts are shown in **Fig. 4.16**.

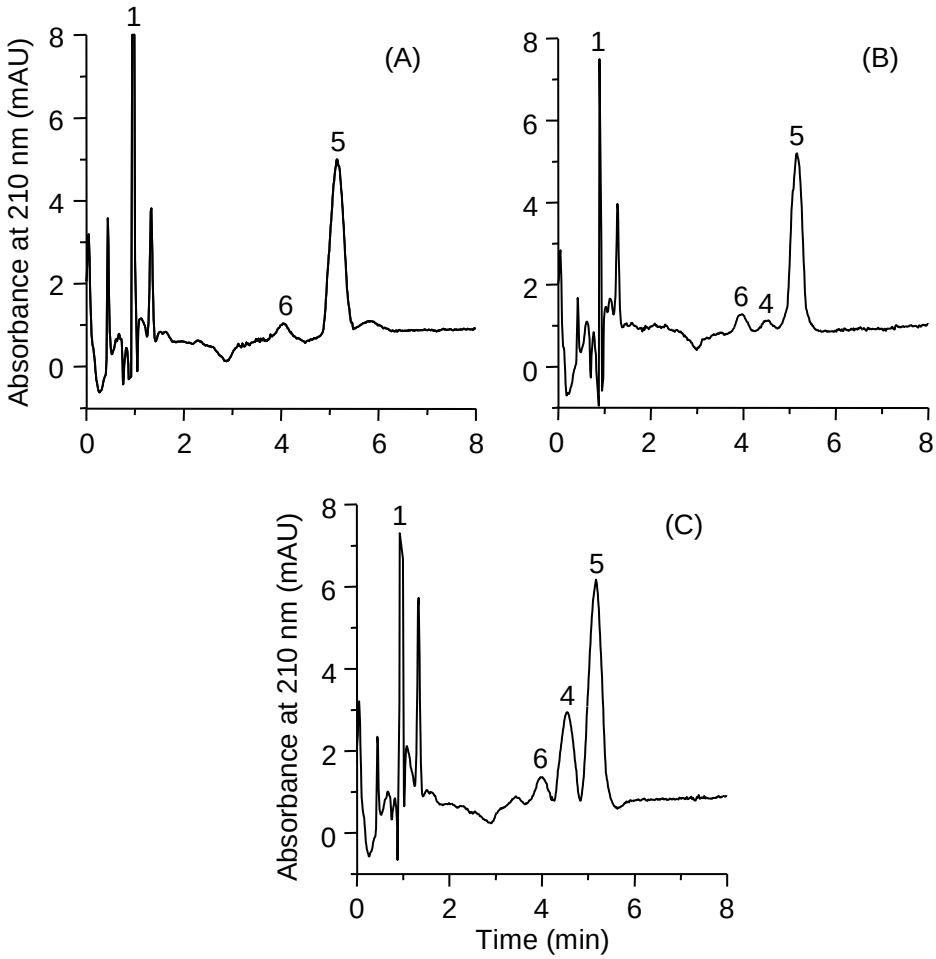

Fig. 4.16. Electrochromatograms of (A) EVOO, (B) hazelnut and (C) soybean oils obtained using an LMA-based monolithic capillary column (column A3). Mobile phase: 85:10:5 (v/v/v) ACN-2-propanol-water containing 5 mM Tris at pH 8.0. Peak identification: 5, β-sitosterol + campesterol; 6, avenasterol. Identification of other peaks and other working conditions as in **Fig. 4.13**.

Peak identification was performed by comparing the retention times with those of the standards or by spiking the sample extracts with the standards. Other

sample peaks observed in the vegetable oils analyzed were tentatively assigned to campesterol and avenasterol, in agreement with their abundance in the oils (Abidi, 2004; Benitez-Sánchez, 2003; Bohacenko, 2001; Cercaci, 2003; Jee, 2002; Martínez-Vidal, 2007; Matthäus, 2008; Parcerisa, 2000). β-Sitosterol and campesterol were assumed to co-elute, as expected from the structural similarity between them. In fact, Mezine et al. (2003) failed to resolve these two compounds using an RP hexyl-phenyl column. However, Abidi et al. (2004) were able to resolve this pair of solutes by CEC using a C_{18} packed column, but at expenses of a long analysis time (> 55 min). Thus, in this work, these two solutes were jointly evaluated.

On the other hand, taking into account the sterol profiles obtained for all oil samples analyzed, and due to the lack of commercial avenasterol standards, the peak located close to 4 min (no. 6 of **Fig. 4.16**) was tentatively assigned to this compound. This peak eluted close to cholesterol peak, which is present in vegetable oils in concentrations below the LOD of the proposed method (Bohacenko, 2001; Cañabate-Díaz, 2007; Cercaci, 2003; Martínez-Vidal, 2007). The co-elution of cholesterol and avenasterol is also consistent with findings reported in literature for RP columns (Martínez-Vidal, 2007).

Due to the similarity between the sensitivities of all sterols (see **Table 4.11**), the β-sitosterol + campesterol and avenasterol contents were estimated using β-sitosterol as reference standard. The found percentages of sterols in the vegetable oils are shown in **Table 4.12**. These results were consistent with reported data (Abidi, 2004; Benitez-Sánchez, 2003; Bohacenko, 2001; Cañabate-Díaz, 2007; Cercaci, 2003; Jee, 2002; Martínez-Vidal, 2007, Matthäus, 2008; Parcerisa, 2000). As it can be seen in **Table 4.12**, soybean and sunflower oils showed large quantities of stigmasterol, being this sterol below the LOD in EVOO (Bohacenko, 2001; Benitez-Sánchez, 2003; Cañabate-Díaz, 2007;

Cercaci, 2003; Jee, 2002; Martínez-Vidal, 2007, Parcerisa, 2000). For this reason, the stigmasterol peak can be used as an adulteration marker (Ballesteros, 1995; Kamm, 2001). To evaluate this possibility, a series of binary mixtures of soybean or sunflower oils with EVOO were prepared and injected. Using the stigmasterol peak area as an adulteration marker, the presence of 8% soybean or sunflower oil in extra virgin olive oil was clearly evidenced (see **Fig. 4.17**).

Table 4.12. Percentage of sterols found in vegetable oils [a].

Oil	Avenasterol, %	Stigmasterol, %	β-Sitosterol+campesterol, %
Sunflower	5	10	85
EVOO	9	ND	91
Soybean	3	19	78
Corn	7	6	87
Peanut	7	9	84
Grapeseed	3	12	85
Hazelnut	5	1	94

[a] ND = Not detected.

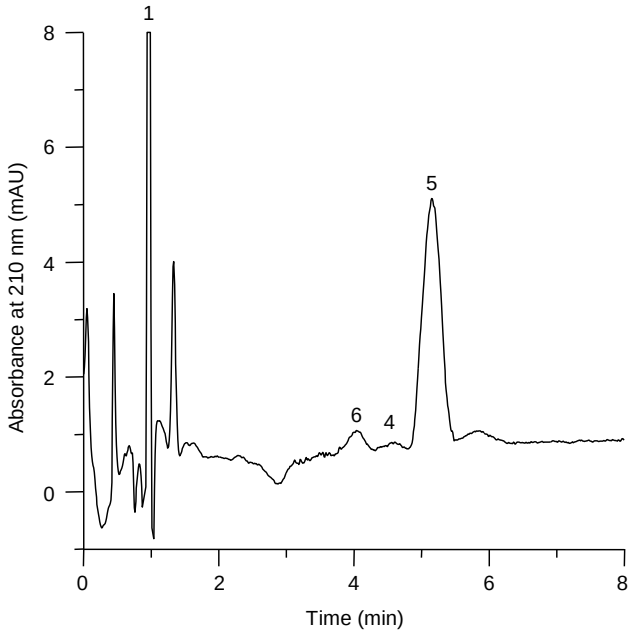

Fig. 4.17. Electrochromatogram of an EVOO containing 8% soybean oil showing the stigmasterol peak (no. 4). Peak identification and other working conditions as in **Fig. 4.16**.

4.5. Determination of sterols by UPLC-MS

In this work, the applicability of UPLC-APCI-MS to characterize the sterol fraction of vegetable oils with different botanical origins has been studied. The developed method was also applied to the identification and determination of the main sterols present in several vegetable oils. The vegetable oils employed in this study are shown in **Table 4.13**.

Table 4.13. Botanical origin, number and brand of the vegetable oil samples used in this work.

Origin	No. of samples	Brand
Avocado	2	Guinama
	2	Marnys
Corn	2	Guinama
	1	Asua
	1	Cristal
Olive	1	Carbonell
	1	Grupo Hojiblanca
	1	Borges
	1	Torrereal
Hazelnut	2	Guinama
	1	Percheron
	1	Flumen
Grapeseed	1	Guinama
	1	Paul Corcelet
	1	Pons
	1	Coosur
Peanut	1	Guinama
	1	Bellsola
	1	Apsara Vital
	1	Maurel
Soybean	1	Coosur
	1	Guinama
	1	Biolasi
	1	Sojola
Sunflower	2	Koipesol
	1	Hacendado
	1	Coosur

4.5.1. Optimization of the separation conditions

In order to optimize sterol separation in terms of mobile phase composition, column temperature and flow rate, a test mixture composed of six sterol standards was used. Ergosterol, stigmasterol, cholesterol and lanosterol concentrations were *ca.* 50 μg mL^{-1}, being 38 and 5 μg mL^{-1} for β-sitosterol and campesterol, respectively.

According to literature (Cañabate-Díaz, 2007), mixtures of ACN/water, both containing 0.01% acetic acid, were tried in gradient elution mode, using a constant column temperature (30 ºC) and a fixed flow rate (0.5 mL min^{-1}). For each sterol standard, two SIR channels, which corresponded to the $[M+H]^+$ and $[M+H-H_2O]^+$ ions, were monitored. However, and as previously reported (Cañabate-Díaz, 2007; Lerma-García, 2008; Segura-Carretero, 2008), the $[M+H-H_2O]^+$ peaks showed higher intensities than the respective $[M+H]^+$ peaks. For this reason, the intensities obtained at the SIR channels of the $[M+H-H_2O]^+$ peaks (379.5, 369.5, 383.5, 395.5, 397.5 and 409.5 for ergosterol, cholesterol, campesterol, stigmasterol, β-sitosterol and lanosterol, respectively) were used for identification and quantification. APCI mass spectra showing the $[M+H-H_2O]^+$ peaks of the six sterol standards are depicted in **Fig. 4.18**. In all the gradient elutions tested, stigmasterol and campesterol peaks overlapped. This was in agreement with previous reports (Lu, 2007). A linear gradient from 80 to 100% ACN for 0.5 min, followed by an isocratic elution with 100% ACN was selected as the best compromise between analysis time and resolution (**Fig. 4.19B**). Under this gradient elution, and a flow rate of 0.5 mL min^{-1}, the influence of column temperature was evaluated.

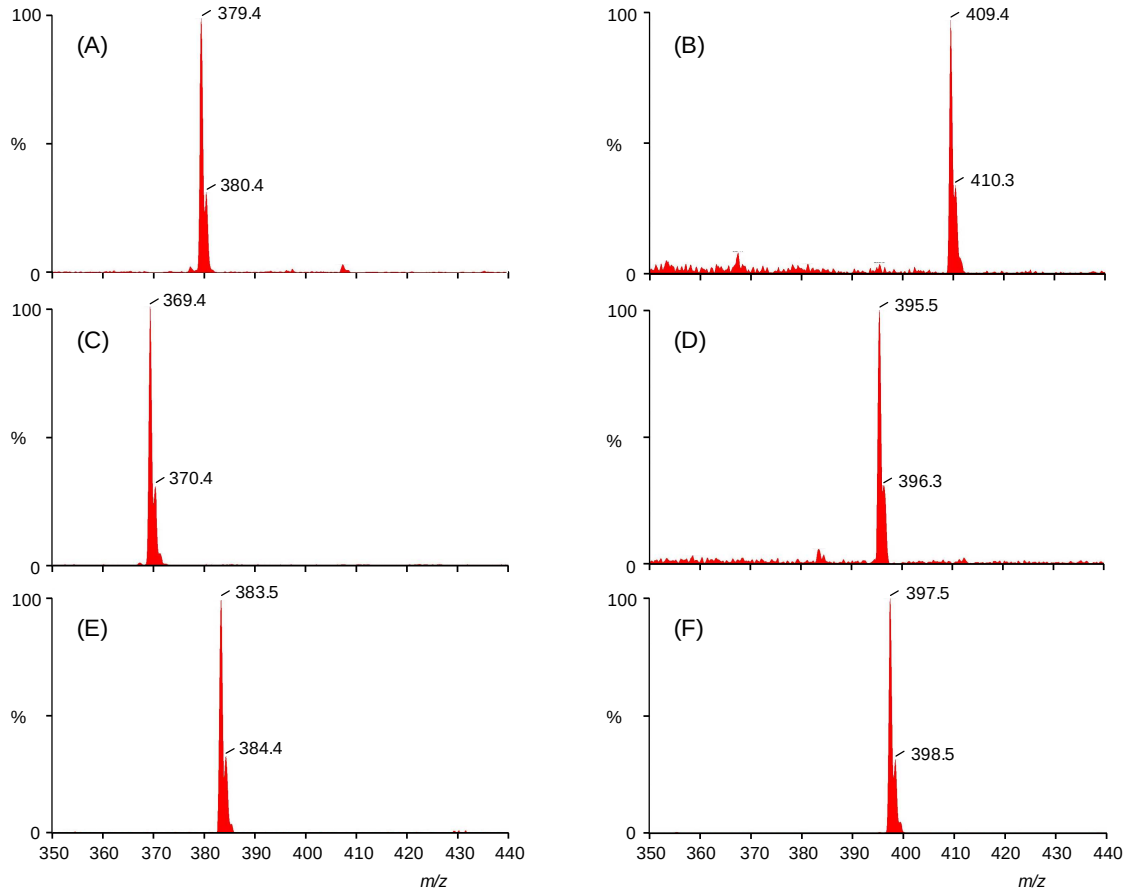

Fig.4.18. Full scan mass spectra of the six sterol standards used in this study. Peak identification: (A), ergosterol; (B), lanosterol; (C), cholesterol; (D), stigmasterol; (E), campesterol; (F), β-sitosterol.

As shown in **Fig. 4.19**, the chromatographic behavior of sterols was modified by increasing the temperature of the column from 10 to 40 ºC. At 40 ºC (**Fig. 4.19A**), lanosterol and cholesterol peaks overlapped. When the temperature was decreased from 30 to 10 ºC (**Fig. 4.19B-D**), a slight decrease in efficiency values jointly with an increase in analysis time was observed. However, the global resolution (measured as the geometrical mean of the resolution between the consecutive sterol pairs) slightly improved (from 1.18 to 1.30). For this reason, a column temperature of 10 ºC was selected for further studies.

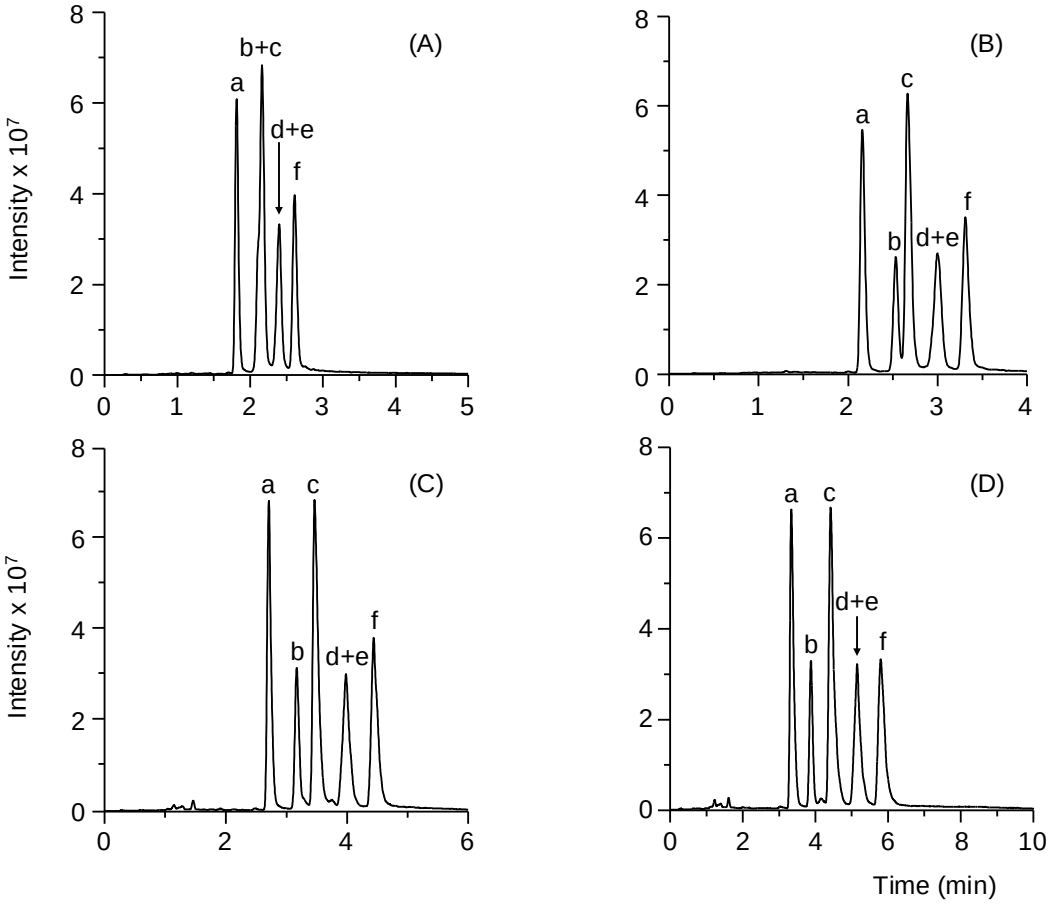

Fig. 4.19. Influence of the column temperature on the separation of sterols: (A) 40 ºC, (B) 30 ºC, (C) 20 ºC and (D) 10 ºC. Chromatographic conditions: linear gradient from 80 to 100% ACN for 0.5 min followed by isocratic elution with 100% ACN for 4.5 more min using a flow rate of 0.5 mL min^{-1}. Peak identification as in **Fig. 4.18**.

Next, the influence of the flow rate on sterol separation was also studied (see **Fig. 4.20**). When the flow rate was increased from 0.4 to 0.8 mL min^{-1} (**Fig. 4.20A-B**), higher efficiencies were obtained, whereas the global resolution decreased from 1.47 to 1.28; a decrease of both parameters was observed when the flow rate was increased up to 1.2 mL min^{-1} (**Fig. 4.20C**). As a result, a flow rate of 0.8 mL min^{-1} was selected as the best compromise between efficiency, resolution and analysis time.

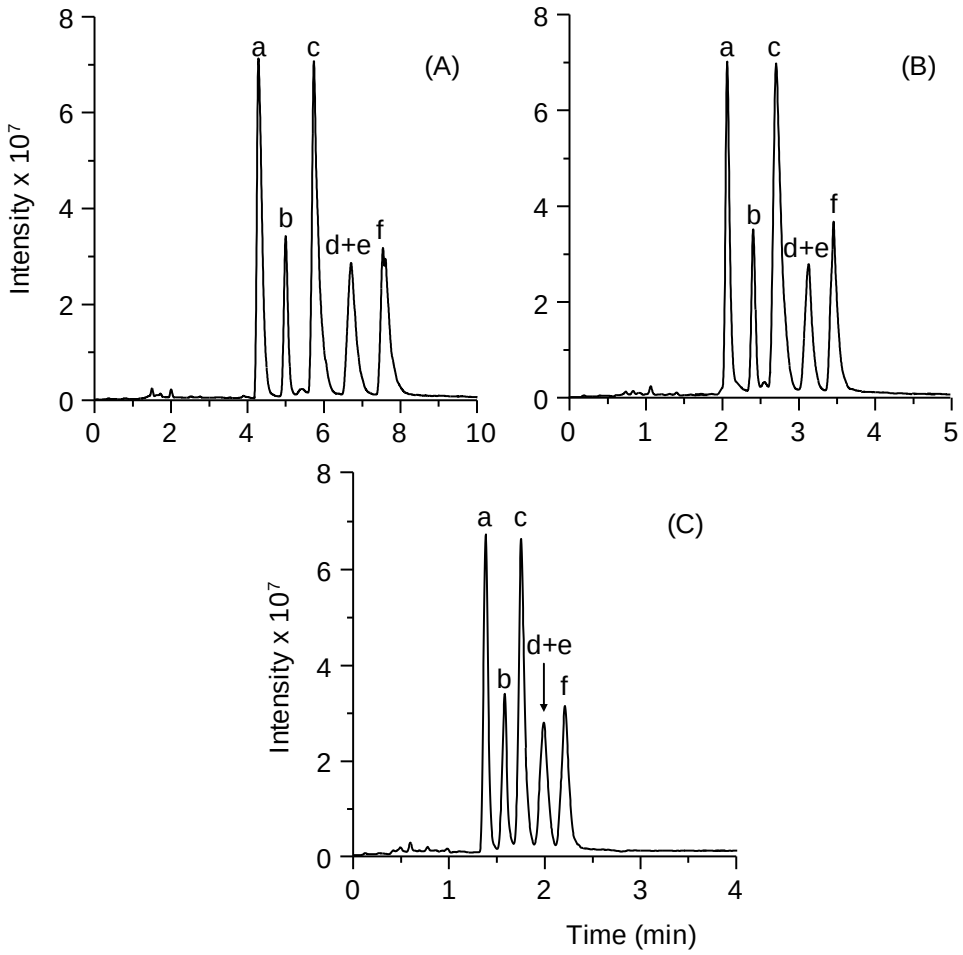

Fig. 4.20. Influence of flow rate on the separation of sterols: (A) 0.4, (B) 0.8 and (C) 1.2 mL min^{-1}. Chromatographic conditions: temperature 10 ºC; gradient elution and peak identification as in **Fig. 4.19**.

4.5.2. Quantitation studies and application to real samples

External calibration curves were constructed by injecting six standard solutions of each solute within its linearity range (0.5-50 μg mL^{-1}, except for β-sitosterol that ranged up to 250 μg mL^{-1}). Straight lines with $r > 0.999$ were obtained. Other analytical figures of merit are given in **Table 4.14**. The intra- and inter-day repeatabilities of peak areas and retention times for all analytes were obtained by injecting the same 1 μg mL^{-1} solution 10 times per day during 3 days. In all cases, the RSD values were lower than 5 and 0.4% for peak areas and retention times, respectively.

Table 4.14. Analytical figures of merit of the proposed UPLC-MS method for the determination of sterols.

Analyte	Intra-day rep[a], %		Inter-day rep[b], %		LOD	LOQ	Relative
	Area	t_R	Area	t_R	(μg mL^{-1})	(μg mL^{-1})	Sensitivity[c]
Ergosterol	2.8	0.08	3.6	0.25	0.04	0.13	1.1
Lanosterol	2.7	0.08	3.2	0.27	0.07	0.25	0.4
Cholesterol	2.7	0.10	4.1	0.30	0.03	0.10	1.2
Stigmasterol	2.6	0.11	3.7	0.30	0.04	0.13	0.9
Campesterol	2.9	0.11	3.8	0.31	0.03	0.10	1.2
β-Sitosterol	2.4	0.12	5.0	0.40	0.04	0.13	1.0

[a] Repeatability (as RSD) for a sterol concentration of 1 μg mL^{-1} (n=10).

[b] Repeatability (as RSD) for a sterol concentration of 1 μg mL^{-1} (3 days).

[c] As the ratio of the slopes of calibration curves of sterols (respect to β-sitosterol).

The relative sensitivities of sterols (respect to β-sitosterol) gave values comprised between 0.9 and 1.2, except for lanosterol that provided a value of 0.4. This behavior was due to differences in sterol structures, which was in agreement with previous studies (Lu, 2007). The LODs, which were estimated for a signal to noise ratio = 3, were comprised between 0.03 and 0.07 μg mL^{-1}, whereas the LOQs, based on a signal to noise ratio = 10, ranged from 0.10 to 0.25 μg mL^{-1}. These values were higher than those reported by Lu (2007) working with the same stationary phase in an UPLC system connected to a triple-quadrupole mass spectrometer. On the other hand, the values obtained in this work were lower than those obtained using a conventional HPLC system connected to a single-quadrupole instrument (Cañabate-Díaz, 2007; Martínez-Vidal, 2007). In any case, a substantial reduction in the analysis time was achieved with the proposed method (between 4- and 10-fold lower than those found in the literature) (Cañabate-Díaz, 2007; Martínez-Vidal, 2007; Segura-Carretero, 2008).

On the other hand, GC methods using FID or MS detection (Cercaci, 2007; Cunha, 2006B; Galeano Díaz, 2005; Parcerisa, 2000; Rivera del Álamo, 2004; Sanchéz-Casas, 2004; Thanh, 2006) showed a superior resolution, especially for some peak pairs as β-sitosterol/Δ^7-stigmastenol and stigmasterol/clerosterol; however, the analysis times were longer (25-30 min) than that found with the proposed method (5 min). In spite of the overlapping of these peak pairs, satisfactory results were achieved in terms of resolution/analysis time ratio. Besides, an additional advantage of the recommended method is that the derivatization step is avoided, which is time-consuming and could be a source of artefacts (Lu, 2007).

Then, the optimized method was applied to the analysis of real samples. All the sterol extracts were injected three times. As the signals of other sterols different from those used as standards were expected in the samples (Cañabate-Díaz, 2007; Lerma-García, 2008; Segura-Carretero, 2008), the *m/z* values corresponding to the $[M+H-H_2O]^+$ ions of these sterols (see **Table 4.15**) were also recorded. As can be deduced from the retention times and *m/z* values of the sterols of **Table 4.15**, by combining chromatographic and spectral information, only 11 sterols or combination of sterol peaks could be distinguished out of a total of 14 expected sterols. These 11 peaks were obtained in less than 5 min.

Table 4.15. Ions observed in the APCI mass spectra of the oil samples with their corresponding retention times (t_R).

Peak no.	Analyte	t_R (min)	Ion $[M+H-H_2O]^+$ (*m/z*)
1	Erythrodiol	1.4	425.5
2	Uvaol	1.4	425.5
3	Ergosterol	2.1	379.5
4	Brassicasterol	2.2	381.5
5	Δ^5-Avenasterol	2.4	395.5
6	Cholesterol	2.7	369.5
7	Campesterol	3.1	383.5
8	Campestanol	3.1	385.5
9	Stigmasterol	3.1	395.5
10	Clerosterol	3.1	395.5
11	$\Delta^{5,24}$-Stigmastadienol	3.3	395.5
12	β-Sitosterol	3.5	397.5
13	Δ^7-Stigmastenol	3.5	397.5
14	Sitostanol	4.5	399.5

The TIC and SIRs of EVOO and hazelnut extracts are shown in **Fig. 4.21** and **Fig. 4.22**, respectively. To quantify the main sterols found in the samples, peak areas were measured from the SIR chromatograms, which were smoothed using a mean algorithm set at window 3 and number 5. On the other hand, the concentrations of those sterols which were not available as standards were estimated as follows: the concentration of the saturated sterols (campestanol and sitostanol) were estimated using the calibration curve of lanosterol, which showed a similar sensitivity to that reported in the literature for compounds of this type (Lu, 2007). Due to the structural resemblance between erythrodiol + uvaol and lanosterol, these solutes were also estimated using the lanosterol calibration curve. The other sterols (brassicasterol, Δ^5-avenasterol and $\Delta^{5,24}$-stigmastadienol) were estimated using the β-sitosterol calibration curve.

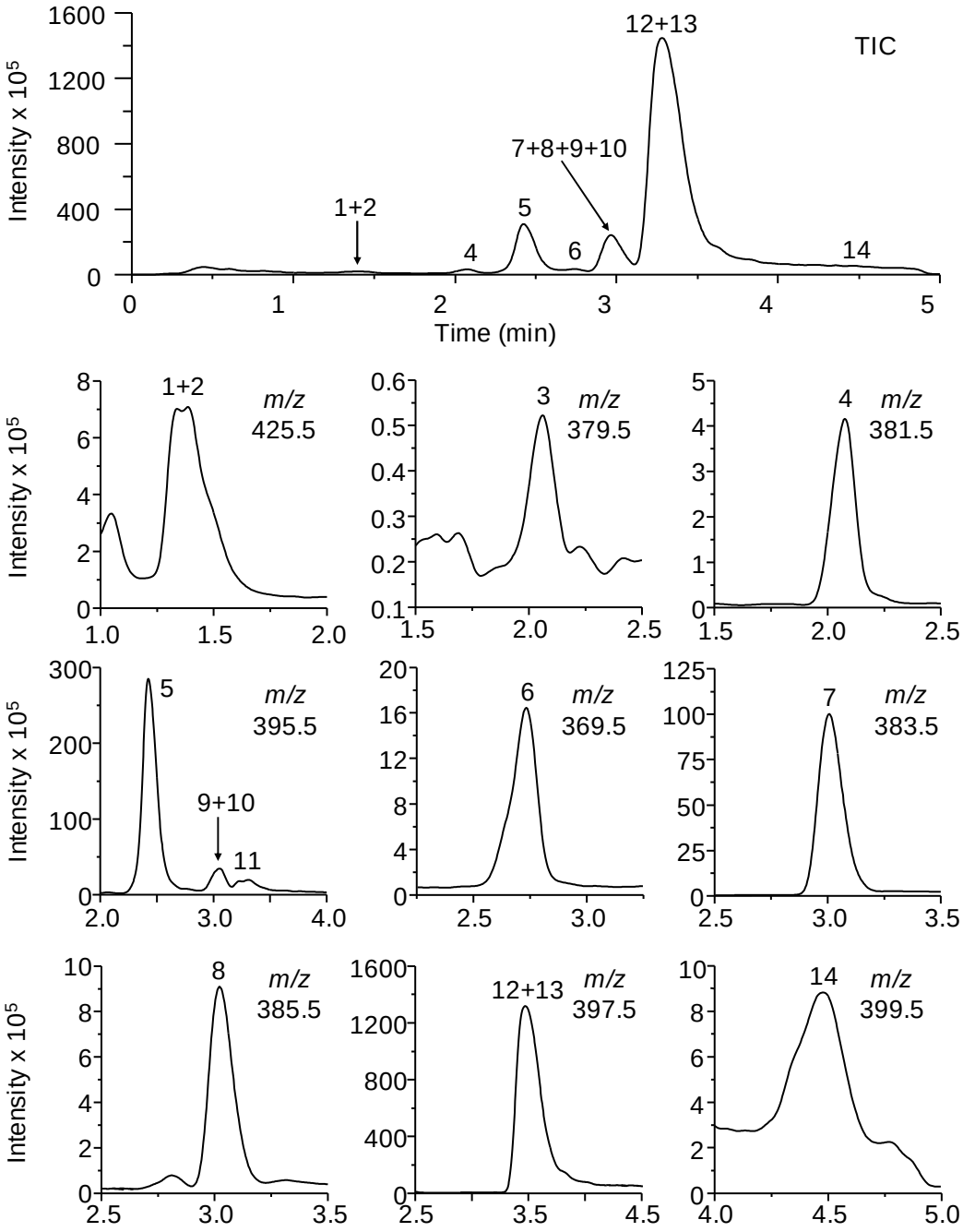

Fig. 4.21. TIC and SIRs of an EVOO extract. Chromatographic conditions: gradient elution as in **Fig. 4.19**; column temperature, 10 ºC; flow rate, 0.8 mL min^{-1}. Peak identification as indicated in **Table 4.14**.

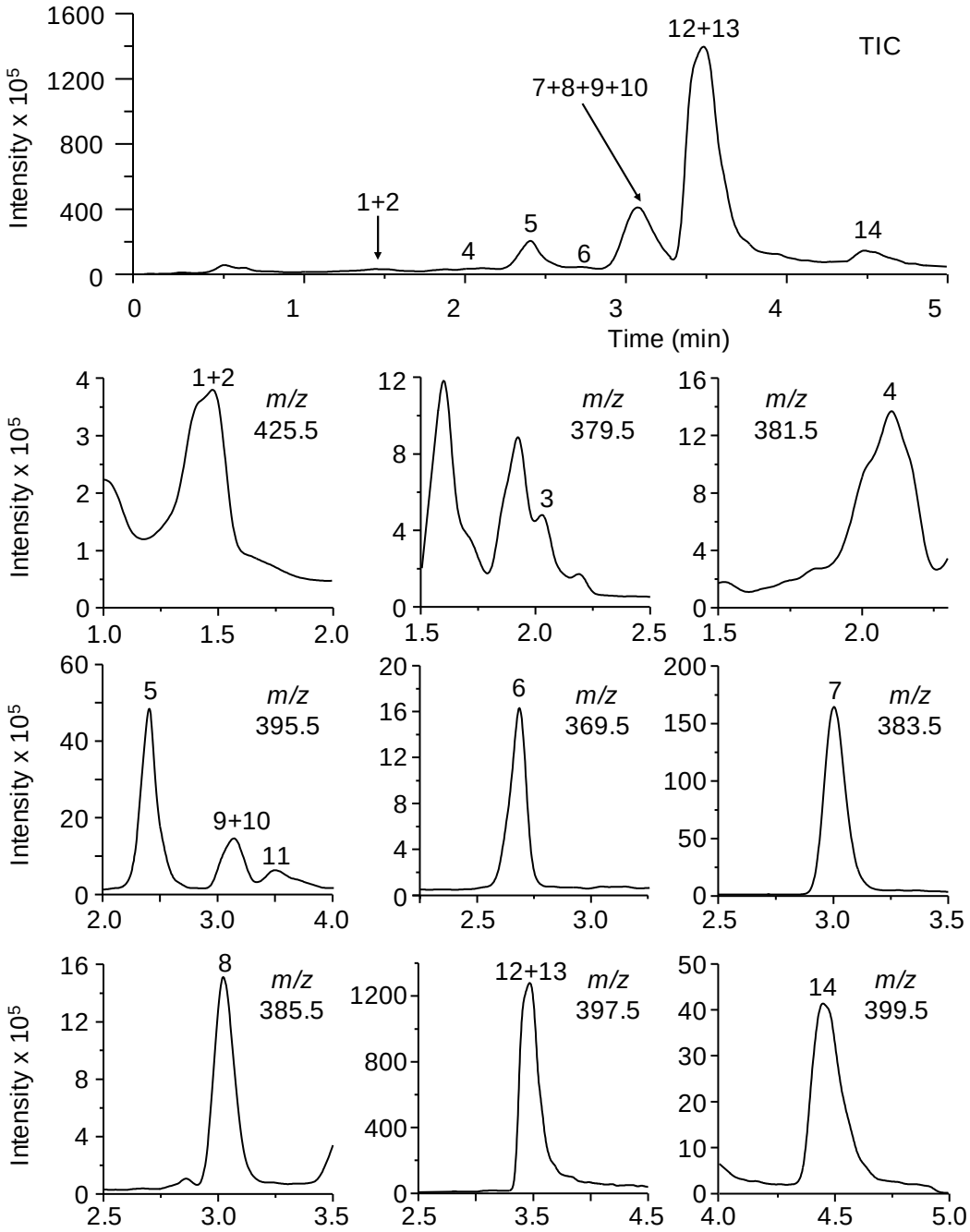

Fig. 4.22. TIC and SIRs of a hazelnut oil extract. Other experimental conditions as in **Fig. 4.21**.

The proportions of sterols found in the vegetable oils analyzed are shown in **Table 4.16**. The range values were obtained from the mean value of three injections of every sample belonging to each category. The levels of sterols found in these samples were in good agreement with data reported in the literature (Abidi, 2004; Cañabate-Díaz, 2007; Jee, 2002; Martínez-Vidal, 2007; Parcerisa, 2000). As observed, β-sitosterol was the main sterol in all the analyzed oils. Soybean oil contained large quantities of campesterol and stigmasterol + clerosterol, whereas corn oil had less amounts of these latter sterols. The contents of these compounds found in EVOO were quite low. Then, the presence of stigmasterol peak could be used as adulteration marker in EVOO. The highest contents of Δ^5-avenasterol were found in avocado followed by EVOO and peanut oils. This sterol was found in much lower amounts in hazelnut than in EVOO; however, sitostanol showed a larger content in hazelnut (see **Fig. 21** and **4.22**). Thus, these peaks could be used to detect the challenging adulteration of EVOO with hazelnut oil. On the other hand, hazelnut and peanut oils showed large ergosterol contents. These high amounts could indicate a fungal activity in the raw material, which also indicates the quality of these oils (Parsia, 2006).

Table 4.16. Proportions of sterols found in total sterol fraction (%).

Sterol	Avocado	Corn	EVOO	Grapeseed	Hazelnut	Peanut	Soybean	Sunflower
Erythrodiol + Uvaol	0.05-0.17	0.27-0.45	0.53-0.90	0.01-0.07	0.16-0.19	0.30-0.35	0.10-0.15	0.25-0.35
Ergosterol	0.01-0.02	0.01-0.02	0.01-0.02	0.00-0.02	0.25-0.34	0.50-0.90	0.01-0.05	0.03-0.05
Brassicasterol	0.25-0.37	0.15-0.18	0.11-0.18	0.10-0.20	0.30-0.40	0.10-0.18	0.28-0.30	0.19-0.23
Δ^5-Avenasterol	17.20-18.15	3.95-5.75	11.00-13.00	2.50-2.80	1.90-2.10	9.18-11.32	3.50-4.00	6.45-9.05
Cholesterol	0.22-0.62	0.31-0.53	0.32-0.47	0.54-0.78	0.30-0.40	0.68-2.10	0.80-0.90	0.78-0.83
Campesterol	4.50-6.30	19.00-19.75	2.74-3.13	12.82-13.14	4.50-5.00	16.47-18.20	17.00-19.00	10.20-10.89
Campestanol	0.31-0.41	0.83-0.91	0.24-0.32	0.58-0.62	0.20-0.23	0.50-0.74	0.60-0.80	0.43-0.53
Stigmasterol + clerosterol	0.44-0.75	6.54-8.08	1.51-3.00	13.94-15.54	0.90-1.00	10.30-11.93	18.40-19.10	8.94-9.37
$\Delta^{5,24}$-Stigmastadienol	ND	0.63-0.70	0.80-0.91	ND	0.95-1.03	0.49-0.51	ND	0.62-0.68
β-Sitosterol + Stigmastenol	72.67-76.54	61.33-66.21	77.69-82.44	64.39-67.27	87.01-88.54	53.27-61.03	54.70-58.61	67.56-71.76
Sitostanol	0.48-0.54	2.10-2.30	0.30-0.38	2.24-2.44	2.00-2.30	0.45-0.50	0.70-1.00	0.35-0.46

ND = Not detected.

CHAPTER 5

DEVELOPMENT OF METHODS FOR THE CLASSIFICATION OF VEGETABLE OILS ACCORDING TO THEIR BOTANICAL ORIGIN

5.1. Classification using FTIR spectroscopy data

The aim of this work was to construct an LDA model able to classify vegetable oils according to their botanical origin using FTIR spectroscopy data. Also, FTIR data treatment by MLR was used to detect and quantify EVOO adulteration with other low cost edible oils. For these purposes, the vegetable oils shown in **Table 5.1** were used. The FTIR spectra of these 30 oil samples were then collected. In all cases, at least two spectra were recorded for each sample. As indicated in this table, four samples of each botanical origin were used for training purposes in the classification studies, being the other two samples of each category reserved in order to evaluate the prediction capability of the classification models.

5.1.1. Data treatment and construction of data matrices

The FTIR spectra were divided in the 26 wavelength regions described in **Table 5.2**. Each spectral region corresponds to a peak or a shoulder, representing structural or functional group information, either about the lipids or minor components of the oil samples; then, the peak/shoulder area of each region was measured. In this study, the normalization procedures A and B, previously described in section 3.7, were used. Then, 26 normalized variables to be used as predictors were obtained by normalization procedure A, whereas 325 predictors were obtained by normalization procedure B. Thus, for classification studies, two matrices containing 20 objects each, which corresponded to the average of the two spectra of each training sample of **Table 5.1**, and either 26 or 325 predictors, according to normalization procedures A and B, respectively, were constructed. A response column, containing the categories corresponding to the five botanical

origins of the oils (corn and corn germ were considered as a single category), was added to the training matrices. The means of the two spectra of each sample instead of the individual spectra were used in order to reduce the internal dispersion of the categories, which was important to also reduce the number of variables selected during model construction.

Table 5.1. Botanical origin, number of samples, brand and use during LDA model construction of the oil samples.

Origin	No. of samples	Brand	LDA set
Hazelnut	2	Guinama	Training
	2	Percheron	Training
	2	Flumen	Evaluation
Sunflower	2	Koipesol	Training
	2	Hacendado	Training
	1	Capicua	Evaluation
	1	Coosol	Evaluation
Corn	1	Guinama	Training
	1	Asua	Training
	1	Artua	Evaluation
	1	Mazola	Evaluation
Corn germ	1	Guinama	Training
	1	Hacendado	Training
EVOO	1	Carbonell	Training
	1	Grupo Hojiblanca	Training
	1	Borges	Training
	1	Torrereal	Training
	1	Coosur	Evaluation
	1	Hacendado	Evaluation
Soybean	2	Guinama	Training
	2	Biolasi	Training
	2	Sojola	Evaluation

Table 5.2. FTIR spectral regions selected as predictor variables for statistical data treatment.

Identification No.	Range, cm^{-1}	Functional group	Nominal frequency	Mode of vibration
1	3029-2989	=C-H (trans)	3025 [a]	stretching
		=C-H (cis)	3006 [a]	stretching
2	2989-2946	-C-H (CH_3)	2953 [a]	stretching (asym)
3	2946-2881	-C-H (CH_2)	2924 [a]	stretching (asym)
4	2881-2782	-C-H (CH_2)	2853 [a]	stretching (sym)
5	1795-1677	-C=O (ester)	1746 [a]	stretching
		-C=O (acid)	1711 [a]	stretching
6	1486-1446	-C-H (CH_2)	1465 [b]	bending (scissoring)
7	1446-1425	-C-H (CH_3)	1450 [b]	bending (asym)
8	1425-1409	=C-H (cis)	1417 [a]	bending (rocking)
9	1409-1396	=C-H	1400 [b]	bending
10	1396-1382	=C-H	- [b]	bending
11	1382-1371	-C-H (CH_3)	1377 [a]	bending (sym)
12	1371-1330	O-H	1359 [b]	bending (in plane)
13	1330-1290	non-assigned	1319 [a]	bending
14	1290-1211	-C-O	1238 [a]	stretching
		$-CH_2-$		bending
15	1211-1147	-C-O	1163 [a]	stretching
		$-CH_2-$		bending
16	1147-1128	-C-O	1138 [b]	stretching
17	1128-1106	-C-O	1118 [a]	stretching
18	1106-1072	-C-O	1097 [a]	stretching
19	1072-1043	-C-O	- [b]	stretching
20	1043-1006	-C-O	1033 [a]	stretching
21	1006-929	-HC=CH- (trans)	968 [a]	bending (out of plane)
22	929-885	-HC=CH- (cis)?	914 [a]	bending (out of plane)
23	885-802	$=CH_2$	850 [b]	wagging
24	802-754	-C-H	- [b]	bending (out of plane)
25	754-701	$-(CH_2)_n-$	723 [a]	rocking
		-HC=CH- (cis)		bending (out of plane)
26	701-640	C⋯C	685 [b]	bending (out of plane)
		O-H	650 [b]	bending (out of plane)

[a] According to Guillén (1998); [b] according to Silverstein (1981).

For evaluation purposes, two more matrices, containing 10 objects each, which corresponded to the average of two spectra of each evaluation sample of **Table 5.1**, and either 26 or 325 predictors, according to normalization procedures A and B, respectively, were constructed.

Fig. 5.1 shows the spectra of five oils, one for each botanical origin, tailored at two absorbance units. As it can be observed, the differences between them were small.

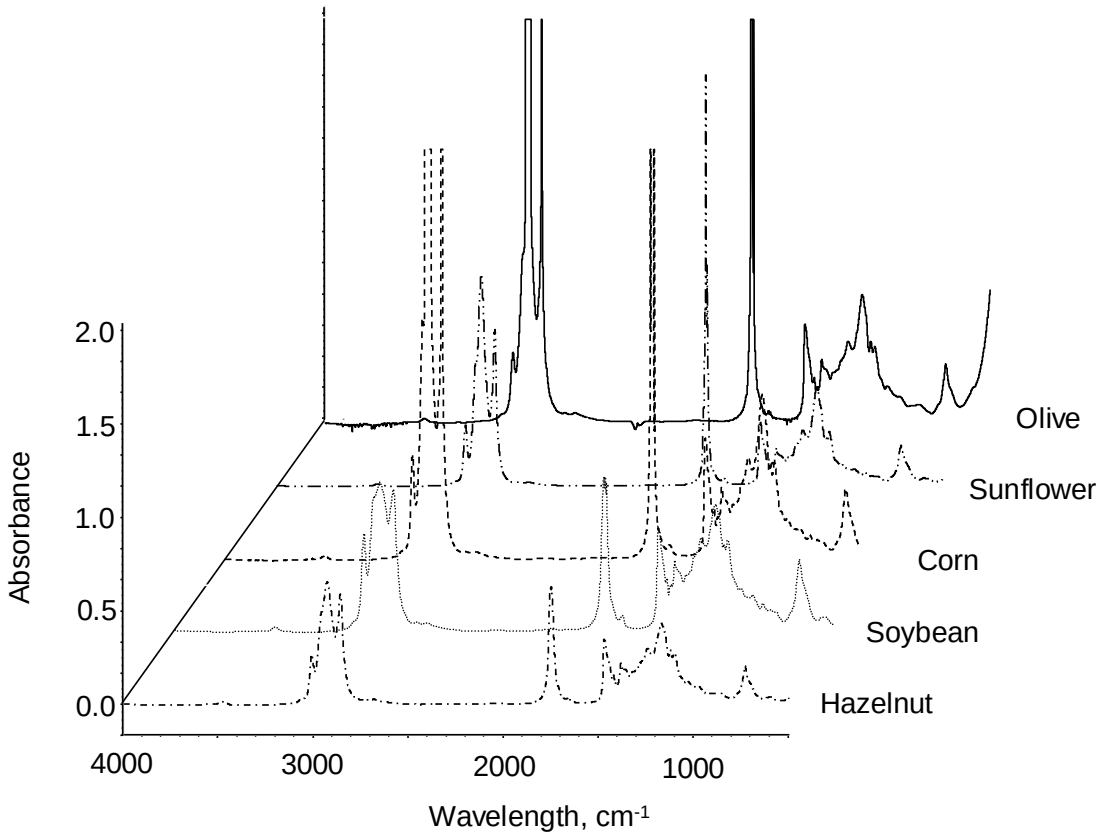

Fig. 5.1. FTIR spectra of representative samples of EVOO, sunflower, corn, soybean and hazelnut oils. Data were tailored at 2 absorbance units to better show the differences among the small peaks.

Interpretation of the absorption bands provides information about the molecular skeleton and functional groups (see **Table 5.2**); however, to obtain information about the botanical origin of the oils, band interpretation is not required. Information related to the origin was obtained by measuring the peak areas at the selected wavelength ranges.

5.1.2. Construction of LDA models

Using these normalized variables, two LDA models, one for each normalization procedure, were constructed. Normalization procedure B, which gave a model with a lower λ_w value and a smaller number of predictors than normalization procedure A, was selected for further studies. As shown in **Fig. 5.2** for normalization procedure B, an excellent resolution between all category pairs was achieved ($\lambda_w = 0.362$).

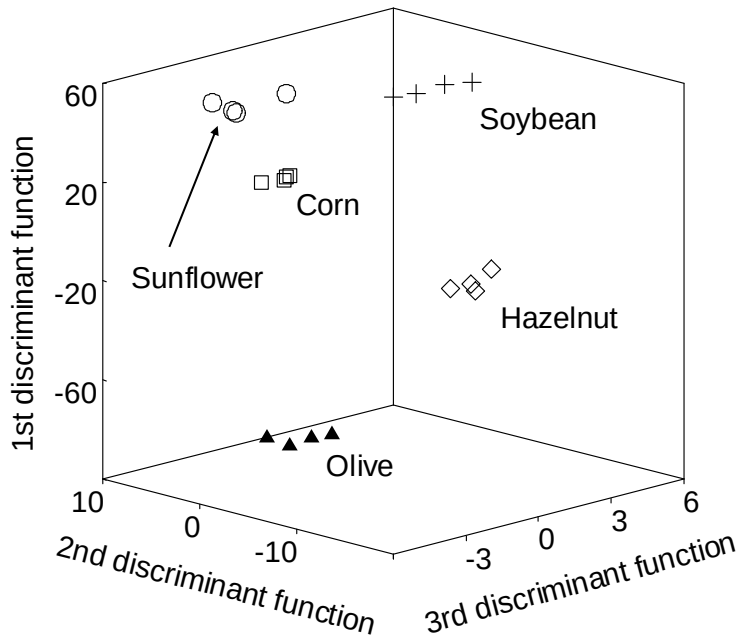

Fig. 5.2. Score plot on an oblique plane of the 3-D space defined by the three first discriminant functions of the LDA model constructed to classify vegetable oils according to their botanical origin.

Taking into account that a large number of categories were simultaneously distinguished, this λ_w value was quite low. The predictors selected by the SPSS stepwise algorithm and the corresponding standardized coefficients of the model, showing the predictors with large discriminant capabilities, are given in **Table 5.3**.

Table 5.3. Predictors selected and corresponding standardized coefficients of the LDA model constructed to predict the botanical origin of vegetable oils.

Predictor[a]	f_1	f_2	f_3	f_4
8/ 9	19.00	8.20	5.14	3.63
10/ 12	0.75	9.37	4.03	0.92
11/ 13	-28.35	5.40	-3.19	-2.13
14/ 17	16.01	-3.49	-1.50	0.65
15/ 17	-6.81	5.74	-1.01	1.68
19/ 25	-13.73	4.33	1.25	0.91
21/ 26	12.51	-3.76	-0.64	-0.95
22/ 24	7.84	-5.13	2.26	-1.36

[a] Pairs of wavelength regions identified according to **Table 5.2**.

According to **Table 5.2**, the main wavelength regions selected by the algorithm to construct the LDA model corresponded to =C-H (bending), O-H (bending in plane), -C-H (CH_3, bending sym), -C-O (stretching), -CH_2- (bending), -HC=CH- (trans, bending out of plane), O-H (bending out of plane) and C$^{\cdots}$C (bending out of plane). When leave-one-out validation was applied, all the objects of the training set were correctly classified. Concerning to the prediction capability of this model, and using a 95% probability, all the objects of the evaluation set were correctly assigned; thus, the prediction capability of the model was 100%.

Finally, an LDA model with all the available objects, including those used above for either training or evaluation, was constructed. The predictors selected by the SPSS stepwise algorithm were basically the same that those selected above, but the λ_w value was smaller (0.202), indicating a satisfactory stability of the model.

5.1.3. Determination of EVOO adulteration by MLR

In order to quantify EVOO adulteration, binary mixtures containing EVOO and increasing percentages of low cost oil (sunflower, corn, soybean or hazelnut) were prepared (**Table 5.1**). To improve robustness of MLR models, the objects of the calibration matrix were prepared using EVOOs and low cost oils from different geographical origins. For instance, for the sunflower-EVOO pair, oils from different geographical origins were selected to prepare a total of seven mixtures containing 0, 5, 10, 30, 50, 75 and 100% sunflower oil. Sets of mixtures containing the same percentages of low cost oil were also prepared for the corn-, soybean- and hazelnut-EVOO pairs. Then, using these mixtures, two calibration matrices for each oil pair were constructed. These matrices contained seven objects each, which corresponded to the averages of the duplicated spectra of the mixtures, and 26 or 325 predictors according to normalization procedures A and B, respectively. A response column, containing the low cost oil percentages of the mixtures, was added to these matrices.

On the other hand, additional mixtures of the sunflower-, corn-, soybean- and hazelnut-EVOO pairs, also using oils from different geographical origins, and containing 5, 50 and 80% low cost oil, were prepared. Using these additional mixtures, two validation matrices of the prediction performance, according to normalization procedure A and B, were constructed for each binary oil pair. These matrices contained 3 objects each, which corresponded to the averages of

triplicate spectra of the additional mixtures, and 26 or 325 predictors.

Thus, MLR models, one for each binary combination of oils, and in each case according to normalization procedures A and B, were constructed. Normalization procedure B, which gave models with higher *r* values than normalization procedure A, was selected. A plot showing the predicted versus the nominal oil percentages for all the binary mixtures is shown in **Fig. 5.3**. The predictors selected and their corresponding non-standardized model coefficients are given in **Table 5.4**. It is interesting to observe that, except in the case of the corn-EVOO mixtures, a single predictor was selected to predict the composition of the other three binary mixtures.

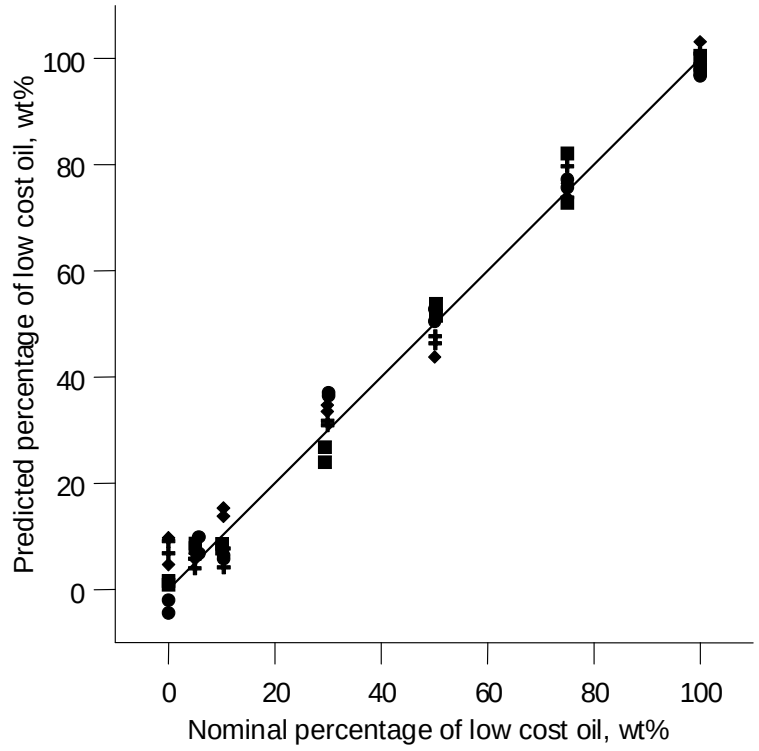

Fig. 5.3. Predicted (MLR) versus nominal oil percentages for binary mixtures of EVOO with sunflower (●), corn (■), soybean (+) and hazelnut (♦) oils. The straight-line is y = x.

Table 5.4. Predictors selected and their corresponding non-standarized model coefficients (coef.), *r* values, average prediction errors (av. pred. error) and LODs obtained for the MLR models constructed to predict EVOO adulteration.

Binary mixture	Predictor	Coef.	*r*	Av. pred. error, %	LOD, %
Hazelnut-EVOO	1/ 15	-1080	0.955	2.0	4.8
	Constant	348			
Sunflower-EVOO	23/ 26	325	0.992	1.7	4.0
	Constant	-270			
Corn-EVOO	1/ 17	-353	0.997	1.5	1.3
	1/ 16	221			
	Constant	309			
Soybean-EVOO	13/ 25	324	0.990	1.9	1.7
	Constant	-228			

According to **Table 5.2**, the main wavelength transitions selected to construct the MLR model for the sunflower-EVOO pair were $=CH_2$ (wagging), O-H (bending out of plane) and C⋯⋯C (bending out of plane). Analogously, for the hazelnut-EVOO pair, the selected transitions were =C-H (trans and cis, stretching), -C-O (stretching) and $-CH_2-$ (bending). Those selected for the soybean-EVOO pair were $-(CH_2)_n-$ (rocking) and -HC=CH- (cis, bending out of plane), and those selected for the corn-EVOO pair were -C-O (stretching) and =C-H (trans and cis, stretching). For all binary combinations of oils, a transition implying a double bond was selected, which suggest that unsaturated fatty acids were important in the quantification of the mixtures. The *r* values, average prediction errors (calculated as the sum of the absolute differences between expected and predicted oil percentages divided by the number of predictions) and the LODs (calculated as 3 times the standard deviation at 5% low cost oil level) are also given in **Table 5.15**. For all the MLR models and using leave-one-out validation, the average prediction errors were lower than 2%. The 4 sets of validation mixtures, one for each binary combination of oils (4 x 3 = 12

mixtures), gave average prediction errors below 5%. LODs were in all cases below 5%, being lower than those previously reported in literature for binary mixtures of the same oils, namely 4% versus 6% (Vlachos, 2006) for sunflower-EVOO, 1.3% versus 9% (Vlachos, 2006) for corn-EVOO, 1.7% versus 6% (Vlachos, 2006) for soybean-EVOO and 4.8% versus 25% (Ozen, 2002) and versus 8% (Baeten, 2005) for hazelnut-EVOO mixtures.

5.2. Classification using sterol profiles established by direct infusion MS

The aim of this work was to develop a simple and quick method for oil classification according to its botanical origin, based on direct infusion of sterol extracts in a mass spectrometer. The vegetable oils employed in this work are shown in **Table 5.5**.

To optimize the MS working conditions, the following sterol standards (β-sitosterol, campesterol, ergosterol, stigmasterol and cholesterol) were used. With both ESI and APPI, peaks at two *m/z* values, corresponding to $[M+H]^+$ and $[M+H-H_2O]^+$ ions, were observed. For all the standards, except to ergosterol with APPI, the $[M+H-H_2O]^+$ peaks showed higher intensities than the respective $[M+H]^+$ peaks. For this reason, the intensities of the $[M+H-H_2O]^+$ peaks were used as the optimization criteria for the working conditions. Under the optimal conditions (see section 3.5.5) and with both ion sources, different standards showed different relationships between the abundances of the corresponding $[M+H]^+$ and $[M+H-H_2O]^+$ peaks. Thus, sterols could be distinguished not only by the different *m/z* values, but also by the different intensity ratios of the $[M+H]^+$ and $[M+H-H_2O]^+$ peaks. Thus, the MS spectra provided information related to the concentrations of all sterols present in the samples, including those having peaks at the same *m/z* values. Since vegetable oils with a different botanical

origin also showed different sterol profiles, the profiles contained the necessary information to predict the origin.

Table 5.5. Botanical origin, number of samples and brand of the vegetable oil samples used in this work.

Origin	No. of samples	Brand
Hazelnut	4	Guinama
Sunflower	2	Koipesol
	2	Hacendado
Corn	2	Guinama
Corn germ	1	Guinama
	1	Hacendado
Olive	1	Carbonell
	1	Grupo Hojiblanca
	1	Borges
	1	Torrereal
Soybean	2	Guinama
	2	Biolasi
Avocado	4	Guinama
Peanut	4	Guinama
Grapeseed	4	Guinama

5.2.1. Selection and normalization of the variables

The spectra obtained with both the ESI and APPI sources showed peaks at the same *m/z* values, which corresponded to the $[M+H]^+$ and the $[M+H-H_2O]^+$ ions of the sterols indicated in **Table 5.6**. From the 42 sterol peaks expected, two for each individual sterol, only 16 peaks were observed in the mass spectra. This low number of peaks was due to the fact that several sterols provided the same *m/z* values. For this reason, only 16 peaks were obtained to be used as variables.

Table 5.6. Molecular mass (most abundant isotopes) and *m/z* values of the $[M+H]^+$ and $[M+H-H_2O]^+$ peaks of the sterols employed in this study.

Sterol	M, Da	$[M+H]^+$	$[M+H-H_2O]^+$	Group
Cholesterol	386.7	387.7	369.7	1
Ergosterol	396.7	397.7	378.7	2
Brassicasterol	398.7	399.7	381.7	3
24-Methylene cholesterol	398.7	399.7	381.7	3
Δ^7-Campesterol	398.7	399.7	381.7	3
Campesterol	400.7	401.7	383.7	4
Campestanol	402.7	403.7	385.7	5
Clerosterol	412.7	413.7	395.7	6
Stigmasterol	412.7	413.7	395.7	6
Δ^7-Avenasterol	412.7	413.7	395.7	6
Δ^5-Avenasterol	412.7	413.7	395.7	6
$\Delta^{5,24}$-Stigmastadienol	412.7	413.7	395.7	6
$\Delta^{7,25}$-Stigmastadienol	412.7	413.7	395.7	6
Fucosterol	412.7	413.7	395.7	6
Isofucosterol	412.7	413.7	395.7	6
Δ^5-Avenastenol	414.7	415.7	397.7	2
Δ^7-Stigmastenol	414.7	415.7	397.7	2
β-Sitosterol	414.7	415.7	397.7	2
Sitostanol	416.7	417.7	399.7	3
Erythrodiol	442.7	443.7	425.7	7
Uvaol	442.7	443.7	425.7	7

[a] Each group is formed by the sterols having peaks with the same *m/z* values.

As it can be observed in **Fig. 5.4** for a soybean oil sample, the $[M+H]^+$ and the $[M+H-H_2O]^+$ peaks obtained with the APPI source showed higher intensities than those provided by the ESI source.

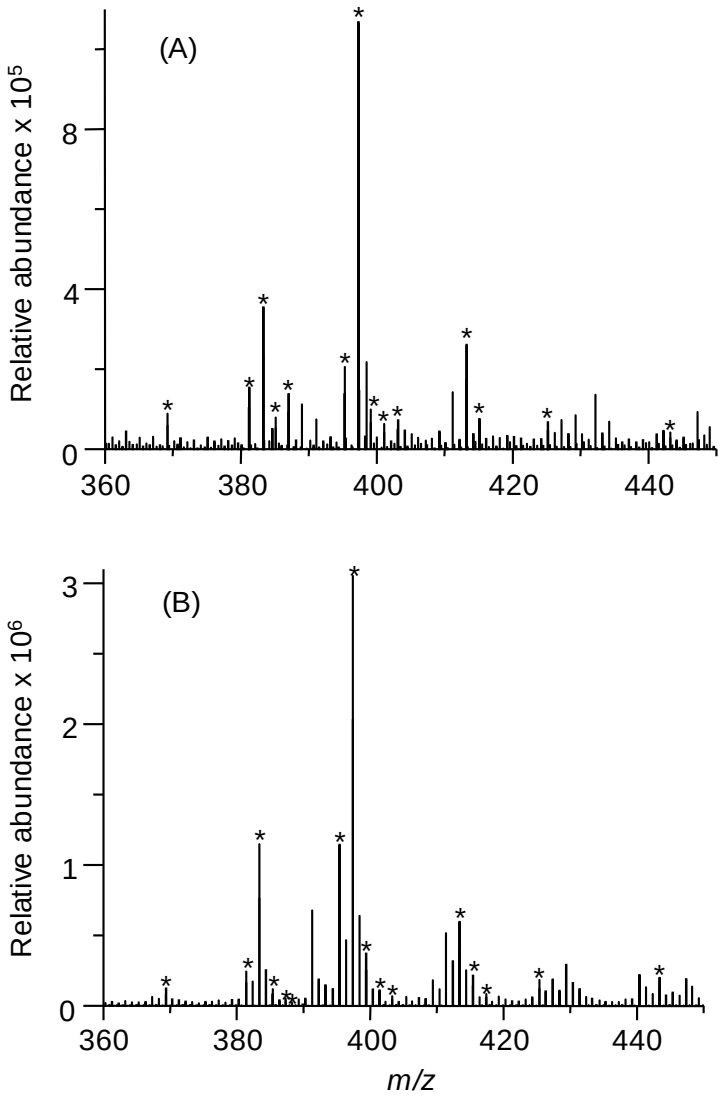

Fig. 5.4. Direct infusion MS spectra of a sterol extract of a soybean oil obtained with the ESI (A) and APPI (B) ion sources. The *m/z* peaks, which correspond to the sterols of **Table 5.6**, are indicated by an asterisk.

In this study, normalized variables obtained by normalization procedure B were used. When this procedure was applied, (16 x 15)/2 = 120 non-redundant peak ratios were obtained.

The same samples employed in MS analysis were also analyzed by the GC-FID official method (Commission Regulation (EEC) No. 2568/91, annex V). A typical gas chromatogram is shown in **Fig. 5.5**.

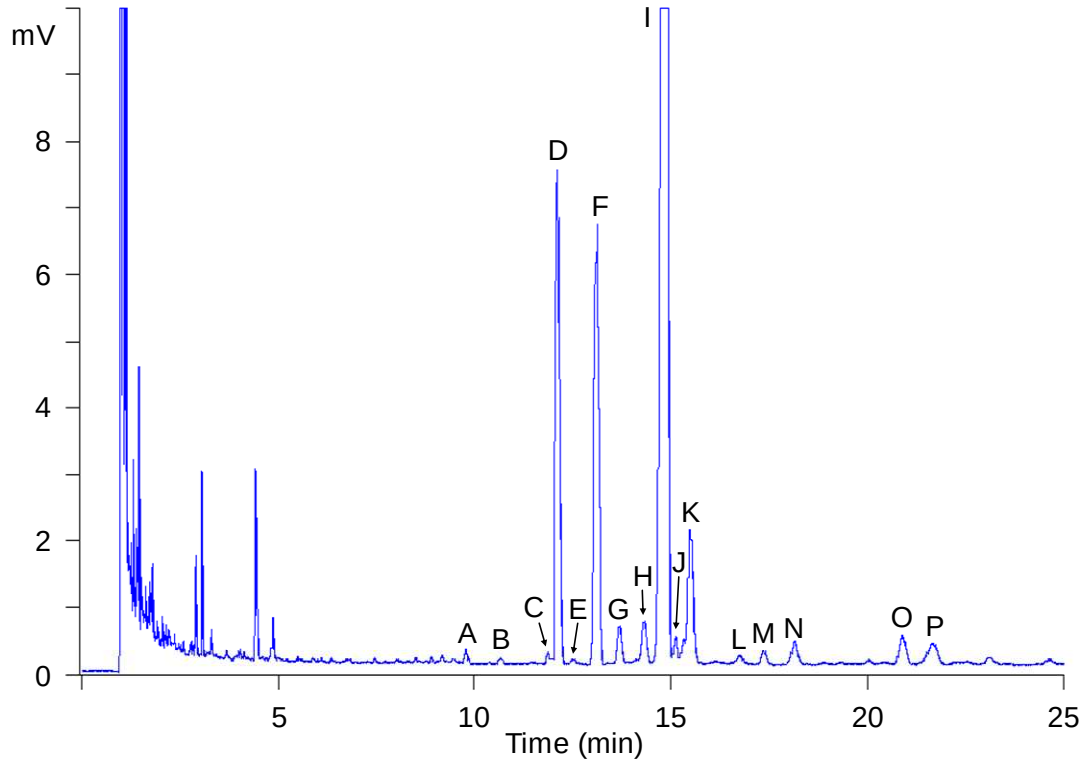

Fig. 5.5. Typical FID gas chromatogram of a sterol extract of a soybean oil. Peak identification: Cholesterol (A), brassicasterol (B), 24-methylene cholesterol (C), campesterol (D), campestanol (E), stigmasterol (F), Δ^7-campesterol (G), clerosterol (H), β-sitosterol (I), sitostanol (J), Δ^5-avenasterol (K), $\Delta^{5,24}$-stigmastadienol (L), Δ^7-stigmastenol (M), Δ^7-avenasterol (N), erythrodiol (O) and uvaol (P). β-Sitosterol peak was tailored to better appreciate small peaks.

The possible correlation between the relative intensities of the MS peaks and the areas of the GC peaks was studied. Owing to the coincidence of the *m/z* values of the peaks of several sterols, a correlation study by using the MS peak intensities and GC peaks areas of individual sterols was not possible. Instead of this, the sterols were arranged into the seven groups that are indicated in **Table 5.6**. Each group was formed by the sterols having peaks with the same *m/z* values. First, for each mass spectrum, the sum of the MS peak intensities of each group was divided by the sum of the peak intensities of all the sterols. Second, for each gas chromatogram, the sum of the areas of the GC peaks of each group

was divided by the sum of the peak areas of all the sterols. The MS and GC data processed in this way for each group of sterols, and for a representative soybean oil sample, were plotted in **Fig. 5.6**.

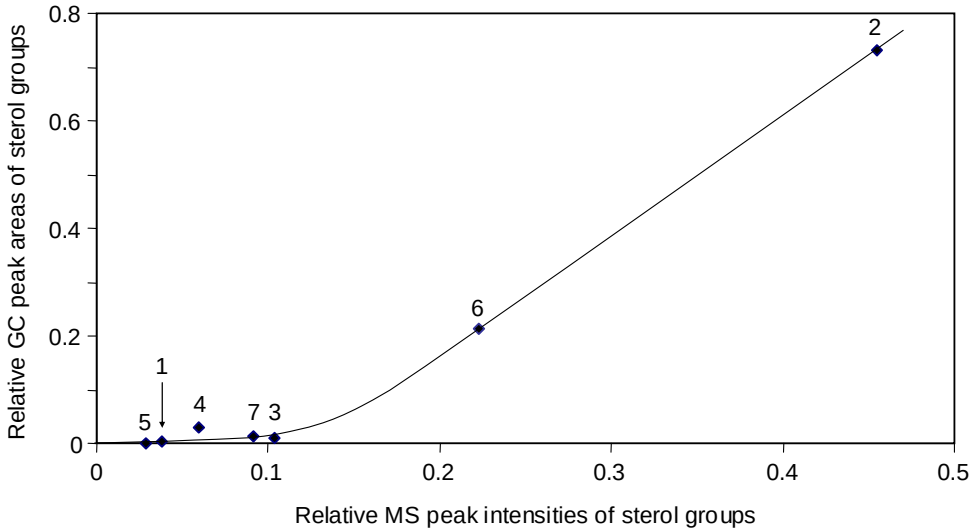

Fig. 5.6. Relative GC peak areas plotted against the relative MS peak intensities of the seven sterol groups indicated in **Table 5.6**.

As shown in this figure, the MS peak intensities and GC peak areas were non-linearly correlated. Non-linearity is probably a consequence of the different response factors of the sterols in both MS and GC; however, **Fig. 5.6** clearly shows that sterols having higher concentration in samples give both large MS peak intensities and large GC peak areas. Similar plots were obtained with the other oil samples.

5.2.2. Construction of data matrices and LDA models

Using the 120 normalized variables, LDA models capable of classifying the oil samples according to their botanical origin were constructed. Since each sterol extract was injected at least four times with each ion source, two matrices,

one for ESI and another for APPI data, containing 128 injections and 120 predictors each, were constructed. A response column, containing the eight categories corresponding to the eight botanical origins of the oils (corn and corn germ were considered as a single category), was added to each matrix. These matrices were used as evaluation sets. To construct LDA training matrices, only the means of the replicates of the samples were included. In this way, the internal dispersion of the categories was reduced, which was important to reduce the number of variables selected by the SPSS stepwise algorithm during model construction.

To classify the oils according to the eight botanical origins, two LDA models, one for each MS ion source data (ESI and APPI), were constructed. With the spectral data obtained with ESI-MS, an excellent resolution between the eight categories was achieved (**Fig. 5.7**, $\lambda_w = 0.294$). Taking into account that a large number of categories were simultaneously distinguished, this λ_w value was quite low.

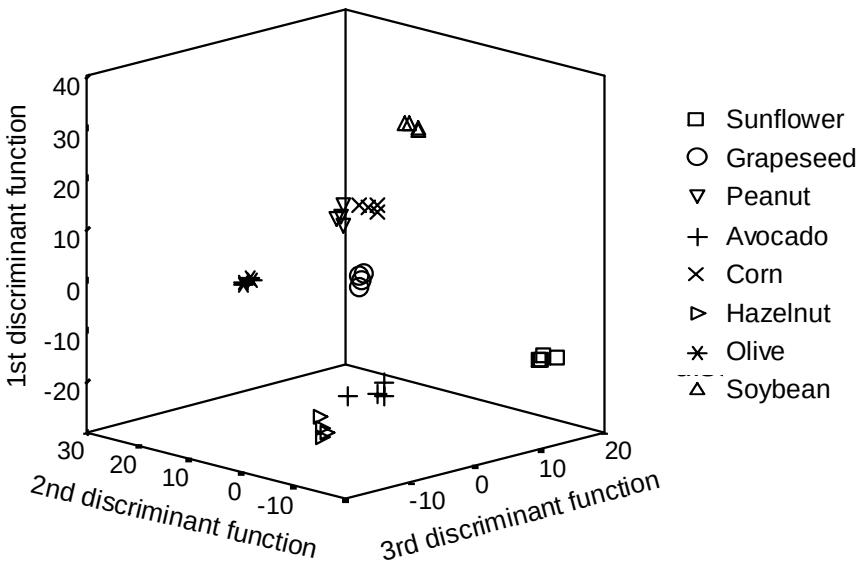

Fig. 5.7. Score plot on an oblique plane of the 3-D space defined by the three first discriminant functions of the LDA model constructed with the ESI-MS data.

The variables selected by the SPSS stepwise algorithm, and the corresponding standardized coefficients of the model, are given in **Table 5.7**.

Table 5.7. Predictors selected and corresponding standardized coefficients of the LDA model constructed to predict the botanical origin of vegetable oils infused in ESI-MS.

Predictors[a]	f_1	f_2	f_3	f_4	f_5	f_6	f_7
395.7/385.7	3.0	6.9	4.8	-1.5	0.9	-0.5	-0.2
395.7/387.7	0.5	-8.2	-1.0	0.8	1.1	1.7	0.5
399.7/397.7	9.4	2.8	3.3	-2.7	3.4	-0.2	0.8
401.7/383.7	4.6	4.4	1.5	1.3	0.8	-0.9	2.3
403.7/397.7	-16.6	-11.5	-5.5	4.6	-1.7	0.1	-4.3
403.7/399.7	14.6	13.3	9.0	-3.9	1.4	1.4	7.0
413.7/369.7	-1.8	-2.4	-0.8	-0.1	2.2	0.3	-0.3
415.7/397.7	-4.5	8.1	2.1	0.7	-4.1	-0.1	2.0
415.7/403.7	2.7	-5.8	1.2	0.3	0.8	0.4	-0.4
417.7/369.7	-1.6	-1.2	-1.1	-0.1	-2.1	0.7	-0.2
425.7/403.7	0.3	3.7	0.9	0.4	0.1	-1.5	0.6
443.7/399.7	-2.1	-5.8	-3.5	0.1	1.9	0.1	-4.7
443.7/403.7	0.6	5.1	2.2	1.2	-0.8	0.8	2.4

[a] Identified by the *m/z* values of the peak pairs.

Along the first discriminant function, f_1, an extremely large separation of the avocado category with respect to all the other categories was observed. As deduced from **Table 5.7**, this function was mainly constructed with the peak intensity ratios taken at *m/z* 403.7/397.7 and 403.7/399.7. As indicated in **Table 5.6**, the *m/z* 403.7 peak belongs to campestanol, and each one of the other two peaks can be due to several sterols. The remaining oil categories were resolved along the second and third discriminant functions, f_2 and f_3.

With the spectral data obtained with APPI-MS, another LDA model was constructed. The eight categories were also very well resolved, being the λ_w value similar to that obtained with the ESI-MS data (**Fig. 5.8**, $\lambda_w = 0.383$).

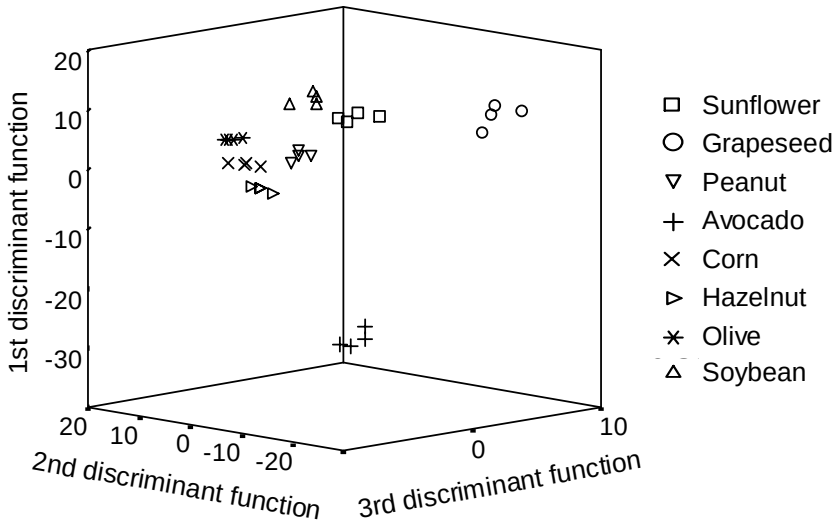

Fig. 5.8. Score plot on an oblique plane of the 3-D space defined by the three first discriminant functions of the LDA model constructed with the APPI-MS data.

The variables selected and the corresponding standardized coefficients of the model are given in **Table 5.8**. Along the first discriminant function, f_1, with the exception of the corn – peanut pair, a remarkable resolution of all the category pairs was produced. This function was mainly constructed with the peak intensity ratios taken at *m/z* 397.7/383.7, 413.7/397.7 and 415.7/383.7. As indicated in **Table 5.6**, the *m/z* 383.7 peak belongs to campesterol, each one of the other *m/z* values corresponding to other sterols. Also, along the f_2 and f_3 (constructed mainly by campestanol) the corn – peanut pair appears overlapped, being the rest of categories well resolved. The corn – peanut pair was resolved along f_4. For the two models constructed with both the ESI- and the APPI-MS data, and using leave-one-out cross-validation, all the points of the respective training sets were correctly classified. The corresponding evaluation sets,

containing 128 original data points each, were used to check the prediction capability of the models. Using a 95% probability, all the objects were correctly assigned; thus, the prediction capability of both models was 100%.

Table 5.8. Predictors selected and corresponding standardized coefficients of the LDA model constructed to predict the botanical origin of vegetable oils injected in APPI-MS.

Predictors[a]	f_1	f_2	f_3	f_4	f_5	f_6	f_7
385.7/383.7	-10.6	1.9	3.6	0.7	-1.2	-0.1	-2.1
397.7/383.7	24.7	15.4	8.0	2.4	5.8	0.8	3.0
401.7/381.7	-9.0	4.7	-4.9	0.2	1.8	2.6	-0.9
413.7/397.7	22.5	4.1	12.9	1.8	4.4	-0.9	2.4
415.7/383.7	-23.6	-12.5	-12.4	-3.1	-1.8	3.3	-1.3
415.7/413.7	16.3	8.5	6.0	0.9	2.0	-2.3	2.3
425.7/369.7	-6.6	-0.8	-2.6	8.7	-0.5	1.7	3.8
425.7/381.7	2.3	-6.9	-4.0	4.1	-4.7	-9.1	1.2
425.7/383.7	10.5	7.5	13.0	-15.0	6.5	9.3	-8.1
425.7/397.7	-15.5	-5.4	-12.9	0.2	0.3	3.2	0.6
443.7/383.7	2.4	2.5	0.7	8.7	-1.7	-8.9	9.6
443.7/399.7	14.5	0.3	3.0	-0.5	-3.2	1.0	-4.0
443.7/401.7	-3.5	2.4	-1.6	-5.2	4.7	2.8	-1.2
443.7/403.7	-1.8	-1.3	0.6	2.0	-0.8	-1.2	-1.6

[a] Identified by the *m/z* values of the peak pairs.

5.3. Classification using alcoholic fraction profiles established by HPLC-MS

The aim of this work was to develop an RP-HPLC method, using both UV-Vis and MS, to characterize the alcoholic fraction extracted from oils with different botanical origins. Previous to HPLC separation, the alcoholic fraction was esterified with diphenic anhydride. Also, LDA models were applied to the

resulting alcohol data profiles obtained by HPLC-MS to classify oils from seven different botanical origins (see **Table 5.9**).

Table 5.9. Botanical origin, number of samples and brand of the vegetable oil samples used in this work.

Origin	No. of samples	Brand
Hazelnut	4	Guinama
Sunflower	2	Koipesol
	2	Hacendado
Corn	2	Guinama
Corn germ	1	Guinama
	1	Hacendado
EVOO	1	Carbonell
	1	Grupo Hojiblanca
	1	Borges
	1	Torrereal
Soybean	2	Guinama
	2	Biolasi
Peanut	4	Guinama
Grapeseed	4	Guinama

5.3.1. Optimization of the esterification procedure

Due to the low absorbance of alcohols in the UV, and due to the fact that fatty alcohols have been not previously detected in MS (Micó-Tormos, 2008A and 2008B), the alcoholic fraction obtained was derivatized with diphenic anhydride, as explained in section 3.3.2. The resulting hemiester (see **Fig. 3.2**) provides not only a chromophore group with a large molar absorptivity, but also a negative charge, which further enhances MS detection. Derivatization of the standards of linear alcohols was performed with a large excess of diphenic anhydride. Owing to the low solubilities of long-chain aliphatic alcohols and triterpenic alcohols in most organic solvents, THF was selected as a reaction

medium. Since the boiling point of THF was quite low (66 ºC), the thermostatic bath temperature was set at 60 ºC; 4 mL portions of a solution containing 10 mg of each alcohol standard were derivatized. Derivatization was performed with and without the presence of finely grinded urea. The peaks of the derivatives increased at least two times when urea was present. Enhancements of the reaction rates and yields have been also reported for the derivatization of fatty alcohols and ethoxylated fatty alcohols with maleic and phthalic anhydrides (Micó-Tormos, 2008A and 2008B). The addition of 0.25 g urea was found to be adequate.

On the other hand, the reaction time and yield were optimized by derivatizing a mixture of the alcohol standards (10 mg each). A series of 8 screw-cap tubes were prepared. From these, a tube was removed from the thermostatic bath every 15 min, diluted, filtered and an aliquot was injected. Isocratic elution with ACN/water 90:10 (v/v) containing 0.1% acetic acid was used. The reaction yield increased when the reaction time increased, and a plateau was reached at 100 min. To assure a maximal reaction yield, 120 min was selected. Using isocratic elution, a linear dependence of log *k* with the number of carbon atoms in the alkyl chain of the alcohols was observed, being the retention time comprised between 6.7 and 56.5 min for C16 and C26, respectively.

5.3.2. Optimization of the separation conditions

Since standards of most aliphatic and triterpene alcohols are either unavailable or have a high-cost, the optimization of the HPLC separation was performed using an extract of EVOO. Under isocratic elution conditions (90:10 ACN/water), straight identification of the peaks of the C24 and C26 alcohols was performed; however, many other peaks were also observed. In order to identify these peaks, MS detection was coupled in series to the HPLC-UV-Vis system.

Using the EICs at the *m/z* values of **Table 5.10**, peaks corresponding to several triterpene alcohols, phytol and 4-methylsterols were identified in the 9-25 min range. Peaks corresponding to linear alcohols having retention times higher than 90 min were also observed. In order to speed up the elution of the heavier alcohols, gradient elution was implemented. Elution was performed first isocratically with 90% ACN for 25 min, followed by a linear gradient from 90 to 100% ACN for 10 min, and by isocratic elution with 100% ACN for 10 more min. The TIC and EICs of an EVOO and sunflower oil extracts are shown in **Figs. 5.9** and **5.10**, respectively. Using the information provided by MS detection, peaks on the chromatograms obtained with UV-Vis detection were also identified. A UV-Vis chromatogram of the EVOO sample (whose mass spectrum is given in **Fig. 5.9**) is shown in **Fig. 5.11**. Then, the derivatized extracts of all the other vegetable oils were also injected in the optimized conditions. Several differences between the peak profiles obtained with oils having different botanical origins were evidenced (see **Figs. 5.9** and **5.10**).

Table 5.10. Type, peak labelling, *m/z* value and possible identification of the alcohols studied in this work.

Type	Peak labelling	*m/z*[a]	Possible compound
Linear alcohols	1	493	1-Octadecanol (C18)
	2a	521	1-Eicosanol (C20)
	3	549	1-Docosanol (C22)
	4	563	1-Tricosanol (C23)
	5	577	1-Tetracosanol (C24)
	6	591	1-Pentacosanol (C25)
	7	605	1-Hexacosanol (C26)
	8	619	1-Heptacosanol (C27)
	9	633	1-Octacosanol (C28)
	10	647	1-Nonacosanol (C29)
	11	661	Tricontanol (C30)
4-Methylsterols	12	513	Geranylgeraniol
	13a-13d	649	Obtusifoliol, cycloeucalenol, citrostadienol
Diterpene alcohol	14	519	Phytol
Triterpene alcohols	13a-13d	649	Cycloartenol, α-amyrin, β-amyrin, taraxerol, dammaradienol, lupeol butyrospermol, parkeol
	15	651	Cycloartanol, lanostenol
	16	661	24-Methylenecycloartanol
	17	663	24-Methylenelanost-9(11)-enol, cyclolaudenol, cyclobranol
Unknown	2b-2c	521	Unknown

[a] *m/z* value corresponding to the $[M-H]^-$ peak of the hemiester of the alcohol.

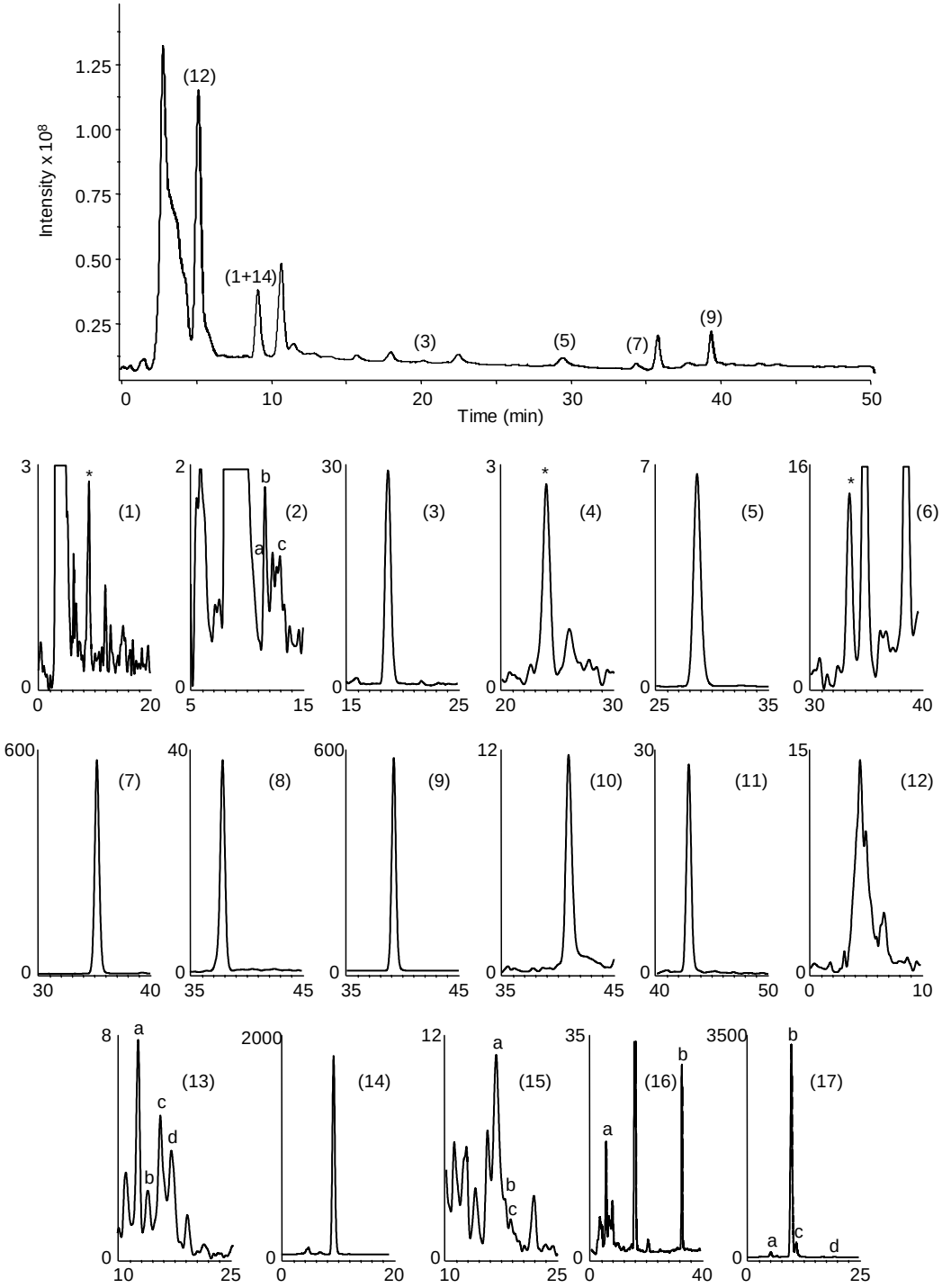

Fig. 5.9. TIC and EICs of an EVOO extract. EIC intensity scales are multiplied by 10^4. Between parenthesis, peak labelling according to **Table 5.10**. The EICs were obtained at the *m/z* values also indicated in **Table 5.10**; when the EIC contains more than one peak, the peak used for data analysis is indicated with an asterisk or with low case characters. Mobile phase: 90% ACN for 20 min, followed by a linear gradient up to 100% ACN for 10 min and 100% ACN for 20 more min.

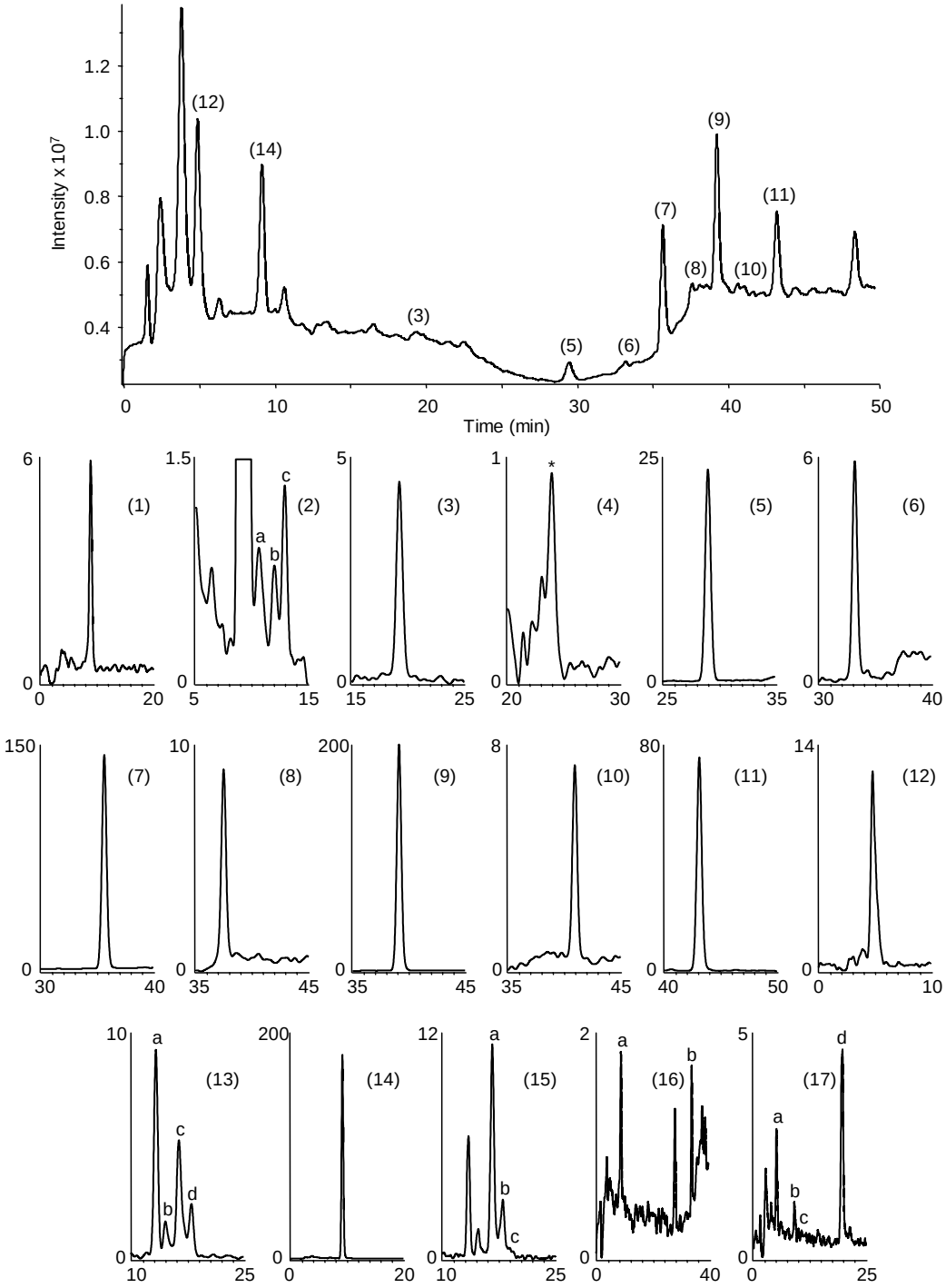

Fig. 5.10. TIC and EICs of a sunflower oil extract. Other details as in **Fig. 5.9**.

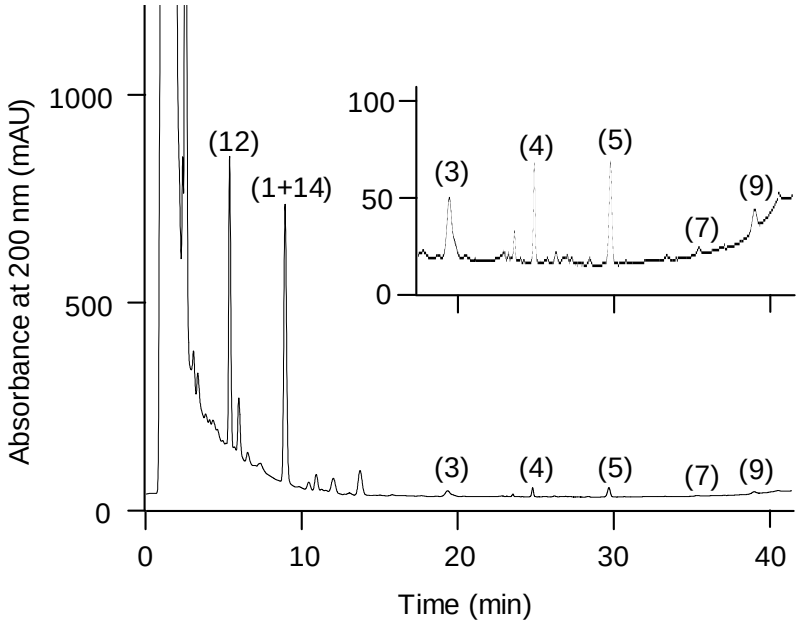

Fig. 5.11. UV-Vis chromatogram of an extract of the same sample of EVOO as in **Fig. 5.9**. Other details as in **Fig. 5.9**.

5.3.3. Construction of data matrices and LDA models

In this work, the original variables (which corresponded to the peak area of each alcohol derivative measured from its corresponding EIC, previously smoothed using a filter set at 9 points) were normalized by procedure B, in which the area of each peak taken from the corresponding EIC was divided by each one of the areas of the other 27 peaks (also taken from their EICs).

Then, using the 378 normalized variables, LDA models capable of classifying the oil samples according to their respective botanical origins were constructed. First, using the 28 samples of **Table 5.9**, matrices containing 84 injections each (all samples were injected three times), were constructed. Oil classification models were constructed by using the peak ratios provided by either linear fatty alcohols, 4-methylsterols plus triterpene alcohols and phytol, or all alcohol peaks at a time. For this purpose, three matrices containing either 55, 136 or 378 predictors, respectively, were constructed. A response column, containing the seven categories corresponding to the seven botanical origins of

the oils (corn and corn germ were considered as a single category), was added to each matrix. These matrices were used as evaluation sets. To construct LDA training matrices, only the means of the replicates of the samples were included (28 objects in each matrix). In this way, and as indicated above, the internal dispersion of the categories was reduced, which was important to reduce the number of variables selected by the SPSS stepwise algorithm during model construction (in this case, the F_{in} and F_{out} values of 3.84 and 2.71, respectively, were adopted).

First, an LDA model was constructed exclusively using the normalized peak areas of the linear alcohols as predictors. A poor resolution between the category pairs ($\lambda_w = 0.708$) was obtained; further, 4 objects of the evaluation set were not correctly assigned. Then, another LDA model was constructed using the normalized peaks of 4-methylsterols, triterpene alcohols and phytol as predictors. With this model, resolution between the category pairs improved largely ($\lambda_w = 0.327$). Finally, another LDA model was constructed using all the available predictors. In this case, an excellent resolution between all the category pairs was achieved (**Fig. 5.12**, $\lambda_w = 0.163$). The variables selected by the SPSS stepwise algorithm, and the corresponding standardized coefficients of this model, are given in **Table 5.11**. As shown in **Fig. 5.12A**, an extremely large resolution among the three following groups of categories was achieved along f_1: corn-hazelnut-grapeseed, olive and soybean-peanut-sunflower. As deduced from **Table 5.11**, f_1 was mainly constructed with the peak area ratios 649d/651b and 649b/513. On the other hand, the variance gathered by f_2 was mainly associated to the resolution between olive oil and the rest of categories as a whole. According to **Fig. 5.12B**, peanut, soybean and grapeseed categories were well resolved from each other and with respect to the rest of categories along f_3. Finally, as illustrated in **Fig. 5.12C** by using a plane oblique to the three first

discriminant functions, all the possible pair of categories were very well resolved from each other. For this model, and using leave-one-out validation, all the points of the training set were correctly classified. The corresponding evaluation set, containing the 84 original data points, was then used to check the prediction capability of the model. Using a 95% probability, all the objects were correctly assigned; thus, the prediction capability of the model was 100%.

Table 5.11. Predictors selected and corresponding standardized coefficients of the LDA model constructed to predict the botanical origin of the oil samples.

Predictors[a]	f_1	f_2	f_3	f_4	f_5	f_6
513/651b	-8.22	7.07	4.33	8.21	7.28	3.96
663c/649a	-1.39	-0.48	16.6	-9.75	-5.37	-1.63
663d/649c	-12.2	-1.23	-1.30	-0.39	-1.50	-0.34
649a/649b	-5.21	-2.10	0.51	-0.77	-1.65	-0.74
649b/493	2.45	-7.24	-2.26	-0.63	-0.78	-0.64
649d/651b	30.7	3.45	1.15	0.57	-1.76	-0.75
521b/591	14.9	-0.43	-0.12	2.07	0.79	-0.21
649b/513	-27.6	5.84	0.02	-5.27	0.01	-0.38
649c/513	15.9	-2.78	-2.99	2.51	0.28	-0.86
521b/519	-18.0	2.12	6.00	1.23	1.47	0.69
549/513	-0.69	13.2	-14.4	12.3	9.50	4.13
549/649b	11.6	-2.02	-4.98	-1.54	-1.68	-0.26

[a] *m/z* values of the peak pairs.

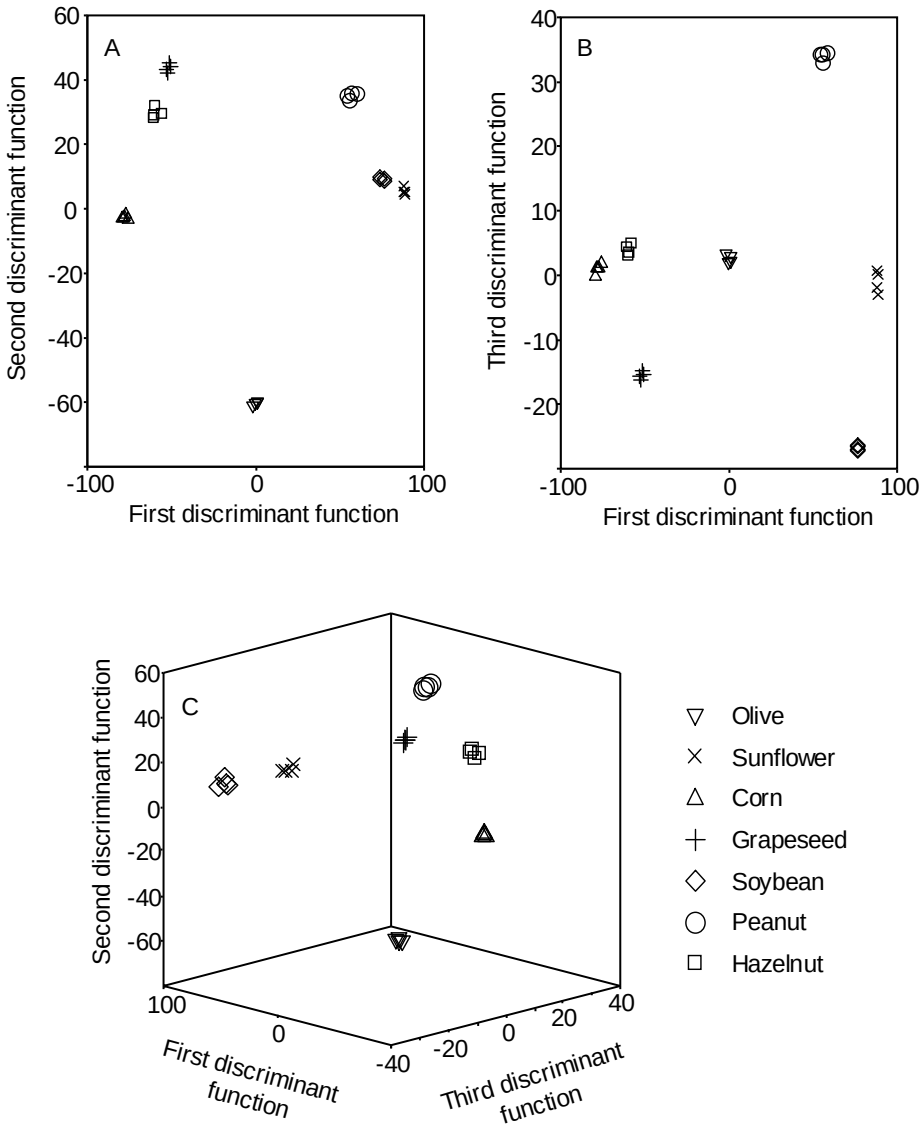

Fig. 5.12. Score plots on the planes of the first and second (A), and first and third discriminant functions (B), and on an oblique plane of the 3-D space defined by the three first discriminant functions (C) of the LDA model constructed to classify vegetable oils according to their botanical origin.

5.4. Classification using amino acid profiles established by direct infusion MS

The aim of this work was the construction of LDA models to classify vegetable oils according to their botanical origin, by using the amino acid profiles obtained by direct infusion MS. For this purpose, the vegetable oils shown in **Table 5.12** were employed. EVOO oil samples of the three most important varieties of the Spanish production, coming from 10 different geographical areas of Spain, and other vegetable oil samples from different areas of Europe and South America were used.

5.4.1. MS amino acid profiles

After protein hydrolysis (see section 3.3.3), the MS spectra of the different oils (**Fig. 5.13**) showed the $[M+H]^+$ peaks of the following amino acids: Gly (*m/z* 76.1), Ala (*m/z* 90.1), Ser (*m/z* 106.1), Pro (*m/z* 116.1), Val (*m/z* 118.1), Thr (*m/z* 120.1), Cys (*m/z* 122.2), Ile + Leu (*m/z* 132.2), Asp (*m/z* 134.1), Lys (*m/z* 147.2), Glu (*m/z* 148.2), Met (*m/z* 150.2), His (*m/z* 156.2), Phe (*m/z* 166.2), Arg (*m/z* 175.2), and Tyr (*m/z* 182.2). Leu and Ile, which have the same MW, gave a single common peak. Asn and Gln were excluded from this study, since hydrolysis converts them into Asp and Glu (Gimeno-Adelantado, 2002). Hydrolysis also leads to a partial conversion of Glu into pyroglutamic acid, and to the degradation of Trp (Gimeno-Adelantado, 2002). The abundances of these 16 peaks were either intermediate or low, but in all cases they were adequate for data analysis.

Table 5.12. Botanical origin, genetic variety, number of samples and brand of the vegetable oil samples used in this work.

Oil sample	Genetic variety	Nº of samples	Brand
Hazelnut	Unknown	4	Guinama S.A.
Sunflower	Unknown	2	Koipesol
		2	Hacendado
Corn	Unknown	2	Guinama S.A.
Corn germen	Unknown	1	Guinama S.A.
		1	Hacendado
Soybean	Unknown	2	Guinama S.A.
		2	Biolasi
EVOO	Arbequina	2	Carbonell
		2	Torrereal
		2	Oleastrum
		1	Coosur
		1	Grupo Hojiblanca
		2	Borges
		1	Romanico
		1	Valderrama
		1	Veà
		1	Aubocassa
		1	Rihuelo
	Hojiblanca	2	Carbonell
		2	Coosur
		3	Borges
		7	Grupo Hojiblanca
		1	Columela
	Picual	2	Carbonell
		2	Coosur
		3	Borges
		1	Grupo Hojiblanca
		1	Castillo Tabernas
		1	Castillo Canena
Avocado	Unknown	4	Guinama S.A.
Peanut	Unknown	4	Guinama S.A.
Grapeseed	Unknown	4	Guinama S.A.

The amino acid profiles observed in the MS spectra differed from the concentration profiles reported by Hidalgo et al. (2001A). The differences were attributed to the different response factors of the amino acids in MS. This was confirmed by directly infusing amino acid stock solutions. The amino acids with low MW, as Gly, Ala and Ser, and also Cys, Thr and Asp, gave low sensitivities, whereas the amino acids with high MW (Lys, Met, His, Phe, Arg and Tyr) gave high sensitivities.

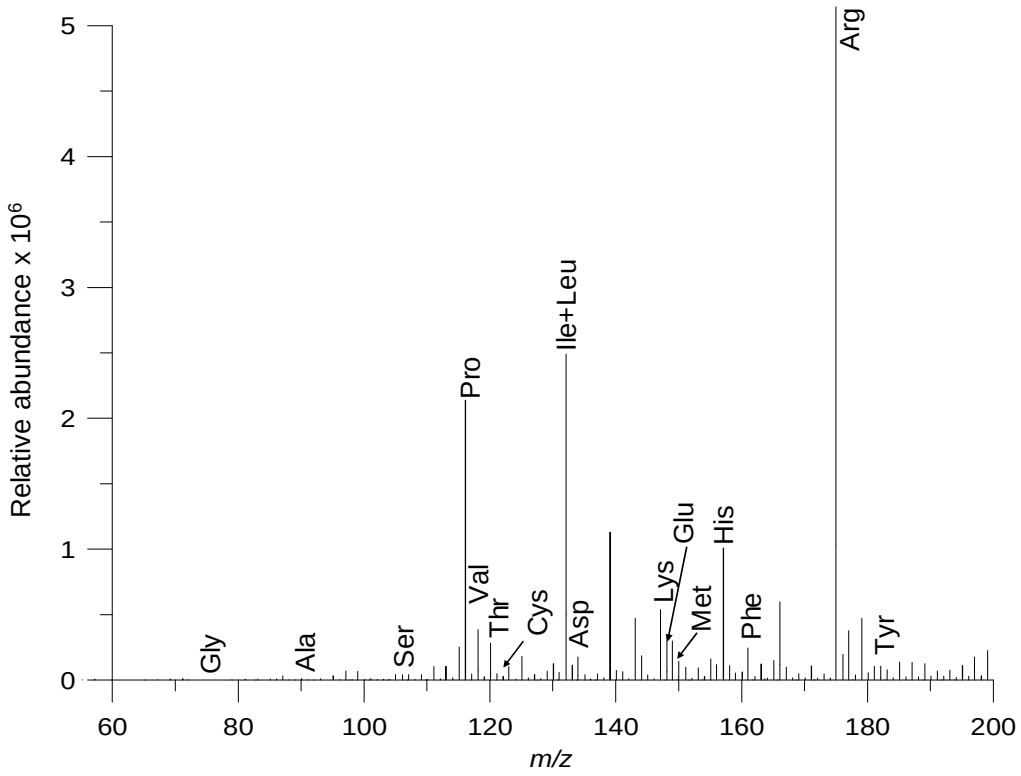

Fig. 5.13. Typical ESI-MS spectrum of an hydrolyzed EVOO oil protein extract. The amino acids studied in this work are indicated.

5.4.2. Construction of data matrices and LDA models

In this work, both normalization procedures, A and B, were applied to the original variables, and then, 16 and (16x15)/2 = 120 normalized variables were obtained to be used as predictors according to normalization procedure A and B, respectively.

Then, using these normalized variables, LDA models capable of classifying the oil samples according to their botanical origin were constructed. For this purpose, each sample was injected four times. Two matrices containing 272 injections each, and either 16 or 120 predictors (according to normalization procedures A and B, respectively) were constructed. A response column, containing the eight categories corresponding to the eight botanical origins of the oils, was added to the matrices. These matrices were used as evaluation sets. To construct LDA training matrices, only the means of the replicates of the samples were included; thus, the internal dispersion of the categories was reduced. In addition, only the means of the replicates of each genetic variety of EVOOs (Arbequina, Hojiblanca and Picual) were included in the training set. In this way, all categories contained a similar number of data points, which is important to achieve a maximal category resolution along the LDA functions. Thus, in the training matrix, the EVOO category was represented by three data points (one for each genetic variety), while the other categories were represented by four data points each.

To classify the oils according to the eight botanical varieties of **Table 5.12**, two LDA models, one for each normalization procedure, were constructed. Normalization procedure B, which led to a better separation between the categories, was selected. With this procedure, the categories hazelnut, EVOO and avocado appeared clearly resolved from each other, and were also well separated from the other five categories (sunflower, corn, soybean, peanut and grapeseed), which overlapped. For this reason, a new LDA model, in which these five categories were grouped in a single one, was constructed. In this case, to maintain a similar number of points in each one of the four categories (hazelnut, EVOO, avocado and the one formed by the other oils), only the means of the sunflower, corn, soybean, peanut and grapeseed oils were included in the new

category. An excellent resolution between these four categories (hazelnut, EVOO, avocado and the one formed by the other oils) was obtained (**Fig. 5.14**, $\lambda_w = 0.056$).

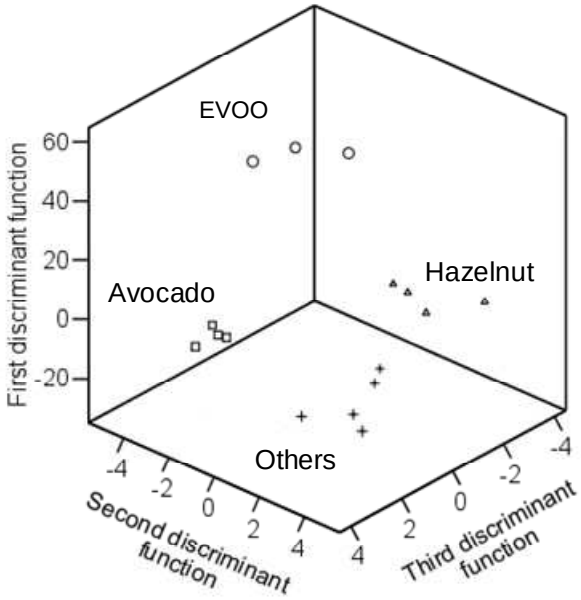

Fig. 5.14. Score plot on an oblique plane of the 3-D space defined by the three discriminant functions of the LDA model constructed to resolve the hazelnut, EVOO, avocado and "others" categories. "Others" is the combined category of the sunflower, corn, soybean, peanut and grapeseed oils.

The variables selected by the SPSS stepwise algorithm, and the corresponding model standardized coefficients, are given in **Table 5.13**. All the points of the training set were correctly classified by leave-one-out cross-validation. The evaluation set, containing the 272 original data points, was used to check the prediction capability of the model. Using a 95% probability, only twelve objects corresponding to replicates of different samples (1 hazelnut, 1 avocado and 10 EVOO) were not correctly assigned; thus, the prediction capability was 96%.

Table 5.13. Predictors selected and the corresponding standardized coefficients of the three sequential LDA models constructed to classify vegetable oils according to their botanical origin.

	Hazelnut/ EVOO/ avocado/ others[b]			*Soybean/ peanut/ others*[c]		*Sunflower/ corn/ grapeseed*	
Predictor[a]	f_1	f_2	f_3	f_1	f_2	f_1	f_2
118.1/76.1	8.07	5.94	0.08	-	-	-	-
150.2/106.1	-	-	-	-	-	-2.18	0.69
148.2/116.1	-1.12	3.85	1.54	-	-	-	-
175.2/116.1	-	-	-	-	-	-3.81	0.26
120.1/118.1	4.56	0.35	0.31	2.93	1.45	-	-
156.2/118.1	-	-	-	-2.17	-1.35	-	-
122.2/120.1	-	-	-	-	-	4.54	-0.87
132.2/122.2	10.42	3.73	3.71	-	-	-	-
175.2/122.2	-13.81	-6.80	-2.72	-	-	-	-
147.2/132.2	-	-	-	-2.17	0.26	-	-
150.2/132.2	7.56	4.88	-0.81	-	-	-	-
156.2/134.1	-	-	-	-	-	2.42	0.46
175.2/156.2	-8.12	-1.18	2.27	-	-	-	-
182.2/156.2	-	-	-	1.43	-0.22	-	-
175.2/166.2	13.09	5.96	-2.42	-	-	-	-

[a] *m/z* values of the ratios of amino acid peaks.

[b] Others = sunflower + corn + soybean + peanut + grapeseed.

[c] Others = sunflower + corn + grapeseed.

Next, the hazelnut, EVOO and avocado categories were removed from the training set, and the remaining categories were used to construct another LDA model. Now, soybean and peanut categories were separated with an excellent resolution, while the other three categories (sunflower, corn and grapeseed) still overlapped. Thus, another LDA model was constructed in which these three unresolved categories were included in a single combined category. As indicated above for the previous LDA model, in order to maintain a similar number of

points per category, only the means of the sunflower, corn and grapeseed oils were included in the new category. As shown in **Fig. 5.15**, an excellent resolution between the new three categories was obtained ($\lambda_w = 0.042$).

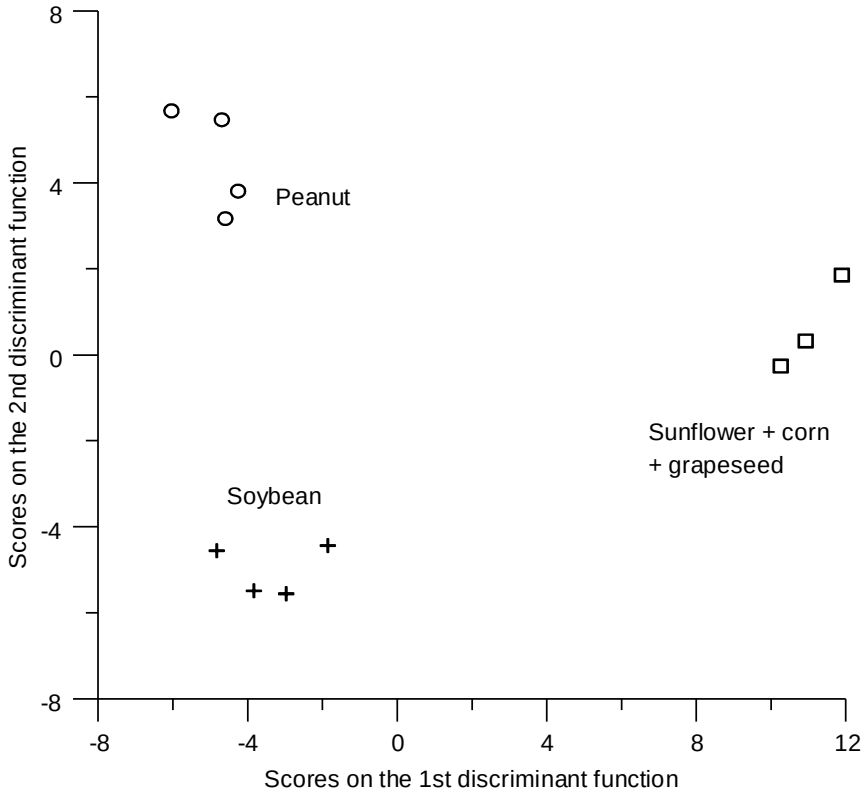

Fig. 5.15. Score plot on the plane of the two discriminant functions of the LDA model constructed to resolve the soybean, peanut and the new combined category (sunflower, corn and grapeseed).

The variables selected and the corresponding model standardized coefficients are given in **Table 5.13**. All the points of the training set were correctly classified by leave-one-out cross-validation. To estimate the prediction capability of the model, the evaluation set, constituted now by 80 original data points, was used. Using a 95% probability, only three objects, which corresponded to replicates of different samples, were not correctly assigned; thus, the prediction capability was 96%.

Finally, to resolve the sunflower, corn and grapeseed categories, a third LDA model was constructed. However, a model with many predictors was obtained. Thus, in order to reduce the number of predictors, the value of the probability of the entrance test was reduced to $F_{in} = 0.02$. As shown in **Fig. 5.16**, the resulting model gave a satisfactory resolution among the three categories ($\lambda_w = 0.279$).

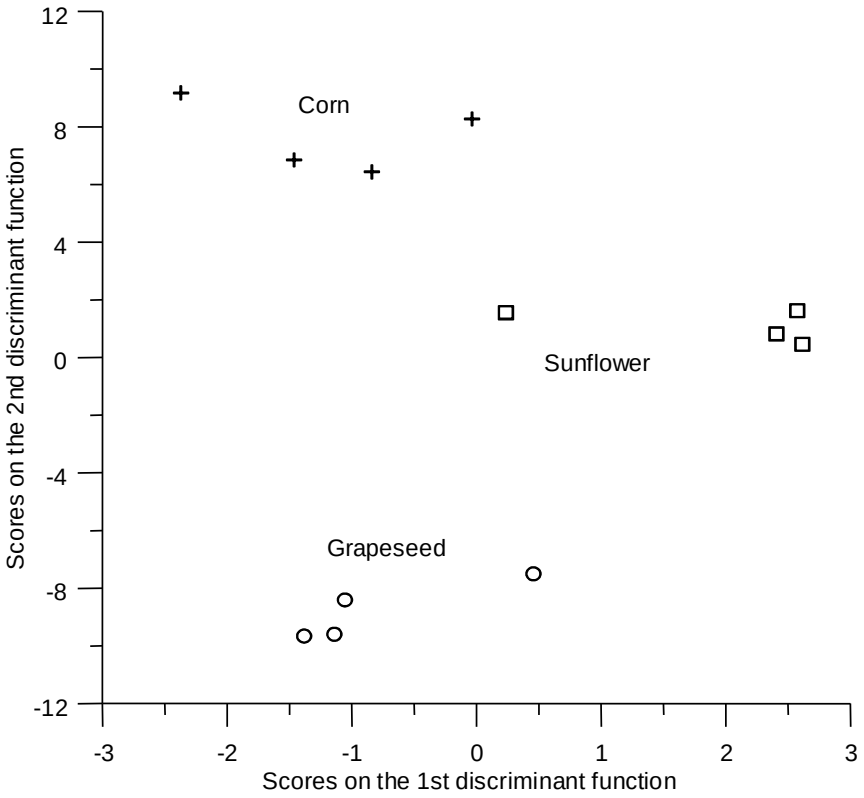

Fig. 5.16. Score plot on the plane of the two discriminant functions of the LDA model constructed to resolve the sunflower, corn and grapeseed categories.

The variables selected and the corresponding model standardized coefficients are also given in **Table 5.13**. All the points of the training set were correctly classified by leave-one-out cross-validation. Using a 95% probability, only three objects out from a total of 48 original data points of the evaluation set,

and corresponding to replicates of different samples, were not correctly assigned; thus, the prediction capability of the model was 94%. Therefore, the vegetable oils belonging to the eight different botanical origins were correctly classified with a high reliability by the sequential application of three LDA models. In terms of resolution between oil origin categories, the proposed method yields similar results to those reported by using ^{31}P- and ^{1}H-NMR of diglycerides (Vigli, 2003).

5.5. Classification using amino acid profiles established by HPLC-UV-Vis

The aim of this work was to construct an LDA model capable of classifying vegetable oils according to their botanical origin by using amino acid profiles obtained by HPLC-UV-Vis. For this purpose, two amino acid extractions, performed as indicated in section 3.3.3, were done to each one of the samples described in **Table 5.14**. These extracts were derivatized with OPA in the presence of NAC prior to HPLC-UV-Vis analysis (see section 3.3.3).

Table 5.14. Botanical origin, number of samples and brand of the oil samples used in this work.

Origin	No. of samples	Brand
Hazelnut	2	Guinama
	2	Percheron
	2	Flumen
Peanut	2	Guinama
	2	Bellsola
	1	Apsara Vital
	1	Maní
Avocado	2	Guinama
	2	Marnys
	2	Serra Vita
Grapeseed	2	Guinama
	1	Coosur
	1	Romulo
	1	Paul Corcelet
	1	Pons
Corn	1	Guinama
	1	Asua
	1	Artua
	1	Mazola
Corn germ	1	Guinama
	1	Hacendado
EVOO	1	Carbonell
	1	Grupo Hojiblanca
	1	Borges
	1	Torrereal
	1	Coosur
	1	Hacendado
Soybean	2	Guinama
	2	Biolasi
	2	Sojola

5.5.1. HPLC-UV-Vis amino acid profiles

Amino acid separation was performed using the experimental conditions indicated in section 3.5.7. Stock solutions containing an amino acid or mixtures of two or three amino acids (1000 μg mL^{-1} each) were prepared, and aliquots were derivatized as indicated (section 3.3.3). After derivatization, these solutions were both directly injected or used to spike the hydrolyzates when required. A chromatogram of the standard mixture is shown in **Fig. 5.17**. As it can be observed, all amino acid peaks were clearly resolved, except the pairs Phe/Leu and the Asn/Ser.

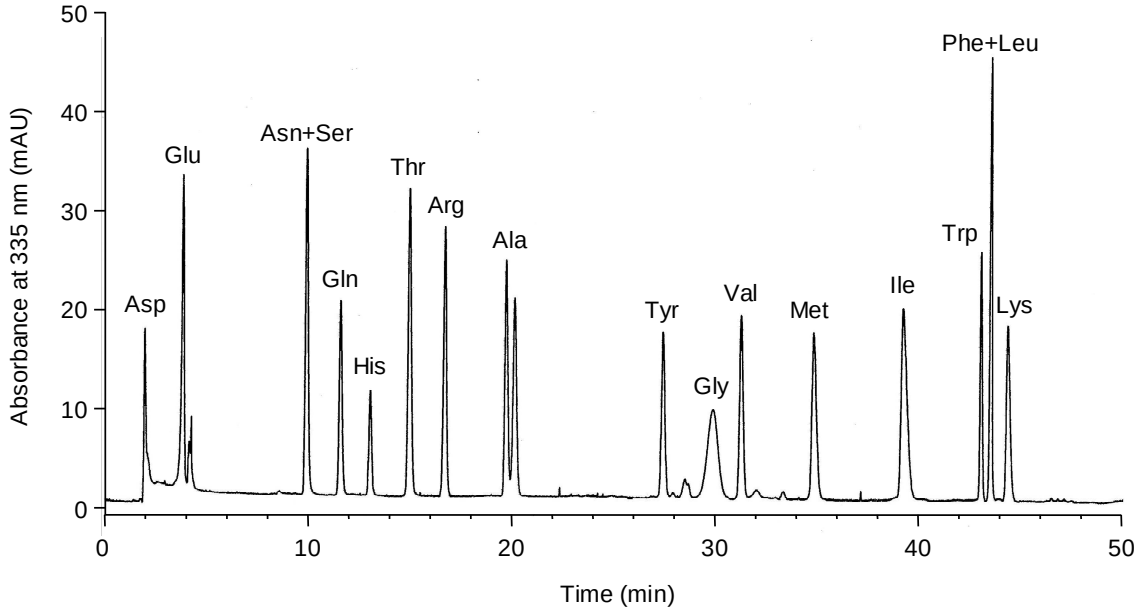

Fig. 5.17. Chromatogram of a standard mixture of derivatized amino acids.

When the extracts of the oil samples were injected (**Fig. 5.17**), several matrix peaks jointly with a baseline disturbance in the last part of the chromatograms were evidenced. Small modifications in the mobile phase composition and in the gradient conditions were tried; however the resolution of these two peak pairs did not improve. A dilution of the amino acid extracts did

not improve either the resolution of these peak pairs. Additionally with the dilution, some minor amino acid peaks were not observed with the subsequent loss of significant information. When comparing the chromatograms of different oil extracts (**Fig. 5.18**), small differences between the amino acid profiles of the different vegetable oils were observed. Thus, to construct LDA models, 16 peak areas, which corresponded to 18 amino acids (Phe/Leu and the Asn/Ser peak pairs were jointly measured), were used as original variables.

5.5.2. Construction of data matrices and LDA models

In this work, both normalization procedures, A and B, were applied to the original variables, and then, 16 and (16x15)/2 = 120 normalized variables were obtained to be used as predictors according to normalization procedure A and B, respectively.

Then, using these normalized variables, LDA models capable of classifying the oil samples according to their botanical origin were constructed. For this purpose, each extract (2 *per* sample) was injected 2 times. Two matrices containing 168 injections each, and either 16 or 120 predictors (according to normalization procedures A and B, respectively) were constructed. A response column, containing the seven categories corresponding to the seven botanical origins of the oils (corn and corn germ were considered as a single category), was added to the matrices. These matrices were randomly divided in two groups, both containing 84 samples. One of the matrices was used as training set, while the other was used to evaluate the model.

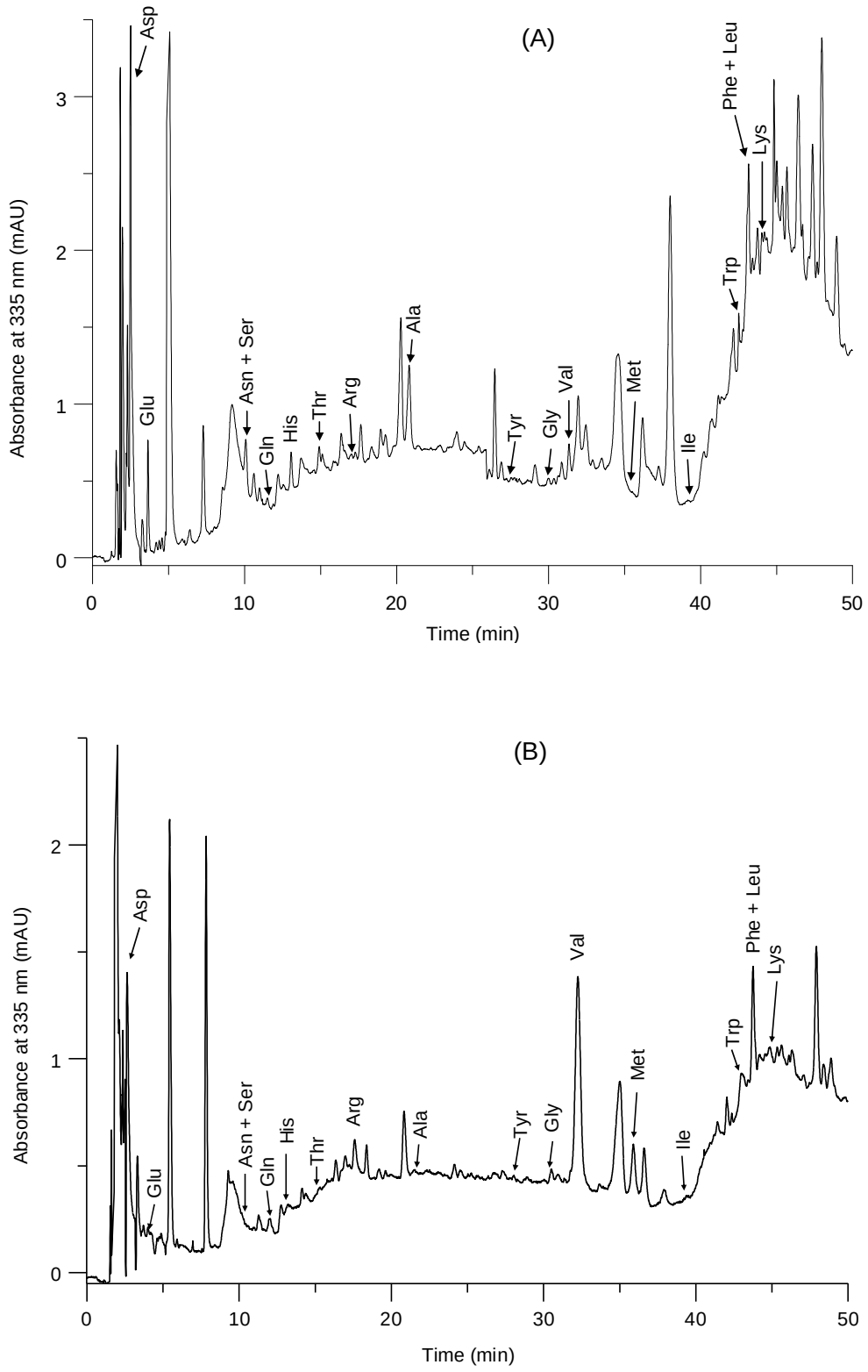

Fig. 5.18. Chromatograms showing the amino acid profiles of an EVOO (A) and hazelnut oil (B) samples. Other working conditions as in **Fig. 5.17**.

To classify the oils according to the seven botanical varieties of **Table 5.14**, two LDA models, one for each normalization procedure, were constructed. The best results according to both, low λ_w values and simplicity (a low number of predictors) were obtained using normalization procedure B, which was selected. An excellent resolution between the seven categories was achieved ($\lambda_w = 0.393$). Taking into account that a large number of categories were simultaneously distinguished, this λ_w value was quite low. The variables selected by the SPSS stepwise algorithm, and the corresponding standardized coefficients of the model, are given in **Table 5.15**.

Table 5.15. Predictors selected and corresponding standardized coefficients of the LDA model constructed to predict the botanical origin of vegetable oils.

Predictors	f_1	f_2	f_3	f_4	f_5	f_6
Asp/Ala	-7.37	1.40	-1.25	0.01	-2.22	-0.35
(Asn+Ser)/Thr	-10.94	0.70	1.46	2.14	-0.58	-0.74
Gln/Thr	6.46	-1.85	-0.20	-1.84	3.35	1.93
His/Gly	16.16	2.00	1.92	1.18	-0.11	0.68
His/Trp	-16.38	-1.03	1.92	0.84	-0.96	1.00
Arg/Ala	-3.43	12.29	2.89	2.21	9.10	4.01
Arg/Val	7.94	-11.50	-1.17	-0.58	-9.83	-5.49
Ala/Val	-4.93	0.37	-0.04	2.54	0.38	0.83
Ala/Trp	2.67	0.31	0.67	-0.95	2.07	-1.03
Gly/Val	29.30	1.75	0.26	1.50	0.07	0.11
Gly/Ile	-6.20	1.17	0.82	-0.56	-0.98	1.62
Val/Ile	24.08	-0.90	-1.21	1.16	1.64	-1.71
Ile/(Leu+Phe)	16.84	0.46	0.72	1.21	1.10	-0.05

As shown in **Fig. 5.19A**, an excellent resolution between the soybean and hazelnut categories, as well as between these and the other categories, was

achieved along f_1. As deduced from **Table 5.15**, f_1 was mainly constructed with the peak area ratios Gly/Val and Val/Ile. On the other hand, the variance gathered by f_2 was mainly associated to the resolution between EVOO and the rest of categories as a whole. According to **Fig. 5.19B**, corn, hazelnut, grapeseed, avocado-EVOO and peanut-soybean categories were resolved along f_3. Finally, as illustrated in **Fig. 5.19C** by using a plane oblique to the three first discriminant functions, all the possible pair of categories were very well resolved from each other.

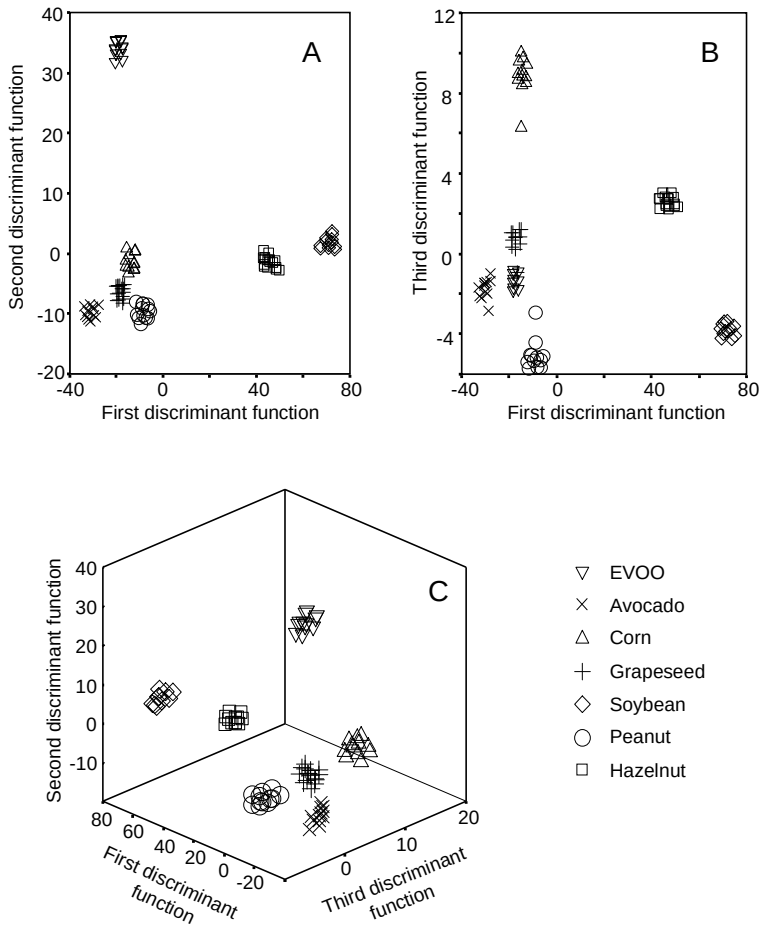

Fig. 5.19. Score plots on the planes of the first and second (A), and second and third discriminant functions (B), and on an oblique plane of the 3-D space defined by the three discriminant functions (C) of the optimal LDA model.

All the points of the training set were correctly classified by leave-one-out cross-validation. The evaluation set, also containing 84 original data points, was used to check the prediction capability of the model. All the objects were correctly assigned with an assignation probability higher than 95%.

CHAPTER 6

DEVELOPMENT OF METHODS FOR OLIVE OIL QUALITY EVALUATION

6.1. Classification of olive oils according to their quality grade using fatty acid profiles obtained by direct infusion MS

In this work, the capability of direct infusion ESI-MS to classify olive oils of different quality grades such as EVOO, VOO, LVOO and ROPO (see **Table 6.1**), and to evaluate mixtures of EVOO and VOO, and binary mixtures of these two oils with olive oils of lower quality grade has been studied. As explained in section 3.3.4, infusion in the ESI interface of the mass spectrometer was performed after dilution of the sample with a miscible alkaline solvent, followed by direct analysis without any previous extraction step.

6.1.1. MS fatty acid profiles

In all cases, the MS spectra of the different oils showed the $[M-H]^-$ peaks of the following fatty acids: myristic (C14:0, *m/z* 227), palmitoleic (C16:1, *m/z* 253), palmitic (C16:0, *m/z* 255), linolenic (C18:3, *m/z* 277), linoleic (C18:2, *m/z* 279), oleic (C18:1, *m/z* 281) and stearic (C18:0, *m/z* 283). The mass spectra were normalized by dividing each peak abundance by the abundance of the C16:0 peak (see **Fig. 6.1**). As observed, oleic acid yielded the most intense signal, whereas palmitic, linoleic and stearic acids gave intermediate abundances. For each quality grade, closely similar peak profiles were obtained, independently of the genetic variety of the oils. The C14:0/C16:0 peak ratio was larger for VOO and LVOO than for the samples of other quality grades. Also, the C18:3/C16:0 peak ratio decreased according to LVOO > EVOO ≈ VOO > ROPO (**Fig. 6.1**). In agreement with these observations, a chemometric study was carried out.

Table 6.1. Olive oils used to construct the LDA models.

Grade	Brand	Genetic variety	Geographical origin	Set type
EVOO	Coosur	Hojiblanca[a]	Luque (Córdoba)	Training
		Arbequina[a]	Estepa (Sevilla) +	Training
			La Roda de Andalucía (Sevilla)	
		Picual[a]	Villanueva del Arzobispo (Jaén) +	Training
			Porcuna (Jaén)	
	Carbonell	Hojiblanca	Estepa (Sevilla)	Evaluation
		Arbequina	Aguadulce (Sevilla)	Evaluation
		Picual	Martos (Jaén)	Evaluation
	Borges	Hojiblanca[a]	Puente Genil (Córdoba)	Training
		Arbequina[a]	Huelva + Zaragoza +	Training
			Palma del Río (Córdoba)	
		Picual[a]	Quesada (Jaén)	Training
	Torrereal	Arbequina	Vila Franca del Penedés (Barcelona)	Evaluation
	Duc	Arbequina	Vila Franca del Penedés (Barcelona)	Evaluation
	Oleastrum	Arbequina	Les Garrigues (Lleida)	Evaluation
	Hipercor	Hojiblanca	Antequera (Málaga)	Evaluation
	Grupo	Hojiblanca[a]	Fuente de Piedra (Málaga)	Training
	Hojiblanca	Arbequina[a]	Antequera (Málaga)	Training
		Picual[a]	Montoro (Córdoba)	Training
VOO	Coosur	Mixture[b]	Vilches (Jaén)	Training
	Grupo	Hojiblanca[a]	Archidona (Málaga)	Training
	Hojiblanca	Arbequina[a]	Antequera (Málaga)	Training
		Picual[a]	Lucena (Córdoba)	Training
LVOO	Coosur	Mixture[a]	Vilches (Jaén)	Training
	Borges	Mixture[a]	Jódar (Jaén)	Training
	Grupo	Hojiblanca[a]	Archidona (Málaga)	Training
	Hojiblanca	Arbequina[a]	Hinojosa del Duque (Córdoba)	Training
		Picual[a]	La Rembla (Córdoba)	Training
ROPO	Coosur S.A	Mixture[a]	Vilches (Jaén)	Training
	Borges	Mixture[a]	Palma del Río (Córdoba)	Training
OPO	*confidential*	Mixture	Unknown	Evaluation[b]

[a] Guaranteed quality.

[b] Used exclusively to evaluate the MLR model.

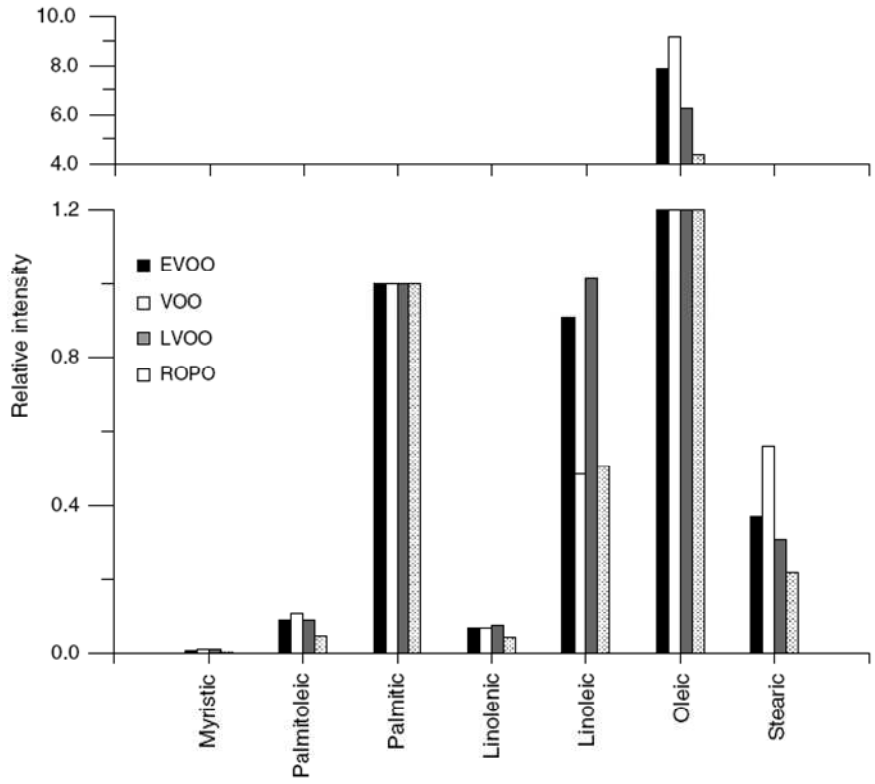

Fig. 6.1. Relative peak intensities of fatty acids observed in the mass spectra of different quality grade olive oils. The palmitic acid peak (*m/z* 255) was used as reference.

6.1.2. Construction of data matrices and LDA models

As indicated in **Table 6.1**, the samples with guaranteed quality grade (9 EVOO, 4 VOO, 5 LVOO and 2 ROPO samples) were used to construct the training set for the LDA models. The other samples, also described in **Table 6.1**, were used as evaluation set. To improve the stability and prediction capability of the models, for each quality grade (EVOO, VOO and LVOO) samples of three genetic varieties (Hojiblanca, Arbequina and Picual), produced in different regions of Spain with rather dissimilar soils and climatic conditions, were used.

About 4-5 injections of each sample were performed; accordingly, two matrices constituted by 123 cases, and by 7 and 21 predictors, after normalization by procedures A and B, respectively, were established. In order to classify the

samples according to their quality grade, LDA models were constructed. The SPSS default values of F_{in} and F_{out}, 3.84 and 2.71, respectively, were used.

Using the samples of the training set (EVOO, VOO, LVOO and ROPO), two LDA models, one for each normalization procedure, were constructed. The best results were obtained using normalization procedure B, which was selected. Using this procedure and a 95% probability, all the evaluation set samples were correctly classified. Then, both the training and evaluation sets were jointly used to construct a new model with an improved prediction capability of the quality grade. In this way, as samples were obtained from different geographical origins, this parameter was also included in the statistical analysis. The λ_w for this model was 0.52. The predictors selected by the SPSS stepwise algorithm, and the corresponding model standardized coefficients, are given in **Table 6.2**. A score plot on the plane of the two first discriminant functions is shown in **Fig. 6.2**. As observed in this figure, EVOO category was very well resolved from the other three categories. Then, to maximize resolution among the VOO, LVOO and ROPO categories, another LDA model was constructed after removing the EVOO category. In this case, λ_w was 0.19, which agrees with the excellent resolution observed between all the category pairs shown in the score plot of **Fig. 6.3**. The model standardized coefficients are also given in **Table 6.2**. Therefore, EVOO, VOO, LVOO and ROPO samples can be unequivocally classified by the sequential application of two LDA models, one constructed with the EVOO category, and the other after removing this category.

At the sight of **Table 6.2** and **Fig. 6.2**, predictors C16:0/C16:1, C18:3/C16:1, C18:1/C16:1, C18:0/C16:0 and C18:1/C18:3 were relevant to distinguish EVOO from the other three categories, whereas predictors C16:0/C16:1, C18:0/C16:1 and C18:1/C16:0 were important to distinguish the category pairs formed by VOO, LVOO and ROPO (**Table 6.2** and **Fig. 6.3**).

Table 6.2. Standardized coefficients of the discriminant functions obtained to predict the quality grade of olive oils.

Predictors	Categories[a]				
	EVOO/VOO/LVOO/ROPO			VOO/LVOO/ROPO	
	f_1	f_2	f_3	f_1	f_2
C16:0/C14:0	-	-	-	3.4	2.5
C18:1/ C14:0	0.042	-1.1	0.53	-	-
C18:0/ C14:0	-	-	-	-2.3	-2.2
C16:0/C16:1	-8.8	-2.3	-1.2	4.5	-3.5
C18:3/C16:1	6.8	1.3	2.3	-	-
C18:2/ C16:1	-	-	-	2.0	-3.3
C18:1/ C16:1	15	2.8	4.1	-	-
C18:0/ C16:1	-1.7	-0.18	-0.65	-6.1	10
C18:1/ C16:0	0.79	-0.71	-1.5	2.5	-7.1
C18:0/ C16:0	-7.7	-0.17	-3.7	-	-
C18:2/ C18:3	-	-	-	0.17	2.4
C18:1/ C18:3	-6.3	0.084	-1.9	-	-
C18:0/ C18:3	3.1	0.69	1.7	-0.68	-0.85
C18:1/ C18:2	0.71	1.1	1.9	-0.72	3.2
C18:0/ C18:1	0.66	-0.38	0.53	2.9	-0.76

[a] Categories included in the training set.

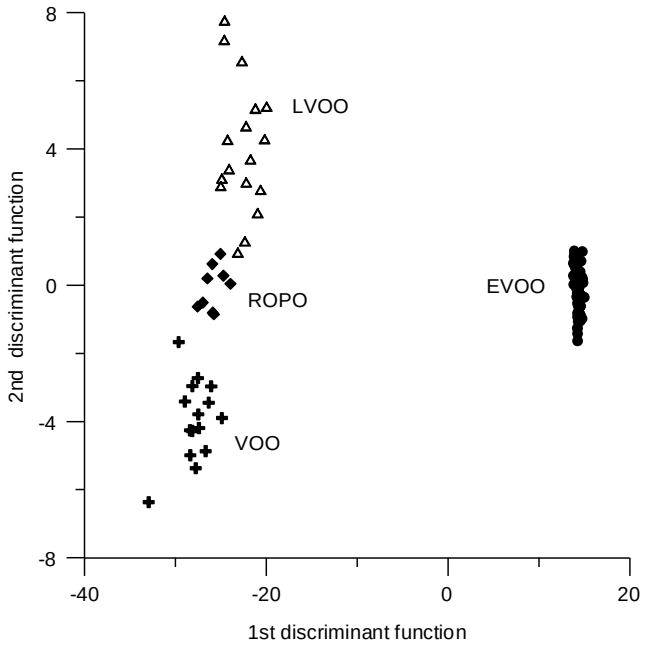

Fig. 6.2. Score plot on the plane of the two first discriminant functions of an LDA model constructed with samples of four different quality grade olive oils using normalization procedure B.

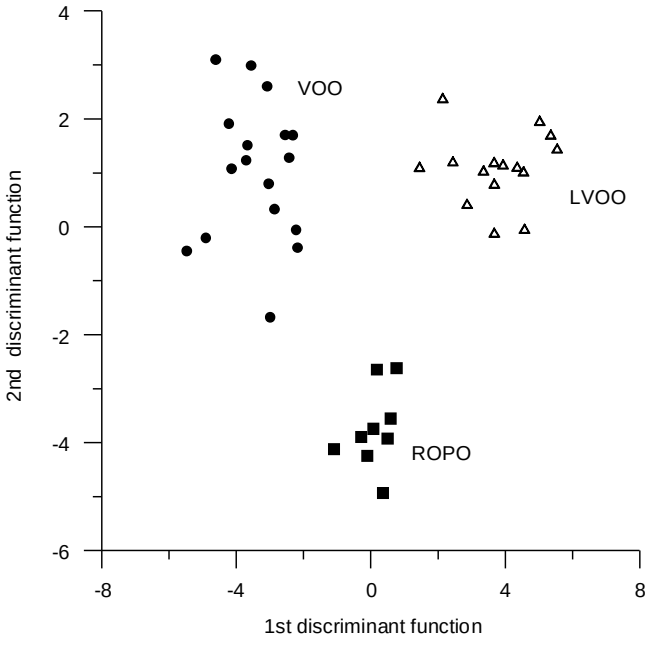

Fig. 6.3. Score plot on the plane of the two discriminant functions of an LDA model constructed with samples of three different quality grade olive oils (EVOO excluded) using normalization procedure B.

6.1.3. Evaluation of binary mixtures of olive oils of different quality grade

Binary mixtures of EVOO and VOO, and either EVOO or VOO with another lower quality grade oil, were prepared. Mixtures with *ca.* 100, 80, 60, 40, 20 and 0 wt% EVOO or VOO, were infused. For each binary combination of oils, the predictors obtained by using normalization procedures A and B were independently used to construct two matrices. Each mixture was injected by triplicate, thus, matrices with a total of 75 cases, and 7 and 21 predictors, respectively, were obtained. A response vector containing the percentage of the higher quality grade oil in the mixture was added to the matrices.

In this case, the SPSS backward algorithm was used to select the predictors in the construction of MLR models. The SPSS default values, F_{in} = 3.84 and F_{out} = 2.71, were again used. The MLR models were constructed both without and with an independent term (a constant). The use of a constant improved the quality of the models constructed with the peak intensity ratios. For all the PLSR1 models, the number of vectors recommended by The Unscrambler after the PLSR1 rotation (*k*-value) was adopted.

The *r* values of the MLR and PLSR1 models are given in **Table 6.3**. In most cases, predictors with large *r* values were common to both models. An average prediction error, calculated as the average absolute difference between the expected and predicted oil percentages, divided by the number of predictions, was used to evaluate model quality. As can be seen in **Table 6.3**, in most cases MLR showed average prediction errors which were slightly better than those obtained by PLSR1. Using MLR, normalization procedure B gave better values of the average prediction errors than procedure A. The MLR regression model for VOO/ROPO mixtures was applied to quantify a guaranteed OPO sample (a commercial mixture of ROPO and VOO). The declared and found percentages in ROPO were 95 ± 3% and 92 ± 5%, respectively.

Table 6.3. *r* values of the MLR and PLSR1[a] models constructed to predict the composition of binary mixtures of oils of different quality grades.

Predictor	EVOO/VOO		EVOO/LVOO		EVOO/ROPO		VOO/LVOO		VOO/ROPO	
	MLR	PLSR1	MLR	PLSR1	MLR	PLSR1	MLR	PLSR1	MLR	PLSR1
C14:0	-0.71	-0.78	0.71	0.63	-0.75	-0.75	-0.32	-0.15	-	0.066
C16:1	-1.2	-0.54	-2.7	-1.3	1.9	0.48	0.45	0.098	-	-0.16
C16:0	1.9	0.31	2.3	0.72	-2.6	-0.48	-	-	-	-0.16
C18:3	2.2	0.67	1.4	0.42	-	0.10	-	0.16	-	-
C18:2	0.41	0.17	0.92	0.061	-	0.11	-1.5	-0.52	1.8	0.465
C18:1	-	-0.20	-1.6	-0.32	2.2	0.078	1.9	0.36	-	-0.23
C18:0	-1.9	-0.23	-	-0.14	-	0.096	-	0.25	-0.94	-0.33
No. of vectors[b]	6	4	6	5	4	4	4	3	2	3
Av. pred. error, %	10	10	9.7	10	9.6	9.0	5.1	5.3	3.4	4.4
C16:1/C14:0	3.0	0.58	-	-0.31	-	0.38	1.4	0.054	-1.1	-
C16:0/C14:0	-5.4	-0.89	-	-0.11	-	-1.2	-	-	-	-
C18:3/C14:0	-	1.8	-	0.15	-	-	2.3	-	-	-
C18:2/ C14:0	-0.64	-1.1	-0.35	-0.14	1.4	0.054	-1.7	-	-	-
C18:1/ C14:0	3.0	1.1	-	-	-	0.24	-	-	1.3	-
C18:0/ C14:0	-	-1.6	-	-	-0.92	-0.85	-1.9	-	-	-
C16:0/C16:1	-	-	-	0.22	-0.44	-0.30	0.82	-	0.54	-
C18:3/C16:1	1.6	0.39	-1.1	-0.20	-	-	-2.9	-	-	0.059
C18:2/ C16:1	-	-0.77	2.0	0.39	-	-0.25	1.2	-0.10	-	0.14
C18:1/ C16:1	-	0.99	0.77	-0.17	-	-1.2	1.2	0.071	-	-
C18:0/ C16:1	-0.69	-0.44	-0.77	-0.14	-	-	-	-	-0.59	-
C18:3/C16:0	-0.69	-0.066	-	-0.17	-	-	0.71	-	0.42	-
C18:2/ C16:0	-1.2	-0.80	-0.71	0.28	-	-	-	-0.169	-	0.168
C18:1/ C16:0	-	0.82	-	-0.17	-	0.080	-	0.095	-	-
C18:0/ C16:0	-	-1.1	-	-0.097	-	-	-	-	-	-0.051
C18:2/ C18:3	2.2	2.0	-	0.20	-	-	-1.2	-0.236	0.95	0.165
C18:1/ C18:3	-0.40	-0.41	-1.2	-0.41	-	1.1	-	0.064	-0.48	-
C18:0/ C18:3	-	0.091	-	-0.38	0.30	-	-0.40	-	0.71	-
C18:1/ C18:2	-	-0.44	-	0.28	0.68	0.19	1.8	0.24	-	-0.14
C18:0/ C18:2	-	-0.20	0.68	0.35	-	-	-2.3	0.18	-	-
C18:0/ C18:1	-	0.71	-	-	-	-	0.98	-	-	-0.11
No. of vectors[b]	10	10	8	7	5	2	14	4	8	3
Av. pred. error, %	5.3	4.8	4.5	5.8	11	15	2.2	7.1	3.0	5.5

[a] PLSR1 coefficients smaller than 0.05 in absolute values are not given.

[b] Number of vectors selected by the forward algorithm of SPSS (MLR), or recommended by The Unscrambler (PLSR1 *k*-values).

6.2. Electronic nose applied to defect detection and quantitation in olive oils and comparison with sensory panel data

The aim of this work was to develop a non-destructive method, based on MOS sensors, capable of classifying oils containing the typical VOO defects (fusty, mouldy, muddy, rancid and winey) according to their sensory threshold as previously established by trained panellists. For this purpose, these defects, available as single standards of the IOC, were added to refined sunflower oil. On the other hand, the electronic nose data were also used to quantify the defect percentage added to sunflower oil.

6.2.1. Establishment of the sensory threshold by trained panelists

As previously explained in section 3.6, ten trained assessors performed eight paired comparison tests between the defected samples and a blank, in order to establish the mean threshold of the panel. The results obtained for the five VOO defects are shown in **Fig. 6.4**. As observed in this figure, the sensory thresholds of the panel (corresponding to the defect percentage perceived by at least a 75% of the judges) followed the order: winey = fusty < mouldy < rancid < muddy. The thresholds were similar for winey (0.09%), fusty (0.09%), mouldy (0.12%) and rancid (0.13%) defects, whereas muddy defect showed a higher threshold (0.80%).

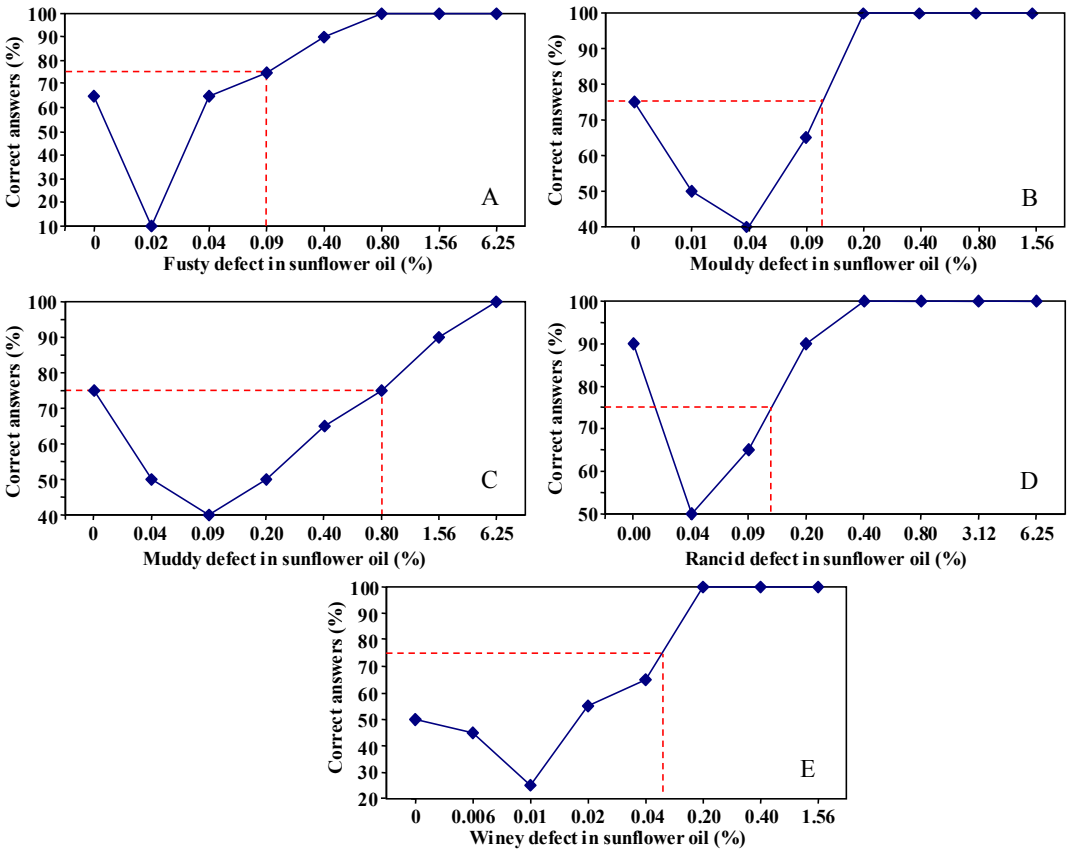

Fig. 6.4. Plots representing the defect (fusty, A; mouldy, B; muddy, C; rancid, D; winey, E) against the correct answer percentages, showing the detection threshold (defect % corresponding to 75% correct answers).

6.2.2. Classification of oils containing VOO defects according to their sensory threshold as established by a sensory panel

According to the panel taster group, the samples with a defect which also yielded a correct answer percentage higher than 75% were grouped as category 1 (samples that were over the sensory threshold), while the remaining samples were grouped as category 2. For example, for the rancid defect, samples prepared with 0.2, 0.4, 0.8, 3.12 and 6.25% defect in sunflower oil corresponded to category 1, while those with 0, 0.04 and 0.09% defect corresponded to category 2.

First, LDA models capable of classifying the samples according to these categories were constructed. The 6 original variables, which corresponded to the response of the 6 sensors of the electronic nose, were normalized according to normalization procedure B. Thus, a total of (6 x 5)/2 = 15 normalized variables to be used as predictors were obtained. Five matrices were then constructed, one for each sensory defect. Each matrix contained 24 points (8 samples x 3 replicates) and 15 predictors. Another column containing the assignments of the samples to one of the two categories described above was added to each matrix. The λ_w values, the variables selected by the SPSS stepwise algorithm, and the corresponding model standardized coefficients, are given in **Table 6.4**. As only two categories were used to construct the model, only one discriminant function was obtained.

Table 6.4. λ_w values and predictors selected with their corresponding standardized coefficients of the LDA models constructed for each sensory defect.

		Fusty	Mouldy	Muddy	Rancid	Winey
				λ_w		
		0.166	0.167	0.029	0.041	0.184
Predictors[a]	S1/S2	2.60	-	-	3.99	-
	S1/S3	-3.63	7.47	5.76	13.91	2.48
	S1/S4	-1.94	10.73	-	-	-
	S1/S5	-	-6.62	-7.33	-17.22	-
	S1/S6	4.55	-11.29	-	-	-
	S2/S3	-	-	-9.82	6.29	-
	S3/S5	-	-	-	-	2.96
	S4/S5	-	-	11.01	-	-

[a] Ratios of sensor signals.

As observed, λ_w values were in all cases lower than 0.2. As also observed, the ratio between sensors 1 and 3 (S1/S3) showed a high discriminant power for all the models. When leave-one-out validation was applied to each model, all the samples were correctly classified. As an example, a plot showing the LDA model constructed for the rancid defect is given in **Fig. 6.5**. As observed, a good resolution was obtained.

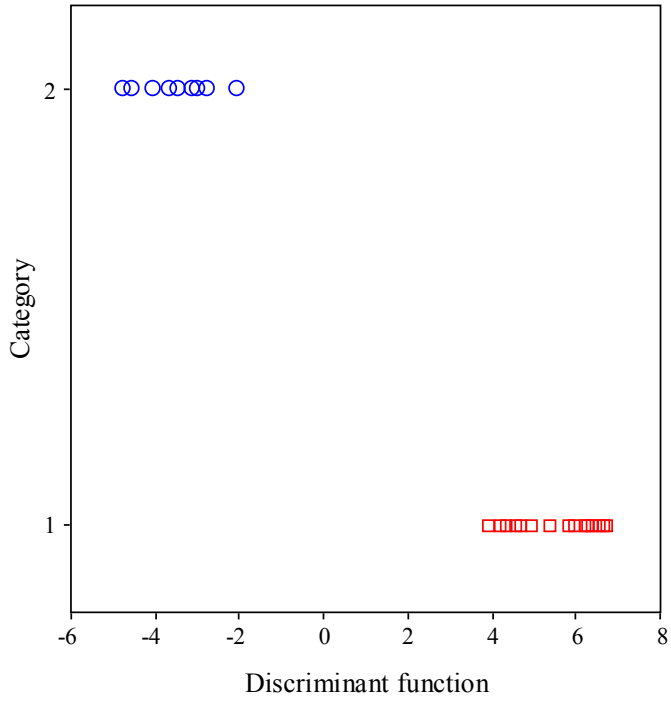

Fig. 6.5. Score plot on the plane of the discriminant function versus the category of the LDA model constructed to classify defected oil samples according to detection threshold of sensory analysis. Samples with a defect higher than detection threshold were grouped as category 1, being the other samples grouped as category 2.

On the other hand, the potential of MLP-ANN for the classification of the samples according to the two categories described above (samples that were over and under the sensory threshold) was also examined. In order to construct the ANN, the sensor responses represented the inputs, whereas a qualitative variable

(containing the two categories) represented the output. Then, the original data set (objects belonging to categories 1 and 2) was randomly divided into training (60% objects), verification (20%) and test (20%) sets. The verification set was used to identify the best ANN on the basis of the network's error performance, as well as to stop training if over-learning occurred. On the other hand the test set was used to give an independent assessment of the ANN capability of classifying samples according to their sensory threshold. The structure of the best MLP-ANN among all the networks tested to classify the samples is shown in **Fig. 6.6**. This ANN was characterized by 8 neurons in the hidden layer. For any oil defect considered, the number of iterations needed to achieve a satisfactory result was 50.

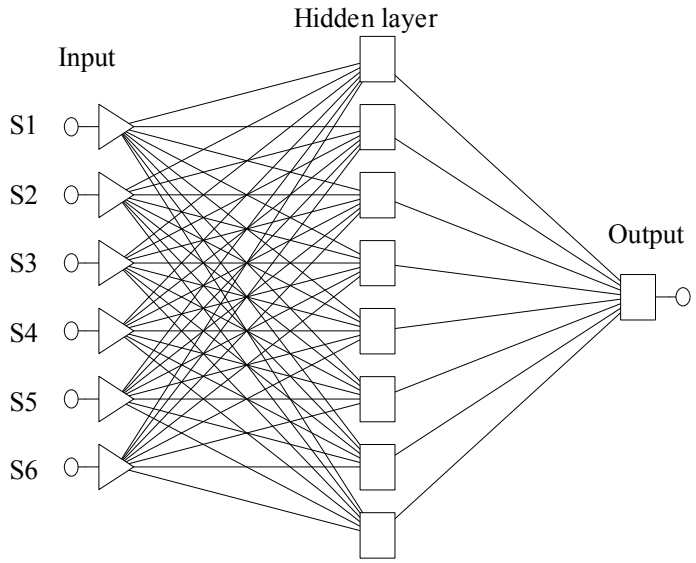

Fig. 6.6. MLP-ANN structures used to classify defected oil samples.

Results of training, verification and test of this MLP-ANN model are summarized in **Table 6.5**. These values were obtained with a momentum value of 0.3 and a learning rate of 0.1. As deduced from the data in **Table 6.5**, the MLP-ANN showed an acceptable performance. In particular, from test

validations, about 100, 85, 85, 80, and 75% of the data set was correctly classified, for rancid, mouldy, fusty, muddy and winey defects, respectively.

Table 6.5. Results of the MLP-ANN: correctly classified cases (%) for each sensory defect for the training, verification and test sets.

	Correctly classified cases (%)		
	Training	*Verification*	*Test*
Rancid	100	100	80
Mouldy	100	85	85
Muddy	100	80	80
Fusty	85	85	85
Winey	75	75	75

6.2.3. Prediction of defect percentage in sunflower oil by electronic nose followed by MLR data analysis

The possibility of predicting the defect percentage added to the sunflower oil using an electronic nose was also investigated. For this purpose, the 8 samples used in the paired comparison tests (8 for each defect) were used. Two additional samples for each defect were added in order to reduce the weight of the samples with higher defect percentages. To construct MLR matrices, only the means of the replicates of the samples were included (10 objects for each model), which was important to reduce the number of variables selected by the SPSS stepwise algorithm during model construction. The 15 signal ratios described above were also used as predictors to construct the MLR models.

The correlation plots of the calculated versus the experimental defect percentages are shown in **Fig. 6.7**. The *r* values, average prediction errors (*av.*

err., calculated as the sum of the absolute differences between expected and calculated defect percentages divided by the number of predictions) and the predictors selected for each MLR model with their corresponding non-standardized coefficients are detailed in **Table 6.6**. As observed, *r* values were in all cases higher than 0.988, being especially higher for fusty, mouldy, muddy and winey defects, were $r > 0.993$. This good correlation is illustrated in **Fig. 6.7**. On the other hand, and as observed in **Table 6.6**, the regression models for the fusty defect (which was mainly characterized by the presence of some volatile compounds originated by fermentation processes, i.e. some branched C5 components as 3-methyl butan-1-ol) and mouldy defect (produced by specific mould enzymes that produce volatile compounds such as 1-octen-3-one and 1-octen-3-ol) were mainly constructed with S4/S6 ratio (being S4 and S6 constructed with SnO_2 catalyzed with Au and WO_3, respectively), muddy defect (which was characterized by some volatile compounds originated by fermentation processes of oils stored for a long time on their sediment, i.e. propyl-propionate, ethyl-butanoate, propyl-butanoate and butyl-butanoate) by S5/S6 (SnO_2 catalyzed with Pd and WO_3, respectively), rancid defect (produced by several saturated and unsaturated aldehydes, such as nonanal and E-2-heptenal, respectively) by S1/S4 (SnO_2 and SnO_2 catalyzed with Ag, respectively) and winey defect (produced by acetic acid and ethyl acetate which were formed by sugar fermentation) by S4/S5 ratio (SnO_2 catalyzed with Ag and Pd, respectively).

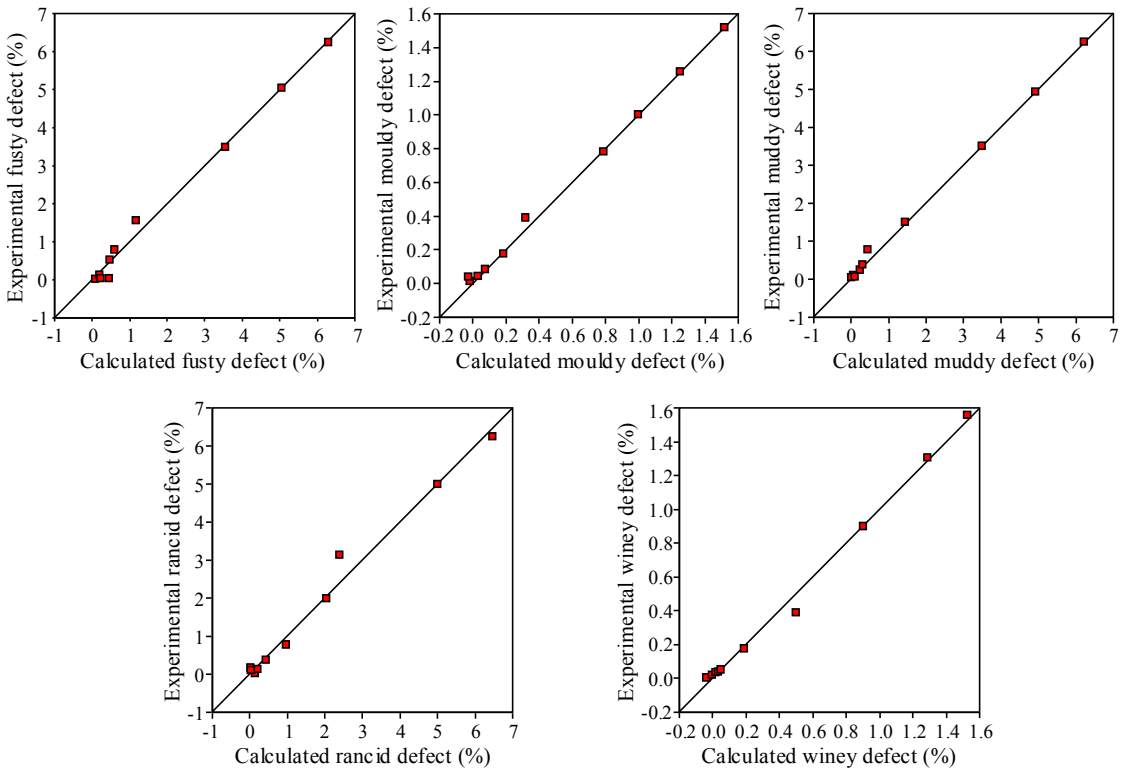

Fig. 6.7. Correlation plots of the calculated versus the experimental defect percentages.

Table 6.6. *r* values, average prediction errors (*av. err.*) and predictors selected with their corresponding non-standardized coefficients for the MLR models constructed to predict defect percentage.

		Fusty	Mouldy	Muddy	Rancid	Winey
	r	0.993	0.997	0.997	0.988	0.996
	Av. err.(%)	0.51	0.22	0.43	0.90	0.39
Predictors[a]	Constant	-651.19	14.74	-440.80	20.18	-66.64
	S1/S4	-	-	-	-61.24	-
	S3/S4	-	-	-	-	27.25
	S3/S6	-	-	-	37.81	-
	S4/S5	-	50.46	177.74	-	41.20
	S4/S6	657.69	-138.47	-	-	-
	S5/S6	-	75.27	271.62	-	-

[a] ratios of sensor signals.

CHAPTER 7

DEVELOPMENT OF METHODS FOR THE CLASSIFICATION OF EVOOS ACCORDING TO THEIR GENETIC VARIETY

7.1. Classification using FTIR spectroscopy data

The aim of this work was to construct an LDA model able to classify EVOOs according to their genetic variety by using FTIR data. In order to construct this LDA model, the EVOOs shown in **Table 7.1** were used. For this purpose, EVOO samples mainly produced at *La Comunitat Valenciana*, Spain, were used. Other samples, such as Hojiblanca and Picual, which were scarcely cultivated at *La Comunitat Valenciana*, were also included in this study because, jointly with the Arbequina variety, are the main varieties of the Spanish market.

7.1.1. Data treatment and construction of data matrices

To obtain the data, FTIR spectra were divided in the 20 wavelength regions which are described in **Table 7.2**. For each region, the peak/shoulder area was measured and used as original variables, which were normalized by normalization procedure B. A matrix containing 76 objects, which corresponded to the average of two replicates (**Table 7.1**), and 190 predictors, was constructed. A response column, containing the categories corresponding to the seven genetic varieties of the oils, was added to this matrix. Only the means of the replicates of the samples were included in this matrix. The matrix was randomly divided in two groups of samples to construct training and evaluation sets. The training set was composed by 6 samples for each genetic variety (6 x 7 = 42 objects), while the evaluation set was constituted with the remaining samples (34 objects).

Table 7.1. Genetic variety, number of samples, geographical origin and supplier of the EVOOs employed in this study.

Genetic variety	Nº of samples	Geographical origin	Supplier	Crop Season
Arbequina	2	Altura (Castellón)	Intercoop	06/07; 07/08
	2	Maestrat *comarca* (Castellón)	Intercoop	06/07; 07/08
	2	Alicante	Intercoop	05/06; 07/08
	2	Palancia *comarca* (Castellón)	Intercoop	06/07; 07/08
Borriolenca	3	Alcalatén *comarca* (Castellón)	Intercoop	05/06; 06/07; 07/08
	4	La Plana *comarca* (Castellón)	Intercoop	05/06; 06/07; 07/08
Canetera	3	Maestrat *comarca* (Castellón)	Intercoop	05/06; 07/08
	2	Adzaneta (Castellón)	Intercoop	06/07; 07/08
	3	La Plana *comarca* (Castellón)	Intercoop	05/06; 06/07; 07/08
Farga	4	Maestrat *comarca* (Castellón)	Intercoop	05/06; 06/07; 07/08
	3	Alcalatén *comarca* (Castellón)	Intercoop	06/07; 07/08
	3	La Plana *comarca* (Castellón)	Intercoop	05/06; 06/07; 07/08
Hojiblanca	2	Estepa (Sevilla)	Carbonell	06/07; 07/08
	2	Luque (Córdoba)	Coosur	06/07; 07/08
	3	Puente Genil (Córdoba)	Borges	06/07; 07/08
	5	Fuente de Piedra (Málaga)	G.Hojiblanca	05/06; 06/07; 07/08
	1	Santaella (Córdoba)	Columela	05/06
Picual	2	Martos (Jaén)	Carbonell	06/07; 07/08
	2	Villanueva del Arzobispo (Jaén) + Porcuna (Jaén)	Coosur	06/07
	3	Quesada (Jaén)	Borges	05/06; 06/07; 07/08
	1	Montoso (Córdoba)	Grupo Hojiblanca	06/07
	1	Tabernas (Almería)	Castillo de Tabernas	06/07
	1	Canena (Jaén)	Castillo de Canena	07/08
Serrana	9	Altura (Castellón)	Cooperativa Altura and Intercoop	05/06; 06/07; 07/08
	3	Artana (Castellón)	Intercoop	06/07; 07/08
	3	Jérica (Castellón)	Intercoop	06/07; 07/08
	5	Viver (Castellón)	Intercoop	05/06; 06/07; 07/08

Table 7.2. FTIR spectral regions selected as predictor variables for statistical data treatment.

Identification No.	Range, cm^{-1}	Functional group	Nominal frequency	Mode of vibration
1	2393-2347	Alcane [b]	-	-
2	2347-2279	Alcane [b]	-	-
3	1870-1712	-C=O (ester)	1746 [a]	stretching
4	1712-1693	-C=O (acid)	1711 [a]	stretching
5	1693-1671	-C=O	- [b]	stretching
6	1671-1590	-C=C- (cis)	1654 [a]	stretching
7	1467-1426	-C-H (CH_2)	1465 [b]	bending (scissoring)
		-C-H (CH_3)	1450 [b]	bending (asym)
8	1426-1407	=C-H (cis)	1417 [a]	bending (rocking)
9	1407-1380	=C-H	1400 [b]	bending
10	1380-1336	-C-H (CH_3)	1377 [a]	bending (sym)
		O-H	1359 [b]	bending (in plane)
11	1336-1309	non-assigned	1319 [a]	bending
12	1309-1292	=C-H (cis)	1294 [c]	bending
13	1292-1257	=C-H	- [c]	bending
14	1257-1216	-C-O	1238 [a]	stretching
		$-CH_2-$		bending
15	1216-1127	-C-O	1163 [a]	stretching
		$-CH_2-$	1163 [a]	bending
		-C-O	1138 [b]	stretching
16	1127-1109	-C-O	1118 [a]	stretching
17	1109-1045	-C-O	1097 [a]	stretching
18	1045-998	-C-O	1033 [a]	stretching
19	998-883	-HC=CH- (trans)	968 [a]	bending (out of plane)
		-HC=CH- (cis)?	914 [a]	bending (out of plane)
20	883-796	$=CH_2$	850 [b]	wagging

[a] According to Guillén (1998).

[b] According to Silverstein (1981).

[c] According to Yang (2005).

FTIR spectra of the 76 EVOO samples shown in **Table 7.1** were collected. The typical spectra of seven oils, corresponding to the seven different genetic varieties, are shown in **Fig. 7.1**. As it can be observed, the FTIR spectra were closely similar. In order to enhance small differences that were not appreciated straight away in the spectra of oils obtained from different genetic varieties, the peak areas of the 20 selected regions were conveniently handled by multivariate statistical techniques.

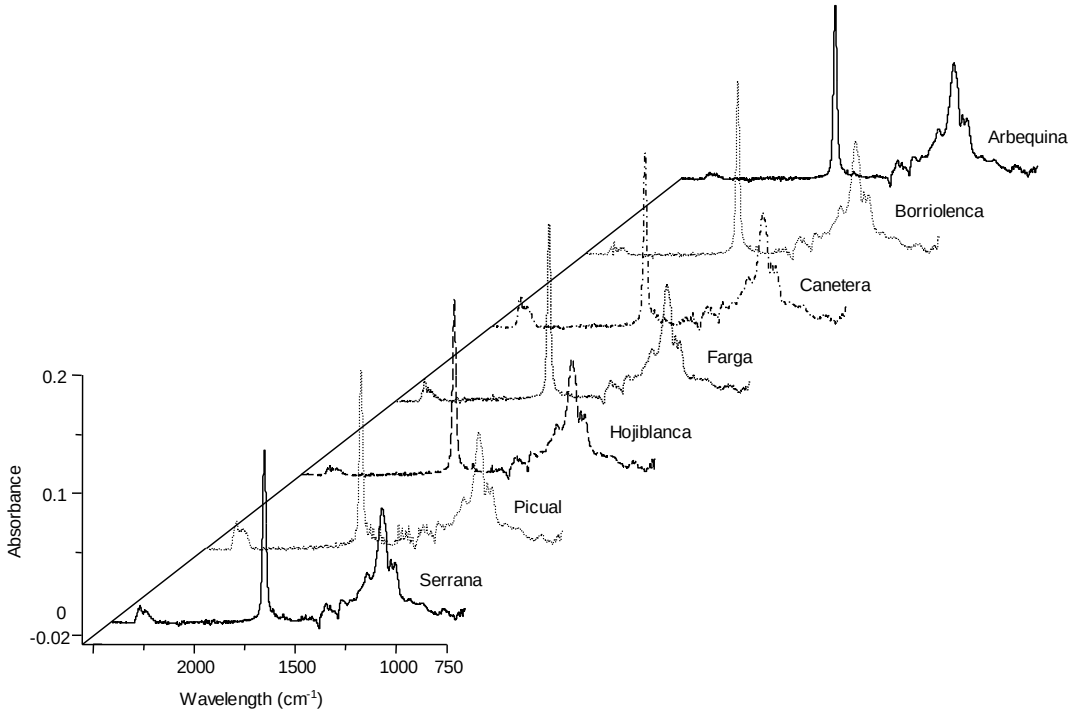

Fig. 7.1. FTIR spectra of EVOO samples of Arbequina from Alicante (crop season 05/06), Borriolenca from Alcalatén *comarca* (crop season 07/08), Canetera from La Plana *comarca* (crop season 06/07), Farga from Maestrat *comarca* (crop season 06/07), Hojiblanca from Luque, Córdoba (crop season 07/08), Picual from Martos, Jaén (crop season 06/07) and Serrana from Altura, Castellón (crop season 05/06).

7.1.2. Construction of LDA models

Using the normalized variables, an LDA model capable of classifying the EVOO samples according to their respective genetic variety was constructed. A good resolution between the seven categories was achieved (λ_w = 0.576). The variables selected by the SPSS stepwise algorithm, and the corresponding standardized coefficients of the model, are given in **Table 7.3**. According to this table, the main IR regions selected by the algorithm to construct the LDA model corresponded to -C=O (acid, stretching), -C-H (CH_2, bending scissoring), -C-H (CH_3, bending sym), =C-H (bending), -C-O (stretching) and -CH_2- (bending).

Table 7.3. Predictors selected and corresponding standardized coefficients of the LDA model constructed to predict the genetic variety of EVOOs.

Predictors[a]	f_1	f_2	f_3	f_4	f_5	f_6
1/5	0.13	-0.91	-0.96	-0.06	-0.60	-2.04
1/7	5.85	4.36	-1.51	4.00	4.07	-2.22
1/9	-6.01	-3.57	3.91	-3.71	-3.11	4.03
3/6	-0.13	0.30	0.47	0.58	0.95	0.76
4/12	9.48	15.43	12.74	16.47	-7.05	-6.22
4/14	-9.00	-14.54	-12.66	-16.58	7.15	6.35
12/15	0.85	1.32	1.25	1.30	-0.89	0.35
13/16	-0.28	-0.55	0.69	-0.11	1.03	-0.48
14/17	1.06	-0.10	-0.37	-0.32	-0.41	0.43

[a] Pairs of wavelength regions identified according to **Table 7.2**.

The projections of the samples on the six discriminant functions allowed the distinction of at least a different category with respect to the other categories. As shown in **Fig. 7.2A**, a large resolution between Farga, Picual and the group formed by the other categories was achieved along f_1. On the other hand, the variance gathered by f_2 was mainly associated to the resolution between Picual

and the rest of categories as a whole. According to **Fig. 7.2B**, Canetera, Picual and Hojiblanca were resolved from the rest of categories along f_3. Finally, **Fig. 7.2C**, shows a score plot projected on an oblique plane of the 3-D space defined by the three first discriminant functions.

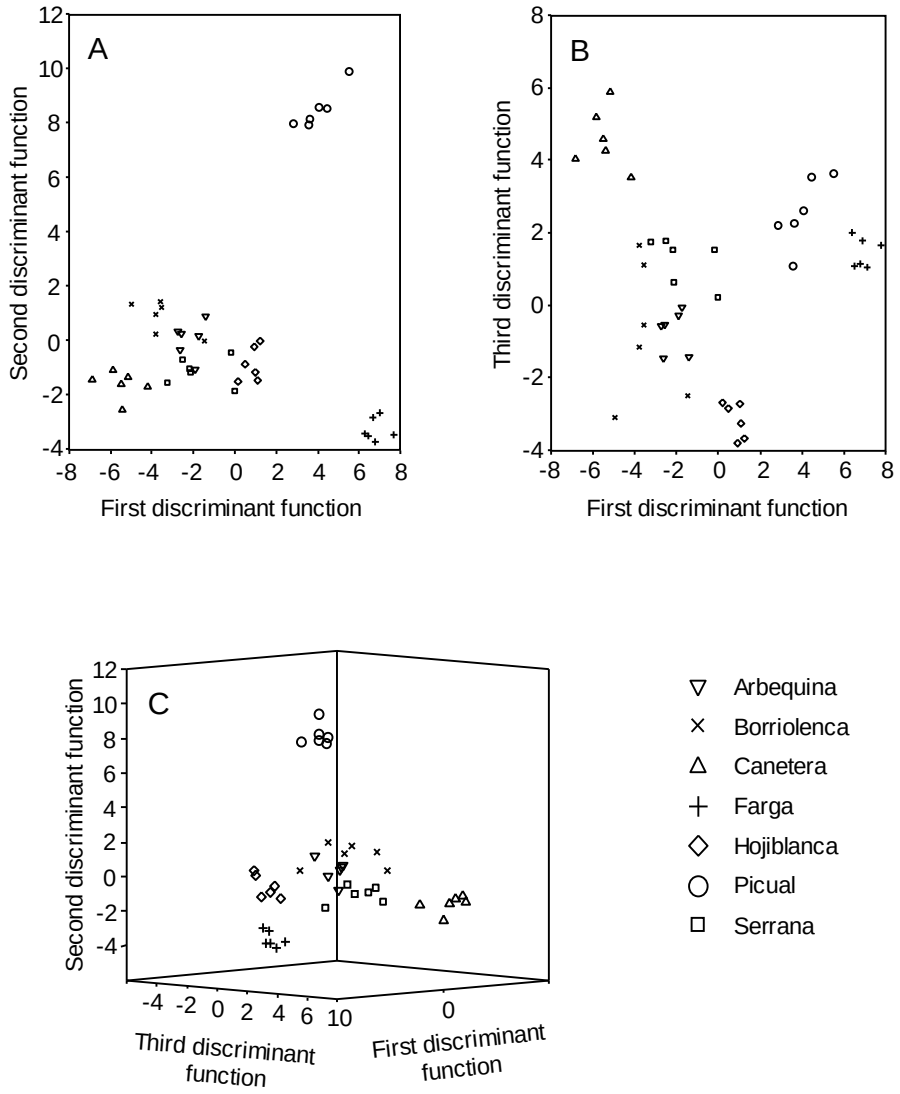

Fig. 7.2. Score plots on the planes of the first and second (A), and first and third discriminant functions (B), and projected on oblique plane of the 3-D space defined by the three discriminant functions (C) of the LDA model constructed to classify EVOOs according to their genetic variety.

When this 3-D figure was rotated, a good resolution between all the category pairs was evidenced. When leave-one-out validation was applied to the training set, all the points were correctly classified. Concerning the evaluation set, all the objects were correctly assigned with an assignment probability higher than 95%, except 4 objects, which corresponded to Borriolenca (2 samples), Hojiblanca (1 sample) and Arbequina (1 sample) varieties.

7.2. Classification using fatty acid and phenolic compound profiles established by direct infusion MS

The aim of this work was to develop a simple and quick method, based on direct infusion MS, capable of classifying Spanish EVOOs according to their genetic variety. For this purpose, EVOOs samples from the three most common monovarietal EVOOs in the Spanish market, Hojiblanca, Arbequina and Picual, were used (see **Table 7.4**).

According to Ríos (2005) and Tripoli (2005), the peaks of seven fatty acids and 28 phenolic compounds were selected as original variables. The selected compounds, and the *m/z* values of the corresponding $[M-H]^-$ peaks, are indicated in **Table 7.5**. Owing to the coincidence of the *m/z* values of several phenolic compounds, these were jointly measured; then, a total of 20 peaks were obtained to be used as variables.

The peak profiles of oils of the three genetic varieties are compared in **Fig. 7.3**. In this figure, and in order to make comparison easier, the spectra were standardized by dividing each peak abundance by the abundance of C16:0 peak; further, the peak of C18:1 (oleic acid), which is the most intense signal in all the genetic varieties, was tailored at 1.2. In this way, the differences between the fatty acid profiles of the three genetic varieties were enhanced. The C18:1 peak intensities, which are not appreciated in the figure due to the indicated cut off,

followed the decreasing order: Hojiblanca > Picual > Arbequina. In comparison to oleic acid, the signals of palmitic, linoleic and stearic acids showed intermediate intensities. The stearic acid peak intensity (C18:0) was lower for Arbequina than for the Hojiblanca and Picual oils, and the intensities of the linoleic acid peak (C18:2) showed the decreasing order: Arbequina > Hojiblanca > Picual.

The peaks of many phenolic compounds were also identified in the MS spectra; however, the intensity of these peaks was several orders of magnitude lower than that of the fatty acids. The spectrum of a Picual oil, with an expanded vertical axis, is shown in **Fig. 7.4**. Similar spectra, showing small differences among the peak profiles, were obtained for the Arbequina and Hojiblanca oils.

Table 7.4. Genetic variety, number of samples, geographical origin and brand of the EVOO samples.

Genetic variety	Nº of samples	Geographical origin	Brand
Arbequina	2	Aguadulce (Sevilla)	Carbonell
	2	Vila Franca del Penedés (Barcelona)	Torrereal
	2	Les Garrigues (Lleida)	Oleastrum
	1	Estepa (Sevilla) + La Roda de Andalucía (Sevilla)	Coosur
	1	Antequera (Málaga)	Grupo Hojiblanca
	2	Huelva + Zaragoza + Palma del Río (Córdoba)	Borges
	1	Les Garrigues (Lleida)	Romanico
	1	La Puebla Nueva (Toledo)	Valderrama
	1	Sarroca de Lleida (Lleida)	Veá
	1	Mallorca	Aubocassa
	1	La Rioja	Rihuelo
Hojiblanca	2	Estepa (Sevilla)	Carbonell
	2	Luque (Córdoba)	Coosur
	3	Puente Genil (Córdoba)	Borges
	5	Fuente de Piedra (Málaga)	Grupo Hojiblanca
	1	Santaella (Córdoba)	Columela
Picual	2	Martos (Jaén)	Carbonell
	2	Villanueva del Arzobispo (Jaén) + Porcuna (Jaén)	Coosur
	3	Quesada (Jaén)	Borges
	1	Montoso (Córdoba)	Grupo Hojiblanca
	1	Tabernas (Almería)	Castillo de Tabernas
	1	Canena (Jaén)	Castillo de Canena

Table 7.5. $[M-H]^-$ peaks of the selected fatty acids and phenolic compounds.

Compound (acronym)	*m/z*
Myristic acid (C14:0)	227
Palmitoleic acid (C16:1)	253
Palmitic acid (C16:0)	255
Linolenic acid (C18:3)	277
Linoleic acid (C18:2)	279
Oleic acid (C18:1)	281
Stearic acid (C18:0)	283
TY	137
p-Hydroxybenzoic acid	137
Cinnamic acid	147
p-Hydroxyphenylacetic acid	151
p-Anisic acid	151
HYTY	153
Gentisic acid	153
Protocatechuic acid	153
Coumaric acid	163
Vanillic acid	167
Gallic acid	169
Caffeic acid	179
Homovanillic acid	181
Ferulic acid	193
Syringic acid	197
Sinapic acid	223
EA	241
Dialdehydic form of deacetoxy ligstroside	303
Deacetoxy ligstroside aglycone	303
Dialdehydic form of deacetoxy oleuropein	319
Deacetoxy oleuropein aglycone	319
Pinoresinol	357
Dialdehydic form of ligstroside	361
LAg	361
Dialdehydic form of oleuropein	377
OA	377
10-Hydroxy-oleuropein aglycone	393
AcPIN	415

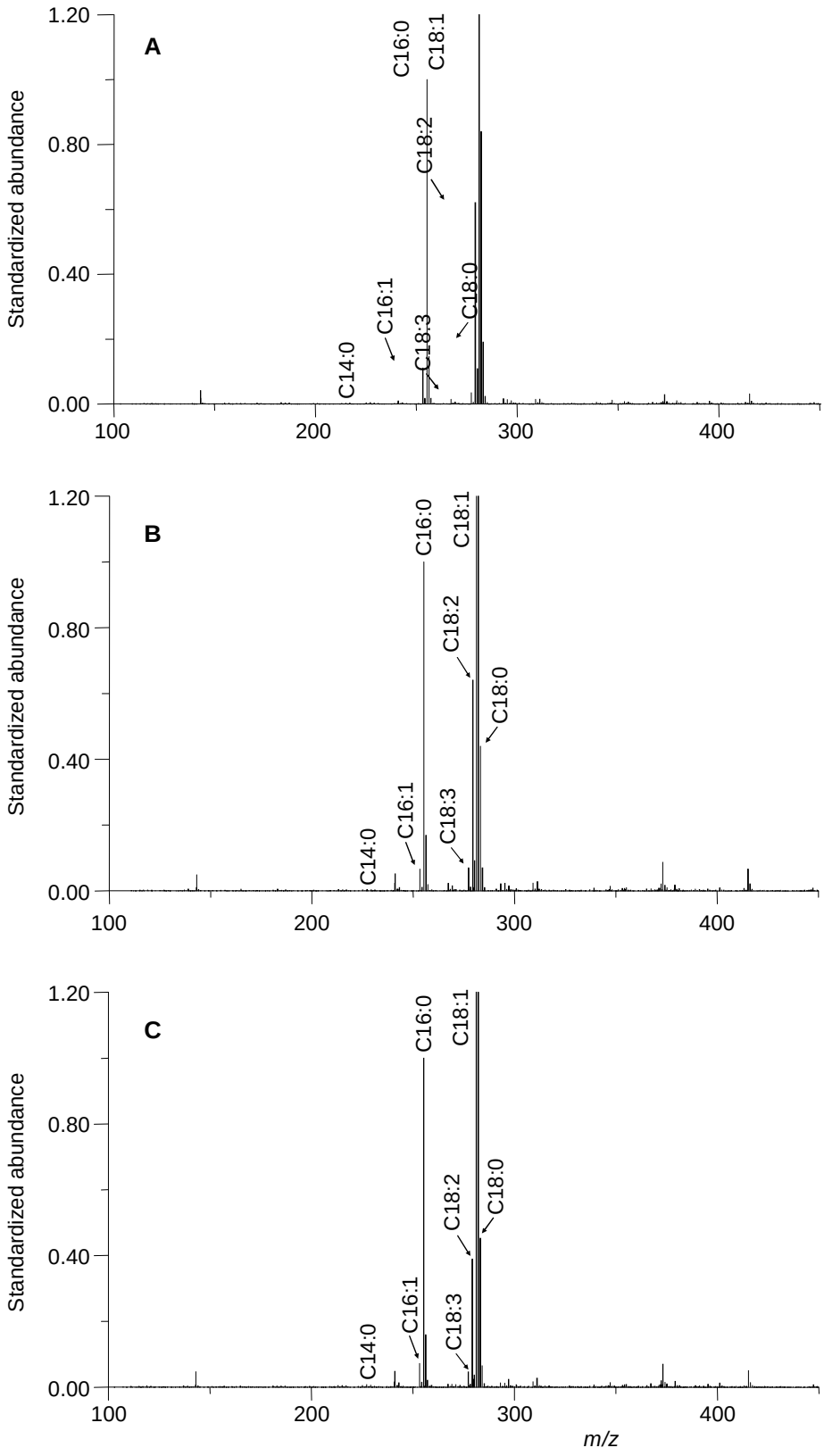

Fig. 7.3. Standardized mass spectra of EVOOs of the three genetic varieties: (A) Arbequina, (B) Hojiblanca and (C) Picual. The intensity of all peaks was divided by the intensity of the C16:0 peak and the C:18:1 peak was tailored at 1.2.

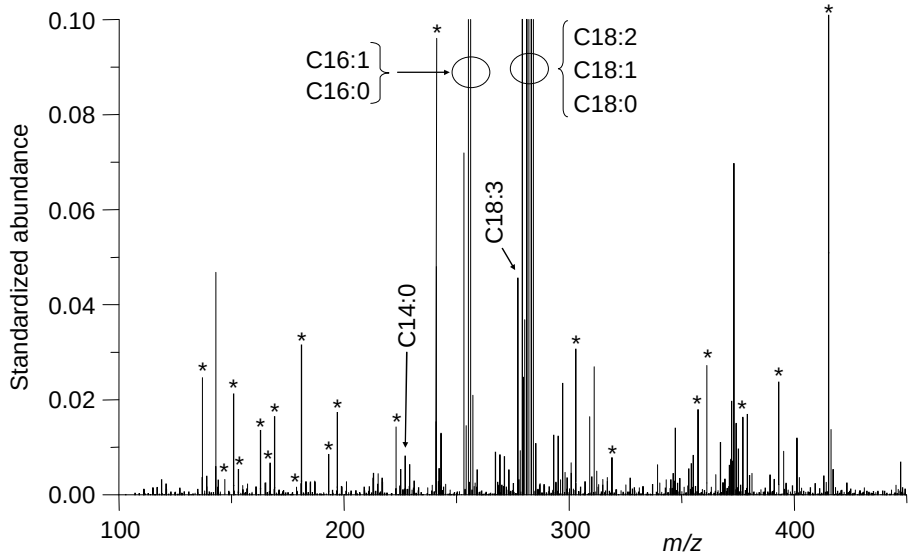

Fig. 7.4. Standardized mass spectrum of a Picual olive oil sample with the vertical axis tailored at 0.1. The peaks of the phenolic compounds of **Table 7.5** are indicated with an asterisk.

7.2.1. Construction of data matrices and LDA models

Owing to the large differences observed between the peak intensities, peaks were divided in two groups, fatty acids and phenolic compounds, and both normalization procedures A and B were independently applied to each group. Then, for the fatty acids, 7 and 21 normalized variables were obtained by normalization procedures A and B, respectively. Similarly, for the phenolic compounds, 20 and 190 normalized variables were respectively obtained.

The 38 samples of the monovarietal EVOOs of **Table 7.4** were used to construct LDA models capable of classifying the EVOO samples according to their genetic variety. To construct the data matrices, each oil sample was injected in two different days, and each day four replicates were accomplished. Two matrices containing 304 injections, and a total of 27 or 211 predictors (according to normalization procedures A and B, respectively) were constructed. A response column, containing the three categories corresponding to the three genetic varieties, was added to the matrices. These matrices were used both to construct

LDA training matrices and to provide evaluation sets. Only the means of the replicates of the samples were included in the training matrices, whereas all the individual injections of the samples were included in the evaluation set.

Initially, the capability for the classification of the studied EVOOs according to their genetic variety, using fatty acids or phenolic compounds, was tested. Both normalization procedures were tried. Normalization procedure B, which led to a better resolution between the category pairs, was selected for further studies. Then, an LDA model constructed exclusively with the ratios of fatty acids showed a clear separation between the three genetic varieties (λ_w = 0.396). The model was constructed with 7 variables, showing the ratios 279/283 and 279/281 predominant weights. All samples were correctly classified. On the other hand, the phenolic compounds were used to construct another LDA model. In this case, 22 variables were selected (λ_w = 0.236); however, resolution between the category pairs was slightly worse than that obtained with the fatty acids. The variables showing predominant weights were 303/241, 303/193 and 393/241. Then, the two sets of variables (fatty acids and phenolic compounds) were jointly used to construct another LDA model. A model with 30 predictors was obtained. Thus, in order to reduce the entrance of predictors in the model, the probability values F_{in} = 0.01 and F_{out}, = 0.20 were used. Now, only 11 predictors were included in the model. An excellent resolution between the three categories was obtained (λ_w = 0.237). A score plot on the plane of the two discriminant functions is shown in **Fig. 7.5**.

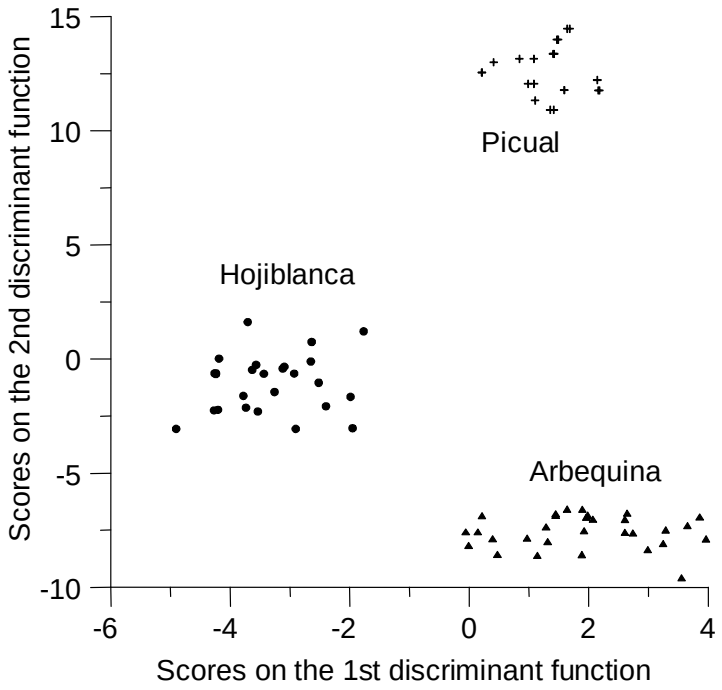

Fig. 7.5. Score plot on the plane of the two LDA discriminant functions obtained to predict EVOO genetic variety after data normalization by procedure B.

The predictors selected by the SPSS stepwise algorithm and the corresponding standardized coefficients of the model are given in **Table 7.6**. The model was used to classify the samples of the evaluation set. Using a 95% probability, all the objects were correctly assigned; thus, the prediction capability was 100%.

Table 7.6. Predictors selected and corresponding standardized coefficients of the LDA model constructed to predict the genetic variety of EVOOs.

Compounds	Predictors[a]	f_1	f_2
Fatty acids	227/279	-0.40	2.78
	227/281	0.63	-1.98
	255/279	-0.32	0.45
	277/279	-1.21	0.16
	279/281	0.35	0.70
	281/283	0.81	1.08
Phenolic compounds	193/167	0.83	0.22
	223/181	0.67	-0.02
	303/197	-0.27	-0.82
	415/197	0.87	0.52
	361/223	-0.28	-0.70

[a] *m/z* values of the ratios of abundances of peak pairs.

7.3. Classification using sterol profiles established by HPLC-MS

The aim of this work was to develop an HPLC-MS method that, jointly with LDA, was able to predict the genetic variety of EVOOs according to six different genetic varieties produced at *La Comunitat Valenciana*, Spain. The sterol profiles were used to classify the samples. The EVOO employed in this study, which covered different crop seasons and geographical origins in order to assure a correct sampling, are shown in **Table 7.7**.

Table 7.7. Genetic variety, number of samples, geographical origin and crop season of the EVOOs employed in this study.

Genetic variety	Nº of samples	Geographical origin	Crop Season
Arbequina	2	Altura (Castellón)	06/07; 07/08
	2	Maestrat *comarca* (Castellón)	06/07; 07/08
	1	Alicante	05/06
	1	Palancia *comarca* (Castellón)	07/08
Borriolenca	3	Alcalatén *comarca* (Castellón)	05/06; 06/07; 07/08
	3	La Plana *comarca* (Castellón)	05/06; 06/07; 07/08
Canetera	2	Maestrat *comarca* (Castellón)	05/06; 07/08
	2	Adzaneta (Castellón)	06/07; 07/08
	2	La Plana *comarca* (Castellón)	05/06; 07/08
Farga	2	Maestrat *comarca* (Castellón)	05/06; 06/07
	2	Alcalatén *comarca* (Castellón)	06/07; 07/08
	2	La Plana *comarca* (Castellón)	05/06; 07/08
Picual	6	Altura (Castellón)	05/06; 06/07; 07/08
Serrana	2	Altura (Castellón)	06/07; 07/08
	1	Artana (Castellón)	06/07
	1	Jérica (Castellón)	07/08
	2	Viver (Castellón)	05/06; 07/08

7.3.1. Optimization of the separation conditions

For each sterol standard used in this study (erythrodiol, β-sitosterol, campesterol, ergosterol and stigmasterol), two peaks, corresponding to $[M+H]^+$ and $[M+H-H_2O]^+$ ions, were observed. However, as previously reported (Cañabate-Díaz, 2007; Lerma-García, 2008; Segura-Carretero, 2008), the $[M+H-H_2O]^+$ peaks showed higher intensities than the respective $[M+H]^+$ peaks. For this reason, only the intensities of the $[M+H-H_2O]^+$ peaks were used for identification and classification. Different gradient elutions using ACN/water mixtures, all containing 0.01% acetic acid, at a constant flow rate of 1.0 mL min^{-1}, were tried. As a result of this study, the linear gradient that provided the best

separation/analysis time ratio was achieved with 90 to 100% ACN for 10 min followed by isocratic elution with 100% ACN for 2 more min. **Fig. 7.6** shows a chromatogram of sterol standards obtained using this gradient. As observed, the total analysis time was 10 min, which was much lower than that reported for sterol separation using GC-FID. On the other hand, an overlapping between campesterol and stigmasterol peaks was observed in all the gradient elutions tried. The overlapping of these two peaks was already reported in other HPLC studies (Sanchéz-Machado, 2004).

Then, all EVOO extracts were injected using the selected optimal conditions. In order to identify other sterol peaks present in the samples, the EICs at the *m/z* values of **Table 7.8**, were obtained. A total of 9 peaks, corresponding to 12 possible sterols, were identified in less than 10 min. The TIC and EICs of two EVOO extracts of the genetic varieties Canetera and Serrana are shown in **Fig. 7.7A** and **B**, respectively. Several differences between the peak profiles of both varieties were evidenced. A quantitative study of the sterols found in the EVOOs is shown in **Table 7.9**. In general, the levels of sterols found in these samples are in good agreement with data reported in literature (Jee, 2002). As shown in this table, several differences between the different genetic varieties were found. Compared to literature, a similar sterol separation performance was observed (Segura-Carretero, 2008); however, lower analysis times were reported in this work (Cañabate-Díaz, 2007; Segura-Carretero, 2008; Martínez-Vidal, 2007).

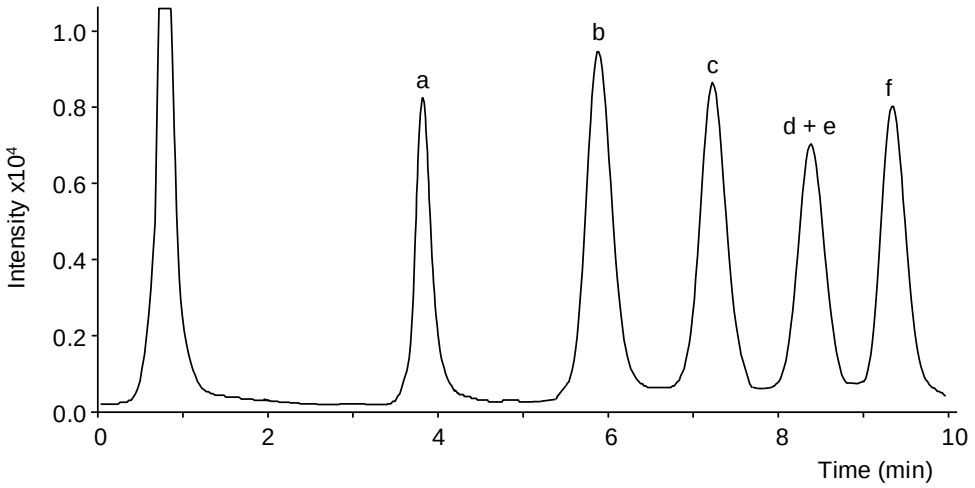

Fig. 7.6. TIC of a standard solution of sterols (*ca.* 100 mg L^{-1}) obtained by using a linear gradient from 90 to 100% ACN for 10 min followed by isocratic elution with 100% ACN for 2 more min. Peak identification: (a) erythrodiol, (b) ergosterol, (c) cholesterol, (d) campesterol, (e) stigmasterol and (f) β-sitosterol.

Table 7.8. Peak labelling, retention time (t_r) and *m/z* value of the sterols studied in this work.

Peak no	Analytes	t_R (min)	*m/z*[a]
1	Erythrodiol	3.90	425
2	Uvaol	3.90	425
3	Brassicasterol	6.10	381
4	Cholesterol	7.25	369
5	Δ^7-Avenasterol	7.25	395
6	Δ^5-Avenasterol	7.25	395
7	Campesterol	8.30	383
8	Campestanol	8.30	385
9	Stigmasterol	8.40	395
10	$\Delta^{5,24}$-Stigmastadienol	9.30	395
11	Δ^7-Stigmastenol	9.40	397
12	β-Sitosterol	9.40	397

[a] *m/z* value corresponding to the $[M+H-H_2O]^+$ peak.

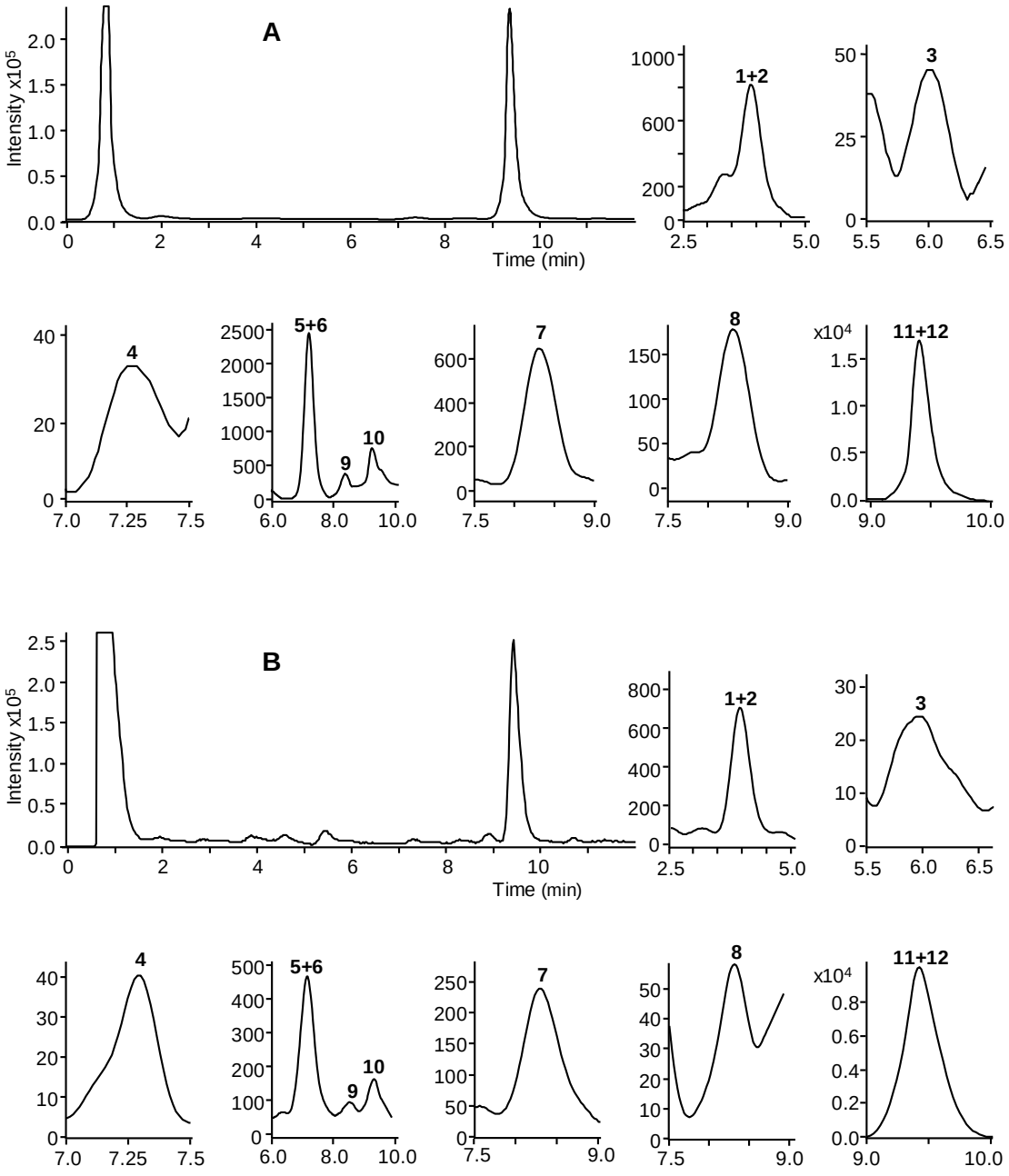

Fig. 7.7. TIC and EICs of Canetera (A) and Serrana (B) EVOO sterol extracts. The EICs were obtained at the *m/z* values indicated in **Table 7.8**. Peak labelling as indicated in **Table 7.8**. Other experimental conditions as in **Fig. 7.6**.

Table 7.9. Proportions of sterols found in the total sterol fraction of EVOOs of different genetic varieties.

Sterol	Arbequina	Borriolenca	Canetera	Farga	Picual	Serrana
Erythrodiol + Uvaol	0.1–0.3	0.0–0.09	2.0–4.0	0.0–0.4	0.2–0.6	5.0–7.7
Brassicasterol	0.08–0.11	0.06–0.09	0.06–0.12	0.09–0.12	0.1–0.2	0.08–0.15
Cholesterol	0.3–0.6	0.3–0.5	0.1–0.2	0.1–0.5	0.4–0.5	0.2–0.4
Δ^7- + Δ^5-Avenasterol	12.1–14.9	7.0–9.9	11.5–12.3	7.8–9.5	4.3–13.2	5.1–6.4
Campesterol	3.7–4.0	3.2–3.7	3.0–3.5	3.2–3.6	2.5–3.1	1.8–2.4
Campestanol	0.2–0.4	0.2–0.3	0.5–0.9	0.2–0.3	0.2–0.3	0.3–0.6
Stigmasterol	0.7–1.5	1.2–2.8	1.5–2.0	1.1–1.9	0.9–1.5	1.0–2.5
$\Delta^{5,24}$-Stigmastadienol	0.7–1.9	0.6–1.0	3.0–3.7	0.8–1.0	0.9–1.3	1.0–1.5
Δ^7-Stigmastenol + β-Sitosterol	76.0–80.0	79.0–82.3	75.0–77.8	78.7–90.8	77.3–90	81.0–82.7

[a] ND = not detected.

7.3.2. Construction of data matrices and LDA models

The original variables were measured on the EICs of the samples. The EICs were previously smoothed using a Gaussian filter set at 5 points, and the peak area of each sterol was measured and normalized by procedure B. In this way, a total of 36 normalized variables were obtained to be used as predictors.

Using the 36 samples of **Table 7.7**, a matrix containing 72 injections (all samples were injected twice) and the 36 predictors, was first constructed. A response column, containing the six categories corresponding to the six genetic varieties of the EVOOs, was added to this matrix. This matrix was used as evaluation set. Only the means of the replicates of the samples were included in the training matrices (36 objects). To classify the EVOOs according to the six genetic varities of **Table 7.7**, an LDA model was constructed. In this case, the SPSS default values of F_{in} and F_{out}, 3.84 and 2.71, respectively, were used. With this model, the categories Arbequina, Borriolenca and Picual appeared clearly resolved from each other, and were also well separated from the other three categories (Canetera, Farga and Serrana), which overlapped (data not shown). For this reason, a new LDA model was constructed in which these three categories were grouped in a single one. An excellent resolution between these four categories (Arbequina, Borriolenca, Picual and the one formed by the other three categories) was obtained (**Fig. 7.8**, $\lambda_w = 0.290$). The variables selected by the SPSS stepwise algorithm and the corresponding model standardized coefficients are given in **Table 7.10**. All the points of the training set were correctly classified by leave-one-out cross-validation. The evaluation set, containing the 72 original data points, was used to check the prediction capability of the model. Using a 95% probability, only 3 objects corresponding to replicates of different samples (1 Borriolenca, 1 Canetera and 1 Farga) were not correctly assigned; thus, the prediction capability was higher than 95%.

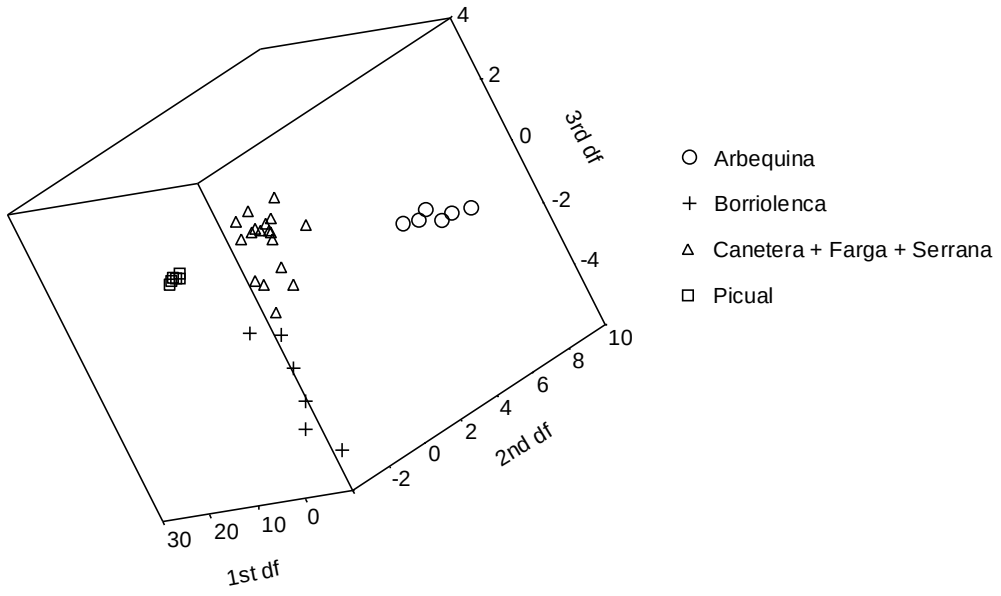

Fig. 7.8. Score plot on an oblique plane of the 3-D space defined by the three discriminant functions of the LDA model constructed to resolve the Arbequina, Borriolenca, Picual and Canetera + Farga + Serrana categories.

Next, the Arbequina, Borriolenca and Picual categories were removed from the training set, and the remaining categories (Canetera, Farga and Serrana) were used to construct another LDA model. Now, the three categories were separated with an excellent resolution (**Fig. 7.9**, λ_w = 0.209). The variables selected and the corresponding model standardized coefficients are also given in **Table 7.10**. All the points of the training set were correctly classified by leave-one-out cross-validation. To estimate the prediction capability of this model, the evaluation set, constituted now by 36 original data points, was used. Using a 95% probability, only 2 objects, which corresponded to replicates of different samples (1 Canetera and 1 Farga), were not correctly assigned; thus, the prediction capability was higher than 88%.

Table 7.10. Predictors selected and the corresponding standardized coefficients of the two sequential LDA models constructed to predict the genetic variety of EVOOs.

Predictor[a]	*Arbequina/Borriolenca/ Picual/ Canetera + Farga + Serrana*			*Canetera/ Farga/ Serrana*	
	f_1	f_2	f_3	f_1	f_2
(1+2)/3	-1.65	0.48	0.02	-2.08	1.32
(1+2)/(5+6)	2.62	-1.12	-0.95	3.86	-3.08
(1+2)/7	3.82	7.47	-0.12	2.13	-1.44
(1+2)/9	-3.30	5.65	-1.29	-5.16	11.45
(1+2)/10	-12.61	-5.83	6.49	12.83	-0.58
(1+2)/(11+12)	24.16	2.47	-5.37	-15.50	1.49
(11+12)/3	-0.80	1.44	2.45	3.60	-1.00
(11+12)/(5+6)	-2.08	0.74	-0.36	-3.59	0.99
(11+12)/7	-4.47	-1.08	-0.13	-	-
(11+12)/9	6.36	-2.86	5.84	4.63	-11.39
(11+12)/10	2.00	0.06	-1.84	3.18	4.81
3/(5+6)	3.27	-2.38	7.39	-	-
3/7	0.83	-7.68	0.54	-	-
3/9	0.93	-0.36	-3.68	-	-
3/10	-20.81	6.40	-6.09	-	-
(5+6)/9	-4.79	-1.77	-0.78	-	-
(5+6)/10	2.79	1.58	0.40	-	-
9/10	4.19	1.25	-0.39	6.51	1.91

[a] *m/z* values of the ratios of sterol peaks labelled as in **Table 7.8**.

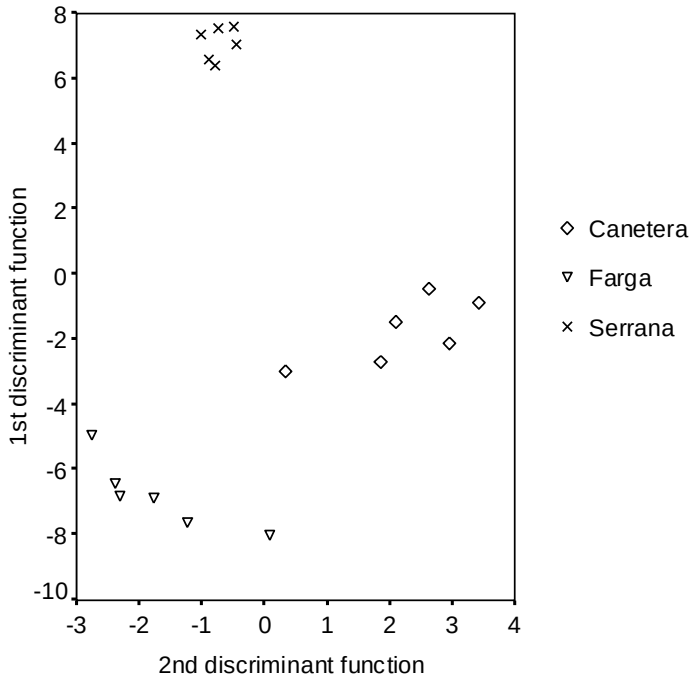

Fig. 7.9. Score plot on the plane of the two discriminant functions of the LDA model constructed to resolve the Canetera, Farga and Serrana categories.

7.4. Classification using sterol profiles established by UPLC-MS

The aim of this work was to obtain an LDA model capable of classifying EVOOs produced at *La Comunitat Valenciana*, Spain, according to their genetic variety. For this purpose, sterol profiles obtained by the UPLC-MS method developed in section 4.5, and the samples shown in **Table 7.7**, were used.

The representative TIC of the sterol standard mixture (*ca.* 50 mg L^{-1}), obtained under the optimal working conditions, is given in **Fig. 4.20B**. As evidenced, the sterol peaks were separated with satisfactory efficiency and resolution in a short analysis time. Under these conditions, all EVOO extracts from different genetic varieties were injected. As indicated in section 4.5, the signals of other sterols different from those used as standards, which were expected in the samples, were also recorded (see **Table 4.15**). As can be deduced

from this table, only 11 sterols or combination of sterol peaks could be distinguished, and then measured. The TIC and SIR chromatograms of two EVOO extracts of the genetic varieties Borriolenca and Farga are shown in **Fig. 7.10** and **7.11**, respectively. Several differences between the peak profiles of both varieties were evidenced. Differences between these varieties and the other varieties were also observed (data not shown).

7.4.1. Construction of data matrices and LDA models

As indicated above, the 11 peaks were measured and used as original variables. These variables were normalized by normalization procedure B, giving a total of 55 predictors to be used in LDA model construction. Then, using these predictors and the 42 samples of **Table 7.7**, a matrix containing 126 injections (all samples were injected three times) and the 55 predictors, was constructed. A response column, containing the seven categories corresponding to the seven genetic varieties of the EVOOs was added to this matrix. This matrix was used as evaluation set. Only the means of the replicates of the samples were used in the construction of the LDA training matrices (42 objects).

To classify the EVOOs according to the seven genetic varieties of **Table 7.7**, an LDA model was constructed. With this model, the categories Arbequina, Borriolenca and Canetera appeared clearly resolved from each other, and were also well separated from the other four categories (Farga, Hojiblanca, Picual and Serrana), which overlapped (data not shown). For this reason, a new LDA model was constructed in which the four non-resolved categories were grouped in a single one. An excellent resolution between the four categories Arbequina, Borriolenca, Canetera and the one formed by the other four categories was obtained (**Fig. 7.12**, $\lambda_w = 0.319$). The variables selected by the SPSS stepwise algorithm, and the corresponding model standardized coefficients, are given in

Table 7.12. All the points of the training set were correctly classified by leave-one-out cross-validation. The evaluation set, containing the 126 original data points, was used to check the prediction capability of the model. Using a 95% probability, only 3 objects corresponding to replicates of different samples (1 Arbequina, 1 Borriolenca and 1 Canetera) were not correctly assigned; thus, the prediction capability was higher than 97%.

Next, the Arbequina, Borriolenca and Canetera categories were removed from the training set, and the remaining categories (Farga, Hojiblanca, Picual and Serrana) were used to construct another LDA model. Now, the four categories were separated with an excellent resolution (**Fig. 7.13**, $\lambda_w = 0.368$). The variables selected and the corresponding model standardized coefficients are also given in **Table 7.11**. All the points of the training set were correctly classified by leave-one-out cross-validation. To estimate the prediction capability of this model, the evaluation set, constituted now by 72 original data points, was used. Using a 95 % probability, only 1 object, which corresponded to a replicate of a Picual sample, was not correctly assigned; thus, the prediction capability was higher than 98%.

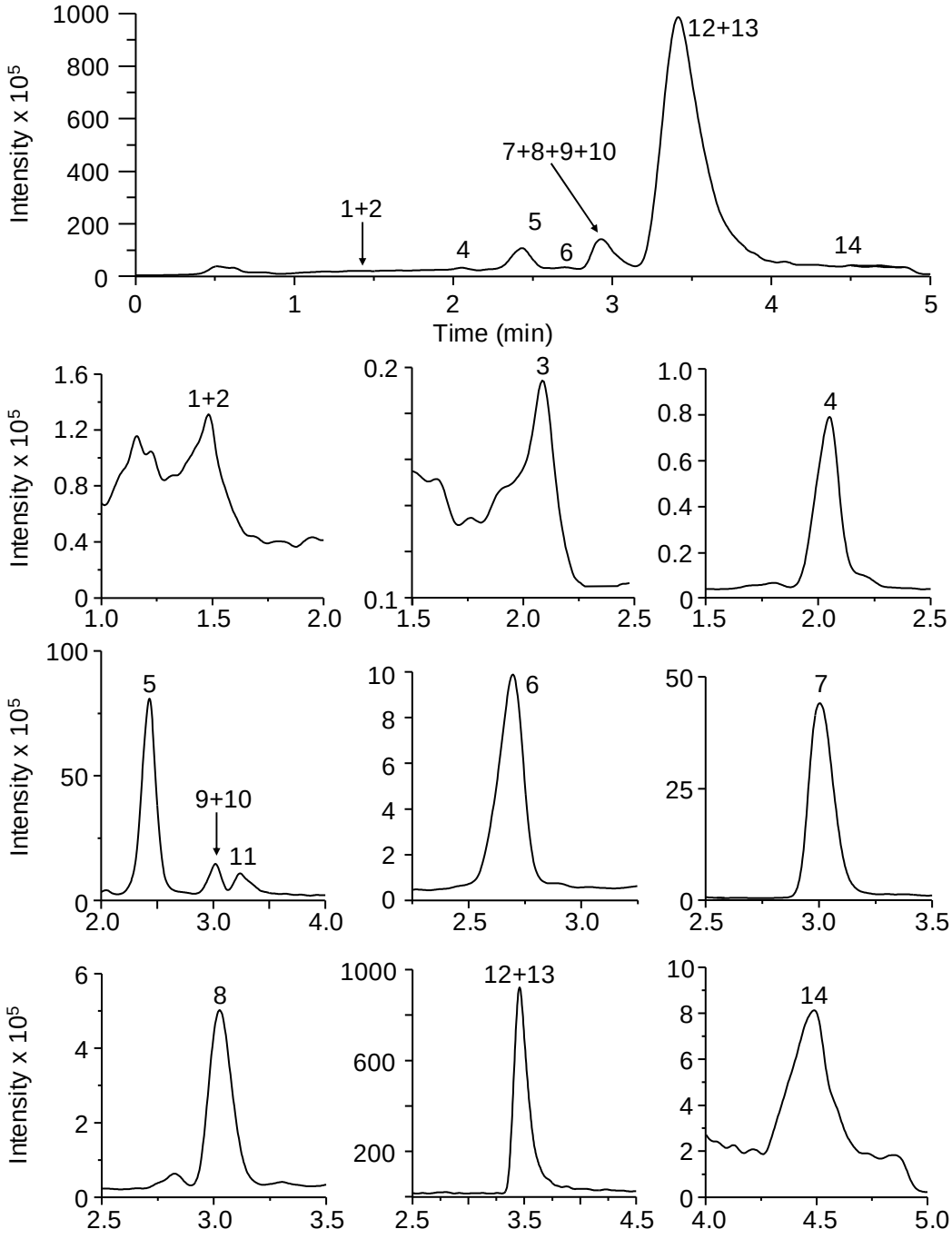

Fig. 7.10. TIC and SIR chromatograms of a Borriolenca EVOO extract. Chromatographic conditions: linear gradient from 80 to 100% ACN for 0.5 min, followed by isocratic elution with 100% ACN for 4.5 more min; flow rate, 0.8 mL min^{-1}; column temperature, 10 ºC. Peak identification as indicated in **Table 4.15**.

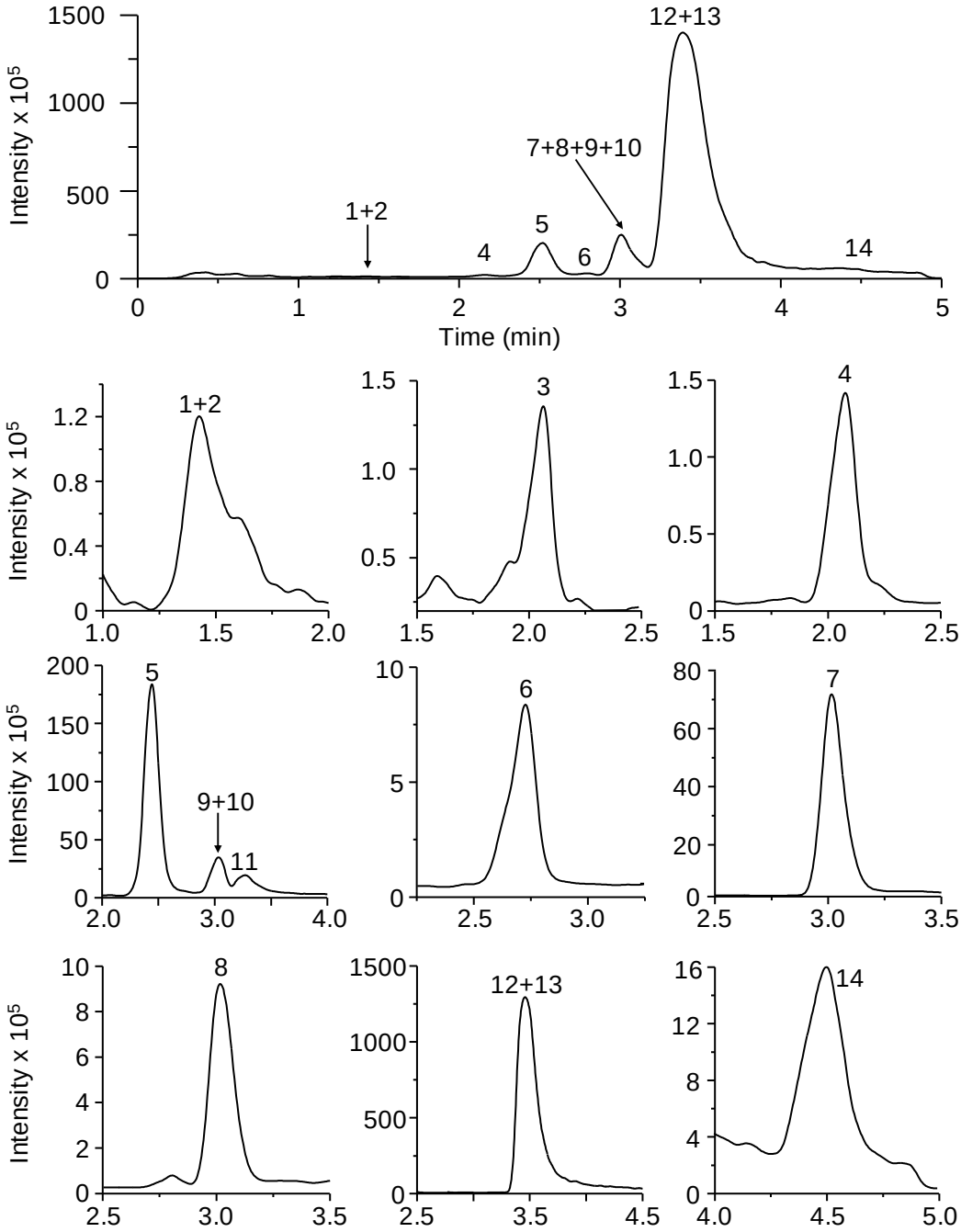

Fig. 7.11. TIC and SIR chromatograms of a Farga EVOO extract. Other experimental conditions as in **Fig. 7.10**.

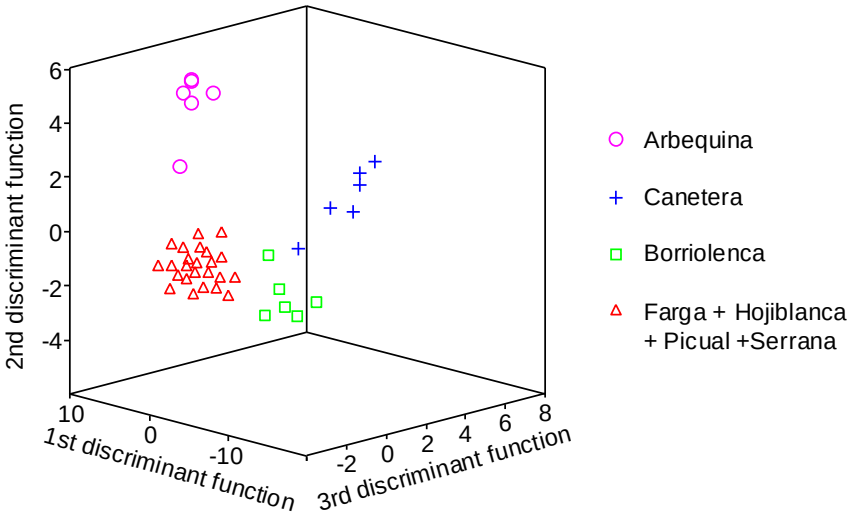

Fig. 7.12. Score plot on an oblique plane of the 3-D space defined by the three discriminant functions of the LDA model constructed to resolve the Arbequina, Borriolenca, Canetera and Farga + Hojiblanca + Picual + Serrana categories.

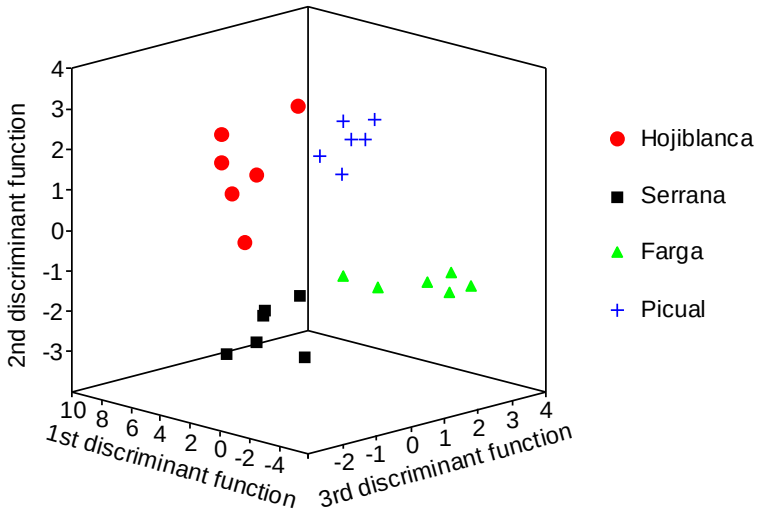

Fig. 7.13. Score plot on an oblique plane of the 3-D space defined by the three discriminant functions of the LDA model constructed to resolve the Farga, Hojiblanca, Picual and Serrana categories.

Table 7.11. Predictors selected and the corresponding standardized coefficients of the two sequential LDA models constructed to predict the genetic variety of EVOOs.

	Arbequina/ Borriolenca/ Canetera/ Farga + Hojiblanca + Picual + Serrana			*Farga/ Hojiblanca/ Picual/ Serrana*		
Predictor[a]	f_1	f_2	f_3	f_1	f_2	f_3
(1+2)/3	0.06	1.09	0.46	0.20	-0.74	-0.91
(1+2)/4	-	-	-	1.37	-1.22	2.45
(1+2)/5	-	-	-	-2.37	2.71	-0.25
(1+2)/6	-	-	-	-2.65	0.06	0.82
(1+2)/7	-	-	-	0.79	1.42	11.66
(1+2)/8	-	-	-	-8.55	3.04	-11.12
(1+2)/(9+10)	-	-	-	1.62	-1.36	-4.23
(1+2)/11	-	-	-	-0.96	10.60	4.14
(1+2)/(12+13)	-	-	-	10.21	-13.67	-0.60
(1+2)/14	-	-	-	-2.60	-0.43	-2.20
3/4	2.36	-1.26	1.07	9.50	0.81	2.88
3/6	3.77	-0.39	3.38	-	-	-
3/7	9.57	0.83	1.17	-9.32	-0.83	-3.33
3/11	-21.37	3.31	-5.92	-	-	-
3/14	6.40	-2.06	1.02	-	-	-
4/7	-	-	-	4.72	1.66	1.45
4/(9+10)	1.56	0.85	0.13	-	-	-
4/(12+13)	-3.66	-1.25	1.27	-	-	-
5/6	1.39	0.21	-1.45	-	-	-
(9+10)/11	1.64	1.06	0.65	-	-	-

[a] *m/z* values of the ratios of sterol peaks labelled as in **Table 4.15**.

7.4.2. Determination of sterols in real samples

The contents of sterols in EVOO samples of different genetic varieties were also established. For this purpose, the external calibration curves described in section 4.5.2 were used. As explain in this section, and in order to quantify the sterols which were not available as standards, the calibration curves of lanosterol

and β-sitosterol were used. Thus, lanosterol calibration curve was used to estimate the saturated sterols campestanol and sitostanol, and erythrodiol + uvaol. The other sterols (brassicasterol, Δ^5-avenasterol and $\Delta^{5,24}$-stigmastadienol) were evaluated using the β-sitosterol calibration curve. The proportions of sterols found in the total sterol fraction of the EVOO samples are given in **Table 7.12**. The range values were obtained from the mean value of the three injections of every sample belonging to each genetic variety. As it can be observed, β-sitosterol was the predominant sterol in all the analyzed oils. Several differences between the sterol contents of the different genetic varieties were found. For instance, Canetera and Serrana oils showed larger quantities of erythrodiol and uvaol than the other genetic varieties. The highest contents of Δ^5-avenasterol were found in Arbequina followed by Canetera variety. Also, this latter variety showed the highest content of $\Delta^{5,24}$-stigmastadienol.

Table 7.12. Proportions of sterols found in the total sterol fraction of EVOOs of different genetic varieties.

Sterol	Arbequina	Borriolenca	Canetera	Farga	Picual	Serrana
Erythrodiol + Uvaol	0.1–0.3	0.0–0.13	1.9–4.2	0.05–0.3	0.2–0.7	5.0 – 6.1
Ergosterol	0.01–0.05	0.01–0.02	0.0–0.08	0.03–0.09	0.01–0.02	0.0–0.02
Brassicasterol	0.05–0.10	0.05–0.09	0.05–0.10	0.08–0.10	0.08–0.11	0.08–0.11
Δ^5-Avenasterol	11.1–14.1	7.3–9.1	11.9–12.7	8.0–10.9	4.0–12.2	5.3–6.9
Cholesterol	0.2–0.5	0.3–0.6	0.1–0.2	0.2–0.6	0.3–0.5	0.2–0.4
Campesterol	3.9–4.5	3.2–4.7	3.2–3.8	3.6–4.7	2.7–3.3	2.1–3.0
Campestanol	0.1–0.4	0.3–0.5	0.4–1.0	0.3–0.7	0.2–0.3	0.2–0.5
Stigmasterol + clerosterol	0.9–1.3	1.6–2.7	1.6–1.9	1.2–1.9	1.0–1.4	1.0–2.4
$\Delta^{5,24}$-Stigmastadienol	0.8 – 1.9	0.5–1.0	3.2–3.8	0.8–2.0	0.8–1.5	1.0–1.6
β-Sitosterol + Δ^7-Stigmastenol	77–82	79.3–83.5	76.0–77.6	77.1–91.1	77.9–91.0	80.8–82.1
Sitostanol	0.5–0.9	0.6–0.8	0.5–1.2	0.9–1.1	0.5–2.5	0.8–1.6

CHAPTER 8

DEVELOPMENT OF METHODS FOR THE CLASSIFICATION OF EVOOS ACCORDING TO THEIR GEOGRAPHICAL ORIGIN

8.1. Classification using phenolic compound profiles obtained by CEC

The aim of this work was to obtain the phenolic profiles of EVOOs by using a simple and reliable CEC method, and to evaluate the use of these profiles in the prediction of the geographical origin of these EVOO samples. For this purpose, monolithic columns containing LA and BDDA monomers were constructed. The EVOO samples employed in this study are summarized in **Table 8.1**. The oils differed in terms of olive cultivar, degree of ripening, area of growth, production system (type, productive capacity and manufacturer) and storage time.

8.1.1. Construction of the monolithic columns and optimization of the separation conditions

The conditions to prepare photo-polymerized LA-based monoliths were adapted from a previous work, where CEC columns were chemically polymerized using LPO as initiator (Cantó-Mirapeix, 2009A). Initially, the selected composition of the polymerization mixture was 40 wt% monomers (69.8 wt% LA, 29.9 wt% BDDA and 0.3 wt% META) and 60 wt% porogens (17 wt% 1,4-butanediol and 83 wt% 1-propanol) in the presence of 0.3 wt% LPO. According to Aturki et al. (2008), an ACN-water mixture (30:70) containing 5 mM formic acid at pH 3.0 was firstly tried as mobile phase. However, at this 1,4-butanediol content in the polymerization mixture (10 wt%), the column exhibited poor permeability, leading to blockage problems. This was evidenced in the SEM picture of this monolith (**Fig. 8.1A**), where small pores and globule sizes were clearly observed.

Table 8.1. Geographical origin, number of samples, genetic variety and suppliers of the EVOOs.

Geographical origin	Nº of samples	Genetic variety	Supplier
Croatia	1	Mastrinka	OLEA
	1	Lastovka	OLEA
	1	Drobnica	OLEA
	3	Oblica	OLEA
	4	Varietal blend	OLEA
			SMS d.o.o
			Zvijezda
Italy	1	Brugnola	OLEA
	1	Ascolana Tenera	OLEA
	1	Correggiolo	OLEA
	1	Raggia	OLEA
	1	Frantoio	OLEA
	1	Brisighella	OLEA
	1	Nocellara	OLEA
	1	Ogliarola	OLEA
	1	Ghiacciola	OLEA
	1	Coratina	OLEA
Spain	1	Serrana	Intercoop
	1	Blanquilla	Intercoop
	1	Canetera	Intercoop
	1	Borriolenca	Intercoop
	1	Farga	Intercoop
	2	Hojiblanca	Coosur
			Carbonell
	2	Arbequina	Carbonell
			Olearum
	1	Picual	Castillo de Taberna

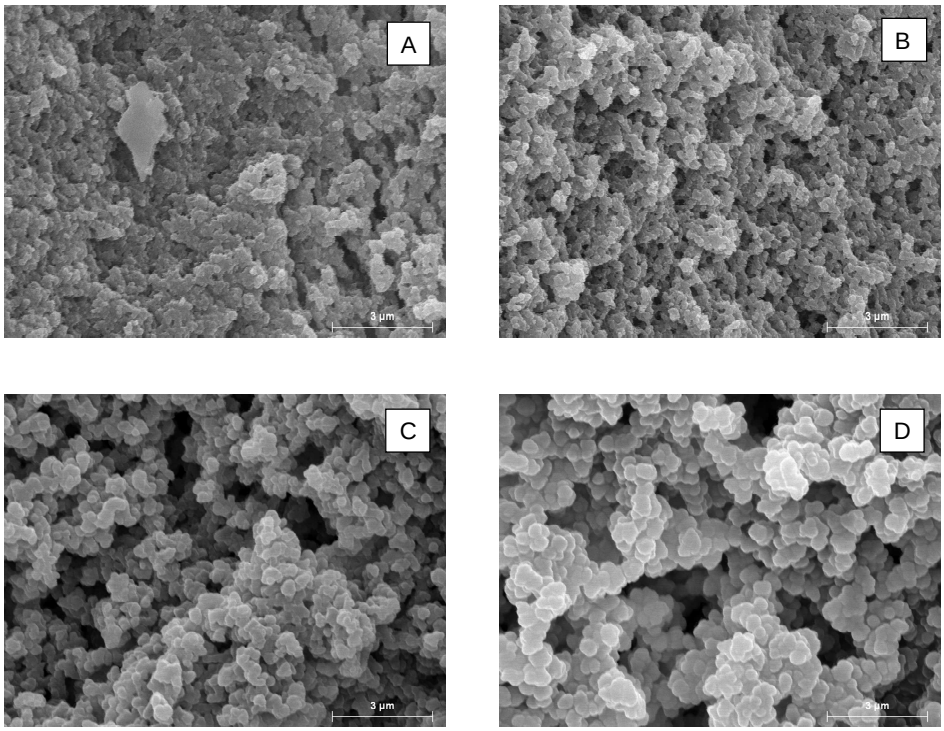

Fig. 8.1. SEM micrographs of LA based monolithic columns prepared with (A) 10 wt%, (B) 12 wt%, (C) 15 wt% and (D) 18 wt% 1,4-butanediol in the polymerization mixture. The bar lengths stand for 3 µm.

For this reason, polymerization mixtures containing higher 1,4-butanediol contents (12-18 wt%) were studied. The monoliths prepared with 12 wt% 1,4-butanediol showed better permeability than those obtained with 10 wt%. This was confirmed by the micrograph of **Fig. 8.1B**, where it can be observed how the monolith constructed with 12 wt% 1,4-butanediol gave larger globules than that obtained with 10 wt%. However, the 12 wt% column showed a tendency to get blocked when attempting to analyze oil samples. In order to overcome this problem, a column containing 15 wt% 1,4-butanediol in the polymerization mixture was prepared. The permeability of this column was quite satisfactory, being its globule size higher than those previously obtained with the other columns (see **Fig. 8.1C**). However, when a phenolic extract (Serrana EVOO variety) was injected in this monolith, a poor resolution between the successive

phenolic compound peaks was obtained (**Fig. 8.2A**). In order to improve resolution, the influence of ACN content on the mobile phase was studied. The results are shown in **Fig. 8.2B-D**. When the concentration of ACN decreased from 20% to 15%, an improvement in the resolution was observed. When 10% ACN was used (**Fig. 8.2D**), a decrease in efficiency and an increase in analysis time was observed. Additionally, a drift in the baseline was evidenced. As a result, a mobile phase composed of 15:85 (v/v) ACN-aqueous buffer containing 5 mM formic acid at pH 3.0 was selected as the best compromise between resolution and analysis time (less than 25 min). Under these conditions, and in order to reduce analysis time, a column with 18 wt% 1,4-butanediol was tried. A loss of resolution and efficiency of phenolic peaks was observed (data not shown). This could be attributed to the larger globule sizes of this monolith (**Fig. 8.1D**) compared with those obtained with a 15 wt% 1,4-butanediol column. Small changes in mobile phase did not lead to a significant separation improvement. At the sight of these results, a monolith prepared with 15 wt% 1,4-butanediol in the polymerization mixture was selected for further studies.

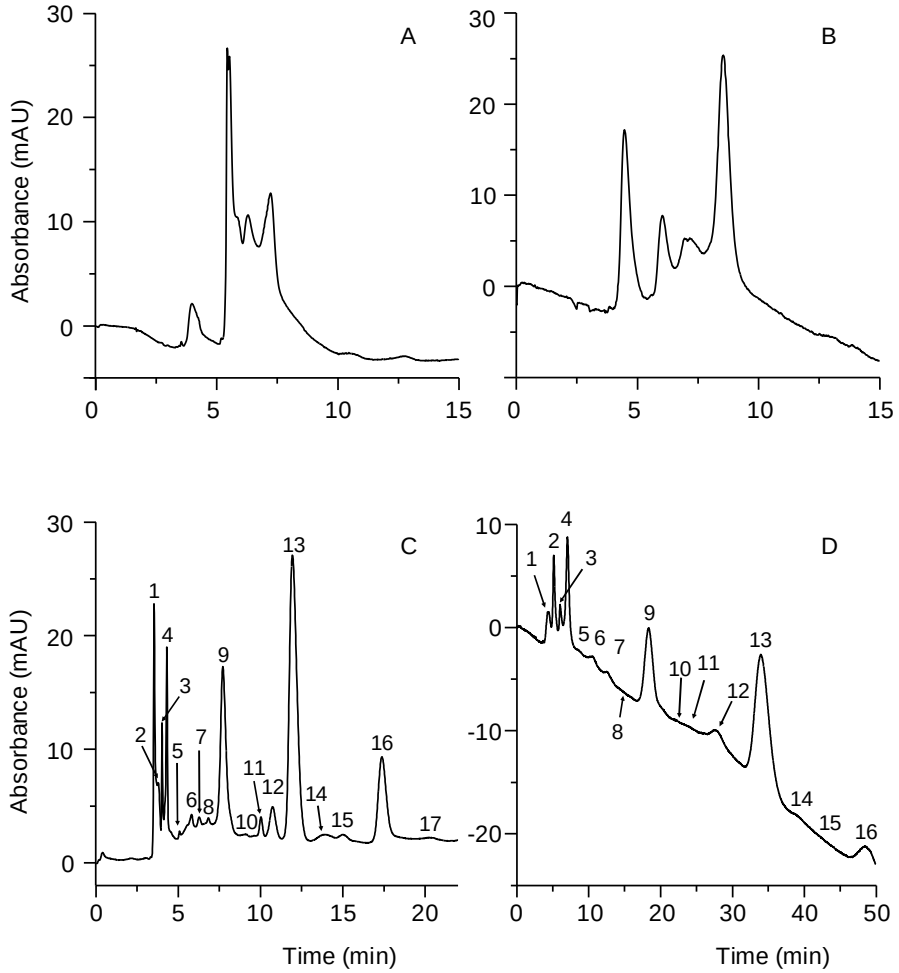

Fig. 8.2. Influence of the mobile phase composition on the separation of phenolic compounds: (A) 30:70, (B) 20:80, (C) 15:85 and (D) 10:90 (v/v) ACN-water mixtures containing 5 mM formic acid at pH 3.0. CEC conditions: LA-based monolithic column prepared with 15 wt% 1,4-butanediol in the polymerization mixture; electrokinetic injection, 10 kV for 2 s; separation voltage, -10 kV; wavelength detection: 280 nm. The 17 peaks labeled were selected as variables.

8.1.2. Characterization of the phenolic compound profiles

The optimized method was applied to the analysis of EVOO samples. Representative electrochromatograms of EVOO from Croatia (A), Italy (B) and Spain (C, D) are shown in **Fig. 8.3**. As it can be observed, 17 peaks, which were present in all the samples, were obtained within 25 min. As previously reported by other authors using different techniques (Brenes, 2002; Carrasco-Pancorbo,

2006), these peaks, which correspond to different phenolic compounds, provided information related to the genetic variety and geographical origin of the EVOOs. On the other hand, the fingerprints of the phenolic compounds of EVOO samples having the same geographical origin (C and D) were closely similar. The little differences observed between the EVOO fingerprints were enhanced when chemometric analysis of the data was performed.

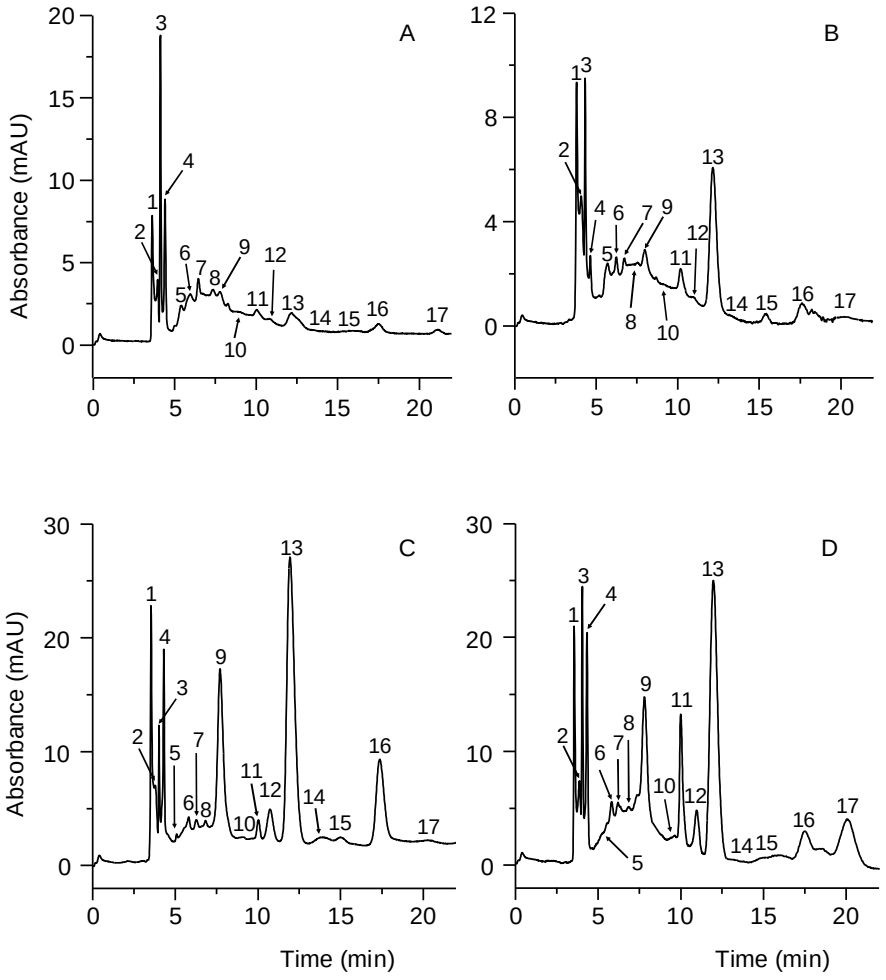

Fig. 8.3. Electrochromatograms of EVOOs from (A) Croatia (Lavstoska), (B) Italy (Frantoio), (C) Spain (Serrana) and (D) Spain (Arbequina) obtained on an LA-based monolithic capillary column under the optimal conditions. CEC conditions: Mobile phase: 15:85 (v/v) ACN-water containing 5 mM formic acid at pH 3.0. Other experimental conditions as in **Fig. 8.2**.

8.1.3. Construction of data matrices and LDA models

The 17 original variables, which corresponded to the 17 peaks labelled in the **Fig. 8.3**, were processed according to normalization procedure B. A total of 136 predictors were obtained. Then, using these normalized variables and the 30 samples of **Table 8.1**, a matrix containing 60 injections (all samples were injected twice), as well as the 136 predictors, was constructed and used for evaluation purposes. To construct the LDA training matrix, only the means of the replicates of the samples were included (30 objects). A response column, containing the three categories corresponding to the three geographical origins of the EVOO, was added to the matrices.

When the LDA model was constructed (using the probability values of F_{in} = 0.01 and F_{out} = 0.10), an excellent resolution between all the category pairs was achieved (**Fig. 8.4**, λ_w = 0.09). The variables selected by the SPSS stepwise algorithm and the corresponding standardized coefficients of this model are given in **Table 8.2**. For this model, and using leave-one-out validation, all the points of the training set were correctly classified. The corresponding evaluation set, containing the 60 original data points, was then used to check the prediction capability of the model. Using a 95% probability, all the objects were correctly assigned.

On the other hand, and in order to validate the model with blind samples, a new LDA model with 24 samples (8 samples x 3 geographical origins), which were randomly selected, was constructed. The predictors selected by this model were mainly the same than those selected in the previous model; however, slight variations in the coefficient values were observed. When the new evaluation set (composed by the means of the duplicates of the remaining 6 samples) was used to check the prediction capability of the model, all the samples were correctly classified using a 95% probability.

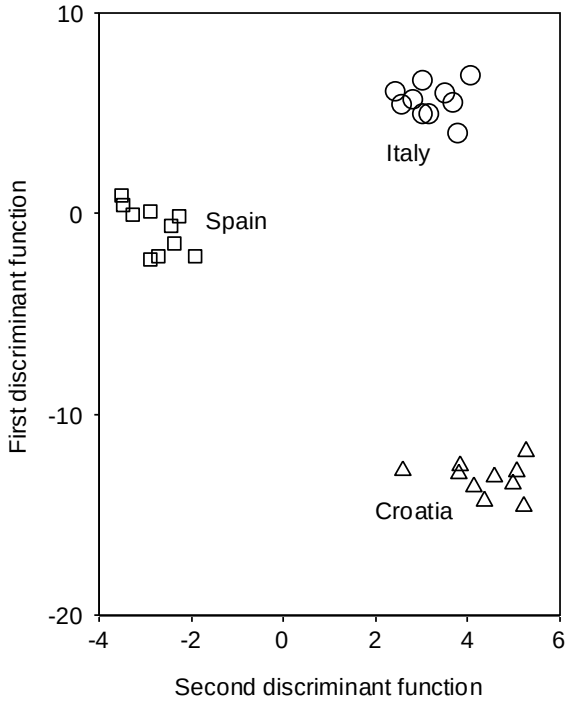

Fig. 8.4. Score plot on the plane of the two LDA discriminant functions obtained to predict the geographical origin of EVOOs.

Table 8.2. Predictors selected and their corresponding standardized coefficients of the LDA model constructed to predict the geographical origin of the EVOOs.

Predictor[a]	f_1	f_2
1/4	3.50	1.91
1/15	-4.51	1.37
2/15	8.02	-2.43
7/13	2.22	2.71
7/14	1.64	-1.04
10/13	-0.97	-1.55
11/17	0.98	1.09
12/14	-4.25	2.19
12/17	-2.90	-2.06
15/17	2.04	1.04

[a] Pairs of peak areas identified according to labels in **Fig. 8.3**.

CHAPTER 9

DEVELOPMENT OF METHODS FOR THE EVALUATION OF OLIVE OIL OXIDATION

9.1. Study of chemical changes produced in VOOs with different phenolic content during an accelerated ageing treatment

The objective of this work was to study the chemical changes produced in an EVOO sample, both in the presence and absence of its phenolic fraction, during an accelerated ageing treatment. Modifications in the concentration of phenolic compounds, as well as changes in several quality parameters (free acidity, peroxide value, UV absorbance, fatty acid composition, OSI and T content) were studied. In addition, transformation of phenolic compounds during the accelerated ageing treatment in EVOO samples with phenolic fraction was also studied. For this purpose, an EVOO sample from the olive fruit variety Brugnola (picked on October 2008 at San Marino) was used. EVOO oxidation was evaluated on two aliquots of the oil sample: EVOO with phenols (EV1) and EVOO without phenols (EV2). This latter was obtained by removing the phenolic compounds as indicated in section 3.3.6. The accelerated ageing treatment was performed as follows (Bendini, 2006; Bonoli-Carbognin, 2008; Lerma-García, 2009A): both samples, EV1 and EV2, were divided in 8 aliquots each, stored in glass bottles and kept in the dark at 60 °C up to 7 weeks. Two bottles, one of EV1 and the other of EV2, were removed every week from the oven and stored at -20 ºC (samples t_0-t_7). Triplicate analyses were carried out in all cases at each storage time on both EV1 and EV2 samples.

9.1.1. Evaluation of the phenolic content

Phenolic fractions of EV1 and EV2 were firstly analyzed to verify the efficiency of phenolic compound stripping. The quantification of the different phenolic compounds was performed by constructing calibration curves of 3,4-

DHPAA for the compounds detected at 280 nm (r = 0.999) and at 240 nm (r = 0.998), whereas the compounds detected at 330 nm were quantified by calibrations curves of API (r = 0.995) and LUT (r = 0.988). Then, considering the sum of all quantified phenolic compounds by HPLC-MS (22 individual phenols), a concentration of 164 mg kg^{-1} oil is obtained in the EV1 sample at zero storage time (t_0), being the concentration of the phenolic compounds in EV2 sample of 0.70 mg kg^{-1} oil at the same storage time. Then, a decrease of 99.6% in phenol content was obtained (see **Fig. 9.1**). A similar extraction yield was reported by Bonoli-Carbognin et al. (2008) using the same extraction procedure.

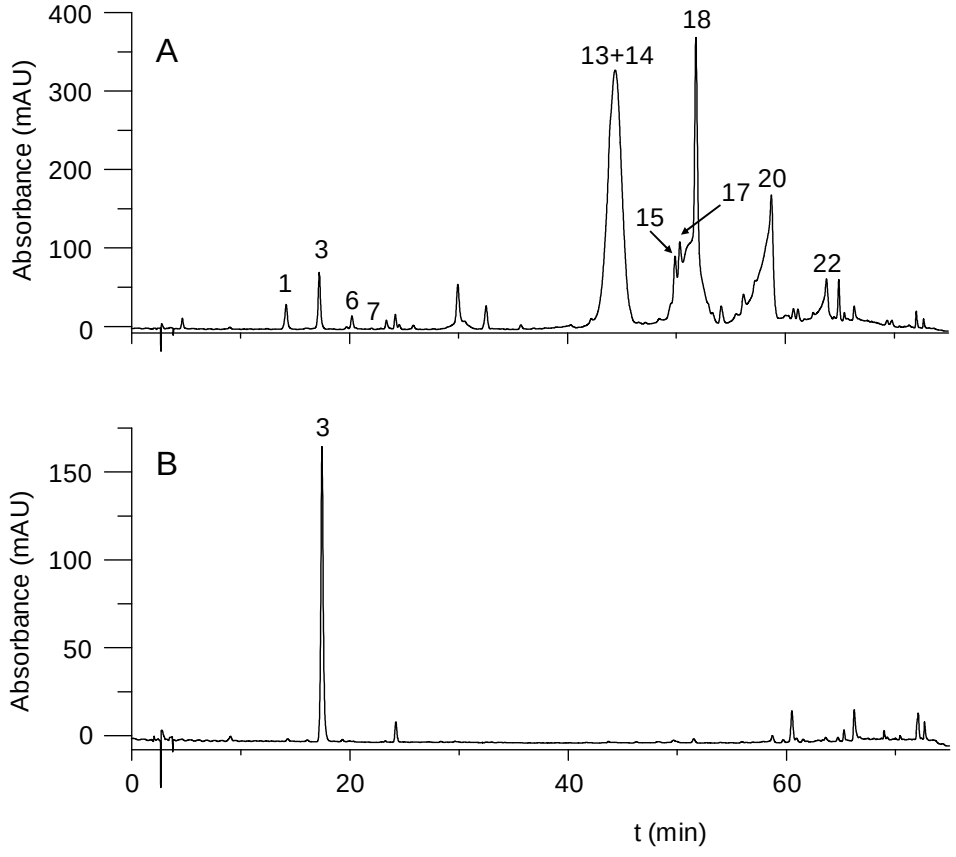

Fig. 9.1. UV-chromatograms of (A) EV1 and (B) EV2 samples at t_0. Peak identification: 1, HYTY; 3, 3,4-DHPAA; 6, Unk; 7, Unk; 13, OxDOA; 14, DOA; 15, OxDLA; 17, DLA; 18, AcPIN; 20, OA and 22, LAg. Detection wavelength: 280 nm.

Differences produced in the chemical parameters of the EV1 and EV2 samples at t_0 have been also studied. As reported in **Table 9.1**, the free acidity percentage of EV1 and EV2 ranged from 0.24 to 0.18 %, respectively, while the peroxide value varied from 11.96 to 12.44 meq O_2 kg^{-1} oil. All these values were within the limits set by the EC Regulation for EVOO (Commission Regulation (EC) No. 1989/2003). The fatty acid composition of both samples at t_0, established by GC-FID, is also reported in **Table 9.1**. EV1 and EV2 showed very similar values in terms of fatty acid composition, which demonstrated that the phenol-removing procedure did not affect this fraction. The high oleic content of both samples was reported to largely contribute to the oxidative stability of EVOOs (Aparicio, 1999).

Table 9.1. Chemical parameters of the EV1 and EV2 samples at t_0.

Parameter	EV1	EV2
Free acidity (%)	0.24	0.18
PV[a] (meq O_2 kg^{-1})	11.96	12.44
Myristic acid (%)	0.01	0.01
Palmitic acid (%)	13.07	13.10
Palmitoleic acid (%)	0.60	0.60
Stearic acid (%)	2.46	2.46
Oleic acid (%)	72.88	72.83
Linoleic acid (%)	9.26	9.28
Linolenic acid (%)	0.41	0.41

[a] PV = peroxide value.

Changes in the oxidative status of EV1 and EV2 are shown in **Table 9.2**. These changes were evaluated by the absortivity of the conjugated dienes (k_{232}) and trienes (k_{270}), as well as by the OSI time and T contents. T content was established by HPLC-UV-Vis after a dilution of 1g oil in 10 mL *n*-hexane.

Quantification was performed by constructing calibration curves of standard solutions of α-T (r = 0.999).

Table 9.2. Chemical parameters for EV1 and EV2 samples at different storage times[a].

Storage time, t_i	k_{232}		k_{270}		OSI time (h)		Ts (mg kg^{-1})	
(weeks)	EV1	EV2	EV1	EV2	EV1	EV2	EV1	EV2
0	2.24 f	2.45 d	0.19 g*	0.16 f	33.65 a*	10.8 a	181.9 a	148.4 a
1	3.51 e	3.67 cd	0.24 f*	0.17 f	22.23 b*	9.03 b	191.1 a	170.6 a
2	4.52 d	5.43 bc	0.26 f	0.23 ef	19.20 c*	6.2 c	195.5 a*	140.8 a
3	5.42 c	6.43 b*	0.34 e	0.29 e	15.78 d*	3.8 d	181.9 a*	90.6 b
4	7.48 b	8.41 a	0.40 d	0.39 d	10.55 e*	1.3 e	139.6 b*	42.0 c
5	9.69 a*	8.48 a	0.51 c	0.47 c	7.28 f*	0 f	85.4 c*	46.9 c
6	7.48 b	8.93 a	0.59 b	0.59 b	5.83 g*	0 f	55.3 d	70.3 bc*
7	7.71 b	9.74 a*	0.68 a	0.67 a	3.43 h*	0 f	25.9 e	97.2 b*

[a] Mean values (n = 3). Means with different letters within the same column were significantly different (p < 0.05). Means with an asterisk for the same parameter and at a given storage time were significantly different (p < 0.05).

The two oil samples at t_0 showed k_{232} and k_{270} values lower than the legal limits established by the EC Regulation for EVOO category (Commission Regulation (EC) No. 1989/2003), which were 2.50 and 0.22, respectively. However, after one week of storage (t_1), both samples exceeded the limit for k_{232}, reaching values of 7.71 and 9.74 for EV1 and EV2, respectively, after 7 weeks (t_7) of storage. After one week of storage (t_1), only the EV1 sample exceeded the EC limit for k_{270}, but one week later (t_2), EV2 also surpassed the legal value. Both samples reached larger values (~ 0.7) after 7 weeks of storage. Similar trends were also found by Bendini et al. under similar experimental conditions (Bendini, 2006).

Regarding OSI time, the EV2 sample at t_0 showed a lower value than the EV1 sample, which was probably due to the different amounts of phenolic compounds present in these samples. In fact, EV2 showed a reduction of the OSI time to one third of its initial value (from 33.7 to 10.8 h). The EV2 OSI value of 10.8 h could be only attributed to the high oleic acid content and to the low amounts of polyunsaturated fatty acids (Aparicio, 1999). Both EV1 and EV2 samples showed a significant decrease of OSI time during the ageing process, being faster for EV2 (in fact after four weeks the OSI time was 100 % reduced), which confirmed the role of the phenolic fraction against the oxidative stability of EV1.

The variation of the T content of both, EV1 and EV2 samples, is also shown in **Table 9.2**. At $t_{0,}$ the two oil samples did not show significant differences in T content. Thus, the alkaline procedure used to wash polar phenols did not affect this lipophilic antioxidant fraction. T content remained substantially unvaried for EV1 from t_0 to t_3; then, a strong decrease was observed until the end of the storage time. The constant loss of oxidative stability (**Table 9.2**) is probably related to the decrease of polar phenols, which during the first three weeks, may act as antioxidant molecules also protecting Ts against oxidation (Baldioli, 1996; Bendini, 2006). On the other hand, Ts started to decrease after two weeks of storage for EV2; however, an oscillating trend was evidenced at higher storage times. This trend could be explained taking into account a synergic effect between α-T and phospholipids (Bandarra, 1999), and the formation of T oxidized derivatives. These latter compounds could overlap with T peaks during HPLC elution, interfering in T determination.

9.1.2. Phenolic compound transformation in EV1 samples during the accelerated ageing treatment

Fig. 9.2, **9.3** and **9.4** report the UV-chromatograms detected at 280, 240 and 330 nm, respectively, showing the 22 phenolic compounds at three storage times (t_0, t_3 and t_7). In particular, at 280 nm (**Fig. 9.2**), the decrease of DOA (peak 14), DLA (peak 17) and LAg (peak 22), the disappearance of OA (peak 20) and the formation of their possible oxidized derivatives (peaks 13, 15, 21 and traces of OxOA) are evidenced. **Fig. 9.3** shows the trend of EA (peak 12) and the appearance of several hypothetical oxidized compounds that absorb only at 240 nm (4, 9, 10 and 11). Finally, **Fig. 9.4** evidences the trend of the loss of LUT (peak 16), and the slightly decreased of API (peak 19), during storage.

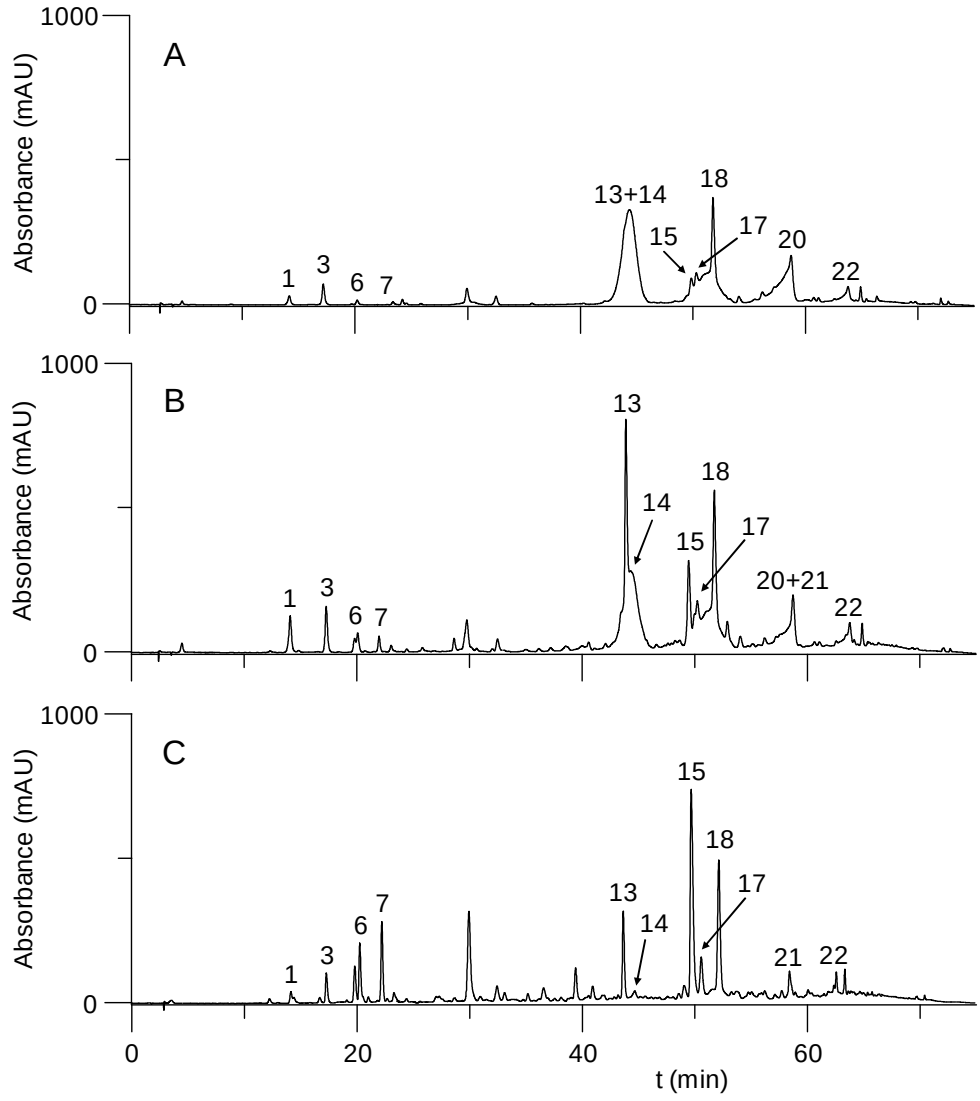

Fig. 9.2. Chromatograms showing the evolution of the EV1 phenolic profile after ageing treatment at 60 ºC: (A) t_0, (B) t_3 and (C) t_7. Peak identification: 21, OxLAg; other peaks as in **Fig. 9.1**. Detection wavelength: 280 nm.

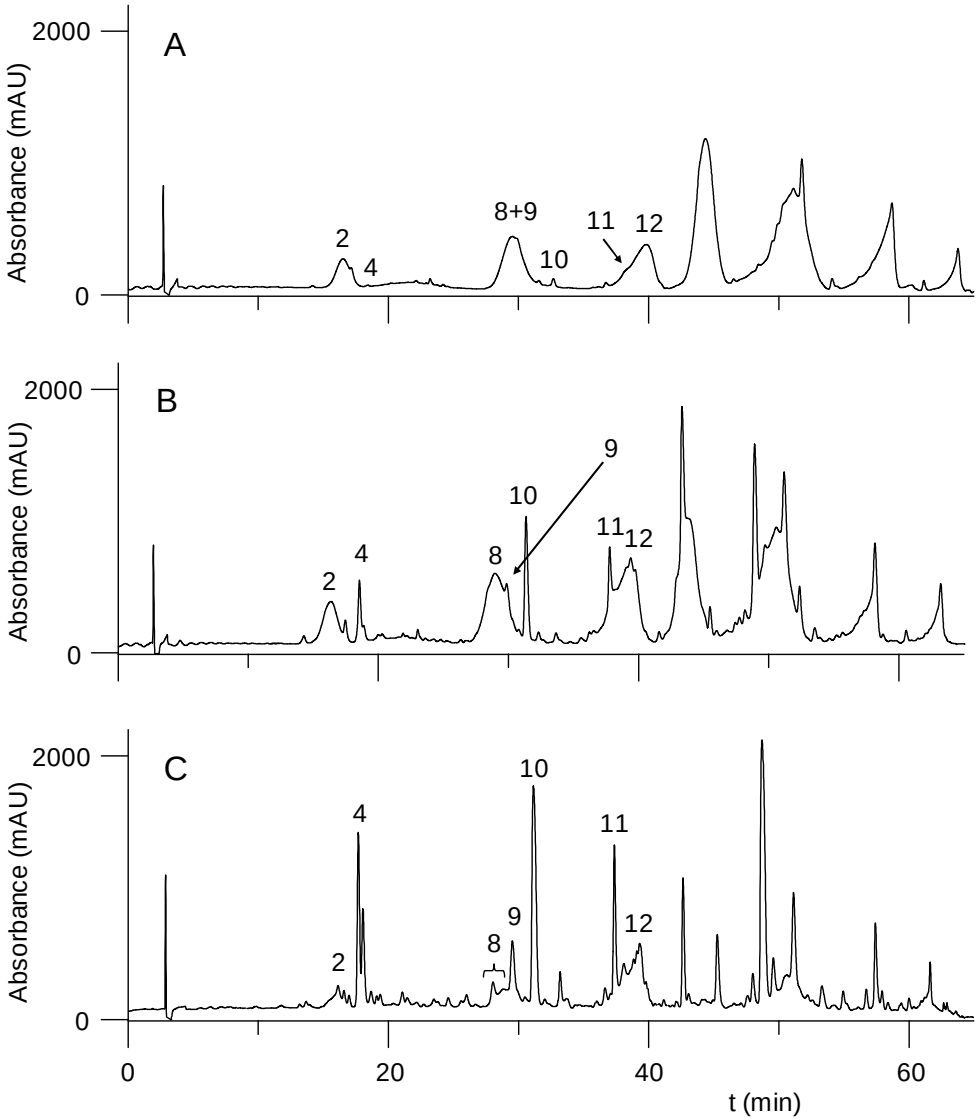

Fig. 9.3. Chromatograms showing the evolution of the EV1 phenolic profile after ageing treatment at 60ºC: (A) t_0, (B) t_3 and (C) t_7. Peak identification: 2, DEA; 4, OxDEA; 8, 9 and 10, Unknown; 11, OxEA and 12, EA. Detection wavelength: 240 nm.

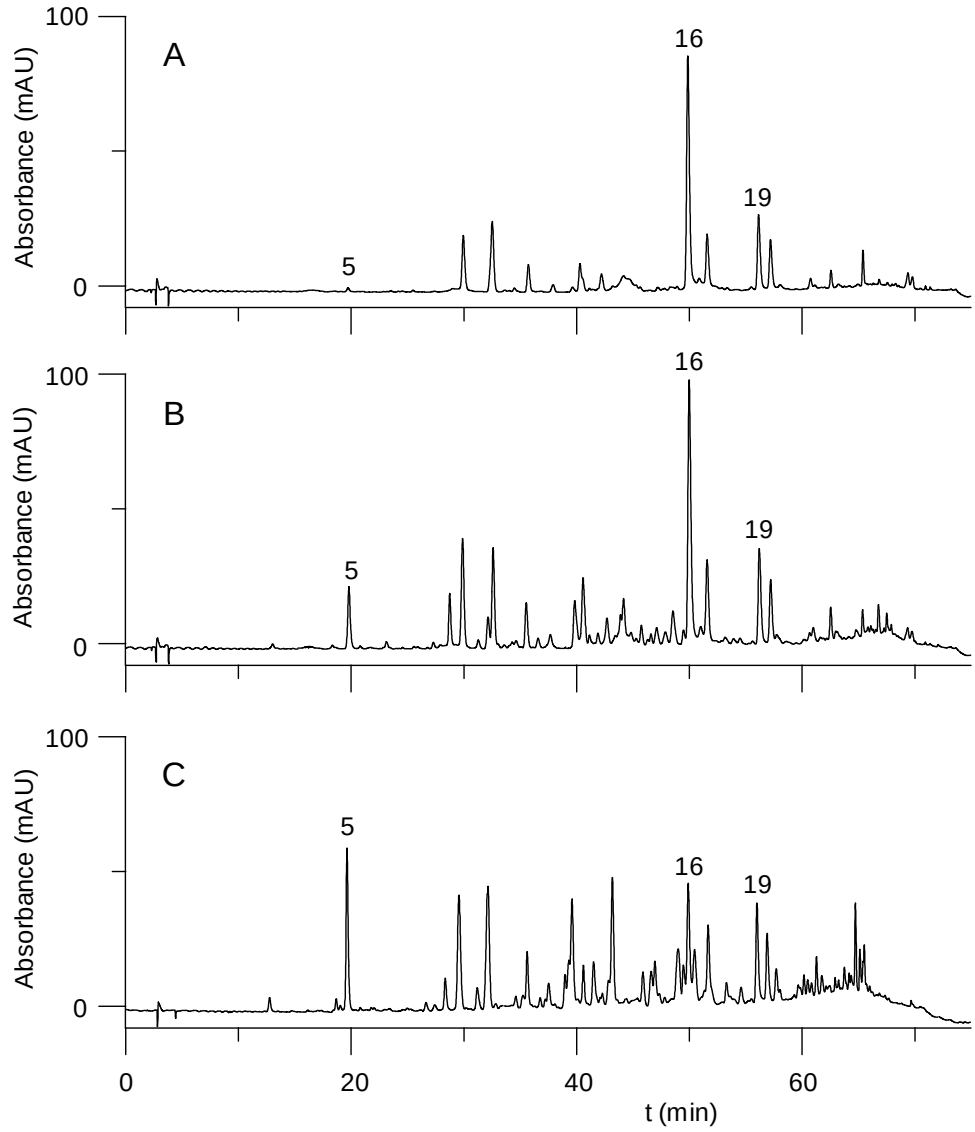

Fig. 9.4. Chromatograms showing the evolution of the EV1 phenolic profile after ageing treatment at 60ºC: (A) t_0, (B) t_3 and (C) t_7. Peak identification: 5, Unknown; 16, LUT and 19, API. Detection wavelength: 330 nm.

A list of the main phenolic compounds studied in this work, as well as their retention times, wavelengths of maxima UV absortivity, MW and MS fragmentation patterns are summarized in **Table 9.3**.

Table 9.3. Retention times, wavelengths of maxima UV absortivity, MW and MS fragmentation patterns of the phenolic compounds.

Analyte	Peak no.	t_R (min)	λ_{max} (nm)	MW	Major fragments ESI positive					
					$[M+H]^+$	$[M+Na]^+$	$[M-H_2O+H]^+$	Loss of PG[b]	Loss of AG[c]	Other fragments
HYTY	1	11.6	232/280	154	-	-	137.1	-	-	-
DEA	2	16.8	230	184	185.1	207.1	-	-	-	-
Unk	3	18.0	232/280	260	-	283.2	-	-	-	299.0 $[M+K]^+$
OxDEA	4	18.5	236	200	-	223.1	-	-	-	123.1/165.0
Unknown	5	20.0	290/310	-	-	-	-	-	-	338.4/321.8/191.1/185.8
Unknown	6	20.1	232/280	-	-	-	-	-	-	177.0/235.1/668.1
Unknown	7	22.0	232/280	-	-	-	-	-	-	113.1/157.1/349.2
Unknown	8	29.5	234	-	-	-	-	-	-	297.1/239.1/221.1/181.1/165.1
Unknown	9	30.4	234	336	-	359.0	-	-	-	375.1 $[M+K]^+$
Unknown	10	36.1	240	-	-	-	-	-	-	237.1/197.1/165.1
OxEA	11	38.9	240	258	259.1	281.1	-	-	-	185.1/227.1/ 241.1 $[M-OH]^+$
EA	12	39.9	240	242	243.1	265.1	-	-	-	211.1 $[M-OCH_3]^+$
OxDOA	13	44.0	234/282	336	337.1	359.1	-	183.1	137.1	375.1 $[M+K]^+$
DOA	14	45.0	234/282	320	-	343.1	-	-	137.1	361.1
OxDLA	15	49.8	242/276	320	-	343.1	-	183.1	121.1	359.1 $[M+K]^+$
LUT	16	50.0	254/348	286	287.1	309.1	-	-	-	-
DLA	17	51.5	236/276	304	-	327.1	-	-	121.1	-
AcPIN	18	53.8	236/280	416	417.1	439.1	-	-	-	455.1 $[M+K]^+$ / 357 $[M-CH_3COOH+H]^+$ / 233 $[M-CH_3COOH-$ phenyl$OCH_3+H]^+$
API	19	56.1	268/338	270	271.1	-	-	-	-	-
OxOA	tr[a]	56.1	236/280	394	395.1	417.1	-	241.1	137.1	439.1
OA	20	58.7	236/282	378	379.1	401.1	-	225.1	137.1	419.1
OxLA	21	60.1	232/276	378	379.1	401.1	-	241.1	121.1	-
LA	22	63.9	230/276	362	363.1	385.1	-	225.1	121.1	-

[a]tr = trace; [b]PG = phenolic group; [c]AG = acidic group.

According to the data given in **Table 9.3**, the following conclusions were obtained:

1. The absorbing band near to 240 nm is typical of a carboxymethyl enol-ether group. Thus, for example, EA (peak 12) is characterized by this band. On the other hand, the bands at 277 and 282 nm are due to a mono-hydroxyphenyl group and to an *ortho*-hydroxyphenyl group, respectively; thus, for example, HYTY (peak 1) and secoiridoid derivatives containing HYTY (OxDOA (peak 13), DOA (peak 14), OxOA (tr), OA (peak 20) and the peaks of unknown compounds 3, 6 and 7) exhibit a secondary UV maximum in the vicinity of 280 nm, whereas those molecules having an mono-hydroxyphenyl group such as TY (OxDLA (peak 15), DLA (peak 17), OxLAg (peak 21) and LAg (peak 22)) show a secondary maximum in the vicinity of 277 nm.

2. HYTY exhibits only an $[M+H-H_2O]^+$ ion. The presence of an initial high percentage of water inhibits a good electrospray ionization of molecules having acidic properties, such as HYTY and TY. As suggested by Rovellini et al. (2002), it is not possible to reveal the pseudo molecular ion for HYTY due to its difficulty to give protonated adducts.

3. Some authors (Ríos, 2005; Rovellini, 2002) have indicated that the oxidation of secoiridoid structures involves the acidic portion (EA) and not the aromatic alcoholic moiety (HYTY and TY); for this reason, the oxidized forms shown in Table 3 maintain the UV specific absorbance of their non oxidized forms.

4. The oxidation involves the conversion of the aldehydic group of EA to a carboxylic group (according to the scheme reported in **Fig. 9.5**).

5. The oxidized forms of secoiridoids, which are more polar than their respective non oxidized derivatives, elute before these latter. In the case of the

couple DEA-OxDEA (peaks 2 and 4 peaks, respectively), the presence of a second carboxylic group in the molecule does not cause an anticipated elution.

6. Under the ESI conditions applied in this study, both the oxidized and non oxidized forms of secoiridoids are characterized by the presence of the sodium adduct $[M+Na]^+$, the loss of the phenolic group (*m/z* 241 and *m/z* 225 for the oxidized and non oxidized forms of secoiridoids, respectively; *m/z* 183 and *m/z* 167 for the oxidized and non oxidized forms of the decarboxymethyl structures of secoiridoids, respectively), and the loss of the acidic group (*m/z* 137 and *m/z* 121 for molecules having HYTY and TY, respectively). A general scheme of the evolution of secoiridoids during storage is shown in **Fig. 9.5**.

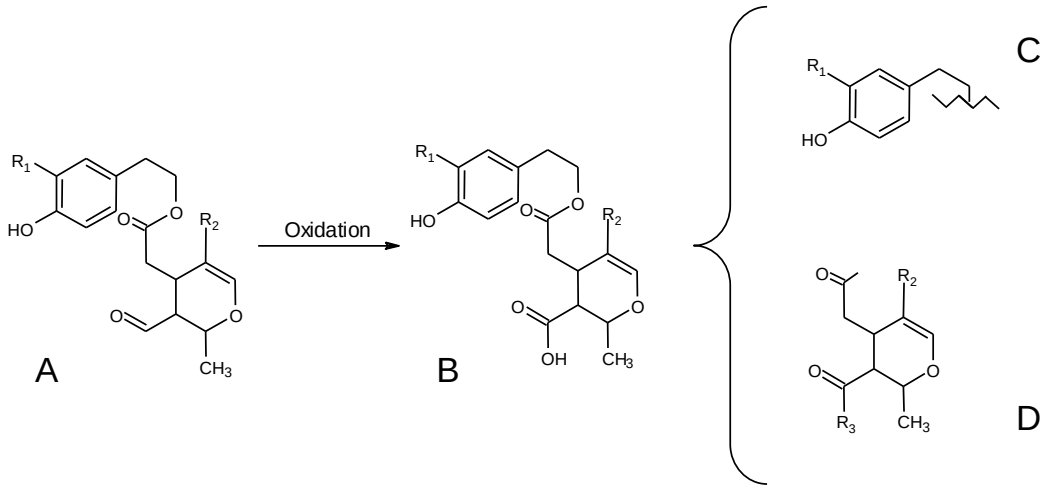

Fig. 9.5. General scheme of the evolution of secoiridoids during ageing treatment. **A**, structure of secoiridoids: LAg (R_1 = H and R_2 = -$COOCH_3$); OA (R_1 = OH and R_2 = -$COOCH_3$); DLA (R_1 = H and R_2 = -H); DOA (R_1 = OH and R_2 = -H). **B**, oxidized forms of secoiridoids: OxLAg (R_1 = H and R_2 = -$COOCH_3$); OxOA (R_1 = OH and R_2 = -$COOCH_3$); OxDLA (R_1 = H and R_2 = -H); OxDOA (R_1 = OH and R_2 = -H). **C**, loss of acidic group during mass fragmentation: R_1 = H fragment with *m/z* = 121; R_1 = OH fragment with *m/z* = 137. **D**, loss of phenolic group during mass fragmentation: R_2 = -$COOCH_3$ and R_3 = OH fragment with *m/z* = 241; R_2 = -$COOCH_3$ and R_3 = H fragment with *m/z* = 225; R_2 = H and R_3 = OH fragment with *m/z* = 183; R_2 = H and R_3 = H fragment with *m/z* = 167.

7. The peaks related to the oxidized forms of secoiridoids are narrower than those related to molecules having one or two aldehydic groups.

Fig. 9.6A showed the trend of the phenolic compounds of EV1 during storage. All areas were divided by the 3,4-DHPAA area (to estimate the extraction recovery), being data expressed as the natural logarithm of the ratios of areas. In this way, the different trends of disappearance of the phenolic compounds could be adequately appreciated. Generally, a decrease of the more abundant compounds (secoiridoids) was observed. Peaks 21 and 22 were jointly evaluated: peak 21 appeared overlapped with peak 22 from t_3 to t_7. At t_7, peak 22 was absent. As previously observed at room temperature (Boselli, 2009; Di Lecce, 2006), transformations of secoiridoids to more simple compounds (for example decarboxymethyl structures), followed by a further conversion to phenyl ethyl alcohols (such as TY and HYTY), occurred. In this work, TY was not found in the EV1 sample at t_0, whereas the concentration of HYTY, which was initially low, increased from t_0 to t_4. This trend was also observed for oils stored at room temperature (Boselli, 2009; Di Lecce, 2006). Concerning lignans, AcPIN (peak 18 of **Fig. 9.2C**) slightly decreased exhibiting a high content also at the end of storage process (t_7). This tendency for lignans has been also observed when oils were heated with conventional or microwave oven (Carrasco-Pancorbo, 2007B; Cerretani, 2009).

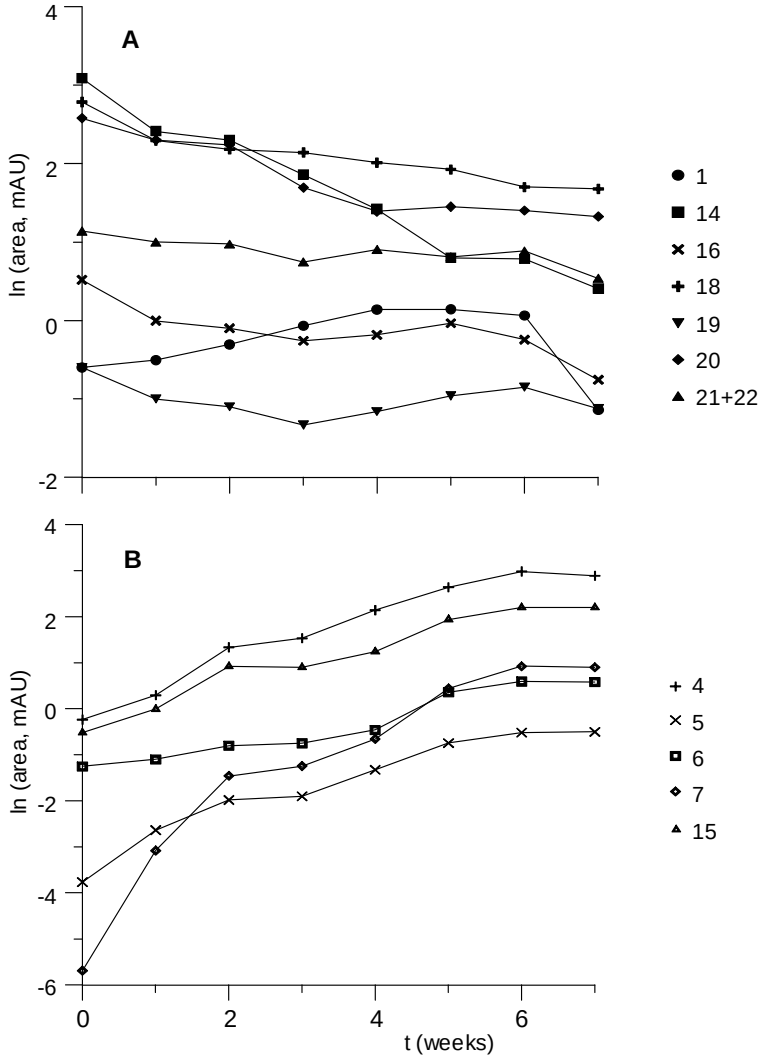

Fig. 9.6. Plots showing the trends of phenolic (A) and neo-formation compounds (B) during storage (from t_0 to t_7) of EV1. Area values were divided by the 3,4-DHPAA area (internal standard). Peak identification as reported in **Table 9.3**.

The trend of the neo-formation compounds during storage is shown in **Fig. 9.6B** (area values were also divided by the 3,4-DHPAA area and expressed as natural logarithms). The most important neo-formation compounds are peaks 4 (oxidation form of decarboxymethyl elenolic acid, OxDEA) and 15 (oxidized form of decarboxymethyl ligstroside aglycon, OxDLA), respectively, followed by peaks 5, 6 and 7 (unknown compounds). Peak 13 (data not reported in **Fig.**

9.6B) was probably due to an oxidized secoiridoid, being tentatively assigned as an oxidized form of DOA (OxDOA).

9.2. Evaluation of the oxidative status of VOOs with different phenolic content by direct infusion MS

The aim of this work was to evaluate the oxidative status of VOOs using direct infusion APCI-MS assisted by LDA. For this purpose, samples at eight levels of oxidation, with and without phenolic compounds, were used. These samples were the EV1 and EV2 described in section 9.1, whose qualitative parameters have been previously described.

9.2.1. MS analysis and selection of the variables

According to a series of recent articles, several markers can be used to monitor the oxidation status of VOOs (Armaforte, 2007; Bendini, 206; Del Carlo, 2004; Lerma-García, 2009B; Rovellini, 1998; Verardo, 2009). In particular, OFA compounds have been used to evaluate the oxidative status of VOOs in several areas of applied research (Armaforte, 2007; Bendini, 206; Del Carlo, 2004; Rovellini, 1998), as well as for the determination of lipid extracts obtained from other matrices, such as spaghetti pasta (Verardo, 2009). At the same time, the oxidized forms of phenolic compounds have been identified as markers of the oxidation level of VOOs, being HPLC-MS methods proposed for their monitoring (Armaforte, 2007; Lerma-García, 2009B). Taking into account these considerations, free fatty acids, OFAs, phenols and their oxidized forms, jointly with α-T, have been selected as target compounds for the present work. Then, the abundances of the $[M-H]^-$ peaks of these compounds (see **Table 9.4**) were measured in the 4 replicates performed for each sample. As observed in

Table 9.4, owing to the coincidence of the *m/z* values of three peak pairs (hydroxy-linoleic acid/keto-oleic acid, DOA/OxDLA and OA/OxLAg), these peaks were measured as the sum of the abundances of the two compounds of each pair; then, a total of 27 peaks was obtained to be used as predictors for LDA construction.

The MS spectra showing the peak profiles of the fatty acid and OFAs of EV1 at t_0 and t_3 are shown in **Fig. 9.7**. The peak intensities of OFAs (peaks 8-12) increased from t_0 to t_3. This trend was also observed at the other storage times.

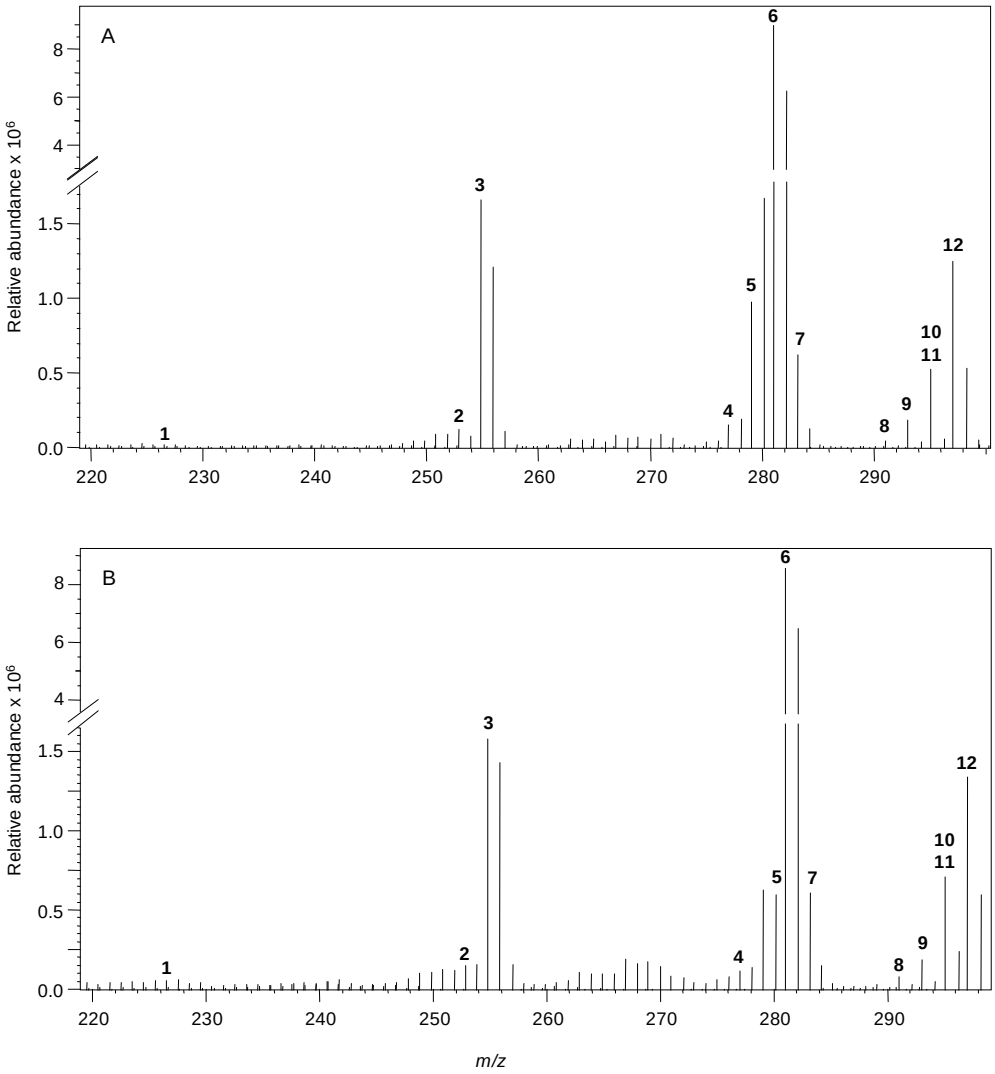

Fig. 9.7. MS spectra showing the peak profiles of fatty acids and their oxidized forms for EV1 at storage times t_0 (A) and t_3 (B). The $[M-H]^-$ peaks are labelled as indicated in **Table 9.4**.

Table 9.4. $[M-H]^-$ peaks of selected fatty acids and antioxidant compounds.

Peak no.	Compound (acronym)	*m/z*
	Fatty acids	
1	Myristic acid (C14:0)	227
2	Palmitoleic acid (C16:1)	253
3	Palmitic acid (C16:0)	255
4	Linolenic acid (C18:3)	277
5	Linoleic acid (C18:2)	279
6	Oleic acid (C18:1)	281
7	Stearic acid (C18:0)	283
	OFAs	
8	Keto-linolenic acid	291
9	Keto-linoleic acid	293
10	Hydroxy-linoleic acid	295
11	Keto-oleic acid	295
12	Hydroxy-oleic acid	297
	Phenolic and T compounds	
13	TY	137
14	HYTY	153
15	DEA	183
16	EA	241
17	API	269
18	LUT	285
19	DLA	303
20	DOA	319
21	LAg	361
22	OA	377
23	AcPIN	415
24	α-T	443
	Oxidized phenols	
25	OxDEA	199
26	OxEA	257
27	OxDLA	319
28	OxDOA	335
29	OxLAg	377
30	OxOA	393

Fig. 9.8 shows the MS spectra of the peak profiles of α-T, phenolic compounds and their oxidized forms (only those whose *m/z* range was between 280 and 450) for the EV1 at t_0 and t_3.

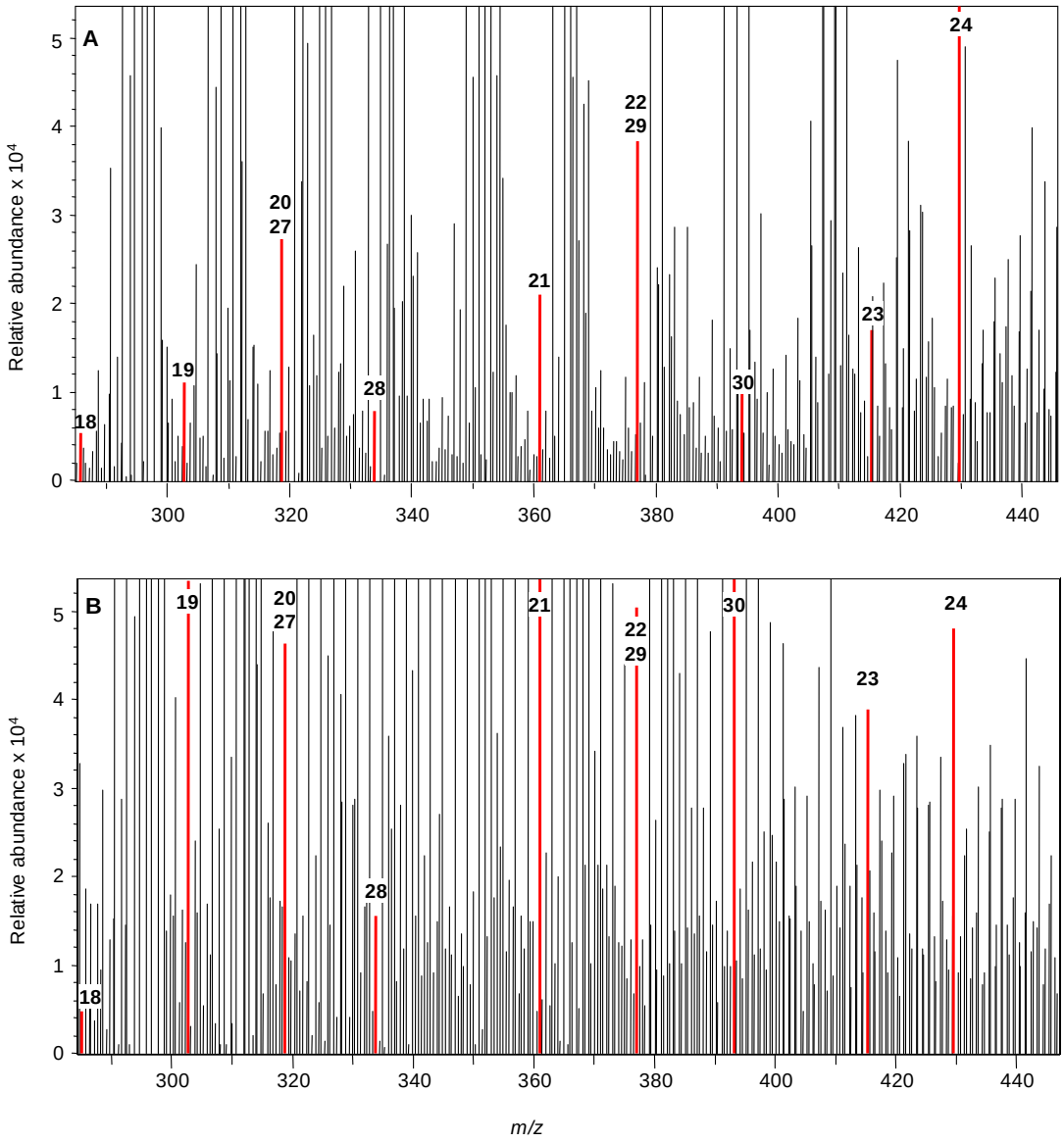

Fig. 9.8. MS spectra showing the peak profiles of tocopherol, phenolic compounds and their oxidized forms for the EV1 at storage times t_0 (A) and t_3 (B). The $[M-H]^-$ peaks are labelled as indicated in **Table 9.4**.

As observed, the intensity of peaks 19 and 21 increased, which was attributed to the transformation of *orto*-diphenolic forms to mono oxydrilic forms. On the other hand, a decrease of the intensity of peak 24 (α-T) is noticeable, while the intensities of peaks 28 and 30 (oxidized forms of phenolic compounds) and the pairs 20/27 and 21/29 increased. For both pairs, the increase is probably due to the contribution of the oxidized form peaks 27 and 29. These trends are in agreement with previous works (Bendini, 2006; Verardo, 2009).

9.2.2. Construction of data matrices and LDA models

After normalization of the 27 original variables by normalization procedure B, LDA models capable of classifying the oil samples according to their oxidative status were performed. For this purpose, two matrices were constructed. The first one was composed by EV1 samples (32 injections) and the 351 predictors. The second one comprised EV1 and EV2 samples (64 injections) and 66 predictors (which corresponded to the α-T, fatty acid and OFA peaks). In this case, this reduced set of 66 predictors was selected because the phenolic compounds were removed by the previous treatment in EV2 samples, and consequently their oxidized forms were not present in the MS spectra. A response column, containing the eight storage times was added to both matrices.

Firstly, an LDA model was constructed using the matrix that contained EV1 samples. An excellent resolution between the eight categories was achieved (**Fig. 9.9**, $\lambda_w = 0.229$). The variables selected by the SPSS stepwise algorithm, showing the predictors with large discriminant capabilities, are given in **Table 9.5**.

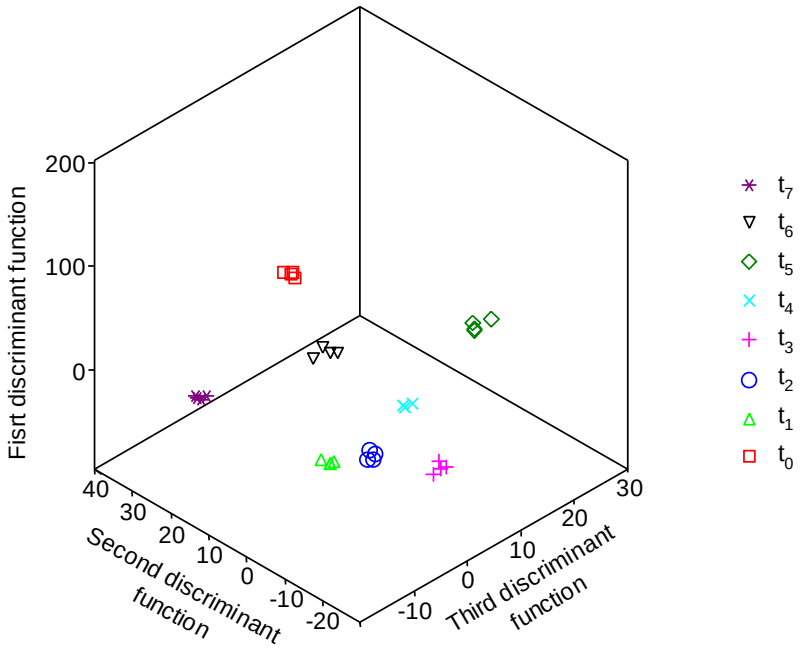

Fig. 9.9. Score plot on an oblique plane of the 3-D space defined by the three first discriminant functions of the LDA model constructed with the EV1 samples.

Table 9.5. Predictors selected and corresponding standardized coefficients of the LDA model constructed with the EV1 samples to predict the oxidative status.

Predictors[a]	f_1	f_2	f_3	f_4	f_5	f_6	f_7
227/277	-0.17	-0.45	-0.64	1.48	1.19	0.64	0.61
227/303	5.81	0.24	0.20	0.03	0.01	-0.35	0.06
255/279	9.83	1.70	2.87	2.25	1.79	0.80	-0.96
255/281	-4.33	1.60	-0.98	-1.96	-0.58	-0.36	0.83
255/361	-0.97	-3.79	-0.10	0.33	-0.20	-0.80	-2.27
277/283	4.65	1.00	-1.09	1.26	1.35	-0.96	-0.14
277/183	-5.48	-1.48	-0.52	0.35	-0.85	2.21	0.76
279/281	5.62	2.82	2.25	0.46	0.72	0.40	-1.72
281/361	4.94	3.66	0.40	-0.62	0.63	0.23	2.13
283/183	8.30	1.51	-0.05	0.22	0.96	-1.71	-0.87
269/257	-0.29	-2.13	-0.07	0.21	0.73	-0.01	0.68
377/335	-0.38	0.32	0.20	0.47	-1.04	0.01	0.20
199/393	-1.89	0.04	-0.09	0.16	0.17	0.27	0.74

[a] *m/z* values of the ratios of abundances of peak pairs.

On the hand, another LDA model was constructed using the matrix that contained the data corresponding to the EV1 and EV2 samples. The eight categories were also very well resolved from each other ($\lambda_w = 0.928$). Taking into account that a large number of categories were simultaneously distinguished, this λ_w value was optimal. As observed in **Fig. 9.10A**, along the first discriminant function, f_1, the t_0 and t_1 appeared well resolved from the other six categories, while the t_0 and t_5 categories appeared resolved along f_2. As observed in **Fig 9.10B**, f_3 was able to resolve t_7 from the other categories, while f_4 resolved the pair t_1/t_6 also from the other categories. Finally, **Fig. 9.10C**, shows a score plot on an oblique plane of the 3-D space defined by the three first discriminant functions. When this 3-D figure was rotated, the separation between all the different categories was clearly evidenced. Due to the large number of categories (seven) included, it was difficult to appreciate the separation between all the category pairs when represented in a plane. The variables selected and the corresponding standardized coefficients of the model are given in **Table 9.6**.

For both LDA models, and using leave-one-out cross-validation, all the points of the respective matrices were correctly classified.

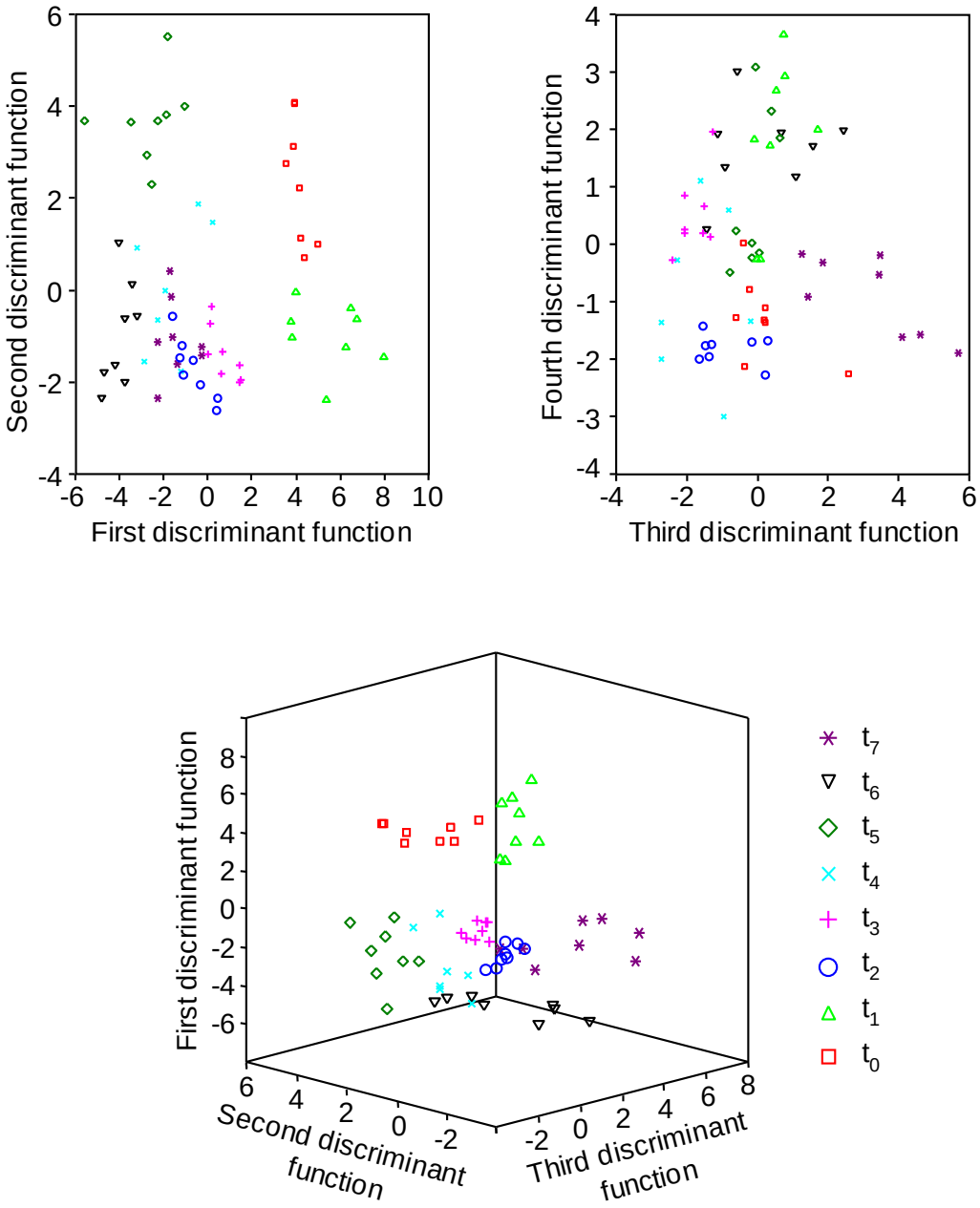

Fig. 9.10. Score plots on the planes of the first and second (A), and third and fourth discriminant functions (B), and on an oblique plane of the 3-D space defined by the three first discriminant functions (C) of the LDA model constructed with the EV1 and EV2 samples.

Table 9.6. Predictors selected and corresponding standardized coefficients of the LDA model constructed with the EV1 and EV2 samples to predict the oxidative status.

Predictors[a]	f_1	f_2	f_3	f_4	f_5	f_6	f_7
255/277	-0.36	-0.33	0.54	1.85	-0.91	0.83	-0.35
255/281	-0.11	-0.34	0.99	1.97	0.84	-1.34	0.55
255/291	-1.17	3.02	-2.94	-8.05	-2.68	-1.73	0.41
277/279	-0.96	-0.02	1.57	0.01	0.85	1.85	0.78
281/283	1.71	-0.18	1.81	2.76	1.26	0.10	0.37
283/291	0.81	-1.90	3.10	7.22	2.96	1.20	-0.17
443/277	-1.38	0.69	0.27	-1.37	3.45	1.23	1.30
443/279	2.91	0.19	-0.22	0.90	-3.26	-1.60	-2.49

[a] *m/z* values of the ratios of abundances of peak pairs

9.3. MOS sensors for monitoring of oxidative status evolution and sensory analysis of VOOs with different phenolic contents

The aim of this work was to establish a non-destructive method based on MOS sensors, in combination with LDA, for the classification of VOOs according to their oxidative level. For this purpose, the EV1 and EV2 samples, previously described in section 9.1, were used. These samples were also evaluated by a panel of testers. Moreover, an additional set of 25 VOO samples, which was also subjected to the panel test assessment, was used to evaluate the LDA model in order to verify if they were well assigned according to sensory data. In order to assure the robustness of the model, these samples were collected by covering different geographical origins and genetic varieties, as well as different years.

9.3.1. Construction of data matrices and LDA models

The signals of the 6 MOS sensors, extracted in this case using the feature

extraction algorithm "classical feature" (see section 3.5.8), were used as predictors for LDA model construction. Three matrices containing 6 predictors each were constructed: one containing EV1 samples (8 x 2 replicates), another containing EV2 samples (8 x 2 replicates), and the third one containing both EV1 and EV2 samples (16 x 2 replicates). A response column containing the 8 categories corresponding to the different storage times was added to the matrices.

Then, a first LDA model was constructed using the matrix containing the EV1 samples. An excellent resolution between all the category pairs was obtained (**Fig. 9.11**, λ_w = 0.049). Taking into account that a large number of categories were simultaneously distinguished, this value was very low.

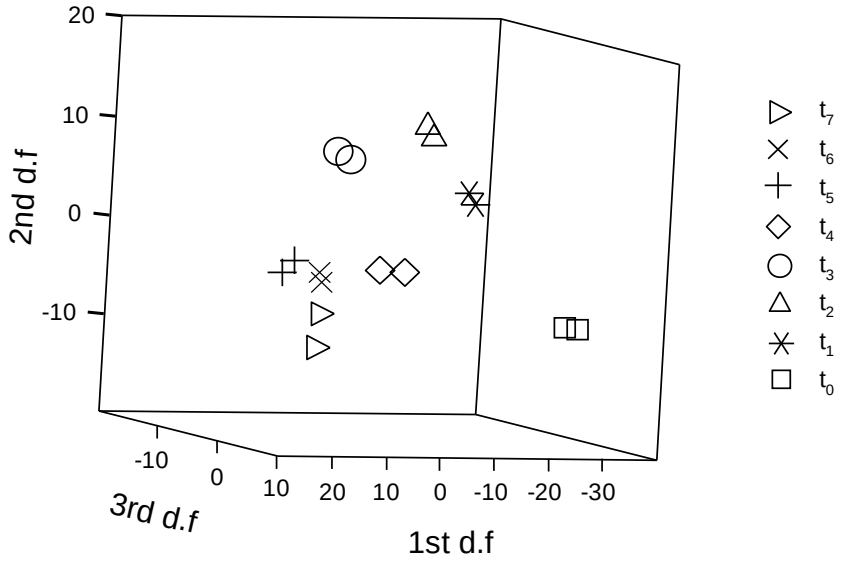

Fig. 9.11. Score plot on an oblique plane of the 3-D space defined by the three first discriminant functions of the LDA model constructed with EV1 samples (d.f., discriminant function).

Next, another LDA model was constructed using the matrix containing the EV2 samples. With this model, resolution between all the category pairs was also excellent (**Fig. 9.12**, λ_w = 0.068).

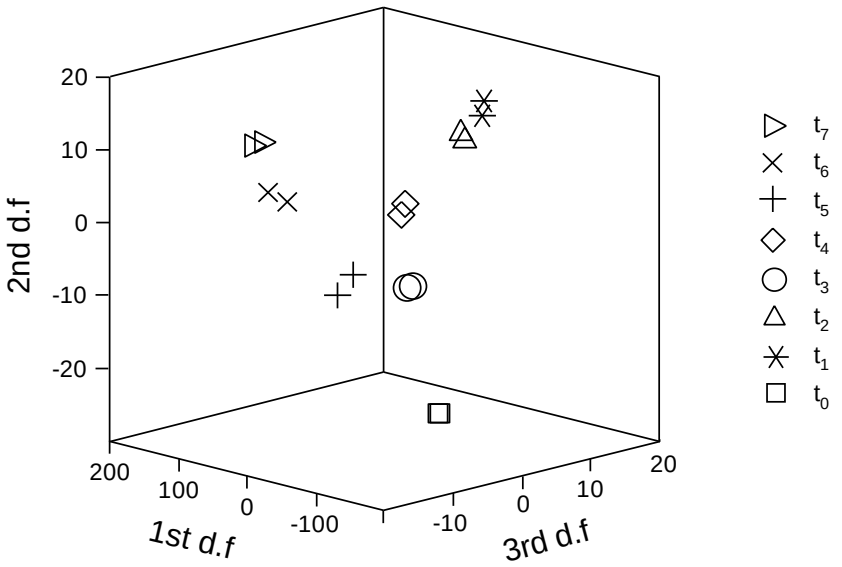

Fig. 9.12. Score plot on an oblique plane of the 3-D space defined by the three first discriminant functions of the LDA model constructed with the EV2 samples. For other comments, see **Fig. 9.11**.

Finally, another LDA model was constructed using all, EV1 and EV2 samples. Again, a satisfactory resolution between all the category pairs was achieved ($\lambda_w = 0.892$). In this case, at any given storage time category, 2 different groups were observed, one for EV1 and the other for EV2 samples (data not shown). This dispersion within the same category could explain the high λ_w value achieved. With this LDA model, it can be concluded that electronic nose data effectively discriminated between samples with and without phenolic compounds at any stage of storage time. The variables selected by the SPSS stepwise algorithm, and the corresponding standardized coefficients of the three models, showing the predictors with large discriminant capabilities, are shown in **Table 9.7**. As can be deduced, the LDA model constructed with the EV1 samples was the only one using sensor 3 as a predictor. For this reason, this sensor was surmised to have a response due to volatile compounds formed after oxidation in the presence of phenolic compounds. For the three models, and using the leave-one-out validation, all points were correctly classified.

Table 9.7. Predictors selected and corresponding standardized coefficients for the three models constructed to predict the storage time.

	Pred.	Sensor 1	Sensor 2	Sensor 3	Sensor 4	Sensor 5
EV1	f_1	1.75	-1.01	0.53	-1.22	-
	f_2	0.50	-0.00	-0.56	1.06	-
	f_3	-1.46	1.27	2.90	-2.39	-
	f_4	3.58	1.47	-3.62	-1.30	-
EV2	f_1	-2.36	-14.51	-	10.73	6.40
	f_2	1.99	0.74	-	-2.30	-0.12
	f_3	0.50	-1.62	-	2.35	-0.30
	f_4	-2.58	0.03	-	0.03	2.93
EV1 and EV2	f_1	-2.83	-5.80	-	4.50	4.16
	f_2	-4.84	-0.90	-	0.96	5.45
	f_3	-2.15	-1.31	-	2.77	1.01
	f_4	4.06	0.33	-	-0.36	-3.25

9.3.2. Sensory analysis and evaluation of the constructed LDA model

The same sets of EV1 and EV2 samples were evaluated by the panel of testers. Only the EV1 sample at t_0 was characterized by a green fruity and leaf and grass attributes, while all other samples had a ripe fruity and any pleasant attributes. Only the EV1 sample at t_1 showed a winey defect, probably masked at t_0 by the green fruity aspect, while rancidity was the only defect noted in all samples during the 7-week period. The evolution of the rancid defect is shown in **Fig. 9.13** (mean values were used instead of median to better show inter-sample variations). As can be observed, rancidity was more pronounced for the EV2 samples, which could be indirectly attributed to the absence of phenolic compounds. Therefore, the model clearly responded to the rancid defect.

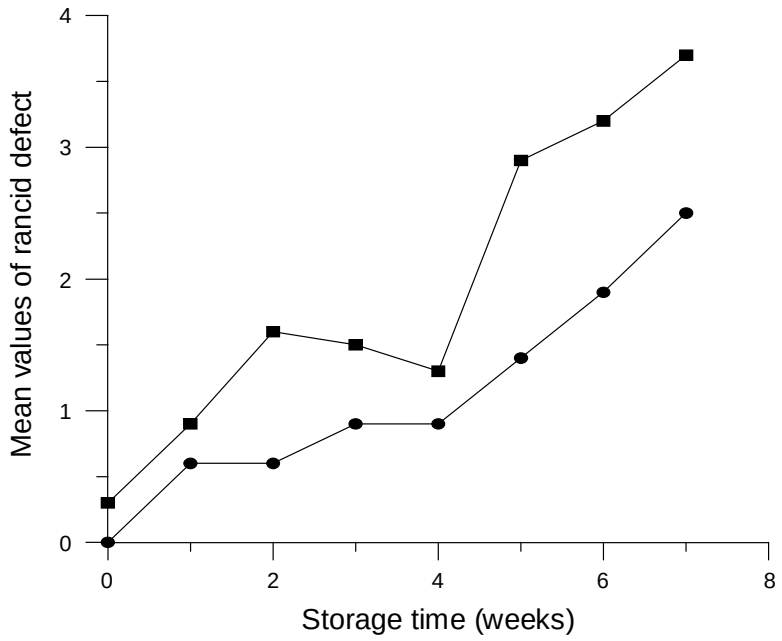

Fig. 9.13. Evolution of the rancid defect expressed as the mean values of the sensory analysis as a function of storage time for EV1 (●) and EV2 (■) samples.

The additional set of 25 VOOs was also subjected to the panel test assessment, being the results of this evaluation used to evaluate the model. The most important sensory attributes of these samples, and the model predicted category, are shown in **Table 9.8**. As observed, the model distinguished all the samples without defects from the other samples, assigning them to the t_0 category. Moreover, **Table 9.8** shows that the model was able to correctly identify 13 defective samples. The two exceptions were samples N16 and N17, which were characterized by a winey defect and fruity absence. In particular, the model responded linearly for the 4 samples characterized by the rancid defect, quite well for N11, N20, and N21, which presented different intensities of fusty, but less for oils with other defects (mouldy, muddy).

Table 9.8. Median values for the sensory attributes and predicted category for the 25 samples used to evaluate the LDA model.

Sample	Fruity (type)	Other pleasant attributes	Defects	Predicted category
N1	3 (green)	2 (grass, tomato)	0	t_0
N2	2 (green)	2 (grass, artichoke, almond)	0	t_0
N3	2 (green)	2 (grass, artichoke)	0	t_0
N4	2 (green)	2 (leaf, almond)	0	t_0
N5	2 (green)	2 (leaf, grass, tomato, almond)	0	t_0
N6	3 (green)	2 (grass, artichoke, tomato)	0	t_0
N7	3 (green)	3 (grass, artichoke, tomato)	0	t_0
N8	3 (green)	2 (grass, artichoke, tomato)	0	t_0
N9	2 (ripe)	2 (other)	0	t_0
N10	2 (ripe)	2 (tomato)	0	t_0
N11	1 (ripe)	0	1.5 (fusty)	t_1
N12	1 (ripe)	0	1 (winey)	t_1
N13	1 (ripe)	0	2 (rancid)	t_1
N14	1 (ripe)	0	5 (3 of muddy, 2 of rancid)	t_2
N15	1 (ripe)	0	2 (rancid)	t_1
N16 [a]	0	0	2 (winey)	t_0
N17 [a]	0	0	3 (winey)	t_0
N18 [a]	0	0	3 (rancid)	t_3
N19 [a]	0	0	5 (rancid)	t_7
N20 [a]	0	0	1 (fusty)	t_1
N21 [a]	0	0	3 (fusty)	t_3
N22 [a]	0	0	1 (muddy)	t_1
N23 [a]	0	0	2 (muddy)	t_1
N24 [a]	0	0	1 (mouldy)	t_1
N25 [a]	0	0	2 (mouldy)	t_1

[a] Official defects provided by IOC.

It is interesting to note that slight differences were observed between the genuinely defected samples (N13 to N15), and between those provided by IOC to recognize the rancid defect (N18 and N19). This could be linked to the differences in total volatile compounds between the profile of VOO and the rancid standard (Aparicio, 2000). In this respect, the near total absence of volatile components responsible for pleasant fruity note (from the LOX pathway), and the presence of high concentrations of several saturated and unsaturated aldehydes in the IOC samples, could have influenced the MOS response.

9.4. Prediction of OFA concentration in VOOs using MOS sensors and MLR

The aim of this work was to develop an electronic nose method capable of predicting, jointly with the use of MLR models, the OFA concentration found in VOOs characterized with different oxidative status. For this purpose, a series of 72 VOOs from different Italian regions (Abruzzo, Emilia-Romagna, Puglia, Sicily and Toscana) were sampled during the harvest seasons 2006-07, 2007-08 and 2008-09. All samples were analyzed between November 2008 and January 2009. The oils differed in terms of olive cultivar, degree of ripening, area of growth, production system (type, productive capacity and manufacturer) and storage time.

9.4.1. OFA content

The HPLC chromatograms in **Fig. 9.14** (A, B and C) showed that the differences in OFA content (low, medium and high) of three VOO samples were related to storage time (2 weeks, 16 months and 34 months after oil production, which correspond to parts A, B and C, respectively). Based on the study of MS spectra, three groups of OFAs were identified (see **Fig. 9.14**): isomeric forms of

keto-linolenic acid (*m/z* 383, 1), isomeric forms of keto-linoleic acid (*m/z* 385, 2) and isomeric forms of keto-oleic acid (*m/z* 387, 3). All these *m/z* values corresponded to the $[M+H]^+$ ions (Rovellini, 1998 and 2004).

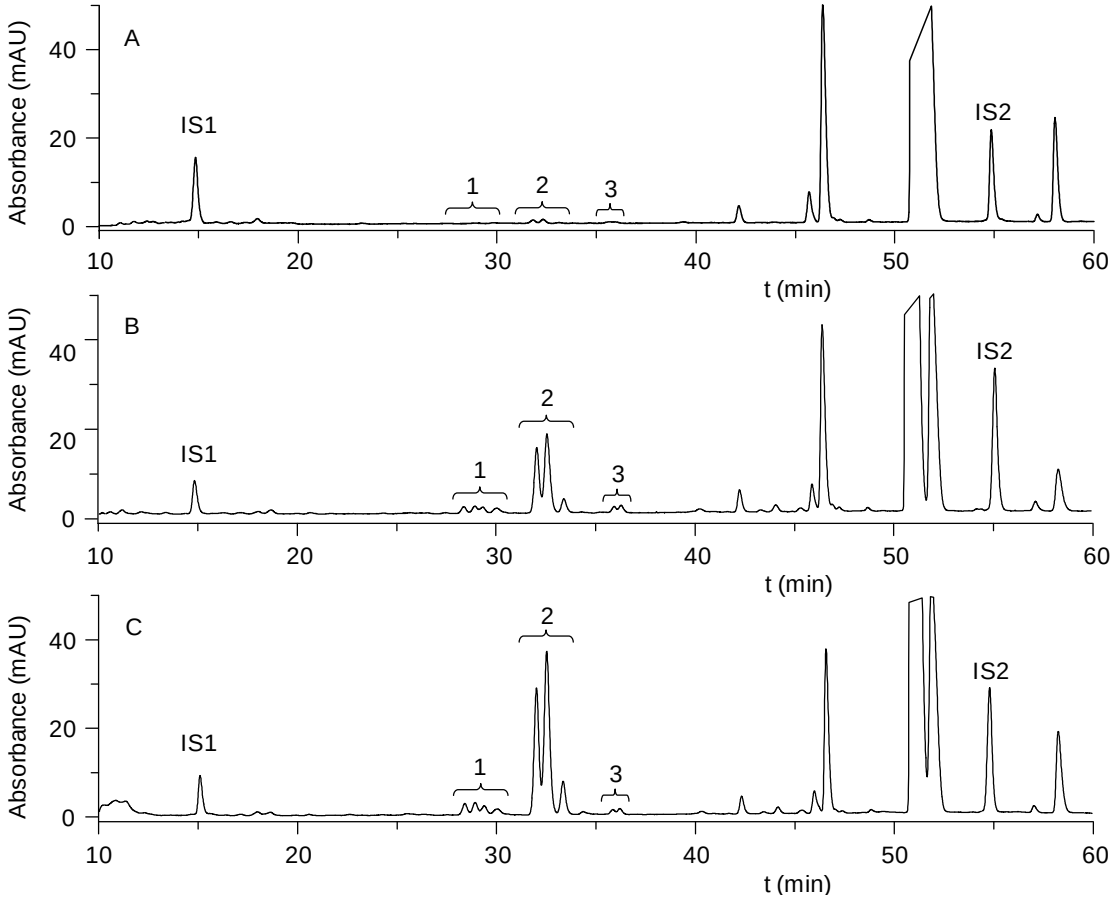

Fig. 9.14. Cromatograms of OFAs in VOOs analyzed after (A) 2 weeks, (B) 16 months and (C) 34 months of oil production. Detection was performed at 255 nm. Peak identification (as benzyl-ester derivatives): 1, group of isomeric forms of keto-linolenic acid; 2 group of isomeric forms of keto-linoleic acid; 3, group of isomeric forms of keto-oleic acid. IS1 and IS2 (internal standards) are benzyl caproate and benzyl heptadecanoate, respectively.

The OFA content was evaluated for the 72 VOO samples, and was found to have a wide range, which varied from 0.3% to 6.5%. This wide range can be attributed to the fact that the oil samples came from different harvest seasons and were analyzed at times ranging from 1 week to 36 months after production. Rovellini (2004) analyzed several VOOs and found that OFA percentages from 2 to 4% are typical for EVOOs stored from 2 to 18 months at room temperature, while oil samples characterized by a total OFA higher than 4% must be considered as "expired".

Taking into account the differences observed in OFA values, samples were divided in 4 groups (**Fig. 9.15A-D**): OFA < 1.0% (**Fig. 9.15A**), 1.0% ≤ OFA < 2.5% (**Fig. 9.15B**), 2.5% ≤ OFA < 4% (**Fig. 9.15C**) and OFA ≥ 4% (**Fig. 9.15D**). Accordingly, the 72 VOOs were subdivided as follows: a first group (G1, n = 23) with a mean of 0.6% OFA; a second group (G2, n = 15) with a mean of 1.8% OFA; a third group (G3, n = 23) with a mean of 3.0% OFA and a fourth group (G4, n = 11) with a mean of 5.3% OFA. All the samples produced within one month before analysis belonged to G1, and exhibited a very narrow range of OFA values (from 0.3 to 0.8%). In contrast, group G4 showed higher OFA percentages and a wider range of variability (from 4.2 to 6.5%). These data confirmed that it is possible to evaluate the freshness of VOOs with a simple OFA assay, thereby reducing the number of analyses (i.e. peroxide values or k_{232} for primary oxidation products, and *p*-anisidine value or volatile content for secondary oxidation products).

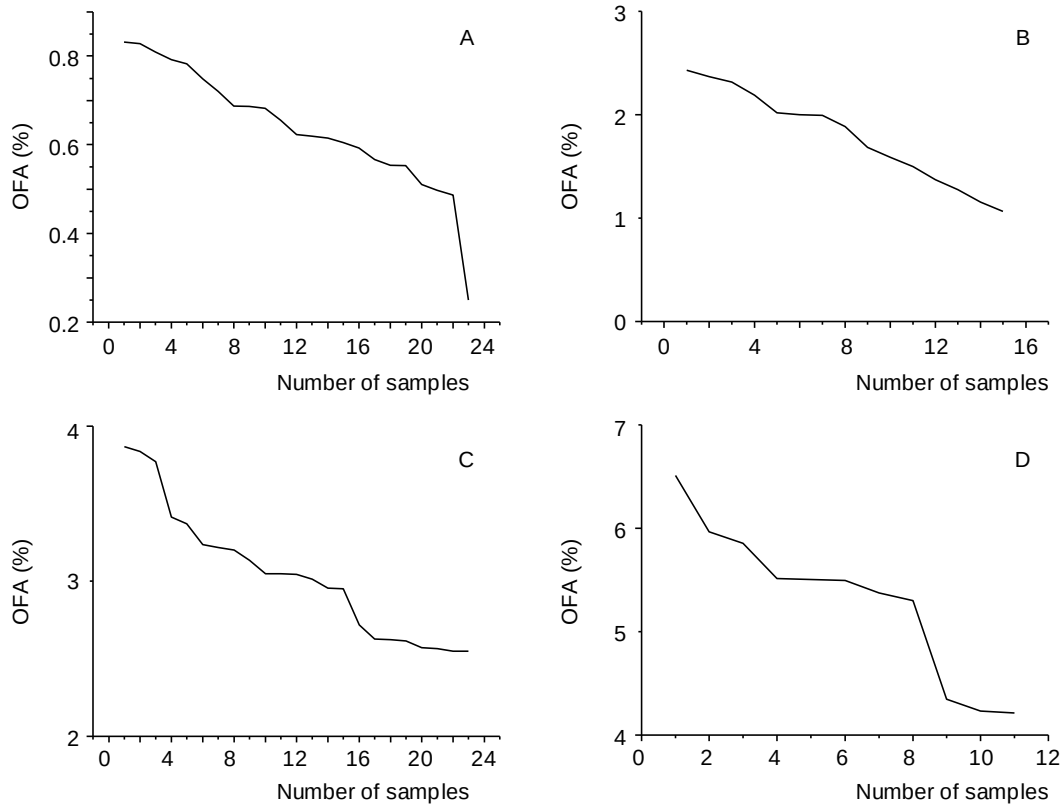

Fig. 9.15. Plots representing the OFA values of the 72 VOOs employed in this study. (A) OFA < 1.0 %; (B), 1.0 % ≤ OFA < 2.5 %; (C), 2.5 % ≤ OFA < 4 % and (D), OFA ≥ 4 %.

9.4.2. Construction of data matrices and MLR models

For MLR studies, calibration and external validation sets were constructed. The calibration matrix contained 60 objects, which were randomly selected, and which corresponded to the average of the duplicates for each sample. The signals of the 6 MOS sensors, extracted using the extraction algorithm "classical feature" (see section 3.5.8), were used as predictors. The external validation matrix was constructed with the remaining 12 objects corresponding to the averages of the duplicates of the samples. Also in this case, the signals of the 6 sensors were added to this matrix. A response column, containing the OFA concentrations (obtained by HPLC), was then added to these matrices.

Using the calibration matrix, two MLR models were constructed, which corresponded to the exclusion and inclusion of an independent term (a constant). Linearity was worse for the model including the constant than for the model without the constant (r = 0.961). For this reason, further studies were performed without the inclusion of the constant. The correlation plot of the calculated versus the experimental OFA percentages is shown in **Fig. 9.16A**. When leave-one-out validation was applied, the average prediction error (calculated as the sum of the absolute differences between expected and calculated OFA percentages divided by the number of predictions) was 30%. In order to obtain information regarding the quality of the model, residual values and/or the relative errors were examined. For this purpose, a plot representing the residual values against the experimental OFA percentages (**Fig. 9.16B**) was obtained.

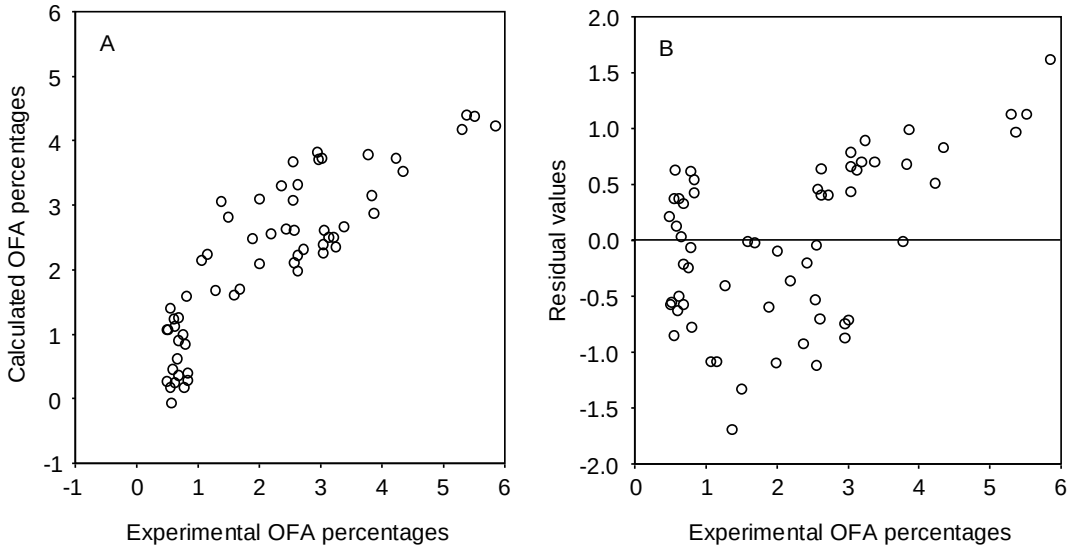

Fig. 9.16. (A) Correlation plot of the calculated versus the experimental OFA percentages. (B) Plot of the residual values versus the experimental OFA percentages.

A dependence of the residuals with the experimental values was observed and therefore, heteroscedasticity (non-constant variance) was evidenced. The problem of heteroscedasticity can be overcome either by applying a transformation of the variables or by using weighted least-squares (Vandeginste, 1998). For this reason, the following transformations were applied to the experimental OFA percentages: natural logarithm and square and cube roots. Homocedasticity was obtained when the cube root transformation was used (see **Fig. 9.17B**). Using the cube root transformation, linearity also improved (r = 0.995). The correlation plot of the calculated versus the experimental OFA percentages obtained using the cube root transformation is shown in **Fig. 9.17A**.

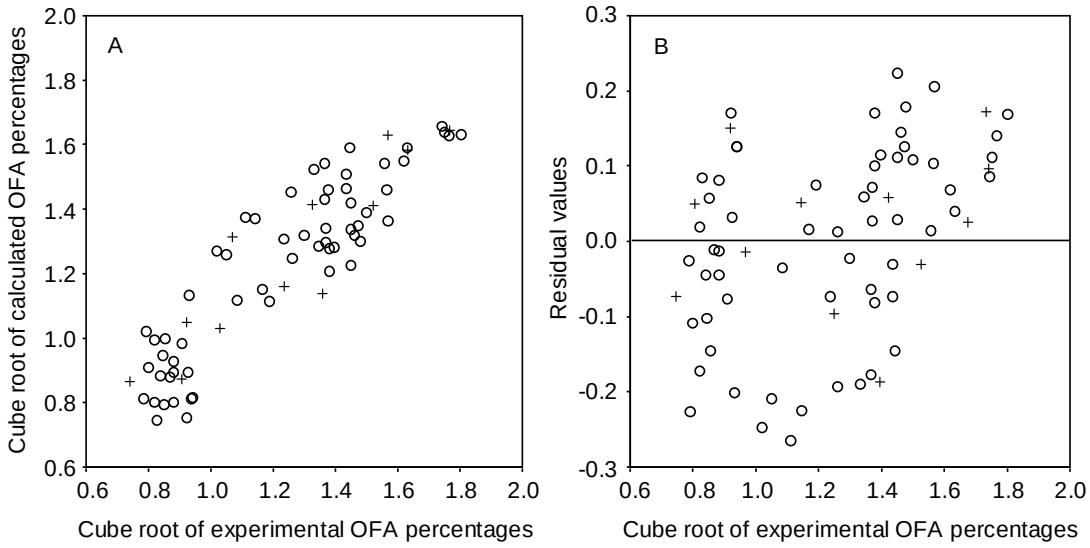

Fig. 9.17. (A) Correlation plot of the calculated versus the experimental OFA percentages obtained after cube root transformation. (B) Plot of the residual values versus the experimental OFA percentages obtained after cube root transformation. For both, A and B, samples were marked as calibration (○) and validation (+).

The predictors selected during model construction, and their corresponding non-standardized coefficients and confidence limits, are detailed in **Table 9.9**. According to this table, sensors 2 - 6 were selected, which

corresponded to $SnO_2 + SiO_2$, to SnO_2 catalyzed with three different metals and to WO_3. When leave-one-out validation was applied, the average prediction error was 8%. When the model was applied to the validation set, a good prediction capability was observed (see **Fig. 9.17A**), being the average validation error 9%.

Table 9.9. Predictors selected and their corresponding non-standardized coefficients (coef.), and confidence limits for the MLR model constructed after a cube root transformation of the variable.

Predictor	Coef.	Confidence limits[a]
Sensor 2	3.18	2.42, 3.94
Sensor 3	10.12	7.67, 12.57
Sensor 4	-8.61	-10.63, -6.58
Sensor 5	-7.98	-10.12, -5.84
Sensor 6	6.16	4.63, 7.69

[a] For a 95 % confidence interval.

9.5. Prediction of OFA concentration in VOOs using FTIR and MLR

The aim of this work was to develop an FTIR method capable of predicting, jointly with the use of MLR models, the OFA concentration found in VOOs characterized by different oxidative statuses. For this purpose, the 72 VOO samples employed in section 9.4 were also used.

9.5.1. Description of FTIR spectra and construction of data matrices and MLR models

The FTIR spectra of the same 3 VOO samples presented in section 9.4.1, which were characterized by different storage times, and thus having different OFA content (see the chromatograms of **Fig. 9.14**), are shown in **Fig. 9.18**.

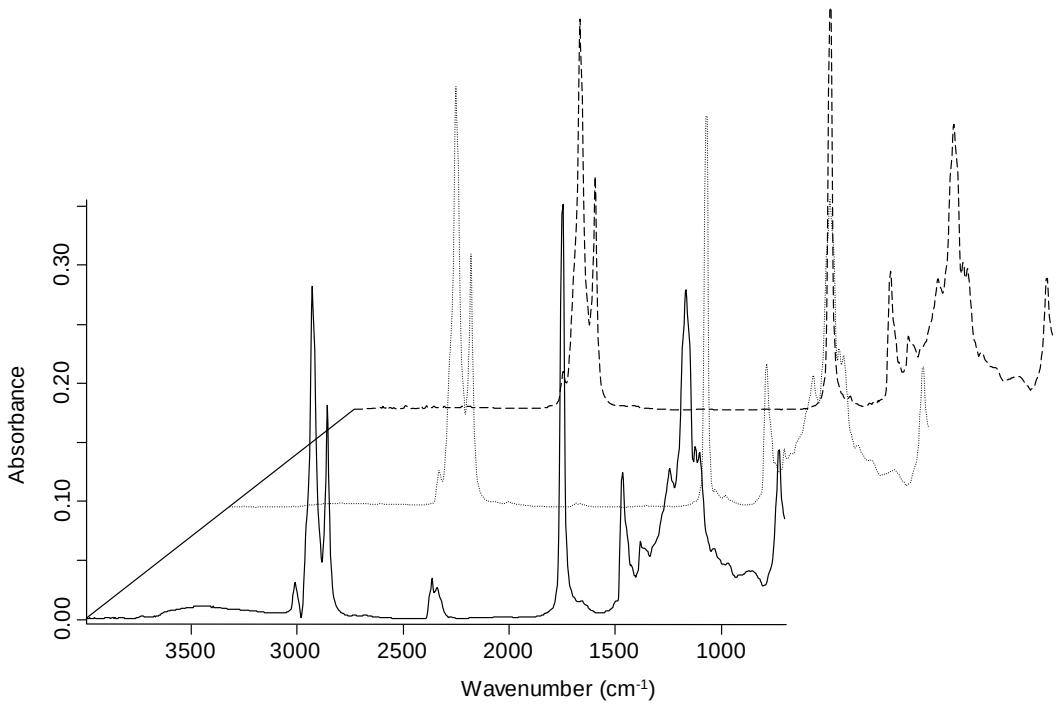

Fig. 9.18. FTIR spectra of VOOs after 2 weeks (—), 16 months (···) and 34 months (---) of oil production.

In order to obtain the variables to be used in MLR model construction, the FTIR spectra were divided in 25 wavelength regions. These regions were described in **Table 5.2**. For each region, the peak or shoulder area was measured and used as original variable. After application of normalization procedure B, a total of 300 normalized variables to be used as predictors were obtained.

Then, for MLR studies, calibration and external validation sets were constructed. The calibration matrix contained 60 objects (which were randomly selected), which corresponded to the average of the three spectra recorded for each sample, as well as the 300 predictors. The external validation matrix was constructed with the remaining 12 samples, also corresponding to the average of three spectra, also having the 300 predictors. A response column, containing the OFA concentrations (obtained by HPLC), was then added to these matrices.

As indicated in section 9.4.2, the calibration matrix was used to construct

two MLR models, which were obtained either with or without the inclusion of a constant. Also in this case, linearity was worse for the model including the constant than for the model without the constant (r = 0.944). For this reason, further studies were performed without the inclusion of the constant. The correlation plot of the predicted versus the experimental OFA percentages, obtained without the inclusion of the constant, is shown in **Fig. 9.19A**.

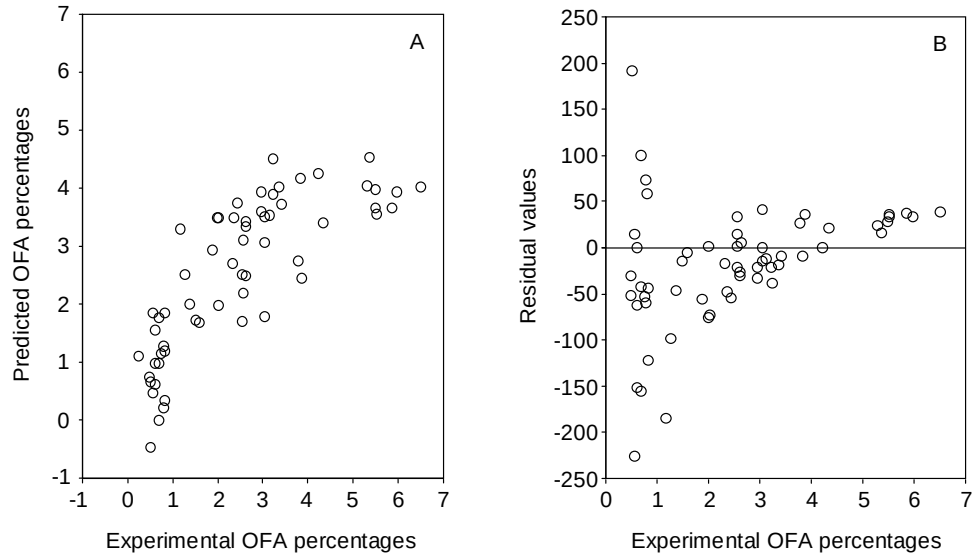

Fig. 9.19. (A) Correlation plot of the predicted versus the experimental OFA percentages. (B) Plot of the residual values versus the experimental OFA percentages.

When leave-one-out validation was applied, the average prediction error (calculated as previously described in section 9.4.2) was 52%. In order to obtain information regarding the quality of the model, residual values were examined. For this purpose, the residual values were plotted against the experimental OFA percentages (**Fig. 9.19B**). Also in this case, the data showed a pronounced heteroscedasticity. For this reason, the following variable transformations were applied to the experimental OFA percentages: natural logarithm and square and

cube roots. An acceptable homoscedasticity was achieved when the cube root transformation was used (see **Fig. 9.20B**). Using the cube root transformation, linearity also improved (r = 0.996). The correlation plot of the predicted versus the experimental OFA percentages obtained using the cube root transformation is shown in **Fig. 9.20A**. The predictors selected for this model and their corresponding non-standardized coefficients are detailed in **Table 9.10**. According to this table, the wavelength regions with a predominant weight in the construction of the MLR model corresponded to =C-H (trans and cis, stretching), -C-H (CH_2, stretching asym), O-H (bending in plane), C-O (stretching), -H-C=C-H- (cis?) and =CH_2 (wagging). These regions were those more affected by oxidation. In fact, most of these regions were characterized by a functional group with an oxygen or a double bond. When leave-one-out validation was applied, the average prediction error was 8%. When the model was applied to the validation set, an excellent prediction capability was observed (see **Fig. 9.20A**), being the average validation error 17%.

Table 9.10. Predictors selected and their corresponding non-standardized coefficients (coef.) for the MLR model constructed after the cubic root transformation of the variable.

Predictor	Coef.
3/17	0.056
3/20	-0.020
1/23	-0.068
19/22	-0.041
6/7	-0.001
14/22	-0.001
5/24	0.003
12/17	0.261

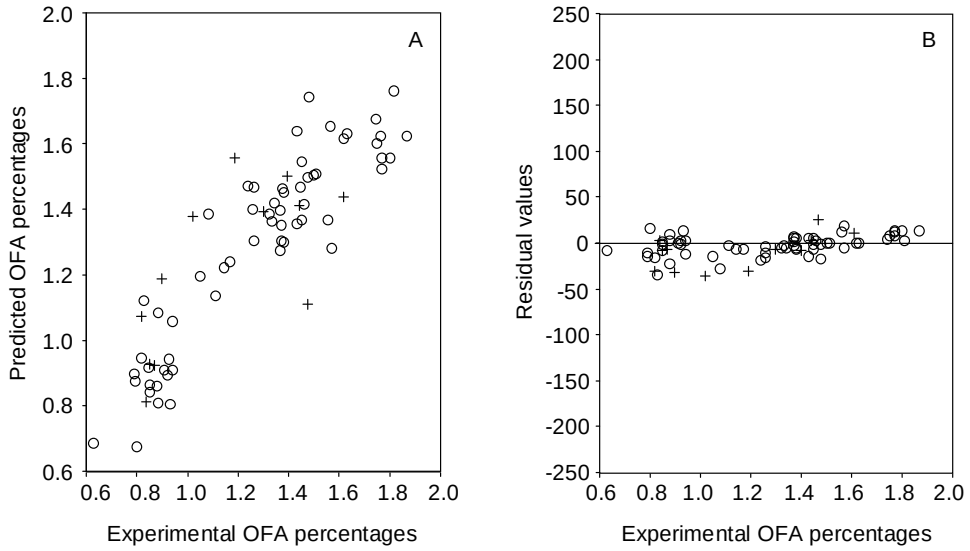

Fig. 9.20. (A) Correlation plot of the predicted versus the experimental OFA percentages obtained after cube root transformation. (B) Plot of the residual values versus the experimental OFA percentages obtained after cube root transformation. For both, A and B, samples were marked as calibration (○) and validation (+).

CAPÍTULO 10

CONCLUSIONES GENERALES

10. Conclusiones generales

10.1. Desarrollo de métodos para la determinación de Ts y T_3s en aceites vegetales

Se han desarrollado diversos métodos para la determinación de Ts y T_3s en aceites vegetales.

Se ha desarrollado un método por CEC usando columnas monolíticas de LMA de fabricación propia. La mezcla de polimerización óptima, con un 12% de 1,4-butanodiol, permitió obtener una columna caracterizada por tamaños de poro pequeños (250 nm). Para la separación de Ts, el mejor compromiso entre resolución y tiempo de análisis (menos de 10 min) se consiguió con una fase móvil constituida por MeOH/agua 99:1 (v/v) amortiguada a pH 8. Por otro lado, para analizar muestras ricas en T_3s, la composición de la fase móvil más adecuada fue una mezcla de MeOH/agua 97:3 (v/v) a pH 8.

También se ha desarrollado un método de nano-LC para la determinación de Ts y T_3s. La separación de los analitos se estudió con 2 columnas monolíticas diferentes, una columna de sílice comercial y una columna de LMA de fabricación propia. Usando la columna monolítica de sílice, el mejor compromiso entre eficacia, resolución y un tiempo de análisis corto (menor de 18 min) se consiguió con una fase móvil constituida por ACN/MeOH/agua 75:8:17 (v/v/v) que contenía un 0,2% de ácido acético. Cuando se utilizó la columna monolítica de LMA, la composición de la fase móvil adecuada fue un 96% de la mezcla ACN/agua (76:24) y un 4% de MeOH. Con esta composición, se obtuvo un

tiempo de análisis similar al obtenido con la columna de sílice. Entre las ventajas del método de nano-LC cabe destacar el bajo consumo de disolventes y de muestra (10 nL).

Ambos métodos, CEC y nano-LC, permiten la detección y evaluación de la adulteración de aceites de oliva con otros aceites vegetales de diferente origen botánico, además de permitir la identificación de la adulteración con aceites ricos en T_3s en un tiempo de análisis corto.

Debido a estas características, estos métodos constituyen una alternativa a los métodos de HPLC, que es la técnica normalmente utilizada en estas determinaciones. Además, se ha demostrado el potencial de las columnas monolíticas, que representan una alternativa competitiva frente a columnas empaquetadas.

10.2. Desarrollo de métodos para la determinación de esteroles en aceites vegetales

Se han desarrollado métodos para la determinación de esteroles en aceites vegetales.

Se ha propuesto un método por CEC usando columnas monolíticas de metacrilato de fabricación propia. Se optimizó la composición de la mezcla de polimerización usándose 2 monómeros diferentes, LMA y ODMA, y variando la relación monómeros/porógenos, monómero/agente entrecruzante y la relación entre los disolventes porogénicos. Los mejores resultados en términos de resolución, eficacia y tiempos de análisis cortos (menos de 7 min) se obtuvieron con una columna de LMA preparada con una relación LMA/EDMA de 60:40 y

60% de porógenos con un 20% de 1,4-butanodiol (12% en la mezcla de polimerización). Como fase móvil óptima se seleccionó una mezcla ACN/2-propanol/agua con 5 mM de Tris a pH 8. En comparación con otros procedimientos de CEC, con el método propuesto se redujo considerablemente el tiempo de análisis, obteniéndose LODs bajos.

También se ha desarrollado un método por UPLC-MS para la determinación de esteroles. Con este método se obtuvo una rápida separación de los analitos (menos de 5 min), obteniéndose picos de elevada eficacia y simetría. Aunque algunos picos de las muestras no aparecieron completamente resueltos en relación al tiempo de retención, la alta selectividad proporcionada por el modo de adquisición SIR del espectrómetro de masas permitió obtener señales bien resueltas para prácticamente todos los analitos.

Los métodos basados en la determinación de los esteroles mediante CEC y UPLC-MS, al igual que los desarrollados para la determinación de Ts y T_3s, permitieron la rápida detección y evaluación de la adulteración de aceites de oliva con otros aceites vegetales de diferente origen botánico.

10.3. Desarrollo de métodos para la clasificación de aceites vegetales en función de su origen botánico

Se han desarrollado métodos rápidos y sencillos, capaces de clasificar aceites vegetales en función de su origen botánico mediante tratamiento de los datos con modelos de LDA.

Para ello y en primer lugar, se han utilizado los datos obtenidos mediante espectroscopia FTIR. Una vez dividido el espectro IR en 26 regiones, se construyó un modelo de LDA capaz de clasificar muestras de aceites vegetales de 5 categorías diferentes mediante el empleo de tan solo 8 regiones espectrales. Por otro lado, se demostró el potencial de la espectroscopia FTIR para la

predicción de la adulteración del EVOO con aceite de girasol, soja, avellana o maíz. Se obtuvieron modelos de MLR construidos con una sola predictora, excepto para la mezcla EVOO-maíz, en la que el modelo se construyó con 2 predictoras. Todos estos modelos fueron capaces de detectar al menos un 5% del aceite adulterante en el EVOO.

En segundo lugar, se utilizaron los perfiles de esteroles obtenidos mediante infusión directa en MS. Con este fin, se utilizaron las interfaces ESI y APPI. En todos los casos, la fuente APPI dio lugar a mayores sensibilidades y mejores relaciones señal-ruido que la fuente ESI. Sin embargo, usando tanto ESI-MS como APPI-MS, se obtuvieron modelos de clasificación capaces de discriminar los aceites vegetales en función de su origen botánico. Por otro lado, se obtuvo una excelente correlación entre los perfiles de esteroles obtenidos mediante el método propuesto y los obtenidos mediante GC-FID (método oficial). Por todo esto, el método propuesto es una buena alternativa frente al método oficial, con la ventaja adicional de que no requiere una separación cromatográfica previa.

En tercer lugar, se utilizaron los perfiles de los alcoholes alifáticos y triterpénicos, obtenidos mediante HPLC-MS, con el mismo propósito clasificatorio. Se obtuvo un modelo de LDA capaz de clasificar correctamente a los aceites con una probabilidad de acierto superior al 95%.

Por último, y con el mismo fin, se utilizó la información proveniente de las proteínas presentes en los aceites. Para ello, las proteínas se aislaron mediante precipitación y se procedió a su hidrólisis. Los aminoácidos resultantes se determinaron mediante infusión directa en MS y mediante HPLC-UV-Vis previa derivatización con OPA-NAC. En el caso de la MS, y mediante la aplicación sucesiva de 3 modelos de LDA, se consiguió clasificar a aceites provenientes de 8 orígenes botánicos. Por otra parte, usando los perfiles obtenidos mediante

HPLC-UV-Vis, y construyendo un único modelo de LDA, fue posible clasificar aceites de 7 orígenes distintos, con una capacidad de predicción del 100%.

10.4. Desarrollo de métodos para la evaluación de la calidad del aceite de oliva

Se ha desarrollado un método rápido y sencillo, basado en infusión directa del aceite en un espectrómetro de masas, capaz de predecir la calidad de los aceites de oliva. Tras una sencilla dilución de las muestras (1:50), los aceites se infunden en el espectrómetro de masas, midiéndose las abundancias de los picos de los ácidos grasos. Los perfiles de estos compuestos se utilizaron con el fin de construir un modelo de LDA que fue capaz de discriminar los aceites en función de su calidad. Por otro lado, usando MLR, se pudieron evaluar mezclas binarias de aceites de diferente calidad con errores de predicción medios comprendidos entre el 3% y el 5%, aunque para mezclas EVOO/ROPO los errores encontraron fueron cercanos al 11%.

Por otro lado, se ha desarrollado un método basado en la respuesta de una matriz de sensores MOS con la finalidad de evaluar la presencia de los principales defectos del VOO. Una vez establecido el umbral sensorial de los diversos defectos por el panel de cata, se construyó un modelo de LDA y una ANN con el fin de diferenciar a los aceites en función de este umbral, obteniéndose excelentes resultados. Además, se consiguieron excelentes predicciones del porcentaje de defecto añadido a cada muestra mediante la construcción de diversos modelos de MLR. Por ello, se puede concluir que la nariz electrónica, si se ha entrenado bien, puede ser considerada como una excelente herramienta con la que trabajar en línea con los catadores. Entre otras características favorables, la nariz electrónica permite discriminar rápidamente aceites con defectos respecto a aceites con buenas propiedades organolépticas.

Además, se puede utilizar para examinar el correcto funcionamiento de un panel de cata.

10.5. Desarrollo de métodos para la clasificación de EVOOs en función de su variedad genética

Se han desarrollado métodos rápidos y sencillos, capaces de clasificar EVOOs en función de su variedad genética mediante el empleo de modelos de LDA.

En primer lugar, se utilizaron los datos obtenidos mediante espectroscopia FTIR. Una vez dividido el espectro IR en 20 regiones, se construyó un modelo de LDA, que fue capaz de clasificar EVOO de 7 variedades genéticas, principalmente cultivadas en la Comunidad Valenciana, España. Mediante el empleo de tan solo 9 variables predictoras, se consiguió una excelente resolución entre todos los pares de categorías.

En segundo lugar, se hizo uso de los datos de MS obtenidos mediante infusión directa de las muestras. Para ello, se procedió a diluir (1:50) las muestras de EVOO, y sin previa extracción, éstas se inyectaron en un espectrómetro de masas, midiéndose los perfiles de ácidos grasos y también de compuestos fenólicos. Usando modelos de LDA construidos con ambos perfiles, los aceites se clasificaron perfectamente según su variedad genética.

Posteriormente, se estudió la posibilidad de clasificar EVOO de acuerdo con su perfil de esteroles establecido mediante HPLC-MS y UPLC-MS. En ambos casos, fueron necesarios 2 modelos de LDA aplicados secuencialmente para clasificar correctamente a todas las muestras, siendo la capacidad de predicción mayor del 88% en todos los casos.

Todos los métodos desarrollados son de interés desde el punto de vista industrial dado que proporcionan una rápida identificación de la variedad genética en EVOOs.

10.6. Desarrollo de métodos para la clasificación de EVOOs en función de su origen geográfico

Se ha desarrollado un método de CEC usando columnas de LA de fabricación propia, que permite predecir el origen geográfico de EVOOs en función del perfil de compuestos fenólicos. La mejor resolución entre los analitos se consiguió usando una columna de LA con un 15% de 1,4-butanodiol en la mezcla de polimerización, y una fase móvil compuesta por una mezcla ACN/agua 15:85 (v/v) que contenía 5 mM de ácido fórmico a pH 3. Usando los datos de CEC y un modelo de LDA, se consiguió una excelente resolución entre las 3 categorías consideradas (EVOOs de España, Italia y Croacia).

10.7. Desarrollo de métodos para la evaluación de la oxidación del aceite de oliva

En primer lugar, se han estudiado los cambios químicos producidos en muestras de VOO que contenían diferente contenido de compuestos fenólicos durante un proceso de envejecimiento acelerado. Ambos tipos de muestras presentaron valores muy diferentes de tiempo OSI, lo que demuestra la alta contribución de los compuestos fenólicos a la estabilidad del aceite. Por otro lado, al estudiar la variación del perfil de compuestos fenólicos durante el envejecimiento, se observó una disminución en la concentración de los secoiridoides más abundantes, así como la formación de algunas de sus formas oxidadas. Por esta razón, se propuso el uso de las concentraciones de estas formas oxidadas como marcadores de la pérdida de frescura en VOOs.

En segundo lugar, las muestras sometidas al proceso de envejecimiento acelerado se han analizado mediante infusión directa en MS, y también mediante una matriz de sensores MOS, con el fin de construir un modelo de LDA capaz de predecir el tiempo de oxidación de cada una de ellas. En el análisis con MS se usaron como variables predictoras las intensidades de ácidos grasos, OFAs y compuestos fenólicos, así como las intensidades de sus productos de oxidación. Estas intensidades, que fueron medidas tras una simple dilución de las muestras con una mezcla alcalina de disolventes, hicieron posible un análisis rápido de las muestras, evitándose así los métodos de extracción convencionales para este tipo de compuestos. Se obtuvo un excelente modelo de LDA que fue capaz de resolver todos los pares de categorías. Por otro lado, cuando el análisis se llevó a cabo con la nariz electrónica se utilizaron las señales de los sensores como variables predictoras. El modelo de LDA construido dio lugar también a una excelente resolución entre todos los pares de categorías. Además, este modelo fue evaluado mediante el análisis de diversas muestras envejecidas cuya categoría fue determinada por análisis sensorial. Se observó una buena correlación entre el modelo de LDA y el análisis sensorial. En particular, el modelo fue capaz de distinguir todos los VOOs sin defectos de los defectuosos, siendo capaz también de responder linealmente a las muestras caracterizadas por rancidez.

Finalmente, mediante la construcción de modelos de MLR, se han desarrollado métodos capaces de predecir la concentración de OFAs en diversas muestras de VOO oxidados de un modo natural. Estas muestras fueron analizadas mediante nariz electrónica y mediante espectroscopia FTIR. Usando ambas técnicas, fue necesario aplicar la raíz cúbica a los datos experimentales de OFAs con el fin de obtener homocedasticidad en los residuales. Usando los datos de la nariz electrónica, se obtuvo un modelo de MLR construido con 5 variables

predictoras con un error promedio del 9%, mientras que usando los datos obtenidos mediante espectroscopia FTIR el modelo se construyo con 8 variables predictoras, siendo su error promedio del 17%.

Los dos métodos propuestos, basados en la nariz electrónica y en la espectroscopia FTIR, son una buena alternativa al método HPLC dado que se evita la extracción de los OFAs y se tienen tiempos de análisis más cortos.

CAPÍTULO 11

REFERENCIAS

11. Referencias

Aballe, M.; López Ruiz, J.; Badía, J. M.; Adeva, P. Microscopía electrónica de barrido y microanálisis por rayos X. CSIC y Ed. Rueda, Madrid, Spain (1996)

Abidi, S. L. J. Chromatogr. A 844 (1999) 67

Abidi, S. L. J. Chromatogr. A 881 (2000) 197

Abidi S. L. J. Chromatogr. A 1059 (2004) 199

Abidi, S. L.; Mounts, T. L. J. Chromatogr. A 782 (1997) 25

Abidi, S. L.; Rennick, K. A. J. Chromatogr. A 913 (2001) 379

Abidi, S. L.; Thiam, S.; Warner, I. M. J. Chromatogr. A 949 (2002) 195

Abou Hadeed, A. M. F.; Kotb, A. R.; Daniels, C. E. J. Food Chem. 35 (1990) 167

Agiomyrgianaki, A.; Petrakis, P. V.; Dais, P. Talanta 80 (2010) 2165

Al-Ismail, K.; Caboni, M. F.; Lercker G. Riv. Ital. Sost. Grasse 75 (1998) 175

Al-Ismail, K.; Caboni, M. F.; Rodríguez-Estrada, M. T.; Lercker, G. Grasas Aceites 50 (1999) 448

Allalout, A.; Krichène, D.; Methenni, K.; Taamalli, A.; Oueslati, I.; Daoud, D.; Zarrouk, M. Scientia Horticulturae, 120 (2009) 77

Alter, M.; Gutfinger, T. Riv. Ital. Sost. Grasse 59 (1982) 14

Aparicio, R.; Alonso, V.; Morales, M. T. Grasas Aceites 45 (1994) 241

Aparicio, R.; Aparicio-Ruíz, R. J. Chromatogr. A 881 (2000) 93

Aparicio, R.; Morales, M. T. J. Sci. Food Agric. 67 (1995) 247

Aparicio, R.; Rocha, S. M.; Delgadillo, I.; Morales, M. T. J. Agric. Food Chem. 48 (2000) 853

Aparicio, R.; Roda, L.; Albi, M. A.; Gutiérrez, F. J. Agric. Food Chem. 47 (1999) 4150

Armaforte, E.; Mancebo-Campos, V.; Bendini, A.; Salvador, M. D.; Fregapane, G.; Cerretani, L. J. Sep. Sci. 30 (2007) 2401

Aturki, Z.; D'Orazio, G.; Fanali, S. Electrophoresis 26 (2005) 798

Aturki, Z.; Fanali, S.; D´Orazio, G.; Rocco, A.; Rosati, C. Electrophoresis 29 (2008) 1643

Azadmard-Damirchi, S.; Savage, G. P.; Dutta, P. C. J. Amer. Oil Chem. Soc. 82 (2005) 717

Baccouri, O.; Bendini, A.; Cerretani, L.; Guerfel, M.; Baccouri, B.; Lercker, G.; Zarrouk, M-; Miled, D. D. B. Food Chem. 111 (2008) 322

Baccouri, O.; Guerfel, M.; Baccouri, B.; Cerretani, L.; Bendini, A.; Lercker, G.; Zarrouk, M.; Daoud Ben Miled, D. Food Chem. 109 (2008B) 743

Baeten, V.; Fernández Pierna, J. A.;Dardenne, P.;Meurens, M.;García-González, D. L.; Aparicio-Ruiz, R. J. Agric. Food Chem. 53 (2005) 6201

Baeuml, F.; Welsh, T. J. Chromatogr. A 961 (2002) 35

Baldioli, M.; Servili, M.; Perretti, G.; Montedoro, G. F. J. Am. Oil Chem. Soc. 73 (1996) 1589

Ballesteros, E.; Gallego, M.; Valcárcel, M. Anal. Chim. Acta 308 (1995) 253

Bandarra, N. M.; Campos, R. M.; Batista, I.; Nunes, M. L.; Empis, J. M. J. Am. Oil Chem. Soc. 76 (1999) 905

Barceló-Barrachina, E.; Moyano, E.; Galceran, M. T. Electrophoresis 25 (2004) 1927

Barranco, D.; Cimato, A.; Florino, P.; Rallo, L.; Touzani, A.; Castañeda, C.; Sefarini, F.; Trujillo, I. Catálogo mundial de variedades de olivo. Ed. Consejo Oleícola Internacional (2001)

Bendini, A.; Bonoli, M.; Cerretani, L.; Biguzzi, B.; Lercker, G.; Gallina-Toschi, T. J. Chromatogr. A 985 (2003) 425

Bendini, A.; Cerretani, L.; Carrasco-Pancorbo, A.; Gómez-Caravaca, A. M.; Segura-Carretero, A.; Fernández-Gutiérrez A., Lercker, G. Molecules 12 (2007) 1679

Bendini, A.; Cerretani, L.; Salvador, M. D.; Fregapane, G.; Lercker, G. Ital. J. Food Sci. 21 (2009) 389

Bendini, A.; Cerretani, L.; Vecchi, S.; Carrasco-Pancorbo, A.; Lercker, G. J. Agric. Food Chem. 54 (2006) 4880

Beneito-Cambra, M.; Bernabé-Zafón, V.; Herrero-Martínez, J. M.; Simó-Alfonso, E. F.; Ramis-Ramos, G. Talanta 79 (2009) 275

Benitez-Sánchez, P. L.; León-Camacho, M.; Aparicio, R. Eur. Food Res. Technol. 218 (2003) 13

Bernabé-Zafón, V.; Cantó-Mirapeix, A.; Simó-Alfonso, E. F.; Ramis-Ramos, G.; Herrero-Martínez, J. M. Electrophoresis 30 (2009) 1929

Blekas, G.; Tsimidou, M.; Bouskou, D. Food Chem. 52 (1995) 289

Bohacenko, I.; Kopicová, Z.; Czech J. Food Sci. 19 (2001) 97

Bonoli, M.; Bendini, A.; Cerretani, L.; Lercker, G.; Gallina-Toschi, T. J. Agric. Food Chem. 52 (2004) 7026

Bonoli-Carbognin, M.; Cerretani, L.; Bendini, A.; Almajano, M. P.; Gordon M. H. J. Agric. Food Chem. 56 (2008) 7076

Boselli, E.; Di Lecce, G.; Strabbioli, R.; Pieralisi, G.; Frega, N.G. LWT - Food Sci. Technol. 42 (2009) 748

Boskou, D. Olive oil, chemistry and technology. AOCS Press, Champaign, IL, USA (1996)

Boskou, D. Olive Oil, in Gunstone, F.D. Vegetable oils in food technology. CRC Press, Blackwell Publishing Ltd., Oxford, UK (2002) pp. 244-277

Brenes, M.; García, A.; García, P.; Garrido, A. J. Agric. Food Chem. 48 (2000) 5178

Brenes, M.; García, A.; Rios, J. J.; García, P.; Garrido, A. Int. J. Food Sci. Technol. 37 (2002) 615

Brunauer, S.; Emmet, P. H.; Teller, E. J. Am. Chem. Soc. 60 (1938) 309

Cahours, X.; Cherkaoui, S.; Rozing, G. P.; Veuthey, J. L. Electrophoresis 23 (2002) 2320

Camurati, F.; Tagliabue, S.; Bresciani, A.; Sberveglieri, G.; Zaganelli, P. Riv. Ital. Sost. Grasse 83 (2006) 205

Cantó-Mirapeix, A.; Herrero-Martínez, J. M.; Mongay-Fernández, C.; Simó-Alfonso, E. F. Electrophoresis 29 (2008) 4399

Cantó-Mirapeix, A.; Herrero-Martínez, J. M.; Mongay-Fernández, C.; Simó-Alfonso, E. F. Electrophoresis 30 (2009) 599

Cañabate-Díaz, B.; Segura Carretero, A.; Fernández-Gutiérrez, A.; Belmonte Vega, A. Garrido Frenich, A.; Martínez Vidal, J. L.; Duran Martos, J. Food Chem. 102 (2007) 593

Caponio, F.; Alloggio, V.; Gomes, T. Food Chem. 64 (1999) 203

Caponio, F.; Pasqualone, A.; Gomes, T. Eur. Food Res. Technol. 215 (2002) 114

Carelli, A. A.; Cert, A. J. Chromatogr. A 630 (1993) 213

Carrasco-Pancorbo, A.; Cerretani, L.; Bendini, A.; Segura-Carretero, A.; Gallina Toschi, T.; Fernández-Gutiérrez, A. J. Sep. Sci. 28 (2005) 837

Carrasco-Pancorbo, A.; Cruces-Blanco, C.; Segura-Carretero, A.; Fernández-Gutiérrez, A. J. Agric. Food Chem. 52 (2004) 6687

Carrasco-Pancorbo, A.; Gómez-Caravaca, A. M.; Cerretani, L.; Bendini, A.; Segura-Carretero, A.; Fernández-Gutiérrez, A. J. Agric. Food Chem. 54 (2006) 7984

Carrasco-Pancorbo, A.; Neusúβ, C.; Pelzing, M.; Segura-Carretero, A.; Fernández-Gutiérrez, A. Electrophoresis 28 (2007A) 806

Carrasco-Pancorbo, A.; Cerretani, L.; Bendini, A.; Segura-Carretero, A.; Lercker, G.; Fernández-Gutiérrez, A. J. Agric. Food Chem. 55 (2007B) 4771

Carney, R. A.; Robson, M. M.; Bartle, K. D.; Myers, P. J. High Resolut. Chromatogr. 22 (1999) 29

Cartoni, G. P.; Coccioli, F.; Jasionowska, R.; Ramires, D. Ital. J. Food Sci. 12 (2000) 163

Cercaci, L.; Passalacqua, G.; Poerio, A.; Rodriguez-Estrada, M. T.; Lercker, G. Food Chem. 102 (2007) 66

Cercaci, L.; Rodríguez-Estrada, M. T.; Lercker, G. J. Chromatogr. A 985 (2003) 211

Cerretani, L.; Bendini, A.; Del Caro, A.; Piga, A.; Vacca, V.; Caboni, M. F.; Gallina Toschi, T. Eur. Food Res. Technol. 222 (2006) 354

Cerretani, L.; Bendini, A.; Rodriguez-Estrada, M.T.; Vittadini, E.; Chiavaro, E. Food Chem. 115 (2009) 1381

Cerretani, L.; Biasini, G.; Bonoli-Carbognin, M.; Bendini, A. J. Sens. Stud. 22 (2007) 403

Chiavaro, E.; Vittadini, E.; Rodriguez-Estrada, M. T.; Cerretani, L.; Bendini, A. Food Chem. 110 (2008) 248

Chirica, G. S.; Remcho, V. T. J. Chromatogr. A 924 (2001) 223

Choe, E.; Min, D. B. Compr. Rev. Food Sci. 5 (2006) 169

Choo, Y. M.; Yap, S. C.; Ooi, C. K.; Ma, A. N.; Goh, S. H.; Ong, A. S. H. J. Am. Oil Chem. Soc. 73 (1996) 599

Choudhary, G.; Horváth, C. J. Chromatogr. A 781 (1997) 161

Choudhary, G.; Apffel, A.; Yin, H.; Hancock, W. J. Chromatogr. A 887 (2000) 85

Christie, W. W. Advances in lipid methodology. The Oily Press, Ayr, UK (1992) pp. 239-271

Christophoridou, S.; Dais, P. Anal. Chim. Acta 633 (2009) 283

Cimato, A.; Dello Monaco, D.; Distante, C.; Epifani, M.; Siciliano, P.; Taurino, A. M.; Zuppa, M.; Sani, G. Sensors Actuat.B 114 (2006) 674

Commission Regulation (EEC) No. 2568/91 of 11 July 1991 on the characteristics of olive oil and olive-residue oil and on the relevant methods of analysis, Off. J. Eur. Union L128 (1991)

Commission Regulation (EC) No. 796/2002 of 6 May 2002 amending Regulation (EEC) No 2568/91 on the characteristics of olive oil and olive-pomace oil and on the relevant methods of analysis and the additional notes in the Annex to Council Regulation (EEC) No 2658/87 on the tariff and statistical nomenclature and on the Common Customs Tariff, Off. J. Eur. Commun. (2002)

Commission Regulation (EC) No. 1989/2003 of 6 November 2003 amending Regulation (ECC) No. 2568/91 on the characteristics of olive oil and olive-residue oil and on the relevant methods of analysis. Off. J. Eur. Commun. L295 (2003) pp. 57-77

Commission Regulation (EC) No. 640/2008 of 4 July 2008 amending Regulation (ECC) No. 2568/91 on the characteristics of olive oil and olive-residue oil and on the relevant methods of analysis. Off. J. Eur. Commun. L178 (2008)

Concha-Herrera, V.; Vivó-Truyols, G.; Torres-Lapasió, J. R.; García-Álvarez-Coque, M. C. J. Chromatogr. A 1063 (2005) 79

Cortesi, N.; Fusetti, M. G.; Fedeli, E. Riv. Ital. Sost. Grasse 64 (1987) 513

Cortesi N.; Rovellini P.; Fedeli E. Riv. Ital. Sost. Grasse 68 (1991) 511

Codex Alimentarius Commission, 1993. Proposed draft standard for named

vegetable oils, CX 1993/16, issued by the Joint FAO/WHO Food Standards Program, Rome, Italy

Cunha, S. C.; Amaral, J. S.; Fernandes, J. O.; Oliveira, M. B. P. P. J. Agr. Food Chem. 54 (2006C) 3351

Cunha, S. C.; Oliveira, M. B. P. P. Food Chem. 95 (2006A) 518

Cunha, S. C.; Fernandes, J. O.; Beatriz, M.; Oliveira, P. P. J. Chromatogr. A 1128 (2006B) 220

Delaunay-Bertoncini, N.; Demesmay, C.; Rocca, J. L. Electrophoresis 25 (2004) 3204

Del Carlo, M.; Sacchetti, G.; Di Mattia, C.; Compagnone, D.; Mastrocola, D.; Liberatore, L.; Cichelli, A. J. Agric. Food Chem. 52 (2004) 4072

Dermaux, A.; Sandra, P.; Ferraz, V. Electrophoresis 20 (1999) 74

Devowsky, J. K. J. Liquid Chromatogr. & Related Tech. 25 (2002) 1875

Di Lecce, G.; Bendini, A.; Cerretani, L.; Bonoli-Carbognin, M.; Lercker, G. Ind. Aliment.-Italy 461 (2006) 873

D'Imperio, M.; Dugo, G.; Alfa, M.; Mannina, L.; Segre, A. L. Food Chem. 102 (2007) 956

Dionisi, F.; Prodolliet, J.; Tagliaferri, E. J. Am. Oil Chem. Soc. 72 (1995) 1505

Doneanu, A.; Chirica, G. C. ; Remcho, V. T. J. Sep. Sci. 25 (2002) 1252

Dood, G. H.; Persaud, K. C. Nature 299 (1982) 352

Dugo, P.; Kumm, T., Crupi, M. L.; Cotroneo, A.; Mondello, L. J. Chromatogr. A 1112 (2006) 269

Eeltink, S.; Herrero-Martínez, J. M.; Rozing, G. P.; Schoenmakers, P. J.; Kok, W. Th. Anal. Chem. 77 (2005) 7342

Eeltink, S.; Svec, F. Electrophoresis 28 (2007) 137

Ericson, C.; Hjertén, S. Anal. Chem. 71 (1999) 1621

Fanali, S.; Camera, E.; Chankvetadze, B.; D'Orazio, G.; Quaglia, M. G. J. Pharmaceut. Biomed. 35 (2004) 331

Farhoosh, R.; Pazhouhanmehr, S. Food Chem. 114 (2009) 1002

Fasciotti, M.; Pereira, N.; Annibal D. Talanta 81 (2010) 1116

Fedeli, E. Lipids of olives, in Ralph, E; Holman, T. Progress on chemistry of fats and other lipids. Pergamon Press, Paris, France (1977) pp. 15-74

Fragaki, G.; Spyros, A.; Siragakis, G.; Salivaras, E.; Dais, P. J. Agric. Food Chem. 53 (2005) 2810

Franceschi, S.; Favero, A.; Conti, E.; Salamini, R.; Volpe, R.; Negri, E.; Barman, L.; La Vecchia, C. British J. Cancer 80 (1999) 614

Frankel, E. N. Chemistry of autoxidation: mechanism, products and flavor significance, in Min, D. B.; Smouse, T. H. Flavor chemistry of fats and oils. AOCS Press, Champaign, IL, USA (1985) pp. 1-37

Frankel, E. N. Lipid Oxidation. The Oily Press, Dundee, UK (1998)

Fronimaki, P.; Spyros, A.; Christophoridou, S.; Dais, P. J. Agric. Food Chem. 50 (2002) 2207

Fujimoto, C.; Kino, J.; Sawada, H. J. Chromatogr. A 716 (1995) 107

Galeano Diaz, T.; Durán Merás, I.; Sánchez Casas, J.; Alexandre Franco, M. F. Food Control 16 (2005) 339

García, A.; Brenes, M.; García, P.; Romero, C.; Garrido, A. Eur. Food Res. Technol. 216 (2003) 520

García-González, D.; Aparicio, R. Food Chem. 120 (2010) 572

Gardner, J. W.; Bartlett, P. N. Sens. Actuators B 18 (1993) 211

Gruszka, J.; Kruk, J. Chromatographia 66 (2007) 909

Guillén, M. D.; Cabo, N. J. Agric. Food Chem. 46 (1998) 1788

Gimeno, E.; Calero, E.; Castellote, A. I.; Lamuela-Raventós, R. M.; De La Torre, M. C.; López-Sabater, M. C. J. Chromatogr. A 881 (2000B)

Gimeno, E.; Castellote, A. I.; Lamuela-Raventós, R. M.; De la Torre, M. C.; López-Sabater, M. C. J. Chromatogr. A 881 (2000A) 255

Gimeno-Adelantado, J. V.; Mateo-Castro, R.; Doménech-Carbó, M. T.; Bosch-Reig, F.; Doménech-Carbó, A.; De la Cruz-Cañizares, J.; Casas-Catalán, M. J. Talanta 56 (2002) 71

Gómez-Caravaca, A. M.; Carrasco-Pancorbo, A.; Cañabate-Díaz, B.; Segura-Carretero, A.; Fernández-Gutiérrez, A. Electrophoresis 26 (2005) 3538

Gordon M. H. Measuring antioxidant activity, in Pokorný, J.; Yanishlieva, N.; Gordon, M. H. Antioxidants in foods. Woodhead Publishing Ltd., Oxford, UK (2001)

Gruszka, J.; Kruk, J. Chromatographia 66 (2007) 909

Gutfinger, J.; Letan, A. Lipids 9 (1974) 658

Gusev, I.; Huang, X.; Horváth, C. J. Chromatogr. A 855 (1999) 273

Guth, H.; Grosch, W. J. Am. Oil Chem. Soc. 70 (1993) 513

Gutiérrez-Rosales, F.; Perdiguero, S.; Gutiérrez, R.; Olías, J. M. J. Am. Oil Chem. Soc. 69 (1992) 394

Gutiérrez-Rosales, F.; Ríos, J. J.; Gómez-Rey, M. L. J. Agric. Food Chem. 51 (2003) 6021

Hajimahmoodia, M.; Vander Heydenb, Y.; Sadeghia, N.; Jannata, B.; Oveisia, M. R.; Shahbaziana, S. Talanta 66 (2005) 1108

Hamilton, R. J. The chemistry of rancidity in foods, in Allen, J. C.; Hamilton, R. J. Rancidity in foods. Blackie Academic & Professional, London, UK (1994) pp. 1–21

Harborne, J. B.; Dey, P. M. Methods in plant biochemistry. Academic Press, London, UK (1989)

Hermle, T.; Weimar, U.; Mitrovics, J.; Rosenmistiel, W.; Göpel, W. Sens. Actuators B 65 (1999) 253

Hidalgo, F. J.; Alaiz, M.; Zamora, R. Anal. Chem. 73 (2001A) 698

Hidalgo, F. J.; Alaiz, M.; Zamora, R. J. Agric. Food Chem. 49 (2001B) 4267

Hidalgo, F. J.; Alaiz, M.; Zamora, R. J. Am. Oil Chem. Soc. 79 (2002) 685

Hidalgo, F. J.; Zamora, R. Trends Food Sci. Technol. 17 (2006) 56

Hjertén, S.; Liao, J. L.; Zhang, R. J. Chromatogr. 473 (1989) 273

Hodge, E.; English, D. R.; McCredie, M. R. E.; Severi, G.; Boyle, P.; Hopper, J. L.; Giles, G.G. Cancer Cause Control 15 (2004) 11

Hoegger, D.; Freitag, R. J. Chromatogr. A 914 (2001) 211

Holčapek, M.; Lísa, M.; Jandera, P.; Kabátová, N. J. Sep. Sci. 28 (2005) 1315

Horstkötter, C.; Jiménez-Lozano, E.; Barrón, D.; Barbosa, J.; Blaschke, G. Electrophoresis 23 (2002) 3078

Institute of food technologists (IFT), Sensory evaluation division, Chicago, IL, USA. Evaluation guide for testing food and beverage products. Food Technology, November 1981, pp. 50-59

Jebe T. A.; Matlock, M. G.; Sleeter, R. T. J. Am. Oil Chem. Soc. 70 (1993) 1055

Jee, M. Oils and fat authentication. Blackwell Publishing, CRC Press, Boca Raton, FL, USA (2002)

Kamm, W.; Dionisi, F.; Hischenhuber, C.; Engel, K. H. Food Rev. Int. 17 (2001) 249

Kiosseoglou, B.; Vlachopoulou, L.; Boskou, D. Grasas Aceites 38 (1987) 102

Kiritsakis, A. Olive oil – second edition. Food and Nutrition Press, Inc., Trumbull, CT, USA (1998)

Kiritsakis, A.; Christie, W. W. Análisis de aceites comestibles, in Aparicio, R.; Hardwood, J. Manual del aceite de oliva. Ed. Mundi-Prensa, Madrid, Spain (2003) pp. 135-162

Kiritsakis, A. K.; Markakis, P. Olive Oil Analysis, in Linskens, H. F.; Jackson, J. F. Modern methods of plant analysis: essential oils and waxes. Springer-Verlag, Berlin, Germany (1991) pp. 1-20

Klampfl, C. W. J. Chromatogr. A 1044 (2004) 131

Knox, J. H. Chromatographia 26 (1988) 329

Kotani, A.; Kusu, F.; Takamura, K. Anal. Chim. Acta 465 (2002) 199

Lanzon, A.; Albi, T.; Cert, A.; Gracian, J. J. Am. Oil Chem. Soc. 71 (1994) 285

Lazzez, A.; Perri, E.; Caravita, M. A.; Khlif, M.; Cossentini, M. J. Agric. Food Chem. 56 (2008) 982

Lercker G.; Capella P. La conservazione delle sostanze grasse, in Capella P.; Fedeli E.; Bonaga G.; Lercker G. Manuale degli oli e dei grassi. Tecniche Nuove, Milano, Italy (1997)

Lerma-García, M. J.; Ramis-Ramos, G.; Herrero-Martínez, J. M.; Simó-Alfonso, E. F. Rapid Commun. Mass Spectrom. 22 (2008) 973

Lerma-García, M. J.; Simó-Alfonso, E. F.; Méndez, A.; Llibería, J. L.; Herrero-Martínez, J. M. J. Agric. Food Chem. 58 (2010) 2771

Lerma-García, M. J.; Simó-Alfonso, E. F.; Ramis-Ramos, G.; Herrero-Martínez, J. M. Electrophoresis 28 (2007) 4128

Lerma-García, M. J.; Simó-Alfonso, E. F.; Ramis-Ramos, G.; Herrero-Martínez, J. M. Electrophoresis 29 (2008) 4603

Lerma-García, M. J.; Simó-Alfonso, E. F.; Bendini, A.; Cerretani, L. Food Chem. 117 (2009A) 608

Lerma-García, M. J.; Simó-Alfonso, E. F.; Chiavaro, E.; Bendini, A.; Lercker, G.; Cerretani, L. J. Agric. Food Chem. 57 (2009B) 7834

Liao, J. L.; Chen, N.; Ericson, C.; Hjertén, A. Anal. Chem. 68 (1996) 3468

Liberatore, L.; Procida, G.; D'Alessandro, N.; Cichelli, A. Food Chem. 73 (2001) 119

Liu, X.; Takahashi, L. H.; Fitch, W. L.; Rozing, G.; Bayle, C.; Couderc, F. J. Chromatogr. A 924 (2001) 323

López-Feria, S.; Cardenas, S.; García-Mesa, J. A.; Valcárcel, M. J. Chromatogr. A 1188 (2008) 308

Lu, B.; Zhang, Y.; Wu, X.; Shi, J. Anal. Chim. Acta 588 (2007) 50

Macher, M. B.; Holmqtvist, A. J. Sep. Sci. 24 (2001) 179

Manzi, P.; Panfili, G.; Esti, M.; Pizzoferrato, L. J. Sci. Food Agric. 77 (1998) 115

Marcos Lorenzo, I.; Pérez Pavón, J. L.; Fernández Laespada, M. E.; García Pinto, C.; Moreno Cordero, B. J. Chromatogr. A 945 (2002) 221

Mariani, C.; Fedeli, E. Riv. Ital. Sost. Grasse 62 (1985) 3

Mariani, C.; Fedeli, E.; Morchio, G. Riv. Ital. Sost. Grasse 64 (1987) 359

Mariani, C.; Bellan, G.; Lestini, E.; Aparicio, R. Eur. Food Res. Technol. 223 (2006) 655

Martínez-Vidal, J. L.; Garrido-Frenich, A.; Escobar-García, M. A.; Romero-González, R. Chromatographia 65 (2007) 695

Maryam, J.; Mahdi, K.; Javad, K. J. Am. Oil Chem. Soc. 86 (2009) 103

Mateos, R.; Trujillo, M.; Pérez-Camino, M. C.; Moreda, W.; Cert. A. J. Agric. Food Chem. 53 (2005) 5766

Matthäus, B. Eur. J. Lipid Sci. Technol. 110 (2008) 645

Medvedovici, A.; David, F.; Sandra, P. Chromatographia 44 (1997) 37

Melchert, H. U.; Pollock, D.; Pabel, E.; Ruback, K.; Stan H. J. J. Chromatogr. A 976 (2002) 215

Melton, S. L.; Jafra, S.; Sykes, D.; Trigiano, M. K. J. Am. Oil Chem. Soc. 71 (1994) 1301

Merthar, M.; Podgornik, A.; Žigon, M.; Štrancar, A. J. Sep. Sci. 26 (2003) 322

Mezine, I.; Zhang, H.; Macku, C.; Lijana, R. J. Agric. Food Chem. 51 (2003) 563

Micó-Tormos, A.; Collado-Soriano, C.; Torres-Lapasió, J. R.; Simó-Alfonso, E.; Ramis-Ramos, G. J. Chromatogr. A 1180 (2008A) 32

Micó-Tormos, A.; Simó-Alfonso, E.; Ramis-Ramos, G. J. Chromatogr. A 1203 (2008B) 47

Miguez-Mosquera, I.; Gandul-Rojas, B.; Garrido-Fernandez, J.; Gallardo-Guerrero, L. J. Am. Oil Chem. Soc. 67 (1990) 192

Morales, M. T.; Aparicio, R.; Rios, J. J. J. Chromatogr. A 668 (1994) 455

Morales, M. T.; Aparicio, R. J. Am. Oil Chem. Soc. 76 (1999) 295

Morales, M. T.; Tsimidou, M. El papel de los compuestos volátiles y polifenoles en la calidad sensorial del aceite de oliva, in Aparicio, R.; Harwood, J. Manual del aceite de oliva. Ed. Mundi-Prensa, Madrid, Spain (2003) pp. 381-442

Norme Grassi e Derivati (NGD). Method NGD C-88 (2007) Stazione Sperimentali degli Oli e dei Grassi, Milano, Italy

Ntsourankoua, H.; Artaud, J.; Guerere, M. Fr. Ann. Fals. Expert. Chim. Toxicol. 87 (1994) 91

Ocakoglu, D.; Tokatli, F.; Ozen, B.; Korel, F. Food Chem. 113 (2009) 401

Ozen, B. F.; Mauer, L. J. J. Agric. Food Chem. 50 (2002) 3898

Paganuzzi. V. J. Am. Oil. Chem. Soc. 56 (1979) 925

Paganuzzi, V. Riv. Ital. Sost. Grasse 59 (1982) 415

Palm, A.; Novotny, M. V. Anal. Chem. 69 (1997) 4499

Panfili, G.; Fratianni, A.; Irano, M. J Agric Food Chem. 51 (2003) 3940

Parcerisa, J.; Boatella, J.; Codony, R.; Rafecas, M.; Castellote, A. I.; García, J.; López, A.; Romero, A. J. Agric. Food Chem. 43 (1995) 13

Parcerisa, J.; Casals, I.; Boatella, J.; Codony, R.; Rafecas, M. J. Chromatogr. A 881 (2000) 149

Parsia, Z.; Górecki, T. J. Chromatogr. A 1130 (2006) 145

Peris-Vicente, J.; Simó-Alfonso, E.; Gimeno-Adelantado, J. V.; Doménech-Carbó, M. T. Rapid Commun. Mass Spectrom. 19 (2005) 3463

Perona, J. S.; Barrón, L. J. R.; Ruiz-Gutierrez, V. J. Chromatogr. A 706 (2001) 173

Peters, E.C. ; Petro, M. ; Svec, F. ; Fréchet, J. M. Anal. Chem. 69 (1997) 3646

Peters, E. C. ; Petro, M. ; Svec, F. ; Fréchet, J. M. J. Anal. Chem. 1998A, 70, 2288

Peters, E. C. ; Petro, M. ; Svec, F. ; Fréchet, J. M. J. Anal. Chem. 1998B, 70, 2296

Petro, M.; Svec, F.; Fréchet, J. M. J. J. Chromatogr. A 752 (1996) 59

Philips, K. M.; Ruggio, D. M.; Toivo, J. I.; Swank, M. A.; Simpkins, A. H. J. Food Compos. Anal. 15 (2002) 123

Poulli, K. I.; Mousdis, G. A.; Georgiou, C. A. Anal. Bioanal. Chem. 386 (2006) 1571

Psomiadou, E.; Tsimidou, M. J. Agric. Food Chem. 46 (1998) 5132

Ranalli, A.; Pollastri, L. ; Contento, S. ; Di Loreto, G. ; Lannucci, E.; Lucera, L.; Russi, F. J. Sci. Food Agric. 82 (2002) 854

Rathore, A. S.; Horváth, C. J. Chromatogr. A 743 (1996) 231

Rathore, A. S.; Horváth, Anal. Chem. 70 (1998) 3271

Rebscher, H.; Pyell, U. Chromatographia 38 (1994) 737

Reiners, J.; Grosch, W. J. Agric. Food Chem. 46 (1998) 2754

Ríos, J. J.; Gil, M. J.; Gutiérrez-Rosales, F. J. Chromatogr. A 1903 (2005) 167

Rivera del Álamo, R. M.; Fregapane, G.; Aranda, F.; Gómez-Alonso, S.; Salvador, M. D. Food Chem. 84 (2004) 533

Robison, J. L.; Tsimidou, M.; Macrae, R. J. Chromatogr. A 324 (1985) 35

Rodríguez-Méndez, M. L.; Apetrei, C.; de Saja, J. A. Electrochim. Acta 53 (2008) 5867

Rossell, J. B. Vegetable oils and fats, in Rossell, J. B.; Pritchard, J. L. R. Analysis of oilseeds, fats and fatty foods. Elsevier Science, London, UK (1991) pp. 261-327

Rovellini, P.; Azzolini, M.; Cortesi, N. Riv. Ital. Sost. Grasse 74 (1997) 1

Rovellini, P.; Cortesi, N. Riv. Ital. Sost. Grasse 69 (2002) 1

Rovellini, P.; Cortesi, N. Ital. J. Food Sci. 16 (2004) 333

Rovellini, P.; Cortesi, N.; Fedeli, E. Riv. Ital. Sost. Grasse 75 (1998) 57

Rozing, G. P.; Dermaux, A.; Sandra, P. Journal of Chromatography Library Series, No. 62, Elsevier Science B.V. Amsterdam, The Netherlands (2001) pp. 39

Saba, A.; Mazzini, F.; Raffaelli, A.; Mattei, A.; Salvadori, P. J. Agric. Food Chem. 53 (2005) 4867

Sacchi, R.; Addeo, F.; Paolillo, L. Magn. Reson. Chem. 35 (1997) S133

Saitta, M.; Salvo, F.; Di Bella, G.; Dugo, G.; La Torre, G. L. Food Chem. 112 (2009) 525

Sakouhia, F.; Harrabia, S.; Absalonb, C.; Sbeia, K.; Boukhchinaa, S.; Kallela, H. Food Chem. 108 (2008) 833

Sánchez-Casas, J.; Osorio Bueno, E.; Montaño García, A. F.; Martinez Cano, M. Food Chem. 87 (2004) 225

Sánchez-Machado, D. I.; López-Hernández, J.; Paseiro-Losada, P.; López-Cervantes, J. Biomed. Chromatogr. 18 (2004) 183

Segura-Carretero, A.; Carrasco-Pancorbo, A.; Cortacero, S.; Gori, A.; Cerretani, L.; Fernández-Gutiérrez, A. Eur. J. Lipid Sci. Technol. 110 (2008) 1142

Serani, A.; Piacenti, D. J. Am. Oil Chem. Soc. 69 (1992) 469

Servili, M.; Montedoro, G. Eur. J. Lipid Sci. Technol. 104 (2002) 602

Sikorska, E.; Gliszczyńska-Świgło, A.; Khmelinskii, I.; Sikorski, M. J. Agr. Food Chem. 53 (2005) 6988

Silva, S. D.; Rosa, N. F.; Ferreira, A. E.; Boas, L. V.; Bronze, M. R. Food Anal. Method 2 (2009) 120

Silverstein, R. M.; Bassler, G. C.; Morrill, T. C. Spectrometric identification of organic compounds. John Wiley & Sons, Chichester, UK (1981)

Sindhu-Kanya, T. C.; Jaganmohan-Rao, L.; Shamanthaka-Sastry, M. C. Food Chem. 101 (2007) 1552

Shamsi, S. A.; Miller, B. E. Electrophoresis 25 (2004) 3927

Solomon, N. W. Nutr. Rev. 56 (1998) 309

Stefanoudaki, E.; Kotsifaki, F.; Koutsaftakis, A. J. Am. Oil Chem. Soc. 76 (1999) 623

Suárez, M.; Macià, A.; Romero, M. P.; Motilva, M. J. J. Chromatogr. A 1214 (2008) 90

Tasioula-Margari, M.; Okogeri, O. Food Chem. 74 (2001) 377

Tateo, E.; Brunelli, N.; Cucurachi, S.; Ferillo, A. New trends in the study of the merits and shortcoming of olive oil in organoleptic terms in correlation with GC/MS analysis of aromas, in Charalampous, G. Food flavors, ingredients and composition. Elsevier Science B. V., Amsterdam, The Netherlands (1993) pp. 301-311

Tena, N.; Lazzez, A.; Aparicio-Ruiz, R.; García-González, D. L. J. Agric. Food Chem. 55 (2007) 7852

Thanh, T. T.; Vergnes, M. F.; Kaloustian, J.; El-Moselhy, T. F.; Amiot-Carlin, M. J.; Portugal, H. J. Sci. Food Agric. 86 (2006) 220

Tiscornia, E.; Fiorina, N.; Evangelisti, F. Riv. Ital. Sost. Grasse 59 (1982) 519

Torres, M. M.; Maestri, D. M. Food Chem. 96 (2006) 507

Tripoli, E., Giammanco, M., Tabacchi, G., Di Majo, D., Giammanco S., La Guardia M. Nutr. Res. Rev. 18 (2005) 98

Tsimidou, M. Ital. J. Food Sci. 10 (1998) 99

Tsimidou, M.; Papadopoulos, G.; Boskou, D. Food Chem. 44 (1992) 53

Tsuda, T. Anal. Chem. 59 (1987) 521

Tura, D.; Gigliotti, C.; Pedo, S.; Failla, O.; Bassi, D.; Serraiocco, A. Scientia Horticulturae 112 (2007) 108

Vandeginste, B. G. M.; Massart, D. L.; Buydens, L. M. C.; De Jong, S.; Lewi, P. J.; Smeyers-Verbeke, J. Data handling in science and technology part B. Elsevier Science B. V, Amsterdam, The Netherlands (1998)

Van der Klift, E. J. C.; Vivó-Truyols, G.; Claassen, F. W.; van Holthoon, F. L.; van Beek, T. A. J. Chromatogr. A, 1178 (2008) 43

Velasco, J.; Dobarganes, C. Eur. J. Lipid Sci. Technol. 104 (2002) 661

Verardo, V.; Ferioli, F.; Riciputi, Y.; Infelice, G.; Marconi, E.; Caboni, M. F. Food Chem. 114 (2009) 472

Vichi, S. ; Pizzale, L.; Conte, L. S.; Buxaderas, S.; López-Tamames, E. J. Agr. Food Chem. 51 (2003) 6564

Vigli, G.; Philippidis, A.; Spyros, A.; Dais, P. J. Agric. Food Chem. 51 (2003) 5715

Vissers, M. N.; Zock, P. L.; Leenen, R.; Roodenburg, A. J. C.; van Putte, K. P. A. M.; Katan, M. B. Free Radical Res. 35 (2001) 619

Vlachos, N.; Skopelitis, Y.; Psaroudaki, M.; Konstantinidou, V.; Chatzilazarou, A.; Tegou, E. Anal. Chim. Acta 573-574 (2006) 459

Waguespack, B. L.; Hodges, S. A.; Bush, M. E.; Sondergeld, L. J.; Bushey, M. M. J. Chromatogr. A 1078 (2005) 171

Wall, W.; Li, J.; el Rassi, Z. J. Sep. Sci. 25 (2002) 1231

Waseem, A.; Rishi, L.; Yaqoob, M.; Nabi, A. Anal. Sci. 25 (2009) 407

Watson, R. R.; Preedy, V. R. Tocotrienols: vitamin E beyond tocopherols. The American Oil Chemist's Society, Urbana, IL, USA (2009)

Xie, S. ; Svec, F. ; Fréchet, J. M. J. J. Chromatogr. A 775 (1997) 65

Yang, H.; Irudayaraj, J.; Paradkar, M. M. Food Chem. 93 (2005) 25

Yu, C.; Xu, M.; Svec, F.; Fréchet, J. M. J. J. Polym. Sci. Pol. Chem. 40 (2001) 755

Zamora, R.; Alaiz, M.; Hidalgo, F. J. J. Agric. Food Chem. 49 (2001) 4267

Zhang, L.; Ping, G.; Zhang, L.; Zhang, W.; Zhang, Y. J. Sep. Sci. 26 (2003) 331

ANEXO I

Electrophoresis 2007, *28*, 4128–4135

María Jesús Lerma-García
Ernesto F. Simó-Alfonso
Guillermo Ramis-Ramos
José M. Herrero-Martínez

Department of Analytical Chemistry,
Faculty of Chemistry,
University of Valencia,
Burjassot, Valencia, Spain

Received March 13, 2007
Revised April 24, 2007
Accepted April 24, 2007

Research Article

Determination of tocopherols in vegetable oils by CEC using methacrylate ester-based monolithic columns

The separation and determination of tocopherols (Ts) in vegetable oils by CEC using methacrylate ester-based monolithic columns has been developed. The effects of pore size of the monolithic columns were studied, and the composition of mobile phase was optimized. The optimal pore size of the monolith was obtained with 12 wt% 1,4-butanediol in the polymerization mixture. Excellent resolution between tocopherols was achieved within 10 min analysis time with a 99:1 v/v MeOH–aqueous buffer containing 5 mM tris(hydroxymethyl)aminomethane at pH 8.0. The LODs were lower than 2.3 μg/mL, and interday and column-to-column reproducibilities at 25 μg/mL were better than 5.6%. Using a 93:7 v/v MeOH–aqueous buffer, both tocopherols and tocotrienols (T_3s) of grapeseed and palm oils were resolved. Application to the detection of olive oil adulteration with low-cost edible oils was demonstrated.

Keywords:
CEC / Food analysis / Methacrylate ester-based monolithic column / Tocopherols / Vegetable oils
DOI 10.1002/elps.200700195

1 Introduction

Vegetable oils contain vitamin E, which is a mixture of tocopherols (Ts) and tocotrienols (T_3s). These important lipid antioxidants are characterized by a two-ring structure known as chromanol (a substituted phenol with a cyclic ether), which is attached to a branched hydrocarbon side chain with 16 carbon atoms. According to the number and position of the methyl substituents in the phenol ring, four tocopherols (α-, β-, γ-, and δ-T) and four tocotrienols (α-, β-, γ-, and δ-T_3) are distinguished. Tocopherols and tocotrienols protect natural oils from oxidation [1–3] and also prevent lipid peroxidation in biological membranes [4, 5]. Their positive influence to retard the development of precancer lesions and tumors [6], and to combat free-radical reactions that can cause DNA mutations [7] has been demonstrated.

Tocopherols are found in variable proportions in vegetable oils, while tocotrienols are present especially in palm oil [8] and in cereal seed oils. The relative concentrations of tocopherols and tocotrienols vary widely from one oil to another, which can be used to distinguish the oils according to their botanical origin. Thus, α-T is the most representative antioxidant in olive oil [9, 10], while γ-, and δ-T contents are high in soybean and sunflower oils, soybean oil being particularly rich in γ-T [11]. Concentrations of tocopherols and/or tocotrienols have been used to detect the adulteration of olive oil with red palm [12] and hazelnut oils [13], and soybean oil with linseed oil [14]. Therefore, rapid and reliable analytical methods, capable of assessing the composition of these compounds in vegetable oils, are important in food quality control and in relation to human health studies.

Vitamin E components have been determined in vegetable oils by GC [15] and HPLC [16]. Although normal-phase columns are more efficient in separating the β- and γ-isomers of tocopherols and tocotrienols [16], RP columns show higher column stability, better reproducibility of the retention times, and shorter analysis times [10, 16, 17].

CEC is a hybrid separation technique, which combines the selectivity of HPLC with the high efficiency of CE [18, 19]. Using CEC, compounds with closely similar properties can be resolved in a short time with minimal solvent consumption. The separation of vitamin E components by CEC using packed columns has been described [20–25]. Quantitation studies of these compounds in edible oils with a CEC-packed column have been reported [24], but application to detect oil adulteration was not demonstrated. However, the fabrication of reproducible CEC-packed columns still remains problematic [26, 27], whereas monolithic capillary columns can be

Correspondence: Dr. José Manuel Herrero Martínez, Department of Analytical Chemistry, Faculty of Chemistry, University of Valencia, E-46100 Burjassot, Valencia, Spain
E-mail: jmherrer@uv.es
Fax: +34-963544436

Abbreviations: AIBN, azobisisobutyronitrile; **BHT,** butylated hydroxytoluene; **EDMA,** ethylene dimethacrylate; **LMA,** lauryl methacrylate; **META,** [2-(methacryloyloxy)ethyl]trimethylammonium chloride; **T,** tocopherol; **T-AcO,** tocopherol acetate

manufactured with an excellent reproducibility. Monolithic columns represent an alternative to packed CEC columns also due to: (i) the easy preparation, (ii) no need of frits, (iii) the nearly total exclusion of bubble formation during operation, and (iv) the wide variety of monomers available for the synthesis of stationary phases with many different functionalities. Silica and acrylamide-, styrene-, and methacrylate ester-based polymeric monolithic materials have been employed as stationary phases in CEC [28–37]. Among these, methacrylate ester-based monolithic columns have several advantages such as an easily adjustable polarity, fine control of pore characteristics, and high stability under extreme pH conditions [33, 34, 36].

The aim of this study was to develop a CEC method for reliable determination of tocopherols in edible oils using methacrylate ester-based monolithic columns. The percentages of the porogenic solvents in the polymerization mixture, and the mobile phase composition, were optimized. The determination of tocopherols and their separation of tocotrienols in vegetable oils of different biological origin was demonstrated and applied to the detection of olive oil adulteration with other low-cost edible oils.

2 Materials and methods

2.1 Reagents

Lauryl methacrylate (LMA), ethylene dimethacrylate (EDMA), [2-(methacryloyloxy)ethyl]trimethyl ammonium chloride (META, 75% in water), 1,4-butanediol, 3-(trimethoxysilyl)propyl methacrylate, and basic alumina were from Aldrich (Milwaukee, WI, USA). 1-Propanol, HPLC-grade ACN, and methanol (MeOH) were from Scharlau (Barcelona, Spain). Azobisisobutyronitrile (AIBN), butylated hydroxytoluene (BHT), and tris(hydroxymethyl)aminoethane (Tris) were from Fluka (Buchs, Switzerland). Hydrochloric acid (37%) was supplied by Panreac Quimica (Barcelona). Deionized water was obtained with a Barnstead deionizer (Sybron, Boston, MA, USA). LMA and EDMA were purified by passing them through activated basic alumina, followed by distillation under reduced pressure. All other chemicals were of analytical grade.

Standards of α-, γ-, δ-T and α-tocopherol acetate (α-T-AcO) were from Sigma (St. Louis, MO, USA). Chemical structures of these compounds are shown in Fig. 1. Stock solutions of the analytes (2000 μg/mL), prepared in MeOH with 0.1% w/v of BHT and were stored at −20°C in amber vials. Working solutions were prepared daily by dilution of the stock solutions with the mobile phase. An EOF marker, thiourea from Riedel-de Haën (Seelze, Germany), was used.

Soybean, sunflower, grapeseed, and extra virgin olive oil samples were kindly donated by Coosur (Vilches, Jaén, Spain). Hazelnut oil was supplied by Guinama (Valencia, Spain). Corn oil (Hacendado, Valencia) and red palm oil (Blue Bay, Equatorial Guinea) were purchased at the local market. Uncoated fused-silica capillaries with 375 μm od × 100 μm id were from Polymicro Technologies (Phoenix, AZ, USA).

2.2 Instrumentation and procedures

CEC experiments were performed on an HP^{3D}CE instrument (Agilent Technologies, Waldbronn, Germany) equipped with a diode array UV detector and external nitrogen pressure. Data acquisition was performed with ChemStation Software (Rev.A.10.01, Agilent). Prior to use, all the eluents for CEC were degassed by ultrasonication. The monolithic column

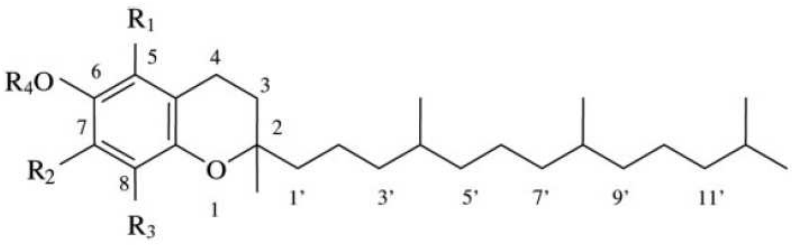

Tocopherol	R_1	R_2	R_3	R_4
α-T	CH_3	CH_3	CH_3	H
β-T	CH_3	H	CH_3	H
γ-T	H	CH_3	CH_3	H
δ-T	H	H	CH_3	H
α-T-AcO	CH_3	CH_3	CH_3	CH_3CO

Figure 1. Chemical structures of tocopherols; the structures of tocotrienols are the same, but with double bonds between carbon atoms 3′-4′, 7′-8′, and 11′-12′.

was placed in the instrument, and equilibrated with the mobile phase as follows. A pressure of 10 bar (1 MPa) was applied to both ends of the column [34–36, 38], and the voltage was stepwise raised, in 5 kV increments, up to 15 kV. Each voltage was maintained until a constant current and a stable baseline were achieved. Separations were performed at 15 kV, with the column kept at 25°C, and the inlet and outlet vials pressurized to 1 MPa with nitrogen. The sample extracts and standard solutions were injected electrokinetically under 20 kV for 3 s. Detection was performed at 205 and 295 nm.

Porosity measurements were obtained with an AutoPore IV 9500 mercury intrusion porosimeter (Micromeritics, Norcross, GA, USA). Nitrogen adsorption measurements were performed with a Sorptomatic 1990 (Thermo Electron, Milan, Italy). Pictures of the monolithic materials were taken with an SEM (S-4100; Hitachi, Ibaraki, Japan) provided with a field emission gun, a BSE Autrata detector, an EMIP 3.0 image data acquisition system, and a microanalysis system (Rontec, Normanton, UK).

2.3 Preparation and characterization of the polymeric monolithic columns

Prior to the preparation of the columns, and in order to enable covalent attachment of the monolith to the wall, surface modification of the inner wall of the fused-silica capillaries with 3-(trimethoxysilyl)propyl methacrylate was performed as described [34, 36]. Monoliths were prepared using polymerization mixtures containing EDMA, META, LMA, and a binary pore-forming solvent constituted by 1,4-butanediol and 1-propanol. AIBN (1 wt% with respect to the monomers) was added as polymerization initiator. After mixing and to obtain a clear solution, sonication for 10 min followed by deaeration with nitrogen for more 10 min were applied. The preconditioned capillary (33.5 cm) was filled with the polymerization mixture to a total length of 8.5 cm by capillary action. After polymerization for 20 h at 70°C, the columns were flushed with MeOH to remove the pore-forming solvents and possible unreacted monomers by using an HPLC pump. A detection window adjacent to the monolithic material was made by burning off the polyimide coating. Prior to CEC experiments, the capillaries were flushed with the mobile phase for 30 min. Simultaneously with the polymerization in the capillaries, batch polymerizations were carried out in 10 mL glass vials. Once the polymerization processes were completed, the monolithic materials were removed from the glass vials, cut into small pieces with a razor blade, and Soxhlet extracted with MeOH for 24 h. After drying at 50°C for 4 h, mercury intrusion porosimetry and nitrogen-adsorption measurements were performed.

2.4 Sample preparation

According to Aturki *et al.* [24], vegetable oil samples (4 g) were extracted twice with 10 mL of MeOH containing 0.1% w/v BHT as antioxidant, and once again with 10 mL of a MeOH/isopropanol mixture 80:20 v/v. All extractions were performed by shaking during 30 s followed by centrifugation at 8000 × *g* for 10 min. The combined extracts were evaporated to dryness using a rotary evaporator at 40°C. The residue was dissolved in 1 mL of MeOH and stored at −20°C in amber vials. These solutions were properly diluted with the mobile phase and injected.

3 Results and discussion

3.1 Influence of the monolith pore size on the separation of tocopherols

Methacrylate ester-based capillary monolithic columns with different pore sizes were prepared from polymerization mixtures constituted by a bulk monomer (LMA), a cross-linker (EDMA), pore-forming solvents (1,4-butanediol and 1-propanol), and AIBN as thermal initiator. A positively charged monomer (META) was also added to generate the EOF. As reported by Svec and co-workers [34, 36–38], the average pore size of methacrylate monoliths can be tailored to the requirements of the analytes by adjusting the polarity of the pore-forming solvents. In our experiments, a series of LMA-based monolithic columns were prepared by modifying the 1,4-butanediol/1-propanol ratio in the polymerization mixture, keeping the proportion of monomers to pore-forming solvents fixed at 40:60 wt%. The content of 1,4-butanediol in the polymerization mixture was varied from 10 to 25 wt%. With less than 10 wt% 1,4-butanediol, small pore sizes (<125 nm), clearly unsuitable for any flow-through applications, were obtained. On the other hand, with more than 25 wt% 1,4-butanediol, the components of the polymerization mixture were not completely solubilized.

The monolithic phases prepared within the 10–25 wt% 1,4-butanediol concentration range were examined by SEM. As observed in Fig. 2, the increase in the 1,4-butanediol percentage led to an increase in both the macropore size and the dimensions of the globules. The monolithic materials were also examined by mercury intrusion porosimetry. The macropore sizes increased from 125 to 250, and to 1800 nm when the percentage of 1,4-butanediol in the polymerization mixture was 10, 12, and 20 wt%, respectively. Also, the surface area of the monoliths was measured by the BET nitrogen adsorption/desorption method. A decrease in the specific surface area from 33.3 to 1.9 m^2/g for monoliths prepared with contents between 10 and 20 wt% 1,4-butanediol was observed. These results were consistent with those obtained with mercury intrusion porosimetry.

Since the pore size and the surface area of the monoliths were highly dependent on the concentration of 1,4-butanediol in the polymerization mixture, the influence of pore size on the separation of the tocopherols was also examined. As shown in Fig. 3, the methacrylate ester-based monolithic column produced with 10 wt% 1,4-butanediol showed the highest resolution of the analytes, but at the expenses of long

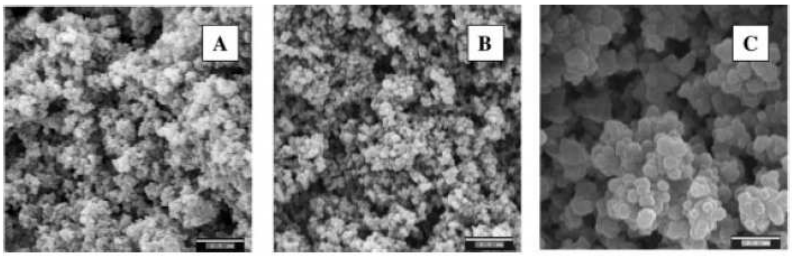

Figure 2. SEM micrographs of the LMA monolithic materials prepared with (a) 10, (b) 12, and (c) 20 wt% 1,4-butanediol in the polymerization mixture, respectively. The bar lengths stand for 2.5 μm.

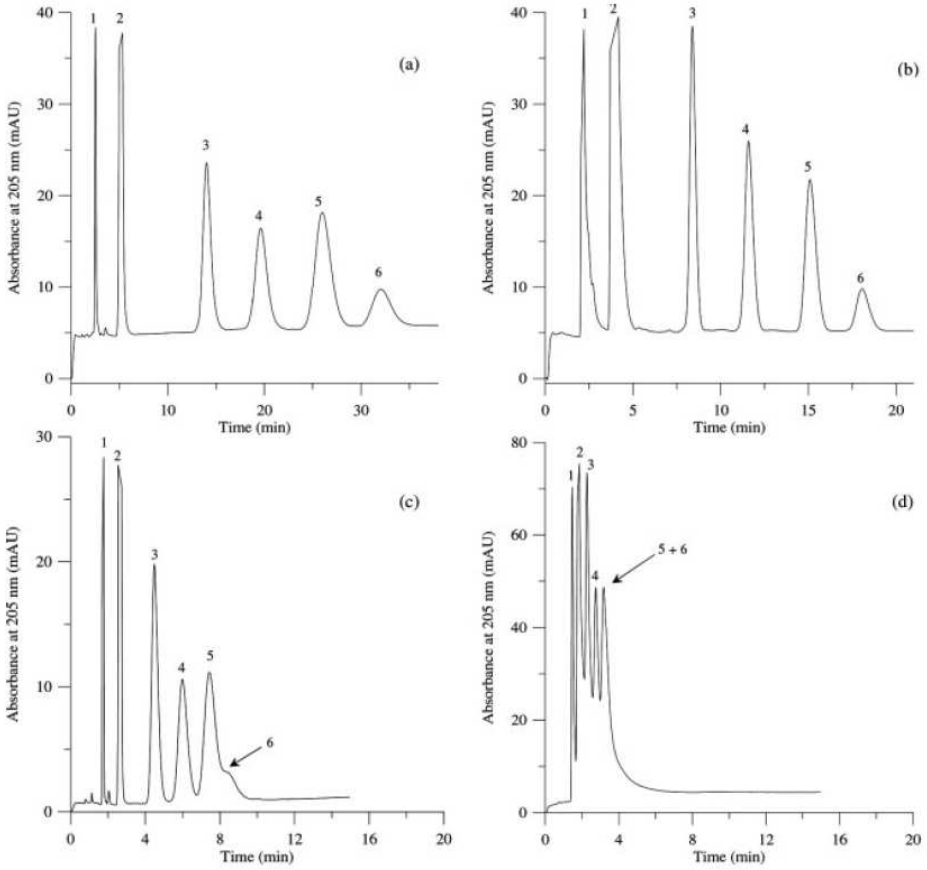

Figure 3. Influence of the percentage of 1,4-butanediol in the polymerization mixture on the CEC separation of tocopherols: (a) 10, (b) 12, (c) 15, and (d) 20 wt% 1,4-butanediol. Working conditions: mobile phase, 95:5 v/v MeOH – 5 mM Tris at pH 8.0; electrokinetic injection, 20 kV for 3 s; separation voltage, 15 kV. Peak identification: 1, thiourea; 2, BHT; 3, δ-T; 4, γ-T; 5, α-T; and 6, α-T-AcO.

separation times (>35 min). With 12 wt% 1,4-butanediol, baseline separations of tocopherols were achieved within 19 min. With 15 wt% 1,4-butanediol, the α-T/α-T-AcO pair was poorly resolved. Monolithic columns prepared with 20 wt% or higher 1,4-butanediol contents were unable to resolve all the analytes pairs, even when the MeOH percentage in the mobile phase was reduced from 95 to 90% (data not shown). Thus, the best resolution was obtained with the lowest 1,4-butanediol content, which was also the monolithic phase with the smallest pore size and the highest surface

area. The monolithic column obtained with 12 wt% 1,4-butanediol was then selected as the best compromise between resolution and analysis time.

Finally, the retention order of the analytes (δ-T > γ-T > α-T > α-T-AcO) revealed that the RP mechanism (hydrophobic interaction with the stationary phase) predominated over other possible interactions. This behavior agrees with other studies on tocopherols eluted with RP-HPLC-packed columns [10, 16, 17].

3.2 Influence of the mobile phase composition on the separation of tocopherols

The influence of the MeOH concentration in the mobile phase was studied using 90:10, 95:5, and 99:1 v/v MeOH–aqueous buffer mixtures at pH 8. The results are shown in Fig. 3, trace b, and in Fig. 4. Resolution decreased when the concentration of MeOH increased; however, resolution of the peak pairs was still higher than 1.5 with 99:1, except for the α-T/α-T-AcO pair which gave $R = 1.3$. Efficiencies also increased and analysis time largely decreased when the methanol content in the mobile phase increased from 90 to 99%. With 99:1 v/v, efficiencies within the 42 000–65 000 plates/m were obtained. This mobile phase was selected as the best compromise between resolution and analysis time (less than 10 min).

3.3 Quantitation studies and application to vegetable oils

Intra- and interday repeatabilities in the selected conditions were obtained by injecting a mixture containing 25 μg/mL of each tocopherol (Table 1). The mixture was injected eight times *per* day during three consecutive days. The column-to-column reproducibility was also tested by repeating the same number of injections on three monolithic columns, which were prepared with the same polymerization mixture. The reproducibility of EOF, retention times, and peak areas are summarized in Table 1. The column-to-column reproducibilities of the retention times and peak areas were better than 4.5 and 5.6%, respectively. About 100 injections of the standard mixture and 60 injections of vegetable oil extracts were performed without the need of replacing the column, therefore, the stability of the columns was satisfactory.

External calibration curves of peak areas were constructed by injecting six standard solutions of each solute within 5–100 μg/mL range. Straight lines with $r > 0.995$ were obtained. The LODs calculated at $S/N = 3$ are also shown in Table 1. The LODs are similar to those reported for packed CEC columns [24].

The optimized method was applied to the determination of tocopherols in several oil samples (Table 2). α-T-AcO was not detected in any of the samples analyzed. Peak identification was performed by comparing the retention times and absorption spectra with those of the standards, and when necessary also by spiking the sample extracts with the standards. Additionally, standard addition calibration curves were obtained by adding to the extracts at least four solutions with increasing concentrations up to 100 μg/mL. The curves were linear with $r > 0.992$, and in all cases the slope of calibration curve did not differ significantly from that obtained with the external calibration method. Representative electrochromatograms of extra virgin olive, corn, and soybean oil extracts are shown in Fig. 5. Different fingerprints of tocopherols were obtained according to the botanical origin of the oil. As indicated above, the monolithic columns used in this work had RP characteristics, being therefore unable to resolve the β-T and γ-T isomers present in the oil samples, which agrees with RP-HPLC studies [10, 16, 17]. Consequently, the sum of the concentrations of the two isomers is

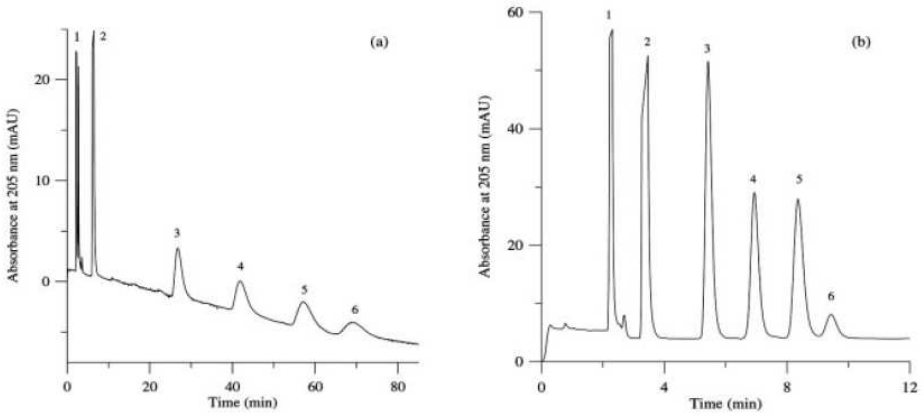

Figure 4. Influence of the MeOH content in the mobile phase on the separation of tocopherols: (a) 90:10 v/v and (b) 99:1 v/v MeOH–aqueous buffer (5 mM Tris at pH 8). The monolithic capillary was prepared with 12 wt% 1,4-butanediol in the polymerization mixture. Other experimental conditions as in Fig. 3.

Table 1. Repeatability and column-to-column reproducibility of retention times and peak areas

Compounds	Intraday repeatability (n = 8) RSD (%)		Interday repeatability (3 days) RSD (%)		Column-to-column reproducibility (n = 3) RSD (%)		LOD (μg/mL)
	t_R	Peak area	t_R	Peak area	t_R	Peak area	
α-T	1.34	2.23	2.15	4.00	4.29	5.60	2.00
γ-T	1.19	1.76	1.92	3.30	3.64	5.20	1.80
δ-T	0.93	1.47	1.68	2.50	2.74	4.52	1.50
α-T-AcO	1.65	2.54	2.76	4.20	4.56	6.20	2.30
BHT	1.02	1.24	1.54	2.76	3.21	3.70	–
EOF	0.64	0.96	1.22	2.35	2.28	3.20	–

Table 2. Contents of tocopherols in vegetable oils (mg/100 g)

Oil	α-T	β-T + γ-T	δ-T
Extra virgin olive	12.2	1.12	ND[a)]
Refined corn	31.2	128	7.1
Refined hazelnut	32.1	3.20	0.80
Refined sunflower	60.0	3.83	1.50
Crude red palm[b)]	14.2	ND	ND
Refined grapeseed[b)]	4.60	ND	ND
Refined soybean	23.1	162	80.4

a) ND = Not detected.
b) Quantitation performed with a mobile phase containing 93:7 v/v MeOH–aqueous buffer (5 mM Tris, pH 8.0), other results were obtained with 99:1 v/v MeOH–aqueous buffer.

given in Table 2. The found concentrations of tocopherols were consistent with those reported for oils of the same botanical origins [11, 12, 39]. Thus, α-T was the major tocopherol present in extra virgin olive oil, while δ-T was not detected (Table 2 and Fig. 5, trace a). In soybean oil, large quantities of β-T + γ-T and δ-T were observed (Table 2 and Fig. 5, trace b). Thus, these tocopherols can be used to detect the presence of soybean oil in virgin olive oil [12]. By injecting a series of mixtures of these two oils, and using the δ-T peak area as an adulteration marker, the presence of 10% soybean oil in virgin olive oil was clearly evidenced. As also shown in Table 2 and Fig. 5, trace c, large quantities of β-T + γ-T and small amounts of α-T and δ-T were present in corn oil. Hazelnut and sunflower oils showed α-T concentrations higher than those of the other tocopherols; however, since α-T also predominates in extra virgin olive oil, this tocopherol is not a good tracer for hazelnut and sunflower oils in olive oil.

Red palm and grapeseed oils constitute important sources of tocotrienols [8, 39]. Thus, these samples were analyzed to provide reference retention times and spectra for the identification of tocotrienols. Using RP, tocopherols and tocotrienols eluted following the same order [21, 22, 40]. In addition, the double bonds of the side chain of tocotrienols are not conjugated, thus, tocopherols and tocotrienols have closely similar UV spectra. These features were employed to assign the additional peaks observed

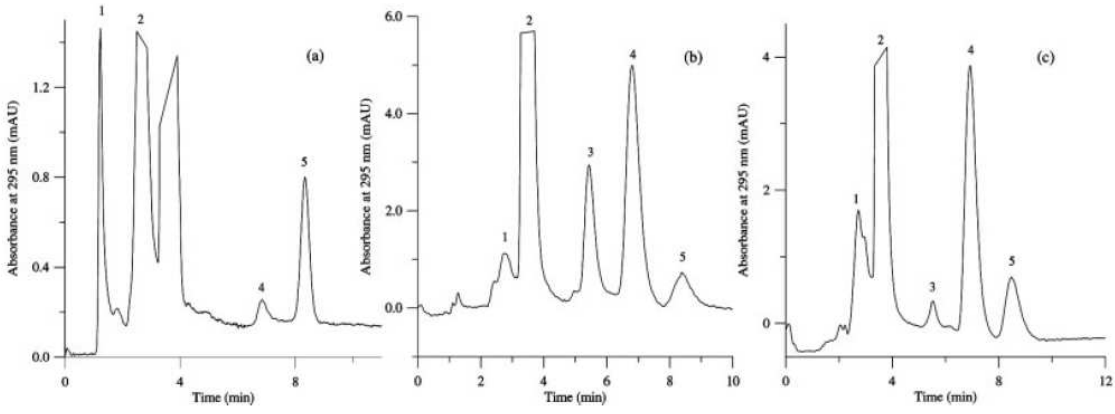

Figure 5. Electrochromatograms of (a) virgin olive, (b) soybean, and (c) corn oils. Mobile phase: 99:1 v/v MeOH–aqueous buffer (5 mM Tris, pH 8.0). Other conditions as in Fig. 3, except the peak labeled as 4 which represents the sum of the β-T and γ-T isomers.

with the grapeseed and palm oils to tocotrienols. Additionally, injections of these oils spiked with the tocopherols standards were performed.

Using a 99:1 v/v MeOH–aqueous buffer mobile phase, the peaks of tocopherols and tocotrienols were partially overlapped; however, an excellent resolution of both compounds in these oil extracts was achieved by using a 93:7 v/v MeOH–aqueous buffer mixture (data not shown). Since tocotrienols did not occur naturally in olive oil, their presence in a sample clearly indicate its adulteration with tocotrienol-rich oils, such as grapeseed or palm oils. An electrochromatogram of an extra virgin olive oil spiked with 10% palm oil is shown in Fig. 6. Although the β-T_3 + γ-T_3 pair was not resolved, the presence of several tocotrienols was definitely evidenced.

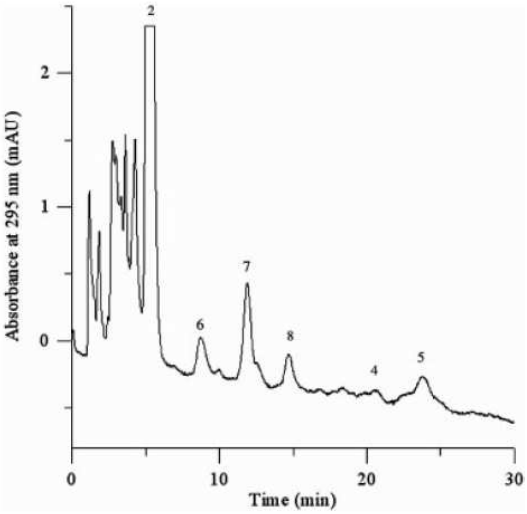

Figure 6. Electrochromatogram of virgin olive oil containing 10% red palm oil. Peak identification: 6, δ-T_3; 7, β-T_3 + γ-T_3; 8, α-T_3. Mobile phase: 93:7 v/v MeOH–aqueous buffer (5 mM Tris, pH 8.0). Other peaks and working conditions as in Fig. 3.

4 Concluding remarks

CEC can be used as alternative to HPLC to determine tocopherols and tocotrienols in vegetable oils and the use of monolithic columns is a competitive alternative to the use of CEC-packed columns. Attending to the state-of-the-art in column technology, an advantage of monolithic columns is the excellent column-to-column reproducibility.

A CEC method using methacrylate ester-based monolithic columns was developed for the analysis of tocopherols and tocotrienols in vegetable oils. The best resolution was obtained with 12 wt% 1,4-butanediol in the polymerization mixture, which yielded a small pore size (250 nm). To resolve tocopherols, mobile phases containing 99:1 v/v MeOH–aqueous buffer at pH 8 gave the best compromise between resolution and analysis time (less than 10 min). To analyze tocotrienols-containing oils, a 93:7 v/v MeOH–aqueous buffer mobile phase is recommended. The method allows the quick detection and evaluation of adulterations of olive oils with other oils of a different biological origin.

The work was supported by Project CTQ2004-06302/BQU (MEC of Spain and FEDER funds). The support of the Generalitat Valenciana (ACOMP06-111) is also acknowledged. M. J. L.-G. thanks the University of Valencia for a grant, and J. M. H.-M. thanks the MEC of Spain and the University of Valencia for a "Ramón y Cajal" research contract.

5 References

[1] Blekas, G., Tsimidou, M., Bouskou, D., *Food Chem.* 1995, *52*, 289–294.

[2] Manzi, P., Panfili, G., Esti, M., Pizzoferrato, L., *J. Sci. Food Agric.* 1998, *77*, 115–120.

[3] Psomiadou, E., Tsimidou, M., *J. Agric. Food Chem.* 1998, *46*, 5132–5138.

[4] Panfili, G., Fratianni, A., Irano, M., *J. Agric. Food Chem.* 2003, *51*, 3940–3944.

[5] Solomon, N. W., *Nutr. Rev.* 1998, *56*, 309–311.

[6] Lupulescu, M., *Int. J. Vitam. Nutr. Res.* 1993, *63*, 3–14.

[7] Gester, H., *Int. J. Vitam. Nutr. Res.* 1993, *63*, 93–141.

[8] Choo, Y. M., Yap, S. C., Ooi, C. K., Ma, A. N et al., *J. Am. Oil Chem. Soc.* 1996, *73*, 599–602.

[9] Tasioula-Margari, M., Okogeri, O., *Food Chem.* 2001, *74*, 377–383.

[10] Gimeno, E., Castellote, A. I., Lamuela-Raventós, R. M., De la Torre, M. C., López-Sabater, M. C., *J. Chromatogr. A* 2000, *881*, 255–259.

[11] Rovellini, P., Azzolini, M., Cortesi, N., *Riv. Ital. Sostanze Grasse* 1997, *74*, 1–5.

[12] Dionisi, F., Prodolliet, J., Tagliaferri, E., *J. Am. Oil Chem. Soc.* 1995, *72*, 1505–1511.

[13] Mariani, C., Bellan, G., Morchio, G., Pellegrino, A., *Riv. Ital. Sostanze Grasse* 1999, *76*, 59–67.

[14] Manandhar, P. P., Nagao, A., Yamazaki, M., *J. Jpn. Oil Chem. Soc.* 1986, *35*, 725–732.

[15] Melchert, H. U., Pollock, D., Pabel, E., Ruback, K., Stan, H. J., *J. Chromatogr. A* 2002, *976*, 215–220.

[16] Abidi, S. L., *J. Chromatogr. A* 2000, *881*, 197–216.

[17] Abidi, S. L., Mounts, T. L., *J. Chromatogr. A* 1997, *782*, 25–32.

[18] Legido-Quigley, C., Marlin, N. D., Melin, V., Manz, A., Smith, N. W., *Electrophoresis* 2003, *24*, 917–944.

[19] Eeltink, S., Kok, W. T., *Electrophoresis* 2006, *27*, 84–96.

[20] Henry III, C. W., Fortier, C. A., Warner, I. M., *Anal. Chem.* 2001, *73*, 6077–6082.

[21] Abidi, S. L., Rennick, K. A., *J. Chromatogr. A* 2001, *913*, 379–386.

[22] Abidi, S. L., Thiam, S., Warner, I. M., *J. Chromatogr. A* 2002, *949*, 195–207.

[23] Fanali, S., Catarcini, P., Quaglia, M. G., Camera, E. *et al.*, *J. Pharm. Biomed. Anal.* 2002, *29*, 973–979.

[24] Aturki, Z., D'Orazio, G., Fanali, S., *Electrophoresis* 2005, *26*, 798–803.

[25] Carabias-Martínez, R., Rodríguez-Gonzalo, E., Smith, N. W., Ruano-Miguel, L., *Electrophoresis* 2006, *27*, 4423–4430.

[26] Fujimoto, C., *Anal. Sci.* 2002, *18*, 19–25.

[27] Siouffi, A. M., *J. Chromatogr. A* 2003, *1000*, 801–818.

[28] Eeltink, S., Decrop, W. M. C., Rozing, G. P., Schoenmakers, P. J., Kok, W. T., *J. Sep. Sci.* 2004, *27*, 1431–1440.

[29] Tanaka, N., Nagayama, H., Kobayashi, H., Ikegami, T. *et al.*, *J. High Resolut. Chromatogr.* 2000, *23*, 111–116.

[30] Dong, J., Xie, C. H., Tian, R. J., Wu, R. A. *et al.*, *Electrophoresis* 2005, *25*, 3452–3459.

[31] Zhang, M., El Rassi, Z., *Electrophoresis* 2001, *22*, 2593–2599.

[32] Huang, H. Y., Lin, H. Y., Lin, S. P., *Electrophoresis* 2006, *27*, 4674–4681.

[33] Svec, F., Fréchet, J. M. J., *Science* 1996, *273*, 205–211.

[34] Peters, E. C., Petro, M., Svec, F., Fréchet, J. M. J., *Anal. Chem.* 1998, *70*, 2288–2295.

[35] Jiang, T., Jiskra, J., Claessens, H. A., Cramers, C. A., *J. Chromatogr. A* 2001, *923*, 215–227.

[36] Peters, E. C., Petros, M., Svec, F., Fréchet, J. M., *Anal. Chem.* 1997, *69*, 3646–3649.

[37] Eeltink, S., Svec, F., *Electrophoresis* 2007, *28*, 137–147.

[38] Eeltink, S., Herrero-Martínez, J. M., Rozing, G. P., Schoenmakers, P. J., Kok, W. T., *Anal. Chem.* 2005, *77*, 7342–7347.

[39] Jee, M., *Oils and Fat Authentication*, Blackwell Publishing, CRC Press, Boca Raton, FL 2000.

[40] Abidi, S. L., *J. Chromatogr. A* 1999, *844*, 67–75.

ANEXO II

JOURNAL OF AGRICULTURAL AND FOOD CHEMISTRY
ARTICLE

J. Agric. Food Chem. 2010, 58, 757–761 757
DOI:10.1021/jf9031537

Determination of Tocopherols and Tocotrienols in Vegetable Oils by Nanoliquid Chromatography with Ultraviolet−Visible Detection Using a Silica Monolithic Column

Lorenzo Cerretani,[†] María Jesús Lerma-García,[‡] José Manuel Herrero-Martínez,[‡] Tullia Gallina-Toschi,[†] and Ernesto Francisco Simó-Alfonso*,[‡]

[†]Dipartimento di Scienze degli Alimenti, Università di Bologna, P. zza Goidanich 60, I-47023 Cesena (FC), Italy, and [‡]Departamento de Química Analítica, Universidad de Valencia, C. Doctor Moliner 50, E-46100 Burjassot, Valencia, Spain

A method for the determination of tocopherols and tocotrienols in vegetable oils by nanoliquid chromatography with UV−vis detection has been developed. The separation of tocopherols was optimized in terms of mobile phase composition on the basis of the best compromise between efficiency, resolution, and analysis time. The optimal conditions were achieved using a C18 silica monolithic column (150 mm × 0.1 mm) with an isocratic elution of acetonitrile/methanol/water (acidified with 0.2% acetic acid) at a flow rate of 0.5 μL min^{-1}, giving a total analysis time below 18 min. The method has been applied to the quantification of tocopherols and tocotrienols present in several vegetable oils with different botanical origins.

KEYWORDS: Botanical origin; nano-LC; silica monolithic columns; tocopherols; tocotrienols; vegetable oils

INTRODUCTION

Vegetable oils contain vitamin E, which is a mixture of tocopherols (Ts) and tocotrienols (T_3s). These important lipid antioxidants are characterized by a two-ring structure known as chromanol (a substituted phenol with a cyclic ether), which is attached to a branched hydrocarbon side chain having 16 carbon atoms. According to the number and position of the methyl substituents in the phenol ring, four Ts (α-, β-, γ-, and δ-T) and four T_3s (α-, β-, γ-, and δ-T_3) are distinguished. Essentially, the family of vitamin E compounds is a major lipid-soluble chain-breaking antioxidant that protects natural oils from oxidation (*1*−*3*) and also prevents lipid peroxidation in biological membranes (*4*, *5*). Their positive influence to retard the development of precancer lesions and tumors (*6*) and to combat free radical reactions that can cause DNA mutations (*7*) has been demonstrated.

Ts are found in variable proportions in vegetable oils, while T_3s are present especially in palm oil (*8*) and in cereal seed oils (*9*). The relative concentrations of Ts and T_3s vary widely from one oil to another, which can be used to distinguish the oils according to their botanical origin. Thus, α-T is the most representative antioxidant in olive oil (*10*, *11*), while γ- and δ-T contents are high in soybean and sunflower oils, with soybean oil particularly rich in γ-T (*12*). Ts and/or T_3s concentrations have been used to detect the adulteration of olive oil with red palm (*13*) and hazelnut oils (*14*) and soybean oil with linseed oil (*15*). Therefore, rapid and reliable analytical methods, capable of assessing the composition of these compounds in vegetable oils, are important in food quality control and in relation to human health studies.

Vitamin E components have usually been determined in vegetable oils by gas chromatography (*16*) and high-performance liquid chromatography (HPLC) (*17*−*20*). Although normal phase columns are more efficient in separating the β- and γ-isomers of Ts and T_3s (*17*), reversed phase columns show higher column stability, better reproducibility, and shorter analysis times (*11*, *17*, *21*). Other techniques, such as Fourier transform infrared spectroscopy (*22*), synchronous fluorescence spectroscopy (*19*), and capillary electrochromatography (CEC) (*23*, *24*) have also been applied to the determination of Ts in vegetable oils.

Miniaturization is one of the present trends in science and technology, especially in the field of analytical chemistry. The use of these miniaturized techniques, such as nanoliquid chromatography (nano-LC), offers several advantages over classical techniques, such as better separation efficiencies, increase in sensitivity, shorter analysis time, and lower sample and reagent consumption (*25*, *26*).

Nano-LC has been applied to the separation of a wide number of compounds in different areas, mainly in proteomics, but also in pharmaceutical or environmental fields (*25*); however, the application of this technique appears very useful in food analysis (*25*, *27*−*32*), especially in quality control or to highlight contamination and/or adulteration. Nano-LC has been applied to the separation of Ts in serum and pharmaceutical preparations using a packed column (*33*); however, as far as we are concerned, it has not been applied to determine Ts in vegetable oils.

*To whom correspondence should be addressed. Tel: +34-963543176. Fax: +34-963544436. E-mail: ernesto.simo@uv.es.

Published on Web 11/19/2009 pubs.acs.org/JAFC

Among the common stationary phases used in nano-LC, silica-modified particles of 3−5 μm, bed monoliths (*34*), or walls coated with appropriate materials (*35*, *36*) have been used. In particular, monolithic materials exhibited important advantages in comparison to packed columns. Some of these benefits are simple preparation, absence of retaining frits, high permeability, adjustable porosity, and pore size and functionality of columns (*37*−*40*).

In this work, a nano-LC-UV−vis method using a C18 silica monolithic column has been developed. After optimization of mobile phase composition, this method has been applied to determine Ts and T_3s in vegetable oils with different botanical origins.

Table 1. Botanical Origin, Number of Samples, and Brand of the Oil Samples Used in This Work

origin	no. of samples	brand
avocado	1	Guinama
	1	Marnys
corn	1	Guinama
	1	Gloria
extra virgin olive	1	Intercoop Oliva[a]
	1	Tenuta Pennita[b]
grapeseed	1	Guinama
	1	Coosur
hazelnut	1	Guinama
	1	Percheron
peanut	1	Guinama
	1	Maurel
red palm	2	Blue Bay
soybean	1	Guinama
	1	Coosur

[a] Oil produced in Spain from the Serrana cultivar. [b] Oil produced in Italy from the Brisighella cultivar.

MATERIALS AND METHODS

Reagents. Used were the following analytical grade reagents: acetonitrile (ACN), methanol (MeOH), 2-propanol (Scharlau, Barcelona, Spain), acetic acid (Panreac, Barcelona), and butylated hydroxytoluene (BHT, Fluka, Buchs, Switzerland). Deionized water was obtained with a Barnstead deionizer (Sybron, Boston, MA). Standards of α-, γ-, and δ-T were from Sigma (St. Louis, MO). Stock solutions of the analytes (ca. 1500 μg mL^{-1}) were prepared in MeOH with 0.1% BHT (w/v) and stored at −20 °C in amber vials. Working solutions were prepared daily by dilution of the stock solutions with the mobile phase. The vegetable oils employed in this study (**Table 1**) were either purchased in the local market or kindly donated by the manufacturers. The botanical origin and quality grade of all of the samples were guaranteed by the suppliers.

Instrumentation and Working Conditions. A 1200 series liquid chromatograph provided with a degasser, a nanopump, and a diode array detector with a micro flow cell (Agilent Technologies, Palo Alto, CA) was used. The column was directly coupled to a 10 nL injector equipped with a microelectric actuator (Valco, Schenkon, Switzerland). Separation was carried out with a Chromolith CapRod RP-18 capillary column (150 mm × 0.1 mm, Merck, Darmstadt, Germany). Elution was performed isocratically with 75:8:17 (ACN/MeOH/water, v/v/v) containing 0.2% acetic acid. UV−vis detection was performed at 295 ± 16 nm (360 ± 100 nm as reference), with a flow rate of 0.5 μL min^{-1}.

Sample Preparation. According to Aturki et al. (*23*), vegetable oil samples (4 g) were extracted twice with 10 mL of MeOH containing 0.1% BHT (w/v) as an antioxidant and once again with 10 mL of a MeOH/2-propanol mixture 80:20 (v/v). All extractions were performed during shaking for 30 s followed by centrifugation at 8000*g* for 10 min. The combined extracts were evaporated to dryness using a rotary evaporator at 40 °C. The residue was dissolved in 1 mL of MeOH and stored at −20 °C in amber vials. For each sample, three extracts were performed. Each extract was properly diluted with the mobile phase and injected three times.

RESULTS AND DISCUSSION

Optimization of Tocopherol Separation. To optimize tocopherol separation in terms of mobile phase composition, a test mixture

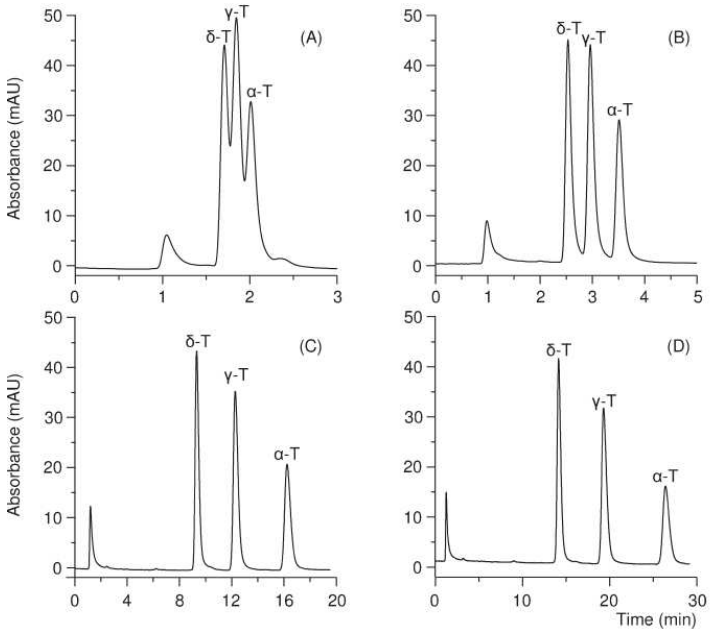

Figure 1. Influence of water content in the mobile phase composition on the separation of tocopherol standards: (**A**) 89:10:1, (**B**) 84:9:7, (**C**) 75:8:17, and (**D**) 71:8:21 ACN/MeOH/water (v/v/v) with 0.2% acetic acid. Chromatographic conditions: flow rate, 0.5 μL min^{-1}; wavelength detection, 295 nm.

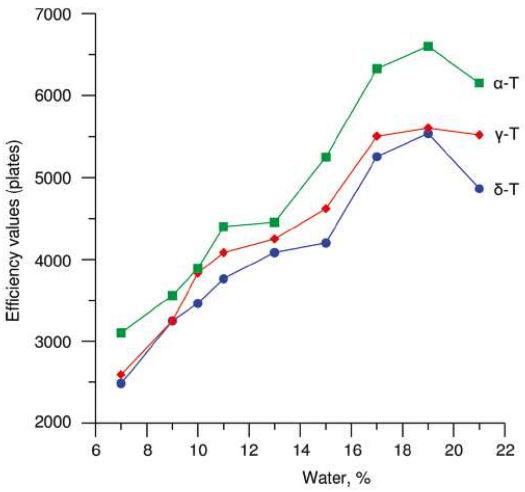

Figure 2. Efficiency values of Ts at several water contents in the mobile phase.

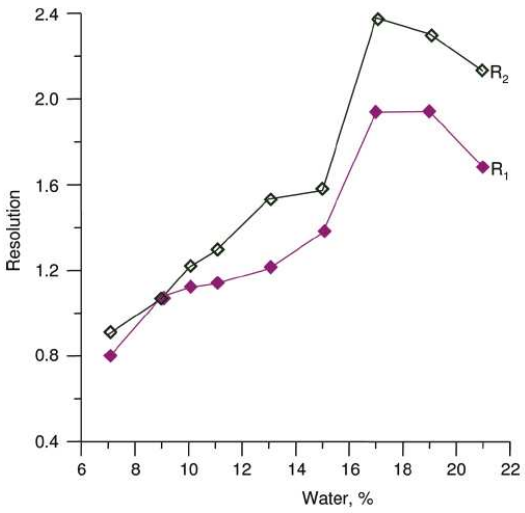

Figure 3. Resolution of Ts at several water contents in the mobile phase (R_1 = resolution between δ- and γ-T; R_2 = resolution between γ- and α-T).

composed of the α-, γ-, and δ-T (ca. 300 μg mL^{-1}) standards was used. According to literature (*20*), an 89:10:1 ACN/MeOH/water mixture (v/v/v) containing 0.2% acetic acid was first tried as a mobile phase in isocratic elution mode using a flow rate of 0.5 μL min^{-1}. As observed in **Figure 1A**, this mobile phase composition was unable to resolve all analyte pairs. To improve this separation, water content was progressively increased from 1 to 21% keeping constant the acetic acid percentage. As shown in **Figure 1**, an increase of analysis time was observed when the water content increased.

To evaluate the quality of tocopherol separation, efficiency (N) and resolution values were calculated (see **Figures 2** and **3**, respectively). It can be seen that both efficiency and resolution are highly dependent on the water content in the mobile phase. As shown in **Figure 2**, a progressive increase in the efficiency values of Ts was observed when the water content was increased, reaching a maximum at 19%. In all cases, theoretical plate values followed the next order: α-T > γ-T > δ-T. On the other hand, resolution also improved when the water content increased, reaching a maximum value at 17% (**Figure 3**). On the basis of these results, a mobile phase containing 75:8:17 (ACN/MeOH/water, v/v/v) was selected as the best compromise between efficiency, resolution, and analysis time (ca. 18 min; see **Figure 1C**).

Quantitation Studies and Application to Vegetable Oils. External calibration curves of peak areas were constructed by injecting six standard solutions in the range 5−500 μg mL^{-1}. Each solution contained the three tocopherol standards. In all cases, an excellent linearity with $r^2 > 0.998$ was obtained. Other analytical figures of merit are shown in **Table 2**. Repeatabilities of peak areas and retention times were obtained by injecting a mixture containing 50 μg mL^{-1} of each standard 10 times per day during 3 days. The limits of detection (LODs) and limits of quantification (LOQs) were estimated for signal-to-noise ratios of 3 and 10, respectively. In all cases, these values were lower than others reported in literature (*24*, *41*). Similar sensitivities were obtained for δ- and γ-T, this value being lower in α-T than in δ- and γ-T. Therefore, a higher LOD was obtained for α-T with respect to the other two Ts assayed. These results are in agreement with the literature (*33*).

The optimized method was applied to the determination of Ts in several oil samples. Peak identification was performed by comparing the retention times and absorption spectra with those of the standards. Representative chromatograms of corn, grapeseed, hazelnut, and soybean oil extracts are shown in **Figure 4**. As indicated above, each extract was injected three times. In all cases, the relative standard deviation was below 2.3%. Different fingerprints of Ts were obtained according to the botanical origin of the oil. The monolithic column used in this work had reversed-phased characteristics and was therefore unable to resolve the β-T and γ-T isomers present in the oil samples, which agrees with RP-HPLC studies (*11*, *17*, *21*). Consequently, the sum of the concentrations of both isomers was considered for quantification. The found concentrations of Ts, expressed as mg kg^{-1} oil, are reported in **Table 3**. These data are consistent with those previously reported for oils of the same botanical origins (*12*, *13*, *42*). As shown in **Table 3** and **Figure 4A**, large quantities of β-T + γ-T and small amounts of α-T and δ-T were present in corn oil. Hazelnut oil showed α-T concentrations higher than those of the other Ts (**Table 3** and **Figure 4C**). In soybean oil, large quantities of β-T + γ-T and δ-T were observed (**Table 3** and **Figure 4D**). Thus, these Ts could be used to detect the presence of soybean oil in virgin olive oil (*13*), whose major isomer was α-T (**Table 3**).

Red palm and grapeseed oils constitute important sources of T_3s (*8*, *42*); these compounds are also present in other oils, such as corn oil (*43*). Thus, T_3s were identified according to their UV spectra (which are closely similar to those of Ts due to the fact that the double bonds of the side chain of T_3s are not conjugated) and comparing the elution order with that previously reported in the literature for C18 reversed-phase analysis (*44*−*46*). These

Table 2. Analytical Figures of Merit for the Nano-LC Method in the Determination of Ts

	repeatability[a] (%)		μg mL^{-1}		
analyte	area	t_R	LOD	LOQ	relative sensitivity[b]
δ-T	2.8	0.1	0.07	0.2	1.81
γ-T	3	0.1	0.07	0.2	1.92
α-T	4.2	0.2	0.16	0.5	1.00

[a] For a tocopherol concentration of 50 μg mL^{-1} (n = 30). [b] As the ratio of the slopes of calibration curves of Ts (respect to α-T).

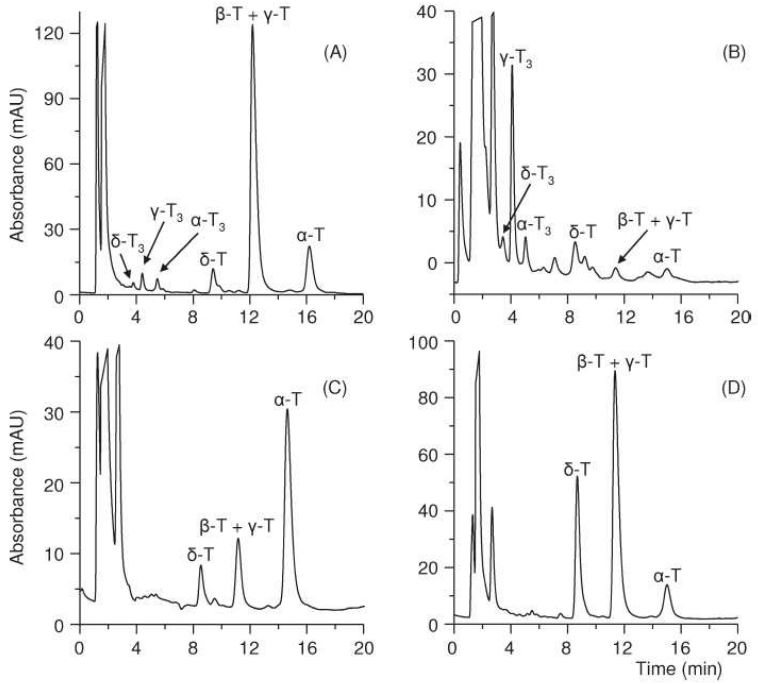

Figure 4. Chromatograms of (**A**) corn, (**B**) grapeseed, (**C**) hazelnut, and (**D**) soybean oil extracts. Chromatographic conditions: 75:8:17 ACN/MeOH/water (v/v/v) with 0.2% acetic acid. Other experimental conditions are as in **Figure 1**.

Table 3. Contents of Ts and T_3s in Vegetable Oils (mg kg^{-1})

oil	δ-T	β-T + γ-T	α-T	δ-T_3	β-T_3 + γ-T_3	α-T_3
avocado	12.2−23.9	6.3−67.6	34.2−55.1	ND[a]−7.9	ND[a]−9.3	ND[a]−5.3
corn	11.1−22.3	125.0−237.0	51.7−82.6	4.8−7.1	4.6−7.3	2.3−12.4
extra virgin olive	ND[a]−5.6	7.5−10.1	52.1−111.7	ND[a]	ND[a]	ND[a]
grapeseed	6.0−10.2	6.3−17.2	5.8−54.8	0−8.2	10.3−31.0	2.1−12.3
hazelnut	7.0−12.1	18.8−32.2	71.5−119.7	ND[a]	ND[a]	ND[a]
peanut	6.9−31.3	36.7−74.1	42.6−44.5	ND[a]	ND[a]	ND[a]
red palm	ND[a]	4.2−8.3	6.8−20.8	8.8−11.3	27.0−40.4	15.2−35.1
soybean	66.9−87.8	95.4−177.1	17.4−52.6	ND[a]	ND[a]	ND[a]

[a] ND, not detected (below the LOD value).

features were employed to assign the additional peaks observed in avocado, corn, grapeseed, and red palm oils. Each T_3 was quantified using the calibration curve of its corresponding tocopherol. Their concentration is also reported in **Table 3**. These T_3 contents were also consistent with those reported in literature (*9*, *42*). Because T_3s did not occur naturally in olive oil, their presence in a sample clearly indicates its adulteration with tocotrienol-rich oils.

LITERATURE CITED

(1) Blekas, G.; Tsimidou, M.; Bouskou, D. Contribution of α-tocopherol to olive oil stability. *Food Chem.* **1995**, *52*, 289–294.

(2) Manzi, P.; Panfili, G.; Esti, M.; Pizzoferrato, L. Natural antioxidants in the unsaponifiable fraction of virgin olive oils from different cultivars. *J. Sci. Food Agric.* **1998**, *77*, 115–120.

(3) Braunrath, R.; Isnardy, B.; Solar, S.; Elmadfa, I. Influence of α-, γ-, and δ-tocopherol on the radiation induced formation of peroxides in rapeseed oil triacylglycerols. *Food Chem.* **2009**, *117*, 349–351.

(4) Panfili, G.; Fratianni, A.; Irano, M. Normal phase high-performance liquid chromatography method for the determination of tocopherols and tocotrienols in cereals. *J. Agric. Food Chem.* **2003**, *51*, 3940–3944.

(5) Solomon, N. W. Plant sources of vitamin A and human nutrition: Red palm oil does the job. *Nutr. Rev.* **1998**, *56*, 309–311.

(6) Lee, H. J.; Ju, J.; Paul, S.; So, J. Y.; DeCastro, A.; Smolarek, A.; Lee, M. J.; Yang, C. S.; Newmark, H. L.; Suh, N. Mixed tocopherols prevent mammary tumorigenesis by inhibiting estrogen action and activating PPAR-γ. *Clin. Cancer Res.* **2009**, *15*, 4242–4249.

(7) Gester, H. Anticarcinogenic effect of common carotenoids. *Int. J. Vitam. Nutr. Res.* **1993**, *63*, 93–121.

(8) Choo, Y. M.; Yapa, S. C.; Ooi, C. K.; Ma, A. N.; Goh, S. H.; Ong, A. S. H. Recovered oil from palm-pressed fiber: A good source of natural carotenoids, vitamin E, and sterols. *J. Am. Oil Chem. Soc.* **1996**, *73*, 599–602.

(9) Watson, R. R.; Preedy, V. R. *Tocotrienols: Vitamin E beyond Tocopherols*; The American Oil Chemist's Society (AOCS): Urbana, IL, 2009.

(10) Tasioula-Margari, M.; Okogeri, O. Simultaneous determination of phenolic compounds and tocopherols in virgin olive oil using HPLC and UV detection. *Food Chem.* **2001**, *74*, 377–383.

(11) Gimeno, E.; Calero, E.; Castellote, A. I.; Lamuela-Raventós, R. M.; De La Torre, M. C.; López-Sabater, M. C. Simultaneous determination of α-tocopherol and β-carotene in olive oil by reversed-phase high-performance liquid chromatography. *J. Chromatogr. A* **2000**, *881*, 255–259.

(12) Rovellini, P.; Azzolini, M.; Cortesi, N. Tocoferoli e tocotrienoli in oli e grassi vegetali mediante HPLC. *Riv. Ital. Sost. Grasse* **1997**, *74*, 1–5.
(13) Dionisi, F.; Prodolliet, J.; Tagliaferri, E. Assessment of olive oil adulteration by reversed-phase high-performance liquid chromatography/amperometric detection of tocopherols and tocotrienols. *J. Am. Oil Chem. Soc.* **1995**, *72*, 1505–1511.
(14) Mariani, C.; Bellan, G.; Morchio, G.; Pellegrino, A. I componenti minori liberi ed esterificati dell'olio di oliva e dell'olio di nocciola: Loro possibile utilizzo nella individuazione di commistioni. Nota 1. *Riv. Ital. Sost. Grasse* **1999**, *76*, 59–67.
(15) Manandhar, P. P.; Nagao, A.; Yamazaki, M. Determination of content of linseed oil in edible soybean oil. *J. Jpn. Oil Chem. Soc.* **1986**, *35*, 725–732.
(16) Melchert, H. U.; Pollock, D.; Pabel, E.; Ruback, K.; Stan, H. J. Determination of tocopherols, tocopherolquinones and tocopherolhydroquinones by gas chromatography−mass spectrometry and preseparation with lipophilic gel chromatography. *J. Chromatogr. A* **2002**, *976*, 215–220.
(17) Abidi, S. L. Chromatographic analysis of tocol-derived lipid antioxidants. *J. Chromatogr. A* **2000**, *881*, 197–216.
(18) Cunha, S. C.; Amaral, J. S.; Fernandes, J. O.; Oliveira, M. B. P. P. Quantification of tocopherols and tocotrienols in Portuguese olive oils using HPLC with three different detection systems. *J. Agric. Food Chem.* **2006**, *54*, 3351–3356.
(19) Sikorska, E.; Gliszczyńska-Świgło, A.; Khmelinskii, I.; Sikorski, M. Synchronous fluorescence spectroscopy of edible vegetable oils. Quantification of tocopherols. *J. Agric. Food Chem.* **2005**, *53*, 6988–6994.
(20) Gruszka, J.; Kruk, J. RP-LC for determination of plastochromanol, tocotrienols and tocopherols in plant oils. *Chromatographia* **2007**, *66*, 909–913.
(21) Abidi, S. L.; Mounts, T. L. Reversed-phase high-performance liquid chromatographic separations of tocopherols. *J. Chromatogr. A* **1997**, *782*, 25–32.
(22) Silva, S. D.; Rosa, N. F.; Ferreira, A. E.; Boas, L. V.; Bronze, M. R. Rapid determination of α-tocopherol in vegetable oils by fourier transform infrared spectroscopy. *Food Anal. Method* **2009**, *2*, 120–127.
(23) Aturki, Z.; D'Orazio, G.; Fanali, S. Rapid assay of vitamin E in vegetable oils by reversed-phase capillary electrochromatography. *Electrophoresis* **2005**, *26*, 798–803.
(24) Lerma-García, M. J.; Simó-Alfonso, E. F.; Ramis-Ramos, G.; Herrero-Martínez, J. M. Determination of tocopherols in vegetable oils by CEC using methacrylate ester-based monolithic columns. *Electrophoresis* **2007**, *28*, 4128–4135.
(25) Hernández-Borges, J. M.; Aturki, Z.; Rocco, A.; Fanali, S. Recent applications in nanoliquid chromatography. *J. Sep. Sci.* **2007**, *30*, 1589–1610.
(26) Luque de Castro, M. D.; Gámiz-Gracia, L. Miniaturisation: A well-defined trend in separation and preconcentration techniques. *Anal. Chim. Acta* **1997**, *351*, 23–40.
(27) Chassaigne, H.; Norgaard, J. V.; Van Hengel, A. J. Proteomics-based approach to detect and identify major allergens in processed peanuts by capillary LC-Q-TOF (MS/MS). *J. Agric. Food Chem.* **2007**, *55*, 4461–4473.
(28) Weber, D.; Raymond, P.; Ben-Rejeb, S.; Lau, B. Development of a liquid chromatography-tandem mass spectrometry method using capillary liquid chromatography and nanoelectrospray ionization-quadrupole time-of-flight hybrid mass spectrometer for the detection of milk allergens. *J. Agric. Food Chem.* **2006**, *54*, 1604–1610.
(29) D'Orazio, G.; Cifuentes, A.; Fanali, S. Chiral nano-liquid chromatography−mass spectrometry applied to amino acids analysis for orange juice profiling. *Food Chem.* **2008**, *108*, 1114–1121.
(30) Hernández-Borges, J.; D'Orazio, G.; Aturki, Z.; Fanali, S. Nano-liquid chromatography analysis of dansylated biogenic amines in wines. *J. Chromatogr. A* **2007**, *1147*, 192–199.
(31) Fanali, S.; Aturki, Z.; D'Orazio, G.; Raggi, M. A.; Quaglia, M. G.; Sabbioni, C.; Rocco, A. Use of nano-liquid chromatography for the analysis of glycyrrhizin and glycyrrhetic acid in licorice roots and candies. *J. Sep. Sci.* **2005**, *28*, 982–986.
(32) Rocco, A.; Fanali, S. Analysis of phytosterols in extra-virgin olive oil by nano-liquid chromatography. *J. Chromatogr. A* **2009**, *1216*, 7173–7178.
(33) Fanali, S.; Camera, E.; Chankvetadze, B.; D'Orazio, G.; Quaglia, M. G. Separation of tocopherols by nano-liquid chromatography. *J. Pharm. Biomed.* **2004**, *35*, 331–337.
(34) Vissers, J. P. C.; Claessens, H. A.; Cramers, C. A. Microcolumn liquid chromatography: instrumentation, detection and applications. *J. Chromatogr. A* **1997**, *779*, 1–28.
(35) Saito, Y.; Jinno, K.; Greibrokk, T. Capillary columns in liquid chromatography: Between conventional columns and microchips. *J. Sep. Sci.* **2004**, *27*, 1379–1390.
(36) Swart, R.; Kraak, J. C.; Poppe, H. Recent progress in open tubular liquid chromatography. *Trends Anal. Chem.* **1997**, *16*, 332–342.
(37) Legido-Quigley, C.; Marlin, N. D.; Melin, V.; Manz, A.; Smith, N. W. Advances in capillary electrochromatography and micro-high performance liquid chromatography monolithic columns for separation science. *Electrophoresis* **2003**, *24*, 917–944.
(38) Svec, F.; Tennikova, T. B.; Deyl, Z. *Monolithic Materials: Preparation, Properties and Applications*; Journal of Chromatography Library, 67; Elsevier: Amsterdam, The Netherlands, 2003.
(39) Núñez, O.; Nakanishi, K.; Tanaka, N. Preparation of monolithic silica columns for high-performance liquid chromatography. *J. Chromatogr. A* **2008**, *1191*, 231–252.
(40) Urbánek, L.; Solichová, D.; Melichar, B.; Dvorák, J.; Svobodová, I.; Solich, P. Optimization and validation of a high performance liquid chromatography method for the simultaneous determination of vitamins A and E in human serum using monolithic column and diode-array detection. *Anal. Chim. Acta* **2006**, *573−574*, 267–272.
(41) Waseem, A.; Rishi, L.; Yaqoob, M.; Nabi, A. Flow-injection determination of retinol and tocopherol in pharmaceuticals with acidic potassium permanganate chemiluminescence. *Anal. Sci.* **2009**, *25*, 407–412.
(42) Jee, M. *Oils and Fat Authentication*; Blackwell Publishing, CRC Press: Boca Raton, FL, 2002.
(43) Gunstone, F. D. TiTulo. *Vegetable Oils in Food Technology: Composition, Properties and Uses*; Blackwell Publishing, CRC Press: Boca Raton, FL, 2002.
(44) Abidi, S. L.; Rennick, K. A. Capillary electrochromatographic evaluation of vitamin E-active oil constituents: Tocopherols and tocotrienols. *J. Chromatogr. A* **2001**, *913*, 379–386.
(45) Abidi, S. L.; Thiam, S.; Warner, I. M. Elution behavior of unsaponifiable lipids with various capillary electrochromatographic stationary phases. *J. Chromatogr. A* **2002**, *949*, 195–207.
(46) Abidi, S. L. Reversed-phase retention characteristics of tocotrienol antioxidants. *J. Chromatogr. A* **1999**, *844*, 67–75.

Received for review September 7, 2009. Revised manuscript received November 6, 2009. Accepted November 9, 2009. This work was supported by Project CTQ2007-61445 (MEC of Spain and FEDER funds). L.C. thanks the University of Valencia for a contract. M.J.L.-G. thanks the Generalitat Valenciana for an FPI grant for Ph.D. studies.

ANEXO III

Electrophoresis 2008, *29*, 4603–4611

María Jesús Lerma-García
Ernesto F. Simó-Alfonso
Guillermo Ramis-Ramos
José M. Herrero-Martínez

Department of Analytical Chemistry, Faculty of Chemistry, University of Valencia, Valencia, Spain

Received April 15, 2008
Revised June 20, 2008
Accepted July 4, 2008

Research Article

Rapid determination of sterols in vegetable oils by CEC using methacrylate ester-based monolithic columns

A method for the determination of sterols in vegetable oils by CEC with UV–Vis detection, using methacrylate ester-based monolithic columns, has been developed. To prepare the columns, polymerization mixtures containing monomers of different hydrophobicities were tried. The influence of composition of polymerization mixture was optimized in terms of porogenic solvent, monomers/porogens and monomer/crosslinker ratios. The composition of the mobile phase was also studied. The optimum monolith was obtained with lauryl methacrylate monomer at 60:40% (wt:wt) lauryl methacrylate/ethylene dimethacrylate ratio and 60 wt% porogens with 20 wt% of 1,4-butanediol (12 wt% 1,4-butanediol in the polymerization mixture). Excellent resolution between sterols was achieved in less than 7 min with an 85:10:5 v/v/v ACN–2-propanol–water buffer containing 5 mM Tris at pH 8.0. The limits of detection were lower than 0.04 mM, and inter-day and column-to-column reproducibilities at 0.75 mM were better than 6.2%. The method was applied to the determination of sterols in vegetable oils with different botanical origins and to detect olive oil adulteration with sunflower and soybean oils.

Keywords:
CEC / Food analysis / Methacrylate ester-based monolithic columns / Sterols / Vegetable oils
DOI 10.1002/elps.200800247

1 Introduction

Genuineness of quality edible oils is of great importance for both commercial value and health impact. The organoleptic properties, high nutritional value and health benefits of quality oils are related to the presence of many components with interesting biochemical properties, including among others, antioxidants and sterols [1, 2]. Sterols, unsaponifiable components of the oils (Fig. 1), may reduce blood cholesterol levels by inhibiting its absorption from the small intestine, and they may have anti-inflammatory, antibacterial and antioxidant activities [3].

A relevant aspect of oil authenticity is adulteration of quality oils with lower price oils of a different botanical origin. The evaluation of sterol profiles and total sterol contents is an excellent tool to assess oil authenticity [4, 5] and to check oil genuineness [6]. Sterol composition of extra virgin olive oils is very characteristic and for this reason, the determination of sterols has become particularly helpful to detect adulterations of extra virgin olive oils with vegetable oils of a different botanical origin [7–10], or with olive oils of a lower-quality grade [11, 12]. To prevent adulteration, several international organizations, including the Codex Alimentarius FAO and WHO and the European Union have established characteristic values for these compounds [12].

Official methods for analysis of sterols in vegetable oils involved saponification of the oil, extraction of the unsaponifiable fraction with diethyl ether and isolation of the sterol fraction by TLC. Quantification of the silanized fraction is performed by GC with flame ionization detection [1, 2, 6, 8, 9, 13–19]. GC with MS detection has been also used [1, 8, 17, 20–22]. The major disadvantage of GC is the requirement of both thermally stable columns and chemical derivatization before analysis. For this reason, the determination of sterols in vegetable oils by HPLC-MS [11, 12, 23] and direct infusion MS [24] has been also proposed.

CEC is a hybrid separation technique, which combines the selectivity of HPLC with the high efficiency of CE [25, 26]. Using CEC, compounds with closely similar properties can be resolved in a short time with minimal solvent consumption. The successful use of packed columns in CEC separation has been demonstrated in many reports [27]. Although a few CEC procedures based on this type of columns have been developed to separate sterols in edible oils [28–30], no application to detect oil adulteration has been demonstrated. However, the fabrication of

Correspondence: Dr. José M. Herrero-Martínez, Department of Analytical Chemistry, Faculty of Chemistry, University of Valencia, 46100-Burjassot, Valencia, Spain
E-mail: jmherrer@uv.es
Fax: +34-963544436

Abbreviations: **EDMA**, ethylene dimethacrylate; **LMA**, lauryl methacrylate; **META**, [2-(methacryloyloxy)ethyl] trimethyl ammonium chloride; **ODMA**, octadecyl methacrylate

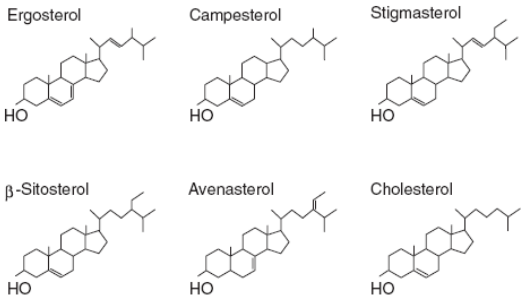

Figure 1. Chemical structures of sterols investigated.

reproducible CEC-packed columns still remains problematic [31, 32]. As an alternative to the conventional CEC-packed columns, monolithic columns have attracted great attention in recent years; their preparation is simple and reproducible, and retaining frits are not needed. So far, silica and several organic polymeric monolithic materials, such as acrylamide, styrene and methacrylate esters, have been employed as stationary phases in CEC [33–42]. Among these, methacrylate ester-based monolithic columns have several advantages such as easily adjustable polarity, fine control of pore characteristics and high stability under extreme pH conditions [38, 39, 41]. In spite of these good features, to our knowledge no CEC method with monolithic columns has been reported for the analysis of sterols in vegetable oils.

In this work, a reliable and fast method to analyze sterols in vegetable oils has been developed. The separation of sterols using methacrylate ester-based monolithic columns was optimized in terms of composition of polymerization mixture (*i.e.* porogenic solvent, monomers/porogens and monomer/crosslinker ratios), monomer hydrophobicity and mobile phase composition. Analytical figures of merit were established, and the application to the detection of olive oil adulteration with sunflower and soybean oils was demonstrated.

2 Materials and methods

2.1 Reagents and samples

Lauryl methacrylate (LMA), octadecyl methacrylate (ODMA), ethylene dimethacrylate (EDMA), [2-(methacryloyloxy)ethyl] trimethyl ammonium chloride (META, 75% in water), 1,4-butanediol, 3-(trimethoxysilyl)propyl methacrylate and basic alumina from Aldrich (Milwaukee, WI, USA), hydrochloric acid (37%) from Panreac (Barcelona, Spain), methanol, ethanol, 1-propanol, 2-propanol, ACN and THF from Scharlau (Barcelona, Spain), AIBN and Tris from Fluka (Buchs, Switzerland), diethyl ether and chloroform from J. T. Baker (Deventer, Holland), potassium hydroxide (Probus, Barcelona, Spain), *n*-hexane (Riedel-de Haën, Seelze, Germany) and 2,7-dichlorofluorescein (Sigma, St. Louis, MO, USA) were employed. Deionized water was obtained with a Barnstead deionizer (Sybron, Boston, MA, USA). Glass plates for TLC, coated with silica gel without fluorescent indicator (0.25 mm plate thickness, Merck, Darmstadt, Germany) were used. Uncoated fused-silica capillaries with 375 μm od × 100 μm id were from Polymicro Technologies (Phoenix, AZ, USA). The sterols used as standards were: β-sitosterol (Sigma), ergosterol, stigmasterol (Acros Organics, Morris Plains, NJ, USA) and cholesterol (Aldrich). Stock solutions of the analytes (*ca.* 5 mM), were prepared in 2-propanol and kept at −20°C in amber vials until their use. Working solutions were prepared daily by dilution of the stock solutions with the mobile phase. Thiourea (Riedel-de Haën) was used as EOF marker.

The following vegetable oils were employed: sunflower (Hacendado, Valencia, Spain), extra virgin olive (Carbonell, Córdoba, Spain), soybean (Biolasi, Ordizia, Guipúzcoa, Spain), corn, peanut, grapeseed and hazelnut oils (Guinama, Valencia, Spain). These oils were either purchased in the local market or kindly donated by the manufacturers. The botanical origin and quality grade of all the oil samples were guaranteed by the suppliers.

2.2 Instrumentation and procedures

CEC experiments were performed on an HP^{3D}CE instrument (Agilent Technologies, Waldbronn, Germany), equipped with a diode array UV–Vis detector and provided with an external nitrogen supply. Data acquisition was performed with ChemStation Software (Rev.A.10.01, Agilent). Before use, all the eluents for CEC were degassed by ultrasonication. The monolithic column was placed in the instrument, and equilibrated with the mobile phase as follows. Using nitrogen, a pressure of 10 bar (1 MPa) was applied to both ends of the column [39–41, 43], and the voltage was stepwise raised from 5 to 20 kV, with increments of 5 kV. Each voltage was maintained until a constant current and a stable baseline were achieved. Separations were performed at 20 kV with the column kept at 25°C, and the inlet and outlet vials pressurized to 1 MPa with nitrogen. The sample extracts and standard solutions were injected electrokinetically under 10 kV for 2 s. Detection was performed at 210 nm.

Pictures of the monolithic materials were taken with a scanning electron microscope (SEM, S-4100, Hitachi, Ibaraki, Japan) provided with a field emission gun, a backscatter electron Autrata detector, an electron microscope image processing 3.0, and a microanalysis system (Rontec, Normanton, UK).

2.3 Preparation and characterization of the polymeric monolithic columns

Before preparation of the columns, and in order to enable covalent attachment of the monolith to the wall, surface modification of the inner wall of the fused-silica capillaries

with 3-(trimethoxysilyl)propyl methacrylate was performed [39, 41]. Monoliths were prepared using polymerization mixtures containing a bulk monomer (LMA or ODMA), a crosslinker (EDMA), pore-forming solvents (1,4-butanediol and 1-propanol) and a positively charged monomer (META), which was added to provide monoliths with the capacity of generating EOF. Before use, LMA, ODMA and EDMA were purified by passing them through activated basic alumina to eliminate polymerization inhibitors, followed by distillation under reduced pressure [38, 39, 41, 43]. AIBN (1 wt% with respect to the monomers) was also added as polymerization thermal initiator. After mixing, and to obtain a clear solution, sonication for 10 min followed by deareation with nitrogen for 10 more min was applied. The preconditioned capillary (33.5 cm) was filled with the polymerization mixture to a total length of 8.5 cm by capillary action. After polymerization for 20 h at 70°C, an HPLC pump was used to flush the columns with methanol, thus to remove the pore-forming solvents and possible unreacted monomers. A detection window adjacent to the monolithic material was made by burning off the polyimide coating. Before CEC experiments, the capillaries were flushed with the mobile phase for 30 min.

2.4 Sample preparation

The extracts containing the sterol fraction of the vegetable oils were obtained following the procedure established by the European Union [44]. Five grams of the oil samples were saponified by refluxing for 20 min with 2 N ethanolic KOH. After this, 50 mL of distilled water was added. Then, the non-saponifiable fraction was extracted three times with diethyl ether. The three ether extracts were introduced into a separating funnel and washed with distilled water (50 mL each time) until neutral reaction. The organic extracts were dried with anhydrous sodium sulfate and filtered. These extracts were evaporated to dryness using a rotatory evaporator. The remaining unsaponifiables were dissolved in 2 mL chloroform and then, sterol fraction was separated by TLC using a plate-developing chamber, which contained hexane/diethyl ether 60:40 v/v. After TLC separation, the plate was sprayed lightly and uniformly with 2,7-dichlorofluorescein. The sterol band was removed from the silica plate using a spatula. This material was dissolved in 10 mL diethyl ether and filtered through a Whatman no. 1 paper using a Buchner funnel. A rotatory evaporator was used to remove this solvent, and the residue was dissolved in 200 µL of 2-propanol and stored at −20°C in amber vials. These solutions were properly diluted with the mobile phase and injected.

3 Results and discussion

3.1 Optimization of the separation of sterols

According to our previous work [45], an LMA-based monolithic column with the following composition was initially selected: 40 wt% of monomers (59.8 wt% of LMA, 39.9 wt% of EDMA and 0.3 wt% of META) and 60 wt% of porogens (80 wt% of 1-propanol and 20 wt% of 1,4-butanediol). A 1 wt% AIBN with respect to the monomers was also added. To obtain an optimal mobile phase for sterol separation, ACN–THF–water ternary mixtures containing 5 mM Tris at pH 8.0 were first tried [28]. For this purpose, several volume fractions of THF in the 5–35% range, keeping a constant water percentage of 5%, were studied. With a mobile phase containing 35% THF, the co-elution of several sterol peaks was observed. By decreasing the THF percentage, peak resolution increased largely; however, with a 5% THF broad peaks were obtained. Then, a mobile phase containing 85:10:5 v/v/v ACN–THF–water gave the best resolution and efficiency values for all the sterol peaks in less than 10 min (see Table 1 and Fig. 2, part A).

A similar study was carried out replacing THF by 2-propanol in the mobile phase composition, since sterols are much more soluble in 2-propanol than in THF. The 2-propanol percentage in the mobile phase was also modified within the 5–35% range. The best results were obtained with a mobile phase constituted by 85:10:5 v/v/v ACN–2-propanol–water (see Fig. 2, part B). A comparison between efficiencies, *k*-values and peak pair resolutions obtained with the two mobile phases alternatively containing 10% THF or 2-propanol is presented in Table 1. As it can be observed, the resolution between sterol peak pairs was similar with both mobile phases; however, better efficiencies and lower *k*-values were obtained for the mobile phase containing 2-propanol, which was selected for the following studies.

The elution order of the analytes (ergosterol, cholesterol, stigmasterol and β-sitosterol) indicated that an RP mechanism (hydrophobic interaction with the stationary phase) predominated over other possible interactions. This behavior agrees with other studies on sterols eluted with RP-packed columns [28].

With the selected mobile phase, and keeping constant the proportion of monomers/porogens and monomers/crosslinker at 40:60 and 60:40% wt/wt, respectively, the effect of porogenic solvent composition on the monolith morphology and chromatographic performance was investigated (Table 2, columns A1–A4). The content of

Table 1. Efficiency, resolution and *k*-values obtained with the two optimal mobile phases using an LMA-based monolithic column with 12 wt% 1,4-butanediol (column A3)

Solutes	ACN–THF–Tris (85:10:5)			ACN–2-propanol–Tris (85:10:5)		
	N (plates/m)	R_s [a)]	*k*	*N* (plates/m)	R_s [a)]	*k*
Ergosterol	28 200	—	3.4	36 300	—	2.2
Cholesterol	34 700	3.4	4.8	46 300	3.3	3.0
Stigmasterol	26 000	1.5	5.7	28 800	1.5	3.4
β-Sitosterol	34 600	1.8	6.7	60 900	2.0	4.1

a) Resolution was calculated between two adjacent peaks

1,4-butanediol in the polymerization mixture was varied from 8 to 15 wt% (14–25 wt% in porogenic solvent). With less than 10 wt% 1,4-butanediol (*e.g.* column A1), too small pore sizes (<125 nm) [45], clearly unsuitable for any flow-through applications, were obtained. In comparison with the use of 12 wt% 1,4-butanediol (column A3), a 10 wt% of this solvent (column A2) led to similar resolutions between the analytes, but with lower efficiencies and longer analysis times (≈15 min). This increase in the retentivity of solutes was due to a strong decrease of both the pore size of the monolith and the dimension of the globules, also implying an increase in the surface area, as observed for polymerization mixtures containing low 1,4-butanediol contents [42, 43]. This behavior can be explained briefly as follows. In a mixture of porogenic solvents with small 1,4-butanediol content (low polarity), phase separation will occur late in the polymerization process, due to the relatively high solubility of the polymer in the solvent. At the time of phase separation, the system contains more polymer that precipitates in the form of numerous nuclei, which are allowed to grow for only a limited period of time before all the monomers are exhausted. Overall, the globules that are formed in such a system are small and, consequently, the voids between them (pores) are small as well. The result would be a polymer with high surface area, and consequently, more retentivity. The low efficiencies obtained at 10 wt% of 1,4-butanediol (column A2) could be explained by the double-layer overlap, as suggested by other authors [39, 43].

To check the possibility of achieving shorter analysis time while maintaining satisfactory resolution between analytes, monolithic columns prepared with 15 wt% 1,4-butanediol (column A4) were also examined. The analysis time was reduced to 5 min; however, cholesterol/stigmasterol peaks co-eluted. Then, a content of 12 wt% of butanediol (20 wt% in the porogenic solvent) was selected for further experiments.

The porogen weight fraction in the polymerization mixture has also some effect on the character of the monolithic structure [42, 43]. In this way, this factor was investigated (Table 2, columns A3, A5 and A6). When the content of the porogenic solvent in the polymerization mixture reached 70 wt% (column A5), an overlapping between cholesterol/stigmasterol peaks was obtained, which

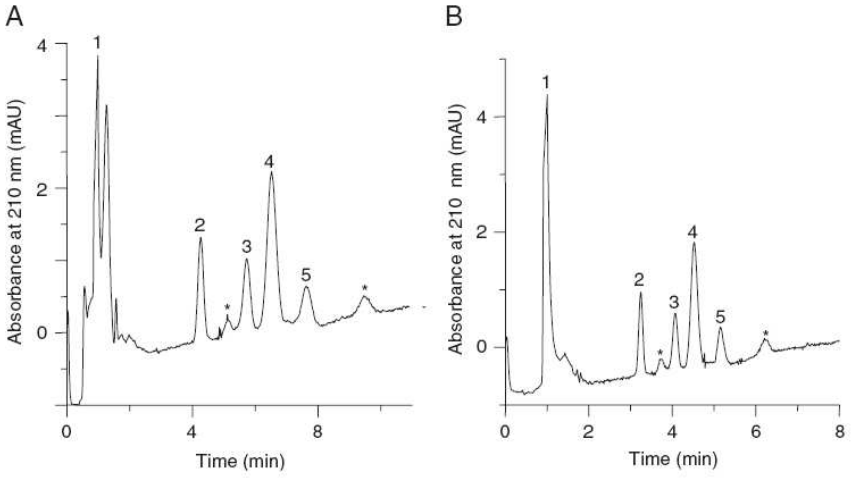

Figure 2. Influence of the mobile phase composition on the separation of sterols: (A) 85:10:5 v/v/v ACN–THF–water and (B) 85:10:5 v/v/v ACN–2-propanol–water, both containing 5 mM Tris at pH 8.0. CEC conditions: LMA-based monolithic column prepared with 12 wt% 1,4-butanediol in the polymerization mixture (column A3) [45]; electrokinetic injection, 10 kV for 2 s; separation voltage, 20 kV. Peak identification: 1, thiourea; 2, ergosterol; 3, cholesterol; 4, stigmasterol; 5, β-sitosterol. Impurities were labeled with an asterisk.

Table 2. Composition of the polymerization mixtures used for the preparation of LMA-based monolithic columns and their efficiency and retention values

Column	Monomers/porogens (% wt/wt)	LMA/EDMA (% wt/wt)	1-Propanol/1,4-butanediol (% wt/wt)	$N_{\beta\text{-sitosterol}}$ (plates/m)	$k_{\beta\text{-sitosterol}}$
A1	40:60	60:40	86:14	NM[a)]	NM[a)]
A2	40:60	60:40	83:17	45200	6.2
A3	40:60	60:40	80:20	60900	4.1
A4	40:60	60:40	75:25	53600	3.9
A5	30:70	60:40	80:20	28200	2.9
A6	50:50	60:40	80:20	NM[a)]	NM[a)]
A7	40:60	70:30	80:20	58700	3.6
A8	40:60	50:50	80:20	NM[a)]	NM[a)]

a) Not measured.

could be attributed to the large globule sizes formed in the polymer network [42, 43]. In contrast, when the content of the porogenic solvent was reduced to 50 wt% (column A6), the bed permeability was significantly reduced, leading to blockage problems of columns, then, a 40:60% wt:wt monomers/porogens was selected for the following research.

Next, the EDMA content in the monomer mixture was also studied (Table 2, columns A3, A7 and A8). When the weight content of porogenic solvent (80:20 wt/wt 1,4-butanediol/1-propanol) was kept constant at 60 wt%, and the weight content of EDMA in the monomer mixture was decreased from 40 (column A3) to 30 wt% (column A7), the efficiency values were similar, but a partial overlapping between sitosterol and cholesterol was obtained. At 50 wt% of EDMA (column A8), the permeability became so poor that it was impossible to flush the column due to the highly dense polymeric bed formed [43]. Looking at these results, column A3 provided the best results in terms of efficiency, resolution and analysis time.

The influence of the nature of the alkyl methacrylate monomer was also investigated. Thus, the bulk monomer (LMA) was substituted by another one with a longer alkyl chain, such as ODMA. A similar optimization study of the composition of the polymerization mixture was also performed with this monomer. Thus, the 1,4-butanediol content in the polymerization mixture was examined in the 4–15 wt% range (7–25 wt% in porogenic solvent) (Table 3, columns B1–B5). With 4 wt% of 1,4-butanediol (column B1), the permeability of the monolith was so poor that it was impossible to flush the column. Columns produced at 6 wt% of 1,4-butanediol (column B2) showed poor efficiencies and long analysis times. As commented above, this was attributed to the double-layer overlap. With 8 wt% (column B3), a peak efficiency of 42 000 for β-sitosterol and resolution values for all analytes comprised between 1.2 and 2.9 were obtained. When 12 wt% (column B4) was tried, the resolution of sterols was similar to that obtained with 8 wt%, but an increase in efficiency values and a decrease in the analysis time was obtained, while a percentage of 15 wt% of 1,4-butanediol (column B5) produced a co-elution of cholesterol/stigmasterol peaks. Thus, the content of 12 wt% of 1,4-butanediol in the polymerization mixture was selected for further studies.

The porogen weight fraction in the polymerization mixture was also studied for ODMA monoliths (Table 3, columns B4, B6 and B7). When the porogen weight fraction increased up to 70 wt% (column B6), all solutes co-eluted in a single peak. When reduced from 60 to 50 wt% (column B7), the column efficiency varied from 46 400 to 43 800 plates/m for β-sitosterol, but its *k*-value increased from 4.6 to 6.2. Consequently, the porogen weight fraction of 60 wt% was selected for further studies.

Next, a change in the monomer/crosslinker ratio was done. The proportion of EDMA in the monomer mixture was varied from 30 to 50 wt% (Table 3, columns B4, B8 and B9). When the content of EDMA was reduced up to 30 wt% (column B8), an overlapping of all solutes (in less than 2 min) was observed, while the percentage of EDMA at 50 wt% gave worse efficiency values (34 200 plates/m for β-sitosterol) and longer retentions times (*ca.* 13 min) than those obtained with 40 wt%. As a result of this study, column B4 was selected. Figure 3 shows the separation of sterol test mixture obtained with this column. As it can be seen, this ODMA-based column gave a slight increase in the retention times compared with the optimum LMA column (Fig. 2, part B), although a more significant increase in *k*-values could be expected due to the longer alkyl chain monomer employed. This retention behavior could be explained taking into account that changes in the polymerization mixture (different bulk monomer) seems to induce not only changes in hydrophobicity but also changes in monolithic structure. This fact was in agreement with previous reports [46, 47]. In fact, at sight of SEM pictures of both columns (Fig. 4), the ODMA-based column (part B) showed voids and globule sizes comparable to those obtained with the LMA-based column. Additionally, the peak efficiencies of analytes achieved in the ODMA-based column were lower (26 000–46 400) than those obtained with the LMA-based column (28 800–60 900 plates/m). Consequently, the monolithic column prepared with LMA containing 12 wt% 1,4-butanediol (column A3) was selected as the best compromise between resolution, efficiency and analysis time.

Table 3. Composition of the polymerization mixtures used for the preparation of ODMA-based monolithic columns and their efficiency and retention values

Column	Monomers/porogens (% wt/wt)	LMA/EDMA (% wt/wt)	1-Propanol/1,4-butanediol (% wt/wt)	$N_{\beta\text{-sitosterol}}$ (plates/m)	$k_{\beta\text{-sitosterol}}$
B1	40:60	60:40	93:7	NM[a)]	NM[a)]
B2	40:60	60:40	90:10	26000	7.6
B3	40:60	60:40	86:14	42000	4.8
B4	40:60	60:40	80:20	46400	4.6
B5	40:60	60:40	75:25	36200	3.9
B6	30:70	60:40	80:20	43800	6.2
B7	50:50	60:40	80:20	NM[a)]	NM[a)]
B8	40:60	70:30	80:20	NM[a)]	NM[a)]
B9	40:60	50:50	80:20	34200	7.1

a) Not measured.

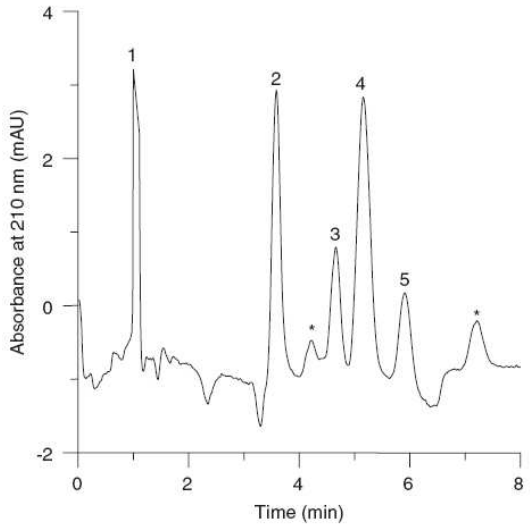

Figure 3. Electrochromatogram obtained with an ODMA-based monolithic column prepared with 12 wt% 1,4-butanediol in the polymerization mixture (column B4). Mobile phase: 85:10:5 v/v/v ACN–2-propanol–water containing 5 mM Tris at pH 8.0. Peak identification and other experimental conditions are as in Fig. 2.

3.2 Quantitation studies and application to vegetable oils

Intra- and inter-day repeatabilities in the optimal conditions were obtained by injecting a mixture containing 0.75 mM of each sterol (Table 4). The mixture was injected ten times *per* day during three consecutive days. The column-to-column reproducibility was also established by ten injections on three different monolithic columns, which were prepared with the same polymerization mixture. The reproducibility of EOF, retention times and peak areas are summarized in Table 4. In all cases, column-to-column RSD values for the retention times and peak areas were lower than 4.4 and 6.2%, respectively. More than 80 injections of the standard mixture and 50 injections of vegetable oil extracts were performed without the need of replacing the column; therefore, the stability of the columns was satisfactory.

External calibration curves using peak areas were constructed by injecting six standard solutions of each solute in the 0.125–5 mM range. Straight lines with $r > 0.994$ were obtained. As it can be seen in Table 4, all the sterols gave closely similar sensitivities. The LODs calculated at $S/N = 3$ are also presented in Table 4.

The optimized method was applied to the analysis of oil samples. Representative electrochromatograms of extra

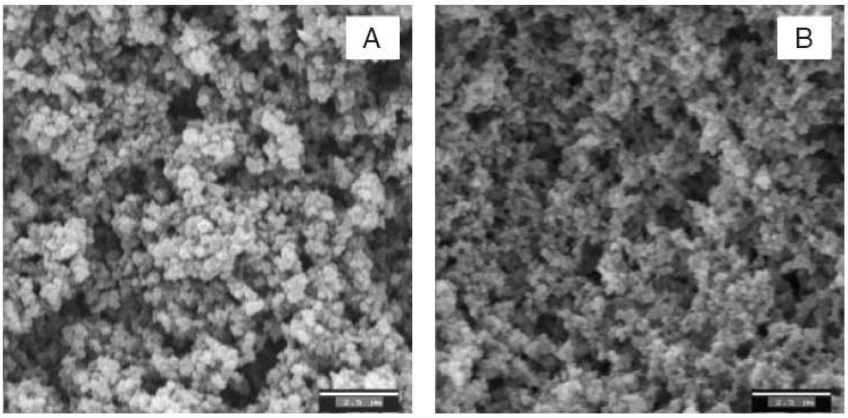

Figure 4. SEM micrographs of the (A) LMA (column A3) and (B) ODMA (column B4) monolithic materials inside the capillary. The bar lengths stand for 2.5 μm.

Table 4. Analytical figures of merit for the sterol standards

Compounds	Intra-day repeatability ($n = 10$) RSD (%)		Inter-day repeatability (3 days) RSD (%)		Column-to-column reproducibility ($n = 3$) RSD (%)		Sensitivities (mM^{-1})	LOD (mM)
	t_R	Peak area	t_R	Peak area	t_R	Peak area		
Ergosterol	0.12	2.62	2.15	4.40	3.81	5.20	31.3	0.037
Cholesterol	0.34	2.92	2.44	5.22	4.26	6.20	28.5	0.030
Stigmasterol	0.27	2.10	2.72	4.92	4.40	5.63	29.6	0.025
β-Sitosterol	0.11	2.84	2.91	4.74	3.73	5.44	31.5	0.029
EOF	0.43	1.92	1.52	3.52	3.10	4.92	—	—

virgin olive, hazelnut and soybean oil extracts are shown in Fig. 5. Peak identification was performed by comparing the retention times with those of the standards or by spiking the sample extracts with the standards. Other sample peaks observed in the vegetable oils analyzed were tentatively assigned to campesterol and avenasterol taking into account their common abundance in the oils [8, 10, 12, 17, 28, 48–51]. β-Sitosterol and campesterol were assumed to co-elute as expected taking into account the structural similarity between them. In fact, Mezine *et al.* [23] failed to resolve these two compounds using an RP hexyl-phenyl column. However, Abidi *et al.* [28] were able to resolve this pair of solutes by CEC using a C_{18}-packed column, but at the expense of a long analysis time (>55 min). Thus, in this work, these two solutes were jointly evaluated.

On the other hand, taking into account the sterol profiles obtained for all oil samples analyzed and due to the lack of commercial avenasterol standards, the peak located close to 4 min (no. 6 of Fig. 5) was tentatively assigned to avenasterol. This peak elutes near to cholesterol, which is present in concentrations lower than our LOD in vegetable oils [8, 10–12]. This co-elution is consistent with findings found in literature in RP columns [12].

Due to the similarity between the sensitivities of all sterols (see Table 4), the β-sitosterol+campesterol and avenasterol contents were estimated using β-sitosterol as reference. The found percentages of sterols in the vegetable oils are presented in Table 5. These results were consistent with other reported data [8, 10–12, 17, 28, 48–51]. As it can be seen in Table 5, soybean and sunflower oils showed large quantities of stigmasterol, this sterol being below the LOD in extra virgin olive oils [8, 10–12, 17, 48, 51]. For this reason, stigmasterol peak could be used as adulteration marker [4, 7]. Consequently, a series of binary mixtures of soybean or sunflower oils with extra virgin olive oil were prepared and injected. Using the stigmasterol peak area as an adulteration marker, the presence of 8% soybean or sunflower oil in extra virgin olive oil was clearly evidenced (see Fig. 6).

4 Concluding remarks

Using methacrylate ester-based monolithic columns, a rapid CEC method for the analysis of sterols in vegetable oils has been developed. The best resolution and efficiency values, maintaining a short analysis time (<7 min), were obtained with an LMA-based column prepared at 60:40% wt:wt LMA/EDMA ratio and 60 wt% porogens with 20 wt% of 1,4-butanediol (12 wt% 1,4-butanediol in the polymerization mixture), and using a mobile phase containing 85:10:5 v/v/v ACN–2-propanol–water buffer (5 mM Tris at pH 8.0). In comparison with other CEC procedures, the proposed method was not able to resolve the β-sitosterol/campesterol pair, but the analysis time was largely reduced and the estimation of sterol percentages in vegetable oils, with low LOD values, was also demonstrated. Additionally, the method allows the quick

Table 5. Percentage of sterols found in vegetable oils[a)]

Oil	Avenasterol (%)	Stigmasterol (%)	β-Sitosterol+campesterol (%)
Sunflower	5	10	85
Extra virgin olive	9	ND	91
Soybean	3	19	78
Corn	7	6	87
Peanut	7	9	84
Grapeseed	3	12	85
Hazelnut	5	1	94

a) ND = Not detected.

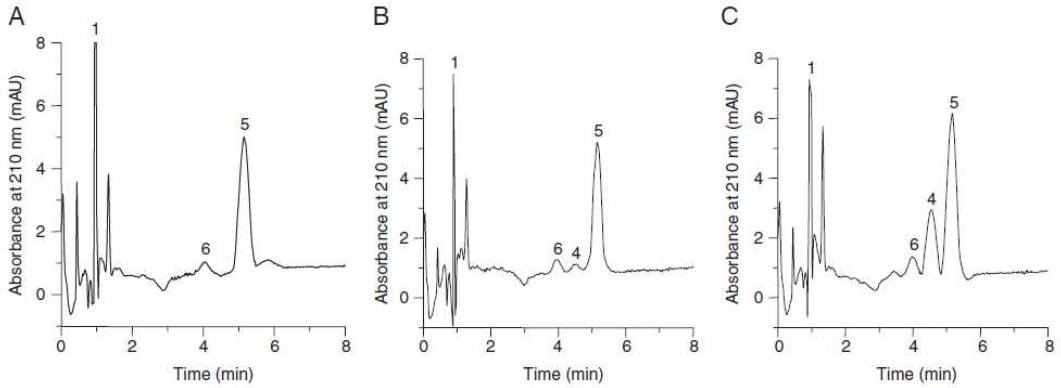

Figure 5. Electrochromatograms of (A) extra virgin olive, (B) hazelnut oil and (C) soybean oil obtained on LMA-based monolithic capillary (column A3). CEC conditions: mobile phase: 85:10:5 v/v/v ACN–2-propanol–water containing 5 mM Tris at pH 8.0. Peak identification: 5, β-sitosterol+campesterol; 6, avenasterol. Other peak identification and experimental conditions are as in Fig. 2.

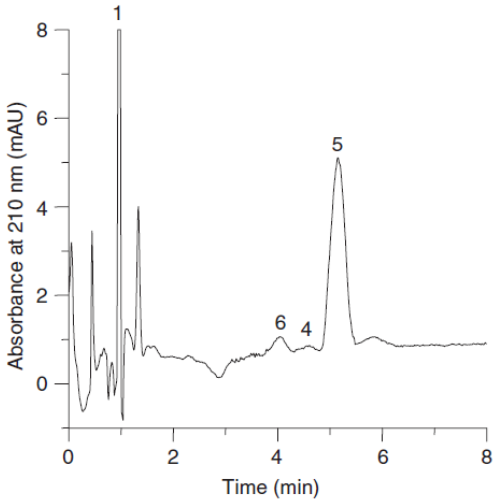

Figure 6. Electrochromatogram of an extra virgin olive oil containing 8% soybean oil showing the stigmasterol peak (no. 4). Peak identification and other experimental conditions are as in Fig. 5.

detection and evaluation of adulterations of olive oil with other oils, such as sunflower and soybean.

This work was supported by project CTQ2007-61445 (MEC and FEDER funds). M. J. L.-G. thanks the Generalitat Valenciana for an FPI grant for PhD studies.

The authors have declared no conflict of interest.

5 References

[1] Cercaci, L., Passalacqua, G., Poerio, A., Rodríguez-Estrada, M. T. *et al.*, *Food Chem.* 2007, *102*, 66–76.

[2] Rui Alves, M., Cunha, S. C., Amaral, J. S., Pereira, J. A., *et al.*, *Anal. Chim. Acta* 2005, *549*, 166–178.

[3] Perona, J. S., Cabello-Moruno, R., Ruiz-Gutierrez, V., *J. Nutr. Biochem.* 2006, *17*, 429–445.

[4] Kamm, W., Dionisi, F., Hischenhuber, C., Engel, K. H., *Food Rev. Int.* 2001, *17*, 249–290.

[5] Aparicio, R., Aparicio-Ruíz, R., *J. Chromatogr. A* 2000, *881*, 93–104.

[6] Ranalli, A., Pollastri, L., Contento, S., Di Loreto, G. *et al.*, *J. Sci. Food Agric.* 2002, *82*, 854–859.

[7] Ballesteros, E., Gallego, M., Valcárcel, M., *Anal. Chim. Acta* 1995, *308*, 253–260.

[8] Cercaci, L., Rodríguez-Estrada, M. T., Lercker, G,, *J. Chromatogr. A* 2003, *985*, 211–220.

[9] Mariani, C., Bellan, G., Lestini, E., Aparicio, R., *Eur. Food Res. Technol.* 2006, *223*, 655–661.

[10] Bohacenko, I., Kopicová, Z., *Czech J. Food Sci.* 2001, *19*, 97–103.

[11] Cañabate-Díaz, B., Segura Carretero, A., Fernández-Gutiérrez, A., Belmonte Vega, A. *et al.*, *Food Chem.* 2007, *102*, 593–598.

[12] Martínez-Vidal, J. L., Garrido-Frenich, A., Escobar-García, M. A., Romero-González, R., *Chromatographia* 2007, *65*, 695–699.

[13] Philips, K. M., Ruggio, D. M., Toivo, J. I., Swank, M. A. *et al.*, *J. Food Compost. Anal.* 2002, *15*, 123–142.

[14] Rivera del Álamo, R. M., Fregapane, G., Aranda, F., Gómez-Alonso, S. *et al.*, *Food Chem.* 2004, *84*, 533–537.

[15] Sánchez-Casas, J., Osorio Bueno, E., Montaño García, A. F., Martínez Cano, M., *Food Chem.* 2004, *87*, 225–230.

[16] Galeano Diaz, T., Durán Merás, I., Sánchez Casas, J., Alexandre Franco, M. F., *Food Control* 2005, *16*, 339–347.

[17] Parcerisa, J., Casals, I., Boatella, J., Codony, R. *et al*, *J. Chromatogr. A* 2000, *881*, 149–158.

[18] Amaral, J. S., Casal, S., Citová, I., Santos, A. *et al*, *Eur. Food Res. Technol.* 2006, *222*, 274–280.

[19] Matos, L. C., Cunha, S. C., Amaral, J. S., Pereira, J. A. *et al.*, *Food Chem.* 2007, *102*, 406–414.

[20] Thanh, T. T., Vergnes, M. F., Kaloustian, J., El-Moselhy, T. F. *et al.*, *J. Sci. Food Agric.* 2006, *86*, 220–225.

[21] Medvedovici, A., David, F., Sandra, P., *Chromatographia* 1997, *44*, 37–42.

[22] Cunha, S. S., Fernandes, J. O., Oliveira, B. P. P., *J. Chromatogr. A* 2006, *1128*, 220–227.

[23] Mezine, I., Zhang, H., Macku, C., Lijana, R., *J. Agric. Food Chem.* 2003, *51*, 5639–5646.

[24] Lerma-García, M. J., Ramis-Ramos, G., Herrero-Martínez, J. M., Simó-Alfonso, E. F., *Rapid Commun. Mass Spectrom.* 2008, *22*, 973–978.

[25] Legido-Quigley, C., Marlin, N. D., Melin, V., Manz, A. *et al. Electrophoresis*, 2003, *24*, 917–944.

[26] Eeltink, S., Kok, WT., *Electrophoresis*, 2006, *27*, 84–96.

[27] Huo, Y., Kok, W. T., *Electrophoresis* 2008, *29*, 80–93.

[28] Abidi, S. L., *J. Chromatogr. A* 2004, *1059*, 199–208.

[29] Abidi, S. L., Thiam, S., Warner, I. M., *J. Chromatogr. A* 2002, *949*, 195–207.

[30] Abidi, S. L., *J. Chromatogr. A* 2001, *935*, 173–201.

[31] Fujimoto, C., *Anal. Sci.* 2002, *18*, 19–25.

[32] Siouffi, A. M., *J. Chromatogr. A* 2003, *1000*, 801–818.

[33] Eeltink, S., Decrop, W. M. C., Rozing, G. P., Schoenmakers, P. J. *et al.*, *J. Sep. Sci.* 2004, *27*, 1431–1440.

[34] Tanaka, N., Nagayama, H., Kobayashi, H., Ikegami, T. *et al.*, *J. High Resol. Chromatogr.* 2000, *23*, 111–116.

[35] Dong, J., Xie, C. H., Tian, R. J., Wu, R. A. *et al.*, *Electrophoresis* 2005, *25*, 3452–3459.

[36] Zhang, M., El Rassi, Z., *Electrophoresis* 2001, *22*, 2593–2599.

[37] Huang, H. Y., Lin, H. Y., Lin, S. P., *Electrophoresis* 2006, *27*, 4674–4681.

[38] Svec, F., Fréchet, J. M. J., *Science* 1996, *273*, 205–211.

[39] Peters, E. C., Petro, M., Svec, F., Fréchet, J. M. J., *Anal. Chem.* 1998, *70*, 2288–2295.

[40] Jiang, T., Jiskra, J., Claessens, H. A., Cramers, C. A., *J. Chromatogr. A* 2001, *923*, 215–227.

[41] Peters, E. C., Petro, M., Svec, F., Fréchet, J. M. J., *Anal. Chem.* 1997, *69*, 3646–3649.

[42] Eeltink, S., Svec, F., *Electrophoresis* 2007, *28*, 137–147.

[43] Eeltink, S., Herrero-Martínez, J. M., Rozing, G. P., Schoenmakers, P. J. *et al.*, *Anal. Chem.* 2005, *77*, 7342–7347.

[44] Commission Regulation (EEC) No. 2568/91 from 11 July 1991, *Off. J. Eur. Union*, annex V.

[45] Lerma-García, M. J., Simó-Alfonso, E. F., Ramis-Ramos, G., Herrero-Martínez, J. M., *Electrophoresis* 2007, *28*, 4128–4135.

[46] Waguespack, B. L., Hodges, S. A., Bush, M. E., Sondergeld, L. J. *et al.*, *J. Chromatogr. A* 2005, *1078*, 171–180.

[47] Delaunay-Bertoncini, N., Demesmay, C., Rocca, J. L., *Electrophoresis* 2004, *25*, 3204–3215.

[48] Jee, M. (Ed.), *Oils and Fat Authentication*, Blackwell Publishing, CRC Press, Boca Raton, FL 2002.

[49] Kim, D. N., Lee, K. T., Reiner, J. M., Thomas, W. A., *J. Lipid Res.* 1974, *15*, 326–331.

[50] Matthäus B., *Eur. J. Lipid Sci. Technol.* 2008, *110* 645–650.

[51] Benitez-Sánchez, P. L., León-Camacho, M., Aparicio, R., *Eur. Food Res. Technol.* 2003, *218*, 13–19.

ANEXO IV

JOURNAL OF AGRICULTURAL AND FOOD CHEMISTRY
ARTICLE

J. Agric. Food Chem. 2010, 58, 2771–2776 2771
DOI:10.1021/jf9043887

Fast Separation and Determination of Sterols in Vegetable Oils by Ultraperformance Liquid Chromatography with Atmospheric Pressure Chemical Ionization Mass Spectrometry Detection

María Jesús Lerma-García,[†] Ernesto Francisco Simó-Alfonso,[†] Alberto Méndez,[‡] Josep Lluís Lliberia,[‡] and José Manuel Herrero-Martínez*,[†]

[†]Department of Analytical Chemistry, Faculty of Chemistry, University of Valencia, E-46100 Burjassot, Valencia, Spain, and [‡]Waters Cromatografía S.A., Ronda de can Fatjó, 7-A, Parc Tecnològic del Vallès, E-08290 Cerdanyola del Vallés, Barcelona, Spain

A method for the determination of sterols in vegetable oils by ultraperformance liquid chromatography (UPLC) with atmospheric pressure chemical ionization mass spectrometry detection has been developed. The separation of sterols was optimized in terms of mobile phase composition, column temperature and flow rate. The optimal conditions were achieved using an Acquity UPLC BEH C18 column (50 × 2.1 mm, 1.7 μm) with a mobile phase consistent of acetonitrile/water (0.01% acetic acid) using a linear gradient, at a flow rate of 0.8 mL min^{-1} and column temperature of 10 °C, giving a total analysis time below 5 min. The determination was performed in selective ion recording mode. The limits of detection were in all cases below 0.07 μg mL^{-1}, with relative standard deviation values of retention times and peak areas below 0.4 and 5%, respectively. The content of main sterols present in several vegetable oils with different botanical origins was also established.

KEYWORDS: Botanical origin; mass spectrometry; sterols; ultraperformance liquid chromatography; vegetable oils

INTRODUCTION

Phytosterols (also called plant sterols) are bioactive components occurring in vegetable oils, constituting the greatest proportion of the unsaponifiable fraction, which represents a total of 1−3% (*1*). Phytosterols have been received particular attention not only regarding their nutritional value but also due to their capacity to decrease the cardiovascular risk of coronary heart disease (*2*), and to reduce blood cholesterol levels, showing anti-inflammatory, antibacterial, and antioxidant activities (*3*).

The nature and quantitative distribution of sterols are characteristic of the original lipid source (*4*−*6*), which could be useful for the identification of the botanical origin of vegetable oils. In fact, the unsaponifiable minor components have been employed as a fingerprint of most vegetable oils (*7*). Moreover, in the same species, content and composition of these components can vary due to the environmental conditions, fruit or seed quality, oil extraction system and refining process (*6*). For these reasons, the determination of these minor components is of great value in establishing the oil genuineness and quality (*6*, *8*), having also a marked influence on typicality, flavor, aroma and shelf life (*9*).

Official methods for analysis of sterols involve saponification of the oil, extraction of the unsaponifiable fraction with diethyl ether and isolation of the sterol fraction by thin layer chromatography (TLC). Quantification of the silanized sterol fraction is commonly performed by GC with flame ionization detection (FID) (*10*−*15*), but GC with MS detection is also used (*10*, *14*, *16*, *17*). The major disadvantage of GC is the requirement of both thermally stable columns and chemical derivatization before analysis. For this reason, other methods such as capillary electrochromatography with UV−vis detection (*18*, *19*), direct infusion MS (*20*) and HPLC−MS (*21*−*23*) have been also developed to determine sterols in vegetable oils.

In the past few years, separation science has been revolutionized with the introduction of ultraperformance liquid chromatography (UPLC). UPLC enables the use of columns packed with 1−2 μm size range, delivering mobile phases at pressures up to 1000 bar (*24*−*28*). According to the Van Deemter equation, when the particle size is lower than 2.5 μm, there is a significant gain in efficiency with increasing flow rates (*25*). Thus, the main advantages of UPLC are (i) a reduction in the analysis time, (ii) an increase in the signal-to-noise ratio and (iii) an enhancement in peak resolution (*26*, *27*). In order to address the very narrow peaks produced by UPLC, a high data capture rate detector is necessary; for this reason, MS detection has been commonly used for UPLC−MS coupling (*25*). The potential of this technique has been tested in different food products (*25*, *28*), such as phytosterols in different food materials (*28*), phenolic compounds in olive oil (*29*) and in olive cakes (*30*).

In this work, the applicability of UPLC−atmospheric pressure chemical ionization (APCI)−MS to characterize the sterol fraction of vegetable oils with different botanical origins has been

*Corresponding author. Tel: +34 96 354 3176. Fax: +34 96 354 44 36. E-mail: jmherrer@uv.es.

Published on Web 02/10/2010 pubs.acs.org/JAFC

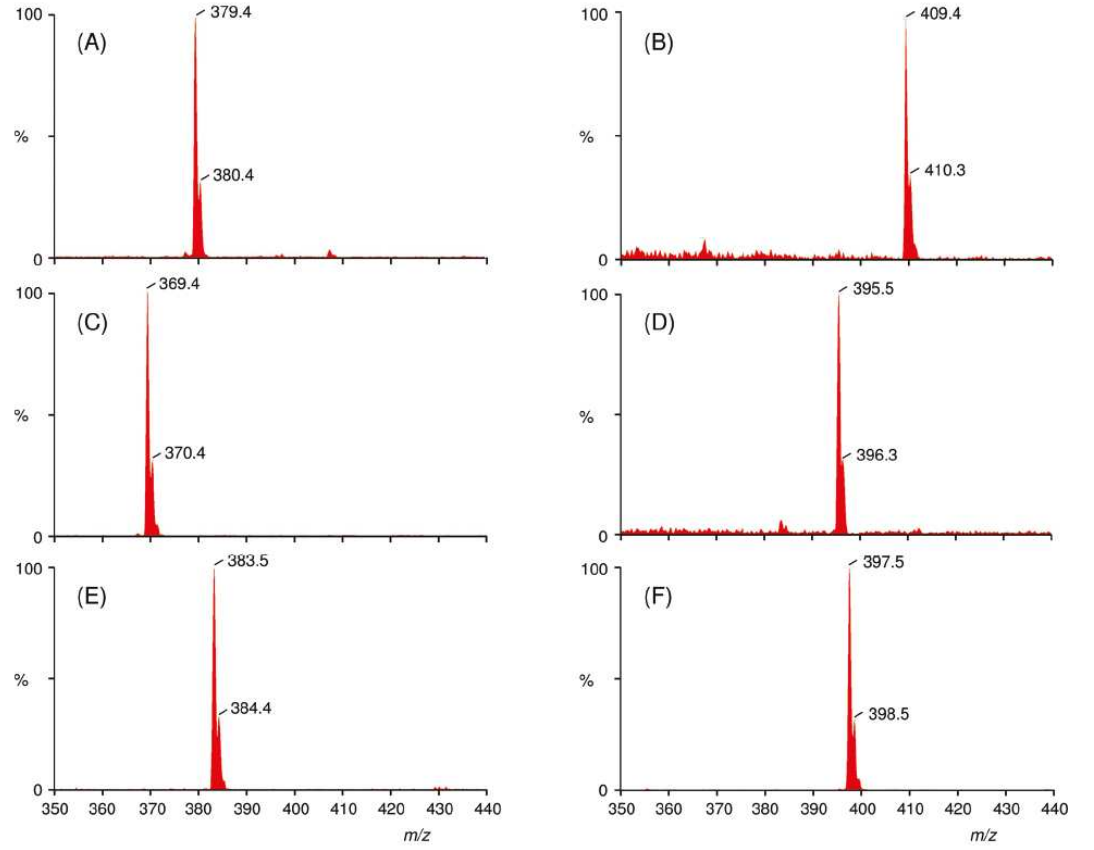

Figure 1. Full scan UPLC−MS spectra of the six sterol standards used in this study. Peak identification: (**A**) ergosterol; (**B**) lanosterol; (**C**) cholesterol; (**D**) stigmasterol; (**E**) campesterol; (**F**) β-sitosterol.

demonstrated. The sterol separation was optimized in terms of mobile phase composition, column temperature and flow rate. The developed method was also applied to the identification and determination of the main sterols present in several vegetable oils.

EXPERIMENTAL PROCEDURES

Reagents and Samples. The following analytical grade reagents were used: ethanol, 2-propanol, acetic acid, acetonitrile (ACN), anhydrous sodium sulfate (Scharlau, Barcelona, Spain), diethyl ether, chloroform (J.T. Baker, Deventer, The Netherlands), potassium hydroxide (KOH, Probus, Barcelona), *n*-hexane (Riedel-de Haën, Seelze, Germany), and 2,7-dichlorofluorescein (Sigma, St. Louis, MO). Glass plates for TLC, coated with silica gel without fluorescent indicator (0.25 mm plate thickness, Merck, Darmstadt, Germany), were used. Deionized water (Barnstead deionizer, Sybron, Boston, MA) was also employed. The sterols used as standards were β-sitosterol (mixture containing 75% β-sitosterol and 10% campesterol), ergosterol, stigmasterol (Acros Organics, Morris Plains, NJ), cholesterol (Aldrich, Milwaukee, WI) and lanosterol (Maybridge Chemical Co., Cornwall, England). A total of 32 vegetable oils were employed in this study, 4 for each botanical origin. These samples, which were either purchased in the local market or kindly donated by the manufacturers, were the following: avocado (Guinama and Marnys), corn (Guinama, Asua and Crystal), olive (Carbonell, Grupo Hojiblanca, Borges and Torrereal), hazelnut (Guinama, Percheron and Flumen), grapeseed (Guinama, Paul Corcelet, Pons and Coosur), peanut (Guinama, Bellsola, Apsara Vital and Maurel), soybean (Coosur, Guinama, Biolasi and Sojola) and sunflower (Koipesol, Hacendado and Coosur). In all cases, the botanical origin and quality grade of all the samples were guaranteed by the suppliers.

Instrumentation and Working Conditions. An AcQuity ultra-performance liquid chromatograph using a binary pump system (Waters, Mildford, MA) was used. The UPLC was coupled to the APCI ion source of a SQD mass spectrometer (Waters Corporation), which was used as detection system. Separation was carried out with an AcQuity UPLC BEH C18 column (50 × 2.1 mm, 1.7 μm, Waters). Mobile phases were prepared by mixing ACN:acetic acid (100:0.01, v/v) (phase A) with water:acetic acid (100:0.01, v/v) (phase B). Elution was performed using a linear gradient from 80 to 100% A for 0.5 min followed by an isocratic elution with 100% A for 4.5 more min. The column temperature was kept at 10 °C, and the flow rate was 0.8 mL min^{-1}. The injection volume was 15 μL.

Ionization was performed in APCI positive-ion mode, and data were collected in the selected ion recording (SIR) mode. Optimization of the source parameters was performed automatically by the Waters Intellistar software (Waters). The ionization source parameters were as follows: corona, 4 kV; source temperature, 120 °C; desolvation gas temperature, 400 °C, with a flow rate of 750 L/h. Nitrogen, supplied by a gas generator (Dominick Hunter generator, Gateshead, England), was used as desolvation gas. The individual cone voltage for each sterol standard was evaluated between 10 and 60 V, by infusing 1 μg mL^{-1} of each compound to obtain the best instrumental conditions, which corresponded to 30 V to each of them. All chromatograms were smoothed using a mean algorithm set at window 3 and number 5. The software used was MassLynx 4.1 (Waters).

Sample Preparation. The sterol fraction of vegetable oils was obtained following the procedure established by the Official Journal of

the European Union (*31*). Briefly, the oil samples were saponified by refluxing with 2 N ethanolic KOH solution, and the nonsaponificable fraction was extracted with diethyl ether. The sterol fraction was isolated using TLC and recovered from the plates with diethyl ether. A rotatory evaporator was used to remove the solvent, and the residue was dissolved in 500 μL of 2-propanol and stored at −20 °C in amber vials. These solutions were diluted with the mobile phase and injected. All the sterol extracts were injected three times. The peak area of each sterol was measured from the smoothed SIR.

RESULTS AND DISCUSSION

Optimization of Sterol Separation. In order to optimize sterol separation in terms of mobile phase composition, column temperature and flow rate, a test mixture composed of six sterol standards (*ca.* 50 μg mL^{-1}, except for β-sitosterol and campesterol that were *ca.* 38 and 5 μg mL^{-1}, respectively) was used. According to literature (*21*), mixtures of mobile phases A and B were tried in gradient elution mode, using a constant column temperature (30 °C) and flow rate (0.5 mL min^{-1}). For each sterol standard, two SIR channels, which corresponded to the $[M + H]^+$ and $[M + H - H_2O]^+$ ions, were monitored. However, and as previously reported (*20*, *21*, *23*), the $[M + H - H_2O]^+$ peaks showed higher intensities than the respective $[M + H]^+$ peaks. For this reason, the intensities obtained at the SIR channels of the $[M + H - H_2O]^+$ peaks (379.5, 369.5, 383.5, 395.5, 397.5, and 409.5 for ergosterol, cholesterol, campesterol, stigmasterol, β-sitosterol and lanosterol, respectively) were used for identification and quantification. The APCI mass spectra showing the $[M + H - H_2O]^+$ peaks of the six sterol standards are depicted in **Figure 1**. In all the gradient elutions tested, stigmasterol and campesterol peaks overlapped. This result was in agreement with previous reports (*28*). A linear gradient from 80 to 100% A for 0.5 min, followed by an isocratic elution with 100% A, was selected as the best compromise between analysis time and separation (**Figure 2B**). Under this gradient elution and using a flow rate of 0.5 mL min^{-1}, the influence of column temperature was evaluated. As shown in **Figure 2**, the chromatographic behavior of sterols was affected by changing the temperature of the column from 10 to 40 °C. At 40 °C (**Figure 2A**), lanosterol and cholesterol peaks overlapped. When the temperature was decreased from 30 to 10 °C (**Figure 2B−D**), a slight decrease in efficiency values jointly with an increase in analysis time was observed. However, the global resolution (measured as the geometrical mean of the resolution between the consecutive sterol pairs) slightly improved (from 1.18 to 1.30). For this reason, a column temperature of 10 °C was selected for further studies. Next, the influence of the flow rate on sterol separation was also studied (see **Figure 3**). When the flow rate was increased from 0.4 to 0.8 mL min^{-1} (**Figure 3A**,**B**), higher efficiency values were obtained whereas the global resolution decreased from 1.47 to 1.28; a decrease of both parameters was observed when flow rate was increased up to 1.2 mL min^{-1} (**Figure 3C**). As a result, a flow rate of 0.8 mL min^{-1} was selected as the best compromise between efficiency, resolution and analysis time.

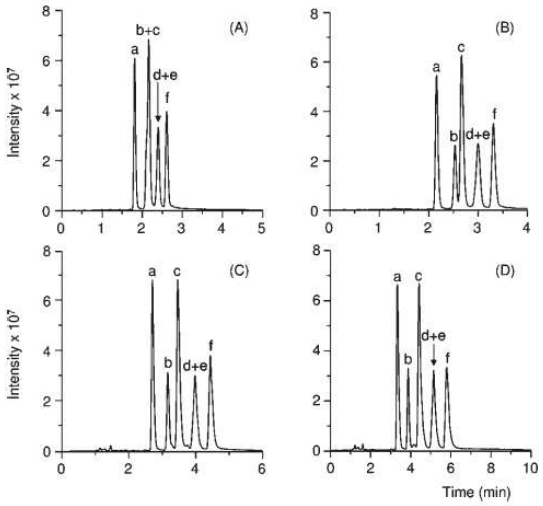

Figure 2. Influence of the column temperature on the separation of sterols: (**A**) 40 °C, (**B**) 30 °C, (**C**) 20 °C and (**D**) 10 °C. Chromatographic conditions: linear gradient from 80 to 100% A for 0.5 min followed by isocratic elution with 100% A for 4.5 more min using a flow rate of 0.5 mL min^{-1}. Peak identification as in **Figure 1**.

Quantitation Studies and Application to Vegetable Oils. External calibration curves were constructed by injecting six standard solutions of each solute within its linearity range (0.5−50 μg mL^{-1}, except for β-sitosterol that ranged up to 250 μg mL^{-1}). Straight lines with $R^2 > 0.998$ were obtained. Other analytical figures of merit are given in **Table 1**. Precision was determined by studying the intra- and interday repeatabilities of peak areas and retention times obtained by injecting the same 1 μg mL^{-1} solution for all analytes, 10 times per day during 3 days. In all cases, the relative standard deviation values were lower than 5 and 0.4% for peak areas and retention times, respectively. The relative sensitivities of sterols (with respect to β-sitosterol) gave values comprised between 0.9 and 1.2, except for lanosterol that provided a value of 0.4. This behavior was due to differences in sterol structures, which was in agreement with previous studies (*28*). The limits of detection, which were estimated for a signal-to-noise ratio of 3, were comprised between 0.03 and 0.07 μg mL^{-1}, whereas the limits

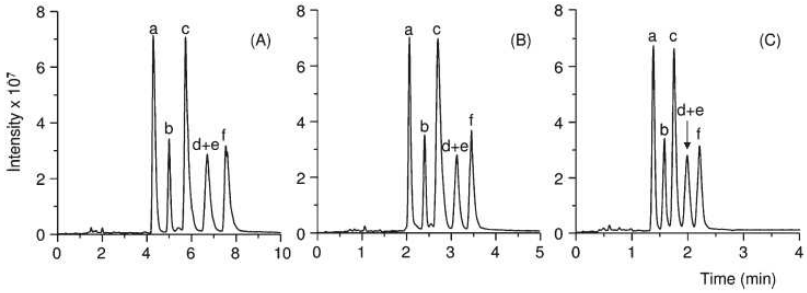

Figure 3. Influence of flow rate on the separation of sterols: (**A**) 0.4, (**B**) 0.8 and (**C**) 1.2 mL min^{-1}. Chromatographic conditions: temperature 10 °C; gradient elution and peak identification as in **Figure 2**.

Table 1. Analytical Figures of Merit for the UPLC–MS Method for the Determination of Sterols

	repeatability, %						
	intraday[a]		interday[b]		LOD	LOQ	rel
analyte	area	t_R	area	t_R	(μg mL^{-1})	(μg mL^{-1})	sensitivity[c]
ergosterol	2.8	0.08	3.6	0.25	0.04	0.13	1.1
lanosterol	2.7	0.08	3.2	0.27	0.07	0.25	0.4
cholesterol	2.7	0.10	4.1	0.30	0.03	0.10	1.2
stigmasterol	2.6	0.11	3.7	0.30	0.04	0.13	0.9
campesterol	2.9	0.11	3.8	0.31	0.03	0.10	1.2
β-sitosterol	2.4	0.12	5.0	0.40	0.04	0.13	1.0

[a] For a sterol concentration of 1 μg mL^{-1} (n = 10). [b] For a sterol concentration of 1 μg mL^{-1} (3 days). [c] As the ratio of the slopes of calibration curves of sterols (respect to β-sitosterol).

Table 2. Ions Observed in the APCI Mass Spectra of the Oil Samples with Their Corresponding Retention Times (t_R)

peak no.	analyte	t_R (min)	ion $[M + H - H_2O]^+$ (m/z)
1	erythrodiol	1.4	425.5
2	uvaol	1.4	425.5
3	ergosterol	2.1	379.5
4	brassicasterol	2.2	381.5
5	Δ^5-avenasterol	2.4	395.5
6	cholesterol	2.7	369.5
7	campesterol	3.1	383.5
8	campestanol	3.1	385.5
9	stigmasterol	3.1	395.5
10	clerosterol	3.1	395.5
11	$\Delta^{5,24}$-stigmastadienol	3.3	395.5
12	β-sitosterol	3.5	397.5
13	Δ^7-stigmastenol	3.5	397.5
14	sitostanol	4.5	399.5

of quantification, based on a signal-to-noise ratio of 10, ranged from 0.10 to 0.25 μg mL^{-1}. These values were higher than those reported by Lu et al. (*28*) working with an UPLC system using the same stationary phase but a triple-quadrupole mass spectrometer, whereas they were lower than those obtained using a conventional HPLC system with a single-quadrupole instrument (*21*, *22*). In any case, a substantial reduction in the analysis time was achieved with the proposed method (between 4- and 10-fold lower than those found in the literature (*21*–*23*)).

On the other hand, GC methods using FID or MS detection (*10*–*14*, *16*, *17*, *31*) showed a superior resolution (especially in some peak pairs as β-sitosterol/Δ^7-stigmastenol and stigmasterol/clerosterol), but longer analysis times (25–30 min) were obtained in comparison to the proposed method (5 min). In spite of these overlappings, satisfactory results were achieved in terms of resolution/analysis time ratio. Besides, an additional advantage of the recommended method is that it avoids the derivatization step, which is time-consuming and could be a source of errors (*28*).

The optimized method was applied to the analysis of oil samples. In addition to the SIR channels of standards, additional signals (see **Table 2**) were also recorded according to the $[M + H - H_2O]^+$ values of other expected sterol compounds in vegetable oil samples (*19*, *21*, *23*). The TIC and SIRs of an extra virgin olive and hazelnut extracts are shown in **Figure 4**. The main sterols found in the samples, with their corresponding retention time and $[M + H - H_2O]^+$ ions, are summarized in **Table 2**. To quantify the main sterols found in samples, those not available as standards were estimated as follows: the saturated sterols (campestanol and sitostanol) were estimated using the calibration curve of lanosterol, which showed a similar sensitivity to that reported in literature for this type of compounds (*28*). Due to the structural resemblance between erythrodiol + uvaol and lanosterol, these solutes were also

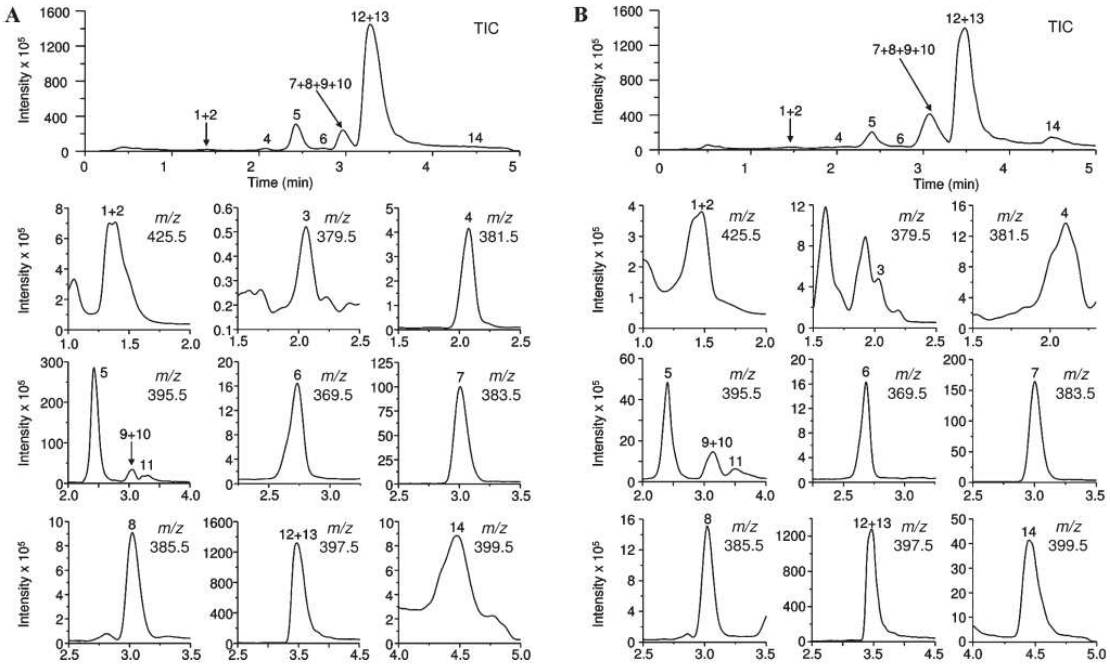

Figure 4. TIC and SIRs of (**A**) extra virgin olive and (**B**) hazelnut oil extracts. Chromatographic conditions: gradient elution as in **Figure 2**; column temperature, 10 °C; flow rate, 0.8 mL min^{-1}. Peak identification as indicated in **Table 1**.

Table 3. Proportions of Sterols Found in Total Sterol Fraction (%)

sterol	avocado	corn	extra virgin olive	grapeseed	hazelnut	peanut	soybean	sunflower
erythrodiol + uvaol	0.05−0.17	0.27−0.45	0.53−0.90	0.01−0.07	0.16−0.19	0.30−0.35	0.10−0.15	0.25−0.35
ergosterol	0.01−0.02	0.01−0.02	0.01−0.02	0.00−0.02	0.25−0.34	0.50−0.90	0.01−0.05	0.03−0.05
brassicasterol	0.25−0.37	0.15−0.18	0.11−0.18	0.10−0.20	0.30−0.40	0.10−0.18	0.28−0.30	0.19−0.23
Δ^5-avenasterol	17.20−18.15	3.95−5.75	11.00−13.00	2.50−2.80	1.90−2.10	9.18−11.32	3.50−4.00	6.45−9.05
cholesterol	0.22−0.62	0.31−0.53	0.32−0.47	0.54−0.78	0.30−0.40	0.68−2.10	0.80−0.90	0.78−0.83
campesterol	4.50−6.30	19.00−19.75	2.74−3.13	12.82−13.14	4.50−5.00	16.47−18.20	17.00−19.00	10.20−10.89
campestanol	0.31−0.41	0.83−0.91	0.24−0.32	0.58−0.62	0.20−0.23	0.50−0.74	0.60−0.80	0.43−0.53
stigmasterol + clerosterol	0.44−0.75	6.54−8.08	1.51−3.00	13.94−15.54	0.90−1.00	10.30−11.93	18.40−19.10	8.94−9.37
$\Delta^{5,24}$-stigmastadienol	nd[a]	0.63−0.70	0.80−0.91	nd	0.95−1.03	0.49−0.51	nd	0.62−0.68
β-sitosterol + stigmastenol	72.67−76.54	61.33−66.21	77.69−82.44	64.39−67.27	87.01−88.54	53.27−61.03	54.70−58.61	67.56−71.76
sitostanol	0.48−0.54	2.10−2.30	0.30−0.38	2.24−2.44	2.00−2.30	0.45−0.50	0.70−1.00	0.35−0.46

[a] Not detected.

estimated using the lanosterol calibration curve. The other sterols (brassicasterol, Δ^5-avenasterol and $\Delta^{5,24}$-stigmastadienol) were estimated using the β-sitosterol calibration curve.

The quantitative results of sterols in the vegetable oils analyzed are shown in **Table 3**. The range values were obtained from the mean value of the three injections of every sample belonging to each category. In general, the levels of sterols found in these samples are in good agreement with data reported in literature (*14*, *18*, *21*, *22*, *32*). As it can be seen, β-sitosterol was the main sterol in all the analyzed oils. Soybean oil contained large quantities of campesterol and stigmasterol + clerosterol, whereas corn oil had less amounts of these latter sterols. The contents of these compounds found in extra virgin olive oil were quite low. Then, the presence of stigmasterol peak could be used as adulteration marker in extra virgin olive oil. The highest contents of Δ^5-avenasterol were found in avocado followed by extra virgin olive and peanut oils. This sterol was found in much low amount in hazelnut than in extra virgin olive oil; however, sitostanol showed a larger content in hazelnut (see **Figure 4A**,**B**). Thus, these peaks could be used to detect the challenging adulteration of extra virgin olive oil with hazelnut. On the other hand, hazelnut and peanut oils showed large ergosterol contents. These high amounts could indicate a fungal activity in the raw material, which also indicates the quality of these oils (*33*).

In conclusion, this method provides a fast and reliable protocol for the separation and identification of sterols in vegetable oils by UPLC−APCI−MS. The separation of sterols could be achieved in less than 5 min, providing narrow peaks with good peak symmetry. Although several peaks in the samples were not completely resolved, the high selectivity provided by the SIR acquisition of MS instrument made it possible to separate most of analytes. The present procedure is of great interest for the routine quality control or adulteration purposes in vegetable oil samples.

LITERATURE CITED

(1) Lercker, G.; Rodriguez-Estrada, M. T. Chromatographic analysis of unsaponifiable compounds of olive oils and fat-containing foods. *J. Chromatogr. A* **2000**, *881*, 105–129.

(2) Piironen, V.; Lindsay, D. G.; Miettinen, T. A.; Toivo, J.; Lampi, A. M. Plant sterols: biosynthesis, biological function and their importance to human nutrition. *J. Sci. Food Agric.* **2000**, *80*, 939.

(3) Perona, J. S.; Cabello-Moruno, R.; Ruiz-Gutierrez, V. The role of virgin olive oil components in the modulation of endothelial function. *J. Nutr. Biochem.* **2006**, *17*, 429.

(4) Morchio, G.; Amelotti, G.; Bocca, A.; Bovio, V.; Conte, L.; Cozzoli, O.; Cremonesi, L.; Fascioli, R.; Giro, L.; Grieco, D.; Lercker, G.; Mariani, C.; Pierattini, G.; Sarti, E; Zunin, P. Analisi gas cromatografica degli steroli con l'impiego di colonne capillari. Risultati di una sperimentazione interlaboratorio. *Riv. Ital. Sostanze Grasse* **1989**, *66*, 531–538.

(5) Mariani, C.; Bellan, G.; Grob, K. On the complexity of sterol fraction in edible fats and oils. Separation of "campesterol" into two epimers. *Riv. Ital. Sostanze Grasse* **1995**, *72*, 97–104.

(6) Cert, A.; Moreda, W.; Pérez-Camino, M. C. Chromatographic analysis of minor constituents in vegetable oils. *J. Chromatogr. A* **2000**, *881*, 131–148.

(7) Aparicio, R.; Aparicio-Ruiz, R. Authentication of vegetable oils by chromatographic techniques. *J. Chromatogr. A* **2000**, *881*, 93–104.

(8) Aparicio, R. In *Handbook of Olive Oil: Analysis and Properties*; Harwood, J. L., Aparicio, R., Eds.; Aspen, Gaithersburg, MD, 1999; p 285.

(9) Kiritsakis, A. K. In *Olive Oil Handbook*; American Oil Chemists' Society: Champaign, IL, 1998; p 20.

(10) Cercaci, L.; Passalacqua, G.; Poerio, A.; Rodriguez-Estrada, M. T.; Lercker, G. Composition of total sterols (4-desmethyl-sterols) in extravirgin olive oils obtained with different extraction technologies and their influence on the oil oxidative stability. *Food Chem.* **2007**, *102*, 66–76.

(11) Rivera del Álamo, R. M.; Fregapane, G.; Aranda, F.; Gómez-Alonso, S.; Salvador, M. D. Sterol and alcohol composition of Cornicabra virgin olive oil: the campesterol content exceeds the upper limit of 4% established by EU regulations. *Food Chem.* **2004**, *84*, 533–537.

(12) Sánchez-Casas, J.; Osorio Bueno, E.; Montaño García, A. F.; Martinez Cano, M. Sterol and erythrodiol + uvaol content of virgin olive oils from cultivars of Extremadura (Spain). *Food Chem.* **2004**, *87*, 225–230.

(13) Galeano Diaz, T.; Durán Merás, I.; Sánchez Casas, J.; Alexandre Franco, M. F. Characterization of virgin olive oils according to its triglycerides and sterols composition by chemometric methods. *Food Control* **2005**, *16*, 339–347.

(14) Parcerisa, J.; Casals, I.; Boatella, J.; Codony, R.; Rafecas, M. Analysis of olive and hazelnut oil mixtures by high-performance liquid chromatography−atmospheric pressure chemical ionisation mass spectrometry of triacylglycerols and gas−liquid chromatography of non-saponifiable compounds (tocopherols and sterols). *J. Chromatogr. A* **2000**, *881*, 149–158.

(15) Matos, L. C.; Cunha, S. C.; Amaral, J. S.; Pereira, J. A.; Andrade, P. B.; Seabra, R. M.; Oliveira, B. P. P. Chemometric characterization of three varietal olive oils (Cvs. Cobrançosa, Madural and Verdeal Transmontana) extracted from olives with different maturation indices. *Food Chem.* **2007**, *102*, 406–414.

(16) Thanh, T. T.; Vergnes, M. F.; Kaloustian, J.; El-Moselhy, T. F.; Amiot-Carlin, M. J.; Portugal, H. Effect of storage and heating on phytosterol concentrations in vegetable oils determined by GC/MS. *J. Sci. Food Agric.* **2006**, *86*, 220–225.

(17) Cunha, S. S.; Fernandes, J. O.; Oliveira, B. P. P. Quantification of free and esterified sterols in Portuguese olive oils by solid-phase extraction and gas chromatography−mass spectrometry. *J. Chromatogr. A* **2006**, *1128*, 220–227.

(18) Abidi, S. L. Capillary electrochromatography of sterols and related steryl esters derived from vegetable oils. *J. Chromatogr. A* **2004**, *1059*, 199–208.
(19) Lerma-García, M. J.; Simó-Alfonso, E. F.; Ramis-Ramos, G.; Herrero-Martínez, J. M. Rapid determination of sterols in vegetable oils by CEC using methacrylate ester-based monolithic columns. *Electrophoresis* **2008**, *29*, 4603–4611.
(20) Lerma-García, M. J.; Ramis-Ramos, G.; Herrero-Martínez, J. M.; Simó-Alfonso, E. F. Classification of vegetable oils according to their botanical origin using sterol profiles established by direct infusion mass spectrometry. *Rapid Commun. Mass Spectrom.* **2008**, *22*, 973–978.
(21) Cañabate-Díaz, B.; Segura-Carretero, A.; Fernández-Gutiérrez, A.; Belmonte Vega, A.; Garrido Frenich, A.; Martínez Vidal, J. L.; Duran Martos, J. Separation and determination of sterols in olive oil by HPLC-MS. *Food Chem.* **2007**, *102*, 593–598.
(22) Martínez-Vidal, J. L.; Garrido-Frenich, A.; Escobar-García, M. A.; Romero-González, R. LC−MS determination of sterols in olive oil. *Chromatographia* **2007**, *65*, 695–699.
(23) Segura-Carretero, A.; Carrasco-Pancorbo, A.; Cortacero, S.; Gori, A.; Cerretani, L.; Fernández-Gutiérrez, A. A simplified method for HPLC-MS analysis of sterols in vegetable oil. *Eur. J. Lipid Sci. Technol.* **2008**, *110*, 1142–1149.
(24) Kawanishi, H.; Toyo'oka, T.; Ito, K.; Maeda, M.; Hamada, T.; Fukushima, T.; Kato, M.; Inagaki, S. Rapid determination of histamine and its metabolites in mice hair by ultra-performance liquid chromatography with time-of-flight mass spectrometry. *J. Chromatogr. A* **2006**, *1132*, 148–156.
(25) Barceló-Barrachina, E.; Moyano, E.; Galcerán, M. T.; Lliberia, J. L.; Bago, B.; Cortes, M. A. Ultra-performance liquid chromatography-tandem mass spectrometry for the analysis of heterocyclic amines in food. *J. Chromatogr. A* **2006**, *1125*, 195–203.
(26) Leandro, C. C.; Hancock, P.; Fussell, R. J.; Keely, B. J. Comparison of ultra-performance liquid chromatography and high-performance liquid chromatography for the determination of priority pesticides in baby foods by tandem quadrupole mass spectrometry. *J. Chromatogr. A* **2006**, *1103*, 94–101.
(27) Li, X.; Xiong, Z.; Ying, X.; Cui, L.; Zhu, W.; Li, F. A rapid ultra-performance liquid chromatography-electrospray ionization tandem mass spectrometric method for the qualitative and quantitative analysis of the constituents of the flower of *Trollius ledibouri* Reichb. *Anal. Chim. Acta* **2006**, *580*, 170–180.
(28) Lu, B.; Zhang, Y.; Wu, X.; Shi, J. Separation and determination of diversiform phytosterols in food materials using supercritical carbon dioxide extraction and ultraperformance liquid chromatography-atmospheric pressure chemical ionization-mass spectrometry. *Anal. Chim. Acta* **2007**, *588*, 50–63.
(29) Suárez, M.; Macià, A.; Romero, M. P.; Motilva, M. J. Improved liquid chromatography tandem mass spectrometry method for the determination of phenolic compounds in virgin olive oil. *J. Chromatogr. A* **2008**, *1214*, 90–99.
(30) Suárez, M.; Romero, M. P.; Ramo, T.; Macià, A.; Motilva, M. J. Methods for preparing phenolic extracts from olive cake for potential application as food antioxidants. *J. Agric. Food Chem.* **2009**, *57*, 1463–1472.
(31) European Community, Commission Regulation 796/2002 of 6 May 2002. *Off. J. Eur. Union* **2002**, *L128*, annex XIX, 23.
(32) Jee, M. In *Oils and fat authentication*; Blackwell Publishing, CRC Press: Boca Raton, FL, **2002**.
(33) Parsia, Z.; Górecki, T. Determination of ergosterol as an indicator of fungal biomass in various samples using non-discriminating flash pyrolysis. *J. Chromatogr. A* **2006**, *1130*, 145–150.

Received for review September 21, 2009. Revised manuscript received January 25, 2010. Accepted January 27, 2010. Work supported by project CTQ2007-61445 (MEC of Spain and FEDER funds). M.J.L.-G. thanks the Generalitat Valenciana for an FPI grant for PhD studies.

ANEXO V

Food Chemistry 118 (2010) 78–83

Contents lists available at ScienceDirect

Food Chemistry

journal homepage: www.elsevier.com/locate/foodchem

Authentication of extra virgin olive oils by Fourier-transform infrared spectroscopy

M.J. Lerma-García *, G. Ramis-Ramos, J.M. Herrero-Martínez, E.F. Simó-Alfonso

Department of Analytical Chemistry, Faculty of Chemistry, University of Valencia, 46100 Burjassot, Valencia, Spain

ARTICLE INFO

Article history:
Received 30 April 2008
Received in revised form 11 March 2009
Accepted 21 April 2009

Keywords:
Botanical origin
Extra virgin olive oil adulteration
Fourier-transform infrared spectroscopy
Linear discriminant analysis
Multiple linear regression

ABSTRACT

Fourier-transform infrared spectroscopy (FTIR), followed by multivariate treatment of the spectral data, was used to classify vegetable oils according to their botanical origin, and also to establish the composition of binary mixtures of extra virgin olive oil (EVOO) with other low cost edible oils. Oil samples corresponding to five different botanical origins (EVOO, sunflower, corn, soybean and hazelnut) were used. The wavelength scale of the FTIR spectra of the oils was divided in 26 regions. The normalized absorbance peak areas within these regions were used as predictors. Classification of the oil samples according to their botanical origin was achieved by linear discriminant analysis (LDA). An excellent resolution among all categories was achieved using an LDA model constructed with eight predictors. In addition, multiple linear regression models were used to predict the composition of binary mixtures of EVOO with sunflower, corn, soybean and hazelnut oils. For all the binary mixtures, models capable of detecting a low cost oil content in EVOO as low as 5% were obtained.

1. Introduction

Oil genuineness is a very important aspect of quality edible oils. Extra virgin olive oil (EVOO) has unique nutritional and sensory characteristics, being also a basic component of the Mediterranean diet. The importance of EVOO is mainly attributed to its high content of oleic acid and its richness in phenolic compounds, which act as natural antioxidants (Bendini et al., 2007). On the other hand, EVOO is expensive owing to the hard and time-consuming tasks involved in the cultivation of olive trees, the harvesting of the fruits, and the extraction of the oil. For these reasons, adulterations of EVOO with olive oils of lower quality, or with oils of a different botanical origin are occasionally detected (Catharino et al., 2005; Chiavaro, Vittadini, Rodriguez-Estrada, Cerretani, & Bendini, 2008; Marcos-Lorenzo, Pérez-Pavón, Fernández-Laespada, García-Pinto, & Moreno-Cordero, 2002; Mariani, Bellan, Lestini, & Aparicio, 2006; Poulli, Mousdis, & Georgiou, 2006; Tay, Singh, Krishnan, & Gore, 2002; Vlachos et al., 2006). For this reason, European Mediterranean countries, which are major suppliers of olive oil in the world market, have adopted common regulations to protect growers and consumers from fraud (European Union Commission, 1991).

To establish the authenticity of edible oils, a number of chromatographic (Brodnjak-Voncina, Kodba, & Novic, 2005; Marcos-Lorenzo et al., 2002; Mariani et al., 2006), thermal (Chiavaro et al., 2008) and spectroscopic methods, including fluorescence (Poulli et al., 2006; Sikorska, Górecki, Khmelinskii, Sikorski, & Kozioł, 2005), NIR (Christy, Kasemsumran, Du, & Ozaki, 2004; Downey, McIntyre, & Davies, 2002; Kasemsumran & Kang, 2005; Sato, 1994; Wesley, Pacheco, & McGill, 1996; Yang, Irudayaraj, & Paradkar, 2005), FTIR (Baeten et al., 2005; Dupuy, Duponchel, Huvenne, Sombret, & Legrand, 1995; Lai, Kemsley, & Wilson, 1999; Ozen & Mauer, 2002; Tay et al., 2002; Vlachos et al., 2006; Yang et al., 2005), FT-Raman (Baeten & Meurens, 1996; López-Díez, Bianchi, & Goodacre, 2003; Yang et al., 2005), NMR (Dais & Spyros, 2007; García-González, Mannina, D'Imperio, Segre, & Aparicio, 2004; Vigli, Philippidis, Spyros, & Dais, 2003) and MS (Catharino et al., 2005; Lay, Liyanage, Durham, & Brooks, 2006; Lerma-García, Ramis-Ramos, Herrero-Martínez, & Simó-Alfonso, 2007, 2008; Lerma-García, Simó-Alfonso, Ramis-Ramos, & Herrero-Martínez, 2007; Marcos-Lorenzo et al., 2002), followed by multivariate statistical analysis of the data, have been described. For this purpose, the contents of fatty acids (Brodnjak-Voncina et al., 2005), tocopherols (Lerma-García, Simó-Alfonso, et al., 2007; Sikorska et al., 2005), volatile compounds (Marcos-Lorenzo et al., 2002), amino acids (Lerma-García, Ramis-Ramos, et al., 2007) and sterols (Lerma-García et al., 2008; Mariani et al., 2006), have been used.

FTIR is a rapid and non-destructive powerful analytical tool for the study of edible oils and fats, requiring minimum sample preparation. FTIR is also an excellent tool for quantitative analysis, since the intensities of the spectral bands are proportional to concentration. For this reason, FTIR has been used to distinguish oils from different botanical origins using non-supervised classificatory techniques (Dupuy et al., 1995; Lai et al., 1999; Rusak, Brown, & Martin, 2003). FTIR has been also used to distinguish EVOOs from different geographical origins (Bendini, Cerretani, et al., 2007; Galtier et al., 2007; Tapp, Defernez, & Kemsley, 2003) and different genetic varieties (Gurdeniz, Tokatli, & Ozen, 2007). FTIR

* Corresponding author. Tel.: +34 96 354 43 34; fax: +34 96 354 44 36.
E-mail address: m.jesus.lerma@uv.es (M.J. Lerma-García).

0308-8146/$ - see front matter © 2009 Elsevier Ltd. All rights reserved.
doi:10.1016/j.foodchem.2009.04.092

applications addressed to detect olive oil adulteration with low cost edible oils (Baeten et al., 2005; Ozen and Mauer, 2002; Tay et al., 2002; Vlachos et al., 2006), to evaluate olive oil freshness (Sinelli, Cosio, Gigliotti, & Casiraghi, 2007), to study changes produced by frying (Valdes & Garcia, 2006) and to assess oil oxidation (Guillén & Cabo, 2002; Muik, Lendl, Molina-Diaz, Valcarcel, & Ayora-Canada, 2007; Vlachos et al., 2006) have been also described.

In this work, FTIR followed by linear discriminant analysis (LDA) of the spectral data was used to classify vegetable oils according to their botanical origin. Also, data treatment by multiple linear regression (MLR) was used to detect and quantify EVOO adulteration with other low cost edible oils, including sunflower, corn, soybean and hazelnut oils.

2. Experimental

2.1. Oil samples and mixtures

The vegetable oils employed in this study (Table 1) were either purchased at the local market or kindly donated by the manufacturers. The botanical origin and quality grade of all the samples were guaranteed by the suppliers. As indicated in Table 1, four samples of each botanical origin were used for training purposes in classification studies, being the other two samples of each category used to evaluate the prediction capability of the classification models. To estimate the adulteration of EVOO with low cost oils by using regression models, binary mixtures containing EVOO and increasing percentages of low cost oil (sunflower, corn, soybean or hazelnut) were prepared. To improve robustness of MLR models, the objects of the calibration matrix were prepared using EVOOs and low cost oils from different geographical origins. For instance, for the sunflower-EVOO pair, oils from different geographical origins were selected to prepare a total of seven mixtures containing 0%, 5%, 10%, 30%, 50%, 75% and 100% sunflower oil. Sets of mixtures containing the same percentages of low cost oil were also prepared for the corn-, soybean- and hazelnut-EVOO pairs. The resulting 28 mixtures were used as calibration set to construct regression models. Additional mixtures of the sunflower-, corn-, soybean- and hazelnut-EVOO pairs, also using oils from different geographical origins, and containing 5%, 50% and 80% low cost oil were prepared. These 12 additional binary mixtures were used to validate the prediction performance of the regression models.

Table 1
Botanical origin, number of samples, brand and use during LDA model construction of the oil samples.

Origin	No. of samples	Brand	LDA set
Hazelnut	2	Guinama	Training
	2	Percheron	Training
	2	Flumen	Evaluation
Sunflower	2	Koipesol	Training
	2	Hacendado	Training
	1	Capicua	Evaluation
	1	Coosol	Evaluation
Corn	1	Guinama	Training
	1	Asua	Training
	1	Artua	Evaluation
	1	Mazola	Evaluation
Corn germ	1	Guinama	Training
	1	Hacendado	Training
Extra virgin olive	1	Carbonell	Training
	1	Grupo Hojiblanca	Training
	1	Borges	Training
	1	Torrereal	Training
	1	Coosur	Evaluation
	1	Hacendado	Evaluation
Soybean	2	Guinama	Training
	2	Biolasi	Training
	2	Sojola	Evaluation

2.2. FTIR spectra

FTIR spectra were obtained using a Nicolet Nexus FTIR spectrophotometer (Thermo Electron Corporation, Waltham, MA, USA) with a resolution of 4 cm^{-1} at 32 scans. A small quantity of the oil samples (≈2 μL) was directly deposited between two well-polished KBr disks, creating a thin film. Duplicated spectra were recorded for all the oil samples and binary mixtures, except the 12 mixtures used as validation set in regression studies which were recorded three times each. Spectra were scanned in the absorbance mode from 4000 to 500 cm^{-1} and the data were handled with the EZ OMNIC 7.3 software (Thermo Electron Corporation).

2.3. Data treatment and construction of matrices

FTIR spectra were divided in the 26 wavelength regions described in Table 2. Each selected spectral region corresponds to a peak or a shoulder, representing structural or functional group information, either about the lipids or minor components of the oil samples (see Table 2). For each region, the peak/shoulder area was measured. In order to reduce the variability associated to the total amount of oil sample used, and to minimize other sources of variance also affecting the intensity of all the peaks, such as the thickness of the sample and radiation source intensity, normalized rather than absolute areas were used. Two normalization procedures were tried. In procedure A, for each spectrum, the area of each region was divided by the sum of the areas of the 26 regions. In procedure B, the area of each region was divided by each one of the areas of the other 25 regions; in this way, and since any pair of areas should be considered only once, $(26 \times 25)/2 = 325$ normalized variables were obtained.

For classification studies, two matrices containing 20 objects each, which corresponded to the averages of the duplicated spectra of the training samples of Table 1, were constructed. These matrices had either 26 or 325 predictors, according to normalization procedures A and B, respectively. A response column, containing the categories corresponding to the five botanical origins of the oils (corn and corn germ were considered as a single category), was added to the training matrices. In order to reduce the internal dispersion of the categories, which was important to reduce the number of variables selected during model construction, the means of the two spectra of each sample, instead of the individual spectra, were used. For evaluation purposes, two more matrices containing 10 objects each, which corresponded to the averages of the duplicated spectra of each evaluation sample of Table 1, were constructed. These matrices also had either 26 or 325 predictors, according to normalization procedures A and B, respectively.

Concerning to the regression studies, and for the sunflower-EVOO pair, two calibration matrices containing seven objects each, which corresponded to the averages of the duplicated spectra of the calibration mixtures, were constructed. According to normalization procedures A and B, the number of predictors was either 26 or 325, respectively. A response column, containing the low cost oil percentages of the mixtures, was added to these matrices. For validation of the prediction performance, two more matrices containing three objects each, which corresponded to the averages of triplicate spectra of validation mixtures, were constructed. The number of predictors was either 26 or 325 predictors, as indicated. Analogously, matrices for the corn-, soybean- and hazelnut-EVOO pairs were also constructed. Statistical treatment of the data was performed using SPSS (v. 12.0.1, Statistical Package for the Social Sciences, Chicago, IL, USA).

Table 2
FTIR spectral regions selected as predictor variables for statistical data treatment.

Identification no.	Range, cm^{-1}	Functional group	Nominal frequency	Mode of vibration
1	3029–2989	=C–H (trans)	3025[a]	Stretching
		=C–H (cis)	3006[a]	Stretching
2	2989–2946	–C–H (CH_3)	2953[a]	Stretching (asym)
3	2946–2881	–C–H (CH_2)	2924[a]	Stretching (asym)
4	2881–2782	–C–H (CH_2)	2853[a]	Stretching (sym)
5	1795–1677	–C=O (ester)	1746[a]	Stretching
		–C=O (acid)	1711[a]	Stretching
6	1486–1446	–C–H (CH_2)	1465[b]	Bending (scissoring)
7	1446–1425	–C–H (CH_3)	1450[b]	Bending (asym)
8	1425–1409	=C–H (cis)	1417[a]	Bending (rocking)
9	1409–1396	=C–H	1400[b]	Bending
10	1396–1382	=C–H	–[b]	Bending
11	1382–1371	–C–H (CH_3)	1377[a]	Bending (sym)
12	1371–1330	O–H	1359[b]	Bending (in plane)
13	1330–1290	Non-assigned	1319[a]	Bending
14	1290–1211	–C–O	1238[a]	Stretching
		$–CH_2–$		Bending
15	1211–1147	–C–O	1163[a]	Stretching
		$–CH_2–$		Bending
16	1147–1128	–C–O	1138[b]	Stretching
17	1128–1106	–C–O	1118[a]	Stretching
18	1106–1072	–C–O	1097[a]	Stretching
19	1072–1043	–C–O	–[b]	Stretching
20	1043–1006	–C–O	1033[a]	Stretching
21	1006–929	–HC=CH– (trans)	968[a]	Bending (out of plane)
22	929–885	–HC=CH– (cis)?	914[a]	Bending (out of plane)
23	885–802	$=CH_2$	850[b]	Wagging
24	802–754	–C–H	–[b]	Bending (out of plane)
25	754–701	$–(CH_2)_n–$	723[a]	Rocking
		–HC=CH– (cis)		Bending (out of plane)
26	701–640	C=C	685[b]	Bending (out of plane)
		O–H	650[b]	Bending (out of plane)

[a] According to Guillén and Cabo (1998).
[b] According to Silverstein, Bassler, and Morrill (1981).

3. Results and discussion

3.1. Classification of vegetable oils according to their botanical origin using LDA

FTIR spectra of the 30 oil samples of Table 1 were collected. Fig. 1 shows the spectra of five oils, one for each botanical origin, tailored at two absorbance units. As it can be observed, the differences between them were small. Interpretation of the absorption bands provides information about the molecular skeleton and functional groups (see Table 2); however, to obtain information about the botanical origin of the oils, band interpretation is not required. Information related to the origin was obtained by measuring the peak areas at the selected wavelength ranges. These data were conveniently handled by multivariate statistical techniques.

LDA, a supervised classificatory technique, is widely recognized as an excellent tool to obtain vectors showing the maximal resolution between sets of objects belonging to previously defined categories. In LDA, vectors minimizing the Wilks' lambda, λ_w, are obtained (Vandeginste et al., 1998). This parameter is calculated as the sum of squares of the distances between points belonging to the same category divided by the total sum of squares. Values of λ_w approaching zero are obtained with well resolved categories, whereas overlapped categories made λ_w to approach one. Up to $N-1$ discriminant vectors are constructed by LDA, being N the lowest value for either the number of predictors or the number of categories.

Using the normalized variables, LDA models capable of classifying the oil samples according to their botanical origin were constructed. To select the variables to be included in the model, the SPSS stepwise algorithm was used. According to this algorithm, a predictor is selected when the reduction of λ_w produced after its inclusion in the model exceeds F_{in}, the entrance threshold of a test of comparison of variances or F-test. However, the entrance of a new predictor modifies the significance of those predictors which are already present in the model. For this reason, after the inclusion of a new predictor, a rejection threshold, F_{out}, is used to decide if one of the other predictors should be removed from the model. The process terminates when there are no predictors entering or being eliminated from the model. The default probability values of F_{in} and F_{out}, 0.05 and 0.10, respectively, were adopted.

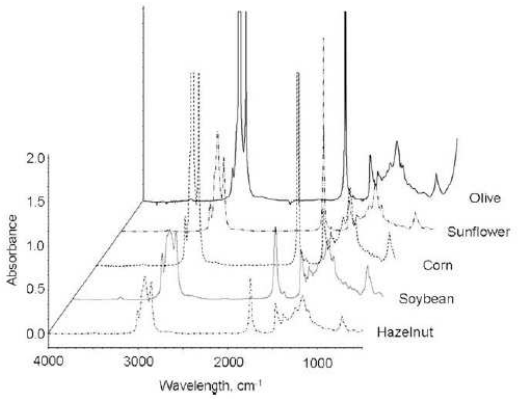

Fig. 1. FTIR spectra of representative samples of EVOO, sunflower, corn, soybean and hazelnut oils. Data were tailored at 2 absorbance units to better show the differences among small peaks.

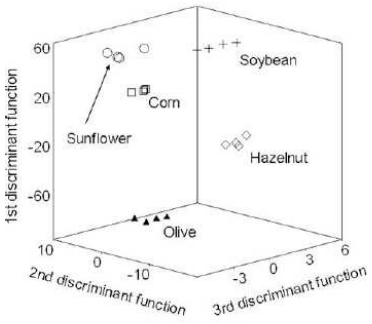

Fig. 2. Score plot on an oblique plane of the 3-D space defined by the three first discriminant functions of the LDA model constructed to classify vegetable oils according to their botanical origin.

Table 3
Predictors selected and corresponding standardized coefficients of the LDA model constructed to predict the botanical origin of vegetable oils.

Predictor[a]	f_1	f_2	f_3	f_4
8/9	19.00	8.20	5.14	3.63
10/12	0.75	9.37	4.03	0.92
11/13	−28.35	5.40	−3.19	−2.13
14/17	16.01	−3.49	−1.50	0.65
15/17	−6.81	5.74	−1.01	1.68
19/25	−13.73	4.33	1.25	0.91
21/26	12.51	−3.76	−0.64	−0.95
22/24	7.84	−5.13	2.26	−1.36

[a] Pairs of wavelength regions identified according to Table 2.

To classify oils according to the five botanical origins, two LDA models, one for each normalization procedure, were constructed. Normalization procedure B, which gave a model with a lower λ_w value and a smaller number of predictors than normalization procedure A, was selected for further studies. As shown in Fig. 2 for normalization procedure B, an excellent resolution between all category pairs was achieved ($\lambda_w = 0.362$). Taking into account that a large number of categories were simultaneously distinguished, this λ_w value was quite low. The predictors selected by the SPSS stepwise algorithm, and the corresponding standardized coefficients of the model, showing the predictors with large discriminant capabilities, are given in Table 3. According to Table 2, the main wavelength regions selected by the algorithm to construct the LDA model corresponded to =C–H (bending), O–H (bending in plane), –C–H (CH_3, bending sym), –C–O (stretching), –CH_2– (bending), –HC=CH– (trans, bending out of plane), O–H (bending out of plane) and c=c (bending out of plane). When leave-one-out validation was applied, all the objects of the training set were correctly classified. Concerning to the prediction capability of this model, and using a 95% probability, all the objects of the evaluation set were correctly assigned; thus, the prediction capability of the model was 100%. On the other hand, the variables obtained by measuring the peak areas along the 26 spectral regions of Table 2 were forced to be included in the model. An improvement of the LDA model was achieved but at the cost of introducing a large number of predictors with low significances. For this reason, variable selection by the stepwise algorithm was maintained.

Finally, an LDA model with all the available objects, including those used above for either training or evaluation, was constructed. The predictors selected by the SPSS stepwise algorithm were basically the same that those selected above, but the λ_w value was smaller (0.202), indicating a satisfactory stability of the model.

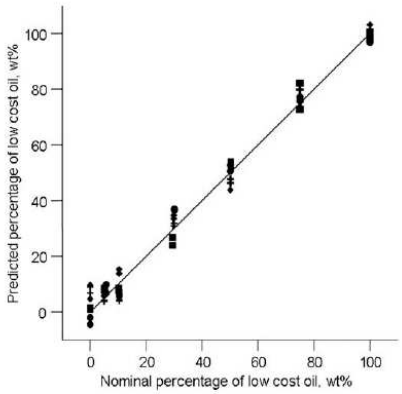

Fig. 3. Predicted (MLR) versus nominal oil percentages for binary mixtures of EVOO with sunflower (●), corn (■), soybean (+) and hazelnut (♦) oils. The straight-line is $y = x$.

3.2. Determination of EVOO adulteration by MLR

In order to quantify EVOO adulteration, the binary mixtures of EVOO with sunflower, corn, soybean and hazelnut oils (Section 2.1), were measured. To select the predictors used in the construction of MLR models, the SPSS stepwise algorithm, with the default probability values of F_{in} and F_{out}, 0.05 and 0.10, respectively, was adopted. MLR models, one for each binary combination of oils, and in each case according to normalization procedures A and B, were constructed. Normalization procedure B, which gave models with higher linear regression coefficients than normalization procedure A, was selected. A plot showing the predicted versus the nominal oil percentages for all the binary mixtures is shown in Fig. 3. The predictors selected and their corresponding non-standardized model coefficients are given in Table 4. It is interesting to observe that, except in the case of the corn-EVOO mixtures, a single predictor was selected to predict the composition of the other three binary mixtures. According to Table 2, the main wavelength transitions selected to construct the MLR model for the sunflower-EVOO pair were =CH_2 (wagging), O–H (bending out of plane) and c=c (bending out of plane). Analogously, for the hazelnut-EVOO pair, the selected transitions were =C–H (trans and cis, stretching), –C–O (stretching) and –CH_2– (bending). Those selected for the soybean-EVOO pair were –$(CH_2)_n$– (rocking) and –HC=CH– (cis, bending out of plane), and those selected for the corn-EVOO pair were –C–O (stretching) and =C–H (trans and cis,

Table 4
Predictors selected and their corresponding non-standardized model coefficients (coef.), linear regression coefficients (R^2), average prediction errors (av. pred. error) and limits of detection (LODs) obtained for the MLR models constructed to predict olive oil adulteration.

Binary mixture	Predictor	Coef.	R^2	Av. pred. error,%	LOD,%
Hazelnut-EVOO	1/15	−1080	0.912	2.0	4.8
	Constant	348			
Sunflower-EVOO	23/26	325	0.989	1.7	4.0
	Constant	−270			
Corn-EVOO	1/17	−353	0.994	1.5	1.3
	1/16	221			
	Constant	309			
Soybean-EVOO	13/25	324	0.980	1.9	1.7
	Constant	−228			

stretching). For all binary combinations of oils, a transition implying a double bond was selected, which suggest that unsaturated fatty acids were important in the quantification of the mixtures. The regression coefficients, average prediction errors (calculated as the sum of the absolute differences between expected and predicted oil percentages divided by the number of predictions) and the limits of detection (LODs, calculated as three times the standard deviation at 5% low cost oil level) are also given in Table 4. For all the MLR models and using leave-one-out validation, the average prediction errors were lower than 2%. The four sets of validation mixtures, one for each binary combination of oils ($4 \times 3 = 12$ mixtures), gave average prediction errors below 5%. LODs were in all cases below 5%, being lower than those previously reported in literature for binary mixtures of the same oils, namely 4% versus 6% (Vlachos et al., 2006) for sunflower-EVOO, 1.3% versus 9% (Vlachos et al., 2006) for corn-EVOO, 1.7% versus 6% (Vlachos et al., 2006) for soybean-EVOO and 4.8% versus 25% (Ozen and Mauer, 2002) and versus 8% (Baeten et al., 2005) for hazelnut-EVOO mixtures.

4. Conclusions

The possibility of classifying vegetable oils according to their botanical origin by using FTIR data has been demonstrated. Using eight wavelength regions, all the oil samples belonging to five different botanical origins were correctly classified with an excellent resolution among the categories. In addition, four MLR models constructed with one predictor for sunflower-, soybean- and hazelnut-EVOO mixtures, and with two predictors for corn-EVOO mixtures, were capable of detecting a low cost oil content in EVOO as low as 5%. Thus, the capability of the proposed method to identify the botanical origin of the oils, and to quantify low cost oils in EVOO has been demonstrated.

Acknowledgements

Project CTQ2007–61445 (MEC and FEDER funds). M.J.L.-G. also thanks the Generalitat Valenciana for an FPI grant for Ph.D. studies.

References

Baeten, V., Fernández Pierna, J. A., Dardenne, P., Meurens, M., García-González, D. L., & Aparicio-Ruiz, R. (2005). Detection of the presence of hazelnut oil in olive oil by FT-Raman and FT-MIR spectroscopy. *Journal of Agricultural and Food Chemistry, 53*, 6201–6206.

Baeten, V., & Meurens, M. (1996). Detection of virgin olive oil adulteration by Fourier transform Raman spectroscopy. *Journal of Agricultural and Food Chemistry, 44*, 2225–2230.

Bendini, A., Cerretani, L., Carrasco-Pancorbo, A., Gómez-Caravaca, A. M., Segura-Carretero, A., Fernández-Gutiérrez, A., et al. (2007). Phenolic molecules in virgin olive oils: a survey of their sensory properties, health effects, antioxidant activity and analytical methods. *An overview of the last decade. Molecules, 12*, 1679–1719.

Bendini, A., Cerretani, L., Di Virgilio, F., Belloni, P., Bonoli-Carbognin, M., & Lercker, G. (2007). Preliminary evaluation of the application of the FTIR spectroscopy to control the geographic origin and quality of virgin olive oils. *Journal of Food Quality, 30*, 424–437.

Brodnjak-Voncina, D., Kodba, Z. C., & Novic, M. (2005). Multivariate data analysis in classification of vegetable oils characterized by the content of fatty acids. *Chemometrics and Intelligent Laboratory Systems, 75*, 31–43.

Catharino, R. R., Haddad, R., Cabrini, L. G., Cunha, I. B. S., Sawaya, A. C. H. F., & Eberlin, M. N. (2005). Characterization of vegetable oils by electrospray ionization mass spectrometry fingerprinting: Classification, quality, adulteration, and aging. *Analytical Chemistry, 77*, 7429–7433.

Chiavaro, E., Vittadini, E., Rodriguez-Estrada, M. T., Cerretani, L., & Bendini, A. (2008). Differential scanning calorimeter application to the detection of refined hazelnut oil in extra virgin olive oil. *Food Chemistry, 110*, 248–256.

Christy, A. A., Kasemsumran, S., Du, Y., & Ozaki, Y. (2004). The detection and quantification of adulteration in olive oil by near-infrared spectroscopy and chemometrics. *Analytical Sciences, 20*, 935–940.

Dais, P., & Spyros, A. (2007). ^{31}P NMR spectroscopy in the quality control and authentication of extra-virgin olive oil: A review of recent progress. *Magnetic Resonance in Chemistry, 45*, 367–377.

Downey, G., McIntyre, P., & Davies, A. (2002). Detecting and quantifying sunflower oil adulteration in extra virgin olive oils from the Eastern Mediterranean by visible and near-infrared spectroscopy. *Journal of Agricultural and Food Chemistry, 50*, 5520–5525.

Dupuy, N., Duponchel, L., Huvenne, J. P., Sombret, B., & Legrand, P. (1995). Classification of edible fats and oils by principal component analysis of Fourier transform infrared spectra. *Food Chemistry, 57*, 245–251.

European Union Commission (1991). Regulation 2568/91, Official Journal of the European Communities.

Galtier, O., Dupuy, N., Le Dréau, Y., Ollivier, D., Pinatel, C., Kister, J., et al. (2007). Geographic origins and compositions of virgin olive oils determinated by chemometric analysis of NIR data. *Analytica Chimica Acta, 595*, 136–144.

García-González, D. L., Mannina, L., D'Imperio, M., Segre, A. L., & Aparicio, R. (2004). Using ^{1}H and ^{13}C NMR techniques and artificial neural networks to detect the adulteration of olive oil with hazelnut oil. *European Food Research and Technology, 219*, 545–548.

Guillén, M. D., & Cabo, N. (1998). Relationships between the composition of edible oils and lard and the ratio of the absorbance of specific bands of their Fourier transform infrared spectra. Role of some bands of the fingerprint region. *Journal of Agricultural and Food Chemistry, 46*, 1788–1793.

Guillén, M. D., & Cabo, N. (2002). Fourier transform infrared spectra data versus peroxide and anisidine values to determine oxidative stability of edible oils. *Food Chemistry, 77*, 503–510.

Gurdeniz, G., Tokatli, F., & Ozen, B. (2007). Differentiation of mixtures of monovarietal olive oils by mid-infrared spectroscopy and chemometrics. *European Journal of Lipid Science and Technology, 109*, 1194–1202.

Kasemsumran, S., & Kang, N. (2005). Partial least squares processing of near-infrared spectra for discrimination and quantification of adulterated olive oils. *Spectroscopy Letters, 38*, 839–851.

Lai, Y. W., Kemsley, E. K., & Wilson, R. H. (1999). Potential of Fourier transform infrared spectroscopy for the authentication of vegetable oils. *Journal of Agricultural and Food Chemistry, 42*, 1154–1159.

Lay, J. O., Liyanage, R., Durham, B., & Brooks, J. (2006). Rapid characterization of edible oils by direct matrix-assisted laser desorption/ionization time-of-flight mass spectrometry analysis using triacylglycerols. *Rapid Communications in Mass Spectrometry, 20*, 952–958.

Lerma-García, M. J., Ramis-Ramos, G., Herrero-Martínez, J. M., & Simó-Alfonso, E. F. (2007). Classification of vegetable oils according to their botanical origin using amino acid profiles established by direct infusion mass spectrometry. *Rapid Communications in Mass Spectrometry, 21*, 3751–3755.

Lerma-García, M. J., Ramis-Ramos, G., Herrero-Martínez, J. M., & Simó-Alfonso, E. F. (2008). Classification of vegetable oils according to their botanical origin using sterol profiles established by direct infusion mass spectrometry. *Rapid Communications in Mass Spectrometry, 22*, 973–978.

Lerma-García, M. J., Simó-Alfonso, E. F., Ramis-Ramos, G., & Herrero-Martínez, J. M. (2007). Determination of tocopherols in vegetable oils by CEC using methacrylate ester-based monolithic columns. *Electrophoresis, 28*, 4128–4135.

López-Díez, E. C., Bianchi, G., & Goodacre, R. (2003). Rapid quantitative assessment of the adulteration of virgin olive oils with hazelnut oils using Raman spectroscopy and chemometrics. *Journal of Agricultural and Food Chemistry, 51*, 6145–6150.

Marcos-Lorenzo, I., Pérez-Pavón, J. L., Fernández-Laespada, M. E., García-Pinto, C., & Moreno-Cordero, B. (2002). Detection of adulterants in olive oil by headspace-mass spectrometry. *Journal of Chromatography A, 945*, 221–230.

Mariani, C., Bellan, G., Lestini, E., & Aparicio, R. (2006). The detection of the presence of hazelnut oil in olive oil by free and esterified sterols. *European Food Research and Technology, 223*, 655–661.

Muik, B., Lendl, B., Molina-Diaz, A., Valcarcel, M., & Ayora-Canada, M. J. (2007). Two-dimensional correlation spectroscopy and multivariate curve resolution for the study of lipid oxidation in edible oils monitored by FTIR and FT-Raman. *Analytica Chimica Acta, 593*, 54–67.

Ozen, B. F., & Mauer, L. J. (2002). Detection of hazelnut oil adulteration using FT-IR spectroscopy. *Journal of Agricultural and Food Chemistry, 50*, 3898–3901.

Poulli, K. I., Mousdis, G. A., & Georgiou, C. A. (2006). Synchronous fluorescence spectroscopy for quantitative determination of virgin olive oil adulteration with sunflower oil. *Analytical and Bioanalytical Chemistry, 386*, 1571–1575.

Rusak, D. A., Brown, L. M., & Martin, S. D. (2003). Classification of vegetable oils by principal component analysis of FTIR spectra. *Journal of Chemical Education, 80*, 541–543.

Sato, T. (1994). Application of principal-component analysis of near-infrared spectroscopic data of vegetable oils for their classification. *Journal of the American Oil Chemists Society, 71*, 293–298.

Sikorska, E., Górecki, T., Khmelinskii, I. V., Sikorski, M., & Koziol, J. (2005). Classification of edible oils using synchronous scanning fluorescence spectroscopy. *Food Chemistry, 89*, 217–225.

Silverstein, R. M., Bassler, G. C., & Morrill, T. C. (1981). *Spectrometric identification of organic compounds*. Chichester: John Wiley & Sons.

Sinelli, N., Cosio, M. S., Gigliotti, C., & Casiraghi, E. (2007). Preliminary study on application of mid infrared spectroscopy for the evaluation of the virgin olive oil freshness. *Analytica Chimica Acta, 598*, 128–134.

Tapp, H. S., Defernez, M., & Kemsley, E. K. (2003). FTIR spectroscopy and multivariate analysis can distinguish the geographic origin of extra virgin olive oils. *Journal of Agricultural and Food Chemistry, 51*, 6110–6115.

Tay, A., Singh, R. K., Krishnan, S. S., & Gore, J. P. (2002). Authentication of olive oil adulterated with vegetable oils using Fourier transform infrared spectroscopy. *Lebensmittel-Wissenschaft und-Technologie, 35*, 99–103.

Valdes, A. F., & Garcia, A. B. (2006). A study of the evolution of the physicochemical and structural characteristics of olive and sunflower oils after heating at frying temperatures. *Food Chemistry, 98*, 214–219.

Vandeginste, B. G. M., Massart, D. L., Buydens, L. M. C., De Jong, S., Lewi, P. J., & Smeyers-Verbeke, J. (1998). *Data handling in science and technology part B* (p. 237). Amsterdam: Elsevier Science B.V.

Vigli, G., Philippidis, A., Spyros, A., & Dais, P. (2003). Classification of edible oils by employing ^{31}P and ^{1}H NMR spectroscopy in combination with multivariate statistical analysis. A proposal for the detection of seed oil adulteration in virgin olive oils. *Journal of Agricultural and Food Chemistry, 51*, 5715–5722.

Vlachos, N., Skopelitis, Y., Psaroudaki, M., Konstantinidou, V., Chatzilazarou, A., & Tegou, E. (2006). Applications of Fourier transform-infrared spectroscopy to edible oils. *Analytica Chimica Acta, 573–574*, 459–465.

Wesley, I. J., Pacheco, F., & McGill, A. E. J. (1996). Identification of adulterants in olive oils. *Journal of the American Oil Chemists Society, 73*, 515–518.

Yang, H., Irudayaraj, J., & Paradkar, M. M. (2005). Discriminant analysis of edible oils and fats by FTIR, FT-NIR and FT-Raman spectroscopy. *Food Chemistry, 93*, 25–32.

ANEXO VI

RAPID COMMUNICATIONS IN MASS SPECTROMETRY
Rapid Commun. Mass Spectrom. 2008; **22**: 973–978
Published online in Wiley InterScience (www.interscience.wiley.com) DOI: 10.1002/rcm.3459

RCM

Classification of vegetable oils according to their botanical origin using sterol profiles established by direct infusion mass spectrometry

María J. Lerma-García*, Guillermo Ramis-Ramos, José M. Herrero-Martínez and Ernesto F. Simó-Alfonso

Department of Analytical Chemistry, Faculty of Chemistry, University of Valencia, 46100 Burjassot, Valencia, Spain

Received 19 December 2007; Revised 28 January 2008; Accepted 28 January 2008

A simple and quick method to classify vegetable oils according to their botanical origin, based on direct infusion of sterol extracts into a mass spectrometer, was developed. Using mass spectrometry (MS) with either an electrospray ionization or an atmospheric pressure photoionization source, followed by linear discriminant analysis of the mass spectral data, oil samples corresponding to eight different botanical origins were perfectly classified with an excellent resolution among all the categories. An excellent correlation between the sterol profiles obtained by MS and by the official gas chromatography (with flame ionization detection) method was obtained. Thus, the proposed method is a promising alternative for sterol fingerprinting of vegetable oils, with the advantage that prior chromatographic separation is not required. Copyright © 2008 John Wiley & Sons, Ltd.

Authentication of edible quality oils is of great importance from the point of view of both commercial value and health impact. The organoleptic properties, high nutritional value and health benefits of quality oils are related to the presence of many components with interesting biochemical properties, including, among others, antioxidants and sterols.[1,2] There is some evidence that plant sterols decrease the cardiovascular risk of coronary heart disease,[3] and that they also reduce blood cholesterol levels, showing anti-inflammatory, antibacterial, and antioxidant activity.[4]

A relevant aspect of oil authenticity is the adulteration of quality oils with lower price oils of a different botanical origin. The evaluation of sterol profiles and total sterol contents are excellent tools to assess oil authenticity.[5,6] Extra virgin olive oils have a highly characteristic sterol composition; for this reason, the determination of sterols has become a helpful tool to detect adulterations of extra virgin olive oils with vegetable oils of a different botanical origin,[7–9] or with olive oils of lower quality.[10,11]

Sterols in vegetable oils have been normally analyzed by gas chromatography with flame ionization detection (GC/FID)[1,2,6,8,9,12–18] and with mass spectrometry detection (GC/MS).[1,8,16,19–21] The major disadvantage of GC is the requirement of thermally stable columns and of chemical derivatization prior to analysis. For this reason, to determine sterols in vegetable oils, capillary electrochromatography (CEC) with diode-array UV-vis detection[22] and high-performance liquid chromatography with mass spectrometry detection (HPLC/MS)[10,11] have also been used.

Sterol contents established by GC, followed by multivariate data treatment, have been used to distinguish between different genetic varieties of extra virgin olive oil.[2,6,13–15,18] Direct infusion into the electrospray ionization (ESI) source of a mass spectrometer, without prior chromatographic separation, has been used to classify vegetable oils according to their botanical origin.[23,24] On the other hand, fatty acid profiles, also obtained by ESI-MS, followed by linear discriminant analysis (LDA) of the mass spectral data, have been employed to classify olive oils according to their quality grade.[25] In addition, the MS profiles of both fatty acids and phenolic compounds have been used to classify extra virgin olive oils according to their genetic variety.[26] The ESI-MS profiles of the triglycerides, followed by principal component analysis (PCA) of the MS and MS^2 data, were used to evaluate the adulteration of olive oils with other fruit and seed oils.[27] In addition, triglyceride profiles, obtained using a quadrupole time-of-flight mass spectrometer and two ion sources (ESI and atmospheric pressure photoionization, APPI), were used to identify mixtures of olive oils with other vegetable oils.[28] Direct infusion ESI-MS, followed by LDA of the spectral data, has also been successfully used to classify binding media in art works[29] and midge larvae.[30]

In this work, a simple and quick method for oil classification according to its botanical origin, based on direct infusion of sterol extracts into a mass spectrometer, was developed. For this purpose, two ion sources, ESI and APPI, were examined. The application of LDA to the resulting sterol profiles in order to distinguish eight different botanical oil origins was performed. The sterol profiles obtained by the proposed MS method and by the official GC/FID method were also compared.

**Correspondence to*: M. J. Lerma-García, Department of Analytical Chemistry, Faculty of Chemistry, University of Valencia, 46100 Burjassot, Valencia, Spain.
E-mail: m.jesus.lerma@uv.es
Contract/grant sponsor: MEC and FEDER; contract/grant number: CTQ2007-61445.
Contract/grant sponsor: Generalitat Valenciana; contract/grant number: ACOMP2007-168.

RCM

Table 1. Botanical origin, number of samples and brand of the vegetable oil samples used in this work

Origin	No. of samples	Brand
Hazelnut	4	Guinama
Sunflower	2	Koipesol
	2	Hacendado
Corn	2	Guinama
Corn germ	1	Guinama
	1	Hacendado
Olive	1	Carbonell
	1	Grupo Hojiblanca
	1	Borges
	1	Torrereal
Soybean	2	Guinama
	2	Biolasi
Avocado	4	Guinama
Peanut	4	Guinama
Grapeseed	4	Guinama

EXPERIMENTAL

Reagents and samples

Ethanol, 2-propanol, anhydrous sodium sulphate (Scharlau, Barcelona, Spain), diethyl ether, chloroform (J.T. Baker, Deventer, The Netherlands), KOH (Probus, Barcelona), n-hexane (Riedel-de Haën, Seelze, Germany), Sylon HTP (3:1:9 mixture of hexamethyldisilazane, trimethylchlorosilane and pyridine; Supelco, Bellefonte, PA, USA) and 2,7-dichlorofluorescein (Sigma, St. Louis, MO, USA) were employed. Glass plates for thin layer chromatography (TLC), coated with silica gel without fluorescent indicator (0.25 mm plate thickness; Merck, Darmstadt, Germany), were used. The sterols used as standards were: β-sitosterol (mixture containing 75% β-sitosterol and 10% campesterol), ergosterol, stigmasterol (Acros Organics, Morris Plains, NJ, USA) and cholesterol (Aldrich, Milwaukee, WI, USA). The vegetable oils employed in this study (Table 1) were either purchased in the local market or kindly donated by the manufacturers. The botanical origin and quality grade of all the samples were guaranteed by the suppliers.

Instrumentation and working conditions

An HP 1100 series ion trap (IT) mass spectrometer provided with an ESI and an APPI source (Agilent Technologies, Waldbronn, Germany) was used. A syringe pump (kdScientific, Holliston, MA, USA) was used to infuse the samples at 0.3 mL h^{-1} (5 μL min^{-1}) through a 50 μm i.d. PEEK tube. The working conditions for the ESI source were: nebulizer gas pressure, 15 psi; drying gas flow rate, 12 L min^{-1} at 365°C; capillary voltage, −4.5 kV; voltages of skimmers 1 and 2, 25.9 V and 6.0 V, respectively. The working conditions for the APPI source were: nebulizer gas pressure, 15 psi; drying gas flow rate, 12 L min^{-1} at 350°C; vaporizer temperature, 275°C; capillary voltage, −4.4 kV; voltages of skimmers 1 and 2, 24.0 V and 7.4 V, respectively. With both sources, nitrogen was used as the nebulizer and drying gas (Gaslab NG LCMS 20 generator; Equcien, Madrid, Spain). The mass spectrometer was scanned within the m/z 200–500 range in the positive ion mode. The ion trap target mass was set at m/z 397 ($[M+H-H_2O]^+$ ion of β-sitosterol). The maximum loading of the ion trap was 3×10^4 counts, and the maximum collection time was 300 ms.

An HP-5890 gas chromatograph provided with a FID detector (Agilent Technologies) was used. Separation was carried out with an HP-5 capillary column (30 m × 0.32 mm × 0.25 μm; J&W Scientific, Folsom, CA, USA). The operation conditions, adapted from the official method,[31] were as follows: oven temperature, 263°C for 30 min; split ratio, 1:10; injector temperature, 290°C; detector temperature, 320°C. Hydrogen was used as the carrier gas at a flow rate of 30 mL min^{-1}.

Procedures

The sterol band of the vegetable oils was obtained following the procedure established by the Official Journal of the European Union.[31] Briefly, the oil samples were saponified by refluxing for 20 min with 2 N ethanolic KOH solution, and the non-saponificable fraction was extracted with diethyl ether. The sterol fraction was isolated using TLC, and recovered from the plates with diethyl ether. A rotary evaporator was used to remove the solvent, and the residue was evenly divided into two portions. One aliquot was dissolved in 200 μL 2-propanol containing 1% acetone for MS analysis, while the second portion was derivatized with 200 μL Sylon for GC analysis. In MS the sterol extracts were infused at least four times into each ion source, and each time the spectrum was averaged for 1 min. For each sterol, the signal intensity of the MS ions was measured, and a data matrix was constructed using the intensities at different m/z values as original variables. After normalization of the variables, the statistical data treatment was performed using SPSS (v. 12.0.1; Statistical Package for the Social Sciences, Chicago, IL, USA).

RESULTS AND DISCUSSION

Optimization of the working conditions

To optimize the ITMS working conditions, the sterol standards indicated above were used. With both ESI and APPI, ions at two m/z values, corresponding to $[M+H]^+$ and $[M+H-H_2O]^+$, were observed. For all the standards, except for ergosterol with APPI, the $[M+H-H_2O]^+$ ions were of higher abundance than the respective $[M+H]^+$ ions. For this reason, the intensities of the $[M+H-H_2O]^+$ ions were used as the optimization criteria for the working conditions. A drying gas temperature of 365°C, a nebulizer pressure of 15 psi, a drying gas flow rate of 12 L min^{-1}, a vaporizer temperature of 275°C and a stability parameter of 50% were selected. Under the optimized conditions and with both ion sources, different standards showed different relationships between the abundances of the corresponding $[M+H]^+$ and $[M+H-H_2O]^+$ ions. Thus, sterols could be distinguished not only by the different m/z values, but also by the different intensity ratios of the $[M+H]^+$ and $[M+H-H_2O]^+$ ions. Thus, the mass spectra provided information related to the concentrations of all sterols present in the samples, including those having ions at the same m/z values. Since vegetable oils of different botanical origin also showed different sterol profiles, the profiles contain the necessary information to distinguish between them.

DOI: 10.1002/rcm

RCM

Table 2. Molecular mass, M, (most abundant isotopes) and *m/z* values of the $[M+H]^+$ and $[M+H-H_2O]^+$ ions of the sterols employed in this study

Sterol	M	$[M+H]^+$	$[M+H-H_2O]^+$	Group
Cholesterol	386.7	387.7	369.7	1
Ergosterol	396.7	397.7	378.7	2
Brassicasterol	398.7	399.7	381.7	3
24-Methylene cholesterol	398.7	399.7	381.7	3
Δ^7-Campesterol	398.7	399.7	381.7	3
Campesterol	400.7	401.7	383.7	4
Campestanol	402.7	403.7	385.7	5
Clerosterol	412.7	413.7	395.7	6
Stigmasterol	412.7	413.7	395.7	6
Δ^7-Avenasterol	412.7	413.7	395.7	6
Δ^5-Avenasterol	412.7	413.7	395.7	6
$\Delta^{5,24}$-Stigmastadienol	412.7	413.7	395.7	6
$\Delta^{7,25}$-Stigmastadienol	412.7	413.7	395.7	6
Fucosterol	412.7	413.7	395.7	6
Isofucosterol	412.7	413.7	395.7	6
Δ^5-Avenastenol	414.7	415.7	397.7	2
Δ^7-Stigmastenol	414.7	415.7	397.7	2
β-Sitosterol	414.7	415.7	397.7	2
Sitostanol	416.7	417.7	399.7	3
Erythrodiol	442.7	443.7	425.7	7
Uvaol	442.7	443.7	425.7	7

[a]Each group is formed by the sterols having ions with the same *m/z* values.

Selection and normalization of the variables

The ESI and the APPI spectra showed ions at the same *m/z* values, corresponding to the $[M+H]^+$ and the $[M+H-H_2O]^+$ ions of the sterols indicated in Table 2. From the 42 sterol ions expected – 2 for each of the 21 individual sterols – only 16 ions were observed in the mass spectra. This low number of ions was because several sterols provided ions of the same *m/z* values. Thus only the 16 ions obtained could be used as variables. As can be observed in Fig. 1 for a soybean oil sample, the $[M+H]^+$ and the $[M+H-H_2O]^+$ ions obtained with the APPI source showed better signal-to-noise ratios than those obtained with the ESI source.

In order to reduce the variability associated with the total amount of sterols recovered from the oil samples, and to minimize other sources of variance, the normalized signal intensities of all the ions rather than the absolute ion abundances were used. In order to obtain the normalized variables for each spectrum, the abundance of each ion was divided by each one of the abundances of the other 15 ions; in this way, and taking into account that each pair of ions should be considered only once, $(16 \times 15)/2 = 120$ non-redundant ion ratios were obtained.

The same samples employed in the MS analysis were also analyzed by the official GC/FID method.[31] A typical gas chromatogram is shown in Fig. 2. The possible correlation between the relative intensities of the MS ions and the areas of the GC peaks was studied. Owing to the coincidence of the *m/z* values of the ions of several sterols, a correlation study using the MS ion intensities and GC peak areas of individual sterols is not possible. Instead, the sterols were arranged into the seven groups that are indicated in Table 2. Each group was formed by the sterols having ions with the same *m/z* values. First, for each mass spectrum, the sum of the MS ion intensities of each group was divided by the sum of the ion intensities of all the sterols. Secondly, for each gas chromatogram, the sum of the areas of the GC peaks of each group was divided by the sum of the peak areas of all the sterols. The MS and GC data processed in this way for each group of sterols, and for a representative soybean oil sample, are plotted in Fig. 3. As shown in this figure, the MS ion intensities and GC peak areas were non-linearly correlated. Non-linearity is probably a consequence of the different response factors of the sterols in MS and GC; however, Fig. 3 clearly shows that sterols having higher concentration in samples give both large MS ion signal intensities and large peak areas. Similar plots were obtained with the other oil samples.

Construction of the data matrices and LDA models

LDA, a supervised classificatory technique, is widely recognized as an excellent tool to obtain vectors showing the maximum resolution between a set of previously defined categories. In LDA, vectors minimizing Wilks' lambda, λ_w, are obtained.[32] This parameter is calculated as the sum of squares of the distances between points belonging to the same category divided by the total sum of squares. Values of

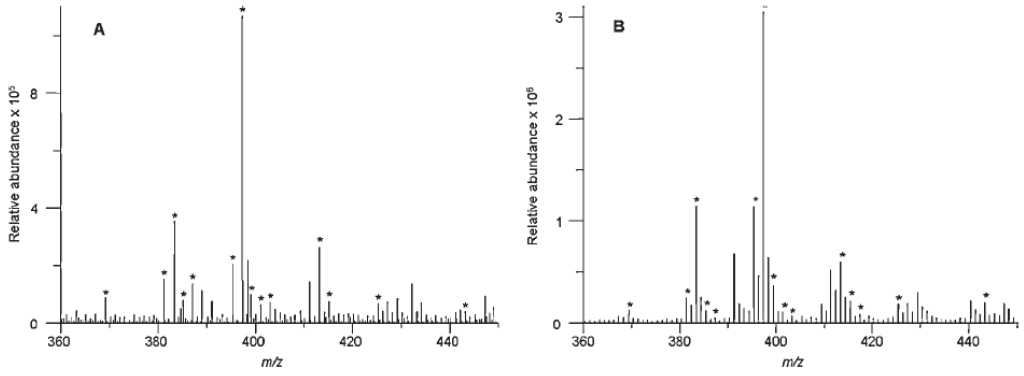

Figure 1. Direct infusion mass spectra of a sterol extract of a soybean oil obtained with the ESI (A) and APPI (B) ion sources. The ions, which correspond to the sterols of Table 2, are indicated by an asterisk.

DOI: 10.1002/rcm

RCM

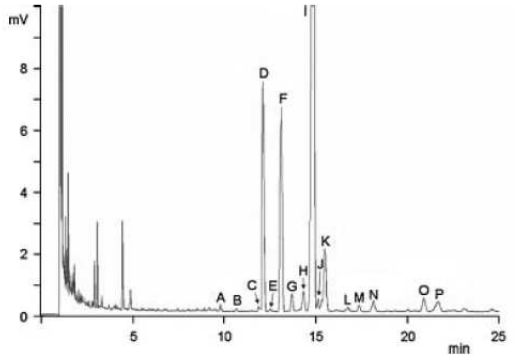

Figure 2. Typical gas chromatogram of a sterol extract of a soybean oil. Peak identification: cholesterol (A), brassicasterol (B), 24-methylene cholesterol (C), campesterol (D), campestanol (E), stigmasterol (F), Δ^7-campesterol (G), clerosterol (H), β-sitosterol (I), sitostanol (J), Δ^5-avenasterol (K), $\Delta^{5,24}$-stigmastadienol (L), Δ^7-stigmastenol (M), Δ^7-avenasterol (N), erythrodiol (O) and uvaol (P). β-Sitosterol peak has been tailored to better appreciate small peaks.

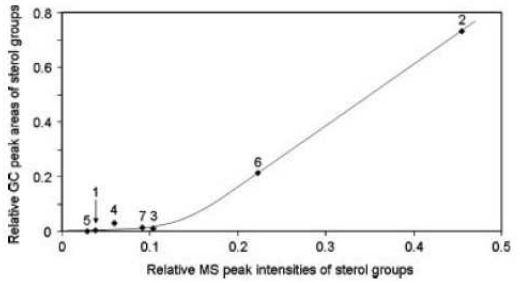

Figure 3. Relative GC peak areas plotted against the relative MS ion signal intensities of the seven sterol groups indicated in Table 2.

λ_w approaching zero are obtained with well-resolved categories, whereas overlapped categories make λ_w approach a value of 1. Up to N – 1 discriminant vectors are constructed

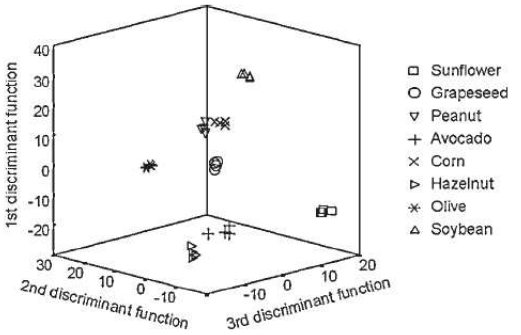

Figure 4. Score plot on an oblique plane of the 3-D space defined by the three first discriminant functions of the LDA model constructed with the ESI-MS data.

by LDA, with N being the lowest value for either the number of predictors or the number of categories.

Using the normalized variables, LDA models capable of classifying the oil samples according to their botanical origin were constructed. Since each sample was injected at least four times with each ion source, two matrices, one for ESI and another for APPI data, containing 128 injections and 120 predictors each, were constructed. A response column, containing the eight categories corresponding to the eight botanical origins of the oils (corn and corn germ were considered as a single category), was added to each matrix. These matrices were used as evaluation sets. To construct LDA training matrices, only the means of the replicates of the samples were included. In this way, the internal dispersion of the categories was reduced, which was important to reduce the number of variables selected by the SPSS stepwise algorithm during model construction. According to this algorithm, a predictor is selected when the reduction of λ_w produced after its inclusion in the model exceeds F_{in}, the entrance threshold of a test of comparison of variances or F-test. However, the entrance of a new predictor modifies the significance of those predictors which are already present in the model. For this reason, after the inclusion of a new predictor, a rejection threshold, F_{out}, is used to decide if one

Table 3. Predictors selected and corresponding standardized coefficients of the LDA model constructed to predict the botanical origin of vegetable oils injected in ESI-MS

Predictors[a]	f_1	f_2	f_3	f_4	f_5	f_6	f_7
395.7/385.7	3.0	6.9	4.8	−1.5	0.9	−0.5	−0.2
395.7/387.7	0.5	−8.2	−1.0	0.8	1.1	1.7	0.5
399.7/397.7	9.4	2.8	3.3	−2.7	3.4	−0.2	0.8
401.7/383.7	4.6	4.4	1.5	1.3	0.8	−0.9	2.3
403.7/397.7	−16.6	−11.5	−5.5	4.6	−1.7	0.1	−4.3
403.7/399.7	14.6	13.3	9.0	−3.9	1.4	1.4	7.0
413.7/369.7	−1.8	−2.4	−0.8	−0.1	2.2	0.3	−0.3
415.7/397.7	−4.5	8.1	2.1	0.7	−4.1	−0.1	2.0
415.7/403.7	2.7	−5.8	1.2	0.3	0.8	0.4	−0.4
417.7/369.7	−1.6	−1.2	−1.1	−0.1	−2.1	0.7	−0.2
425.7/403.7	0.3	3.7	0.9	0.4	0.1	−1.5	0.6
443.7/399.7	−2.1	−5.8	−3.5	0.1	1.9	0.1	−4.7
443.7/403.7	0.6	5.1	2.2	1.2	−0.8	0.8	2.4

[a]Identified by the *m/z* values of the ion pairs.

Rapid Commun. Mass Spectrom. 2008; **22**: 973–978
DOI: 10.1002/rcm

RCM

of the other predictors should be removed from the model. The process terminates when there are no predictors entering or being eliminated from the model. The probability values of F_{in} and F_{out}, 0.05 and 0.10, respectively, were adopted.

To classify the oils according to the eight botanical origins, two LDA models, one for each set of MS ion source data, were constructed. With the ESI-MS data, excellent resolution among the eight categories was achieved (Fig. 4, $\lambda_w = 0.294$). Taking into account the fact that a large number of categories were simultaneously distinguished, this λ_w value was quite low. The variables selected by the SPSS stepwise algorithm, and the corresponding standardized coefficients of the model, showing the predictors with large discriminant capabilities, are given in Table 3. Along the first discriminant function, f_1, an extremely large separation of the avocado category with respect to all the other categories was observed. As deduced from Table 3, this function was mainly constructed with the ion intensity ratios taken at m/z 403.7/397.7 and 403.7/399.7. As indicated in Table 2, the m/z 403.7 ion belongs to campestanol, and each of the other two ions can be due to several sterols. The remaining oil categories were resolved along the second and third discriminant functions, f_2 and f_3.

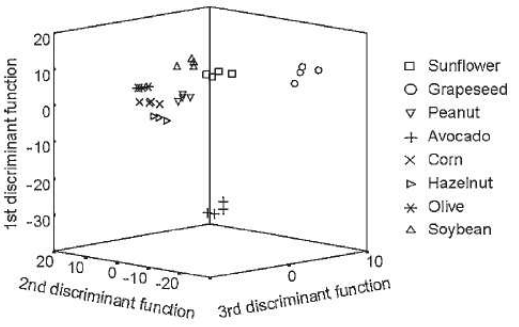

Figure 5. Score plot on an oblique plane of the 3-D space defined by the three first discriminant functions of the LDA model constructed with the APPI-MS data.

With the APPI-MS spectral data, another LDA model was constructed. The eight categories were also very well resolved, with the λ_w value being similar to that obtained with the ESI-MS data (Fig. 5, $\lambda_w = 0.383$). The variables selected and the corresponding standardized coefficients of the model are given in Table 4. Along the first discriminant function, f_1, with the exception of the corn/peanut pair, remarkable resolution of all the category pairs was produced. This function was mainly constructed with the ion intensity ratios taken at m/z 397.7/383.7, 413.7/397.7 and 415.7/383.7. As indicated in Table 2, the m/z 383.7 ion belongs to campesterol, with each of the other m/z values corresponding to several sterols. In addition, along the f_2 and f_3 (constructed mainly by campestanol) the corn/peanut pair appears to be overlapped, with the rest of the categories being well resolved. The corn/peanut pair was resolved along f_4. For the two models constructed with both the ESI and the APPI data, and using leave-one-out cross-validation, all the points of the respective training sets were correctly classified. The corresponding evaluation sets, containing 128 original data points each, were used to check the prediction capability of the models. Using a 95% probability, all the objects were correctly assigned; thus, the prediction capability of both models was 100%.

CONCLUSIONS

The possibility of classifying vegetable oils according to their botanical origin by using sterol profiles established by direct infusion MS has been demonstrated. The ESI and APPI ion sources have been compared, with APPI giving higher sensitivities and better signal-to-noise ratios for all the ions. However, using both the ESI-MS and the APPI-MS data, all oil samples belonging to the eight different botanical origins were perfectly classified with excellent resolution among the categories. Excellent correlation between the sterol profiles obtained by the proposed method and those obtained by GC/FID was found. Thus, the proposed method is a promising alternative for sterol fingerprinting applied to the classification of vegetable oils, with the additional

Table 4. Predictors selected and corresponding standardized coefficients of the LDA model constructed to predict the botanical origin of vegetable oils injected in APPI-MS

Predictors[a]	f_1	f_2	f_3	f_4	f_5	f_6	f_7
385.7/383.7	−10.6	1.9	3.6	0.7	−1.2	−0.1	−2.1
397.7/383.7	24.7	15.4	8.0	2.4	5.8	0.8	3.0
401.7/381.7	−9.0	4.7	−4.9	0.2	1.8	2.6	−0.9
413.7/397.7	22.5	4.1	12.9	1.8	4.4	−0.9	2.4
415.7/383.7	−23.6	−12.5	−12.4	−3.1	−1.8	3.3	−1.3
415.7/413.7	16.3	8.5	6.0	0.9	2.0	−2.3	2.3
425.7/369.7	−6.6	−0.8	−2.6	8.7	−0.5	1.7	3.8
425.7/381.7	2.3	−6.9	−4.0	4.1	−4.7	−9.1	1.2
425.7/383.7	10.5	7.5	13.0	−15.0	6.5	9.3	−8.1
425.7/397.7	−15.5	−5.4	−12.9	0.2	0.3	3.2	0.6
443.7/383.7	2.4	2.5	0.7	8.7	−1.7	−8.9	9.6
443.7/399.7	14.5	0.3	3.0	−0.5	−3.2	1.0	−4.0
443.7/401.7	−3.5	2.4	−1.6	−5.2	4.7	2.8	−1.2
443.7/403.7	−1.8	−1.3	0.6	2.0	−0.8	−1.2	−1.6

[a]Identified by the m/z values of the ion pairs.

DOI: 10.1002/rcm

advantage that previous chromatographic separation is not required.

Acknowledgements

We acknowledge funds from MEC and FEDER (Project No. CTQ2007-61445) and Generalitat Valenciana (Project No. ACOMP2007-168). MJL-G also thanks the Generalitat Valenciana for an FPI grant for PhD studies.

REFERENCES

1. Cercaci L, Passalacqua G, Poerio A, Rodriguez-Estrada MT, Lercker G. *Food Chem.* 2007; **102**: 66.
2. Rui Alves M, Cunha SC, Amaral JS, Pereira JA, Beatriz Oliveira M. *Anal. Chim. Acta* 2005; **549**: 166.
3. Piironen V, Lindsay DG, Miettinen TA, Toivo J, Lampi AM. *J. Sci. Food Agric.* 2000; **80**: 939.
4. Perona JS, Cabello-Moruno R, Ruiz-Gutierrez V. *J. Nutr. Biochem.* 2006; **17**: 429.
5. Kamm W, Dionisi F, Hischenhuber C, Engel KH. *Food Rev. Int.* 2001; **17**: 249.
6. Ranalli A, Pollastri L, Contento S, Di Loreto G, Iannucci E, Lucera L, Russi F. *J. Sci. Food Agric.* 2002; **82**: 854.
7. Ballesteros E, Gallego M, Valcárcel M. *Anal. Chim. Acta* 1995; **308**: 253.
8. Cercaci L, Rodríguez-Estrada MT, Lercker G. *J. Chromatogr. A* 2003; **985**: 211.
9. Mariani C, Bellan G, Lestini E, Aparicio R. *Eur. Food Res. Technol.* 2006; **223**: 655.
10. Cañabate-Díaz B, Segura Carretero A, Fernández-Gutiérrez A, Belmonte Vega A, Garrido Frenich A, Martínez Vidal JL, Duran Martos J. *Food Chem.* 2007; **102**: 593.
11. Martínez-Vidal JL, Garrido-Frenich A, Escobar-García MA, Romero-González R. *Chromatographia* 2007; **65**: 695.
12. Philips KM, Ruggio DM, Toivo JI, Swank MA, Simpkins AH. *J. Food Compos. Anal.* 2002; **15**: 123.
13. Rivera del Álamo RM, Fregapane G, Aranda F, Gómez-Alonso S, Salvador MD. *Food Chem.* 2004; **84**: 533.
14. Sánchez-Casas J, Osorio Bueno E, Montaño García AF, Martinez Cano M. *Food Chem.* 2004; **87**: 225.
15. Galeano Diaz T, Durán Merás I, Sánchez Casas J, Alexandre Franco MF. *Food Control* 2005; **16**: 339.
16. Parcerisa J, Casals I, Boatella J, Codony R, Rafecas M. *J. Chromatogr. A* 2000; **881**: 149.
17. Amaral JS, Casal S, Citová I, Santos A, Seabra RM, Oliveira BPP. *Eur. Food Res. Technol.* 2006; **222**: 274.
18. Matos LC, Cunha SC, Amaral JS, Pereira JA, Andrade PB, Seabra RM, Oliveira BPP. *Food Chem.* 2007; **102**: 406.
19. Thanh TT, Vergnes MF, Kaloustian J, El-Moselhy TF, Amiot-Carlin MJ, Portugal H. *J. Sci. Food Agric.* 2006; **86**: 220.
20. Medvedovici A, David F, Sandra P. *Chromatographia* 1997; **44**: 37.
21. Cunha SS, Fernandes JO, Oliveira BPP. *J. Chromatogr. A* 2006; **1128**: 220.
22. Abidi SL. *J. Chromatogr. A* 2004; **1059**: 199.
23. Catharino RR, Haddad R, Cabrini LG, Cunha IBS, Sawaya ACHF, Eberlin MN. *Anal. Chem.* 2005; **77**: 7429.
24. Lerma-García MJ, Ramis-Ramos G, Herrero-Martínez JM, Simó-Alfonso EF. *Rapid Commun. Mass Spectrom.* 2007; **21**: 3751.
25. Lerma-García MJ, Herrero-Martínez JM, Ramis-Ramos G, Simó-Alfonso EF. *Food Chem.* 2008; **107**: 1307.
26. Lerma-García MJ, Herrero-Martínez JM, Ramis-Ramos G, Simó-Alfonso EF. *Food Chem.* 2007; DOI: 10.1016/j.food-chem.2007.11.065.
27. Goodacre R, Vaidyanathan S, Bianchi G, Kell DB. *Analyst* 2002; **11**: 1457.
28. Gómez-Ariza JL, Arias-Borrego A, García-Barrera T, Beltran R. *Talanta* 2006; **70**: 859.
29. Peris-Vicente J, Simó-Alfonso E, Gimeno-Adelantado JV, Domenech-Carbó MT. *Rapid Commun. Mass Spectrom.* 2005; **19**: 3463.
30. Gama Melão MG, Simó-Alfonso E, Ramis-Ramos G, Vicente E. *Rapid Commun. Mass Spectrom.* 2006; **20**: 1039.
31. Commission Regulation (EEC) No. 2568/91 from 11 July 1991, *Off. J. Eur. Union*, annex V.
32. Vandeginste BGM, Massart DL, Buydens LMC, De Jong S, Lewi PJ, Smeyers-Verbeke J. *Data Handling in Science and Technology*, part B. Elsevier Science: Amsterdam, 1998; 237.

ANEXO VII

Journal of Chromatography A, 1216 (2009) 230–236

Contents lists available at ScienceDirect

Journal of Chromatography A

journal homepage: www.elsevier.com/locate/chroma

Characterization of the alcoholic fraction of vegetable oils by derivatization with diphenic anhydride followed by high-performance liquid chromatography with spectrophotometric and mass spectrometric detection

M.J. Lerma-García, G. Ramis-Ramos, J.M. Herrero-Martínez, J.V. Gimeno-Adelantado, E.F. Simó-Alfonso*

Department of Analytical Chemistry, Faculty of Chemistry, University of Valencia, 46100 Burjassot, Valencia, Spain

ARTICLE INFO

Article history:
Received 7 August 2008
Received in revised form
20 November 2008
Accepted 21 November 2008
Available online 27 November 2008

Keywords:
Aliphatic alcohols
Botanical origin
Linear discriminant analysis
Mass spectrometry
Triterpene alcohols
Vegetable oil authentication

ABSTRACT

Aliphatic and triterpene alcohols present in vegetable oils have been identified and determined by HPLC using UV–vis and MS detection after previous derivatization with diphenic anhydride. The alcoholic fraction was obtained by saponification, extraction and TLC (according to the European Union official procedure). Derivatization was performed in tetrahydrofuran in the presence of suspended grinded urea, which increases the reaction rate and yield. Derivatized extracts were chromatographed on a C8 column using gradient elution with acetonitrile/water mixtures containing 0.1% acetic acid, with UV–vis followed by negative-ion mode MS detection. Using linear discriminant analysis of the HPLC-MS data (extracted ion chromatograms), oil samples belonging to seven botanical origins (hazelnut, sunflower, corn, extra virgin olive, soybean, peanut and grapeseed) were correctly classified with excellent resolution among all the categories.

1. Introduction

Vegetable oils are mainly constituted by triacylglycerols, also containing an unsaponifiable fraction which amounts to 1–3%. Among other compounds, this fraction contains aliphatic and triterpene alcohols. The nature and quantitative distribution of these components are characteristic of the original lipid source [1,2,3], thus being useful for the identification of the biological origin of the lipid matrix from which they were extracted. In fact, the unsaponifiable minor components have been employed as a fingerprint of most vegetable oils [4]. Moreover, in the same species, content and composition of these components can vary due to the environmental conditions, fruit or seed quality, oil extraction system and refining process [3]. For these reasons, the determination of these minor components is of great value in establishing the oil genuineness and quality [3,5], having also a marked influence on typicality, flavour, aroma and shelf-life [6].

Vegetable oils contain linear alcohols [7], which are constituted by primary fatty alcohols having generally 20–32 carbon atoms in the alkyl chain. Triterpene alcohols, also known as 4,4′-dimethylsterols, have a steroid structure and are present at different levels in all vegetable lipids [7]. Other alcohols, as phytol, are generated as artifacts of lipid saponification [7].

Long chain aliphatic and triterpene alcohols in vegetable oils have been normally analyzed by GC with flame ionization detection (FID) [8–23] and with MS detection [8,9,12,13,22–24]. Their contents, established by GC-FID, jointly with the contents of other minor components, have been used to distinguish virgin olive oils according to their genetic variety [14–18,20], geographical origin [21] and maturity stage [21], and to detect olive oil adulteration with hazelnut oil [19,22,25–26]. The differences in the contents of these alcohols in olive seed, pulp and fruit oils have been also described [17].

On the other hand, HPLC has been scarcely used to analyze the alcoholic fraction of oils [27]. Due to the low absorbance of these compounds in the UV, Cortesi et al. [27] have derivatized aliphatic and triterpene alcohols with 3,5-dinitrobenzoyl chloride. By using MS with either electrospray ionization (ESI) or atmospheric pressure chemical ionization (APCI), fatty alcohols are not detected [28,29]. Along the last years, APCI-MS has gained interest in sterol characterization [30–33].

The derivatization of fatty alcohols with symmetric cyclic anhydrides, including maleic [28] and phthalic [29,34,35] anhydrides, previous to RP-HPLC has been proposed. Fatty alcohol derivatization with these anhydrides is speeded up by suspending grinded urea in the reaction medium [28,29].

* Corresponding author. Tel.: +34 9635 43176; fax: +34 9635 44436.
E-mail address: ernesto.simo@uv.es (E.F. Simó-Alfonso).

0021-9673/$ – see front matter © 2008 Elsevier B.V. All rights reserved.
doi:10.1016/j.chroma.2008.11.056

Table 1
Botanical origin, number of samples and brand of the vegetable oil samples used in this work.

Origin	Number of samples	Brand
Hazelnut	4	Guinama
Sunflower	2	Koipesol
	2	Hacendado
Corn	2	Guinama
Corn germ	1	Guinama
	1	Hacendado
Extra	1	Carbonell
virgen olive	1	Grupo Hojiblanca
	1	Borges
	1	Torrereal
Soybean	2	Guinama
	2	Biolasi
Peanut	4	Guinama
Grapeseed	4	Guinama

In this work, an RP-HPLC method to characterize the alcoholic fraction extracted from oils with different botanical origins has been developed. Previous to HPLC separation, the alcoholic fraction was esterified with diphenic anhydride. Esterification was carried out in tetrahydrofuran (THF), and was shown to be speeded up in the presence of urea. Both UV–vis and MS detection were implemented. The application of linear discriminant analysis (LDA) to the resulting alcohol data profiles obtained by HPLC-MS was used to classify oils from seven different botanical origins.

2. Experimental

2.1. Reagents and samples

The following analytical grade reagents were used: ammonium hydroxide, acetic acid, methanol (MeOH), ethanol, acetonitrile (ACN), THF, anhydrous sodium sulphate (Sharlau, Barcelona, Spain), urea (99.5%, Fluka, Buchs, Switzerland), diethyl ether, chloroform (J.T. Baker, Deventer, The Netherlands), KOH (Probus, Barcelona, Spain), *n*-hexane (Riedel-de Haën, Seelze, Germany), 2,7-dichlorofluorescein (Sigma, St. Louis, MO, USA) and diphenic anhydride (98%, Aldrich, Milwaukee, WI, USA). The following linear alcohols were used as standards: 1-hexadecanol (C16, Sigma–Aldrich), 1-octadecanol (C18, Fluka), 1-docosanol (C22), 1-tetracosanol (C24) and 1-hexacosanol (C26) (Sigma). Glass plates for thin-layer chromatography (TLC), coated with silica gel without fluorescent indicador (0.25 mm plate thickness, Merck, Darmstadt, Germany) were used. Deionized water (Barnstead deionizer, Sybron, Boston, MA, USA) was also used. The vegetable oils employed in this study (Table 1) were either purchased at the local market or kindly donated by the manufacturers. The botanical origin and quality grade of all the samples were guaranteed by the suppliers.

2.2. Instrumentation and working conditions

A 1100 series liquid chromatograph provided with a quaternary pump and UV–vis diode array detection (Agilent Technologies, Waldbronn, Germany), was used. Separation was carried out with a C8 fused-core type column (Ascentis-Express, 2.7 μm, 15 cm × 4.6 mm I.D., Supelco, Bellefonte, PA, USA). Mobile phases were prepared by mixing ACN and water, both containing 0.1% acetic acid. Elution was performed isocratically with 90% ACN for 25 min, followed by a linear gradient from 90% to 100% ACN for 10 min, and by isocratic elution with 100% ACN for 10 more min. UV–vis detection was performed at 200 ± 10 nm (360 ± 60 nm as reference). In all cases, 40 μL was injected, being the flow rate 1 mL min^{-1}.

The liquid chromatograph was also coupled (in series with the UV–vis detector) to the ESI source of an HP 1100 series ion trap mass spectrometer (ITMS) (Agilent). The ITMS working conditions were: nebulizer gas pressure, 0.24 MPa (35 psi); drying gas flow, 7 L min^{-1} at 300 °C; capillary voltage, 2.5 kV; voltages of skimmers 1 and 2, −41.0 and −6.0 V, respectively. Nitrogen was used as nebulizer and drying gas (Gaslab NG LCMS 20 generator, Equcien, Madrid, Spain). The mass spectrometer was scanned within the *m/z* 300–800 range in the negative-ion mode. The ion trap target mass was set at *m/z* 605 ($[M-H]^-$ peak of the diphenic hemiester of C26). Maximum loading of the ion trap was 3×10^4 counts, and maximum collection time was 300 ms. To enhance sensitivity in the detection of the $[M-H]^-$ ions of the hemiesters, the pH of the eluate was increased. For this purpose, a T union located after the UV–vis detector and before the ESI source, and an auxiliary isocratic HPLC pump set at 0.1 mL min^{-1}, were used to mix the eluate with a 0.01 M NH_3 stream. Total ion chromatograms (TIC) and extracted ion chromatograms (EIC) were smoothed using a gaussian filter set at 9 points.

2.3. Sample preparation and data treatment

The alcoholic fraction of vegetable oils was obtained following the procedure established by the European Union [36]. Accordingly, 5 g oil was saponified by refluxing with 2 M ethanolic KOH for 20 min; 50 mL distilled water was added and the non-saponifiable fraction was extracted three times with diethyl ether. The extracts were combined and washed in a separatory funnel with distilled water (50 mL each time) until neutral reaction. The organic layer was dried with anhydrous sodium sulphate, filtered and evaporated to dryness using a rotatory evaporator. The remaining unsaponifiables were dissolved in 2 mL chloroform and the alcoholic fraction was separated by TLC using a plate-developing chamber containing 60:40 (v/v) hexane/diethyl ether. After TLC separation, the silica plate was sprayed lightly and uniformly with 2,7-dichlorofluorescein. The two bands containing, respectively, the aliphatic and triterpene alcohols were removed from the plate using a spatula. Both bands were jointly suspended in 4 mL THF and introduced in a screw-cap tube (15 mL, 15 cm long) also containing 0.45 g diphenic anhydride and 0.25 g finely grinded urea. The tube was shaken and introduced in a thermostatic bath at 60 °C for 120 min. After cooling, 2 mL of a 2:1 (v/v) MeOH/water mixture containing 0.1 M NH_3 was added. The suspension was sonicated for 15 min and passed through a 0.45 μm pore-size nylon filter (Albet, Barcelona, Spain). The solution was immediately injected in the chromatograph or stored in a freezer.

All the alcoholic extracts were injected at least three times. The peak area of each alcohol derivative was measured from the smoothed EIC, and a data matrix was constructed using the areas of all the peaks as original variables. After normalization of the variables, statistical data treatment was performed using SPSS (v. 15.0, Statistical Package for the Social Sciences, Chicago, IL, USA).

3. Results and discussion

3.1. Optimization of the esterification procedure

The esterification reaction is illustrated in Fig. 1. The resulting hemiester provides not only a chromophore group with a large molar absorptivity, but also a negative charge, which further

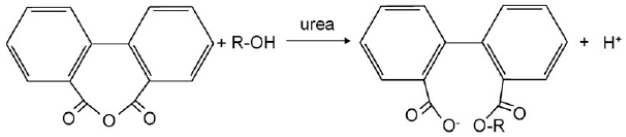

Fig. 1. Esterification reaction with diphenic anhydride.

enhances MS detection. Derivatization of the standards of linear alcohols was performed with a large excess of diphenic anhydride. Owing to the low solubilities of long-chain aliphatic alcohols and triterpenic alcohols in most organic solvents, THF was selected as a reaction medium. Since the boiling point of THF was quite low (66 °C), the thermostatic bath temperature was set at 60 °C; 4 mL portions of a solution containing 10 mg of each alcohol standard were derivatized. Derivatization was performed with and without the presence of finely grinded urea. The peaks of the derivatives increased at least two times when urea was present. Enhancements of the reaction rates and yields have been also reported for the derivatization of fatty alcohols and ethoxylated fatty alcohols with maleic and phthalic anhydrides [28,29]. The addition of 0.25 g urea was found to be adequate.

As described in Section 2.3, the reaction time and yield were optimized by derivatizing a mixture of the alcohol standards (10 mg each). A series of eight screw-cap tubes were prepared. From these, a tube was removed from the thermostatic bath every 15 min, diluted, filtered and an aliquot was injected. Isocratic elution with ACN/water (90:10) containing 0.1 % acetic acid was used. The reaction yield increased when the reaction time increased, and a plateau was reached at 100 min. To assure a maximal reaction yield, 120 min was selected. Using isocratic elution, a linear dependence of log k with the number of carbon atoms in the alkyl chain of the alcohols was observed, being the retention time comprised between 6.7 and 56.5 min for C16 and C26, respectively.

3.2. Optimization of the HPLC separation of the hemiesters

Since the standards of most aliphatic and triterpene alcohols are either unavailable or have a high-cost, the optimization of the HPLC separation was performed using an extract of extra virgin olive oil. Under isocratic elution conditions (90:10 ACN/water), straight identification of the peaks of the C24 and C26 alcohols was performed; however, many other peaks were also observed. In order to identify these peaks, MS detection was coupled in series to the HPLC-UV–vis system. Using the EICs at the m/z values of Table 2, peaks corresponding to several triterpene alcohols, phytol and 4-methylsterols were identified in the 9–25 min range. Peaks corresponding to linear alcohols having retention times higher than 90 min were also observed. In order to speed up the elution of the heavier alcohols, gradient elution was implemented. Elution was performed isocratically with 90% ACN for 25 min, followed by a linear gradient from 90% to 100% ACN for 10 min, and by isocratic elution with 100% ACN for 10 min more. The TIC and EICs of an extra virgin olive and sunflower oil extracts are shown in Figs. 2 and 3, respectively. Using the information provided by MS detection, peaks on the chromatograms obtained with UV–vis detection were also identified. A UV–vis chromatogram of the extra virgin olive oil sample (whose mass spectrum is shown in Fig. 2) is shown in Fig. 4. Then, the derivatized extracts of all the other vegetable oils were also injected in the optimized conditions. Several differences between the peak profiles obtained with oils having different botanical origins were evidenced (see Figs. 2 and 3).

3.3. Selection and normalization of the variables for LDA classification

In order to reduce the variability associated to the total amount of alcohols recovered from the oil samples, and to minimize other sources of variance also affecting the sum of the areas of all the peaks, normalized rather than absolute peak areas were used. In order to normalize the variables, the area of each peak taken from the corresponding EIC was divided by each one of the areas of the other 27 peaks (also taken from their EICs); in this way, and taking into account that each pair of peaks should be considered only once,

Table 2
Type, peak labelling, m/z value and possible compound of the alcohols studied in this work.

Type	Peak labelling	m/z[a]	Possible compound
Linear alcohols	1	493	1-Octadecanol (C18)
	2a	521	1-Eicosanol (C20)
	3	549	1-Docosanol (C22)
	4	563	1-Tricosanol (C23)
	5	577	1-Tetracosanol (C24)
	6	591	1-Pentacosanol (C25)
	7	605	1-Hexacosanol (C26)
	8	619	1-Heptacosanol (C27)
	9	633	1-Octacosanol (C28)
	10	647	1-Nonacosanol (C29)
	11	661	Tricontanol (C30)
4-Methylsterols	12	513	Geranylgeraniol
	13a–13d	649	Obtusifoliol, cycloeucalenol, citrostadienol
Diterpene alcohol	14	519	Phytol
Triterpene alcohols	13a–13d	649	Cycloartenol, α-amyrin, β-amyrin, taraxerol, dammaradienol, lupeol butyrospermol, parkeol
	15	651	Cycloartanol, lanostenol
	16	661	24-Methylenecycloartanol
	17	663	24-Methylenelanost-9(11)-enol, cyclolaudenol, cyclobranol
Unknown	2b–2c	521	Unknown

[a] m/z Value corresponding to the $[M-H]^-$ peak of the hemiester of the alcohol.

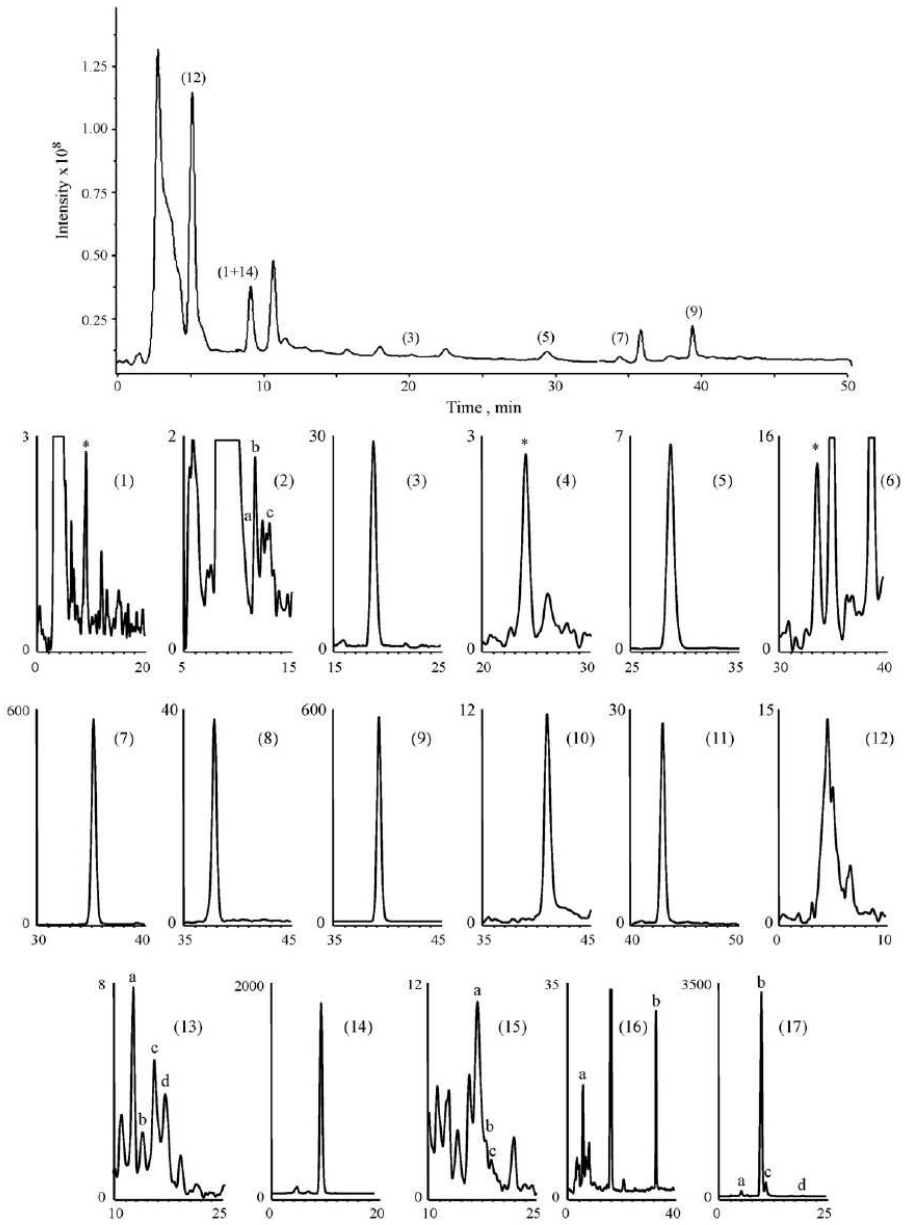

Fig. 2. TIC and EICs of an extract of a sample of extra virgin olive oil. EIC intensity scales are multiplied by 10^4. Between parenthesis, peak labelling according to Table 2. The EICs were obtained at the *m/z* values also indicated in Table 2; when the EIC contains more than one peak, the peak used for data analysis is indicated with an asterisk or with low case characters. Mobile phase: 90% ACN for 20 min, followed by a linear gradient up to 100% ACN for 10 min and 100% ACN for 20 min more.

$(28 \times 27)/2 = 378$ non-redundant peak ratios were obtained to be used as variables.

3.4. Construction of the data matrices and LDA models

LDA, a supervised classificatory technique, is widely recognized as an excellent tool to obtain vectors showing the maximal resolution between a set of previously defined categories. In LDA, vectors minimizing the Wilks' lambda, $\lambda_{w,}$ are obtained [37]. This parameter is calculated as the sum of squares of the distances between points belonging to the same category divided by the total sum of squares. Values of λ_w approaching zero are obtained with well-resolved categories, whereas overlapped categories made λ_w to approach one. Up to N-1 discriminant vectors are constructed by

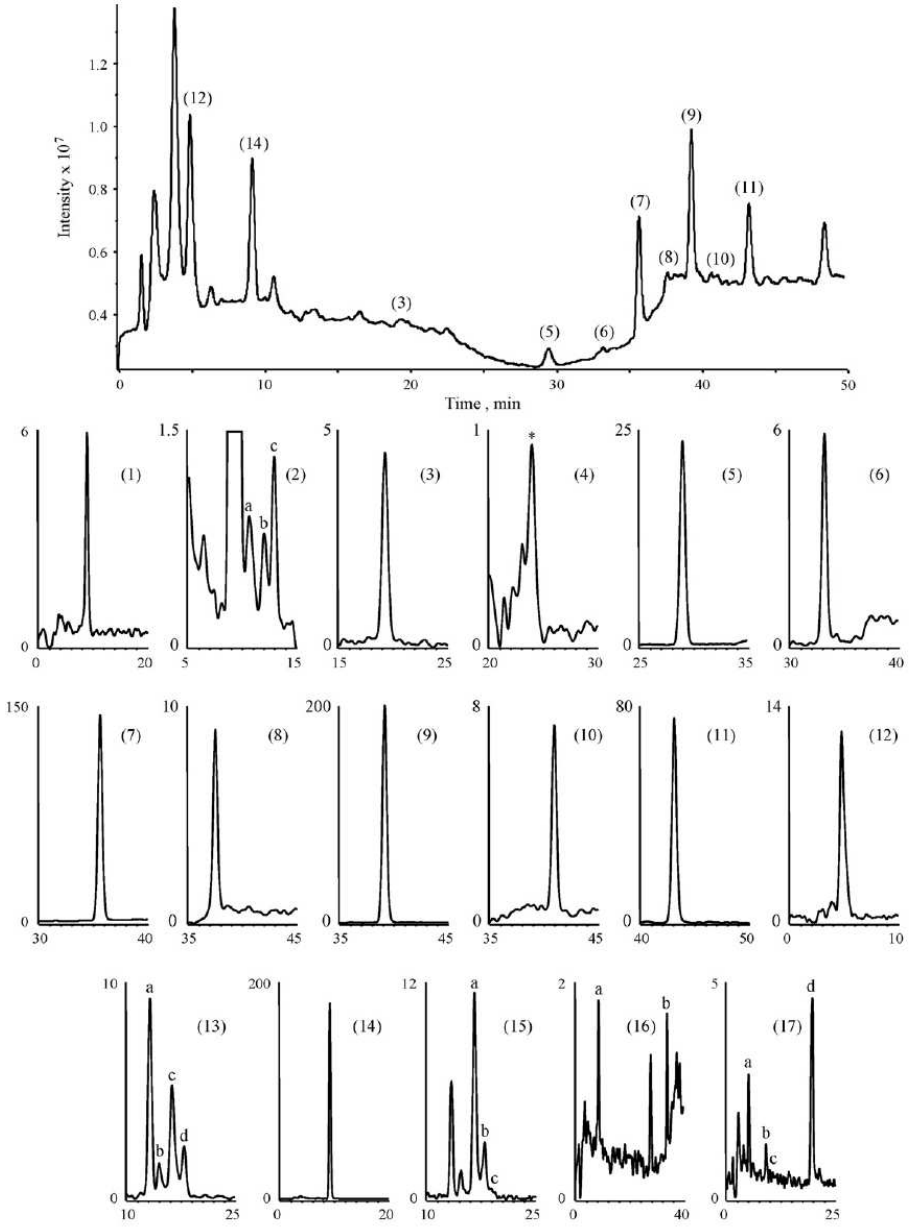

Fig. 3. TIC and EICs of a sunflower oil extract. Other details are as in Fig. 2.

LDA, N being the lowest value for either the number of predictors or the number of categories.

Using the normalized variables, LDA models capable of classifying the oil samples according to their respective botanical origins were constructed. First, from the 28 samples of Table 1, matrices containing 84 injections each (all samples were injected three times), were constructed. Oil classification models were constructed by using the peak ratios provided either by the linear fatty alcohols, the 4-methylsterols plus the triterpene alcohols and phytol, or all the alcohol peaks at a time. For this purpose, three matrices containing either 55, 136 or 378 predictors, respectively, were constructed. A response column, containing the seven categories corresponding to the seven botanical origins of the oils (corn and corn germ were considered as a single category), was added to each matrix. These matrices were used as evaluation sets. To construct LDA training matrices, only the means of the replicates

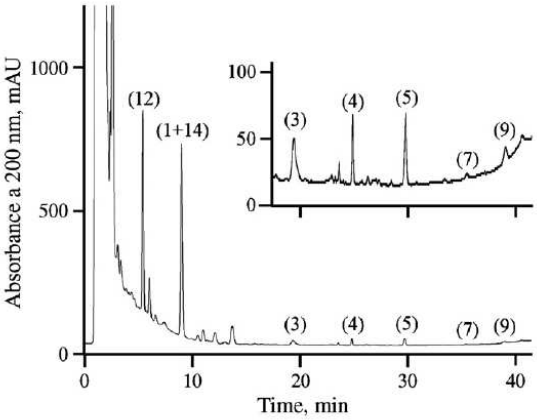

Fig. 4. UV–vis chromatogram of an extract of the same sample of extra virgin olive oil as in Fig. 2. Other details are as in Fig. 2.

of the samples were included (28 objects in each matrix); in this way, the internal dispersion of the categories was reduced, which was important to reduce the number of variables selected by the SPSS stepwise algorithm during model construction. According to this algorithm, a predictor is selected when the reduction of λ_w produced after its inclusion in the model exceeds F_{in}, the entrance threshold of a test of comparison of variances or F-test. However, the entrance of a new predictor modifies the significance of those predictors which are already present in the model. For this reason, after the inclusion of a new predictor, a rejection threshold, F_{out}, is used to decide if one of the other predictors should be removed from the model. The process terminates when there are no predictors entering or being eliminated from the model. The values of F_{in} and F_{out}, 3.84 and 2.71, respectively, were adopted.

First, an LDA model was constructed exclusively using the normalized peak areas of the linear alcohols as predictors. A poor resolution between the category pairs ($\lambda_w = 0.708$) was obtained; further, four objects of the evaluation set were not correctly assigned. Then, another LDA model was constructed using the normalized peaks of 4-methylsterols, triterpene alcohols and phytol as predictors. With this model, resolution between the category pairs improved largely ($\lambda_w = 0.327$). Finally, another LDA model was constructed using all the available predictors. In this case, an excellent resolution between all the category pairs was achieved (Fig. 4, $\lambda_w = 0.163$). The variables selected by the SPSS stepwise algorithm, and the corresponding standardized coefficients of this model, showing the predictors with large discriminant capabilities, are given in Table 3. As shown in Fig. 5A, an extremely large resolution among the three following groups of categories was achieved along f_1: corn–hazelnut–grapeseed,

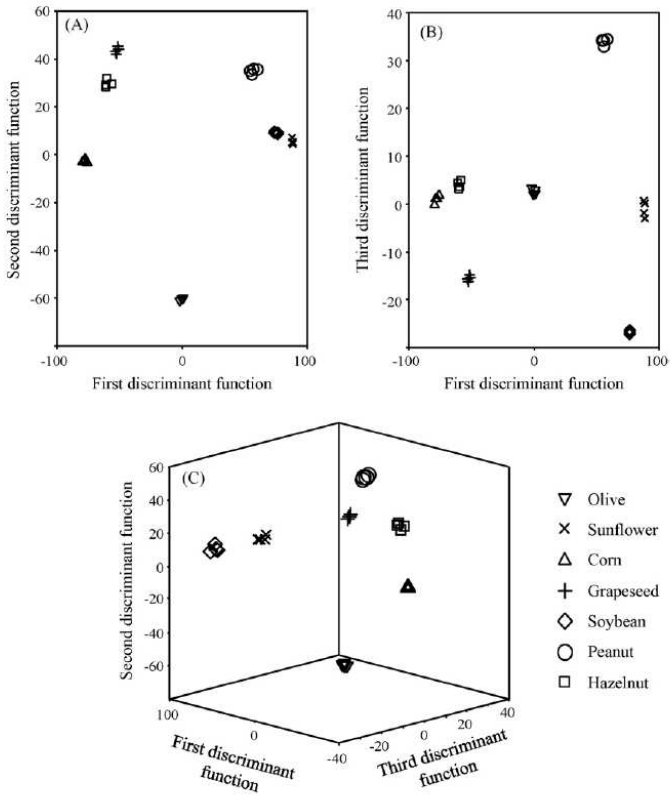

Fig. 5. Score plots on the planes of the first and second (A), and first and third discriminant functions (B), and on an oblique plane of the three-dimensional space defined by the three first discriminant functions (C) of the LDA model constructed to classify vegetable oils according to their botanical origin.

Table 3
Predictors selected and corresponding standardized coefficients of the LDA model constructed to predict the botanical origin of the oil samples.

Predictors[a]	f_1	f_2	f_3	f_4	f_5	f_6
513/651b	−8.22	7.07	4.33	8.21	7.28	3.96
663c/649a	−1.39	−0.48	16.6	−9.75	−5.37	−1.63
663d/649c	−12.2	−1.23	−1.30	−0.39	−1.50	−0.34
649a/649b	−5.21	−2.10	0.51	−0.77	−1.65	−0.74
649b/493	2.45	−7.24	−2.26	−0.63	−0.78	−0.64
649d/651b	30.7	3.45	1.15	0.57	−1.76	−0.75
521b/591	14.9	−0.43	−0.12	2.07	0.79	−0.21
649b/513	−27.6	5.84	0.02	−5.27	0.01	−0.38
649c/513	15.9	−2.78	−2.99	2.51	0.28	−0.86
521b/519	−18.0	2.12	6.00	1.23	1.47	0.69
549/513	−0.69	13.2	−14.4	12.3	9.50	4.13
549/649b	11.6	−2.02	−4.98	−1.54	−1.68	−0.26

[a] m/z Values of the peak pairs.

olive and soybean–peanut–sunflower. As deduced from Table 3, f_1 was mainly constructed with the peak area ratios 649d/651b and 649b/513. On the other hand, the variance gathered by f_2 was mainly associated to the resolution between olive oil and the rest of categories as a whole. According to Fig. 5B, peanut, soybean and grapeseed categories were well resolved from each other and with respect to the rest of categories along f_3. Finally, as illustrated in Fig. 5C, by using a plane oblique to the three first discriminant functions, all the possible pair of categories were very well resolved from each other. For this model, and using leave-one-out validation, all the points of the training set were correctly classified. The corresponding evaluation set, containing the 84 original data points, was then used to check the prediction capability of the model. Using a 95% probability, all the objects were correctly assigned; thus, the prediction capability of the model was 100%.

4. Conclusions

A method for the separation and identification of aliphatic and triterpenic alcohols in vegetable oils by RP-HPLC with UV–vis and MS detection, in a single run, has been described. To enhance UV–vis and MS sensitivities, derivatization with diphenic anhydride, which simultaneously provides both a chromophore and a charge, has been developed. Further, it has been shown how vegetable oils can be successfully classified according to their botanical origin by multivariate LDA of the resulting HPLC-MS data. By using leave-one-out cross-validation all the samples were correctly classified with a prediction probability higher than 95%. Thus, the proposed method is of interest for quality control purposes in the vegetable oil industry.

Acknowledgements

Work supported by project CTQ2007-61445 (MEC of Spain and FEDER funds). M.J.L.-G. thanks the Generalitat Valenciana for an FPI grant for PhD studies.

References

[1] G. Morchio, G. Amelotti, A. Bocca, V. Bovio, L. Conte, O. Cozzoli, L. Cremonesi, R. Fascioli, L. Giro, D. Grieco, G. Lercker, C. Mariani, G. Pierattini, E. Sarti, P. Zunin, Riv. Ital. Sostanze Grasse 66 (1989) 531.
[2] C. Mariani, G. Bellan, K. Grob, Riv. Ital. Sostanze Grasse 72 (1995) 97.
[3] A. Cert, W. Moreda, M.C. Pérez-Camino, J. Chromatogr. A 881 (2000) 131.
[4] R. Aparicio, R. Aparicio-Ruiz, J. Chromatogr. A 881 (2000) 93.
[5] R. Aparicio, in: J.L. Harwood, R. Aparicio (Eds.), Handbook of Olive Oil: Analysis and Properties, Aspen, Gaithersburg, MD, 1999, p. 285.
[6] A.K. Kiritsakis, Olive Oil Handbook, American Oil Chemists' Society, Champaign, IL, 1998, p. 20.
[7] G. Lercker, M.T. Rodriguez-Estrada, J. Chromatogr. A 881 (2000) 105.
[8] T. Itoh, K. Yoshida, T. Yatsu, T. Tamura, T. Matsumoto, G.H. Spencer, J. Am. Oil Chem. Soc. 58 (1981) 545.
[9] A.M.F. Abou Hadeed, A.R. Kotb, C.E.J. Daniels, Food Chem. 35 (1990) 167.
[10] C. Mariani, E. Fedeli, K. Grob, Riv. Ital. Sostanze Grasse 68 (1991) 233.
[11] D. Chryssafidis, P. Maggos, V. Kiosseoglou, D. Boskou, J. Sci. Food Agric. 58 (1992) 581.
[12] H. Ntsourankoua, J. Artaud, M. Guerere, Fr. Ann. Fals. Expert. Chim. Toxicol 87 (1994) 91.
[13] A. Lanzon, T. Albi, A. Guinda, J. Am. Oil Chem. Soc. 76 (1999) 1421.
[14] E. Stefanoudaki, F. Kotsifaki, A. Koutsaftakis, J. Sci. Food Agric. 80 (2000) 381.
[15] J. Giacometti, Analyst 126 (2001) 472.
[16] G. Bianchi, L. Giansante, A. Shaw, D.B. Kell, Eur. J. Lipid Sci. Technol. 103 (2001) 141.
[17] A. Ranalli, L. Pollastri, S. Contento, G. Di Loreto, E. Lannucci, L. Lucera, F. Russi, J. Sci. Food Agric. 82 (2002) 854.
[18] L. Giansante, D. Di Vicenzo, G. Bianchi, J. Sci. Food Agric. 83 (2003) 905.
[19] P.L. Benitez-Sánchez, M. León-Camacho, R. Aparicio, Eur. Food Res. Technol. 218 (2003) 13.
[20] R.M. Rivera del Álamo, G. Fregapane, F. Aranda, S. Gómez-Alonso, M.D. Salvador, Food Chem. 84 (2004) 533.
[21] A. Lazzez, E. Perri, M.A. Caravita, M. Khlif, M. Cossentini, J. Agric. Food Chem. 56 (2008) 982.
[22] S. Azadmard-Damirchi, G.P. Savage, P.C. Dutta, J. Am. Oil Chem. Soc. 82 (2005) 717.
[23] T.C. Sindhu-Kanya, L. Jaganmohan-Rao, M.C. Shamanthaka-Sastry, Food Chem. 101 (2007) 1552.
[24] S.S. Cunha, J.O. Fernandes, M. Beatriz, P.P. Oliveira, J. Chromatogr. A 1128 (2006) 220.
[25] C. Mariani, G. Bellan, G. Morchio, A. Pellegrino, Riv. Ital. Sostanze Grasse 76 (1999) 297.
[26] S. Vichi, L. Pizzale, E. Toffano, R. Bortolomeazzi, L. Conte, J. Assoc. Offic. Anal. Chem. Int. 84 (2001) 1534.
[27] N. Cortesi, M.G. Fusetti, E. Fedeli, Riv. Ital. Sostanze Grasse 64 (1987) 513.
[28] A. Micó-Tormos, C. Collado-Soriano, J.R. Torres-Lapasió, E. Simó-Alfonso, G. Ramis-Ramos, J. Chromatogr. A 1180 (2008) 32.
[29] A. Micó-Tormos, E. Simó-Alfonso, G. Ramis-Ramos, J. Chromatogr. A 1203 (2008) 47–53.
[30] K. Nagy, D. Bongiorno, G. Avellone, P. Agozzino, L. Ceraulo, J. Vékey, J. Chromatogr. A 1078 (2005) 90.
[31] J.L. Martinez-Vidal, A. Garrido-Frenich, M.A. Escobar-Garcia, R. Romero-Gonzalez, Chromatographia 65 (2007) 695.
[32] B. Canabate-Diaz, A. Segura-Carretero, A. Fernandez-Gutierrez, A. Belmonte-Vega, A. Garrido-Frenich, J.L. Martinez-Vidal, J. Duran-Martos, Food Chem. 102 (2007) 593.
[33] B. Lu, Y. Zhang, X. Wu, J. Shi, Anal. Chim. Acta 588 (2007) 50.
[34] R.A. Wallingford, Anal. Chem. 68 (1996) 2541.
[35] C.J. Sparham, I.D. Bromilow, J.R. Dean, J. Chromatogr. A 1062 (2005) 39.
[36] Commission Regulation (EC) no. 796/2002 of 6 May 2002, European Union, Brussels, Off. J. Eur. Union, L128 annex XIX (2002) 23.
[37] B.G.M. Vandeginste, D.L. Massart, L.M.C. Buydens, S. De Jong, P.J. Lewi, J. Smeyers-Verbeke, Data Handling in Science and Technology, Part B, Elsevier, Amsterdam, 1998, p. 237.

ANEXO VIII

RAPID COMMUNICATIONS IN MASS SPECTROMETRY
Rapid Commun. Mass Spectrom. 2007; **21**: 3751–3755
Published online in Wiley InterScience (www.interscience.wiley.com) DOI: 10.1002/rcm.3272

RCM

Classification of vegetable oils according to their botanical origin using amino acid profiles established by direct infusion mass spectrometry

María J. Lerma-García*, Guillermo Ramis-Ramos, José M. Herrero-Martínez and Ernesto F. Simó-Alfonso

Department of Analytical Chemistry, Faculty of Chemistry, University of Valencia, 46100 Burjassot, Valencia, Spain

Received 23 July 2007; Revised 14 September 2007; Accepted 14 September 2007

Amino acid profiles, established by direct infusion mass spectrometry, have been used to classify vegetable oils according to their botanical origin. The proteins present in hazelnut, sunflower, corn, soybean, olive, avocado, peanut and grapeseed oils were precipitated with acetone, and the residue was hydrolyzed in acid medium, diluted in a hydrochloric acid/ethanol mixture, and infused into the mass spectrometer. The spectra of the hydrolyzed protein extracts showed $[M+H]^+$ ions of the following amino acids: glycine, alanine, serine, proline, valine, threonine, cysteine, isoleucine + leucine, aspartic acid, lysine, glutamic acid, methionine, histidine, phenylalanine, arginine and tyrosine. These ions were used to construct linear discriminant analysis (LDA) models. The ratios of the ion signal intensities selected by pairs were used as predictors. With the sequential application of three LDA models, the eight botanical origin categories of the samples were well resolved. Copyright © 2007 John Wiley & Sons, Ltd.

Oil authenticity is a very important aspect of quality edible oils. Extra virgin olive oil, due to its high price, is occasionally adulterated with olive oils of lower quality, or with oils of a different botanical origin.[1–6] To establish the authenticity of edible oils a number of chromatographic methods[1,2,6–8] and spectroscopic techniques including fluorescence,[4,9] FTNIR,[10] FTIR,[5,10] FT-Raman,[10] NMR,[11–15] and MS,[1,3,16] followed by multivariate statistical analysis of the data, have been applied. For this purpose, the contents of fatty acids,[8] tocopherols,[9] volatile compounds,[1] and sterols[6] have been used.

The presence of different enzyme activities, which implies the presence of proteins, has been demonstrated in olive oils;[17,18] however, only in few reports have proteins been recognized as components of olive oils.[19–21] The influence of proteins in olive oil stability has been studied. Proteins react with lipid oxidation products, yielding endogenous antioxidants in food systems.[22–24] However, due to their low concentrations, proteins do not seem to play a clear role in oil stability.[25] Polypeptides similar to those found in olive oils have been detected in other vegetable oils,[19] which opens the way to use polypeptides and amino acids to classify the oils according to their botanical origin. Amino acid profiles obtained by protein hydrolysis have been used to classify different categories of samples in art works[26–29] and rice cultivars.[30] The contents of free amino acids have also been used to classify tea samples,[31] to establish the quality of beer,[32] and to characterize fortified wines.[33]

Hidalgo *et al.*[19,20] have developed a method to determine peptides and proteins in fats and oils by precipitation and hydrolysis, followed by amino acid analysis by high-performance liquid chromatography (HPLC) with ultraviolet (UV) detection. Reported protein contents in edible oils vary widely, depending on the type and source of the oil, as well as on the methodology used for extraction and analysis.[25] The total protein content and the amino acid composition in olive fruits of the Arbequina and Picual varieties at three stages of ripening have been studied; significant differences according to either the cultivar or the fruit ripening stage were not found.[21]

In this work, the amino acid profiles of oils of eight different botanical origins, as well as olive oils of different genetic varieties, have been obtained by direct infusion mass spectrometry. The spectral data were used to construct linear discriminant analysis (LDA) models. With the sequential application of three LDA models, the oil samples were well classified with an excellent resolution according to their category of origin.

**Correspondence to*: M. J. Lerma-García, Department of Analytical Chemistry, Faculty of Chemistry, University of Valencia, 46100, Burjassot, Valencia, Spain.
E-mail: mlergar@alumni.uv.es
Contract/grant sponsor: MEC and FEDER; contract/grant number: CTQ2004-06302.
Contract/grant sponsor: Generalitat Valenciana; contract/grant number: ACOMP07-168.

RCM

EXPERIMENTAL

Reagents and samples

Reagent grade acetone, tetrahydrofuran (THF), absolute ethanol (Scharlau, Barcelona, Spain), hydrochloric acid (37%) and 1,4-dioxane (Panreac, Barcelona, Spain) were employed. The amino acids used as standards were alanine (Ala), arginine (Arg), aspartic acid (Asp), glutamic acid (Glu), glycine (Gly), histidine (His), isoleucine (Leu), lysine (Lys), methionine (Met), phenylalanine (Phe), serine (Ser), threonine (Thr), tyrosine (Tyr), valine (Val), proline (Pro) and cysteine (Cys) (Sigma, St. Louis, MO, USA). The vegetable oils and their commercial brands are shown in Table 1. Olive oil samples of the three most important varieties of Spanish production, coming from ten different geographical areas of Spain, and other vegetable oil samples from different areas of Europe and South America, were used. The genetic variety of the olive oils and the botanical and geographical origin of all the samples were guaranteed by the suppliers.

Instrumentation and working conditions

An HP 1100 series ion trap mass spectrometer provided with an electrospray ionization (ESI) source (Agilent Technologies, Waldbronn, Germany) was used. A syringe pump (kdScientific, Holliston, MA, USA) was used to infuse the samples at 0.3 mL h^{-1} (5 μL min^{-1}) through a 50 μm i.d. fused-silica capillary. The mass spectrometer working conditions (adapted from Peris-Vicente *et al.*[29]) were: nebulizer gas pressure, 25 psi; drying gas flow rate, 8 L min^{-1} at a temperature of 250°C; capillary voltage, 3.5 kV; voltages of skimmers 1 and 2, −26.8 V and −6.0 V, respectively. Nitrogen was used as the nebulizer and drying gas (Gaslab NG LCMS 20 generator, Equcien, Madrid, Spain). The mass spectrometer was scanned within the *m/z* 50–300 range in the positive ion mode. The ion trap target mass was set at *m/z* 122 ($[M+H]^+$ of Cys). The maximum loading of the ion trap was 3×10^4 counts, and the maximum collection time was 300 ms.

Table 1. Botanical origin, genetic variety, number of samples and brand of the vegetable oil samples used in this work

Oil sample	Genetic variety	N° of samples	Brand
Hazelnut	Unknown	4	Guinama S.A.
Sunflower	Unknown	2	Koipesol
		2	Hacendado
Corn	Unknown	2	Guinama S.A.
Corn germen	Unknown	1	Guinama S.A.
		1	Hacendado
Soybean	Unknown	2	Guinama S.A.
		2	Biolasi
Olive	Arbequina	2	Carbonell
		2	Torrereal
		2	Oleastrum
		1	Coosur
		1	Grupo Hojiblanca
		2	Borges
		1	Romanico
		1	Valderrama
		1	Veá
		1	Aubocassa
		1	Rihuelo
	Hojiblanca	2	Carbonell
		2	Coosur
		3	Borges
		7	Grupo Hojiblanca
		1	Columela
	Picual	2	Carbonell
		2	Coosur
		3	Borges
		1	Grupo Hojiblanca
		1	Castillo Tabernas
		1	Castillo Canena
Avocado	Unknown	4	Guinama S.A.
Peanut	Unknown	4	Guinama S.A.
Grapeseed	Unknown	4	Guinama S.A.

Procedures

The procedure for the isolation of proteins was taken from Hidalgo *et al.*[19] Briefly, to precipitate the proteins, 40 g oil were weighed and cooled at 18°C for at least 90 min prior to the addition of 98 mL acetone, which had also previously been cooled at 4°C. The mixture was kept at 4°C for 30 min and filtered through a Whatman no. 1 filter paper using a Buchner funnel. The filter paper was extracted by shaking with 5 mL THF followed by 5 mL 1,4-dioxane. The extracts were combined and evaporated to dryness under a nitrogen stream. The residue was dissolved in 100 μL concentrated hydrochloric acid and hydrolyzed for 24 h at 110°C.[29,34] After being allowed to cool, 1 mL aqueous 0.1 M HCl and 1 mL ethanol were added. The mixture was manually shaken, filtered through a 0.45 μm Nylon filter and directly infused into the mass spectrometer. All the extracts were infused at least four times, and each time the spectrum was averaged for 1 min. The statistical treatment of the data was performed using the SPSS package (v. 12.0.1, Statistical Package for the Social Sciences Inc., Chicago, IL, USA).

RESULTS AND DISCUSSION

Amino acid profiles

After protein hydrolysis, the mass spectra of the different oils (Fig. 1) showed the $[M+H]^+$ ions of the following amino acids: Gly (*m/z* 76.1), Ala (*m/z* 90.1), Ser (*m/z* 106.1), Pro (*m/z* 116.1), Val (*m/z* 118.1), Thr (*m/z* 120.1), Cys (*m/z* 122.2), Ile + Leu (*m/z* 132.2), Asp (*m/z* 134.1), Lys (*m/z* 147.2), Glu (*m/z* 148.2), Met (*m/z* 150.2), His (*m/z* 156.2), Phe (*m/z* 166.2), Arg (*m/z* 175.2), and Tyr (*m/z* 182.2). Leu and Ile, which have the same molecular mass, gave a single common peak. Aspargine and glutamine were excluded from this study, since hydrolysis converts them into Asp and Glu.[34] Hydrolysis also leads to a partial conversion of Glu into pyroglutamic acid,[34] and to the degradation of tryptophan.[34] The abundances of these 16 ions were either intermediate or low, but in all cases they were adequate for data analysis. The amino acid profiles observed in the mass spectra differed from the concentration profiles reported by Hidalgo *et al.*[19] The differences were attributed to the different mass spectrometric response factors of the amino acids. This was confirmed by directly infusing amino acid stock solutions. The amino acids with low molecular masses, such as Gly, Ala and Ser, and also Cys, Thr and Asp, gave low sensitivities, whereas the amino acids with high molecular masses (Lys, Met, His, Phe, Arg and Tyr) gave high sensitivities.

DOI: 10.1002/rcm

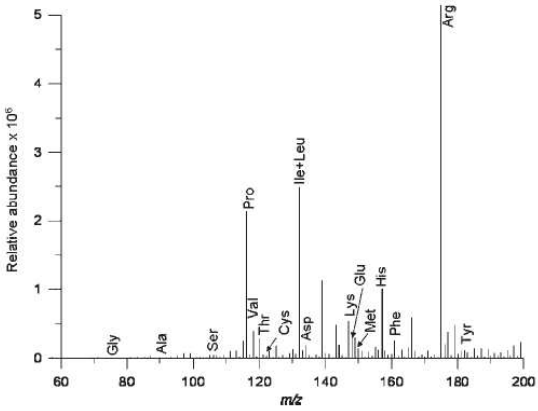

Figure 1. Typical mass spectrum of a hydrolyzed olive oil protein extract. The amino acids studied in this work are indicated.

Normalization of the variables

In order to reduce the variability associated with the total amount of proteins recovered from the oil samples, and to consequently minimize the sources of variance, the normalized rather than the absolute ion abundances were used. Two normalization procedures were tried. In procedure A, the ion abundance of each amino acid peak was divided by the sum of the ion abundances of all the amino acid peaks. In procedure B, the ion abundance of each amino acid peak was divided by each one of the abundances of the other 15 amino acid peaks; in this way, and since any pair of peaks should be considered only once, $(16 \times 15)/2 = 120$ non-redundant peak ratios were obtained.

Construction of the data matrices and LDA models

LDA, a supervised classificatory technique, is an excellent tool for obtaining vectors showing the maximal resolution between categories. In LDA, vectors minimizing the Wilks' lambda, λ_w, are obtained.[35] The λ_w is calculated as the sum of squares of the distances between points belonging to the same category divided by the total sum of squares. Values of λ_w approaching zero are obtained with well-resolved categories, whereas overlapped categories give λ_w approaching one. Up to N – 1 discriminant vectors are constructed by using LDA, with N being the lowest value for either the number of predictors or the number of categories.

Using the normalized variables, LDA models capable of classifying the oil samples according to their botanical origin were constructed. For this purpose, each sample was injected at least four times. Two matrices containing 272 injections each, and 15 or 120 predictors (according to normalization procedures A and B, respectively), were constructed. A response column, containing the eight categories corresponding to the eight botanical origins of the oils, was added to the matrices. These matrices were used as evaluation sets. To construct LDA training matrices, only the means of the replicates of the samples were included; thus, the internal dispersion of the categories was reduced, which was also important in reducing the number of variables selected by the stepwise algorithm during model construction. In addition, only the means of the replicates of each genetic variety of olive oils (Arbequina, Hojiblanca and Picual) were included in the training set. In this way, all categories contained a similar number of data points, which is important to achieve a maximal category resolution along the LDA functions. Thus, in the training matrix, the olive oil category was represented by three data points (one for each genetic variety), while the other categories were represented by four data points each.

To select the predictors to be included in the models, the SPSS stepwise algorithm was used. In this algorithm, a predictor is selected when the reduction of λ_w produced after its inclusion in the model exceeds the entrance threshold of a test of comparison of variances or F-test, F_{in}. However, the entrance of a new predictor modifies the significance of those predictors which are already present in the model. For this reason, after the inclusion of a new predictor, a rejection threshold, F_{out}, is used to decide if one of the other predictors should be removed from the model. The process terminates when there are no predictors entering or being eliminated from the model. The default probability values of F_{in} and F_{out} provided by SPSS, 0.05 and 0.10, respectively, were adopted.

To classify the oils according to the eight botanical varieties of Table 1, two LDA models, one for each normalization procedure, were constructed. Normalization procedure B, which led to a better separation between the categories, was selected. With this procedure, the categories hazelnut, olive and avocado appeared clearly resolved from each other, and were also well separated from the other five categories (sunflower, corn, soybean, peanut and grapeseed), which overlapped. For this reason, a new LDA model was constructed in which these five categories were grouped in a single category. To maintain a similar number of points in the four categories considered in this model (hazelnut, olive, avocado and the one formed by the other oils) only the means of the sunflower, corn, soybean, peanut and grapeseed oils were included in the new category. Excellent resolution between these four categories (hazelnut, olive, avocado and the one formed by the other oils) was obtained (Fig. 2, $\lambda_w = 0.056$). The variables selected by the SPSS stepwise algorithm, and the corresponding model standardized coefficients, showing the predictors with large discriminant capabilities, are given in Table 2. All the points of the training set were correctly classified by leave-one-out cross-validation. The evaluation set, containing the 272 original data points, was used to check the prediction capability of the model. Using a 95% probability, only twelve objects corresponding to replicates of different samples (1 hazelnut, 1 avocado and 10 olive) were not correctly assigned; thus, the prediction capability was 96%.

Next, the hazelnut, olive and avocado categories were removed from the training set, and the remaining categories were used to construct another LDA model. Now, the soybean and peanut categories were separated with excellent resolution, while the other three categories (sunflower, corn and grapeseed) still overlapped. Thus, another LDA model was constructed considering these three unresolved categories as a single one. To maintain a similar number

DOI: 10.1002/rcm

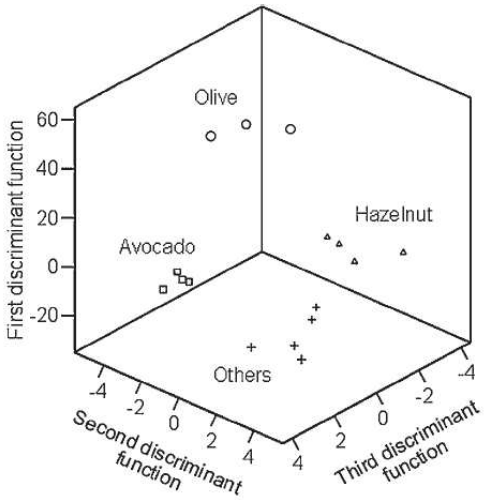

Figure 2. Score plot on an oblique plane of the 3-D space defined by the three discriminant functions of the LDA model constructed to resolve the hazelnut, olive, avocado and 'others' categories. 'Others' is the combined category of the sunflower, corn, soybean, peanut and grapeseed oils.

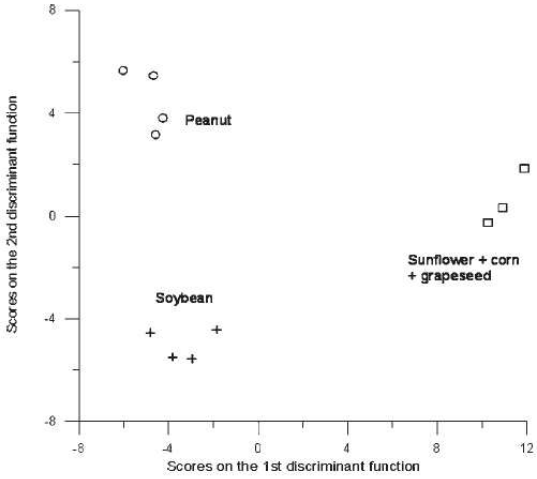

Figure 3. Score plot on the plane of the two discriminant functions of the LDA model constructed to resolve the soybean, peanut and the combined category (sunflower, corn and grapeseed).

of points per category, only the means of the sunflower, corn and grapeseed oils were included in the new category. As shown in Fig. 3, excellent resolution between the three categories was obtained ($\lambda_w = 0.042$). The variables selected and the corresponding model standardized coefficients are also given in Table 2. All the points of the training set were correctly classified by leave-one-out cross-validation. To estimate the prediction capability of the model, the evaluation set, constituted now by 80 original data points, was used. Using a 95% probability, only three objects, which corresponded to replicates of different samples, were not correctly assigned; thus, the prediction capability was 96%.

Finally, to resolve the sunflower, corn and grapeseed categories, a third LDA model was constructed. However, a model with many predictors was obtained. Thus, in order to reduce the number of predictors in the model, the value of the probability of the entrance test was reduced to $F_{in} = 0.02$. As shown in Fig. 4, satisfactory resolution among the three categories was achieved ($\lambda_w = 0.279$). The variables selected and the corresponding model standardized coefficients are also given in Table 2. All the points of the training set were correctly classified by leave-one-out cross-validation. Using a 95% probability, only three objects from a total of 48

Table 2. Predictors selected and the corresponding standardized coefficients of the three sequential LDA models constructed

	Hazelnut/olive avocado/sunflower + corn + soybean + peanut + grapeseed			Soybean/peanut/ sunflower + corn + grapeseed		Sunflower/corn/ grapeseed	
Predictor[a]	f_1	f_2	f_3	f_1	f_2	f_1	f_2
118.1/76.1	8.07	5.94	0.08	—	—	—	—
150.2/106.1	—	—	—	—	—	−2.18	0.69
148.2/116.1	−1.12	3.85	1.54	—	—	—	—
175.2/116.1	—	—	—	—	—	−3.81	0.26
120.1/118.1	4.56	0.35	0.31	2.93	1.45	—	—
156.2/118.1	—	—	—	−2.17	−1.35	—	—
122.2/120.1	—	—	—	—	—	4.54	−0.87
132.2/122.2	10.42	3.73	3.71	—	—	—	—
175.2/122.2	−13.81	−6.80	−2.72	—	—	—	—
147.2/132.2	—	—	—	−2.17	0.26	—	—
150.2/132.2	7.56	4.88	−0.81	—	—	—	—
156.2/134.1	—	—	—	—	—	2.42	0.46
175.2/156.2	−8.12	−1.18	2.27	—	—	—	—
182.2/156.2	—	—	—	1.43	−0.22	—	—
175.2/166.2	13.09	5.96	−2.42	—	—	—	—

[a] m/z values of the amino acid ions used in calculation of ratios.

Rapid Commun. Mass Spectrom. 2007; **21**: 3751–3755
DOI: 10.1002/rcm

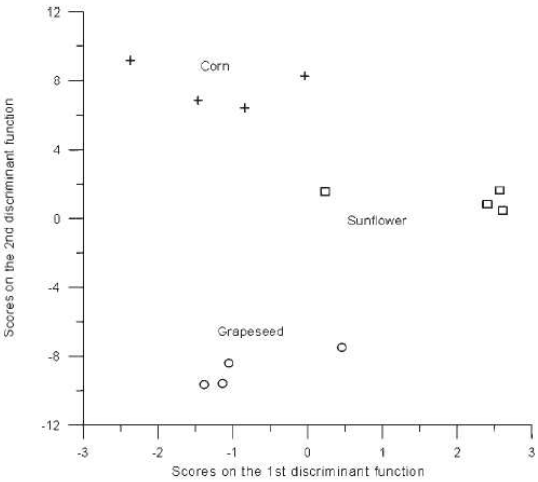

Figure 4. Score plot on the plane of the two discriminant functions of the LDA model constructed to resolve the sunflower, corn and grapeseed categories.

original data points of the evaluation set, corresponding to replicates of different samples, were not correctly assigned; thus, the prediction capability of the model was 94%. Therefore, the vegetable oils belonging to the eight different botanical origins were correctly classified with high reliability by the sequential application of three LDA models. In terms of resolution between oil origin categories, the proposed method yields similar results to those reported by using ^{31}P- and ^{1}H-NMR of diglycerides.[12]

In addition, an attempt to classify olive oils according to their genetic variety was made. All the replicates of the olive oil samples of Table 1 were used; however, an LDA model capable of classifying the genetic varieties of olive oils according to their amino acid profiles was not found ($\lambda_w = 0.982$). This agrees with the results reported by Zamora *et al.*,[21] who did not find a significant variability between the amino acid concentration profiles belonging to different genetic varieties.

CONCLUSIONS

The possibility of classifying vegetable oils according to their botanical origin by using amino acid profiles has been demonstrated. After precipitation and hydrolysis of the proteins, the peak profiles obtained by direct infusion of the amino acid extracts into a mass spectrometer were used. We have shown that vegetable oils belonging to a large number of botanical origins can be correctly classified with a high reliability by the sequential application of LDA models. The wide variety of geographical origins and genetic varieties warrants the applicability of the proposed methodology. However, and in agreement with Zamora *et al.*,[21] olive oils with different genetic varieties were not distinguished.

Acknowledgements

Supported by Projects CTQ2004-06302 (MEC and FEDER funds) and ACOMP07-168 (Generalitat Valenciana). MJL-G also thanks the Generalitat Valenciana for a FPI grant for PhD studies.

REFERENCES

1. Marcos-Lorenzo I, Pérez-Pavón JL, Fernández-Laespada ME, García-Pinto C, Moreno-Cordero B. *J. Chromatogr. A* 2002; **945**: 221.
2. Hajimahmoodi M, Vander Heyden Y, Sadeghi N, Jannat B, Oveisi MR, Shahbazian S. *Talanta* 2005; **66**: 1108.
3. Catharino RR, Haddad R, Cabrini LG, Cunha IBS, Sawaya CHF, Eberlin MN. *Anal. Chem.* 2005; **77**: 7429.
4. Poulli KI, Mousdis GA, Georgiou CA. *Anal. Bioanal. Chem.* 2006; **386**: 1571.
5. Vlachos N, Skopelitis Y, Psaroudaki M, Konstantinidou V, Chatzilazarou A, Tegou E. *Anal. Chim. Acta* 2006; **573**: 459.
6. Mariani C, Bellan G, Lestini E, Aparicio R. *Eur. Food Res. Technol.* 2006; **223**: 655.
7. Cert A, Moreda W, Pérez-Camino MC. *J. Chromatogr. A* 2000; **881**: 131.
8. Brodnjak-Voncina D, Kodba ZC, Novic M. *Chemom. Intell. Lab. Syst.* 2005; **75**: 31.
9. Sikorska E, Górecki T, Khmelinskii IV, Sikorski M, Koziol J. *Food Chem.* 2005; **89**: 217.
10. Yang H, Irudayaraj J, Paradkar MM. *Food Chem.* 2005; **93**: 25.
11. Zamora R, Gómez G, Dobarganes MC, Hidalgo FJ. *J. Am. Oil Chem. Soc.* 2002; **79**: 267.
12. Vigli G, Philippidis A, Spyros A, Dais P. *J. Agric. Food Chem.* 2003; **51**: 5715.
13. García-González DL, Mannina L, DImperio M, Segre AL, Aparicio R. *Eur. Food Res. Technol.* 2004; **219**: 545.
14. Fragaki G, Spyros A, Siragakis G, Salivaras E, Dais P. *J. Agric. Food Chem.* 2005; **53**: 2810.
15. Dais P, Spyros A. *Magn. Reson. Chem.* 2007; **45**: 367.
16. Lay JO, Liyanage R, Durham B, Brooks J. *Rapid Commun. Mass Spectrom.* 2006; **20**: 952.
17. Georgalaki MD, Sotiroudis TG, Xenakis A. *J. Am. Oil Chem. Soc.* 1998; **75**: 155.
18. Georgalaki MD, Bachmann A, Sotiroudis TG, Xenakis A, Porzel A, Feussner I. *Fett/Lipid* 1998; **100**: 554.
19. Hidalgo FJ, Zamora R. *Anal. Chem.* 2001; **73**: 698.
20. Hidalgo FJ, Alaiz M, Zamora R. *J. Am. Oil Chem. Soc.* 2002; **7**: 685.
21. Zamora R, Alaiz M, Hidalgo FJ. *J. Agric. Food Chem.* 2001; **49**: 4267.
22. Zamora R, Alaiz M, Hidalgo FJ. *Biochemistry* 1997; **36**: 15765.
23. Alaiz M, Hidalgo FJ, Zamora R. *J. Am. Oil Chem. Soc.* 1998; **75**: 1127.
24. Hidalgo FJ, Zamora R. *Grasas Aceites* 2000; **51**: 35.
25. Hidalgo FJ, Zamora R. *Trends Food Sci. Technol.* 2006; **17**: 56.
26. Colombini MP, Modugno F, Giacomelli M, Francesconi S. *J. Chromatogr. A* 1999; **846**: 113.
27. Colombini MP, Modugno F, Menicagli E, Fuoco R, Giacomelli A. *Microchem. J.* 2000; **67**: 291.
28. Letí R, Sarabia A, Ortiz MC, Todeschini R, Colombini MP. *Analyst* 2003; **128**: 281.
29. Peris-Vicente J, Simó-Alfonso E, Gimeno-Adelantado JV, Doménech-Carbó MT. *Rapid Commun. Mass Spectrom.* 2005; **19**: 3463.
30. Wang GY, Abe T, Sasahara T. *Breeding Sci.* 1998; **48**: 129.
31. Alcazar A, Ballesteros O, Jurado JM, Pablos F, Martin MJ, Vilches JL, Navalon A. *J. Agric. Food Chem.* 2007; **55**: 5960.
32. Erbe T, Brückner H. *J. Chromatogr. A* 2000; **881**: 81.
33. Patzold R, Nieto-Rodriguez A, Bruckner H. *Chromatographia* 2003; **57**: 207.
34. Gimeno-Adelantado JV, Mateo-Castro R, Doménech-Carbó MT, Bosch-Reig F, Doménech-Carbó A, De la Cruz-Cañizares J, Casas-Catalán MJ. *Talanta* 2002; **56**: 71.
35. Vandeginste BGM, Massart DL, Buydens LMC, De Jong S, Lewi PJ, Smeyers-Verbeke J. *Data Handling in Science and Technology*, part B. Elsevier Science: Amsterdam, 1998; 237.

DOI: 10.1002/rcm

ANEXO IX

Food Chemistry 120 (2010) 1149–1154

Contents lists available at ScienceDirect

Food Chemistry

journal homepage: www.elsevier.com/locate/foodchem

Analytical Methods

Classification of vegetable oils according to their botanical origin using amino acid profiles established by High Performance Liquid Chromatography with UV–vis detection: A first approach

V. Concha-Herrera [a], M.J. Lerma-García [b], J.M. Herrero-Martínez [b], E.F. Simó-Alfonso [b,*]

[a] Unidad Académica de Ciencias Químicas, Universidad Autónoma de Zacatecas, 98160 Zacatecas, Mexico
[b] Department of Analytical Chemistry, Faculty of Chemistry, University of Valencia, 46100 Burjassot, Valencia, Spain

ARTICLE INFO

Article history:
Received 20 January 2009
Received in revised form 12 May 2009
Accepted 21 November 2009

Keywords:
Amino acid profiles
Botanical origin
Linear discriminant analysis
o-Phthaldialdehyde
Vegetable oils

ABSTRACT

A preliminary study using amino acid profiles to classify oils according to their botanical origin has been performed. Amino acid profiles were obtained from hydrolysis of proteins present in vegetable oils, and established by High Performance Liquid Chromatography (HPLC) with UV–vis detection. Proteins present in hazelnut, corn, soybean, olive, avocado, peanut and grapeseed oils were precipitated with acetone, and the residue was hydrolysed in acid medium. The amino acids obtained were derivatized with *o*-phthaldialdehyde and separated by HPLC. Peaks corresponding to 18 amino acids were observed using a C18 column and a gradient of acetonitrile–water in the presence of a 5 mM citric/citrate buffer at pH 6.5. The 16 peaks observed in each sample (arginine–serine and phenylalanine–leucine peaks appeared overlapped) were used to construct linear discriminant analysis (LDA) models. Ratios of the peak areas selected by pairs were used as predictors. With a LDA model, the oils were correctly classified with assignment probabilities higher than 99%.

1. Introduction

Authenticity of edible oils is a very important aspect from the point of view of marketing and quality, also having a significant influence in human health and economy. To establish authenticity, a number of chromatographic methods (Arvanitoyannis & Vlachos, 2007; Brodnjak-Voncina, Kodba, & Novic, 2005; Marcos Lorenzo, Pérez Pavón, Fernández Laespada, García Pinto, & Moreno Cordero, 2002; Mariani, Bellan, Lestini, & Aparicio, 2006; Mildner-Szkudlarz & Jelen, 2008) and spectroscopic techniques including fluorescence (Sikorska, Górecki, Khmelinskii, Sikorski, & Koziol, 2005), FTNIR (Yang, Irudayaraj, & Paradkar, 2005), FTIR (Yang et al., 2005), FT-Raman (Yang et al., 2005), NMR (Dais & Spyros, 2007; García-González, Mannina, Ólmperio, Segre, & Aparicio, 2004; Zamora, Gómez, Dobarganes, & Hidalgo, 2002) and mass spectrometry (MS, Lay, Liyanage, Durham, & Brooks, 2006; Lerma-García, Ramis-Ramos, Herrero-Martínez, & Simó-Alfonso, 2007; Lerma-García, Simó-Alfonso, Ramis-Ramos, & Herrero-Martínez, 2008; Marcos Lorenzo et al., 2002) followed by multivariate statistical analysis of the data, have been applied. Other techniques, such as calorimetry (Chiavaro, Vittadini, Rodriguez-Estrada, Cerretani, & Bendini, 2008) have been also used. The content of fatty acids (Brodnjak-Voncina et al., 2005), tocopherols (Lerma-García, Simó-Alfonso, Ramis-Ramos, & Herrero-Martínez, 2007; Sikorska et al., 2005) volatile compounds (Marcos Lorenzo et al., 2002; Mildner-Szkudlarz & Jelen, 2008), sterols (Lerma-García, Ramis-Ramos, Herrero-Martínez, & Simó-Alfonso, 2008; Lerma-García, Simó-Alfonso, et al., 2008; Mariani et al., 2006), tryacylglycerols (Lay et al., 2006) and more recently amino acids (Lerma-García, Ramis-Ramos, et al., 2007), has been used in these authentication studies.

Determination of peptides and proteins in fats and oils has been carried out by their previous hydrolysis followed by amino acid derivatization with diethyl ethoxymethylenemalonate and analysis of the derivatized amino acids by HPLC with UV detection (Hidalgo, Alaiz, & Zamora, 2002; Hidalgo & Zamora, 2001).

Amino acid concentration profile in other kind of matrices has been also established by different analytical techniques, such as GC previous derivatization with different reagents (De la Cruz-Cañizares, Doménech-Carbó, Gimeno-Adelantado, Mateo-Castro, & Bosch-Reig, 2004; Rampazzi, Cariati, Tanda, & Colombini, 2002) and HPLC (Concha-Herrera, Vivó-Truyols, Torres-Lapasió, & García-Álvarez-Coque, 2005; Hanczkó, Jámbor, Perl, & Molnár-Perl, 2007; Molnár-Perl, 2000, 2001; Pereira, Pontes, Camara, & Marques, 2008). Amongst these, RP-HPLC with pre-column derivatization using either phenylisothiocyanate or *o*-phthaldialdehyde (OPA), in the presence of a reagent containing an –SH group, is the method most frequently used (Molnár-Perl, 2000). Amongst

* Corresponding author. Tel.: +34 963543176; fax: +34 963544436.
E-mail address: ernesto.simo@uv.es (E.F. Simó-Alfonso).

0308-8146/$ - see front matter © 2009 Elsevier Ltd. All rights reserved.
doi:10.1016/j.foodchem.2009.11.046

Table 1
Botanical origin, number of samples and brand of the oil samples used in this work.

Origin	No. of samples	Brand
Hazelnut	2	Guinama
	2	Percheron
	2	Flumen
Peanut	2	Guinama
	2	Bellsola
	1	Apsara Vital
	1	Maní
Avocado	2	Guinama
	2	Marnys
	2	Serra Vita
Grapeseed	2	Guinama
	1	Coosur
	1	Romulo
	1	Paul Corcelet
	1	Pons
Corn	1	Guinama
	1	Asua
	1	Artua
	1	Mazola
Corn germ	1	Guinama
	1	Hacendado
Extra virgin olive	1	Carbonell
	1	Grupo Hojiblanca
	1	Borges
	1	Torrereal
	1	Coosur
	1	Hacendado
Soybean	2	Guinama
	2	Biolasi
	2	Sojola

the SH-group-containing additives, 3-mercaptopropionic acid, *N*-acetylcysteine (NAC) (Beneito-Cambra, Bernabé-Zafón, Herrero-Martínez, Simó-Alfonso, & Ramis-Ramos, 2009; Concha-Herrera, Vivó-Truyols, Torres-Lapasió, & García-Álvarez-Coque, 2004; Concha-Herrera et al., 2005; Molnár-Perl, 2001) and ethanethiol (Hanczkó et al., 2007), which yield rather stable isoindoles, have been recommended.

In this work, a preliminary study based on the amino acid profiles obtained from vegetable oils with different botanical origins was performed. Amino acids were derivatized with OPA in the presence of NAC prior to HPLC–UV–vis analysis. These profiles were used to construct linear discriminant analysis (LDA) models, which were able to correctly classify oils according to their botanical origins.

2. Experimental

2.1. Reagents and samples

Reagent grade acetone, tetrahydrofuran (THF), ethanol, acetonitrile (ACN, HPLC grade), sodium hydroxide, 1,4-dioxane anhydrous (Scharlau, Barcelona, Spain), and hydrochloric acid (HCl 37%, Panreac, Barcelona) were employed. Others reagents as OPA, NAC (Fluka, Buchs, Switzerland), citric acid (Sigma, St. Louis, MO, USA) and boric acid (Panreac) were also used. All solutions were prepared using nanopure water (Barnstead, Sybron, Boston, MA).

The amino acids used as standards were: Alanine (Ala), aspartic acid (Asp), glutamic acid (Glu), glycine (Gly), glutamine (Gln), leucine (Leu), valine (Val), tryptophan (Trp), phenylalanine (Phe) (Aldrich, Steinheim, Germany); arginine (Arg), asparagine (Asn), histidine (His), lysine (Lys), threonine (Thr), (Fluka, Buchs, Switzerland), methionine (Met), tyrosine (Tyr), (Merck, Darmstadt, Germany), isoleucine (Ile), (Guinama) and serine (Ser) (Scharlab, Barcelona).

The vegetable oils and their commercial brands are shown in Table 1. The genetic variety of the olive oils and the botanical and geographical origin of all the samples were guaranteed by the suppliers.

2.2. Instrumentation and HPLC conditions

A 1100 series liquid chromatograph (Agilent Technologies, Waldbronn, Germany), provided with a quaternary pump, thermostated column compartment, automatic sampler, and UV–vis variable multiwavelength detector was used. Separation was carried out with a Kromasil C18 column (250 mm × 4 mm I.D., 5 μm particle size, Análisis Vínicos, Tomelloso, Spain). The HPLC conditions were adapted from Beneito-Cambra et al. (2009) and Concha-Herrera et al. (2005). Briefly, mobile phases were prepared by mixing ACN and water, both containing 5 mM citric acid adjusted at pH 6.5 with sodium hydroxide. A gradient elution from 5% to 30% ACN in 30 min, followed by an increase from 30% to 50% ACN in another 5 min, was used. Detection was performed at 335 ± 10 nm (450 ± 30 nm as reference). In all cases, 20 μL was injected, being the flow rate 1 mL min^{-1}. Peak areas were measured with the ChemStation

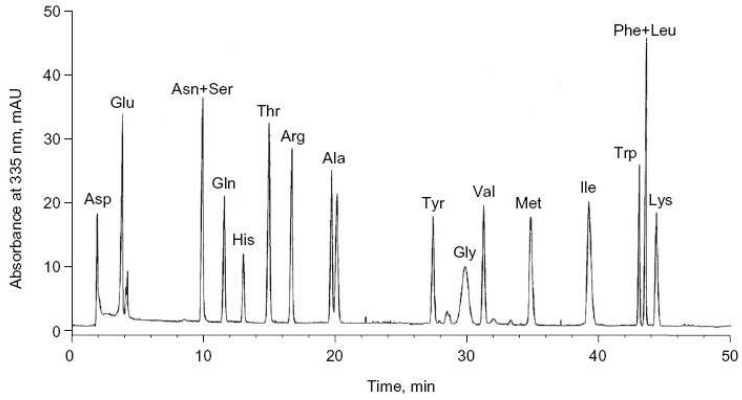

Fig. 1. Chromatogram of a standard mixture of derivatized amino acids. Experimental conditions as indicated in Section 2.2.

for LC v.10.02 software (Agilent). The statistical treatment of the data was performed using the SPSS package (v. 12.0.1, Statistical Package for the Social Sciences Inc., Chicago, IL, USA).

2.3. Proteins isolation, hydrolysis and derivatization procedure

The procedure for the isolation of proteins was taken from Hidalgo and Zamora (2001). Briefly, to precipitate the proteins, 40 g oil were weighed and cooled at 18 °C for at least 90 min prior to the addition of 98 mL acetone, which was also previously cooled at 4 °C. The mixture was kept at 4 °C for 30 min and filtered through a Whatman No. 1 filter paper using a Buchner funnel. The filter paper was extracted by shaking with 5 mL THF followed by 5 mL 1,4-dioxane. The extracts were combined and evaporated to dryness under a nitrogen stream. The residue was dissolved in 100 mL concentrated HCl and hydrolysed for 24 h at 110 °C (Peris-Vicente, Simó-Alfonso, Gimeno-Adelantado, & Domenech-Carbó, 2005). After cooling, 1 mL aqueous 0.1 M HCl and 1 mL ethanol were added. Two amino acid extractions were performed for each sample.

The derivatization reagent, containing 1.25×10^{-2} M OPA and 2.5×10^{-2} M NAC, was buffered with 1 M boric acid at pH 9.5 (Concha-Herrera et al., 2005). This mixture, protected from light with aluminium foil, was stored at 4 °C and renewed weekly. Ali-

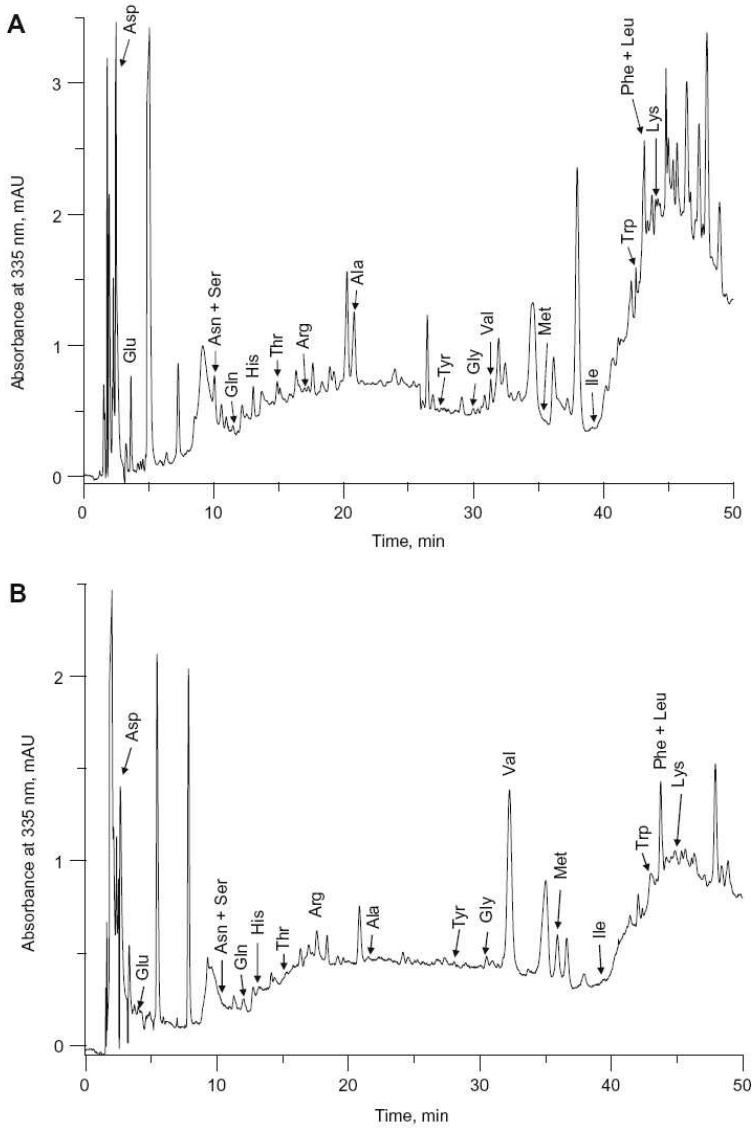

Fig. 2. Chromatograms showing the amino acid profiles of an extra virgin olive (A) and hazelnut oil (B) samples. Experimental conditions as indicated in Section 2.2.

Table 2
Predictors selected and corresponding standardised coefficients of the LDA model constructed to predict the botanical origin of vegetable oils.

Predictors	f_1	f_2	f_3	f_4	f_5	f_6
Asp/Ala	−7.37	1.40	−1.25	0.01	−2.22	−0.35
(Asn + Ser)/Thr	−10.94	0.70	1.46	2.14	−0.58	−0.74
Gln/Thr	6.46	−1.85	−0.20	−1.84	3.35	1.93
His/Gly	16.16	2.00	1.92	1.18	−0.11	0.68
His/Trp	−16.38	−1.03	1.92	0.84	−0.96	1.00
Arg/Ala	−3.43	12.29	2.89	2.21	9.10	4.01
Arg/Val	7.94	−11.50	−1.17	−0.58	−9.83	−5.49
Ala/Val	−4.93	0.37	−0.04	2.54	0.38	0.83
Ala/Trp	2.67	0.31	0.67	−0.95	2.07	−1.03
Gly/Val	29.30	1.75	0.26	1.50	0.07	0.11
Gly/Ile	−6.20	1.17	0.82	−0.56	−0.98	1.62
Val/Ile	24.08	−0.90	−1.21	1.16	1.64	−1.71
Ile/(Leu + Phe)	16.84	0.46	0.72	1.21	1.10	−0.05

quots of 100 μL of the hydrolyzates were mixed with 1 mL OPA–NAC solution. To identify amino acid peaks along the chromatograms, stock solutions containing an amino acid or mixtures of two or three amino acids (1000 μg mL^{-1} each) were prepared, and aliquots were derivatized as indicated. After derivatization, these solutions were both directly injected or used to spike the hydrolyzates when required.

3. Results and discussion

3.1. Amino acid separation and normalisation of the variables

Using the separation conditions indicated in Section 2.2, the derivatized amino acid standards were injected. A chromatogram of the standard mixture is shown in Fig. 1. As it can be observed, all amino acid peaks were clearly separated, except the pairs Phe/Leu and the Asn/Ser. When oil samples were injected (Fig. 2, parts A and B), several matrix peaks jointly with a baseline disturbance in the last part of the chromatograms were evidenced. Small modifications in the mobile phase composition and in the gradient conditions were done, but non-enhancement of the resolution of these peaks was obtained. A dilution of amino acid extracts did not either improved the resolution of these peaks. Additionally with this dilution, some minor amino acid peaks were not observed with the subsequent loss of significant information. When comparing oil sample chromatograms (Fig. 2), small differences between the amino acid profiles of the different vegetable oils were observed. Thus, to construct LDA models, 16 peak areas, which corresponded to 18 amino acids (Phe/Leu and the Asn/Ser peak pairs were jointly measured), were used as original variables. Similar results in terms of separation, efficiency and analysis times have been obtained by other authors using as derivatization reagent diethyl ethoxymethylenemalonate (Hidalgo & Zamora, 2001; Hi-

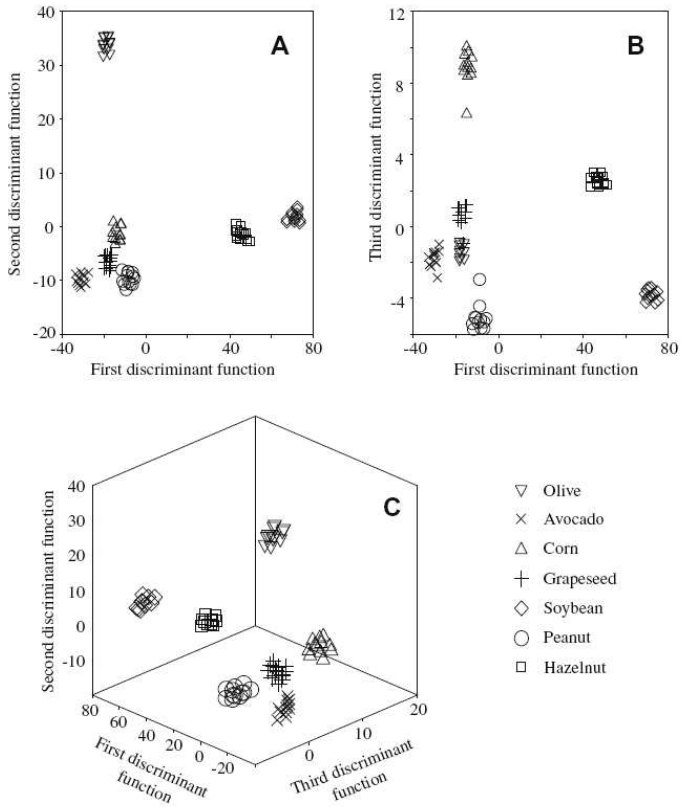

Fig. 3. Score plots on the planes of the first and second (A), and second and third discriminant functions (B), and on an oblique plane of the 3-D space defined by the three discriminant functions (C) of the optimal LDA model.

dalgo et al., 2002). Longer analysis times were obtained when the system OPA + NAC was used (Concha-Herrera et al., 2005).

In order to reduce the variability associated to the total amount of proteins recovered from the oil samples, and consequently minimise the sources of variance, the normalised rather than the absolute peak areas were used. For this purpose, two normalisation procedures were tried. In procedure A, the area of each amino acid peak was divided by the sum of the areas of all the amino acid peaks of the chromatogram. In procedure B, the area of each amino acid peak was divided by each one of the areas of the other 15 amino acid peaks; in this way, and taking into account that a pair of peaks should be considered only once, $(16 \times 15)/2 = 120$ non-redundant ratios of peak areas were obtained.

3.2. Construction of the data matrices and LDA models

Using the normalised variables, LDA models capable of classifying the oil samples according to their botanical origin were constructed. For this purpose, each extract (2 *per* sample) was injected two times. Two matrices containing 168 injections each, and 16 or 120 predictors (according to normalisation procedures A and B, respectively) were constructed. A response column, containing the seven categories corresponding to the seven botanical origins of the oils (corn and corn germ were considered as a single category), was added to the matrices. These matrices were randomly divided in two groups (training and evaluation sets) with the same size (84 samples each). To select the predictors to be included in the models, the SPSS stepwise algorithm was used. The default probability values of F_{in} and F_{out} provided by SPSS, 0.05 and 0.10, respectively, were adopted.

To classify the oils according to the seven botanical varieties of Table 1, two LDA models, one for each normalisation procedure, were constructed. The best results according to both, low λ_w values and simple models having a small number of predictors were obtained using normalisation procedure B, which was selected. An excellent resolution between the seven categories was achieved ($\lambda_w = 0.393$). Taking into account that a large number of categories were simultaneously distinguished, this λ_w value was quite low. The variables selected by the SPSS stepwise algorithm, and the corresponding standardised coefficients of the model, showing the predictors with large discriminant capabilities, are given in Table 2. As shown in Fig. 3, part A, a large resolution between soybean, hazelnut from the other categories was achieved along f_1. As deduced from Table 2, f_1 was mainly constructed with the peak area ratios Gly/Val and Val/Ile. On the other hand, the variance gathered by f_2 was mainly associated to the resolution between olive oil and the rest of categories as a whole. According to Fig. 3, part B, corn, hazelnut, grapeseed, avocado-olive and peanut-soybean categories were resolved along f_3. Finally, as illustrated in Fig. 3, part C, by using a plane oblique to the three first discriminant functions, all the possible pair of categories were very well resolved from each other.

All the points of the training set were correctly classified by leave-one-out cross-validation. The evaluation set, containing the 84 original data points, was used to check the prediction capability of the model. All the objects were correctly assigned with an assignation probability higher than 95%.

Classification of vegetable oils according to amino acid profiles obtained by direct MS has been also performed in a previous work (Lerma-García, Ramis-Ramos, et al., 2007). Using MS data, a sequential use of three LDA models was required in order to correctly classify vegetable oils. However, in the present work, a good resolution between the seven botanical origins was obtained using only an LDA model.

4. Conclusions

A preliminary study for the classification of vegetable oils according to its botanical origin using amino acid profiles established by HPLC–UV–vis has been developed. For this purpose, after precipitation and hydrolysis, the amino acids were derivatized with OPA–NAC and aliquots were chromatographed. A C18 column and multi-segmented gradient elution with ACN/water were used to separate the isoindoles of the amino acids. An LDA model with an excellent prediction capability was obtained by using ratios of the areas of the peaks taken by pairs as predictors. All the objects of the evaluation set were correctly assigned. Thus, the prediction capability was 100%.

Acknowledgements

Project CTQ2007-61445 (MEC of Spain and FEDER funds). V. C.-H. thanks to the University of Valencia for a contract. M.J. L.-G. also thanks the Generalitat Valenciana for an FPI grant for PhD studies.

References

Arvanitoyannis, I. S., & Vlachos, A. (2007). Implementation of physicochemical and sensory analysis in conjunction with multivariate analysis towards assessing olive oil authentication/adulteration. *Critical Reviews in Food Science and Nutrition, 47*, 441–498.

Beneito-Cambra, M., Bernabé-Zafón, V., Herrero-Martínez, J. M., Simó-Alfonso, E. F., & Ramis-Ramos, G. (2009). Enzyme class identification in cleaning products by hydrolysis followed by derivatization with o-phthaldialdehyde, HPLC and linear discriminant analysis. *Talanta*. doi:10.1016/j.talanta.2009.03.048.

Brodnjak-Voncina, D., Kodba, Z. C., & Novic, M. (2005). Multivariate data analysis in classification of vegetable oils characterized by the content of fatty acids. *Chemometrics and Intelligent Laboratory Systems, 75*, 31–43.

Chiavaro, E., Vittadini, E., Rodriguez-Estrada, M. T., Cerretani, L., & Bendini, A. (2008). Differential scanning calorimeter application to the detection of refined hazelnut oil in extra virgin olive oil. *Food Chemistry, 110*, 248–256.

Concha-Herrera, V., Vivó-Truyols, G., Torres-Lapasió, J. R., & García-Álvarez-Coque, M. C. (2004). Enhancement of retention predictions in reversed-phase liquid chromatography using reference compounds. *Analytica Chimica Acta, 518*, 191–197.

Concha-Herrera, V., Vivó-Truyols, G., Torres-Lapasió, J. R., & García-Álvarez-Coque, M. C. (2005). Limits of multi-linear gradient optimisation in reversed-phase liquid chromatography. *Journal of Chromatography A, 1063*, 79–88.

Dais, P., & Spyros, A. (2007). P-31 NMR spectroscopy in the quality control and authentication of extra-virgin olive oil: A review of recent progress. *Magnetic Resonance in Chemistry, 45*, 367–377.

De la Cruz-Cañizares, J., Doménech-Carbó, M. T., Gimeno-Adelantado, J. V., Mateo-Castro, R., & Bosch-Reig, F. (2004). Suppression of pigment interference in the gas chromatographic analysis of proteinaceous binding media in paintings with EDTA. *Journal of Chromatography A, 1025*, 277–285.

García-González, D. L., Mannina, L., DImperio, M., Segre, A. L., & Aparicio, R. (2004). Using H-1 and C-13 NMR techniques and artificial neural networks to detect the adulteration of olive oil with hazelnut oil. *European Food Research and Technology, 219*, 545–548.

Hanczkó, R., Jámbor, A., Perl, A., & Molnár-Perl, I. (2007). Advances in the omicron-phthalaldehyde derivatizations comeback to the omicron-phthalaldehyde-ethanethiol reagent. *Journal of Chromatography A, 1163*, 25–42.

Hidalgo, F. J., Alaiz, M., & Zamora, R. (2002). Low molecular weight polypeptides in virgin and refined olive oils. *Journal of the American Oil Chemists' Society, 7*, 685–689.

Hidalgo, F. J., & Zamora, R. (2001). Determination of peptides and proteins in fats and oils. *Analytical Chemistry, 73*, 698–702.

Lay, J. O., Liyanage, R., Durham, B., & Brooks, J. (2006). Rapid characterization of edible oils by direct matrix-assisted laser desorption/ionization time-of-flight mass spectrometry analysis using triacylglycerols. *Rapid Communications in Mass Spectrometry, 20*, 952–958.

Lerma-García, M. J., Ramis-Ramos, G., Herrero-Martínez, J. M., & Simó-Alfonso, E. F. (2007). Classification of vegetable oils according to their botanical origin using amino acid profiles established by direct infusion mass spectrometry. *Rapid Communications in Mass Spectrometry, 21*, 3751–3755.

Lerma-García, M. J., Ramis-Ramos, G., Herrero-Martínez, J. M., & Simó-Alfonso, E. F. (2008). Classification of vegetable oils according to their botanical origin using sterol profiles established by direct infusion mass spectrometry. *Rapid Communications in Mass Spectrometry, 22*, 973–978.

Lerma-García, M. J., Simó-Alfonso, E. F., Ramis-Ramos, G., & Herrero-Martínez, J. M. (2007). Determination of tocopherols in vegetable oils by CEC using methacrylate ester-based monolithic columns. *Electrophoresis, 28*, 4128–4135.

Lerma-García, M. J., Simó-Alfonso, E. F., Ramis-Ramos, G., & Herrero-Martínez, J. M. (2008). Rapid determination of sterols in vegetable oils by CEC using methacrylate ester-based monolithic columns. *Electrophoresis, 29*, 4603–4611.

Marcos Lorenzo, I., Pérez Pavón, J. L., Fernández Laespada, M. E., García Pinto, C., & Moreno Cordero, B. (2002). Detection of adulterants in olive oil by headspace–mass spectrometry. *Journal of Chromatography A, 945*, 221–230.

Mariani, C., Bellan, G., Lestini, E., & Aparicio, R. (2006). The detection of the presence of hazelnut oil in olive oil by free and esterified sterols. *European Food Research and Technology, 223*, 655–661.

Mildner-Szkudlarz, S., & Jelen, H. H. (2008). The potential of different techniques for volatile compounds analysis coupled with PCA for the detection of adulteration of olive oil with hazelnut oil. *Food Chemistry, 110*, 751–761.

Molnár-Perl, I. (2000). Role of chromatography in the analysis of sugars, carboxylic acids and amino acids in food. *Journal of Chromatography A, 891*, 1–32.

Molnár-Perl, I. (2001). Derivatization and chromatographic behavior of the o-phthaldialdehyde amino acid derivatives obtained with various SH-group-containing additives. *Journal of Chromatography A, 913*, 283–302.

Pereira, V., Pontes, M., Camara, J. S., & Marques, J. C. (2008). Simultaneous analysis of free amino acids and biogenic amines in honey and wine samples using in loop orthophthalaldeyde derivatization procedure. *Journal of Chromatography A, 1189*, 435–443.

Peris-Vicente, J., Simó-Alfonso, E., Gimeno-Adelantado, J. V., & Domenech-Carbó, M. T. (2005). Direct infusion mass spectrometry as a fingerprint of protein-binding media used in works of art. *Rapid Communications in Mass Spectrometry, 19*, 3463–3467.

Rampazzi, L., Cariati, F., Tanda, G., & Colombini, M. P. (2002). Characterisation of wall painting in the Sos Furrighesos necropolis (Anela, Italy). *Journal of Cultural Heritage, 3*, 237–240.

Sikorska, E., Górecki, T., Khmelinskii, I. V., Sikorski, M., & Koziol, J. (2005). Classification of edible oils using synchronous scanning fluorescence spectroscopy. *Food Chemistry, 89*, 217–225.

Yang, H., Irudayaraj, J., & Paradkar, M. M. (2005). Discriminant analysis of edible oils and fats by FTIR, FT-NIR and FT-Raman spectroscopy. *Food Chemistry, 93*, 25–32.

Zamora, R., Gómez, G., Dobarganes, M. C., & Hidalgo, F. J. (2002). Oil fractionation as a preliminary step in the characterization of vegetable oils by high-resolution ^{13}C NMR spectroscopy. *Journal of the American Oil Chemists' Society, 79*, 261–266.

ANEXO X

Available online at www.sciencedirect.com
ScienceDirect
Food Chemistry 107 (2008) 1307–1313
Food Chemistry
www.elsevier.com/locate/foodchem

Analytical Methods

Evaluation of the quality of olive oil using fatty acid profiles by direct infusion electrospray ionization mass spectrometry

M.J. Lerma-García, J.M. Herrero-Martínez, G. Ramis-Ramos, E.F. Simó-Alfonso *

Department of Analytical Chemistry, Faculty of Chemistry, University of Valencia, Cl Doctor Moliner 50, 46100 Burjassot, Valencia, Spain

Received 18 May 2007; received in revised form 17 September 2007; accepted 4 October 2007

Abstract

Electrospray ionization mass spectrometry is used to predict the olive oil quality according to European Union marketing standards. Samples were 1:50 diluted in an alkaline 85:15 (v/v) propanol/methanol mixture and directly infused into the electrospray ionization source of an ion trap mass spectrometer. The establishment of ratios of the peak abundances of the free fatty acids followed by linear discriminant analysis was employed to predict the olive oil quality grade. In addition, using multiple linear regression and partial least-squares regression, the percentages of extra virgin and virgin olive oils in binary mixtures were predicted with 5–11% average prediction errors.

Keywords: Olive oil; Quality control; Mass spectrometry; Fatty acids; Linear discriminant analysis

1. Introduction

Olive oil is a fine product with high nutritional value and significant health benefits (Owen et al., 2000). Quality olive oils are expensive owing to the hard and time-consuming tasks involved in the cultivation of olive trees, the harvesting of the fruits, and the extraction of the oil. For this reason, adulteration of higher quality olive oils with either seed oils or olive oils of lower quality is a relatively common fraudulent practice. European Mediterranean countries, which are major suppliers of olive oils on the world market, have adopted common regulations to protect olive oil growers and consumers from fraud. According to the European Union Legislation (European Union Commission, 2003), there are several types of virgin olive and olive pomace oils. Thus, virgin olive oils are classified as extra virgin olive oil (EVOO), virgin olive oil (VOO) and lampante virgin olive oil (LVOO). Two further types of olive oils are distinguished: refined olive oil (ROO, obtained by refining virgin olive oils, and having a maximal free acidity of 0.5 g per 100 g), and olive oil (OO, a mixture of refined and virgin olive oils, excluding lampante oil, and having a maximal free acidity of 1.5 g per 100 g). Finally, three categories of olive pomace oil are recognized: crude olive pomace oil (COPO, obtained by treating olive pomace with solvents), refined olive pomace oil (ROPO, obtained by refining crude olive pomace oil, and having a maximal free acidity of 0.5 g per 100 g), and olive pomace oil (OPO, a mixture of refined olive pomace and virgin olive oils, excluding lampante oil, and having a maximal free acidity of 1.5 g per 100 g).

The authenticity of olive oils covers many aspects, including genetic variety, geographical origin and quality grade (Bianchi, 2002). Oil authentication can be carried out by a variety of methods, which have been recently reviewed (Aparicio & Aparicio-Ruíz, 2000; Aparicio & Luna, 2002). Many factors such as latitude, climatic conditions, irrigation regime, fruit ripening, harvesting and extraction technologies affect both the total fatty acid composition (particularly, the concentration of oleic acid), and the concentration profiles of many other oil components (Aparicio & Luna, 2002; Bruni, Cortesi, & Fiorino, 1994;

* Corresponding author. Tel.: +34 963543176; fax: +34 963544436.
E-mail address: ernesto.simo@uv.es (E.F. Simó-Alfonso).

0308-8146/$ - see front matter © 2007 Elsevier Ltd. All rights reserved.
doi:10.1016/j.foodchem.2007.10.020

Caponio, Alloggio, & Gomes, 1999; Di Giovacchino, Solinas, & Miccoli, 1994; Guimet, Boqué, & Ferré, 2004; Morello, Romero, & Motilva, 2004; Ranalli, Tombesi, De Mattia, Ferrante, & Giansante, 1997; Salvador, Aranda, Gómez-Alonso, & Fregapane, 2003; Torres & Maestri, 2006; Tura, Prenzler, Bedgood, Antolovich, & Robards, 2004; Vichi, Pizzale, Conte, Buxaderas, & Lopez-Tamames, 2003).

Traditional methods, that employ organoleptic features to classify olive oils according to genetic variety and quality grade, are affected by assessor bias. For this reason, chemometric approaches constitute promising tools to classify olive oils. Fluorimetry at different excitation wavelengths, followed by cluster analysis, has been used to classify VOO, pure olive oil and olive pomace oil (Guimet et al., 2004). In order to distinguish between edible virgin olive oil from lampante olive oil, synchronous fluorescence and total luminiscence spectroscopy, followed by data analysis using principal component analysis and hierarchical cluster analysis, have been proposed (Poulli, Mousdis, & Georgiu, 2005). A 2% olive pomace oil has been estimated in EVOO by using Fourier transform-Raman spectroscopy, followed by partial least-squares regression (PLS) (Yang & Irudayaraj, 2001).

Olive oil adulterations have been also investigated using NMR (Fragaki, Spyros, Siragakis, Salivaras, & Dais, 2005; Fronimaki, Spyros, Christophoridou, & Dais, 2002; Zamora, Alba, & Hidalgo, 2001). The relationship between the ratio of 1,2-diglycerides with respect to the total amount of diglycerides, and the total amount of diglycerides determined by ^{31}P NMR spectroscopy has been used to classify commercial Cretan olive oils, ROO and pomace oils (Fronimaki et al., 2002). Also, ^{31}P NMR followed by multivariate supervised and non-supervised statistical techniques, has been used to classify Greek oils from different regions according to quality grade, and to detect EVOO adulteration with LVOO (Fragaki et al., 2005). The quality of edible oils has been also established by using sensor arrays (García-Gonzalez & Aparicio, 2002a, 2002b, 2003; Guadarrama, Rodríguez-Méndez, Sanz, Ríos, & De Saja, 2001). García-Gonzalez and Aparicio (2003) have used an array of seven metal oxide sensors and neural networks to detect LVOO in VOO with a 4.5% validation error. Guadarrama, Rodriguez-Mendez, De Saja, Rios, and Olias (2000) and Guadarrama et al. (2001) have described an array constructed with eight polymeric sensors to discriminate EVOO, VOO, LVOO and four deodorized oils. The adulteration of VOO with deodorized oils has also been studied using gas chromatography (CG) coupled to chemical ionization-mass spectrometry (CI-MS) (Saba, Mazzini, Raffaelli, Mattei, & Salvadori, 2005). Mixtures of high quality olive oils with lower quality grade olive oils, and with other vegetable oils, have also been studied by headspace-mass spectrometry (Marcos Lorenzo, Pérez Pavón, Fernández Laespada, García Pinto, & Moreno Cordero, 2002).

Direct infusion electrospray ionization mass spectrometry (ESI-MS) followed by linear discriminant analysis (LDA) of peak intensities and peak ratios has been successfully used to classify different types of samples into categories (Gama Melão, Simó-Alfonso, Ramis-Ramos, & Vicente, 2006; Peris-Vicente, Simó-Alfonso, Gimeno-Adelantado, & Domenech-Carbó, 2005). Direct infusion ESI-MS has been also used to classify vegetable oils according to biological origin, and to detect the adulteration of olive oil with soybean oil (Catharino et al., 2005).

In this work, the capability of ESI-MS to classify commercial olive oils of different quality grades (EVOO, VOO, LVOO and ROPO), and to evaluate mixtures of EVOO and VOO, and binary mixtures of these two oils with olive oils of lower quality grade has been studied. Infusion was performed with a simple dilution of the sample in a miscible alkaline solvent, and analyzed directly without any previous extraction step. Classification and evaluation studies were performed on the basis of fatty acid fingerprints obtained by direct infusion using ESI-MS in the negative-ion mode. Several chemometric techniques, including LDA, multiple linear regression (MLR) and PLS, were used to treat the data. The regression models provided fairly reliable predictions of the percentage of extra virgin and virgin olive oils in several oil mixtures.

2. Experimental

2.1. Instrumentation and working conditions

An HP 1100 series ion trap mass spectrometer (ITMS) provided with an ESI source (Agilent Technologies, Waldbronn, Germany) was used. A syringe pump (kd Scientific, Holliston, MA, USA) was used to infuse the samples at 0.3 ml h^{-1} (5 μl min^{-1}) through a 50 μm i.d. fused silica capillary. The MS working conditions were: nebulizer gas pressure, 25 psi; dry temperature, 200 °C; dry gas, 5 L min^{-1}; capillary voltage, 3.5 kV; voltages of skimmers 1 and 2, −26.8 V and −6.0 V, respectively. Nitrogen was used as nebulizer and dry gas (Gaslab NG LCMS 20 generator, Equcien, Madrid, Spain). The mass spectrometer was scanned within the *m/z* 100–800 range in the negative-ion mode. The target mass was set at *m/z* 281 ([M−H]$^-$ oleic acid peak). Maximum loading of the ion trap was 3×10^4 counts, and maximum collection time was 300 ms.

2.2. Reagents and samples

Analytical grade KOH (Probus, Barcelona, Spain), propanol (PrOH) and methanol (MeOH) (Scharlau, Barcelona, Spain) were used. Olive oil samples of the following quality grades were used: EVOO, VOO, LVOO and ROPO (European Union Commission, 2003). Samples of guaranteed quality, where the genetic variety was also known, were kindly donated by Coosur (Vilches, Jaén, Spain), Borges (Tàrrega, Lleida, Spain) and Grupo Hojiblanca (Antequera, Málaga, Spain). These samples were used to construct the models (see Table 1). Other samples, purchased at the local market (Table 1), were used to evaluate

Table 1
Olive oils used to construct LDA models

Grade	Brand	Genetic variety	Geographical origin	Set type
EVOO	Coosur	Hojiblanca[a]	Luque (Córdoba)	Training
		Arbequina[a]	Estepa (Sevilla) + La Roda de Andalucía (Sevilla)	Training
		Picual[a]	Villanueva del Arzobispo (Jaén) + Porcuna (Jaén)	Training
	Carbonell	Hojiblanca	Estepa (Sevilla)	Evaluation
		Arbequina	Aguadulce (Sevilla)	Evaluation
		Picual	Martos (Jaén)	Evaluation
	Borges	Hojiblanca[a]	Puente Genil (Córdoba)	Training
		Arbequina[a]	Huelva + Zaragoza + Palma del Río (Córdoba)	Training
		Picual[a]	Quesada (Jaén)	Training
	Torrereal	Arbequina	Vila Franca del Penedés (Barcelona)	Evaluation
	Duc	Arbequina	Vila Franca del Penedés (Barcelona)	Evaluation
	Oleastrum	Arbequina	Les Garrigues (Lleida)	Evaluation
	Hipercor	Hojiblanca	Antequera (Málaga)	Evaluation
	Grupo Hojiblanca	Hojiblanca[a]	Fuente de Piedra (Málaga)	Training
		Arbequina[a]	Antequera (Málaga)	Training
		Picual[a]	Montoro (Córdoba)	Training
VOO	Coosur	Mixture[b]	Vilches (Jaén)	Training
	Grupo Hojiblanca	Hojiblanca[a]	Archidona (Málaga)	Training
		Arbequina[a]	Antequera (Málaga)	Training
		Picual[a]	Lucena (Córdoba)	Training
LVOO	Coosur	Mixture[a]	Vilches (Jaén)	Training
	Borges	Mixture[a]	Jódar (Jaén)	Training
	Grupo Hojiblanca	Hojiblanca[a]	Archidona (Málaga)	Training
		Arbequina[a]	Hinojosa del Duque (Córdoba)	Training
		Picual[a]	La Rembla (Córdoba)	Training
ROPO	Coosur	Mixture[a]	Vilches (Jaén)	Training
	Borges	Mixture[a]	Palma del Río (Córdoba)	Training
OPO	*Confidential*	Mixture	Unknown	Evaluation[b]

[a] Guaranteed quality.
[b] Used exclusively to evaluate the MLR model.

the prediction capability of the models and to detect possible adulterations.

2.3. Procedures

A mixture of EVOO and VOO, and binary mixtures of these oils with lower quality grade oils, were prepared by weighing the appropriate amounts of the guaranteed oil samples provided by Coosur. An 85:15 (v/v) PrOH/MeOH mixture, containing 40 mM KOH, was used to dilute the oil samples and their mixtures in a 1:50 ratio (v/v). Lower dilutions led to a significant increase in background noise. MS experiments with saponified samples were also performed. However, the signal-to-noise ratios did not improve after saponification (data not shown). Thus, unsaponified samples were used. Between samples, the capillary was rinsed for 5 min with the alkaline PrOH/MeOH mixture. Before data acquisition, the diluted sample was infused until the signal remained constant. All samples were injected 4–5 times, and each time the data were averaged for 1 min. LDA and MLR models were constructed using the SPSS statistical package (v. 12.0.1, SPSS Inc., Chicago, IL, USA), and PLS1 models (for the prediction of a single response) were established with The Unscrambler (v. 7.6, CAMO Technologies Inc., Bergen, Norway).

3. Results and discussion

3.1. Normalization of the variables

In all cases, the MS spectra showed the $[M-H]^-$ peaks of the following fatty acids: myristic (C14:0, *m/z* 227), palmitoleic (C16:1, *m/z* 253), palmitic (C16:0, *m/z* 255), linolenic (C18:3, *m/z* 277), linoleic (C18:2, *m/z* 279), oleic (C18:1, *m/z* 281) and stearic (C18:0, *m/z* 283). The mass spectra were normalized by dividing each peak abundance by the abundance of the C16:0 peak (Fig. 1). As observed, oleic acid yielded the most intense signal, whereas palmitic, linoleic and stearic acids gave intermediate abundances. For each quality grade, closely similar peak profiles were obtained, independently of the genetic variety of the oils. The C14:0/C16:0 peak ratio was larger for VOO and LVOO than for the samples of other quality grades. Also, the C18:3/C16:0 peak ratio decreased according to LVOO > EVOO ≈ VOO > ROPO (Fig. 1). In agreement with these observations a chemometric study was carried out.

In order to reduce signal fluctuations between measurements, two normalization procedures were tried. First, the abundance of each fatty acid in each mass spectrum was divided by the total sum of the abundances of the seven

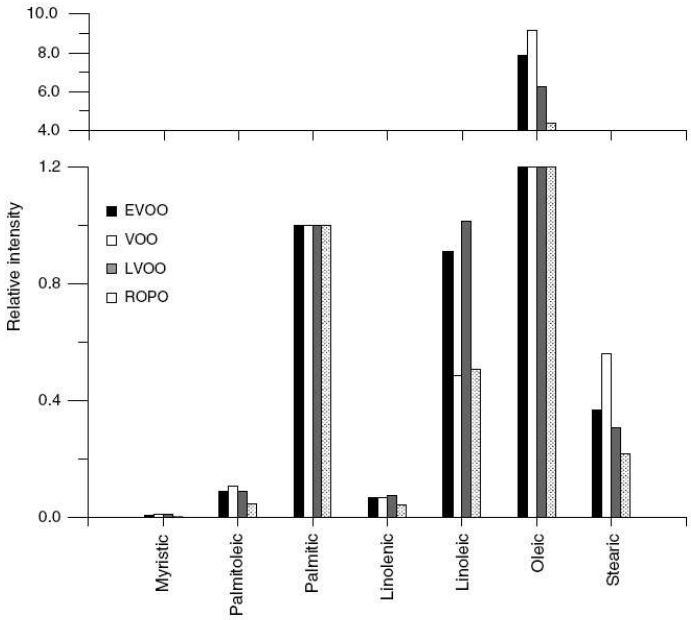

Fig. 1. Relative peak intensities of fatty acids observed in the mass spectra of different quality grade olive oils. The palmitic acid peak (*m/z* 255) was used as reference.

fatty acids (procedure A). Second, the abundance of each fatty acid was divided by each one of the abundances of the other six fatty acids; in this way, $(7 \times 6)/2 = 21$ non-redundant peak ratios to be used as predictors were obtained (procedure B).

3.2. Construction of the data matrix and quality grade prediction by LDA

As indicated above and in Table 1, the samples with guaranteed quality grade (9 EVOO, 4 VOO, 5 LVOO and 2 ROPO samples) were used to construct the training set for the LDA models. The other samples, also described in Table 1, were used as evaluation set. To improve the stability and prediction capability of the models, for each quality grade (EVOO, VOO and LVOO) samples of three genetic varieties (Hojiblanca, Arbequina and Picual), produced in different regions of Spain with rather dissimilar soils and climatic conditions, were used.

According to 4–5 injections of each sample, two matrices constituted by 123 cases, and by 7 and 21 predictors, after normalization by procedures A and B, respectively, were established. In order to classify the samples according to their quality grade, LDA models were constructed. In LDA, vectors minimizing Wilks' lambda (λ_w) are obtained (Vandeginste et al., 1998). To select the predictors to be included in the models, the SPSS stepwise algorithm was used. Using this algorithm, a predictor is selected when the reduction of λ_w produced by including the predictor in the model exceeds the entrance threshold of an *F*-test, F_{in}. However, the entrance of a new predictor modifies the significance of those predictors which are already present in the model. For this reason, after the inclusion of a new predictor, a rejection threshold, F_{out}, is used to decide if one of the other predictors should be removed from the model. The process terminates when there are no predictors entering or being eliminated from the model. The SPSS default values of F_{in} and F_{out}, 3.84 and 2.71, were respectively used.

Using the samples of the training set (EVOO, VOO, LVOO and ROPO), two LDA models, one for each normalization procedure, were constructed. The best results were obtained using normalization procedure B, which was selected. Using this procedure, the evaluation set samples were correctly classified with a probability higher than 95%. Then, both the training and evaluation sets were jointly used to construct a new model with an improved prediction capability. In this way, the geographical origin of the samples was also included in the statistical analysis. The λ_w for this model was 0.52. The predictors selected by the SPSS stepwise algorithm, and the corresponding model standardized coefficients, which show their discriminant capabilities, are given in Table 2. A score plot on the plane of the two first discriminant functions is shown in Fig. 2. EVOO category was very well resolved from the other three categories. To maximize resolution among the VOO, LVOO and ROPO categories, another LDA model was constructed without EVOO category. In this case, λ_w was

Table 2
Standardised coefficients of the discriminant functions obtained to predict the quality grade of olive oils

Predictors	Categories[a]				
	EVOO/VOO/LVOO/ROPO			VOO/LVOO/ROPO	
	f_1	f_2	f_3	f_1	f_2
C16:0/C14:0	–	–	–	3.4	2.5
C18:1/C14:0	0.042	−1.1	0.53	–	–
C18:0/C14:0	–	–	–	−2.3	−2.2
C16:0/C16:1	−8.8	−2.3	−1.2	4.5	−3.5
C18:3/C16:1	6.8	1.3	2.3	–	–
C18:2/C16:1	–	–	–	2.0	−3.3
C18:1/C16:1	15	2.8	4.1	–	–
C18:0/C16:1	−1.7	−0.18	−0.65	−6.1	10
C18:1/C16:0	0.79	−0.71	−1.5	2.5	−7.1
C18:0/C16:0	−7.7	−0.17	−3.7	–	–
C18:2/C18:3	–	–	–	0.17	2.4
C18:1/C18:3	−6.3	0.084	−1.9	–	–
C18:0/C18:3	3.1	0.69	1.7	−0.68	−0.85
C18:1/C18:2	0.71	1.1	1.9	−0.72	3.2
C18:0/C18:1	0.66	−0.38	0.53	2.9	−0.76

[a] Categories included in the training set.

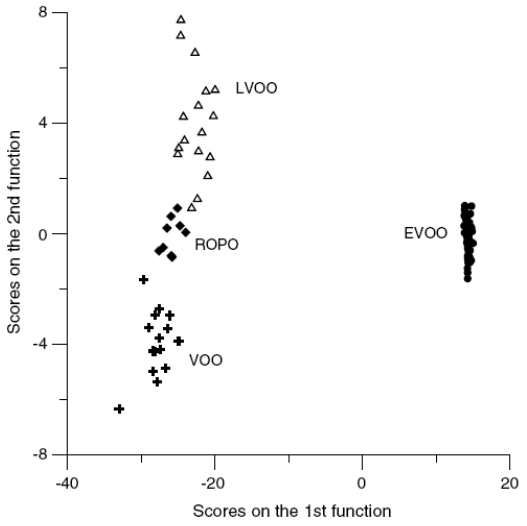

Fig. 2. Score plot on the plane of the two first discriminant functions of an LDA model constructed with four different quality grade olive oils using normalization procedure B.

0.19, which agrees with the excellent resolution between the three categories shown in the score plot of Fig. 3. The model standardized coefficients are also given in Table 2. Therefore, EVOO, VOO, LVOO and ROPO oil samples can be unequivocally classified by the sequential application of two LDA models, one constructed with and the other without EVOO category.

At the sight of Table 2 and Fig. 2, predictors C16:0/C16:1, C18:3/C16:1, C18:1/C16:1, C18:0/C16:0 and

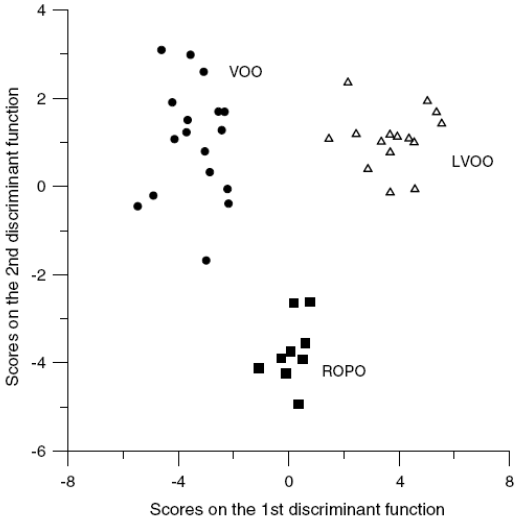

Fig. 3. Score plot on the plane of the two discriminant functions of an LDA model constructed with three different quality grade olive oils (EVOO excluded) using normalization procedure B.

C18:1/C18:3 were relevant to distinguish EVOO from the other three categories. Among these predictors, only C16:0/C16:1 was significant to distinguish VOO, LVOO and ROPO categories when EVOO was excluded from model construction (Fig. 3). The ratios C18:3/C16:1, C18:1/C16:1, C18:0/C16:0 and C18:1/C18:3 were characteristic to distinguish EVOO from the other categories. In addition to C16:0/C16:1, predictors C18:0/C16:1 and C18:1/C16:0 were also important to distinguish VOO, LVOO and ROPO categories.

3.3. Evaluation of binary mixtures of olive oils of different quality grade

Binary mixtures of EVOO and VOO, and either EVOO or VOO with another lower quality grade oil, were prepared. Mixtures with *ca.* 100%, 80%, 60%, 40%, 20% and 0% EVOO or VOO, were infused. For each binary combination of oils, the predictors obtained by using normalization procedures A and B were independently used to construct two matrices. Each mixture was injected in triplicate, thus, matrices with a total of 75 cases, and 7 and 21 predictors, were respectively obtained. A response vector containing the percentage of the higher quality grade oil in the mixture was added to the matrices.

To select the predictors used in the construction of MLR models, the SPSS backward algorithm was used. With this algorithm, all the predictors are initially introduced in the model, and then are sequentially eliminated according to an F-test. The SPSS default values, $F_{in} = 3.84$ and $F_{out} = 2.71$, were again used. The MLR models were constructed both without and with an

Table 3
Regression coefficients of the MLR and PLS1[a] models constructed to predict the composition of binary mixtures of oils of different quality grades

Predictor	EVOO/VOO		EVOO/LVOO		EVOO/ROPO		VOO/LVOO		VOO/ROPO	
	MLR	PLS1	MLR	PLS1	MLR	PLS1	MLR	PLS1	MLR	PLS1
C14:0	−0.71	−0.78	0.71	0.63	−0.75	−0.75	−0.32	−0.15	–	0.066
C16:1	−1.2	−0.54	−2.7	−1.3	1.9	0.48	0.45	0.098	–	−0.16
C16:0	1.9	0.31	2.3	0.72	−2.6	−0.48	–	–	–	−0.16
C18:3	2.2	0.67	1.4	0.42	–	0.10	–	0.16	–	–
C18:2	0.41	0.17	0.92	0.061	–	0.11	−1.5	−0.52	1.8	0.465
C18:1	–	−0.20	−1.6	−0.32	2.2	0.078	1.9	0.36	–	−0.23
C18:0	−1.9	−0.23	–	−0.14	–	0.096	–	0.25	−0.94	−0.33
Number of vectors[b]	6	4	6	5	4	4	4	3	2	3
Average prediction error (%)	10	10	9.7	10	9.6	9.0	5.1	5.3	3.4	4.4
C16:1/C14:0	3.0	0.58	–	−0.31	–	0.38	1.4	0.054	−1.1	–
C16:0/C14:0	−5.4	−0.89	–	−0.11	–	−1.2	–	–	–	–
C18:3/C14:0	–	1.8	–	0.15	–	–	2.3	–	–	–
C18:2/C14:0	−0.64	−1.1	−0.35	−0.14	1.4	0.054	−1.7	–	–	–
C18:1/C14:0	3.0	1.1	–	–	–	0.24	–	–	1.3	–
C18:0/C14:0	–	−1.6	–	–	−0.92	−0.85	−1.9	–	–	–
C16:0/C16:1	–	–	–	0.22	−0.44	−0.30	0.82	–	0.54	–
C18:3/C16:1	1.6	0.39	−1.1	−0.20	–	–	−2.9	–	–	0.059
C18:2/C16:1	–	−0.77	2.0	0.39	–	−0.25	1.2	−0.10	–	0.14
C18:1/C16:1	–	0.99	0.77	−0.17	–	−1.2	1.2	0.071	–	–
C18:0/C16:1	−0.69	−0.44	−0.77	−0.14	–	–	–	–	−0.59	–
C18:3/C16:0	−0.69	−0.066	–	−0.17	–	–	0.71	–	0.42	–
C18:2/C16:0	−1.2	−0.80	−0.71	0.28	–	–	–	−0.169	–	0.168
C18:1/C16:0	–	0.82	–	−0.17	–	0.080	–	0.095	–	–
C18:0/C16:0	–	−1.1	–	−0.097	–	–	–	–	–	−0.051
C18:2/C18:3	2.2	2.0	–	0.20	–	–	−1.2	–0.236	0.95	0.165
C18:1/C18:3	−0.40	−0.41	−1.2	−0.41	–	1.1	–	0.064	−0.48	–
C18:0/C18:3	–	0.091	–	−0.38	0.30	–	−0.40	–	0.71	–
C18:1/C18:2	–	−0.44	–	0.28	0.68	0.19	1.8	0.24	–	−0.14
C18:0/C18:2	–	−0.20	0.68	0.35	–	–	−2.3	0.18	–	–
C18:0/C18:1	–	0.71	–	–	–	–	0.98	–	–	−0.11
Number of vectors[b]	10	10	8	7	5	2	14	4	8	3
Average prediction error (%)	5.3	4.8	4.5	5.8	11	15	2.2	7.1	3.0	5.5

[a] PLS1 coefficients smaller than 0.05 in absolute values are not given.
[b] Number of vectors selected by the forward algorithm of SPSS (MLR), or recommended by The Unscrambler (PLS1 *k*-values).

independent term (a constant). The use of a constant improved the quality of the models constructed with the peak intensity ratios. For all the PLS1 models, the number of vectors recommended by The Unscrambler after the PLS1 rotation (*k*-value) was adopted.

The regression coefficients of the MLR and PLS1 models are given in Table 3. In most cases, predictors with large regression coefficients were common to both models. An average prediction error, calculated as the average absolute difference between the expected and predicted oil percentages, divided by the number of predictions, was used to evaluate model quality. As can be seen in Table 3, in most cases MLR showed average prediction errors slightly better than PLS1. Using MLR, normalization procedure B gave better values of the average prediction errors than procedure A. The MLR regression model for VOO/ROPO mixtures was applied to quantify a guaranteed OPO sample (a commercial mixture of ROPO and VOO). The declared and found percentages in ROPO were $95 \pm 3\%$ and $92 \pm 5\%$, respectively.

4. Conclusions

A quick ESI-MS method, capable of predicting the olive oil quality grade has been developed. After a simple 1:1 dilution, the oil samples were infused in a mass spectrometer, and the peak abundances of the fatty acids were measured. Using LDA, the oils were unequivocally classified according to European Union marketing standards. Using MLR, binary mixtures of different quality grade oils can be evaluated with average prediction errors within the 3–5% range; however, errors of the order of 11% should be expected for EVOO/ ROPO mixtures. The present procedure can be easily applied to the quality control of legal mixtures and in fraud detection.

Acknowledgements

Work supported by Project CTQ2004-06302/BQU (Ministry of Education and Science (MEC) of Spain and FEDER funds). The support of the Generalitat Valenciana

(ACOMP07-168) is also acknowledged. MJL-G thanks the Generalitat Valenciana for an FPI Grant, and JMH-M thanks the MEC of Spain and the University of Valencia for a Ramón y Cajal Research Contract.

References

Aparicio, R., & Aparicio-Ruíz, R. (2000). Authentication of vegetable oils by chromatographic techniques. *Journal of Chromatography A, 881*, 93–104.

Aparicio, R., & Luna, G. (2002). Characterisation of monovarietal virgin olive oils. *European Journal of Lipid Science and Technology, 104*, 614–627.

Bianchi, G. (2002). Adulteration and authentication of oils and fats: An overview. In M. Jee (Ed.), *Oils and fats, authentication* (pp. 25–65). Boca Raton, FL: CRC Press.

Bruni, U., Cortesi, N., & Fiorino, P. (1994). Influence of agricultural techniques, cultivar and area of origin on characteristics of virgin olive oil and on levels of some of its minor components. *Olivae, 53*, 28–41.

Caponio, F., Alloggio, V., & Gomes, T. (1999). Phenolic compounds of virgin olive oil: Influence of paste preparation techniques. *Food Chemistry, 64*, 203–209.

Catharino, R. R., Haddad, R., Cabrini, L. G., Cunha, I. B. S., Sawaya, A. C. H. F., & Eberlin, M. N. (2005). Characterization of vegetable oils by electrospray ionization mass spectrometry fingerprinting: Classification, quality, adulteration, and aging. *Analytical Chemistry, 77*, 7429–7433.

Di Giovacchino, L., Solinas, M., & Miccoli, M. (1994). Effects of extraction systems on the quality of virgin olive oil. *Journal of American Oil and Chemical Society, 71*, 1189–1194.

European Union Commission, (2003). Regulation EEC/1989/2003, Off. Journal of European Union, L295.

Fragaki, G., Spyros, A., Siragakis, G., Salivaras, E., & Dais, P. (2005). Detection of extra virgin olive oil adulteration with lampante olive oil and refined olive oil using nuclear magnetic resonance spectroscopy and multivariate statistical analysis. *Journal of Agricultural and Food Chemistry, 53*, 2810–2816.

Fronimaki, P., Spyros, A., Christophoridou, S., & Dais, P. (2002). Determination of the diglyceride content in Greek virgin olive oils and some commercial olive oils by employing ^{31}P NMR spectroscopy. *Journal of Agricultural and Food Chemistry, 50*, 2207–2213.

Gama Melão, M. G., Simó-Alfonso, E. F., Ramis-Ramos, G., & Vicente, E. (2006). Determination of aerobic–anaerobic metabolism-related compounds in a Chaoborus flavicans population by infusion ion trap mass spectrometry of extracts of individual larvae. *Rapid Communications in Mass Spectrometry, 20*, 1039–1044.

García-Gonzalez, D. L., & Aparicio, R. (2002a). Detection of vinegary defect in virgin olive oils by metal oxide sensors. *Journal of Agricultural and Food Chemistry, 50*, 1809–1814.

García-Gonzalez, D. L., & Aparicio, R. (2002b). Detection of defective virgin olive oils by metal–oxide sensors. *European Food Research and Technology, 215*, 118–123.

García-Gonzalez, D. L., & Aparicio, R. (2003). Virgin olive oil quality classification combining neural network and MOS sensors. *Journal of Agricultural and Food Chemistry, 51*, 3515–3519.

Guadarrama, A., Rodriguez-Mendez, M. L., De Saja, J. A., Rios, J. L., & Olias, J. M. (2000). Array of sensors based on conducting polymers for the quality control of the aroma of the virgin olive oil. *Journal Sensors and Actuators B, 69*, 276–282.

Guadarrama, A., Rodríguez-Méndez, M. L., Sanz, C., Ríos, J. L., & De Saja, J. A. (2001). Electronic nose based on conducting polymers for the quality control of the olive oil aroma: Discrimination of quality, variety of olive and geographic origin. *Analytica Chimica Acta, 432*, 283–292.

Guimet, F., Boqué, R., & Ferré, J. (2004). Cluster analysis applied to the exploratory analysis of commercial Spanish olive oils by means of excitation-emission fluorescence spectroscopy. *Journal of Agricultural and Food Chemistry, 52*, 6673–6679.

Marcos Lorenzo, I., Pérez Pavón, J. L., Fernández Laespada, M. E., García Pinto, C., & Moreno Cordero, B. (2002). Detection of adulterants in olive oil by headspace-mass spectrometry. *Journal of Chromatography A, 945*, 221–230.

Morello, J. R., Romero, M. P., & Motilva, M. J. (2004). Effect of the maturation process of the olive fruit on the phenolic fraction of drupes and oils from Arbequina, Farga, and Morrut cultivars. *Journal of Agricultural and Food Chemistry, 52*, 6002–6009.

Owen, R. W., Giacosa, A., Hull, W. E., Haubner, R., Wurtele, G., Spiegelhalder, B., & Bartsch, H. (2000). Olive oil consumption and health: The possible role of antioxidants. *Lancet Oncology, 1*, 107–112.

Peris-Vicente, J., Simó-Alfonso, E. F., Gimeno-Adelantado, J. V., & Domenech-Carbó, M. T. (2005). Direct infusion mass spectrometry as a fingerprint of protein-binding media used in works of art. *Rapid Communications in Mass Spectrometry, 19*, 3463–3467.

Poulli, K. I., Mousdis, G. A., & Georgiu, C. A. (2005). Classification of edible and lampante virgin olive oil based on synchronous fluorescence and total luminescence spectroscopy. *Analytica Chimica Acta, 542*, 151–156.

Ranalli, A., Tombesi, A., De Mattia, G., Ferrante, M. L., & Giansante, L. (1997). Incidence of olive cultivation area on the analytical characteristics of the oil. *Rivista Italiana delle Sostanze Grasse, 74*, 501–508.

Saba, A., Mazzini, F., Raffaelli, A., Mattei, A., & Salvadori, P. (2005). Identification of 9(E),11(E)-18:2 fatty acid methyl ester at trace level in thermal stressed olive oils by GC coupled to acetonitrile CI-MS and CI-MS/MS, a possible marker for adulteration by addition of deodorized olive oil. *Journal of Agricultural and Food Chemistry, 53*, 4867–4872.

Salvador, M. D., Aranda, F., Gómez-Alonso, S., & Fregapane, G. (2003). Influence of extraction system, production year and area on Cornicabra virgin olive oil: A study of five crop seasons. *Food Chemistry, 80*, 359–366.

Torres, M. M., & Maestri, D. M. (2006). The effects of genotype and extraction methods on chemical composition of virgin olive oils from Traslasierra Valley (Córdoba, Argentina). *Food Chemistry, 96*, 507–511.

Tura, D., Prenzler, P. D., Bedgood, D. R., Antolovich, M., & Robards, K. (2004). Varietal and processing effects on the volatile profile of Australian olive oils. *Food Chemistry, 84*, 341–349.

Vandeginste, B. G. M., Massart, D. L., Buydens, L. M. C., De Jong, S., Lewi, P. J., & Smeyers-Verbeke, J. (1998). Suppervised pattern recognition. In B. G. M. Vandeginste & S. C. Rutan (Eds.), *Data Handling in Science and Technology 20 Part B* (pp. 207–241). Amsterdam, Netherlands: Elsevier Science.

Vichi, S., Pizzale, L., Conte, L. S., Buxaderas, S., & Lopez-Tamames, E. (2003). Solid-phase microextraction in the analysis of virgin olive oil volatile fraction: Characterization of virgin olive oils from two distinct geographical areas of northern Italy. *Journal of Agricultural and Food Chemistry, 51*, 6572–6577.

Yang, H., & Irudayaraj, J. (2001). Comparison of near-infrared, fourier transform-infrared, and fourier transform-Raman methods for determining olive pomace oil adulteration in extra virgin olive oil. *Journal of American Oil and Chemical Society, 78*, 889–895.

Zamora, R., Alba, V., & Hidalgo, F. J. (2001). Use of high-resolution C-13 nuclear magnetic resonance spectroscopy for the screening of virgin olive oils. *Journal of American Oil and Chemical Society, 78*, 89–94.

ANEXO XI

Sensors and Actuators B 147 (2010) 283–289

Contents lists available at ScienceDirect

Sensors and Actuators B: Chemical

journal homepage: www.elsevier.com/locate/snb

Use of electronic nose to determine defect percentage in oils. Comparison with sensory panel results

M.J. Lerma-García [a], L. Cerretani [b,c,*], C. Cevoli [c], E.F. Simó-Alfonso [a], A. Bendini [b], T. Gallina Toschi [b]

[a] Departamento de Química Analítica, Universidad de Valencia, C. Doctor Moliner 50, E-46100 Burjassot, Valencia, Spain
[b] Dipartimento di Scienze degli Alimenti, Università di Bologna, P. zza Goidanich 60, I-47521 Cesena (FC), Italy
[c] Dipartimento di Economia e Ingegneria Agrarie, Università di Bologna, P. zza Goidanich 60, I-47521 Cesena (FC), Italy

ARTICLE INFO

Article history:
Received 11 December 2009
Received in revised form 16 March 2010
Accepted 17 March 2010
Available online 25 March 2010

Keywords:
Electronic nose
Sensory defect
Sensory threshold
Olive oil
Statistical analysis

ABSTRACT

An electronic nose based on an array of 6 metal oxide semiconductor sensors was used, jointly with linear discriminant analysis (LDA) and artificial neural network (ANN) method, to classify oils containing the five typical virgin olive oil (VOO) sensory defects (fusty, mouldy, muddy, rancid and winey). For this purpose, these defects, available as single standards of the International Olive Council, were added to refined sunflower oil. According to the LDA models and the ANN method, the defected samples were correctly classified. On the other hand, the electronic nose data was used to predict the defect percentage added to sunflower oil using multiple linear regression models. All the models were able to predict the defect percentage with average prediction errors below 0.90%. Then, the develop is a useful tool to work in parallel to panellists, for realizing a rapid screening of large set of samples with the aim of discriminating defective oils.

1. Introduction

Food industry, especially dairy industry, has been one of the earliest users of sensory analysis, which is an extremely useful tool for flavour researchers [1]. There are two major types of sensory analysis: affective and analytical. Affective sensory tests are based on consumers and their perceptions of acceptability, and are important to the food industry because they explain the role of flavour, texture, and appearance in influencing consumer acceptability. These types of techniques can only measure what untrained consumers think; they tend to suffer from extensive person-to-person variability. Therefore, polling a large number of consumers (>50) is typically done to improve the statistical validity of the information obtained [1]. On the other hand, analytical sensory techniques are based on trained panelists. Discriminatory tests (difference and threshold), as well as descriptive sensory analysis, are perhaps the most powerful sensory tools. Analytical techniques are well suited for both identifying flavours in a product and discriminating sensory properties between products [1].

The most important phase of olive oil sensory analysis is represented by its aroma. Aroma is a very complex sensation, being identified more than 7100 volatile compounds in foods overall [2,3]. Each volatile compound may *potentially* contribute to aroma perception, depending upon their concentrations and sensory thresholds. The definition of sensory threshold was introduced in sensory analysis as a threshold in which any sensation was perceived. Regarding olive oil sensory analysis, the olfactory sensory threshold of a panel with respect to some defects is evaluated to habilitate the panel as official, recognized by the International Olive Council (IOC) or by the Ministry of the different European Countries. On the other hand, the sensory analysis is one of the most important tools useful to classify the virgin olive oils (VOOs) in different commercial categories (extra virgin, virgin and lampante), which is mainly evaluated with the presence of sensory defects [4]. The most frequent off-flavours of VOO are grouped into five main defects: fusty, muddy, mouldy, winey and rancid. Several works in literature have focused the correlation between defects perceived by a trained panel in VOOs and the presence of specific volatile compounds in the head-space of these samples. Morales et al. [5] have studied VOOs differently defected by dynamic headspace high-resolution gas chromatography coupled with mass spectrometry detection and olfactometry, identifying the volatile compounds mainly responsible for the off-flavours. Considering the ratio between the volatile concentration and its odour threshold in oil the mouldy defect resulted strictly related to the presence of some C_8 compounds produced by specific mould enzymes as 1-octen-3-one and 1-octen-3-ol. On the other hand, the winey defect, due to sugar fermentation, was well described by acetic acid and ethyl acetate whereas

* Corresponding author at: Dipartimento di Scienze degli Alimenti, Università di Bologna, P. zza Goidanich 60, I-47521 Cesena (FC), Italy. Tel.: +39 0547338121; fax: +39 0547382348.
E-mail address: lorenzo.cerretani@unibo.it (L. Cerretani).

0925-4005/$ – see front matter © 2010 Elsevier B.V. All rights reserved.
doi:10.1016/j.snb.2010.03.058

the fusty unpleasant odour was linked with some branched C_5 components as 3-methyl butan-1-ol as a consequence of an anomalous aminoacid degradation; with regard to rancid sensory defect several saturated and unsaturated aldehydes, as nonanal and *E*-2-heptenal respectively, have been detected as characteristic compounds.

The human being is exceptionally sensitive to some volatiles (such as 2-isobutyl-3-methoxypyrazine, which has an odour detection threshold in water of 0.002 ppb [6] and 0.015 ppb in wine [7], and 1-octen-3-ol, with a detection threshold of 1 ppb in oil) [5], but insensitive to many other volatiles (e.g., ethanol has an odour threshold in water and in oil of 100,000 ppb and 30,000 ppb respectively, and a taste threshold of 52,000 ppb in water) [5,6]. A person's ability to detect odours is also influenced by many other factors such as genetic variability, olfactory fatigue, and naturally occurring and unpredictable factors such as temperature and humidity. The complexity of food aromas and sensitivity required, plus the fact that the olfactory system must be able to respond to unknown odorants (it cannot be learned response), make this a most complex phenomenon. For this reason, considerable interest exists in the development of instrumental techniques, non-invasive and non-destructive, in order to make more objective, faster and less expensive the assessments of olive oil sensory quality [8].

Recently, metal oxide semiconductor (MOS) sensors have been applied in VOO aroma control to detect a variety of sensory defects [9–14] and to authenticate VOOs according to varietal or geographical origin of olives [15]. On the other hand, MOS sensors have a low cost and can work on-line without sample pretreatment [16,17]. These sensors do not provide a quali-quantitative analysis of volatile compounds of the samples, but responds to the whole set of volatiles in a unique digital pattern. These patterns are a signature of the particular set of aromatic compounds such as these should determine a specific olfactory perception [18].

Aparicio et al. [9] have used MOS sensors to detect the rancid defect in VOOs, using the information on volatile compounds responsible for rancidity and the sensory evaluation of the samples by assessors for explaining the mathematical selection of sensors. The same studies have been also performed by Garcia-Gonzalez et al. [11] for the detection of vinegary defect. More recently, Cimato et al. [19] have studied 12 monovarietal extra VOOs from Tuscany by means of three different methodological approaches: metal oxide sol–gel thin films based electronic nose and multivariate data analysis (PCA), headspace-solid phase micro-extraction/gas chromatography/mass spectrometry (HS-SPME/GC/MS) and sensory analysis with the aim to discriminate the different samples. Authors evidenced that HS-SPME/GC/MS was possible to obtain the chemical map of the different samples, while with electronic nose samples were separated in clusters.

More recently, Lopez-Feria et al. [20] have developed a fast method based on the direct coupling of HS-MS without chromatographic separation and multivariate tools (SIMCA and PLS) to determine the presence of negative attributes and to classify VOO. Authors analyzed a training set composed by refined olive samples spiked at different levels (from 20 to 100%) with standard defects whereas the prediction set was made up of several unknown samples belonging to different VOO classes. Despite the good results, it should be considered that this type of instrumentation is more complex and expensive than an electronic nose.

The aim of the present study was to develop a non-destructive method, based on MOS sensors, capable of classifying oils containing the typical virgin olive oil defects according to their sensory threshold previously established by trained panellists. For this purpose, linear discriminant analysis (LDA) models and artificial neural network (ANN) method were used. On the other hand, multiple linear regression (MLR) models were also constructed to predict the defect percentage added to sunflower oil.

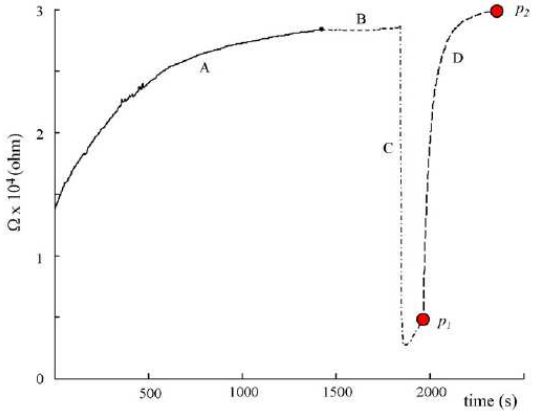

Fig. 1. Plot representing the electric resistance (Ω) of a MOS sensor during oil evaluation: (A) conditioning phase, (B) before injection phase, (C) measurement cycle and (D) recovery phase.

2. Materials and methods

2.1. Instrumentation and working conditions

An electronic olfactory system (EOS 507, Sacmi Imola S.C., Imola, Bologna, Italy) composed of a measuring chamber with 6 metal oxide sensors and a personal computer was used for the acquisition and analysis of the data generated by the EOS 507. The sensors used were: sensor 1 (SnO_2), sensor 2 ($SnO_2 + SiO_2$), sensor 3, 4 and 5 (catalyzed SnO_2 with Au, Ag and PD, respectively) and sensor 6 (WO_3). During the analysis, sensors were maintained at a temperature range of 350–450 °C. The EOS 507 was controlled by an integrated PDA equipped with proprietary software, and was connected to an automatic sampling apparatus (Model HT500H) which had a carousel of 10 sites for loading samples. Samples were kept at controlled temperature (37 °C) and placed in a chamber provided by a system that removes humidity from the surrounding environment.

2.2. MOS sensor array procedure

For each sample, 15 g were placed in 100 mL Pyrex vials equipped with a pierceable silicon/Teflon cap. For each sensor, signal is divided in four parts (see Fig. 1): (A) conditioning phase (25 min period employed to obtain a constant baseline), (B) before injection phase (in which samples were incubated at 37 °C for 7 min before injection), (C) measurement cycle (in which the oil headspace, sampled with an automatic syringe, was then pumped over the sensor surfaces for 2 min during which the sensor signals were recorded; in this phase, sensors were exposed to filtered air at a constant flow rate of 50 sccm (standard cubic cm per min) to obtain the baseline) and (D) recovery phase (another 7 min period applied to restore the original MOS conditions). Ambient air filtered with activated silica and charcoal was used as a reference gas during the recovery phase of the measurement cycle. The previous conditions ensured that the baseline reading had indeed been recovered before the next analysis was performed.

The experimental conditions adapted from Camurati et al. [10] were used, being each sample evaluated in triplicate in different days.

2.3. Determination of the sensory threshold by trained panelists

Sensory analysis was performed according to the European normative reported in Reg. 2568/91/EEC (Annex XII) [21]. Thresholds of the following defects (fusty, mouldy, muddy, rancid and winey) were assessed by ten trained assessors working as the professional panel of the Dipartimento di Scienze degli Alimenti (recognized by Italian Ministry-Mipaaf on 20 July 2006) according to the method described by Doc. 14, Rev. 2 (International Olive Council, 2007) [22]. The panel leader has used as reference defected oils those provided by IOC. A series of 12–15 samples of each of the defected oils were performed at descending concentrations by making successive dilutions in sunflower oil until the defect is not perceived. Then, paired comparison tests were carried out between these defected samples and a blank to establish the mean threshold of the panel. Up to a total of 8 pairs (the 8 samples with lower defect and 8 blanks) were randomly presented in successive independent tastings. After each tasting, the assessors were asked whether the two samples are identical or different. Upon completion of the test, the panel leader noted down the correct answers of the tasters for each concentration and expressed them as a percentage. The leader plotted the concentrations tested along the x-axis and the percentages of correct answers along the y-axis and then, by interpolation of the curve, shall determine the detection threshold which is the concentration corresponding to 75% correct answers.

2.4. Data treatment and statistical analysis

The data from the electronic nose was extracted and analyzed with the statistical package "Nose Pattern Editor" (Sacmi Imola S.C.). A feature extraction algorithm called "classical after feature" was applied to the data before other statistical treatments.

The response extracted by each sensor was defined by:

$$X = \frac{p_1}{p_2}$$

where p_1 was the resistance (see Fig. 1) of a sensor in the presence of the volatile compounds emitted from the VOO headspace, p_2 was the resistance of the sensor after the measurement (see Fig. 1), and X was the response of each sensor recorded.

In order to reduce the variability associated to possible fluctuations in the electronic nose signals, and to minimize other sources of variance also affecting the total signal of the sensors, normalized rather than absolute signals were used to construct LDA and MLR models. In order to normalize the variables, the signal of each sensor was divided by each one of the signals of the other 5 sensors; in this way, and taking into account that each pair of signals should be considered only once, $(6 \times 5)/2 = 15$ non-redundant signal ratios were obtained to be used as predictors.

LDA and MLR models were constructed using SPSS (v. 11.5, Statistical Package for the Social Sciences, Chicago, IL, USA). LDA, a supervised classificatory technique, is widely recognized as an excellent tool to obtain vectors showing the maximal resolution between a set of previously defined categories. In LDA, vectors minimizing the Wilks' lambda, λ_w, are obtained [23]. This parameter is calculated as the sum of squares of the distances between points belonging to the same category divided by the total sum of squares. Values of λ_w approaching zero are obtained with well resolved categories, whereas overlapped categories approach a λ_w of one. Up to N-1 discriminant vectors are constructed by LDA, and N has the lowest value for either the number of predictors or the number of categories. The selection of the predictors to be included in the LDA models was performed using the SPSS stepwise algorithm. According to this algorithm, a predictor is selected when the reduction of λ_w produced after its inclusion in the model exceeds F_{in}, the entrance threshold of a test of comparison of variances or F-test. However, the entrance of a new predictor modifies the significance of those predictors which are already present in the model. For this reason, after the inclusion of a new predictor, a rejection threshold, F_{out}, is used to decide if one of the other predictors should be removed from the model. The process terminates when there are no predictors entering or being eliminated from the model. Probability values of F_{in} and F_{out}, 0.05 and 0.10, respectively, were adopted. On the other hand, to select the predictors used in the construction of MLR models, the SPSS stepwise algorithm with probability values, $F_{in} = 0.05$ and $F_{out} = 0.10$, was again used.

ANN models were constructed using STATISTICA Neural Networks 4.0 (Statsoft Inc.) ANN is a mathematical algorithm which has the capability of relating the input and output parameters, learning from examples through iteration without requiring a prior knowledge on the relationships between the process variables [24]. Studies have been reported for the classification of several agricultural products, such as fruit [25,26], fish and meat [27], and vegetables [28,29].

A MLP with Back-propagation learning algorithm was performed to set up networks capable of classifying samples with a defect and samples without defect (classified according to the panel sensory thresholds). The input values were represented by the response extracted by each sensor. Two nominal output variables (V_1 and V_2) were used to perform classification tasks: V_1 for the samples with a defect (category 1) and V_2 for the samples without defect (category 2).

The original dataset (category 1 and category 2 cases) was randomly divided into *training set* (60%), *verification set* (20%) and *test set* (20%). The *verification set* was used to identify the best network on the basis of the network's error performance and to stop *training* if over-learning occurs; the *test set* was performed to give an independent assessment of the network capability of classifying samples with a defect and samples without defect.

3. Results and discussion

3.1. Establishment of the sensory threshold by the sensory panel

The evaluation of olfactory sensory threshold of a panel is necessary to know the sensory capability of the assessors. In fact, this estimation represents the first step that drives the panel to receive the habilitation as official or professional panel (certified by a certification organism).

Fig. 2 shows the results of the evaluation of the sensory thresholds of the professional panel of the Dipartimento di Scienze degli Alimenti for the five VOO defects. In particular, the sensory thresholds of the panel (corresponding to the defect percentage perceived from at least 75% of the judges) followed the order: winey = fusty < mouldy < rancid < muddy. The thresholds were similar for winey (0.09%), fusty (0.09%), mouldy (0.12%) and rancid (0.13%) defects, whereas for muddy defect this value was higher (0.80%). As reported by Morales et al. [5] each defect is characterized by the contemporary presence in the head-space of the sample of several volatile compounds, but only some of these really contribute to the specific perception as a consequence of their individual concentrations and odour thresholds [5].

3.2. Classification of the oils containing the VOO defects according to their sensory threshold establish by the sensory panel

According to the panel taster group, the samples with a defect and a correct answer percentage higher than 75% were grouped as category 1 (samples that were over the sensory threshold), while the remaining samples were grouped as category 2. For example, for the rancid defect, samples prepared with 0.2, 0.4, 0.8, 3.12 and 6.25%

Table 1
Wilk's lambda (λ_w) values and predictors selected with their corresponding standardized coefficients of the LDA models constructed for each sensory defect.

	Fusty	Mouldy	Muddy	Rancid	Winey
			λ_w		
	0.166	0.167	0.029	0.041	0.184
Predictors[a]					
S1/S2	2.60	–	–	3.99	–
S1/S3	−3.63	7.47	5.76	13.91	2.48
S1/S4	−1.94	10.73	–	–	–
S1/S5	–	−6.62	−7.33	−17.22	–
S1/S6	4.55	−11.29	–	–	–
S2/S3	–	–	−9.82	6.29	–
S3/S5	–	–	–	–	2.96
S4/S5	–	–	11.01	–	–

[a] Ratios of sensor signals.

Table 2
Results of ANN: correct classified cases (%) for each sensory defect. training, verification and test.

	Correct classified cases (%)		
	Training	*Verification*	*Test*
Rancid	100	100	80
Mouldy	100	85	85
Muddy	100	80	80
Fusty	85	85	85
Winey	75	75	75

defect in sunflower oil corresponded to category 1, while those with 0, 0.04 and 0.09% corresponded to category 2. Then, using the normalized variables, LDA models capable of classifying the samples according to these categories were constructed. Five matrices were performed, one for each sensory defect. Each matrix contained 24 points (8 samples × 3 replicates) and 15 predictors. Another column containing the two categories previously described was added to each matrix.

The λ_w values, the variables selected by the SPSS stepwise algorithm and the corresponding model standardized coefficients, showing the predictors with large discriminant capabilities for each defect, are given in Table 1. As only two categories were used to construct the model, only one discriminant function can be obtained. As observed, λ_w values were in all cases lower than 0.2. As also observed, the ratio between sensors 1 and 3 (S1/S3) showed a high discriminant power for all the models. When leave-one-out validation was applied to each model, all the samples were correctly classified. As an example, a plot showing the LDA model constructed for the rancid defect is shown in Fig. 3. As observed, a good resolution was obtained.

The structure of the best MLP neural networks tested to classify samples with a defect and samples without defect is shown in Fig. 4. The structure is characterized by 6 neurons in the input layer and 8 neurons in the hidden layer. For any defect considered, the number of iterations needed to achieve the best result is 50. Results of *training*, *verification* and *test* of the best MLP neural networks are summarized in Table 2. These values were obtained with a momentum value of 0.3 and a learning rate of 0.1.

As showed in Table 2, the performed MLP neural networks appear to classify the samples with an acceptable performance. In particular, from *test* validations, about 100, 85, 85, 80, and 75% of the data set is correctly classified, respectively for rancid, mouldy, fusty, muddy and winey defect.

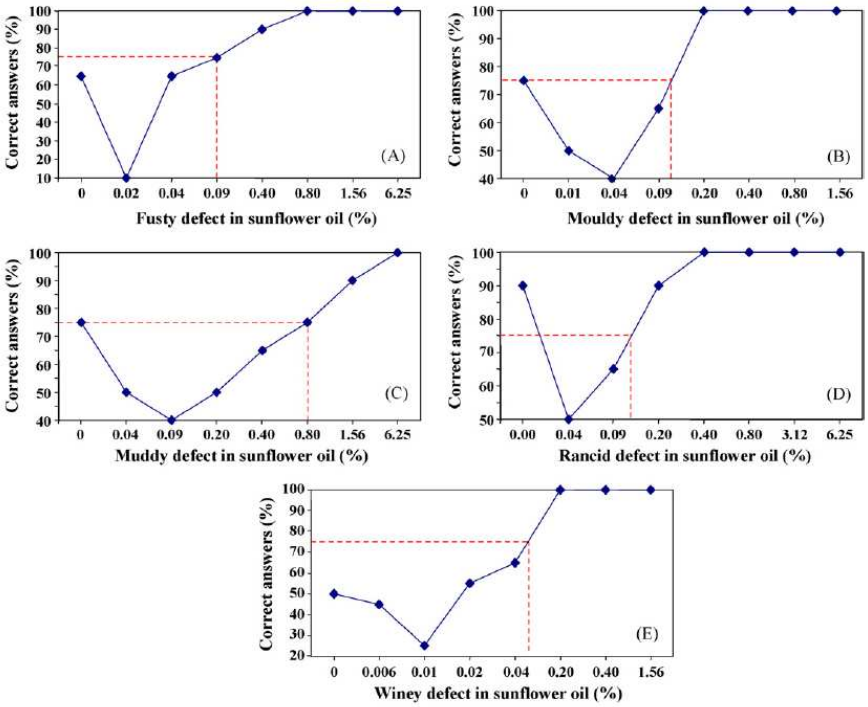

Fig. 2. Plots representing the defect (fusty, A; mouldy, B; muddy, C; rancid, D; winey, E) against the correct answer percentages, showing the detection threshold (defect % corresponding to 75% correct answers).

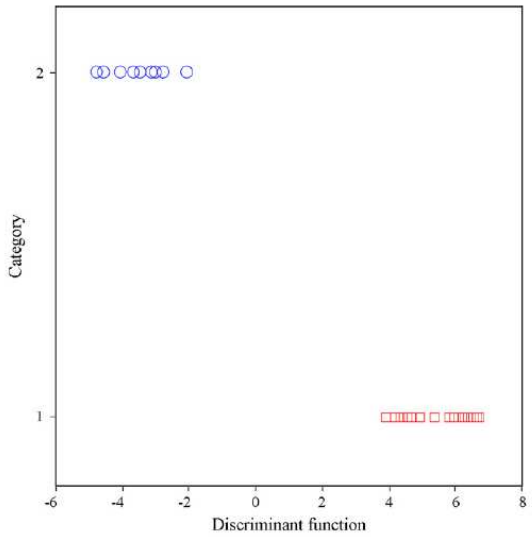

Fig. 3. Score plot on the plane of the discriminant function versus the category of the LDA model constructed to classify defected oil samples according to detection threshold of sensory analysis. Samples with a defect higher than detection threshold were grouped as category 1, the lower as category 2.

3.3. Prediction of the defect percentage in sunflower oil by electronic nose data and MLR analysis

The possibility of predicting the defect percentage added to the sunflower oil using electronic nose data was tried. For this purpose, the samples firstly described (8 samples for each defect) were used. Two additional samples were performed for each defect in order to reduce the weight of the samples with higher defect percentages. To construct MLR matrices, only the means of the replicates of the samples were included (10 objects for each model), which was important to reduce the number of variables selected by the SPSS stepwise algorithm during model construction. The 15 signal ratios described in Section 3.2 were also used as predictors to construct the MLR models.

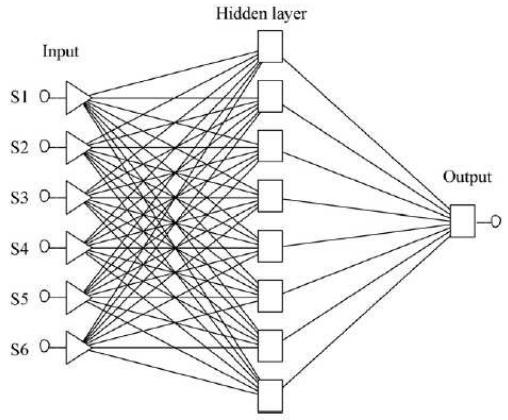

Fig. 4. MLP neural network structures used to classify defected oil samples.

The correlation plots of the calculated versus the experimental defect percentages are shown in Fig. 4. The regression coefficients (r), average prediction errors (*av. err.*, calculated as the sum of the absolute differences between expected and calculated defect percentages divided by the number of predictions) and the predictors selected for each MLR model with their corresponding non-standardized coefficients are detailed in Table 3. As observed, r values were in all cases higher than 0.988, being especially higher

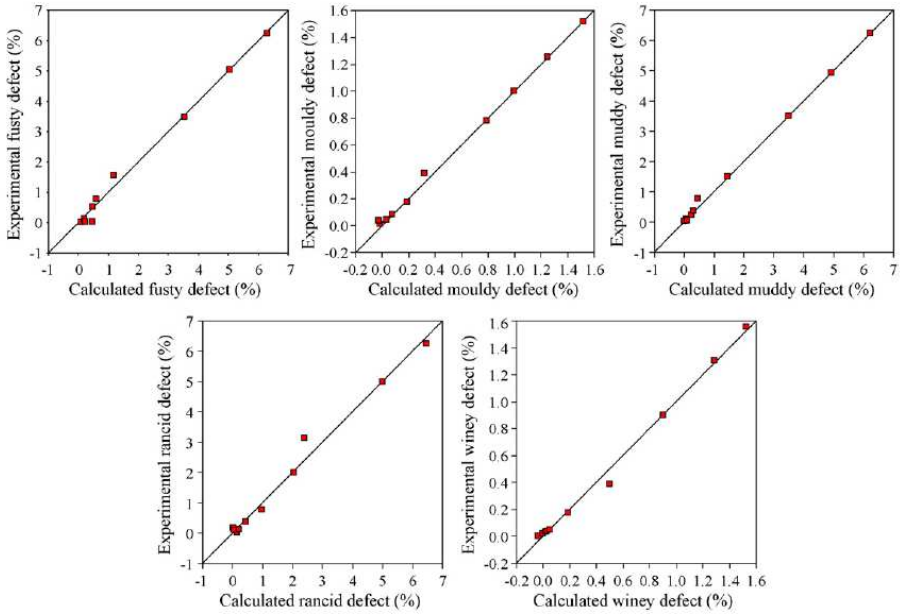

Fig. 5. Correlation plots of the calculated versus the experimental defect percentages.

Table 3
Regression coefficients (*r*), average prediction errors (av. err.) and predictors selected with their corresponding non-standardized coefficients for the MLR models constructed to predict defect percentage.

	Fusty	Mouldy	Muddy	Rancid	Winey
r	0.993	0.997	0.997	0.988	0.996
Av. err.(%)	0.51	0.22	0.43	0.90	0.39
Predictors[a]					
Constant	−651.19	14.74	−440.80	20.18	−66.64
S1/S4	–	–	–	−61.24	–
S3/S4	–	–	–	–	27.25
S3/S6	–	–	–	37.81	–
S4/S5	–	50.46	177.74	–	41.20
S4/S6	657.69	−138.47	–	–	–
S5/S6	–	75.27	271.62	–	–

[a] Ratios of sensor signals.

for fusty, mouldy, muddy and winey defects, with values higher than 0.993. This good correlation can be observed in Fig. 5. On the other hand, and as observed in Table 3, the regression models for the fusty defect (which was mainly characterized by the presence of some volatile compounds originated by fermentation processes, i.e. some branched C_5 components as 3-methyl butan-1-ol) and mouldy defect (produced by specific mould enzymes that produce volatile compounds such as 1-octen-3-one and 1-octen-3-ol) were mainly constructed with S4/S6 ratio (being S4 and S6 constructed with SnO_2 catalyzed with Au and WO_3, respectively), muddy defect (which was characterized by some volatile compounds originated by fermentation processes of oils stored for a long time on their sediment, i.e. propyl-propionate, ethyl-butanoate, propyl-butanoate and butyl-butanoate) by S5/S6 (SnO_2 catalyzed with Pd and WO_3, respectively), rancid defect (produced by several saturated and unsaturated aldehydes, such as nonanal and *E*-2-heptenal, respectively) by S1/S4 (SnO_2 and SnO_2 catalyzed with Ag, respectively) and winey defect (produced by acetic acid and ethyl acetate which were formed by sugar fermentation) by S4/S5 ratio (SnO_2 catalyzed with Ag and Pd, respectively).

4. Conclusions

This work demonstrates the ability of the electronic nose to evaluate the presence of the most common defects of VOO (fusty, mouldy, muddy, rancid and winey) when tested in different concentrations. The sensory analysis performed by a panel of trained assessors could be made more robust by the jointly use of an electronic nose, which was able to test singular defects one-by-one and to classify the defected oils according to their sensory threshold. On the other hand, excellent predictions of the defect percentage were obtained using MLR models. Then, the electronic nose, if correctly trained, could be considered an useful tool to work in parallel to panellists, for example to realize a rapid screening of large set of samples with the aim to discriminate defective oils. Under this point of view it could be helpful to test the panel performance.

Acknowledgements

The authors gratefully acknowledge Sacmi Imola S.C. who kindly allowed us to use the MOS 340 system (EOS 507), and Ibanez Riccò for technical assistance. Project CTQ2007-61445 (MEC and FEDER funds) is also acknowledged. M.J. Lerma-García thanks the Generalitat Valenciana for an FPI grant for PhD studies.

References

[1] R.T. Marsili, Comparing sensory and analytical chemistry flavor analysis, in: R. Marsili (Ed.), Sensory-Directed Flavor Analysis, CRC Press, Boca Raton, FL (USA), 2007.
[2] H. Maarse, C.A. Visscher, L.C. Willemsens, L.M. Nijssen, M.H. Boelens, Volatile Compounds in Food: Qualitative and Quantitative Data, TNO Nutrition and Food Research, Zeist (The Netherlands), 1994.
[3] L.M. Nijssen, C.A. Visscher, H. Maarse, L.C. Willemsens, M.H. Boelens, Volatile Compounds in Food-Qualitative and Quantitative Data, 7th ed., TNO Nutrition and Food Research Institute, Zeist (The Netherlands), 1996.
[4] European Community, Commission Regulation 640/2008 of 4 July 2008 amending Regulation No. 2568/91/EEC, Off. J. Eur. Communities L178 (2008) 11–16.
[5] M.T. Morales, G. Luna, R. Aparicio, Comparative study of virgin olive oil sensory defects, Food Chem. 91 (2005) 293–301.
[6] Leffingwell & Associates, Flavor-Base, Canton, GA, 1998, Accessed December 11, 2009 (http://www.leffingwell.com/odorthre.htm).
[7] D. Roujou De Boubee, C.V. Leeuwen, D. Dubourdieu, Organoleptic impact of 2-methoxy-3-isobutylpyrazine on red Bordeaux and Loire wines: effect of environmental conditions on concentrations in grapes during ripening, J. Agric. Food Chem. 48 (2000) 4830–4834.
[8] M.J. Lerma-García, C. Lantano, E. Chiavaro, L. Cerretani, J.M. Herrero-Martínez, E.F. Simó-Alfonso, Classification of extra virgin olive oils according to their geographical origin using phenolic compound profiles obtained by capillary electrochromatography, Food Res. Int. 42 (2009) 1446–1452.
[9] R. Aparicio, S.M. Rocha, I. Delgadillo, M.T. Morales, Detection of rancid defect in virgin olive oil by the electronic nose, J. Agric. Food Chem. 48 (2000) 853–860.
[10] F. Camurati, S. Tagliabue, A. Bresciani, G. Sberveglieri, P. Zaganelli, Sensory analysis of virgin olive oil by means of organoleptic evaluation and electronic olfactory system, Riv. Ital. Sost. Grasse 83 (2006) 205–211.
[11] D.L. García-González, R. Aparicio, Detection of vinegary defect in virgin olive oils by metal oxide sensors, J. Agric. Food Chem. 50 (2002) 1809–1814.
[12] D.L. García-González, R. Aparicio, Virgin olive oil quality classification combining neural network and MOS sensors, J. Agric. Food Chem. 51 (2003) 3515–3519.
[13] M.J. Lerma-García, E.F. Simó-Alfonso, A. Bendini, L. Cerretani, Metal oxide semiconductor sensors for monitoring of oxidative status evolution and sensory analysis of virgin olive oils with different phenolic content, Food Chem. 117 (2009) 608–614.
[14] M.J. Lerma-García, E.F. Simó-Alfonso, A. Bendini, L. Cerretani, Rapid evaluation of oxidized fatty acid concentration in virgin olive oils using metal oxide semiconductor sensors and multiple linear regression, J. Agric. Food Chem. 57 (2009) 9365–9369.
[15] N. Tena, A. Lazzez, R. Aparicio-Ruiz, D.L. García-González, Volatile compounds characterizing Tunisian Chemlali and Chétoui virgin olive oils, J. Agric. Food Chem. 55 (2007) 7852–7858.
[16] M.E. Escuderos, M. Uceda, S. Sánchez, A. Jiménez, Instrumental technique evolution for olive oil sensory analysis, Eur. J. Lipid Sci. Technol. 109 (2007) 536–546.
[17] S. Esposto, G.F. Montedoro, R. Selvaggini, I. Riccò, A. Taticchi, S. Urbani, M. Servili, Monitoring of virgin olive oil volatile compounds evolution during olive malaxation by an array of metal oxide sensors, Food Chem. 113 (2009) 345–350.
[18] H. Zhang, M. Chang, J. Wang, S. Ye, Evaluation of peach quality indices using an electronic nose by MLR, QPST and BP network, Sens. Actuators B Chem. 134 (2008) 332–338.
[19] A. Cimato, D. Dello Monaco, C. Distante, M. Epifani, P. Siciliano, A.M. Taurino, M. Zuppa, G. Sani, Analysis of single-cultivar extra virgin olive oils by means of an Electronic Nose and HS-SPME/GC/MS methods, Sens. Actuators B 114 (2006) 674–680.
[20] S. Lopez-Feria, S. Cardenas, J.A. García-Mesa, M. Valcárcel, Simple and rapid instrumental characterization of sensory attributes of virgin olive oil based on the direct coupling headspace-mass spectrometry, J. Chromatogr. A 1188 (2008) 308–313.
[21] European Community, Commission Regulation, No. 2568/91/EEC July 11, Off. J. Eur. Communities L248 (1991) 1–83.
[22] International Olive Council, Sensory analysis of olive oil—standard guide for the selection, training and monitoring of skilled virgin olive oil tasters, COI/T.20/Doc. No. 14/2nd Review, IOC, Madrid (Spain), September 2007.
[23] B.G.M. Vandeginste, D.L. Massart, L.M.C. Buydens, S. De Jong, P.J. Lewi, J. Smeyers-Verbeke, Data Handling in Science and Technology Part B, Elsevier Science B.V., Amsterdam (The Netherlands), 1998.
[24] M. Smith, Neural Networks for Statistical Modelling, International Thomson Computer Press, London, 1996.
[25] R. Diaz, L. Gil, C. Serrano, M. Blasco, E. Moltó, J. Blasco, Comparison of three algorithms in the classification of table olives by means of computer vision, J. Food Eng. 61 (1) (2004) 101–107.
[26] W.M. Miller, Optical defect analysis of Florida citrus, Applied Engineering in Agriculture, ASAE 11 (6) (1995) 855–860.
[27] M.R. Chandraratne, D. Kulasiri, S. Samarasinghe, Classification of lamb carcass using machine vision: comparison of statistical and neural network analyses, J. Food Eng. 82 (2007) 26–34.
[28] J.R. Brandon, M.S. Howarth, S.W. Searcy, N. Kehtarnavaz, A neural network for carrot tip classification, ASAE (1990), 90–7549, ASAE, St Joseph, MI.
[29] J. Paliwal, N.S. Visen, D.S. Jayas, Evaluation of neural network architectures for cereal grain classification using morphological features, J. Agric. Eng. Res. 79 (4) (2001) 361–370.

Biographies

M.J. Lerma-García obtained her bachelor degree in chemistry at the University of Valencia (Spain) in 2005. She is now finishing her PhD studies in the Department

of Analytical Chemistry at the same University. Her research interests include the development of analytical methods to authenticate vegetable oils, especially olive oil. At the moment she has published 25 research articles regarding this topic, some of them related to sensory analysis (she is oil taster) and electronic nose.

L. Cerretani received master's degree in 2002 and PhD in 2006 in food science from University of Bologna. He is a post-doctoral researcher at the Department of Food Science at University of Bologna and his current research interests are in the area of science and technology of lipids. He is panel leader of official panel taster group of Dipartimento di Scienze degli Alimenti of University of Bologna recognized by Italian Ministry of Agriculture (MiPAAF). He is author and co-author of over 100 scientific papers, published on national and international journals, and of chapters of books.

C. Cevoli received bachelor degree in food science and technology on 2005 at the University of Bologna. She is now finishing her PhD studies in agricultural engineering at the same University. Her research interests include numerical simulation in food processing, statistical elaboration of data about measures on food materials by neural network and other methods of multivariate statistical and thermal, physical and rheological characterization of biological materials.

E.F. Simó-Alfonso is professor in the Department of Analytical Chemistry at the University of Valencia (Spain) since 1997. He received his PhD in chemistry at the same University in 1992. His research activity is focused on: development of analytical methods to authenticate foods (as cheese, ham, wheat flour and vegetable oils), quality control of clean products and development of stationary phases for HPLC and CEC. He has published more than 90 research articles regarding these topics.

A. Bendini is an assistant professor in the Department of Food Science at the University of Bologna. She received her PhD in food biotechnology from the University of Firenze and Bologna. Her research activity is focused on: lipid analysis of vegetable oils; composition of food lipids, modification and degradation of components caused by processing and preservation; identification and quantification by chromatographic methods of volatiles and phenols; sensory characteristics linked to minor components of virgin olive oil; application of in vitro tests to value the antioxidant activity of phenols in different vegetable matrices; application of sensory analysis to virgin olive oil and other food matrices.

T. Gallina Toschi received bachelor degree in pharmaceutical chemistry on 1990. From 1990 to 1993 she studied for a post-doctoral degree in food technology of the University of Bologna and she worked on cholesterol and fatty acids oxidation. She is an assistant professor in the Department of Food Science at the University of Bologna since 1995. Her research activity is focused on: lipid analysis of vegetable oils; composition of food lipids, modification and degradation of components caused by processing and preservation. She worked using various absolute (FT-IR, FT-NIR), preparative (TLC, SPE) simple and hyphenated (GC, GC–MS, HPLC-UV–VIS, HPLC-ELSD, HPLC-DAD/FD, HPLC–MS-ES, HPLC–MS-APCI and LC–GC) analytical techniques.

ANEXO XII

JOURNAL OF AGRICULTURAL AND FOOD CHEMISTRY
ARTICLE

J. Agric. Food Chem. **2009,** *57,* 9985–9989 **9985**
DOI:10.1021/jf901730p

Prediction of the Genetic Variety of Extra Virgin Olive Oils Produced at *La Comunitat Valenciana*, Spain, by Fourier Transform Infrared Spectroscopy

VICTORIA CONCHA-HERRERA,[†] MARÍA JESÚS LERMA-GARCÍA,[‡] JOSÉ MANUEL HERRERO-MARTÍNEZ,[‡] AND ERNESTO FRANCISCO SIMÓ-ALFONSO*[,‡]

[†]Unidad Académica de Ciencias Químicas, Universidad Autónoma de Zacatecas, 98160 Zacatecas, México, and [‡]Department of Analytical Chemistry, Faculty of Chemistry, University of Valencia, 46100 Burjassot, Valencia, Spain

Fourier transform infrared spectroscopy (FTIR), followed by multivariate treatment of the spectral data, was used to classify extra virgin olive oils (EVOOs) according to their genetic variety. EVOO samples corresponding to seven different genetic varieties (Arbequina, Borriolenca, Canetera, Farga, Hojiblanca, Picual, and Serrana) were analyzed. The wavelength scale of the FTIR spectra of the oils was divided into 20 regions. The normalized absorbance peak areas within these regions were used as predictor variables. Classification of the EVOO samples according to their genetic variety was achieved by linear discriminant analysis (LDA). A good resolution among all categories was achieved using a LDA model constructed with only nine predictor variables. With this LDA model, 88% of the EVOOs were correctly classified, with assignment probabilities higher than 95%. This method is helpful for olive oil producers because it provides useful information related to the genetic variety of EVOOs, which is required by European Community regulations.

KEYWORDS: Extra virgin olive oil; genetic variety; Fourier transform infrared spectroscopy; linear discriminant analysis

INTRODUCTION

Extra virgin olive oil (EVOO) is a traditional Mediterranean food product, whose market has recently been expanded because of its highly appreciated organoleptic attributes and its health and nutritional properties (*1*). Along the last few years, the consumption of EVOOs has increased considerably in relation to the consumption of virgin and refined olive oils. Owing to its distinctive and peculiar intense taste, EVOOs obtained from some pure genetic varieties are highly appreciated.

To establish the authenticity of edible oils, a number of chromatographic (*2*−*4*), thermal (*5*), and spectroscopic methods, including fluorescence (*6*), near-infrared spectroscopy (*7*, *8*), Fourier transform infrared spectroscopy (FTIR) (*8*−*14*), FT-Raman (*8*), nuclear magnetic resonance (*15*), and mass spectrometry (MS) (*16*−*18*), followed by multivariate statistical analysis of data, have been described. For this purpose, the contents of fatty acids (*2*, *14*), tocopherols (*6*), volatile compounds (*4*), amino acids (*17*), and sterols (*3*, *18*), among others, have been used.

The development of methods to distinguish the genetic variety and also the geographical origin of EVOOs is important because, according to the European Community (EC) regulation 182/2009 (*19*), olive oil producers have to include in their manufactured products the genetic variety and also the geographical origin of the olives. In fact, authentication methods for genetic varieties of EVOO have been mainly addressed by gas chromatography (*20*−*28*) and high-performance liquid chromatography (*20*−*24*). Other techniques, such as MS (*29*), have also been used for these purposes.

FTIR is a rapid and nondestructive powerful analytical tool for the study of edible oils and fats, requiring minimum sample preparation. FTIR is also an excellent tool for quantitative analysis, because the intensities of the spectral bands are proportional to the concentration. For this reason, FTIR has mainly been used to distinguish oils from different botanical origins using non-supervised classificatory techniques (*10*, *11*), to distinguish EVOOs from different geographical origins (*30*,*31*), and to detect olive oil adulteration with other low-cost edible oils (*9*, *12*, *13*). FTIR has also been used to distinguish mixtures of three Turkish monovarietal olive oils using principal component analysis (*32*).

In this work, FTIR, jointly with the application of linear discriminant analysis (LDA), is used to classify EVOOs from seven different genetic varieties, commonly produced at *La Comunitat Valenciana*, Spain. For this purpose, FTIR spectra were divided into 20 wavelength regions, using the normalized absorbance peak areas as predictor variables.

EXPERIMENTAL PROCEDURES

Oil Samples. The EVOO samples employed in this study were mainly produced at *La Comunitat Valenciana*, Spain. Other samples, such as Hojiblanca and Picual, which were not commonly cultivated at *La Comunitat Valenciana*, were also included in this study because, jointly with the Arbequina variety, they are the main varieties in the

*To whom correspondence should be addressed. Telephone: +34-96-354-3176. Fax: +34-96-354-44 36. E-mail: ernesto.simo@uv.es.

Published on Web 10/08/2009

Table 1. Genetic Variety, Number of Samples, Geographical Origin, and Supplier of the EVOOs

genetic variety	number of samples	geographical origin	supplier	crop season
Arbequina	2	Altura (Castellón)	Intercoop	06/07, 07/08
	2	Maestrat comarca (Castellón)	Intercoop	06/07, 07/08
	2	Alicante	Intercoop	05/06, 07/08
	2	Palancia comarca (Castellón)	Intercoop	06/07, 07/08
Borriolenca	3	Alcalatén comarca (Castellón)	Intercoop	05/06, 06/07, 07/08
	4	La Plana comarca (Castellón)	Intercoop	05/06, 06/07, 07/08
Canetera	3	Maestrat comarca (Castellón)	Intercoop	05/06, 07/08
	2	Adzaneta (Castellón)	Intercoop	06/07, 07/08
	3	La Plana comarca (Castellón)	Intercoop	05/06, 06/07, 07/08
Farga	4	Maestrat comarca (Castellón)	Intercoop	05/06, 06/07, 07/08
	3	Alcalatén comarca (Castellón)	Intercoop	06/07, 07/08
	3	La Plana comarca (Castellón)	Intercoop	05/06, 06/07, 07/08
Hojiblanca	2	Estepa (Sevilla)	Carbonell	06/07, 07/08
	2	Luque (Córdoba)	Coosur	06/07, 07/08
	3	Puente Genil (Córdoba)	Borges	06/07, 07/08
	5	Fuente de Piedra (Málaga)	Grupo Hojiblanca	05/06, 06/07, 07/08
	1	Santaella (Córdoba)	Columela	05/06
Picual	2	Martos (Jaén)	Carbonell	06/07, 07/08
	2	Villanueva del Arzobispo (Jaén) and Porcuna (Jaén)	Coosur	06/07
	3	Quesada (Jaén)	Borges	05/06, 06/07, 07/08
	1	Montoso (Córdoba)	Grupo Hojiblanca	06/07
	1	Tabernas (Almería)	Castillo de Tabernas	06/07
	1	Canena (Jaén)	Castillo de Canena	07/08
Serrana	9	Altura (Castellón)	Cooperativa Altura and Intercoop	05/06, 06/07, 07/08
	3	Artana (Castellón)	Intercoop	06/07, 07/08
	3	Jérica (Castellón)	Intercoop	06/07, 07/08
	5	Viver (Castellón)	Intercoop	05/06, 06/07, 07/08

Spanish market. The genetic variety, number of samples, geographical origin, sample suppliers, and crop season are shown in **Table 1**. All Valencian samples were kindly donated by *Intercoop Oliva*l (Almassora, Castellón, Spain) and the *Cooperativa de Altura* (Castellón, Spain). Other samples were purchased at the local market, with their genetic variety and geographical origin being certified by the suppliers. All of the samples were stored in amber glass bottles at −20 °C prior to their analysis.

FTIR Spectra. FTIR spectra were obtained using a Jasco 4100 type A spectrophotometer (Jasco, Easton, MD) fitted with a single reflection attenuated total reflectance (ATR) accessory. The ATR accessory (ATR-PRO410-S, Jasco) was equipped with a ZnSe reflection crystal. All analyses were carried out at room temperature. Measurements were obtained using 15 scans at 2 cm^{-1} resolution. Spectra were recorded in the absorbance mode from 4000 to 600 cm^{-1}, with only the regions being from 2500 to 750 cm^{-1} considered in this study. Data handling was performed with the Spectra Manager version 2.07.00 software (Jasco).

For each sample (ca. 20 μL were put on the crystal surface), the absorbance spectrum was collected against a background obtained with a dry and empty ATR cell. Two spectra were recorded for each sample. Before each spectrum was acquired, the ATR crystal was cleaned with a cellulose tissue soaked in *n*-hexane, rinsed with acetone, and dried.

Data Treatment and Construction of Data Matrices. FTIR spectra were divided into the 20 wavelength regions described in **Table 2**. Each selected region corresponds to a peak or a shoulder, which represent structural or functional group information, either about the lipids or minor components of the oil samples (see **Table 2**). For each region, the peak/shoulder area was measured. To reduce the variability associated with the total amount of oil sample used and to minimize other sources of variance also affecting the intensity of all of the peaks, such as the radiation source intensity, normalized rather than absolute areas were used. To normalize the variables, the area of each region was divided by each one of the areas of the other 19 regions; in this way and because any pair of areas should be considered only once, $(20 \times 19)/2 = 190$ normalized variables were obtained.

A matrix containing 76 objects, which corresponded to the average of 2 replicates (**Table 1**), and 190 predictors, was constructed. A response column, containing the categories corresponding to the 7 genetic varieties of the oils, was added to this matrix. Only the means of the replicates of the samples were included in this matrix; in this way, the internal dispersion of the categories was reduced, which was important to reduce the number of variables selected during model construction. The matrix was randomly divided into two groups, training and evaluation sets. The training set was composed of 6 samples for each genetic variety ($6 \times 7 = 42$ objects), while the evaluation set was performed with the remaining samples (34 objects). Statistical data treatment of the normalized variables was performed using the SPSS package (version 12.0.1, Statistical Package for the Social Sciences, Chicago, IL).

RESULTS AND DISCUSSION

FTIR spectra of the 76 EVOO samples shown in **Table 1** were collected. **Figure 1** shows the spectra of seven oils, corresponding to the seven genetic varieties. As it can be observed, FTIR spectra were closely similar. To enhance small differences that were not appreciated straight away in the spectra of oils obtained from different genetic varieties, the peak areas of the 20 selected regions were conveniently handled by multivariate statistical techniques.

Classification of EVOOs According to Their Genetic Variety Using LDA. LDA, a supervised classificatory technique, is widely recognized as an excellent tool to obtain vectors showing the maximal resolution between a set of previously defined categories. In LDA, vectors minimizing Wilks' lambda, λ_w, are obtained (*35*). This parameter is calculated as the sum of squares of the distances between points belonging to the same category

Table 2. FTIR Spectral Regions Selected as Predictor Variables for Statistical Data Treatment

identification number	range (cm^{-1})	functional group	nominal frequency	mode of vibration
1	2393−2347	alcane[a]		
2	2347−2279	alcane[a]		
3	1870−1712	−C═O (ester)	1746[b]	stretching
4	1712−1693	−C═O (acid)	1711[b]	stretching
5	1693−1671	−C═O	[a]	stretching
6	1671−1590	−C═C− (*cis*)	1654[b]	stretching
7	1467−1426	−C−H (CH_2)	1465[a]	bending (scissoring)
		−C−H (CH_3)	1450[a]	bending (asym)
8	1426−1407	═C−H (*cis*)	1417[b]	bending (rocking)
9	1407−1380	═C−H	1400[a]	bending
		−C−H (CH_3)	1377[b]	bending (sym)
10	1380−1336	O−H	1359[a]	bending (in plane)
11	1336−1309	non-assigned	1319[b]	bending
12	1309−1292	═C−H (*cis*)	1294[c]	bending
13	1292−1257	═C−H	−[c]	bending
14	1257−1216	−C−O		stretching
		$-CH_2-$	1238[b]	bending
		−C−O	1163[b]	stretching
15	1216−1127	$-CH_2-$	1163[b]	bending
		−C−O	1138[a]	stretching
16	1127−1109	−C−O	1118[b]	stretching
17	1109−1045	−C−O	1097[b]	stretching
18	1045−998	−C−O	1033[b]	stretching
		−HC═CH− (*trans*)	968[b]	bending (out of plane)
19	998−883	−HC═CH− (*cis*)?	914[b]	bending (out of plane)
20	883−796	$═CH_2$	850[a]	wagging

[a] According to ref *34*. [b] According to ref *33*. [c] According to ref *8*.

divided by the total sum of squares. Values of λ_w approaching 0 are obtained with well-resolved categories, whereas overlapped categories made λ_w approach 1. Up to $N-1$ discriminant vectors are constructed by LDA, with N being the lowest value for either the number of predictors or the number of categories.

Using the normalized variables, a LDA model capable of classifying the EVOO samples according to their genetic varieties was constructed. To select the variables to be included in the model, the SPSS stepwise algorithm was used. According to this algorithm, a predictor is selected when the reduction of λ_w produced after its inclusion in the model exceeds F_{in}, the entrance threshold of a test of comparison of variances or F test. However, the entrance of a new predictor modifies the significance of those predictors that are already present in the model. For this reason, after the inclusion of a new predictor, a rejection threshold, F_{out}, is used to decide if one of the other predictors should be removed from the model. The process terminates when there are no predictors entering or being eliminated from the model. The default probability values of F_{in} and F_{out}, 0.05 and 0.10, respectively, were adopted.

A good resolution between the seven categories was achieved when the LDA model was constructed ($\lambda_w = 0.576$). This λ_w value was higher than those previously reported in our previous work (*29*); however, in this previous study, just three categories were simultaneously distinguished. The variables selected by the SPSS stepwise algorithm and the corresponding standardized coefficients of the model, showing the predictors with large discriminant capabilities, are given in **Table 3**. According to this table, the main IR regions selected by the algorithm to construct the LDA model corresponded to −C═O (acid, stretching), −C−H (CH_2, bending scissoring), −C−H (CH_3, bending sym), ═C−H (bending), −C−O (stretching), and $-CH_2-$ (bending).

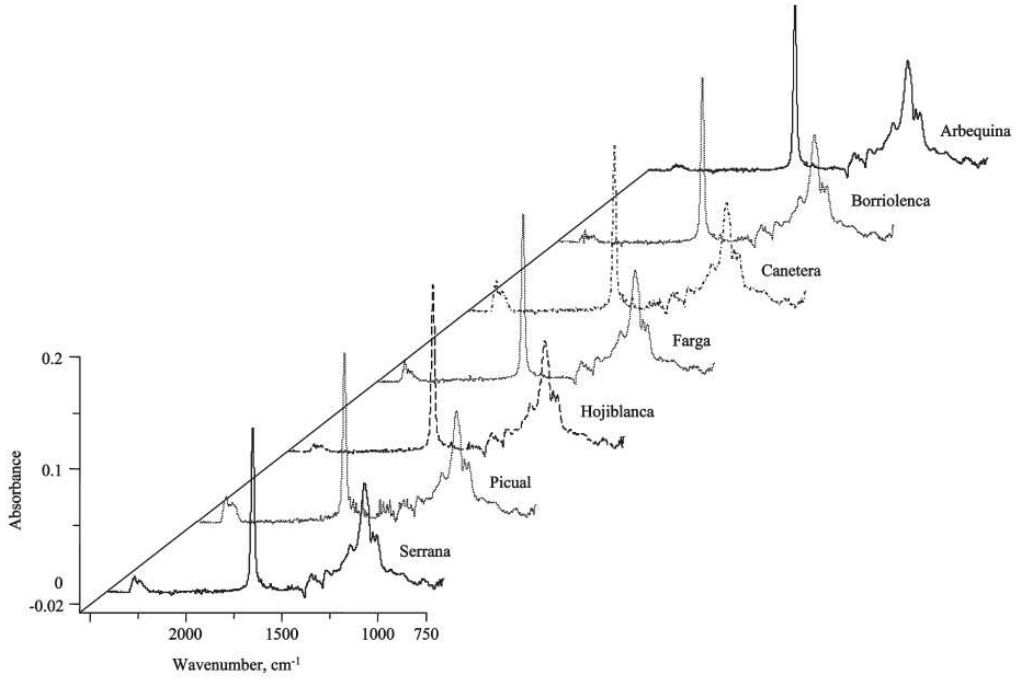

Figure 1. FTIR spectra of EVOO samples of (A) Arbequina from Alicante (crop season 05/06), (B) Borriolenca from Alcalatén comarca (crop season 07/08), (C) Canetera from La Plana comarca (crop season 06/07), (D) Farga from Maestrat comarca (crop season 06/07), (E) Hojiblanca from Luque, Córdoba (crop season 07/08), (F) Picual from Martos, Jaén (crop season 06/07), and (G) Serrana from Altura, Castellón (crop season 05/06).

Table 3. Predictors Selected and Corresponding Standardized Coefficients of the LDA Model Constructed To Predict the Genetic Variety of EVOOs

predictors[a]	f_1	f_2	f_3	f_4	f_5	f_6
1/5	0.13	−0.91	−0.96	−0.06	−0.60	−2.04
1/7	5.85	4.36	−1.51	4.00	4.07	−2.22
1/9	−6.01	−3.57	3.91	−3.71	−3.11	4.03
3/6	−0.13	0.30	0.47	0.58	0.95	0.76
4/12	9.48	15.43	12.74	16.47	−7.05	−6.22
4/14	−9.00	−14.54	−12.66	−16.58	7.15	6.35
12/15	0.85	1.32	1.25	1.30	−0.89	0.35
13/16	−0.28	−0.55	0.69	−0.11	1.03	−0.48
14/17	1.06	−0.10	−0.37	−0.32	−0.41	0.43

[a] Pairs of wavelength regions were identified according to **Table 2**.

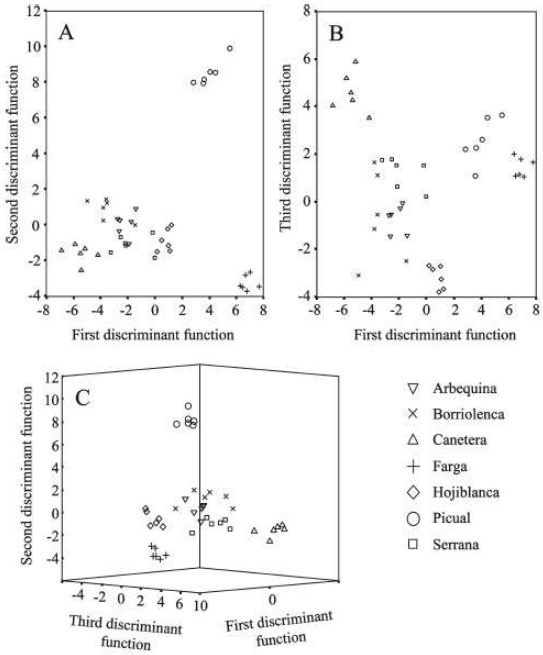

Figure 2. Score plots on the planes of the (A) first and second and (B) first and third discriminant functions and (C) an oblique perspective of the 3D space defined by the three discriminant functions of the LDA model constructed to classify EVOOs according to their genetic variety.

The projections of the samples on the six discriminant functions allowed for the distinction of at least a different category. As shown in **Figure 2A**, a large resolution between Farga, Picual, and the other categories was achieved along f_1. On the other hand, the variance gathered by f_2 was mainly associated with the resolution between Picual and the rest of categories as a whole. According to **Figure 2B**, Canetera, Picual, and Hojiblanca were resolved from the rest of categories along f_3. Finally, **Figure 2C** shows a score plot from an oblique perspective of the 3D space defined by the three first discriminant functions. When this 3D figure was rotated, the separation between all of the different categories was evident. Because of the fact that a large number of categories (seven) were included in this work in relation to the three categories described in our previous work (*29*), it is logical that it was more difficult to appreciate separation between categories when represented in a plane. When the leave-one-out validation method was applied to the training set, all of the points were correctly classified. Concerning the evaluation set, all of the objects were correctly assigned to an assignment probability higher than 95%, except four objects, which corresponded to two Borriolenca, one Hojiblanca, and one Arbequina samples.

Thus, the possibility of classifying EVOO samples according to their genetic variety using FTIR data has been demonstrated. Using only nine predictors, all of the EVOO samples belonging to seven different genetic varieties mainly produced at *La Comunitat Valenciana* were correctly classified with a good resolution among the categories. According to the EC regulation (*19*), this reliable procedure provides useful information regarding the genetic varieties, which is important for olive oil producers.

On the other hand, this method is faster than other methods described in the literature (*20*−*23*, *26*), which are based on chromatographic separations, using fatty acids (*20*−*22*, *26*), sterols (*21*), *n*-alkanes (*23*), and triglycerides (*22*) as variables. For classification purposes, these methods have used both nonsupervised and supervised statistical tools. The first one just led to a preliminary distribution according to the genetic varieties (*20*). The second approach produced satisfactory resolution among the categories (*21*−*23*, *26*); however, in these studies, no more than five categories were simultaneously resolved.

ABBREVIATIONS USED

EVOO, extra virgin olive oil; LDA, linear discriminant analysis; MS, mass spectrometry.

LITERATURE CITED

(1) Bendini, A.; Cerretani, L.; Carrasco-Pancorbo, A.; Gómez-Caravaca, A. M.; Segura-Carretero, A.; Fernández-Gutiérrez, A.; Lercker, G. Phenolic molecules in virgin olive oils: A survey of their sensory properties, health effects, antioxidant activity and analytical methods. An overview of the last decade. *Molecules* **2007**, 12, 1679–1719.

(2) Brodnjak-Voncina, D.; Kodba, Z. C.; Novic, M. Multivariate data analysis in classification of vegetable oils characterized by the content of fatty acids. *Chemom. Intell. Lab. Syst.* **2005**, 75, 31–43.

(3) Mariani, C.; Bellan, G.; Lestini, E.; Aparicio, R. The detection of the presence of hazelnut oil in olive oil by free and esterified sterols. *Eur. Food Res. Technol.* **2006**, 223, 655–661.

(4) de Koning, S.; Kaal, E.; Janssen, H.-G.; van Platerink, C.; Brinkman, U. A. T. Characterization of olive oil volatiles by multi-step direct thermal desorption−comprehensive gas chromatography−time-of-flight mass spectrometry using a programmed temperature vaporizing injector. *J. Chromatogr., A* **2008**, 1186, 228–235.

(5) Chiavaro, E.; Vittadini, E.; Rodriguez-Estrada, M. T.; Cerretani, L.; Bendini, A. Differential scanning calorimeter application to the detection of refined hazelnut oil in extra virgin olive oil. *Food Chem.* **2008**, 110, 248–256.

(6) Sikorska, E.; Górecki, T.; Khmelinskii, I. V.; Sikorski, M.; Koziol, J. Classification of edible oils using synchronous scanning fluorescence spectroscopy. *Food Chem.* **2005**, 89, 217–225.

(7) Kasemsumran, S.; Kang, N. Partial least squares processing of near-infrared spectra for discrimination and quantification of adulterated olive oils. *Spectrosc. Lett.* **2005**, 38, 839–851.

(8) Yang, H.; Irudayaraj, J.; Paradkar, M. M. Discriminant analysis of edible oils and fats by FTIR, FT-NIR and FT-Raman spectroscopy. *Food Chem.* **2005**, 93, 25–32.

(9) Baeten, V.; Fernández Pierna, J. A.; Dardenne, P.; Meurens, M.; García-González, D. L.; Aparicio-Ruiz, R. Detection of the presence of hazelnut oil in olive oil by FT-Raman and FT-MIR spectroscopy. *J. Agric. Food Chem.* **2005**, 53, 6201–6206.

(10) Dupuy, N.; Duponchel, L.; Huvenne, J. P.; Sombret, B.; Legrand, P. Classification of edible fats and oils by principal component analysis of Fourier transform infrared spectra. *Food Chem.* **1995**, 57, 245–251.

(11) Lai, Y. W.; Kemsley, E. K.; Wilson, R. H. Potential of Fourier transform infrared spectroscopy for the authentication of vegetable oils. *J. Agric. Food Chem.* **1999**, 42, 1154–1159.

(12) Ozen, B. F.; Mauer, L. J. Detection of hazelnut oil adulteration using FT-IR spectroscopy. *J. Agric. Food Chem.* **2002**, 50, 3898–3901.
(13) Vlachos, N.; Skopelitis, Y.; Psaroudaki, M.; Konstantinidou, V.; Chatzilazarou, A.; Tegou, E. Applications of Fourier transform-infrared spectroscopy to edible oils. *Anal. Chim. Acta* **2006**, 573−574, 459–465.
(14) Maggio, R. M.; Kaufman, T. S.; Del Carlo, M.; Cerretani, L.; Bendini, A.; Cichelli, A.; Compagnone, D. Monitoring of fatty acid composition in virgin olive oil by Fourier transformed infrared spectroscopy coupled with partial least squares. *Food Chem.* **2009**, 114, 1549–1554.
(15) Dais, P.; Spyros, A. ^{31}P NMR spectroscopy in the quality control and authentication of extra-virgin olive oil: A review of recent progress. *Magn. Reson. Chem.* **2007**, 45, 367–377.
(16) Lay, J. O.; Liyanage, R.; Durham, B.; Brooks, J. Rapid characterization of edible oils by direct matrix-assisted laser desorption/ionization time-of-flight mass spectrometry analysis using triacylglycerols. *Rapid Commun. Mass Spectrom.* **2006**, 20, 952–958.
(17) Lerma-García, M. J.; Ramis-Ramos, G.; Herrero-Martínez, J. M.; Simó-Alfonso, E. F. Classification of vegetable oils according to their botanical origin using amino acid profiles established by direct infusion mass spectrometry. *Rapid Commun. Mass Spectrom.* **2007**, 21, 3751–3755.
(18) Lerma-García, M. J.; Ramis-Ramos, G.; Herrero-Martínez, J. M.; Simó-Alfonso, E. F. Classification of vegetable oils according to their botanical origin using sterol profiles established by direct infusion mass spectrometry. *Rapid Commun. Mass Spectrom.* **2008**, 22, 973–978.
(19) Commission regulation (EC) number 182/2009 of 6 March 2009 amending regulation (EC) number 1019/2002 on marketing standards for olive oil. *Off. J. Eur. Union* **2009**, *L63*, 6−8.
(20) Stefanoudaki, E.; Kotsifaki, F.; Koutsaftakis, A. Classification of virgin olive oils of the two major Cretan cultivars based on their fatty acid composition. *J. Am. Oil Chem. Soc.* **1999**, 76, 623–626.
(21) Bucci, R.; Magri, A. D.; Magri, A. L.; Marini, D.; Marini, F. Chemical authentication of extra virgin olive oil varieties by supervised chemometric procedures. *J. Agric. Food Chem.* **2002**, 50, 413–418.
(22) Aranda, F.; Gómez-Alonso, S.; Rivera del Álamo, R. M.; Salvador, M. D.; Fregapane, G. Triglyceride, total and 2-position fatty acid composition of Cornicabra virgin olive oil: Comparison with other Spanish cultivars. *Food Chem.* **2004**, 86, 485–492.
(23) Koprivnjak, O.; Moret, S.; Populin, T.; Lagazio, C.; Conte, L. S. Variety differentiation of virgin olive oil based on *n*-alkane profile. *Food Chem.* **2005**, 90, 603–608.
(24) Krichene, D.; Taamalli, W.; Daoud, D.; Salvador, M. D.; Fregapane, G.; Zarrouk, M. Phenolic compounds, tocopherols and other minor components in virgin olive oils of some Tunisian varieties. *J. Food Biochem.* **2007**, 31, 179–194.
(25) Luna, G.; Morales, M. T.; Aparicio, R. Characterisation of 39 varietal virgin olive oils by their volatile compositions. *Food Chem.* **2006**, 98, 243–252.
(26) D'Imperio, M.; Dugo, G.; Alfa, M.; Mannina, L.; Segre, A. L. Statistical analysis on Sicilian olive oils. *Food Chem.* **2007**, 102 (3), 956–965.
(27) Baccouri, O.; Bendini, A.; Cerretani, L.; Guerfel, M.; Baccouri, B.; Lercker, G.; Zarrouk, M.; Ben Miled, D. D. Comparative study on volatile compounds from Tunisian and Sicilian monovarietal virgin olive oils. *Food Chem.* **2008**, 111, 322–328.
(28) Ben Temime, S.; Manai, H.; Methenni, K.; Baccouri, B.; Abaza, L.; Daoud, D.; Sánchez-Casas, J.; Osorio-Bueno, E.; Zarrouk, M. Sterolic composition of Chétoui virgin olive oil: Influence of geographical origin. *Food Chem.* **2008**, 110, 368–374.
(29) Lerma-García, M. J.; Herrero-Martínez, J. M.; Ramis-Ramos, G.; Simó-Alfonso, E. F. Prediction of the genetic variety of Spanish extra virgin olive oils using fatty acid and phenolic compound profiles established by direct infusion mass spectrometry. *Food Chem.* **2008**, 108, 1142–1148.
(30) Bendini, A.; Cerretani, L.; Di Virgilio, F.; Belloni, P.; Bonoli-Carbognin, M.; Lercker, G. Preliminary evaluation of the application of the FTIR spectroscopy to control the geographic origin and quality of virgin olive oils. *J. Food Qual.* **2007**, 30, 424–437.
(31) Galtier, O.; Dupuy, N.; Le Dréau, Y.; Ollivier, D.; Pinatel, C.; Kister, J.; Artaud, J. Geographic origins and compositions of virgin olive oils determinated by chemometric analysis of NIR data. *Anal. Chim. Acta* **2007**, 595, 136–144.
(32) Gurdeniz, G.; Tokatli, F.; Ozen, B. Differentiation of mixtures of monovarietal olive oils by mid-infrared spectroscopy and chemometrics. *Eur. J. Lipid Sci. Technol.* **2007**, 109, 1194–1202.
(33) Guillén, M. D.; Cabo, N. Relationships between the composition of edible oils and lard and the ratio of the absorbance of specific bands of their Fourier transform infrared spectra. Role of some bands of the fingerprint region. *J. Agric. Food Chem.* **1998**, 46, 1788–1793.
(34) Silverstein, R. M.; Bassler, G. C.; Morrill, T. C. In *Spectrometric Identification of Organic Compounds*; John Wiley and Sons: Chichester, U.K., 1981.
(35) Vandeginste, B. G. M.; Massart, D. L.; Buydens, L. M. C.; De Jong, S.; Lewi, P. J.; Smeyers-Verbeke, J. In *Data Handling in Science and Technology Part B*; Elsevier Science B.V.: Amsterdam, The Netherlands, 1998; p 237.

Received for review February 25, 2009. Revised manuscript received September 11, 2009. Accepted September 22, 2009. This work was supported by Project CTQ2007-61445 (MEC and FEDER funds). V. Concha-Herrera thanks the University of Valencia for a contract. M. J. Lerma-García also thanks the Generalitat Valenciana for a FPI grant for Ph.D. studies.

ANEXO XIII

Available online at www.sciencedirect.com
ScienceDirect
Food Chemistry 108 (2008) 1142–1148
Food Chemistry
www.elsevier.com/locate/foodchem

Analytical Methods

Prediction of the genetic variety of Spanish extra virgin olive oils using fatty acid and phenolic compound profiles established by direct infusion mass spectrometry

M.J. Lerma-García *, J.M. Herrero-Martínez, G. Ramis-Ramos, E.F. Simó-Alfonso

Department of Analytical Chemistry, Faculty of Chemistry, University of Valencia, C/Doctor Moliner 50, 46100 Burjassot, Valencia, Spain

Received 18 September 2007; received in revised form 20 November 2007; accepted 24 November 2007

Abstract

The genetic varieties of Spanish extra virgin olive oils (Arbequina, Hojiblanca and Picual) were predicted by direct infusion of the samples in the electrospray ionization source of a mass spectrometer, followed by linear discriminant analysis of the spectral data. The samples were 1:50 diluted (v/v) with an 85:15 propanol/methanol (v/v) mixture containing 40 mM KOH and infused. The abundances of the $[M–H]^-$ peaks of the free fatty acids (7 peaks) and 28 phenolic compounds (20 peaks) were measured. Ratios of pairs of peak abundances were used as predictors in the construction of the linear discriminant analysis models. An excellent resolution between the three genetic varieties was achieved.

Keywords: Fatty acids; Genetic variety; Mass spectrometry; Olive oil authentication; Phenolic compounds

1. Introduction

Olive oil is a product of significant nutritional value, and a very important ingredient of the Mediterranean diet. The beneficial effects of olive oil can be attributed not only to the high relationship between unsaturated and saturated fatty acids, but also to the antioxidant properties of its phenolic compounds (Ríos, Gil, & Gutiérrez-Rosales, 2005; Tripoli et al., 2005). Along the last years, the consumption of extra virgin olive oils has increased considerably in relation to the consumption of virgin and refined olive oils. Owing to its distinctive and peculiar intense taste, extra virgin olive oils obtained from some pure genetic varieties are highly appreciated.

Oil authentication (Lees, 1999) can be carried out by a variety of methods which have been recently reviewed (Aparicio & Aparicio-Ruíz, 2000; Aparicio & Luna, 2002). The concentration profiles of saturated and unsaturated fatty acids (Aranda, Gómez-Alonso, Rivera del Álamo, Salvador, & Fregapane, 2004; Bucci, Magri, Magri, Marini, & Marini, 2002; Caponio, Alloggio, & Gomes, 1999; D'Imperio et al., 2007; Krichene et al., 2007; Marini et al., 2004; Ranalli et al., 2002; Salvador, Aranda, Gómez-Alonso, & Fregapane, 2003; Stefanoudaki, Kotsifaki, & Koutsaftakis, 1999; Torres & Maestri, 2006), triglycerides (Aranda et al., 2004; Stefanoudaki, Kotsifaki, & Koutsaftakis, 1997), diacylglycerols and tryacylglycerols (Nagy et al., 2005; Ranalli et al., 2002), sterols (Bucci et al., 2002; Marini et al., 2004; Nagy et al., 2005; Salvador et al., 2003), phenolic compounds (Caponio et al., 1999; Gómez-Alonso, Salvador, & Fregapane, 2002; Krichene et al., 2007; Morelló, Romero, & Motilva, 2004; Ríos et al., 2005; Saitta, Lo-Curto, Salvo, Di-Bella, & Dugo, 2002; Salvador et al., 2003; Torres & Maestri, 2006), hydrocarbons (Koprivnjak, Moret, Populin, Lagazio, & Conte, 2005), pigments (Cichelli & Pertesana, 2004; Krichene et al., 2007) and volatile components (Guadarrama, Rodríguez-Méndez, Sanz, Ríos, & De Saja, 2001; Luna, Morales,

* Corresponding author. Tel.: +34 963543176; fax: +34 963544436.
E-mail address: mlergar@alumni.uv.es (M.J. Lerma-García).

0308-8146/$ - see front matter © 2007 Elsevier Ltd. All rights reserved.
doi:10.1016/j.foodchem.2007.11.065

& Aparicio, 2006; Tura, Prenzler, Bedgood, Antolovich, & Robards, 2004) differ according to the fruit variety. Other factors as latitude, climatic conditions, irrigation regime, fruit ripening, and harvesting and extraction technologies also affect the distributions of the fatty acids (D'Imperio et al., 2007; Stefanoudaki et al., 1999; Torres & Maestri, 2006) and triglycerides (Stefanoudaki et al., 1997). The concentration profiles of other minor oil components, such as phenolic compounds (Caponio et al., 1999; Gómez-Alonso et al., 2002; Morelló et al., 2004; Salvador et al., 2003; Torres & Maestri, 2006; Tripoli et al., 2005), hydrocarbons (Koprivnjak et al., 2005) and volatile components (Tura et al., 2004), are also affected.

Authentication methods for genetic varieties of olive oils have been most frequently established using GC (Aranda et al., 2004; Bucci et al., 2002; Caponio et al., 1999; D'Imperio et al., 2007; Koprivnjak et al., 2005; Krichene et al., 2007; Luna et al., 2006; Ríos et al., 2005; Saitta et al., 2002; Stefanoudaki et al., 1999; Torres & Maestri, 2006; Tura et al., 2004) and HPLC (Aranda et al., 2004; Bucci et al., 2002; Caponio et al., 1999; Cichelli & Pertesana, 2004; Gómez-Alonso et al., 2002; Koprivnjak et al., 2005; Krichene et al., 2007; Morelló et al., 2004; Nagy et al., 2005; Ranalli et al., 2002; Ríos et al., 2005; Salvador et al., 2003; Stefanoudaki et al., 1997, 1999). The fatty acid composition of two olive oil varieties from Crete, Koroneiki and Mastoides, were studied by GC (Stefanoudaki et al., 1999). In comparison to the Mastoides variety, the Koroneiki oils were characterized by their lower concentrations of oleic and heptadecanoic acids, and higher concentrations of linoleic and palmitic acids. In the same study, oils from high-altitude locations were rich in mono-unsaturated fatty acids, whereas oils from low-altitude locations were mainly richer in saturated fatty acids. Also, the contents of both palmitic and palmitoleic acids increased with the altitude in both cultivars. In addition, the classification of olive oils according to the cultivar and geographical origin using factor analysis and linear discriminant analysis (LDA) of the fatty acid concentrations, was demonstrated. D'Imperio et al. (2007) have analyzed a large number of Sicilian extra virgin olive oils from 22 cultivars of different geographical areas and harvesting times using GC. Oleic, linoleic and palmitic fatty acids were crucial in the characterization of the olive oil varieties. Using GC and solid phase extraction followed by RP–HPLC, Krichene et al. (2007) have determined the contents of fatty acids and 14 phenolic compounds, as well as other olive oil minor components, in six Tunisian olive varieties; the concentrations of these compounds differed between the genetic varieties.

Direct infusion in the electrospray ionization source (ESI) of a mass spectrometer (MS) without prior chromatographic separation, followed by principal component analysis (PCA), were used to evaluate the adulteration of olive oils with oils of others fruits and seeds (Goodacre, Vaidyanathan, Bianchi, & Kell, 2002); using the triglyceride profile and their daughter ions, refined olive and hazelnut oils, and unrefined peanut and sunflower oils, appeared as four resolved groups. Two ion sources, ESI and atmospheric pressure photoionization (APPI), coupled to a quadrupole time-of-flight mass spectrometer, applied to the control of olive oil adulteration (Gómez-Ariza, Arias-Borrego, García-Barrera, & Beltran, 2006), were compared. Using PCA and LDA of the triglyceride profile, mixtures of olive oils with other vegetable oils were distinguished.

Direct infusion ESI–MS, followed by LDA, has been successfully used to classify binding media in art works (Peris-Vicente, Simó-Alfonso, Gimeno-Adelantado, & Domenech-Carbó, 2005) and midge larvae (Gama Melão, Simó-Alfonso, Ramis-Ramos, & Vicente, 2006). Direct infusion ESI–MS has been also used to classify vegetable oils according to their biological origin, and to detect the adulteration of olive oil with soybean oil (Catharino et al., 2005).

In this work, a simple and quick method based on direct infusion MS, followed by LDA of the ratios of peak pairs of both free fatty acids and a large number of phenolic compounds, capable of reliably classifying the three most common monovarietal olive oils in the Spanish market (Hojiblanca, Arbequina and Picual), was developed.

2. Materials and methods

2.1. Instrumentation and working conditions

An HP 1100 series ion trap mass spectrometer (ITMS) provided with an ESI source (Agilent Technologies, Waldbronn, Germany) was used. A syringe pump (kdScientific, Holliston, MA, USA) was used to infuse the samples at 0.3 mL h^{-1} (5 μL min^{-1}) through a 50 μm i.d. fused silica capillary. The MS conditions were: nebulizer gas pressure, 25 psi; drying gas flow, 5 L min^{-1} at a temperature of 200 °C; capillary voltage, 3.5 kV; skimmers 1 and 2 V, −26.8 V and −6.0 V, respectively. Nitrogen was used as the nebulizer and drying gas (Gaslab NG LCMS 20 generator, Equcien, Madrid, Spain). The MS was scanned within the m/z 100–800 range in the negative-ion mode. The target mass was set at m/z 281 ($[M–H]^-$ peak of oleic acid). Maximum loading of the ion trap was 3×10^4 counts, and maximum collection time was 300 ms. All samples were injected at least four times, and each time the data were averaged during 1 min. The four replicates of each sample were always performed in different days.

2.2. Reagents, samples and procedures

Methanol (MeOH) and *n*-propanol (PrOH) (Scharlau, Barcelona, Spain) and KOH (Probus, Barcelona, Spain) were used. The extra virgin olive oil samples employed in this study are indicated in Table 1. The genetic variety and geographical origin of the oils were certified by the suppliers. The oil samples were 1:50 (v/v) diluted with an 85:15 PrOH/MeOH (v/v) mixture containing 40 mM KOH. This mixture was also used to rinse and clean the

Table 1
Genetic variety, number of samples, geographical origin and brand of the extra virgin olive oil samples

Genetic variety	No. of samples	Geographical origin	Brand
Arbequina	2	Aguadulce (Sevilla)	Carbonell
	2	Vila Franca del Penedés (Barcelona)	Torrereal
	2	Les Garrigues (Lleida)	Oleastrum
	1	Estepa (Sevilla) + La Roda de Andalucía (Sevilla)	Coosur
	1	Antequera (Málaga)	Grupo Hojiblanca
	2	Huelva + Zaragoza + Palma del Río (Córdoba)	Borges
	1	Les Garrigues (Lleida)	Romanico
	1	La Puebla Nueva (Toledo)	Valderrama
	1	Sarroca de Lleida (Lleida)	Veá
	1	Mallorca	Aubocassa
	1	La Rioja	Rihuelo
Hojiblanca	2	Estepa (Sevilla)	Carbonell
	2	Luque (Córdoba)	Coosur
	3	Puente Genil (Córdoba)	Borges
	5	Fuente de Piedra (Málaga)	Grupo Hojiblanca
	1	Santaella (Córdoba)	Columela
Picual	2	Martos (Jaén)	Carbonell
	2	Villanueva del Arzobispo (Jaén) + Porcuna (Jaén)	Coosur
	1	Quesada (Jaén)	Borges
	1	Montoso (Córdoba)	Grupo Hojiblanca
		Tabernas (Almería)	Castillo de Tabernas
		Canena (Jaén)	Castillo de Canena

Table 2
$[M–H]^-$ peaks of the selected fatty acids and phenolic compounds

Compound (acronym)	*m/z*
Myristic acid (C14:0)	227
Palmitoleic acid (C16:1)	253
Palmitic acid (C16:0)	255
Linolenic acid (C18:3)	277
Linoleic acid (C18:2)	279
Oleic acid (C18:1)	281
Stearic acid (C18:0)	283
Tyrosol	137
p-Hydroxybenzoic acid	137
Cinnamic acid	147
p-Hydroxyphenylacetic acid	151
p-Anisic acid	151
Hydroxytyrosol	153
Gentisic acid	153
Protocatechuic acid	153
Coumaric acid	163
Vanillic acid	167
Gallic acid	169
Caffeic acid	179
Homovanillic acid	181
Ferulic acid	193
Syringic acid	197
Sinapic acid	223
Elenolic acid	241
Dialdehydic form of deacetoxy ligstroside	303
Deacetoxy ligstroside aglycone	303
Dialdehydic form of deacetoxy oleuropein	319
Deacetoxy oleuropein aglycone	319
Pinoresinol	357
Dialdehydic form of ligstroside	361
Ligstroside aglycone	361
Dialdehydic form of oleuropein	377
Oleuropein aglycone	377
10-Hydroxyoleuropein aglycone	393
1-Acetoxypinoresinol	415

capillary at 10 bar between successive infusions. Rinsing for 5 min was enough to achieve a satisfactory reduction of the background noise and reproducible oil profiles. The LDA models were constructed using the SPSS software (v. 12.0.1, SPSS Inc., Chicago, IL, USA).

3. Results and discussion

3.1. Optimization of the ITMS working conditions

To optimize the ITMS working conditions, a sample of Hojiblanca oil was used.

The peaks of seven fatty acids and those of 28 phenolic compounds selected according to Ríos et al. (2005) and Tripoli et al. (2005) were used as variables. The selected compounds, and the *m/z* values of the corresponding $[M–H]^-$ peaks, are indicated in Table 2. Owing to the coincidence of the *m/z* values of several phenolic compounds, these were jointly measured; then, a total of 20 peaks were obtained to be used as variables. Most peaks showed a slight intensity increase when the drying gas temperature was increased from 150 to 200 °C. No further improvement was observed at higher temperatures up to 350 °C, then 200 °C was selected. Most peak intensities also improved by increasing the nebulizer pressure from 5 to 25 psi, but a plateau was reached at higher pressures; then, 25 psi was selected. The influence of the drying gas flow was negligible, thus 5 L min^{-1} was selected. The stability parameter was set at 75%, since no further sensitivity improvement was observed at lower values.

3.2. Construction of the data matrices

The peak profiles of oils of the three genetic varieties are compared in Fig. 1. In this Figure, and in order to make comparison easier, the spectra were standardized by dividing each peak abundance by the abundance of C16:0 peak; further, the peak of C18:1 (oleic acid), which is the most intense signal in all the genetic varieties, was tailored at 1.2. In this way, the differences between the fatty acid profiles of the three genetic varieties were enhanced. The C18:1 peak intensities, which cannot be appreciated in the Figure due to the cut off, followed the decreasing order: Hojiblanca > Picual > Arbequina. In comparison to oleic acid, the signals of palmitic, linoleic and stearic acids showed intermediate intensities. The stearic acid peak (C18:0) was

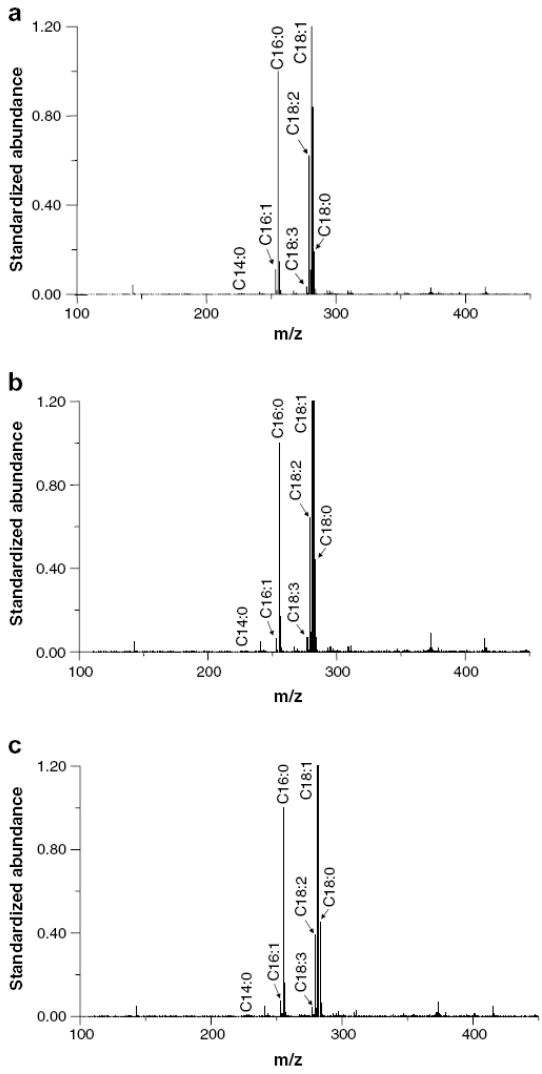

Fig. 1. Standardized mass spectra of olive oils of the three genetic varieties: (a) Arbequina, (b) Hojiblanca and (c) Picual. The intensity of all peaks was divided by the intensity of the C16:0 peak; also the C18:1 peak was tailored at 1.2.

lower for Arbequina than for the Hojiblanca and Picual oils, and the intensities of the linoleic acid peak (C18:2) showed the decreasing order: Arbequina > Hojiblanca > Picual. The peaks of many phenolic compounds were also identified in the MS spectra; however, the intensity of these peaks was several orders of magnitude lower than that of the fatty acids. The spectrum of a Picual oil, with an expanded vertical axis, is shown in Fig. 2. Similar spectra, showing small differences among the peak profiles, were obtained for the Arbequina and Hojiblanca oils.

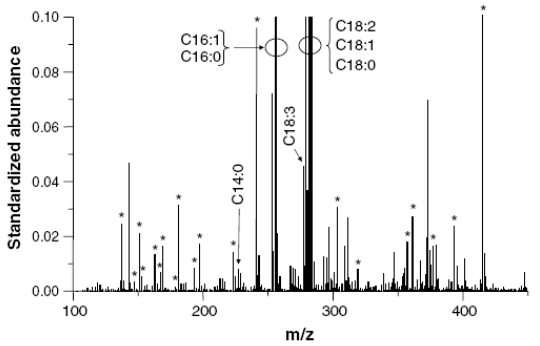

Fig. 2. Standardized mass spectrum of a Picual olive oil sample with the vertical axis tailored at 0.1. The peaks of the phenolic compounds of Table 2 are indicated with an asterisk.

In order to reduce the variability associated with the infusion in the mass spectrometer, and consequently minimize the influence of sources of variance non-associated to the origin and history of the oils, normalized ion abundances were employed for data analysis. Owing to the large differences between the peak intensities, the peaks were divided in two groups, fatty acids and phenolic compounds, and two normalization procedures were independently applied to each group. First, for each spectrum, the peak abundance of each fatty acid was divided by the sum of the peak abundances of the seven fatty acids, and the peak abundance of each phenolic compound was divided by the sum of the 20 peak abundances of the phenolic compounds (normalization procedure A). Second, the peak abundance of each fatty acid was divided by each one of the peak abundances of the other six fatty acids, and the peak abundance of each phenolic compound was divided by each one of the abundances of the other 19 peaks of the other phenolic compounds (normalization procedure B). To avoid perfectly correlated variables, each pair of peak abundances was divided only once. Then, for the fatty acids, 7 and 21 normalized variables were obtained by normalization procedures A and B, respectively. Similarly, for the phenolic compounds, 20 and 190 normalized variables were, respectively obtained.

3.3. Prediction of the genetic variety by LDA

LDA, a supervised classificatory technique, is widely recognized as an excellent tool to obtain vectors showing the maximal resolution between categories. In LDA, vectors minimizing the Wilks' lambda, λ_w, are obtained. This parameter is defined as:

$$\lambda_w = S_{intra}/(S_{intra} + S_{inter})$$

where S_{intra} is the sum of squares of data points belonging to the same category, and $S_{intra} + S_{inter}$ is the total sum of squares (Vandeginste et al., 1998). Values of λ_w approach-

ing zero are obtained when all the categories are well resolved, whereas overlapped categories make λ_w to approach one. Up to N-1 discriminant vectors are constructed by using LDA, being N the lowest value of either the number of predictors or the number of categories. The 38 samples of the monovarietal oils of Table 1 were used to construct LDA models capable of classifying olive oil samples according to their genetic variety.

Selection of the variables during model construction was made with the stepwise algorithm of SPSS. Using this algorithm, the predictor causing the most significant decrease of λ_w is first introduced in the model, this criterion being successively applied to all the predictors. Acceptation of the predictors is performed with an *F*-test. In order to avoid the introduction of variables with reduced discriminant capability, an entrance threshold, F_{in}, is adopted. However, the entrance of a new predictor modifies the significance of the predictors which are already present in the model. Then, in the stepwise algorithm, a rejection threshold, F_{out}, is used to resolve if a predictor should be removed from the model. The process terminates when there are no predictors entering or being eliminated from the model.

To construct the data matrices, each oil sample was injected in two different days, and each day four replicates were accomplished. Two matrices containing 304 injections, and a total of 27 or 211 predictors (according to normalization procedures A and B, respectively) were constructed. A response column, containing the three categories corresponding to the three genetic varieties, was added to the matrices. These matrices were used both to construct LDA training matrices and to provide evaluation sets. Only the means of the replicates of the samples were included in the training matrices; in this way, the internal dispersion of the categories was reduced, which was important to also reduce the number of variables selected by the stepwise algorithm during model construction. In the evaluation set, all the individual injections of the samples were included.

Initially, the capability for the classification of the studied olive oils according to their genetic variety, using fatty acids or phenolic compounds, was tested. Both normalization procedures were tried. Normalization procedure B, which led to a better separation of the categories, was selected in further studies. Then, an LDA model constructed exclusively with the fatty acids ratios showed a clear separation between the three genetic varieties ($\lambda_w = 0.396$). Using the SPSS default probability values of $F_{in} = 0.05$ and $F_{out} = 0.10$, the model was constructed with 7 variables and mainly with the variables 279/283 and 279/281. All samples were correctly classified. On the other hand, the phenolic compounds were used to construct another LDA model. In this case, 22 variables were selected ($\lambda_w = 0.236$), but with an apparent lower separation between categories. The variables showing higher weight in the model construction were 303/241, 303/193 and 393/241. Then, both variables sets were jointly used to construct another LDA model. A model with 30 predictors was obtained. Thus, in order to reduce the entrance of predictors in the model, the probability values $F_{in} = 0.01$ and $F_{out} = 0.20$ were used. Now, only 11 predictors were included in the model. An excellent resolution between the three categories was obtained ($\lambda_w = 0.237$). A score plot on the plane of the two discriminant functions is shown in Fig. 3. The predictors selected by the SPSS stepwise algorithm, and the corresponding standardized coefficients of the model, which indicate the discriminant capabilities of the predictors, are given in Table 3. The model was used to classify the samples of the evaluation set. Using a 95% probability, all the objects were correctly assigned; thus, the prediction capability was 100%.

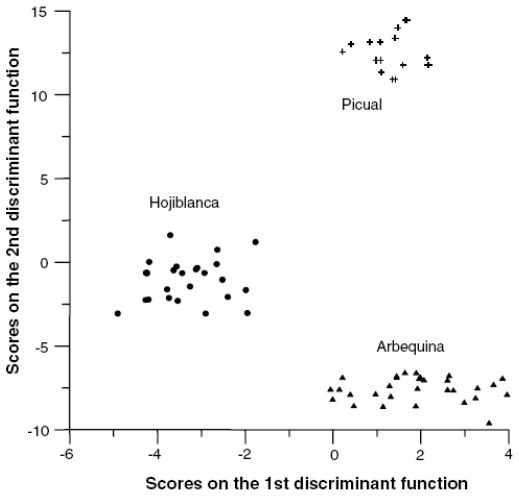

Fig. 3. Score plot on the plane of the two LDA discriminant functions obtained to predict olive oil varieties after data normalization by procedure B.

Table 3
Predictors selected and corresponding standardized coefficients of the LDA model constructed to predict the genetic variety of extra virgin olive oils

Compounds	Predictors[a]	f_1	f_2
Fatty acids	227/279	−0.4	2.78
	227/281	0.63	−1.98
	255/279	−0.32	0.45
	277/279	−1.21	0.16
	279/281	0.35	0.7
	281/283	0.81	1.08
Phenolic compounds	193/167	0.83	0.22
	223/181	0.67	−0.02
	303/197	−0.27	−0.82
	415/197	0.87	0.52
	361/223	−0.28	−0.7

[a] *m*/*z* values of the ratios of abundances of peak pairs.

4. Conclusions

With the jointly use of the peaks of both fatty acids and phenolic compounds, direct infusion MS spectra of monovarietal extra virgin olive oils provide the necessary information to predict the genetic variety with a high reliability. For this purpose, the use of LDA models constructed using the intensity ratios of peak pairs as predictor is recommended. The MS intensities of the free fatty acids and many phenolic compounds can be measured after a simple dilution of the oil samples with a miscible alkaline solvent mixture. In this way, the conventional laborious extraction protocols commonly reported for phenolic compounds are avoided, being only necessary to rinse the spectrometer for 5 min between successive infusions to achieve low backgrounds and reproducible oil profiles. Thus, an extremely quick and simple procedure, which can be easily automatized, has been described.

Acknowledgements

Projects CTQ2004-06302 (MEC and FEDER funds), ACOMP07-168 (Generalitat Valenciana). MJL-G also thanks the Generalitat Valenciana for a FPI grant for PhD studies.

References

Aparicio, R., & Aparicio-Ruíz, R. (2000). Authentication of vegetable oils by chromatographic techniques. *Journal of Chromatography A, 881*, 93–104.

Aparicio, R., & Luna, G. (2002). Characterisation of monovarietal virgin olive oils. *European Journal of Lipid Science and Technology, 104*, 614–627.

Aranda, F., Gómez-Alonso, S., Rivera del Álamo, R. M., Salvador, M. D., & Fregapane, G. (2004). Triglyceride, total and 2-position fatty acid composition of Cornicabra virgin olive oil: Comparison with other Spanish cultivars. *Food Chemistry, 86*, 485–492.

Bucci, R., Magri, A. D., Magri, A. L., Marini, D., & Marini, F. (2002). Chemical authentication of extra virgin olive oil varieties by supervised chemometric procedures. *Journal of Agricultural and Food Chemistry, 50*, 413–418.

Caponio, F., Alloggio, V., & Gomes, T. (1999). Phenolic compounds of virgin olive oil: influence of paste preparation techniques. *Food Chemistry, 64*, 203–209.

Catharino, R. R., Haddad, R., Cabrini, L. G., Cunha, I. B. S., Sawaya, A. C. H. F., & Eberlin, M. N. (2005). Characterization of vegetable oils by electrospray ionization mass spectrometry fingerprinting: Classification, quality, adulteration, and aging. *Analytical Chemistry, 77*, 7429–7433.

Cichelli, A., & Pertesana, G. P. (2004). High-performance liquid chromatographic analysis of chlorophylls, pheophytins and carotenoids in virgin olive oils: Chemometric approach to variety classification. *Journal of Chromatography A, 1046*, 141–146.

D'Imperio, M., Dugo, G., Alfa, M., Mannina, L., & Segre, A. L. (2007). Statistical analysis on Sicilian olive oils. *Food Chemistry, 102*(3), 956–965.

Gama Melão, M. G., Simó-Alfonso, E., Ramis-Ramos, G., & Vicente, E. (2006). *Determination of aerobic-anaerobic metabolism-related compounds in a Chaoborus flavicans population by infusion ion trap mass spectrometry of extracts of individual larvae*. Rapid Communications in Mass Spectrometry.

Gómez-Alonso, S., Salvador, M. D., & Fregapane, G. (2002). Phenolic compounds profile of Cornicabra virgin olive oil. *Journal of Agricultural and Food Chemistry, 50*, 6812–6817.

Gómez-Ariza, J. L., Arias-Borrego, A., García-Barrera, T., & Beltran, R. (2006). Comparative study of electrospray and photospray ionization sources coupled to quadrupole time-of-flight mass spectrometer for olive oil authentication. *Talanta, 70*(4), 859–869.

Goodacre, R., Vaidyanathan, S., Bianchi, G., & Kell, D. B. (2002). Metabolic profiling using direct infusion electrospray ionisation mass spectrometry for the characterisation of olive oils. *Analyst, 11*, 1457–1462.

Guadarrama, A., Rodríguez-Méndez, M. L., Sanz, C., Ríos, J. L., & De Saja, J. A. (2001). Electronic nose based on conducting polymers for the quality control of the olive oil aroma: Discrimination of quality, variety of olive and geographic origin. *Analytica Chimica Acta, 432*, 283–292.

Koprivnjak, O., Moret, S., Populin, T., Lagazio, C., & Conte, L. S. (2005). Variety differentiation of virgin olive oil based on *n*-alkane profile. *Food Chemistry, 90*, 603–608.

Krichene, D., Taamalli, W., Daoud, D., Salvador, M. D., Fregapane, G., & Zarrouk, M. (2007). Phenolic compounds, tocopherols and other minor components in virgin olive oils of some Tunisian varieties. *Journal of Food Biochemistry, 31*, 179–194.

Lees, M. (1999). Food Authenticity: Issues and Methodologies. Nantes: Eurofins Scientific.

Luna, G., Morales, M. T., & Aparicio, R. (2006). Characterisation of 39 varietal virgin olive oils by their volatile compositions. *Food Chemistry, 98*, 243–252.

Marini, F., Balestrieri, F., Bucci, R., Magri, A. D., Magri, A. L., & Marini, D. (2004). Supervised pattern recognition to authenticate Italian extra virgin olive oil varieties. *Chemometrics and Intelligent Laboratory Systems, 73*, 85–93.

Morelló, J. R., Romero, M. P., & Motilva, M. J. (2004). Effect of the maturation process of the olive fruit on the phenolic fraction of drupes and oils from Arbequina, Farga, and Morrut cultivars. *Journal of Agricultural and Food Chemistry, 52*, 6002–6009.

Nagy, K., Bongiorno, D., Avellone, G., Agozzino, P., Ceraulo, L., & Vékey, K. (2005). High performance liquid chromatography–mass spectrometry based chemometric characterization of olive oils. *Journal of Chromatography A, 1078*, 90–97.

Peris-Vicente, J., Simó-Alfonso, E., Gimeno-Adelantado, J. V., & Domenech-Carbó, M. T. (2005). *Direct infusion mass spectrometry as a fingerprint of protein-binding media used in works of art*. Rapid Communications in Mass Spectrometry.

Ranalli, A., Pollastri, L., Contento, S., Di-Loreto, G., Iannucci, E., Lucera, L., & Russi, F. (2002). Acylglycerol and fatty acid components of pulp, seed, and whole olive fruit oils. Their use to characterize fruit variety by chemometrics. *Journal of Agricultural and Food Chemistry, 50*, 3775–3779.

Ríos, J. J., Gil, M. J., & Gutiérrez-Rosales, F. (2005). Solid-phase extraction gas chromatography-ion-trap-mass spectrometry qualitative method for evaluation of phenolic compounds in virgin olive oil and structural confirmation of oleuropein and ligstroside aglycons and their oxidation products. *Journal of Chromatography A, 1093*, 167–176.

Saitta, M., Lo-Curto, S., Salvo, F., Di-Bella, G., & Dugo, G. (2002). Gas chromatographic – tandem mass spectrometric identification of phenolic compounds in Sicilian olive oils. *Analytica Chimica Acta, 466*, 335–344.

Salvador, M. D., Aranda, F., Gómez-Alonso, S., & Fregapane, G. (2003). Influence of extraction system, production year and area on Cornicabra virgin olive oil: a study of five crop seasons. *Food Chemistry, 80*, 359–366.

Stefanoudaki, E., Kotsifaki, F., & Koutsaftakis, A. (1997). The potential of HPLC trygliceride profiles for the classification of Cretan olive oils. *Food Chemistry, 60*, 425–432.

Stefanoudaki, E., Kotsifaki, F., & Koutsaftakis, A. (1999). Classification of virgin olive oils of the two major Cretan cultivars based on their

fatty acid composition. *Journal of the American Oil Chemical Society, 76*, 623–626.

Torres, M. M., & Maestri, D. M. (2006). The effects of genotype and extraction methods on chemical composition of virgin olive oils from Traslasierra Valley, Córdoba, Argentina. *Food Chemistry, 96*, 507–511.

Tripoli, E., Giammanco, M., Tabacchi, G., Di Majo, D., Giammanco, S., & La Guardia, M. (2005). The phenolic compounds of olive oil: structure, biological activity and beneficial effects on human health. *Nutrition Research Reviews, 18*, 98–112.

Tura, D., Prenzler, P. D., Bedgood, D. R., Antolovich, M., & Robards, K. (2004). Varietal and processing effects on the volatile profile of Australian olive oils. *Food Chemistry, 84*, 341–349.

Vandeginste, B. G. M., Massart, D. L., Buydens, L. M. C., De Jong, S., Lewi, P. J., & Smeyers-Verbeke, J. (1998). *Data Handling in Science and Technology Part B*. Amsterdam: Elsevier Science, 237.

ANEXO XIV

10512 J. Agric. Food Chem. 2009, 57, 10512–10517
DOI:10.1021/jf902322c

JOURNAL OF AGRICULTURAL AND FOOD CHEMISTRY
ARTICLE

Classification of Extra Virgin Olive Oils Produced at *La Comunitat Valenciana* According to Their Genetic Variety Using Sterol Profiles Established by High-Performance Liquid Chromatography with Mass Spectrometry Detection

María Jesús Lerma-García,[†] Victoria Concha-Herrera,[‡] José Manuel Herrero-Martínez,[†] and Ernesto Francisco Simó-Alfonso*,[†]

[†]Department of Analytical Chemistry, Faculty of Chemistry, University of Valencia, E-46100 Burjassot, Valencia, Spain, and [‡]Unidad Académica de Ciencias Químicas, Universidad Autónoma de Zacatecas, 98160 Zacatecas, Mexico

A method to classify extra virgin olive oils (EVOOs) according to their genetic variety using sterol profiles obtained by high-performance liquid chromatography (HPLC) with mass spectrometry (MS) detection has been developed. Sterol extracts were chromatographed on a dC_{18} Atlantis column (100 × 3 mm, 3 μm) with a gradient of acetonitrile/water (0.01% acetic acid) at a flow rate of 1.0 mL min^{-1} and positive-ion mode MS detection. Using linear discriminant analysis of the HPLC-MS data (extracted ion chromatograms), EVOO samples belonging to six genetic varieties cultivated at *La Comunitat Valenciana*, Spain (Arbequina, Borriolenca, Canetera, Farga, Picual, and Serrana), were correctly classified with an excellent resolution among all of the categories.

KEYWORDS: Extra virgin olive oil; genetic variety; high-performance liquid chromatography; linear discriminant analysis; mass spectrometry; sterols

INTRODUCTION

Extra virgin olive oil (EVOO) is a traditional Mediterranean food product, the market for which has been recently expanded due to its highly appreciated organoleptic attributes and its health and nutritional properties (*1*). During recent years, the consumption of EVOO has increased considerably in relation to the consumption of virgin and refined olive oils. Owing to its distinctive and peculiar intense taste, EVOOs obtained from some pure genetic varieties are highly appreciated.

EVOOs are mainly constituted by triacylglycerols, also containing an unsaponifiable matter which amounts to 1−3%. Within this unsaponifiable matter, sterols constitute the greatest and most studied fraction (*2*). The content of these components depends on the kind of olive oil (*3*), but can also vary due to environmental conditions, fruit quality, oil extraction system, and refining process (*4*). For these reasons, the determination of these minor components is of great value in establishing the oil genuineness and quality (*4*, *5*), having also a marked influence on typicality, flavor, aroma, and shelf life (*6*). On the other hand, sterols are supposed to decrease the cardiovascular risk of coronary heart disease (*7*),and also reduce blood cholesterol levels, showing anti-inflammatory, antibacterial, and antioxidant activities (*8*).

Official methods for the analysis of sterols involve saponification of the oil, extraction of the unsaponifiable fraction with diethyl ether, and isolation of the sterol fraction by thin layer chromatography (TLC). Quantification of the silanized sterol fraction is commonly performed by gas chromatography (GC) with flame ionization detection (FID) (*9*−*20*), but GC with mass spectrometry (MS) detection is also used (*9*, *12*, *18*, *21*−*23*). The major disadvantage of GC is the requirement of both thermally stable columns and chemical derivatization before analysis. For this reason, other methods such as capillary electrochromatography with diode array UV−vis detection (*24*, *25*), direct infusion mass spectrometry (*26*), and high-performance liquid chromatography (HPLC)-MS (*3*, *27*, *28*) have been also developed to determine sterols in vegetable oils. These HPLC-MS methods have been applied to both the analysis of olive oil samples of different qualities (*3*, *27*) and the analysis of several botanical oil varieties (*28*). To our knowledge, no study about the analysis of different EVOO genetic varieties using HPLC-MS sterol profiles has been previously reported.

On the other hand, sterol contents established by GC, followed by multivariate data treatment, have been used to distinguish different genetic varieties of EVOO (*10*, *11*, *15*−*17*, *20*). The contents of other compounds, such as *n*-alkanes (*29*), triglycerides (*30*), tocopherols (*31*), volatile compounds (*32*, *33*), fatty acids (*30*, *34*, *35*), and phenolic compounds (*31*, *35*), established by GC (*29*−*34*), HPLC (*29*−*31*, *34*), and direct infusion MS (*35*), have been also used as authentication methods for genetic varieties of EVOO.

In this work, sterol profiles of EVOOs from six different genetic varieties produced at *La Comunitat Valenciana*, Spain, have been obtained by HPLC-MS. The normalized peak areas have been used as predictors to construct linear discriminant (LDA) models

*Author to whom correspondence should be addressed (telephone +34-963543176; fax +34-963544436; e-mail ernesto.simo@uv.es).

 Published on Web 11/02/2009

Table 1. Genetic Variety, Number of Samples, Geographical Origin, and Crop Season of the EVOOs Employed in This Study

genetic variety	no. of samples	geographical origin	crop season (2005−2008)
Arbequina	2	Altura (Castellón)	06/07; 07/08
	2	Maestrat *comarca* (Castellón)	06/07; 07/08
	1	Alicante	05/06
	1	Palancia *comarca* (Castellón)	07/08
Borriolenca	3	Alcalatén *comarca* (Castellón)	05/06; 06/07; 07/08
	3	La Plana *comarca* (Castellón)	05/06; 06/07; 07/08
Canetera	2	Maestrat *comarca* (Castellón)	05/06; 07/08
	2	Adzaneta (Castellón)	06/07; 07/08
	2	La Plana *comarca* (Castellón)	05/06; 07/08
Farga	2	Maestrat *comarca* (Castellón)	05/06; 06/07
	2	Alcalatén *comarca* (Castellón)	06/07; 07/08
	2	La Plana *comarca* (Castellón)	05/06; 07/08
Picual	6	Altura (Castellón)	05/06; 06/07; 07/08
Serrana	2	Altura (Castellón)	06/07; 07/08
	1	Artana (Castellón)	06/07
	1	Jérica (Castellón)	07/08
	2	Viver (Castellón)	05/06; 07/08

capable of classifying the EVOO samples according to their genetic variety.

EXPERIMENTAL PROCEDURES

Reagents and Samples. The following analytical grade reagents were used: ethanol, 2-propanol, acetic acid, acetonitrile (ACN), anhydrous sodium sulfate (Scharlau, Barcelona, Spain); diethyl ether, chloroform (J. T. Baker, Deventer, The Netherlands); KOH (Probus, Barcelona, Spain); *n*-hexane (Riedel-de Haën, Seelze, Germany); and 2,7-dichlorofluorescein (Sigma, St. Louis, MO). Glass plates for TLC, coated with silica gel without fluorescent indicador (0.25 mm plate thickness, Merck, Darmstadt, Germany) were used. Deionized water (Barnstead deionizer, Sybron, Boston, MA) was also used. The sterols used as standards were erythrodiol (Fluka, Buchs, Switzerland); β-sitosterol (mixture containing 75% β-sitosterol and 10% campesterol), ergosterol, and stigmasterol (Acros Organics, Morris Plains, NJ); and cholesterol (Aldrich, Milwaukee, WI). The EVOOs employed in this study (**Table 1**) were kindly donated by *Intercoop Olival* (Almassora, Castellón, Spain) and by the *Cooperativa de Altura* (Altura, Castellón) from different crop seasons, also specified in **Table 1**. The genetic variety, quality grade, and geographical origin of all EVOO samples were guaranteed by the suppliers.

Instrumentation and Working Conditions. An 1100 series liquid chromatograph provided with a quaternary pump (Agilent Technologies, Waldbronn, Germany) was used. Separation was carried out with a dC_{18} column (Atlantis, 3 μm, 100 × 3 mm, Waters, Milford, MA). Mobile phases were prepared by mixing ACN and water, both containing 0.01% acetic acid. A linear gradient at a flow rate of 1 mL min^{-1} from 90 to 100% ACN for 10 min, followed by isocratic elution with 100% ACN for 2 more min, was used. In all cases, 20 μL was injected. The mass spectrometer system was an HP 1100 series ion trap mass spectrometer (Agilent) equipped with an atmospheric pressure photoionization source. The MS working conditions were as follows: nebulizer gas pressure, 15 psi; drying gas flow, 12 L min^{-1} at 350 °C; vaporizer temperature, 275 °C; capillary voltage, −1.9 kV; voltages of skimmers 1 and 2, 25.9, and 6.0 V, respectively. Nitrogen was used as nebulizer and drying gas (Gaslab NG LCMS 20 generator, Equcien, Madrid, Spain). The mass spectrometer was scanned within the m/z 200−500 range in the positive ion mode. The ion trap target mass was set at m/z 397 ($[M + H - H_2O]^+$ peak of β-sitosterol). Maximum loading of the ion trap was 3×10^4 counts, and maximum collection time was 300 ms. Total ion chromatograms (TIC) and extracted ion chromatograms (EIC) were smoothed using a Gaussian filter set at 5 points.

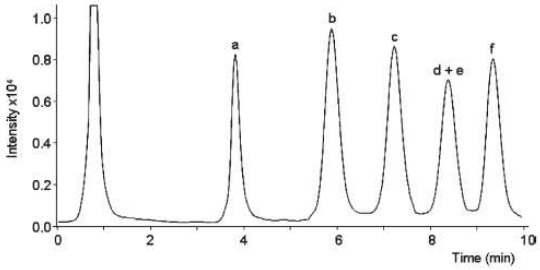

Figure 1. TIC of a standard solution of sterols (ca. 100 mg L^{-1}) using a linear gradient from 90 to 100% ACN for 10 min, followed by isocratic elution with 100% ACN for an additional 2 min. Peaks: (a) erythrodiol; (b) ergosterol; (c) cholesterol; (d) campesterol; (e) stigmasterol; (f) β-sitosterol.

Table 2. Peak Labeling, Retention Time (t_R), and m/z Value of the Sterols Studied in This Work

peak	analyte	t_R (min)	m/z[a]
1	erythrodiol	3.90	425
2	uvaol	3.90	425
3	brassicasterol	6.10	381
4	cholesterol	7.25	369
5	Δ^7-avenasterol	7.25	395
6	Δ^5-avenasterol	7.25	395
7	campesterol	8.30	383
8	campestanol	8.30	385
9	stigmasterol	8.40	395
10	$\Delta^{5,24}$-stigmastadienol	9.30	395
11	Δ^7-stigmastenol	9.40	397
12	β-sitosterol	9.40	397

[a] m/z value corresponding to the $[M + H - H_2O]^+$ peak.

Sample Preparation. The sterol fraction of the EVOO samples was obtained following the procedure established by EC Regulation (*36*). Accordingly, 5 g of oil was saponified by refluxing with 2 M ethanolic KOH for 20 min; 50 mL of distilled water was added, and the non-saponifiable fraction was extracted three times with diethyl ether. The three ether extracts were introduced into a separating funnel and washed with distilled water (50 mL each time) until neutral reaction. The organic extracts were dried with anhydrous sodium sulfate and filtered. These extracts were evaporated to dryness using a rotatory evaporator. The remaining unsaponifiables were dissolved in 2 mL of chloroform, and then the sterol fraction was separated by TLC using a plate-developing chamber, which contained hexane/diethyl ether 60:40 (v/v). After TLC separation, the silica plate was sprayed lightly and uniformly with 2,7-dichlorofluorescein. The sterol band was removed from the silica plate using a spatula. This material was dissolved in 10 mL of diethyl ether and filtered through a Whatman no. 1 paper using a Büchner funnel. A rotatory evaporator was used to remove this solvent, and the residue was dissolved in 500 μL of 2-propanol and stored at −20 °C in amber vials. These solutions were properly diluted with the mobile phase and injected two times.

Data Treatment and Statistical Analysis. The peak area of each sterol was measured from the smoothed EIC, and a data matrix was constructed using the areas of all peaks as original variables. After

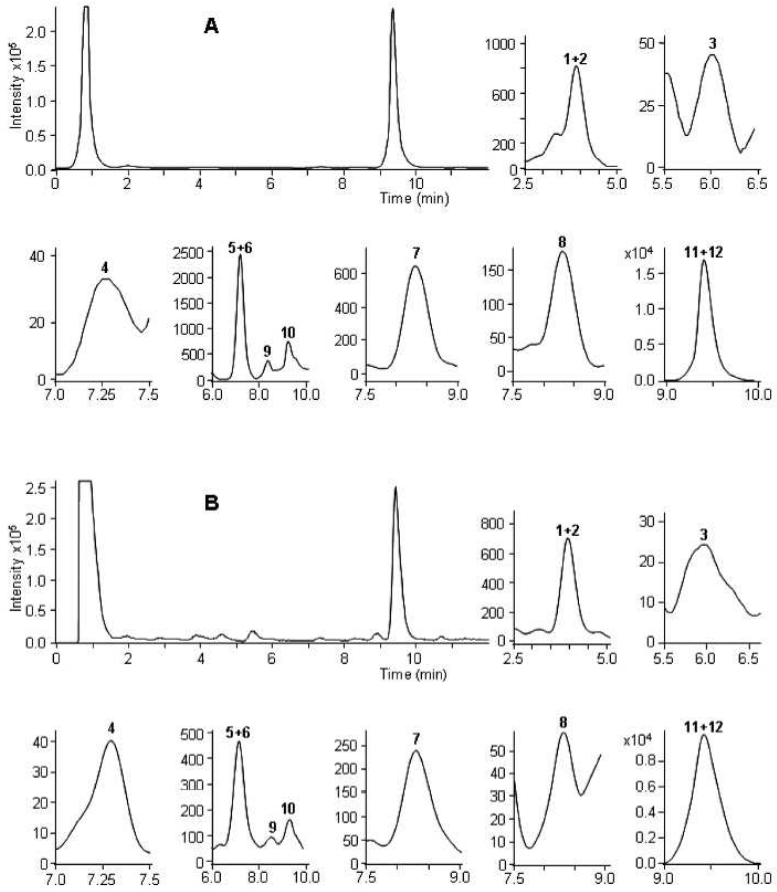

Figure 2. TIC and EICs of Canetera (**A**) and Serrana (**B**) EVOO sterol extracts. EICs were obtained at the *m/z* values indicated in **Table 2**. Peak labeling is as indicated in **Table 2**. Other experimental conditions were as in **Figure 1**.

normalization of the variables, statistical data treatment was performed using SPSS (v. 15.0, Statistical Package for the Social Sciences, Chicago, IL). LDA, a supervised classificatory technique, is widely recognized as an excellent tool to obtain vectors showing the maximal resolution between a set of previously defined categories. In LDA, vectors minimizing Wilks' lambda, λ_w, are obtained (*37*). This parameter is calculated as the sum of squares of the distances between points belonging to the same category divided by the total sum of squares. Values of λ_w approaching 0 are obtained with well-resolved categories, whereas overlapped categories made λ_w approach 1. Up to N − 1 discriminant vectors are constructed by LDA, *N* being the lowest value for either the number of predictors or the number of categories. The selection of the predictors to be included in the LDA models was performed using the SPSS stepwise algorithm. According to this algorithm, a predictor is selected when the reduction of λ_w produced after its inclusion in the model exceeds F_{in}, the entrance threshold of a test of comparison of variances or *F* test. However, the entrance of a new predictor modifies the significance of those predictors that are already present in the model. For this reason, after the inclusion of a new predictor, a rejection threshold, F_{out}, is used to decide if one of the other predictors should be removed from the model. The process terminates when there are no predictors entering or being eliminated from the model. The values of F_{in} and F_{out}, 3.84 and 2.71, respectively, were adopted.

RESULTS AND DISCUSSION

Optimization of the Sterol Separation. For each sterol standard peak, two *m/z* values, corresponding to $[M + H]^+$ and $[M + H - H_2O]^+$ ions, were observed. However, and as previously reported (*3*, *25*, *28*), the $[M + H - H_2O]^+$ peaks showed higher intensities than the respective $[M + H]^+$ peaks. For this reason, the intensities of the $[M + H - H_2O]^+$ peaks were used for identification and classification. Different gradient elutions using ACN/water mixtures, both containing 0.01% acetic acid, at a constant flow rate of 1.0 mL min^{-1} were tried. As a result of this study, the linear gradient that provided the best separation/analysis time ratio was achieved with 90−100% ACN for 10 min, followed by isocratic elution with 100% ACN for an additional 2 min. **Figure 1** shows a chromatogram of sterol standards using this gradient elution. As observed, the total analysis time was 10 min, which was much lower than that reported for sterol separation using GC-FID. On the other hand, an overlapping between campesterol and stigmasterol peaks was observed in all of the gradient elutions tried. This finding was in agreement with some previous HPLC results (*38*).

Then, all EVOO extracts were injected using these optimal conditions. To identify other sterol peaks present in the samples, the EICs at the *m/z* values of **Table 2** were performed. A total of 9 peaks, corresponding to 12 possible sterols, were identified in < 10 min. The TIC and EICs of two EVOO extracts of different genetic varieties, Canetera and Serrana, are shown in panels **A** and **B**, respectively, of **Figure 2**. Several differences between the peak profiles of both varieties were evidenced. The quantitative results of sterols in the vegetable oils analyzed are shown in

Table 3. Proportions of Sterols Found in Total Sterol Fraction of EVOO of Different Genetic Varieties

sterol	Arbequina	Borriolenca	Canetera	Farga	Picual	Serrana
erythrodiol + uvaol	0.1−0.3	0−0.09	2.0−4.0	0.0−0.4	0.2−0.6	5.0−7.7
brassicasterol	0.08−0.11	0.06−0.09	0.06−0.12	0.09−0.12	0.1−0.2	0.08−0.15
cholesterol	0.3−0.6	0.3−0.5	0.1−0.2	0.1−0.5	0.4−0.5	0.2−0.4
Δ^7- + Δ^5-avenasterol	12.1−14.9	7.0−9.9	11.5−12.3	7.8−9.5	4.3−13.2	5.1−6.4
campesterol	3.7−4.0	3.2−3.7	3.0−3.5	3.2−3.6	2.5−3.1	1.8−2.4
campestanol	0.2−0.4	0.2−0.3	0.5−0.9	0.2−0.3	0.2−0.3	0.3−0.6
stigmasterol	0.7−1.5	1.2−2.8	1.5−2.0	1.1−1.9	0.9−1.5	1.0−2.5
$\Delta^{5,24}$-stigmastadienol	0.7−1.9	0.6−1.0	3.0−3.7	0.8−1.0	0.9−1.3	1.0−1.5
Δ^7-stigmastenol + β-sitosterol	76−80	79.0−82.3	75.0−77.8	78.7−90.8	77.3−90.0	81.0−82.7

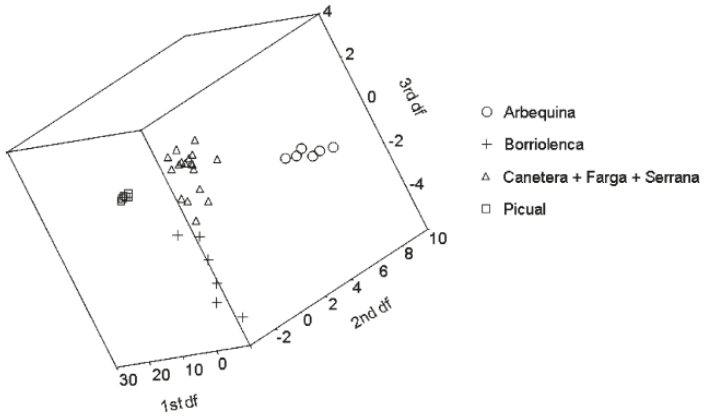

Figure 3. Score plot on an oblique plane of the three-dimensional space defined by the three discriminant functions of the LDA model constructed to resolve the Arbequina, Borriolenca, Picual, and Canetera + Farga + Serrana categories.

Table 3. In general, the levels of sterols found in these samples are in good agreement with data reported in the literature (*39*). As shown in this table, several differences between the contents of the different genetic varieties were found. Similar sterol separation performance was observed compared to the literature (*28*), but lower analysis times were obtained (*3*, *27*, *28*).

Normalization of the Variables for LDA Classification. To reduce the variability associated with the total amount of sterols recovered from the oil samples and to minimize other sources of variance also affecting the sum of the areas of all peaks, normalized rather than absolute peak areas were used. To normalize the variables, the area of each peak taken from the corresponding EIC was divided by each of the areas of the other eight peaks (also taken from their EICs); in this way, and taking into account that each pair of peaks should be considered only once, $(9 \times 8)/2 = 36$ nonredundant peak ratios were obtained to be used as predictors.

Construction of the Data Matrices and LDA Models. Using the normalized variables, LDA models capable of classifying the EVOO samples according to their respective genetic varieties were constructed. First, from the 36 samples of **Table 1**, a matrix containing 72 injections (all samples were injected two times) and 36 predictors, was constructed. A response column, containing the six categories corresponding to the six genetic varieties of the EVOOs, was added to this matrix. This matrix was used as an evaluation set. To construct LDA training matrices, only the means of the replicates of the samples were included (36 objects); in this way, the internal dispersion of the categories was reduced, which was important to reduce the number of variables selected by the SPSS stepwise algorithm during model construction.

To classify the EVOOs according to the six genetic varities of **Table 1**, an LDA model was constructed. With this model, the categories Arbequina, Borriolenca, and Picual appeared to be clearly resolved from each other and were also well separated from the other three categories (Canetera, Farga, and Serrana), which overlapped (data not shown). For this reason, a new LDA model was constructed in which these three categories were grouped into a single one. An excellent resolution between these four categories (Arbequina, Borriolenca, Picual, and the one formed by the other three categories) was obtained (**Figure 3**, $\lambda_w = 0.290$). The variables selected by the SPSS stepwise algorithm, and the corresponding model standardized coefficients, showing the predictors with large discriminant capabilities, are given in **Table 4**. All of the points of the training set were correctly classified by leave-one-out cross-validation. The evaluation set, containing the 72 original data points, was used to check the prediction capability of the model. Using a 95% probability, only three objects corresponding to replicates of different samples (one Borriolenca, one Canetera, and one Farga) were not correctly assigned; thus, the prediction capability was $>95\%$.

Next, the Arbequina, Borriolenca, and Picual categories were removed from the training set, and the remaining categories (Canetera, Farga, and Serrana) were used to construct another LDA model. Now, the three categories were separated with excellent resolution (**Figure 4**, $\lambda_w = 0.209$). The variables selected and the corresponding model standardized coefficients are also given in **Table 4**. All of the points of the training set were correctly classified by leave-one-out cross-validation. To estimate the prediction capability of this model, the evaluation set, constituted now by 36 original data points, was used. Using a 95% probability, only two objects, which corresponded to replicates of

Table 4. Predictors Selected and Corresponding Standardized Coefficients of the Two Sequential LDA Models Constructed

	Arbequina/Borriolenca/Picual/Canetera + Farga + Serrana			Canetera/Farga/ Serrana	
predictor[a]	f_1	f_2	f_3	f_1	f_2
p1 + 2/3	−1.65	0.48	0.02	−2.08	1.32
p1 + 2/5 + 6	2.62	−1.12	−0.95	3.86	−3.08
p1 + 2/7	3.82	7.47	−0.12	2.13	−1.44
p1 + 2/9	−3.30	5.65	−1.29	−5.16	11.45
p1 + 2/10	−12.61	−5.83	6.49	12.83	−0.58
p1 + 2/11 + 12	24.16	2.47	−5.37	−15.50	1.49
p11 + 12/3	−0.80	1.44	2.45	3.60	−1.00
p11 + 12/5 + 6	−2.08	0.74	−0.36	−3.59	0.99
p11 + 12/7	−4.47	−1.08	−0.13		
p11 + 12/9	6.36	−2.86	5.84	4.63	−11.39
p11 + 12/10	2.00	0.06	−1.84	3.18	4.81
p3/5 + 6	3.27	−2.38	7.39		
p3/7	0.83	−7.68	0.54		
p3/9	0.93	−0.36	−3.68		
p3/10	−20.81	6.40	−6.09		
p5 + 6/9	−4.79	−1.77	−0.78		
p5 + 6/10	2.79	1.58	0.40		
p9/10	4.19	1.25	−0.39	6.51	1.91

[a] *m/z* values of the ratios of sterol peaks.

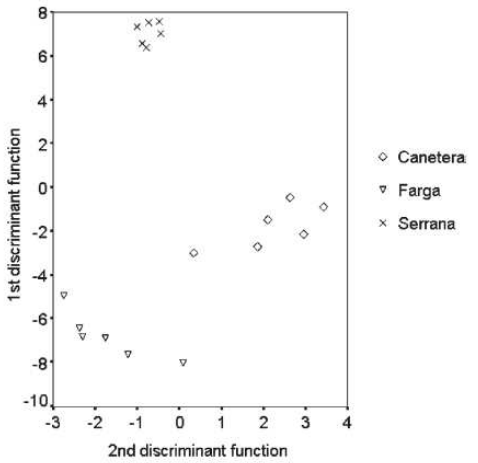

Figure 4. Score plot on the plane of the two discriminant functions of the LDA model constructed to resolve the Canetera, Farga, and Serrana categories.

different samples (one Canetera and one Farga), were not correctly assigned; thus, the prediction capability was >88%. Therefore, the possibility of classifying EVOOs according to their genetic variety by using sterol profiles obtained by HPLC-MS has been demonstrated, when a sequential application of two LDA models was performed. Thus, the proposed method is of interest to control the genetic origin of the olives used to obtain the EVOOs.

ACKNOWLEDGMENT

We acknowledge *Intercoop Olival* and the *Cooperativa de Altura* for the EVOO samples kindly donated.

LITERATURE CITED

(1) Bendini, A.; Cerretani, L.; Carrasco-Pancorbo, A.; Gómez-Caravaca, A. M.; Segura-Carretero, A.; Fernández-Gutiérrez, A.; Lercker, G. Phenolic molecules in virgin olive oils: a survey of their sensory properties, health effects, antioxidant activity and analytical methods. An overview of the last decade. *Molecules* **2007**, *12*, 1679–1719.

(2) Lercker, G.; Rodriguez-Estrada, M. T. Chromatographic analysis of unsaponifiable compounds of olive oils and fat-containing foods. *J. Chromatogr., A* **2000**, *881*, 105–129.

(3) Cañabate-Díaz, B.; Segura-Carretero, A.; Fernández-Gutiérrez, A.; Belmonte Vega, A.; Garrido Frenich, A.; Martínez Vidal, J. L.; Duran Martos, J. Separation and determination of sterols in olive oil by HPLC-MS. *Food Chem.* **2007**, *102*, 593–598.

(4) Cert, A.; Moreda, W.; Pérez-Camino, M. C. Chromatographic analysis of minor constituents in vegetable oils. *J. Chromatogr., A* **2000**, *881*, 131–148.

(5) Aparicio, R. In *Handbook of Olive Oil: Analysis and Properties*; Harwood, J. L., Aparicio, R., Eds.; Aspen: Gaithersburg, MD, 1999; pp 285.

(6) Kiritsakis, A.K. In *Olive Oil Handbook*; American Oil Chemists' Society: Champaign, IL, 1998; pp 20.

(7) Piironen, V.; Lindsay, D. G.; Miettinen, T. A.; Toivo, J.; Lampi, A. M. Plant sterols: biosynthesis, biological function and their importance to human nutrition. *J. Sci. Food Agric.* **2000**, *80*, 939.

(8) Perona, J. S.; Cabello-Moruno, R.; Ruiz-Gutierrez, V. The role of virgin olive oil components in the modulation of endothelial function. *J. Nutr. Biochem.* **2006**, *17*, 429.

(9) Cercaci, L.; Passalacqua, G.; Poerio, A.; Rodriguez-Estrada, M. T.; Lercker, G. Composition of total sterols (4-desmethyl-sterols) in extravirgin olive oils obtained with different extraction technologies and their influence on the oil oxidative stability. *Food Chem.* **2007**, *102*, 66–76.

(10) Rui Alves, M.; Cunha, S. C.; Amaral, J. S.; Pereira, J. A.; Beatriz Oliveira, M. Classification of PDO olive oils on the basis of their sterol composition by multivariate analysis. *Anal. Chim. Acta* **2005**, *549*, 166–178.

(11) Ranalli, A.; Pollastri, L.; Contento, S.; Di Loreto, G.; Lannucci, E.; Lucera, L.; Russi, F. Sterol and alcohol components of seed, pulp and whole olive fruit oils. Their use to characterise olive fruit variety by multivariates. *J. Sci. Food Agric.* **2002**, *82*, 854–859.

(12) Cercaci, L.; Rodríguez-Estrada, M. T.; Lercker, G. Solid-phase extraction−thin-layer chromatography−gas chromatography method for the detection of hazelnut oil in olive oils by determination of esterified sterols. *J. Chromatogr., A* **2003**, *985*, 211–220.

(13) Mariani, C.; Bellan, G.; Lestini, E.; Aparicio, R. The detection of the presence of hazelnut oil in olive oil by free and esterified sterols. *Eur. Food Res. Technol.* **2006**, *223*, 655–661.

(14) Philips, K. M.; Ruggio, D. M.; Toivo, J. I.; Swank, M. A.; Simpkins, A. H. Free and esterified sterol composition of edible oils and fats. *J. Food Compos. Anal.* **2002**, *15*, 123–142.

(15) Rivera del Álamo, R. M.; Fregapane, G.; Aranda, F.; Gómez-Alonso, S.; Salvador, M. D. Sterol and alcohol composition of Cornicabra virgin olive oil: the campesterol content exceeds the upper limit of 4% established by EU regulations. *Food Chem.* **2004**, *84*, 533–537.

(16) Sánchez-Casas, J.; Osorio Bueno, E.; Montaño García, A. F.; Martinez Cano, M. Sterol and erythrodiol + uvaol content of virgin olive oils from cultivars of Extremadura (Spain). *Food Chem.* **2004**, *87*, 225–230.

(17) Galeano Díaz, T.; Durán Merás, I.; Sánchez Casas, J.; Alexandre Franco, M. F. Characterization of virgin olive oils according to its triglycerides and sterols composition by chemometric methods. *Food Control* **2005**, *16*, 339–347.

(18) Parcerisa, J.; Casals, I.; Boatella, J.; Codony, R.; Rafecas, M. Analysis of olive and hazelnut oil mixtures by high-performance liquid chromatography−atmospheric pressure chemical ionisation mass spectrometry of triacylglycerols and gas−liquid chromatography of non-saponifiable compounds (tocopherols and sterols). *J. Chromatogr., A* **2000**, *881*, 149–158.

(19) Amaral, J. S.; Casal, S.; Citová, I.; Santos, A.; Seabra, R. M.; Oliveira, B. P. P. Characterization of several hazelnut (*Corylus avellana* L.) cultivars based in chemical, fatty acid and sterol composition. *Eur. Food Res. Technol.* **2006**, *222*, 274–280.

(20) Matos, L. C.; Cunha, S. C.; Amaral, J. S.; Pereira, J. A.; Andrade, P. B.; Seabra, R. M.; Oliveira, B. P. P. Chemometric characterization

of three varietal olive oils (cvs. Cobrançosa, Madural and Verdeal Transmontana) extracted from olives with different maturation indices. *Food Chem.* **2007**, *102*, 406–414.
(21) Thanh, T. T.; Vergnes, M. F.; Kaloustian, J.; El-Moselhy, T. F.; Amiot-Carlin, M. J.; Portugal, H. Effect of storage and heating on phytosterol concentrations in vegetable oils determined by GC/MS. *J. Sci. Food Agric.* **2006**, *86*, 220–225.
(22) Medvedovici, A.; David, F.; Sandra, P. Analysis of sterols in vegetable oils using off-line SFC/capillary GC-MS. *Chromatographia* **1997**, *44*, 37–42.
(23) Cunha, S. S.; Fernandes, J. O.; Oliveira, B. P. P. Quantification of free and esterified sterols in Portuguese olive oils by solid-phase extraction and gas chromatography−mass spectrometry. *J. Chromatogr., A* **2006**, *1128*, 220–227.
(24) Abidi, S. L. Capillary electrochromatography of sterols and related steryl esters derived from vegetable oils. *J. Chromatogr., A* **2004**, *1059*, 199–208.
(25) Lerma-García, M. J.; Simó-Alfonso, E. F.; Ramis-Ramos, G.; Herrero-Martínez, J. M. Rapid determination of sterols in vegetable oils by CEC using methacrylate ester-based monolithic columns. *Electrophoresis* **2008**, *29*, 4603–4611.
(26) Lerma-García, M. J.; Ramis-Ramos, G.; Herrero-Martínez, J. M.; Simó-Alfonso, E. F. Classification of vegetable oils according to their botanical origin using sterol profiles established by direct infusion mass spectrometry. *Rapid Commun. Mass Spectrom.* **2008**, *22*, 973–978.
(27) Martínez-Vidal, J. L.; Garrido-Frenich, A.; Escobar-García, M. A.; Romero-González, R. LC−MS determination of sterols in olive oil. *Chromatographia* **2007**, *65*, 695–699.
(28) Segura-Carretero, A.; Carrasco-Pancorbo, A.; Cortacero, S.; Gori, A.; Cerretani, L.; Fernández-Gutiérrez, A. A simplified method for HPLC-MS analysis of sterols in vegetable oil. *Eur. J. Lipid Sci. Technol.* **2008**, *110*, 1142–1149.
(29) Koprivnjak, O.; Moret, S.; Populin, T.; Lagazio, C.; Conte, L. S. Variety differentiation of virgin olive oil based on *n*-alkane profile. *Food Chem.* **2005**, *90*, 603–608.
(30) Aranda, F.; Gómez-Alonso, S.; Rivera del Álamo, R. M.; Salvador, M. D.; Fregapane, G. Triglyceride, total and 2-position fatty acid composition of Cornicabra virgin olive oil: comparison with other Spanish cultivars. *Food Chem.* **2004**, *86*, 485–492.
(31) Krichene, D.; Taamalli, W.; Daoud, D.; Salvador, M. D.; Fregapane, G.; Zarrouk, M. Phenolic compounds, tocopherols and other minor components in virgin olive oils of some Tunisian varieties. *J. Food Biochem.* **2007**, *31*, 179–194.
(32) Luna, G.; Morales, M. T.; Aparicio, R. Characterisation of 39 varietal virgin olive oils by their volatile compositions. *Food Chem.* **2006**, *98*, 243–252.
(33) Baccouri, O.; Bendini, A.; Cerretani, L.; Guerfel, M.; Baccouri, B.; Lercker, G.; Zarrouk, M.; Ben Miled, D. D. Comparative study on volatile compounds from Tunisian and Sicilian monovarietal virgin olive oils. *Food Chem.* **2008**, *111*, 322–328.
(34) Stefanoudaki, E.; Kotsifaki, F.; Koutsaftakis, A. Classification of virgin olive oils of the two major Cretan cultivars based on their fatty acid composition. *J. Am. Oil Chem. Soc.* **1999**, *76*, 623–626.
(35) Lerma-García, M. J.; Herrero-Martínez, J. M.; Ramis-Ramos, G.; Simó-Alfonso, E. F. Prediction of the genetic variety of Spanish extra virgin olive oils using fatty acid and phenolic compound profiles established by direct infusion mass spectrometry. *Food Chem.* **2008**, *108*, 1142–1148.
(36) Commission Regulation (EC) No. 796/2002 of 6 May 2002, *Off. J. Eur. Union* **2002**, *L128*, annex XIX, 23.
(37) Vandeginste, B. G. M.; Massart, D. L.; Buydens, L. M. C.; De Jong, S.; Lewi, P. J.; Smeyers-Verbeke, J. In *Data Handling in Science and Technology Part B*; Elsevier Science: Amsterdam, The Netherlands, 1998; pp 237.
(38) Sánchez-Machado, D. I.; López-Hernández, J.; Paseiro-Losada, P.; López-Cervantes, J. An HPLC method for the quantification of sterols in edible seaweeds. *Biomed. Chromatogr.* **2004**, *18*, 183–190.
(39) Jee, M. In *Oils and Fat Authentication*.; Blackwell Publishing, CRC Press: Boca Raton, FL, 2002.

Received for review July 7, 2009. Revised manuscript received October 6, 2009. Accepted October 14, 2009. Work supported by Project CTQ2007-61445 (MEC of Spain and FEDER funds). M.J.L.-G. thanks the Generalitat Valenciana for an FPI grant for Ph.D. studies. V.C.-H. thanks the University of Valencia for a contract.

ANEXO XV

Food Research International 42 (2009) 1446–1452

Contents lists available at ScienceDirect

Food Research International

journal homepage: www.elsevier.com/locate/foodres

Classification of extra virgin olive oils according to their geographical origin using phenolic compound profiles obtained by capillary electrochromatography

M.J. Lerma-García [a], C. Lantano [b], E. Chiavaro [b], L. Cerretani [c], J.M. Herrero-Martínez [a], E.F. Simó-Alfonso [a,*]

[a] Departamento de Química Analítica, Universidad de Valencia, C. Doctor Moliner 50, E-46100 Burjassot, Valencia, Spain
[b] Dipartimento di Ingegneria Industriale, Università degli Studi di Parma, viale Usberti, 181/A, I-43100 Parma, Italy
[c] Dipartimento di Scienze degli Alimenti, Università di Bologna, P. zza Goidanich 60, I-47023 Cesena (FC), Italy

ARTICLE INFO

Article history:
Received 21 May 2009
Accepted 26 July 2009

Keywords:
CEC
Extra virgin olive oils
Geographical origin
Lauryl acrylate-based monolithic columns
Linear discriminant analysis
Phenolic compounds

ABSTRACT

A simple and reliable method for the evaluation of the phenolic fraction of extra virgin olive oils (EVOO) by capillary electrochromatography (CEC) with UV–Vis detection, using lauryl acrylate (LA) ester-based monolithic columns, has been developed. The percentages of the porogenic solvents in the polymerization mixture, and the mobile phase composition, were optimized. The optimum monolith was obtained with a monomers/porogens ratio of 40:60% (wt/wt) using a LA/1,3-butanediol diacrylate ratio of 70:30% (wt/wt) and a 1,4-butanediol/1-propanol ratio of 25:75% (wt/wt). A satisfactory resolution between the phenolic compounds was achieved in less than 25 min with a 15:85 (v/v) ACN–water buffer containing 5 mM formic acid at pH 3.0. The method was applied to the analysis of the phenolic fraction of EVOO samples. Using linear discriminant analysis of the CEC phenolic profiles, the EVOO samples belonging to three different geographical origins (Croatia, Italy and Spain) were correctly classified with an excellent resolution among all the categories.

1. Introduction

Virgin olive oils (VOOs) are defined by the regulation of the European Communities as those "oils obtained from the fruit of the olive tree solely by mechanical or other physical means" (European Union Commission, 2001).

VOO is unique among other vegetable oils due to its high levels of monounsaturated fatty acids (mainly oleic acid) and to the presence of minor components, such as phenolic compounds among others. The content of phenolic compounds is an important factor to be considered when evaluating the quality of VOO (Servili & Montedoro, 2002), since these compounds have potent antioxidant activity and contribute significantly to the extraordinary stability of VOOs against oxidation (Tura et al., 2007). The high phenolic levels found are possible because VOO is obtained from mechanical pressing of ripe olive fruits without any further refining process. These compounds have shown chemoprotective properties (such as anticancer, antioxidant and anti-inflammatory) in human beings (Bendini et al., 2007; Cicerale, Conlan, Sinclair & Keast, 2009), and have also contributed to the sensorial properties of VOOs by conferring bitterness, pungency and astringency (Andrewes, Busch, De Joode, Groenewegen, & Alexandre, 2003; Cerretani, Salvador, Bendini, & Fregapane, 2008; Gutierrez-Rosales, Rios, & Gomez-Rey, 2003).

The concentration and composition of phenolic compounds in VOO are strongly affected by agronomical and technological factors, such as olive cultivar (Baccouri et al., 2008; Tura et al., 2007), place of cultivar (Cerretani et al., 2006), climate, degree of maturation (Baccouri et al., 2008), crop season (Gómez-Alonso, Salvador, & Fregapane, 2002) and production process (Cerretani et al., 2006; Ranalli, Contento, Schiavone, & Simone, 2001).

Traditionally, separation and determination of phenolic compounds in extracts obtained from VOO by liquid–liquid extraction or solid phase extraction have been carried out by HPLC analysis coupled mostly with UV detection (Allalout et al., 2009; Andrewes et al., 2003; Baccouri et al., 2008; Bendini et al., 2003; Bonoli, Bendini, Cerretani, Lercker, & Gallina-Toschi, 2004; Cerretani et al., 2006; Gutierrez-Rosales et al., 2003; Gómez-Alonso et al., 2002; Ocakoglu, Tokatli, Ozen, & Korel, 2009; Tura et al., 2007), electrochemical (Brenes, García, García, & Garrido, 2000), fluorescence (Cartoni, Coccioli, Jasionowska, & Ramires, 2000; García, Brenes, García, Romero, & Garrido, 2003) and mass spectrometry (MS) detection systems (Andejelkovic et al., 2008; Baccouri et al., 2008; Bendini et al., 2003; Bonoli et al., 2004; Carrasco-Pancorbo, Neusúβ, Pelzing, Segura-Carretero, & Fernández-Gutiérrez, 2007; Gutierrez-Rosales et al., 2003; Suárez, Macià, Romero, & Motilva, 2008). GC (Angerosa, D'Alessandro, Corana, & Mellerio, 1996; Carrasco-Pancorbo, Cerretani et al., 2005; Liberatore, Procida,

* Corresponding author. Tel.: +34 963543176; fax: +34 963544436.
E-mail address: ernesto.simo@uv.es (E.F. Simó-Alfonso).

0963-9969/$ - see front matter © 2009 Elsevier Ltd. All rights reserved.
doi:10.1016/j.foodres.2009.07.027

D'Alessandro, & Cichelli, 2001; Ranalli et al., 2001; Ríos, Gil, & Gutiérrez-Rosales, 2005; Saitta, Salvo, Di Bella, Dugo, & La Torre, 2009) and capillary electrophoresis (CE) (Bendini et al., 2003; Bonoli et al., 2004; Carrasco-Pancorbo, Arráez-Román, Segura-Carretero, & Fernández-Gutiérrez, 2006; Carrasco-Pancorbo, Cruces-Blanco, Segura-Carretero, & Fernández-Gutiérrez, 2004; Carrasco-Pancorbo, Segura-Carretero, & Fernández-Gutiérrez, 2005; Carrasco-Pancorbo, Gómez-Caravaca et al., 2006; Carrasco-Pancorbo et al., 2007; Gómez-Caravaca, Carrasco-Pancorbo, Cañabate-Díaz, Segura-Carretero, & Fernández-Gutiérrez, 2005) coupled both with different detection systems have been also used for these purposes. More recently, other techniques such as voltammetric sensors (Rodríguez-Méndez, Apetrei, & de Saja, 2008) and high resolution ^{1}H nuclear magnetic resonance spectroscopy (Christophoridou & Dais, 2009) have been also applied to phenolic compound determination in VOOs.

Using mainly HPLC and phenolic compound profiles, several studies have been reported on the study of VOOs according to their cultivar or geographical origin (Allalout et al., 2009; Andejelkovic et al., 2008; Ocakoglu et al., 2009).

Capillary electrochromatography (CEC) is a hybrid separation technique, which combines the selectivity of HPLC with the high efficiency of CE. Among CEC supports, the use of monolithic columns has extensively grown in the last few years. Their advantages compared with CEC packed columns are: (i) simple preparation, (ii) absence of retaining frits, (iii) adjustable porosity and pore size, allowing the use of long columns to achieve highly efficient separations, and (iv) the wide variety of monomers available for the synthesis of stationary phases with different functionalities (Legido-Quigley, Marlin, Melin, Manz, & Smith, 2003; Svec, Tennikova, & Deyl, 2003). Briefly, monolithic materials can be classified into two categories, organic polymer- and silica-based monoliths (Svec et al., 2003). Among these polymeric stationary phases, acrylate- (Cantó-Mirapeix, Herrero-Martínez, Mongay-Fernández, & Simó-Alfonso, 2009a; Augustin, Jardy, Gareil, & Hennion, 2006; Barrioulet, Delaunay-Bertoncini, Demesmay, & Rocca, 2005; Bedair & El Rassi, 2003; Ngola, Fintschenko, Choi, & Shepodd, 2001) and methacrylate-based (Cantó-Mirapeix, Herrero-Martínez, Mongay-Fernández, & Simó-Alfonso, 2009b; Eeltink, Herrero-Martínez, Rozing, Schoenmakers, & Kok, 2005; Peters, Petro, Svec, & Fréchet, 1998; Yu, Xu, Svec, & Fréchet, 2002) monoliths are the most popular materials used for CEC applications. These monoliths are usually prepared by *in situ* polymerization of a mixture composed of functional monomer/s, cross-linker, porogens, and a free radical initiator. Polymerization reaction is commonly initiated thermally (Bedair & El Rassi, 2003; Eeltink et al., 2005; Peters et al., 1998; Yu et al., 2002), by UV irradiation (Augustin et al., 2006; Barrioulet et al., 2005; Bedair & El Rassi, 2003; Ngola et al., 2001; Yu et al., 2002), or by a chemical system (Cantó-Mirapeix et al., 2009a, 2009b). Advantages of photo-initiation are speed and easy selection of polymerization regions by using masks, which is particularly important in relation to the manufacturing of microfluidic chips.

The potential of this monolithic technology was demonstrated when applied to tocopherol (Lerma-García, Simó-Alfonso, Ramis-Ramos, & Herrero-Martínez, 2007) and sterol (Lerma-García, Simó-Alfonso, Ramis-Ramos, & Herrero-Martínez, 2008) determination in vegetable oils. On the other hand, CEC using packed columns has been used to separate phenolic compounds in VOO (Aturki, Fanali, ÓOrazio, Rocco, & Rosati, 2008); however, the use of monolithic columns has not been reported for this purpose.

The aim of this work was to evaluate the phenolic profiles of extra virgin olive oils (EVOO) from different geographical origins by using a simple and reliable CEC method. The characterization of the phenolic profile using lauryl acrylate (LA) ester-based monolithic columns was optimized in terms of composition of polymerization mixture (i.e. porogenic solvents) and mobile phase composition. The classification of EVOO samples according to their geographical origin was performed by linear discriminant analysis (LDA).

2. Materials and methods

2.1. Reagents and samples

LA, 1,3-butanediol diacrylate (BDDA), lauroyl peroxide (LPO), [2-(methacryloyloxy)ethyl] trimethyl ammonium chloride (75% in water, META), 1,4-butanediol and 3-(trimethoxysilyl)propyl methacrylate from Aldrich (Milwaukee, WI, USA), hydrochloric acid (37%) from Panreac (Barcelona, Spain), methanol, 1-propanol and ACN from Scharlau (Barcelona), thiourea and *n*-hexane (Riedel-de Haën, Seelze, Germany) were employed. Deionized water was obtained with a Barnstead deionizer (Sybron, Boston, MA, USA). Fused-silica capillaries of 33.5 cm length and 375 μm O.D. × 100 μm I.D. with UV-transparent external coating (Polymicro Technologies, Phoenix, AZ, USA) were used.

The EVOO samples employed in this study are summarized in Table 1. These oils were either purchased or kindly donated by the manufacturers. The geographical origin and quality grade of all the EVOO samples were guaranteed by the suppliers. The oils differed in terms of olive cultivar, degree of ripening, area of growth, production system (type, productive capacity and manufacturer) and storage time.

2.2. Instrumentation

CEC experiments were performed on an HP^{3D}CE instrument (Agilent Technologies, Waldbronn, Germany), equipped with a diode array UV–Vis detector and provided with an external nitrogen supply. Data acquisition was performed with ChemStation Software (Rev.A.10.01, Agilent). Before use, all the eluents for CEC were degassed with a D-78224 ultrasonic bath (Elma, Germany). To photoinitiate polymerization, capillaries were placed into an UV crosslinker (model CL1000) from UVP Inc. (Upland, CA, USA)

Table 1
Geographical origin, number of samples, genetic variety and suppliers of the EVOOs.

Geographical origin	No. of samples	Genetic variety	Supplier
Croatia	1	Mastrinka	OLEA[a]
	1	Lastovka	OLEA[a]
	1	Drobnica	OLEA[a]
	3	Oblica	OLEA[a]
	4	Varietal blend	OLEA[a], SMS d.o.o, Zvijezda
Italy	1	Brugnola	OLEA[a]
	1	Ascolana Tenera	OLEA[a]
	1	Correggiolo	OLEA[a]
	1	Raggia	OLEA[a]
	1	Frantoio	OLEA[a]
	1	Brisighella	OLEA[a]
	1	Nocellara	OLEA[a]
	1	Ogliarola	OLEA[a]
	1	Ghiacciola	OLEA[a]
	1	Coratina	OLEA[a]
Spain	1	Serrana	Intercoop
	1	Blanquilla	Intercoop
	1	Canetera	Intercoop
	1	Borriolenca	Intercoop
	1	Farga	Intercoop
	2	Hojiblanca	Coosur, Carbonell
	2	Arbequina	Carbonell, Olearum
	1	Picual	Castillo de Taberna

[a] Italian organization of olive oil tasters (http://www.olea.info).

equipped with five UV lamps (5 × 8 W, 254 nm). Scanning electron microscope (SEM) photographs of monolithic materials were taken with a SEM model S-4100 (Hitachi, Ibaraki, Japan) provided with a field emission gun, a BSE AUTRATA detector and an EMIP 3.0 image data acquisition system.

2.3. Preparation and characterization of the polymeric monolithic columns

Before preparation of the columns, and in order to enable covalent attachment of the monolith to the wall, surface modification of the inner wall of the fused-silica capillaries with 3-(trimethoxysilyl)propyl methacrylate was performed (Peters et al., 1998). Monoliths were prepared using polymerization mixtures containing a bulk monomer (LA), a cross-linker (BDDA), pore-forming solvents (1,4-butanediol/1-propanol) and a positively charged monomer (META), which was added to assure EOF. LPO (1 wt.% with respect to the monomers) was employed as initiator. After mixing, and to obtain a clear solution, sonication for 10 min followed by deareation with nitrogen for 10 more min was applied. The preconditioned capillary (33.5 cm) was filled with the polymerization mixture up to a total length of 25 cm. Photo-polymerization was accomplished by irradiation of the capillaries inside the UV cross-linker at 0.9 J/cm^2 for 10 min (Bernabé-Zafón, Cantó-Mirapeix, Simó-Alfonso, Ramis-Ramos, & Herrero-Martínez, 2009). After polymerization and using an HPLC pump, the resulting columns were flushed first with methanol to remove the pore-forming solvents and possible unreacted monomers or oligomers, and then with mobile phase for 30 min.

2.4. CEC procedures

The monolithic column was placed in the instrument and equilibrated with the mobile phase as follows. Using nitrogen, a pressure of 10 bar (1 MPa) was applied to both ends of the column (Eeltink et al., 2005; Peters et al., 1998), and the voltage was stepwise raised from −5 to −20 kV, with increments of 5 kV. Each voltage was kept until a constant current and a stable baseline were achieved. Separations were performed at −10 kV with the column kept at 25 °C, and the inlet and outlet vials pressurized to 1 MPa with nitrogen. Sample extracts were injected electrokinetically under −20 kV for 3 s. Detection was performed at 240, 280 and 330 nm, being quantification performed at 280 nm.

2.5. Sample preparation and data treatment

The liquid–liquid extraction procedure to obtain the phenolic fraction was adapted from Carrasco-Pancorbo et al. (2004). Briefly, 50 g of oil were dissolved in 50 mL *n*-hexane, and the solution was extracted successively with four 20 mL portions of methanol/water (60:40, v/v). The combined extracts of the hydrophilic layer were brought to dryness in a rotary evaporator under pressure at 40 °C. Finally, the residue was re-dissolved in 1 mL methanol/water (50:50, v/v) and filtered through a 0.45 μm filter. These solutions were properly diluted with the mobile phase and injected. All the phenolic extracts were injected two times. The peak area of each compound was measured, and a data matrix was constructed using the areas of all the peaks as original variables. After normalization of the variables, statistical data treatment was performed using SPSS (v. 15.0, Statistical Package for the Social Sciences, Chicago, IL, USA).

3. Results and discussion

3.1. Optimization of the separation of phenolic compounds

The conditions to prepare photo-polymerized LA-based monoliths were adapted from a previous work, where CEC columns were chemically polymerized using LPO as initiator (Cantó-Mirapeix et al., 2009a). Initially, the selected composition of the polymerization mixture was 40 wt.% monomers (69.8 wt.% LA, 29.9 wt.% BDDA and 0.3 wt.% META) and 60 wt.% porogens (17 wt.% 1,4-butanediol and 83 wt.% 1-propanol) in the presence of 0.3 wt.% LPO. According to Aturki et al. (2008), an ACN–water mixture

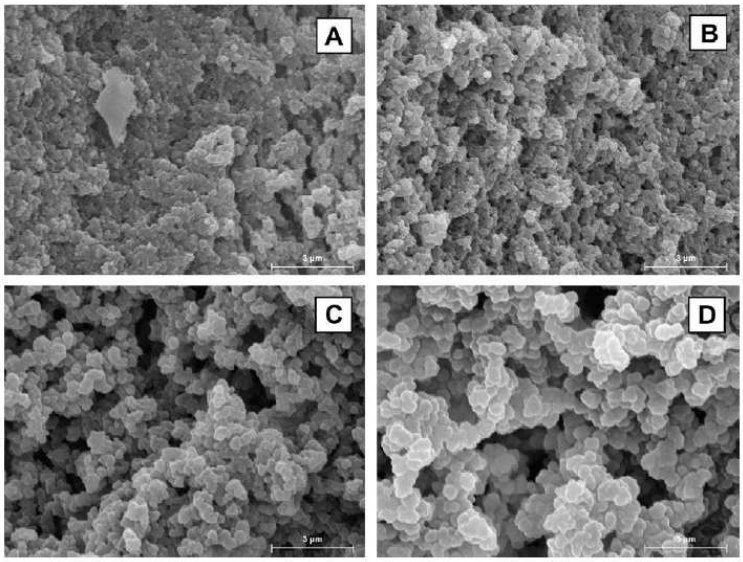

Fig. 1. SEM micrographs of LA-based monolithic columns prepared with (A) 10%, (B) 12%, (C) 15% and (D) 18% 1,4-butanediol in the polymerization mixture. The bar lengths stand for 3 μm.

(30:70) containing 5 mM formic acid at pH 3.0 was firstly tried as mobile phase. However, at this 1,4-butanediol content in the polymerization mixture (10 wt.%), the column exhibited poor permeability, leading to blockage problems. This is well evidenced in the SEM picture of this monolith (Fig. 1A), where small pore and globule size can be clearly observed. For this reason, polymerization mixtures containing higher 1,4-butanediol contents (12–18 wt.%) were studied. Monolith prepared with 12 wt.% 1,4-butanediol showed better permeability than 10 wt.%, as confirmed in Fig. 1B, where slightly larger globules can be evidenced. However, this column showed a tendency to get blocked when attempting to analyze oil samples. In order to overcome this problem, a column containing 15 wt.% 1,4-butanediol in the polymerization mixture was prepared. The permeability of this column was quite satisfactory, being its globule size higher than previous column (see Fig. 1C). When a phenolic extract (Serrana EVOO variety) was injected in this monolith, a poor separation was obtained (Fig. 2A). In order to improve the quality of separation, the influence of ACN content in the mobile phase was studied from 20% to 10%. The results are shown in Fig. 2B–D. When the concentration of ACN decreased, an improvement in the resolution was observed. When a content of 10% ACN was used (Fig. 2D), a decrease in efficiency values and an increase in analysis time was observed. Additionally, a drift in the baseline was evidenced. As a result, a mobile phase composed of 15:85 (v/v) ACN-aqueous buffer containing 5 mM formic acid at pH 3.0 was selected as the best compromise between resolution and analysis time (less than 25 min).

Under these conditions and in order to speed up the analysis, a column with 18 wt.% 1,4-butanediol was tried. A loss of resolution and efficiency of phenolic peaks was obtained (data not shown). It could be attributed to the larger globule sizes of this monolith (Fig. 1D) compared with that made with 15 wt.% 1,4-butanediol. Small changes in mobile phase did not lead to a significant separation improvement. At the sight of these results, a monolith prepared with 15 wt.% 1,4-butanediol in the polymerization mixture was selected for further studies.

3.2. Characterization of the phenolic profiles of EVOO

The optimized method was applied to the analysis of EVOO samples. Representative electrochromatograms of EVOO from Croatia (A), Italy (B) and Spain (C, D) are shown in Fig. 3. As it can be observed, 17 common peaks were obtained for the three different geographical origins in less than 25 min. These peaks, which correspond to different phenolic compounds, should be related with the different olive varieties coming from different geographical areas, as previously reported by other authors using different techniques (Brenes, García, Rios, García, & Garrido, 2002; Carrasco-Pancorbo, Gómez-Caravaca et al., 2006). On the other hand, phenol fingerprints for EVOO samples from the same geographical origin (C and D) were closely similar. The little differences observed in EVOO fingerprints were enhanced when chemometric analysis of the data was performed.

3.3. Selection and normalization of the variables for LDA classification

In order to reduce the variability associated to the total amount of phenolic compounds recovered from the EVOO samples, and to minimize other sources of variance also affecting the sum of the areas of all the peaks, normalized rather than absolute peak areas were used. In order to normalize the variables, the area of each peak was divided by each one of the areas of the other 16 peaks; in this way, and taking into account that each pair of peaks should

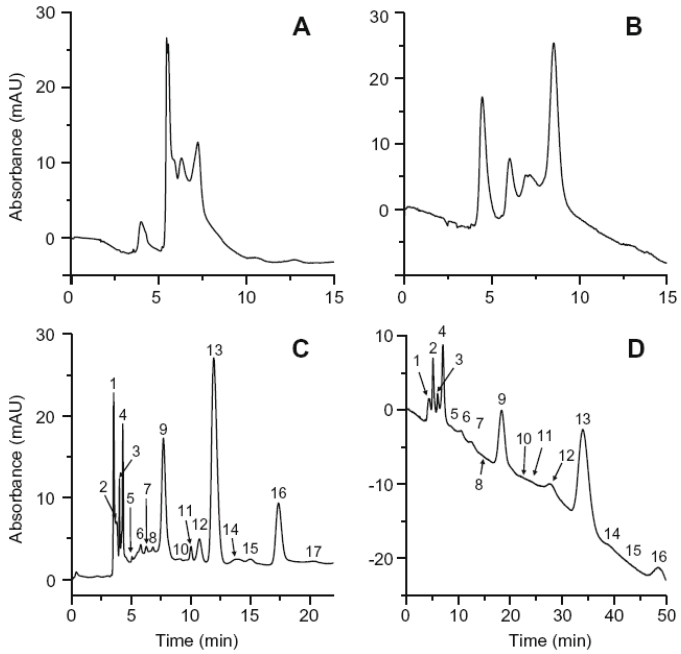

Fig. 2. Influence of the mobile phase composition on the separation of phenolic compounds: (A) 30:70, (B) 20:80, (C) 15:85 and (D) 10:90 (v/v) ACN–water mixtures containing 5 mM formic acid at pH 3.0. CEC conditions: LA-based monolithic column prepared with 15 wt.% 1,4-butanediol in the polymerization mixture; electrokinetic injection, 10 kV for 2 s; separation voltage, −10 kV; wavelength detection: 280 nm. The 17 peaks labeled were selected as variables.

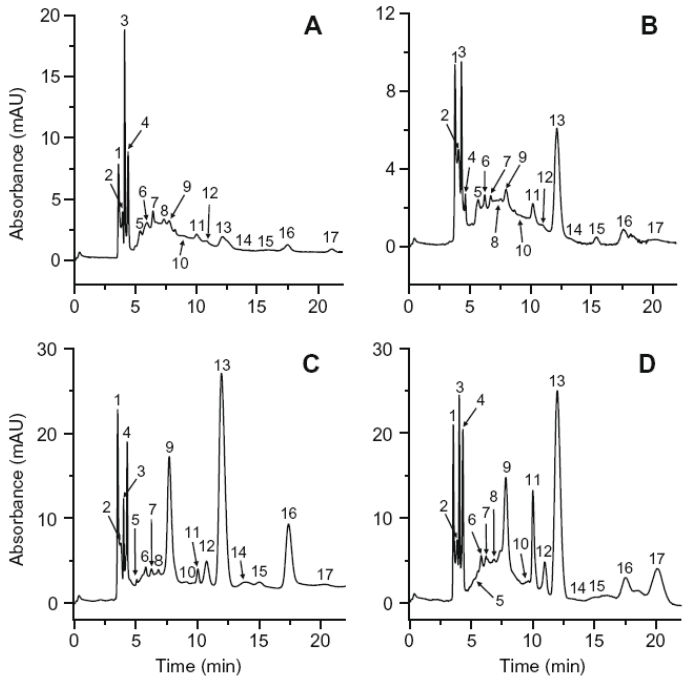

Fig. 3. Electrochromatograms of EVOO from (A) Croatia (Lavstoska), (B) Italy (Frantoio), (C) Spain (Serrana) and (D) Spain (Arbequina) obtained on an LA-based monolithic capillary under the optimal conditions. CEC conditions: mobile phase: 15:85 (v/v) ACN–water containing 5 mM formic acid at pH 3.0. Other experimental conditions as in Fig. 2.

be considered only once, $(17 \times 16)/2 = 136$ non-redundant peak ratios were obtained to be used as predictors.

3.4. Construction of the data matrices and LDA model

LDA, a supervised classificatory technique, is widely recognized as an excellent tool to obtain vectors showing the maximal resolution between a set of previously defined categories. In LDA, vectors minimizing the Wilks' lambda, λ_w, are obtained (Vandeginste et al., 1998). This parameter is calculated as the sum of squares of the distances between points belonging to the same category divided by the total sum of squares.

Using the normalized variables, an LDA model capable of classifying the EVOO samples according to their respective geographical origin was constructed. From the 30 samples of Table 1, a matrix containing 60 injections (all samples were injected twice), was constructed and used for evaluation purposes. To construct the LDA training matrix, only the means of the replicates of the samples were included (30 objects); in this way, the internal dispersion of the categories was reduced, which was important to reduce the number of variables selected by the SPSS stepwise algorithm during model construction. A response column, containing the three categories corresponding to the three geographical origins of the EVOO, was added to both matrices. According to the SPSS stepwise algorithm, a predictor is selected when the reduction of λ_w produced after its inclusion in the model exceeds F_{in}, the entrance threshold of a test of comparison of variances or F-test. However, the entrance of a new predictor modifies the significance of those predictors which are already present in the model. For this reason, after the inclusion of a new predictor, a rejection threshold, F_{out}, is used to decide if one of the other predictors should be removed from the model. The process terminates when there are no predictors entering or being eliminated from the model. The

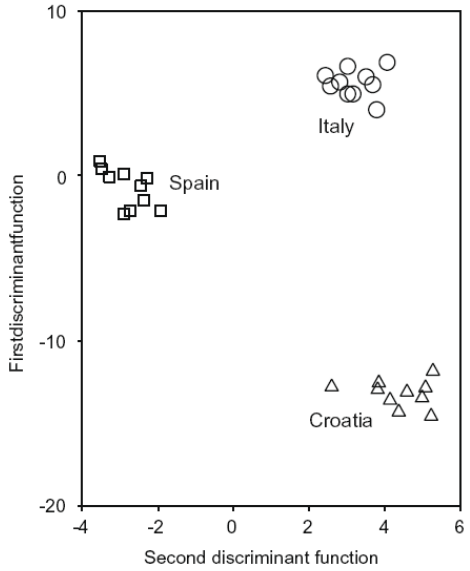

Fig. 4. Score plot on the plane of the two LDA discriminant functions obtained to predict the geographical origin of EVOOs.

Table 2
Predictors selected and their corresponding standardized coefficients of the LDA model constructed to predict the geographical origin of the EVOOs.

Predictor[a]	f_1	f_2
1/4	3.50	1.91
1/15	−4.51	1.37
2/15	8.02	−2.43
7/13	2.22	2.71
7/14	1.64	−1.04
10/13	−0.97	−1.55
11/17	0.98	1.09
12/14	−4.25	2.19
12/17	−2.90	−2.06
15/17	2.04	1.04

[a] Pairs of peak areas identified according to figure labels.

probability values of F_{in} and F_{out}, 0.01 and 0.10, respectively, were adopted.

When the LDA model was constructed, an excellent resolution between all the category pairs was achieved (Fig. 4, $\lambda_W = 0.09$). The variables selected by the SPSS stepwise algorithm, and the corresponding standardized coefficients of this model, showing the predictors with large discriminant capabilities, are given in Table 2. For this model, and using leave-one-out validation, all the points of the training set were correctly classified. The corresponding evaluation set, containing the 60 original data points, was then used to check the prediction capability of the model. Using a 95% probability, all the objects were correctly assigned.

On the other hand, and in order to validate the model with blind samples, a new LDA model with 24 samples, eight of each geographical origin, which were randomly selected, was constructed. The predictors selected by this model were mainly the same than those selected in the previous model; however, slightly variations in the coefficients were observed. When the new evaluation set (composed by the mean of the remaining six samples) was used to check the prediction capability of the model, all the samples were correctly classified.

4. Conclusions

Using LA ester-based monolithic columns, a simple and reliable CEC method for the analysis of the phenolic fraction of EVOOs has been developed. The best separations keeping an optimal analysis time (<25 min), were obtained with an LA-based column prepared with 15 wt.% 1,4-butanediol in the polymerization mixture, and using a mobile phase containing 15:85 (v/v) ACN–water (5 mM formic acid at pH 3.0). Using CEC data and LDA, the EVOO samples belonging to the three different geographical origins (Croatia, Italy and Spain) were correctly classified with an excellent resolution among all the categories. A next step of this work will be the identification of the 17 phenolic compounds by interfacing CEC with MS or by injection of single phenolic compounds previously collected by HPLC.

Acknowledgements

Work supported by Project CTQ2007-61445 (MEC and FEDER funds). M. J. Lerma García thanks the Generalitat Valenciana for an FPI Grant for PhD studies. Authors also acknowledge *Intercoop Olival* and the *Cooperativa de Altura* for the EVOO samples kindly donated.

References

Allalout, A., Krichène, D., Methenni, K., Taamalli, A., Oueslati, I., Daoud, D., et al. (2009). Characterization of virgin olive oil from super intensive Spanish and Greek varieties grown in Northern Tunisia. *Scientia Horticulturae, 120,* 77–83.

Andejelkovic, M., Van Camp, J., Pedra, M., Renders, K., Socaciu, C., & Verhé, R. (2008). Correlations of the phenolic compounds and the phenolic content in some Spanish and French olive oils. *Journal of Agricultural and Food Chemistry, 56,* 5181–5187.

Andrewes, P., Busch, J. L. H. C., De Joode, T., Groenewegen, A., & Alexandre, H. (2003). Sensory properties of virgin olive oil polyphenols: Identification of deacetoxy-ligstroside aglycon as a key contributor to pungency. *Journal of Agricultural and Food Chemistry, 51,* 1415–1420.

Angerosa, F., D'Alessandro, N., Corana, F., & Mellerio, G. (1996). Characterization of phenolic and secoiridoid aglycons present in virgin olive oil by gas chromatography–chemical ionization mass spectrometry. *Journal of Chromatography A, 736,* 195–203.

Aturki, Z., Fanali, S., ÓOrazio, G., Rocco, A., & Rosati, C. (2008). Analysis of phenolic compounds in extra virgin olive oil by using reversed-phase capillary electrochromatography. *Electrophoresis, 29,* 1643–1650.

Augustin, V., Jardy, A., Gareil, P., & Hennion, M. C. (2006). In situ synthesis of monolithic stationary phases for electrochromatographic separations: Study of polymerization conditions. *Journal of Chromatography A, 1119,* 80–87.

Baccouri, O., Guerfel, M., Baccouri, B., Cerretani, L., Bendini, A., Lercker, G., Zarrouk, M., & Daoud Ben Miled, D. (2008). Chemical composition and oxidative stability of Tunisian monovarietal virgin olive oils with regard to fruit ripening. *Food Chemistry, 109,* 743–754.

Barrioulet, M. P., Delaunay-Bertoncini, N., Demesmay, C., & Rocca, J. L. (2005). Development of acrylate-based monolithic stationary phases for electrochromatographic separations. *Electrophoresis, 26,* 4104–4115.

Bedair, M., & El Rassi, Z. (2003). Capillary electrochromatography with monolithic stationary phases: II. Preparation of cationic stearyl-acrylate monoliths and their electrochromatographic characterization. *Journal of Chromatography A, 1013,* 35–45.

Bendini, A., Bonoli, M., Cerretani, L., Biguzzi, B., Lercker, G., & Gallina-Toschi, T. (2003). Liquid–liquid and solid-phase extractions of phenols from virgin olive oil and their separation by chromatographic and electrophoretic methods. *Journal of Chromatography A, 985,* 425–433.

Bendini, A., Cerretani, L., Carrasco-Pancorbo, A., Gómez-Caravaca, A. M., Segura-Carretero, A., Fernández-Gutiérrez, A., et al. (2007). Phenolic molecules in virgin olive oils: A survey of their sensory properties, health effects, antioxidant activity and analytical methods. An overview of the last decade. *Molecules, 12,* 1679–1719.

Bernabé-Zafón, V., Cantó-Mirapeix, A., Simó-Alfonso, E. F., Ramis-Ramos, G., & Herrero-Martínez, J. M. (2009). Comparison of thermal and photo-polymerization of lauryl methacrylate monolithic columns for CEC. *Electrophoresis, 30,* 1929–1936.

Bonoli, M., Bendini, A., Cerretani, L., Lercker, G., & Gallina-Toschi, T. (2004). Qualitative and semiquantitative analysis of phenolic compounds in extra virgin olive oil as a function of the ripening degree of fruits by different analytical techniques. *Journal of Agricultural and Food Chemistry, 52,* 7026–7032.

Brenes, M., García, A., García, P., & Garrido, A. (2000). Rapid and complete extraction of phenols from olive oil and determination by means of a coulometric electrode array system. *Journal of Agricultural and Food Chemistry, 48,* 5178–5183.

Brenes, M., García, A., Rios, J. J., García, P., & Garrido, A. (2002). Use of 1-acetoxypinoresinol to authenticate Picual olive oils. *International Journal of Food Science and Technology, 37,* 615–625.

Cantó-Mirapeix, A., Herrero-Martínez, J. M., Mongay-Fernández, C., & Simó-Alfonso, E. F. (2009a). Chemical initiation for butyl and lauryl acrylate monolithic columns for CEC. *Electrophoresis, 30,* 599–606.

Cantó-Mirapeix, A., Herrero-Martínez, J. M., Mongay-Fernández, C., & Simó-Alfonso, E. F. (2009b). CEC column behaviour of butyl and lauryl methacrylate monoliths prepared in non-aqueous media. *Electrophoresis, 30,* 607–615.

Carrasco-Pancorbo, A., Arráez-Román, D., Segura-Carretero, A., & Fernández-Gutiérrez, A. (2006). Capillary electrophoresis–electrospray ionization–mass spectrometry method to determine the phenolic fraction of extra-virgin olive oil. *Electrophoresis, 27,* 2182–2196.

Carrasco-Pancorbo, A., Cerretani, L., Bendini, A., Segura-Carretero, A., Gallina Toschi, T., & Fernández-Gutiérrez, A. (2005). Analytical determination of polyphenols in olive oils. *Journal of Separation Science, 28,* 837–858.

Carrasco-Pancorbo, A., Cruces-Blanco, C., Segura-Carretero, A., & Fernández-Gutiérrez, A. (2004). Sensitive determination of phenolic acids in extra-virgin olive oils by capillary zone electrophoresis. *Journal of Agricultural and Food Chemistry, 52,* 6687–6693.

Carrasco-Pancorbo, A., Gómez-Caravaca, A. M., Cerretani, L., Bendini, A., Segura-Carretero, A., & Fernández-Gutiérrez, A. (2006). Rapid quantification of the phenolic fraction of Spanish virgin olive oils by capillary electrophoresis with UV detection. *Journal of Agricultural and Food Chemistry, 54,* 7984–7991.

Carrasco-Pancorbo, A., Neusúβ, C., Pelzing, M., Segura-Carretero, A., & Fernández-Gutiérrez, A. (2007). CE- and HPLC-TOF-MS for the characterization of phenolic compounds in olive oil. *Electrophoresis, 28,* 806–821.

Carrasco-Pancorbo, A., Segura-Carretero, A., & Fernández-Gutiérrez, A. (2005). Co-electroosmotic capillary electrophoresis determination of phenolic acids in commercial olive oil. *Journal of Separation Science, 28,* 925–934.

Cartoni, G. P., Coccioli, F., Jasionowska, R., & Ramires, D. (2000). HPLC analysis of the benzoic and cinnamic acids in edible vegetable oils. *Italian Journal of Food Science, 12,* 163–173.

Cerretani, L., Bendini, A., Del Caro, A., Piga, A., Vacca, V., Caboni, M. F., & Gallina Toschi, T. (2006). Preliminary characterisation of virgin olive oils obtained from

different cultivars in Sardinia. *European Food Research and Technology, 222*, 354–361.
Cerretani, L., Salvador, M. D., Bendini, A., & Fregapane, G. (2008). Relationship between sensory evaluation performed by Italian and Spanish official panels and volatile and phenolic profiles of virgin olive oils. *Chemosensory Perception, 1*, 258–267.
Christophoridou, S., & Dais, P. (2009). Detection and quantification of phenolic compounds in olive oil by high resolution 1H nuclear magnetic resonance spectroscopy. *Analytica Chimica Acta, 633*, 283–292.
Cicerale, S., Conlan, X. A., Sinclair, A. J., & Keast, R. S. J. (2009). Chemistry and health of olive oil phenolics. *Critical Reviews in Food Science and Nutrition, 49*, 218–236.
Eeltink, S., Herrero-Martínez, J. M., Rozing, G. P., Schoenmakers, P. J., & Kok, W. Th. (2005). Tailoring the morphology of methacrylate ester-based monoliths for optimum efficiency in liquid chromatography. *Analytical Chemistry, 77*, 7342–7347.
European Union Commission (2001). Council Regulation (EC) No 1513/2001 of 23 July 2001 amending Regulations No 136/66/EEC and (EC) No 1638/98 as regards the extension of the period of validity of the aid scheme and the quality strategy for olive oil. *Official Journal of European Communities, L201*, 4–7.
García, A., Brenes, M., García, P., Romero, C., & Garrido, A. (2003). Phenolic content of commercial olive oils. *European Food Research and Technology, 216*, 520–525.
Gómez-Alonso, S., Salvador, M. D., & Fregapane, G. (2002). Phenolic compounds profile of Cornicabra virgin olive oil. *Journal of Agricultural and Food Chemistry, 50*, 6812–6817.
Gómez-Caravaca, A. M., Carrasco-Pancorbo, A., Cañabate-Díaz, B., Segura-Carretero, A., & Fernández-Gutiérrez, A. (2005). Electrophoretic identification and quantification of compounds in the polyphenolic fraction of extra-virgin olive oil. *Electrophoresis, 26*, 3538–3551.
Gutierrez-Rosales, F., Rios, J. J., & Gomez-Rey, M. A. L. (2003). Main polyphenols in the bitter taste of virgin olive oil. Structural confirmation by on-line high-performance liquid chromatography electrospray ionization mass spectrometry. *Journal of Agricultural and Food Chemistry, 51*, 6021–6025.
Legido-Quigley, C., Marlin, N. D., Melin, V., Manz, A., & Smith, N. W. (2003). Advances in capillary electrochromatography and micro-high performance liquid chromatography monolithic columns for separation science. *Electrophoresis, 2003*, 24, 917–944.
Lerma-García, M. J., Simó-Alfonso, E. F., Ramis-Ramos, G., & Herrero-Martínez, J. M. (2007). Determination of tocopherols in vegetable oils by CEC using methacrylate ester-based monolithic columns. *Electrophoresis, 28*, 4128–4135.
Lerma-García, M. J., Simó-Alfonso, E. F., Ramis-Ramos, G., & Herrero-Martínez, J. M. (2008). Rapid determination of sterols in vegetable oils by CEC using methacrylate ester-based monolithic columns. *Electrophoresis, 29*, 4603–4611.
Liberatore, L., Procida, G., D'Alessandro, N., & Cichelli, A. (2001). Solid phase extraction and gas chromatographic analysis of phenolic compounds in virgin olive oil. 2. *Food Chemistry, 73*, 119–124.
Ngola, S. M., Fintschenko, Y., Choi, W. Y., & Shepodd, T. J. (2001). Conduct-as-cast polymer monoliths as separation media for capillary electrochromatography. *Analytical Chemistry, 73*, 849–856.
Ocakoglu, D., Tokatli, F., Ozen, B., & Korel, F. (2009). Distribution of simple phenols, phenolic acids and flavonoids in Turkish monovarietal extra virgin olive oils for two harvest years. *Food Chemistry, 113*, 401–410.
Peters, E. C., Petro, M., Svec, F., & Fréchet, J. M. J. (1998). Molded rigid polymer monoliths as separation media for capillary electrochromatography. 1. Fine control of porous properties and surface chemistry. *Analytical Chemistry, 70*, 2288–2295.
Ranalli, A., Contento, S., Schiavone, C., & Simone, N. (2001). Malaxing temperature affects volatile and phenol composition as well as other analytical features of virgin olive oil. *European Journal of Lipid Science and Technology, 103*, 228–238.
Ríos, J. J., Gil, M. J., & Gutiérrez-Rosales, F. (2005). Solid-phase extraction gas chromatography–ion-trap-mass spectrometry qualitative method for evaluation of phenolic compounds in virgin olive oil and structural confirmation of oleuropein and ligstroside aglycons and their oxidation products. *Journal of Chromatography A, 1903*, 167–176.
Rodríguez-Méndez, M. L., Apetrei, C., & de Saja, J. A. (2008). Evaluation of the polyphenolic content of extra virgin olive oils using an array of voltammetric sensors. *Electrochimica Acta, 53*, 5867–5872.
Saitta, M., Salvo, F., Di Bella, G., Dugo, G., & La Torre, G. L. (2009). Minor compounds in the phenolic fraction of virgin olive oils. *Food Chemistry, 112*, 525–532.
Servili, M., & Montedoro, G. (2002). Contribution of phenolic compounds to virgin olive oil quality. *European Journal of Lipid Science and Technology, 104*, 602–613.
Suárez, M., Macià, A., Romero, M. P., & Motilva, M. J. (2008). Improved liquid chromatography tandem mass spectrometry method for the determination of phenolic compounds in virgin olive oil. *Journal of Chromatography A, 1214*, 90–99.
Svec, F., Tennikova, T. B., & Deyl, Z. (2003). *Monolithic materials: Preparation, properties and applications. Journal of Chromatography Library* (Vol. 67). .
Tura, D., Gigliotti, C., Pedo, S., Failla, O., Bassi, D., & Serraiocco, A. (2007). Influence of cultivar and site of cultivation on levels of lipophilic and hydrophilic antioxidants in virgin olive oils (*Olea europea* L) and correlations with oxidative stability. *Scientia Horticulturae, 112*, 108–119.
Vandeginste, B. G. M., Massart, D. L., Buydens, L. M. C., De Jong, S., Lewi, P. J., & Smeyers-Verbeke, J. (1998). *Data handling in science and technology – Part B*. Amsterdam: Elsevier Science BV.
Yu, C., Xu, M., Svec, F., & Fréchet, J. M. J. (2002). Preparation of monolithic polymers with controlled porous properties for microfluidic chip applications using photoinitiated free radical polymerization. *Journal of Polymer Science, Part A: Polymer Chemistry, 40*, 755–769.

ANEXO XVI

7834 J. Agric. Food Chem. 2009, 57, 7834–7840
DOI:10.1021/jf901346n

JOURNAL OF AGRICULTURAL AND FOOD CHEMISTRY
ARTICLE

Study of Chemical Changes Produced in Virgin Olive Oils with Different Phenolic Contents during an Accelerated Storage Treatment

María Jesús Lerma-García,*,† Ernesto F. Simó-Alfonso,† Emma Chiavaro,§ Alessandra Bendini,# Giovanni Lercker,# and Lorenzo Cerretani*,#

†Departamento de Química Analítica, Universidad de Valencia, C. Doctor Moliner 50, E-46100 Burjassot, Valencia, Spain, §Dipartimento di Ingegneria Industriale, Università degli Studi di Parma, viale Usberti 181/A, I-43100 Parma, Italy, and #Dipartimento di Scienze degli Alimenti, Università di Bologna, P. zza Goidanich 60, I-47521 Cesena (FC), Italy

Chemical changes produced in an extra virgin olive oil sample in the presence (EVOO) and absence (EVOOP) of its phenolic fraction during an accelerated storage treatment at 60 °C up to 7 weeks were studied. Modifications in phenol content, as well as changes in several quality parameters (free acidity, peroxide value, UV absorbance, fatty acid composition, oxidative stability index, and tocopherol content) were also evaluated under the same storage conditions and compared to those of the same sample deprived of phenolic compounds. When the phenolic extract of the EVOO was studied, a decrease of the antioxidants first present in the sample and an increase of the oxidized products were observed. In addition, oxidation seemed to produce the transformation of such phenolic compounds as secoiridoids and the appearance of oxidized forms of them. These latter compounds could be used as molecular markers of the lack of extra virgin olive oil freshness.

KEYWORDS: Aging; HPLC; oxidation; phenolic compounds; virgin olive oil

INTRODUCTION

Several studies regarding natural antioxidants from vegetable matrices have shown that olives and olive derivatives play an important role in the Mediterranean diet and, along these lines, are now considered as a source of natural phenolic antioxidants (*1*, *2*). These compounds are supposed to have chemoprotective properties in human beings (anticancer, antioxidant, and anti-inflammatory properties) (*3*, *4*) and also to contribute to the sensorial properties of virgin olive oils (VOO) by conferring bitterness, pungency, and astringency (*5*−*7*). Moreover, the high oxidative stability of VOO is related not only to the high monounsatured/polyunsatured ratio but also to the presence of phenolic compounds with antioxidant action.

During storage, the phenolic compounds present in VOO could undergo oxidative degradation; for this reason, the molecules that appeared after oxidation are being investigated. Rovellini and Cortesi have proposed several oxidized forms derived from phenolic compounds of VOO exposed to light for 2 years (*8*). More recently, Ríos et al. (*9*) have collected individual oxidation products from an oxidized VOO sample (at 100 °C for 8 h under an air flow) by preparative high-performance liquid chromatography (HPLC) and determined the structures of these oxidized forms by gas chromatography (GC)−mass spectrometry (MS) after their conversion to trimethylsilyl ethers. However, oxidation conditions applied in these studies do not often reflect the real storage conditions of VOO. In addition, the results of the analytical methods used to evaluate natural antioxidants must be carefully interpreted depending on the conditions of oxidation (i.e., temperature or oxygen availability), as suggested by Frankel (*10*).

The extraction procedure of the phenolic fraction of VOO may offer several problems in the presence of their oxidation forms. For this reason, Armaforte et al. (*11*), comparing different methods usually employed to extract the phenolic fraction of VOO, proved that the solid phase extraction procedure (by means of diol phase) was not appropriate when VOOs contain significant amounts of polar oxidation products from phenols or lipids; in fact, these polar products could interfere with the retention mechanism of phenols during their extraction.

As shown by several authors (*11*−*15*), modifications due to hydrolysis/oxidation reactions during VOO storage or as consequence of heating treatments produce changes of the total antioxidant power of the phenolic fraction and, thus, of the oxidative stability of VOO. Five different kinds of reactions that involve phenols are generally described (*12*−*15*): (1) lysis of complex phenols, which increase the content of low molecular weight (MW) phenolics such as hydroxytyrosol (HYTY) and tyrosol (TY); (2) increase of the dialdehydic forms of decarboxymethyl oleuropein aglycon (DOA) and decarboxymethyl ligstroside aglycon (DLA); (3) hydrolysis of the acetic ester

*Corresponding authors [(M.J.L.-G.) telephone +34963544334, fax +34963544436, e-mail m.jesus.lerma@uv.es; (L.C.) telephone +390-547338121, fax +390547382348, e-mail lorenzo.cerretani@unibo.it].

 Published on Web 08/14/2009

occurring for HYTY; (4) cleavage of elenolic acid (EA) with loss of the carboxymethyl moiety and conversion of the monoaldehyde form to its dialdehyde form; and (5) appearance of oxidation products of phenolics (especially the oxidized derivatives of dialdehyde forms of DOA and DLA).

In particular, several authors have studied the presence of the closed aldehydic form of oleuropein aglycon (OA) and the open dialdehydic form of DOA by NMR (*16*, *17*), LC-MS (*8*, *9*, *18*), and GC-MS (*9*, *19*, *20*). The analogous forms for ligstroside aglycon (LA) have been also suggested (*8*, *9*, *20*). Rovellini et al. (*8*) have confirmed the presence of the dialdehydic open structures of the OA and LA without the loss of the carboxymethyl group by exposing a monovarietal Coratina extra VOO to light for 2 years and evaluating its phenolic extract by means of HPLC-MS equipped with both electrospray ionization (ESI) and atmospheric pressure chemical ionization (APCI) sources.

These authors (*8*) proposed that the ratio between aldehydic (due to enzymatic natural reaction) and dialdehydic (due to hydrolytic chemical reaction) forms of secoiridoids and their oxidized derivatives could be used to evaluate the incidence of technological/storage processes. Moreover, they identified the major oxidized derivatives of secoiridoid molecules, underscoring that, for this type of analysis, the ESI source in the positive-ion mode was better than the APCI, due to the capacity of ESI to form adduct ions, which gave more diagnostic information. However, and as far as we are concerned, no research has monitored the evolution of oxidized phenolic compounds during storage treatment.

The objective of this work is to study the chemical changes produced in an extra VOO sample in the presence and absence of its phenolic fraction during storage. For this purpose, an accelerated storage treatment at 60 °C for up to 7 weeks was performed. Modifications in phenol content, as well as changes in several quality parameters [free acidity, peroxide value (PV), UV absorbance, fatty acid (FA) composition, oxidative stability index (OSI), and tocopherol content] were studied. In addition, phenol transformation during the accelerated storage treatment in extra VOO samples with phenolic fraction was also studied.

MATERIALS AND METHODS

Reagents. The following reagents were used: sodium hydroxide (NaOH), sodium chloride (NaCl), potassium hydroxide (Carlo Erba, Milan, Italy); *n*-hexane, methanol, diethyl ether, α-tocopherol, apigenin (API), luteolin (LUT) (Sigma-Aldrich, St. Louis, MO); chloroform, acetonitrile (ACN), hydrochloric acid (HCl), anhydrous sodium sulfate, formic acid, ethanol, phenolphthalein, sodium thiosulfate, starch indicator (Merck, Darmstadt, Germany); iso-octane, potassium iodide, 3,4-dihydroxyphenylacetic acid (3,4-DHPAA), and acetic acid (Fluka, Buchs, Switzerland).

Instruments. HPLC analyses were performed with an 1100 series liquid chromatograph (Agilent Technologies, Palo Alto, CA) provided with a binary pump delivery system, a degasser, an autosampler, and a diode array UV−Vis detector (DAD). The liquid chromatograph was also coupled (in series with the DAD) to the ESI source of an HP 1100 series quadrupole mass spectrometer (MS) (Agilent). Phenol separation was carried out with a reverse phase C18 Luna column (5 μm, 25 cm × 3 mm i.d., Phenomenex, Torrance, CA), with a C18 precolumn (Phenomenex), whereas tocopherol separation was performed using a CN Luna 100A column (5 μm, 15 cm × 4.6 mm i.d., Phenomenex).

Fatty acid (FA) composition of samples was established by capillary GC employing a fused silica capillary column BPX70 (50 m × 0.22 mm i.d., 0.25 μm film thickness) from SGE Forte (Palo Alto, CA) that was fitted on a Clarus 500 gas chromatograph from Perkin-Elmer (Waltham, MA) equipped with a flame ionization detector (FID).

The oxidative stability of samples was evaluated by the OSI, using an eight-channel oxidative stability instrument (Omnion, Decatur, IL).

Sample Preparation. An extra VOO sample from the olive fruit variety Brugnola (picked on October 2008 at San Marino) was used. The olives were processed using an Oliomio 150 extraction machine (Tem, Tavernelle Val di Pesa, Florence, Italy) to obtain extra VOO sample. Samples oxidation was evaluated on two aliquots of the oil sample: extra VOO with phenols (EVOO) and extra VOO without phenols (EVOOP). Phenolic compounds were removed from EVOO according to the procedure described by Bonoli-Carbognin et al. (*21*). Briefly, 35 g of EVOO was washed with several aliquots of 0.5 M NaOH (4 × 15 mL). To eliminate the aqueous phase, the mixture was centrifuged (1000*g*, 5 min) after each washing. Combined olive oil fractions were then washed with 0.5 M HCl (2 × 10 mL) and saturated NaCl solution (5 × 10 mL), centrifuged at 1000*g* for 5 min, dried with anhydrous sodium sulfate, and finally filtered under vacuum. Dried EVOOP was then obtained.

Storage Treatment. According to several authors (*21*−*23*), both samples, EVOO and EVOOP, were divided in eight aliquots each (250 mL, 228.8 g) and kept in the dark at 60 °C for up to 7 weeks. Each aliquot was stored in an individual open glass bottle of 300 mL (i.d. = 6 cm; surface area exposed to the air = 28.3 cm^2). Two bottles, one of EVOO and the other of EVOOP, were removed every week from the oven and then analyzed. Triplicate analyses were carried out for each analytical determination at each storage time on both EVOO and EVOOP samples.

Quality Parameters. The chemical parameters measured were free acidity (free fatty acid content of the oil expressed as the percentage of oleic acid), PV (amount of hydroperoxides expressed as mequiv of O_2 kg^{-1}), and UV absorbance at 232 and 270 nm (k_{232} and k_{270}, which provide a measurement of the state of oxidation of the oils). These analyses were performed according to the official methods of the European Commission (*24*).

FA composition has been also established according to the method of Bendini et al. (*22*). The methyl esters of FAs were obtained after a cold basic transmethylation procedure and then analyzed by GC-FID. The results were expressed as percentage of saturated, monounsaturated, and polyunsaturated. The ratio of oleic/linoleic acids was also calculated.

Oxidative Stability. A stream of purified air (120 mL min^{-1} air flow rate) was passed through a 5 g oil sample, and the effluent air for the oil sample was then bubbled through a vessel containing deionized water. The effluent air contains especially volatile organic acids as formic acid and other volatile compounds formed during thermal oxidation of the oil, which increased the conductivity of the water. The temperature at which this test was carried out was 110 °C. The OSI (or OSI time) was expressed in hours.

Liquid−Liquid Extraction (LLE) of Phenolic Compounds from EVOO and EVOOP. The LLE procedure was adapted from that of Carrasco-Pancorbo et al. (*14*). Briefly, 50 g of oil containing 200 μL of 3,4-DHPAA (1000 mg L^{-1}, used as internal standard to evaluate the extraction recovery) were dissolved in 50 mL of *n*-hexane, and the solution was extracted successively with four 20 mL portions of methanol/water (60:40, v/v). The combined extracts of the hydrophilic layer were brought to dryness in a rotary evaporator under pressure at 40 °C. Finally, the residue was redissolved in 1 mL of methanol/water (50:50, v/v) and filtered through a 0.45 μm filter.

Tocopherol Extraction. One gram of oil sample was dissolved in 10 mL of *n*-hexane, these extracts being filtered through a 0.45 μm nylon filter.

HPLC Analysis. *Phenolic Compounds.* Mobile phases were prepared by mixing water containing 0.5% formic acid and ACN. A gradient elution was performed according to the conditions described by Carrasco-Pancorbo et al. (*14*). UV−Vis detection was set at 240, 280, and 330 nm. In all cases, 10 μL was injected, the flow rate being 0.5 mL min^{-1}. The MS working conditions were as follows: ESI interface; nebulizer gas pressure, 50 psi; drying gas flow, 9 L min^{-1} at 350 °C; capillary voltage, 3 kV. Nitrogen was used as nebulizer and drying gas. The MS scanned within the m/z 50−800 range in the positive-ion mode. The calibration curves were constructed with standard solutions of 3,4-DHPAA to quantify compounds detected at 280 (r^2 = 0.999) and 240 nm (r^2 = 0.998) and API (r^2 = 0.995) and LUT (r^2 = 0.988) to quantify these compounds at 330 nm. Results are given in milligrams per kilogram of oil.

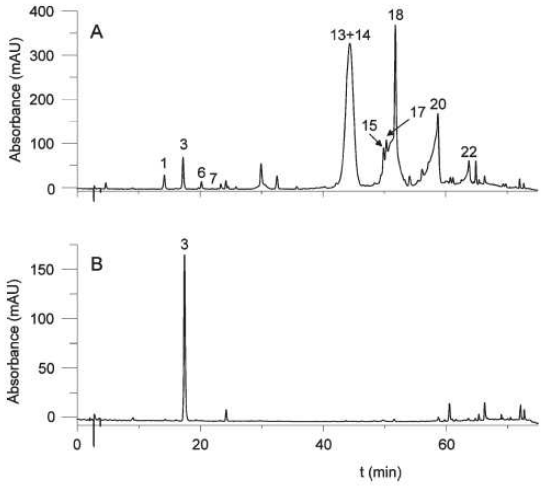

Figure 1. UV chromatograms of (**A**) EVOO and (**B**) EVOOP samples at t_0. Peaks: 1, HYTY; 3, 3,4-DHPAA; 6, unknown; 7, unknown; 13, OxDOA; 14, DOA; 15, OxDLA; 17, DLA; 18, AcPIN; 20, OA; 22, LA. Detection wavelength was 280 nm.

Tocopherols. α-, β-, and γ-tocopherols were determined using isocratic conditions with *n*-hexane/dichloromethane (95:5, v/v). UV−Vis detection was performed at 295 nm. In all cases, 10 μL was injected, the flow rate being 1.0 mL min^{-1}. Analyses were carried out at room temperature. The total run time was 10 min. The calibration curves were constructed with standard solutions of α-tocopherol ($r^2 = 0.999$) and used for quantification. Results are given in milligrams of α-tocopherol per kilogram of oil.

Statistical Analysis. Means and standard deviations were calculated with SPSS (version 15.0, SPSS Inc., Chicago, IL) statistical software. SPSS was used to perform one-way analysis of variance and Tukey's honest significant difference test at a 95% confidence level ($p < 0.05$) to identify differences in the samples at different storage times. A Student *t* test ($p < 0.05$) was also used to identify differences between samples for the same parameter at each storage time.

RESULTS AND DISCUSSION

Evaluation of the Differences Observed between EVOO and EVOOP Samples during the Accelerated Storage Treatment. Phenolic fractions of EVOO and EVOOP were first analyzed to verify the efficiency of phenolic compound stripping. Considering the sum of all quantified phenolic compound (22 individual phenols), a concentration of 164 mg kg^{-1} oil is obtained in EVOO sample at storage time zero (t_0), being the concentration of EVOOP sample of 0.70 mg kg^{-1} oil at the same storage time. Then, a decrease of 99.6% in phenol content was obtained (see **Figure 1**). A similar effect has been previously observed by Bonoli-Carbognin et al. (*21*).

Differences produced in the chemical parameters of the EVOO and EVOOP samples at t_0 have been also studied. As reported in **Table 1**, the free acidity percentage of EVOO and EVOOP ranged from 0.24 to 0.18%, respectively, whereas the PV varied from 11.96 to 12.44 mequiv O_2 kg^{-1} of oil. All of these values were below the limits set by EC regulation for extra VOO (*24*).

The FA composition of both samples at t_0 is also reported in **Table 1**. EVOO and EVOOP showed very similar values in terms of FA composition, which demonstrated that the phenol-removing procedure did not affect this fraction. Both samples were also characterized by high values of MUFA and oleic/linoleic acid ratio, as expected. The high oleic content of both samples was reported to give a large contribution to the oxidative stability of this oil (*25*).

Table 1. Chemical Parameters of the EVOO and EVOOP Samples at Storage Time Zero

parameter	EVOO	EVOOP
free acidity (%)	0.24	0.18
PV (mequiv of O_2 kg^{-1})	11.96	12.44
oleic/linoleic acid	7.87	7.85
MUFA[a] (%)	73.80	73.75
PUFA[b] (%)	9.67	9.68
SFA[c] (%)	16.53	16.57

[a] Monounsaturated fatty acids. [b] Polyunsaturated fatty acids. [c] Saturated fatty acids.

Changes in the oxidative status of EVOO and EVOOP are shown in **Table 2** as conjugated dienes (k_{232}), trienes (k_{270}), and OSI time. The two oil samples at t_0 showed k_{232} and k_{270} values lower than the legal limit values established by EC regulation for the extra VOO category (*24*) (2.50 and 0.22, respectively). However, after 1 week of storage (t_1), both samples exceeded the limit for k_{232}, reaching values of 7.71 and 9.74 for EVOO and EVOOP, respectively, after 7 weeks (t_7) of storage. After 1 week of storage (t_1), only the EVOO sample exceeded the EC limit for k_{270}, but 7 days later (t_2), EVOOP also surpassed the legal value, reaching both after 7 weeks (t_7) of storage the final value of ~0.7. Similar trends were also found by Bendini et al. under comparable experimental conditions (*22*). With regard to OSI time, the EVOOP sample at t_0 showed a lower value than the EVOO sample, probably related to the different amounts of phenolic compounds. EVOOP exhibited a OSI value of about 10 h that could only be related to the FA composition of the oil (high oleic acid content, low amounts of polyunsaturated FA, and the high oleic/linoleic acid ratio), as previously reported (*25*). Both EVOO and EVOOP samples showed a significant decrease of oxidative stability (OSI time value) during the storage process, being more evident for EVOOP, confirming the role of the phenolic fraction in the oxidative stability of EVOO.

The tocopherol content for both EVOO and EVOOP samples is also shown in **Table 2**. At t_0, the two oil samples did not show significant differences in tocopherol content. Thus, the alkaline procedure used to wash polar phenols did not affect this lipophilic antioxidant fraction. Tocopherol content remained substantially unvaried for EVOO from t_0 to t_3; then, a strong decrease was observed until the end of the storage time. The constant loss of oxidative stability (**Table 2**) is probably related to the decrease of polar phenols, which during the first 3 weeks, may act as antioxidant molecules also protecting tocopherols against oxidation (*22*, *26*). On the other hand, tocopherols started to decrease after 2 weeks of storage for EVOOP, but at higher storage times an oscillating trend was evidenced. This trend could be explained by taking into account a synergic effect between α-tocopherol and phospholipids (*27*) and the formation of tocopherol oxidized derivatives. These last compounds could overlap with tocopherol peaks during HPLC elution, interfering in tocopherol determination and not allowing their correct quantification.

Phenolic Compound Transformation in EVOO Samples during the Accelerated Storage Treatment. Figures 2, **3**, and **4** report the UV chromatograms detected at 280, 240, and 330 nm, respectively, showing the 22 phenolic compounds at three times of the storage process (t_0, t_3, and t_7). In particular, at 280 nm (**Figure 2**), the decrease of DOA (peak 14), DLA (peak 17), and LA (peak 22), the disappearance of OA (peak 20), and the formation of their possible oxidized derivatives (peaks 13, 15, and 21 and traces of OxOA) are evident. **Figure 3** shows the trend of EA (peak 12) and the appearance of several hypothetical oxidized compounds

Table 2. Chemical Parameters for EVOO and EVOOP Samples at Different Storage Times[a]

	k_{232}		k_{270}		OSI time (h)		tocopherols (mg kg^{-1})	
storage time (weeks)	EVOO	EVOOP	EVOO	EVOOP	EVOO	EVOOP	EVOO	EVOOP
t_0	2.24 f	2.45 d	0.19 g*	0.16 f	33.65 a*	10.8 a	181.9 a	148.4 a
t_1	3.51 e	3.67 cd	0.24 f*	0.17 f	22.23 b*	9.03 b	191.1 a	170.6 a
t_2	4.52 d	5.43 bc	0.26 f	0.23 ef	19.20 c*	6.2 c	195.5 a*	140.8 a
t_3	5.42 c	6.43 b*	0.34 e	0.29 e	15.78 d*	3.8 d	181.9 a*	90.6 b
t_4	7.48 b	8.41 a	0.40 d	0.39 d	10.55 e*	1.3 e	139.6 b*	42.0 c
t_5	9.69 a*	8.48 a	0.51 c	0.47 c	7.288 f	0 f	85.48 c	46.9 c
t_6	7.48 b	8.93 a	0.59 b	0.59 b	5.83 g*	0 f	55.3 d	70.3 bc*
t_7	7.71 b	9.74 a*	0.68 a	0.67 a	3.438 h	0 f	25.9 e	97.2 b*

[a] Mean values ($n = 3$). Means followed by different letters in the same column are significantly different ($p < 0.05$). Means with an asterisk for the same parameter at each storage time are significantly different ($p < 0.05$).

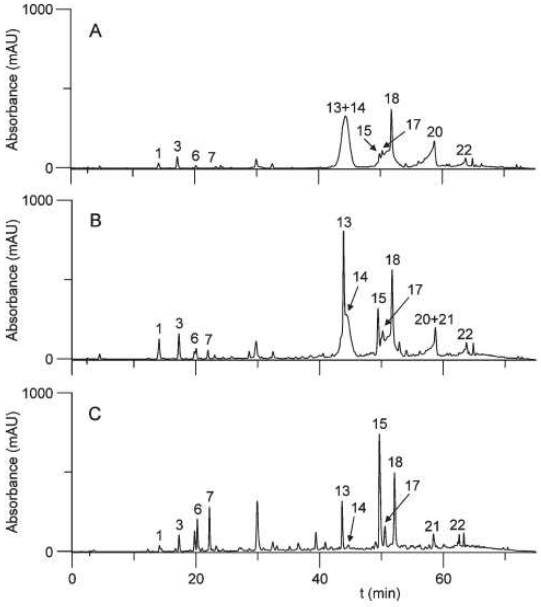

Figure 2. UV chromatograms showing the evolution of the EVOO phenolic profile after storage treatment at 60 °C: (**A**) t_0; (**B**) t_3; (**C**) t_7. Peaks: 21, OxLA; other peaks as in **Figure 1**. Detection wavelength was 280 nm.

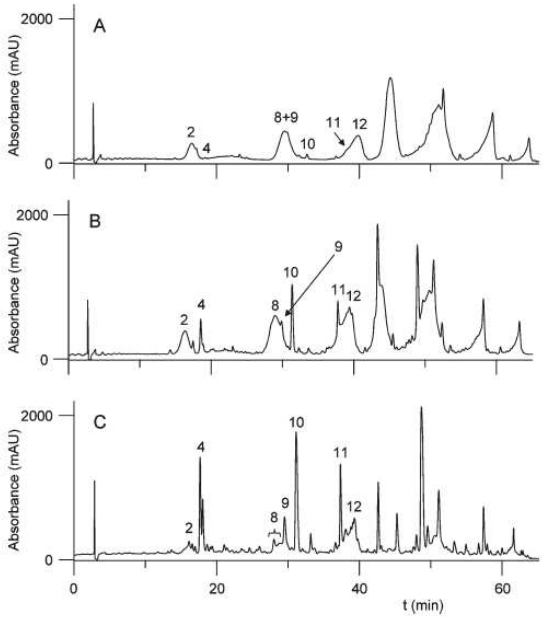

Figure 3. UV chromatograms showing the evolution of the EVOO phenolic profile after storage treatment at 60 °C: (**A**) t_0, (**B**) t_3; (**C**) t_7. Peaks: 2, DEA; 4, OxDEA; 8, unknown; 9, unknown; 10, unknown; 11, OxEA; 12, EA. Detection wavelength was 240 nm.

that absorb only at 240 nm (4, 9, 10, and 11). Finally, **Figure 4** shows the trend at 330 nm of the loss of LUT (peak 16) and the slightly decreased of API (peak 19) during storage.

A list of the main phenolic compounds studied in this work as well as their retention times, UV absorbance maxima, molecular weights, and MS fragmentation patterns is summarized in **Table 3**. From the information shown in this table it is possible to summarize some general concepts:

(1) The absorbing band near 240 nm is typical of a carboxymethyl enol-ether group. Thus, for example, EA (peak 12) is characterized by this band. On the other hand, the bands at 277 and 282 nm are due to a monohydroxyphenyl group and to an *o*-hydroxyphenyl group, respectively; so, for example, HYTY (peak 1) and secoiridoid derivatives containing HYTY [OxDOA (peak 13), DOA (peak 14), OxOA (tr), OA (peak 20), and the unknown peaks 3, 6, and 7] exhibit the second UV maximum near 280 nm, whereas the molecules having a monohydroxyphenyl group such as TY [OxDLA (peak 15), DLA (peak 17), OxLA (peak 21), and LA (peak 22)] show the second maximum near 277 nm.

(2) HYTY exhibits only the ion derived by the neutral loss of water, because the presence of a high initial percentage of water inhibits a good electrospray ionization of molecules such as HYTY and TY having acidic properties. As suggested by Rovellini et al. (*8*), it is not possible to reveal the pseudomolecular ion for HYTY due to its difficulty in giving protonated adducts.

(3) Some authors (*8*, *9*) have indicated that the oxidation of secoiridoid structures involves the acidic portion (EA) and not the aromatic alcoholic moiety (HYTY and TY); for this reason, the oxidized forms shown in **Table 3** maintain the UV specific absorbance of their nonoxidized forms.

(4) The oxidation involves the conversion of the aldehydic group of EA to carboxylic group (according to the scheme reported in **Figure 5**).

(5) The oxidized forms of secoiridoids, which are more polar than their respective nonoxidized derivatives, elute before them. In the case of the couple DEA−OxDEA (peaks 2 and 4 , respectively), the presence of a second carboxylic group in the molecule does not cause the anticipated elution.

(6) Under the ESI conditions applied in this study, both the oxidized and nonoxidized forms of secoiridoids are characterized by the presence of the sodium adduct $[M + Na]^+$, the loss of the phenolic group (m/z 241 and 225 for the oxidized and nonoxidized forms of secoiridoids, respectively; m/z 183 and 167 for the oxidized and nonoxidized forms of the decarboxymethyl structures of secoiridoids, respectively), and the loss of the acidic group (m/z 137 and m/z 121 for molecules having HYTY and TY, respectively), according to the scheme reported in **Figure 5**.

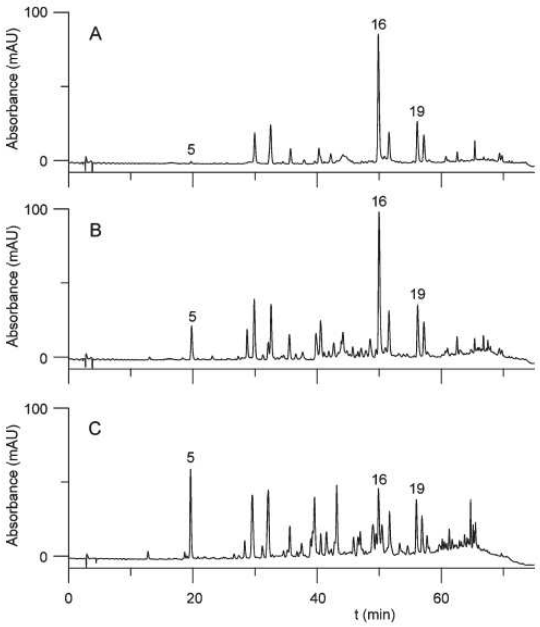

Figure 4. UV chromatograms showing the evolution of the EVOO phenolic profile after storage treatment at 60 °C: (**A**) t_0; (**B**) t_3; (**C**) t_7. Peaks: 5, unknown; 16, LUT; 19, API. Detection wavelength was 330 nm.

(7) The peaks related to the oxidized forms of secoiridoids are characterized by a narrower profile than for the molecules having one or two aldehydic groups.

Figure 6A shows the trend of the phenolic compounds of EVOO during the storage treatment. Area values were divided by 3,4-DHPAA area (to estimate the extraction recovery) and expressed as natural logarithm for a better evaluation of the different trends of disappearance of the phenolic compounds. Generally, a decrease of the more abundant compounds (secoiridoids) is observed. Peaks 21 and 22 were jointly evaluated: peak 21 appeared overlapped with peak 22 from t_3 to t_7. At t_7, only peak 21 was present. As previously observed at room temperature (*12*, *28*), transformations of secoiridoids to simpler compounds (for example, decarboxymethyl structures) followed by a further conversion to phenylethyl alcohols such as TY and HYTY occurred. In this work, TY was not found in EVOO sample at t_0, whereas HYTY, which was initially found at low concentrations, increased from t_0 to t_4. This tendency was also observed for oils stored at room temperature (*12*, *28*). Among lignans, in particular AcPIN (peak 18 of **Figure 2C**) slightly decreased, exhibiting a high content also at the end of storage process (t_7). This tendency for lignans has been also observed when oils were heated in a conventional or microwave oven (*14*, *29*).

The trend of the neoformation compounds during the storage treatment is shown in **Figure 6B** (area values were also divided by the 3,4-DHPAA area and expressed as natural logarithm). The most important neoformation compounds are peaks 4 (oxidation form of decarboxymethyl elenolic acid, OxDEA) and 15 (oxidized form of decarboxymethyl ligstroside aglycon, OxDLA),

Table 3. Retention Times, UV Absorbance Maxima, Molecular Weights (MW), and MS Fragmentation Patterns of the Phenolic Compounds

					major fragments ESI positive					
analyte	peak	t_r (min)	λ_{max} (nm)	MW	$[M + H]^+$	$[M + Na]^+$	$[M - H_2O + H]^+$	loss of phenolic group	loss of acidic group	other fragments
HYTY	1	11.6	232/280	154			137.1			
DEA	2	16.8	230	184	185.1	207.1				
unknown	3	18.0	232/280	260		283.2				299.0 $[M + K]^+$
OxDEA	4	18.5	236	200		223.1				123.1/165.0
unknown	5	20.0	290/310							338.4/321.8/191.1/185.8
unknown	6	20.1	232/280							177.0/235.1/668.1
unknown	7	22.0	232/280							113.1/157.1/349.2
unknown	8	29.5	234							297.1/239.1/221.1/181.1/165.1
unknown	9	30.4	234	336		359.0				375.1 $[M + K]^+$
unknown	10	36.1	240							237.1/197.1/165.1
OxEA	11	38.9	240	258	259.1	281.1				185.1/227.1/241.1 $[M - OH]^+$
EA	12	39.9	240	242	243.1	265.1				211.1 $[M - OCH_3]^+$
OxDOA	13	44.0	234/282	336	337.1	359.1		183.1	137.1	375.1 $[M + K]^+$
DOA	14	45.0	234/282	320		343.1			137.1	361.1
OxDLA	15	49.8	242/276	320		343.1		183.1	121.1	359.1 $[M + K]^+$
LUT	16	50.0	254/348	286	287.1	309.1				
DLA	17	51.5	236/276	304		327.1			121.1	
AcPIN	18	53.8	236/280	416	417.1	439.1				455.1 $[M + K]^+$/357 $[M - CH_3COOH + H]^+$/233 $[M - CH_3COOH - \text{phenylOCH}_3 + H]^+$
API	19	56.1	268/338	270	271.1					
OxOA	tr[a]	56.1	236/280	394	395.1	417.1		241.1	137.1	439.1
OA	20	58.7	236/282	378	379.1	401.1		225.1	137.1	419.1
OxLA	21	60.1	232/276	378	379.1	401.1		241.1	121.1	
LA	22	63.9	230/276	362	363.1	385.1		225.1	121.1	

[a] tr, trace.

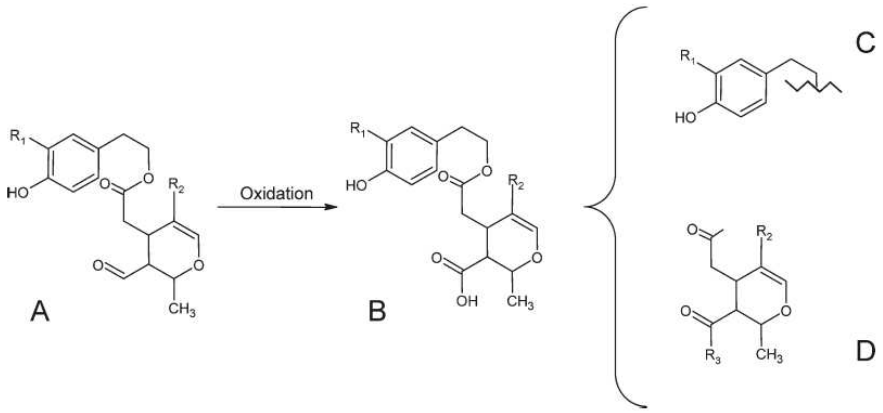

Figure 5. General scheme of storage treatment of secoiridoids: **A**, structure of secoiridoids [LA (R_1 = H and R_2 = −$COOCH_3$); OA (R_1 = OH and R_2 = −$COOCH_3$); DLA (R_1 = H and R_2 = −H); DOA (R_1 = OH and R_2 = −H)]; **B**, oxidized forms of secoiridoids [OxLA (R_1 = H and R_2 = −$COOCH_3$); OxOA (R_1 = OH and R_2 = −$COOCH_3$); OxDLA (R_1 = H and R_2 = −H); OxDOA (R_1 = OH and R_2 = −H)]; **C**, loss of acidic group during mass fragmentation (R_1 = H fragment with m/z = 121; R_1 = OH fragment with m/z = 137); **D**, loss of phenolic group during mass fragmentation (R_2 = −$COOCH_3$ and R_3 = OH fragment with m/z = 241; R_2 = −$COOCH_3$ and R_3 = H fragment with m/z = 225; R_2 = H and R_3 = OH fragment with m/z = 183; R_2 = H and R_3 = H fragment with m/z = 167).

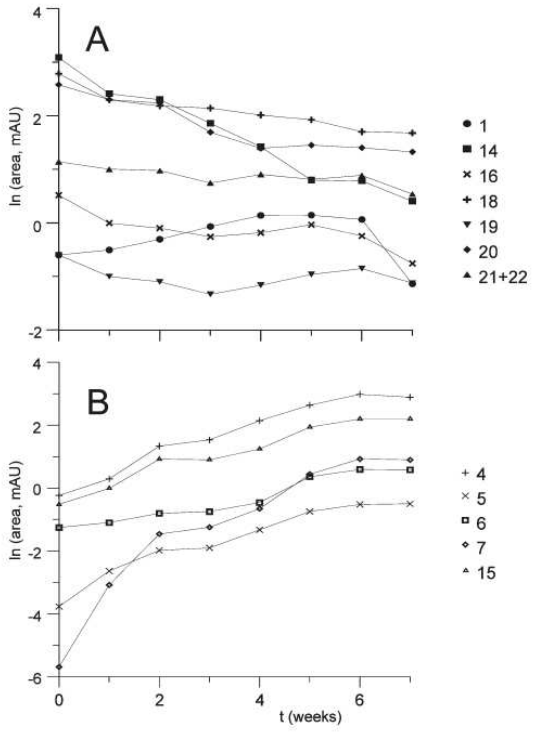

Figure 6. Plots showing the trends of phenolic (**A**) and neoformation compounds (**B**) during the storage treatment (from t_0 to t_7) of EVOO. Area values were divided by 3,4-DHPAA area (internal standard). Peak identification is as reported in **Table 3**.

respectively, followed by peaks 5, 6, and 7 (unknown peaks). Peak 13 (data not reported in **Figure 6B**) probably represents an oxidized secoiridoid compound, being tentatively assigned as an oxidized form of DOA (OxDOA).

In this work, the importance of the role of phenolic compounds in oil stability against oxidation has been demonstrated. The differences observed between EVOO and EVOOP samples enforced this agreement due to the different OSI values obtained that demonstrated a high contribution of polar phenolic compounds to oil shelf life.

In EVOO samples, a decrease of the major secoiridoids and the formation of some of their oxidized forms were observed during the storage treatment. For this reason, these latter compounds could be considered as potential markers of the loss of extra VOO freshness.

A next step of this work will be the investigation of the residual antioxidant activity (in vitro) of these oxidized derivatives, in particular OxDOA and OxOA, which could be of great interest due to the fact that these molecules appeared to maintain unchanged the *o*-hydroxyphenyl part of the original molecular structure. Another challenge will be the identification of other peaks observed but still not identified using other techniques such as TOF-MS or NMR.

ABBREVIATIONS USED

3,4-DHPAA, 3,4-dihydroxyphenylacetic acid; AcPIN, (+)-1-acetoxypinoresinol; API, apigenin; APCI, atmospheric pressure chemical ionization; DEA, decarboxymethylated form of elenolic acid; DLA, decarboxymethyl ligstroside aglycon; DOA, decarboxymethyl oleuropein aglycon; EA, elenolic acid; ESI, electrospray ionization; EVOO, extra virgin olive oil sample with phenols; EVOOP, extra virgin olive oil sample without phenols; FA, fatty acid; FID, flame ionization detector; HYTY, hydroxytyrosol; LA, ligstroside aglycon; LUT, luteolin; MUFA, monounsaturated fatty acid; MW, molecular weight; OA, oleuropein aglycon; OxDEA, oxidized form of decarboxymethyl elenolic acid; OxDLA, oxidized form of decarboxymethyl ligstroside aglycon; OxDOA, oxidized form of decarboxymethyl oleuropein aglycon; OxLA, oxidized form of ligstroside aglycon; OxOA, oxidized form of oleuropein aglycon; OSI, oxidative stability index; OxEA, oxidized form of elenolic acid; PUFA, polyunsaturated fatty acid; PV, peroxide value; SFA, saturated fatty acid; TY, tyrosol; VOO, virgin olive oil.

LITERATURE CITED

(1) Wahrburg, U.; Kratz, M.; Cullen, P. Mediterranean diet, olive oil and health. *Eur. J. Lipid Sci. Technol.* **2002**, *104*, 698–705.

(2) Pellegrini, N.; Serafini, M.; Colombi, B.; Del Rio, D.; Salvatore, S.; Bianchi, M. Total antioxidant capacity of plant foods, beverages and oils consumed in Italy assessed by three different in vitro assays. *J. Nutr.* **2003**, *133*, 2812–2819.

(3) Beauchamp, G. K.; Keast, R. S. J.; Morel, D.; Lin, J.; Pika, J.; Han, Q.; Lee, C.; Smith, A. B.; Breslin, P. A. S. Ibuprofen-like activity in extra-virgin olive oil. *Nature* **2005**, *437*, 45–46.

(4) Bendini, A.; Cerretani, L.; Carrasco-Pancorbo, A.; Gómez-Caravaca, A. M.; Segura-Carretero, A.; Fernández-Gutiérrez, A.; Lercker, G. Phenolic molecules in virgin olive oils: a survey of their sensory properties, health effects, antioxidant activity and analytical methods. An overview of the last decade. *Molecules* **2007**, *12*, 1679–1719.

(5) Andrewes, P.; Busch, J. L. H. C.; De Joode, T.; Groenewegen, A.; Alexandre, H. Sensory properties of virgin olive oil polyphenols: identification of deacetoxy-ligstroside aglycon as a key contributor to pungency. *J. Agric. Food Chem.* **2003**, *51*, 1415–1420.

(6) Gutierrez-Rosales, F.; Rios, J. J.; Gomez-Rey, M. A. L. Main polyphenols in the bitter taste of virgin olive oil. Structural confirmation by on-line high-performance liquid chromatography electrospray ionization mass spectrometry. *J. Agric. Food Chem.* **2003**, *51*, 6021–6025.

(7) Cerretani, L.; Salvador, M. D.; Bendini, A.; Fregapane, G. Relationship between sensory evaluation performed by Italian and Spanish official panels and volatile and phenolic profiles of virgin olive oils. *Chemosens. Percept.* **2008**, *1*, 258–267.

(8) Rovellini, P.; Cortesi, N. Liquid chromatography−mass spectrometry in the study of oleuropein and ligstroside aglycons in virgin olive oils: aldehydic, dialdehydic forms and their oxidized products. *Riv. Ital. Sostanze Grasse* **2002**, *69*, 1–14.

(9) Ríos, J. J.; Gil, M. J.; Gutiérrez-Rosales, F. Solid-phase extraction gas chromatography−ion trap−mass spectrometry qualitative method for evaluation of phenolic compounds in virgin olive oil and structural confirmation of oleuropein and ligstroside aglycons and their oxidation products. *J. Chromatogr., A* **2005**, *1093*, 167–176.

(10) Frankel, E. N. Search of better methods to evaluate natural antioxidants and oxidative stability in food lipids. *Trends Food Sci. Technol.* **1993**, *4*, 220–225.

(11) Armaforte, E.; Mancebo-Campos, V.; Bendini, A.; Salvador, M. D.; Fregapane, G.; Cerretani, L. Retention effects of oxidized polyphenols during analytical extraction of phenolic compounds of virgin olive oil. *J. Sep. Sci.* **2007**, *30*, 2401–2406.

(12) Boselli, E.; Di Lecce, G.; Strabbioli, R.; Pieralisi, G.; Frega, N. G. Are virgin olive oils obtained below 27 °C better than those produced at higher temperatures? *LWT−Food Sci. Technol.* **2009**, *42*, 748–757.

(13) Brenes, M.; García, A.; García, P.; Garrido, A. Acid hydrolysis of secoiridoid aglycons during storage of virgin olive oil. *J. Agric. Food Chem.* **2001**, *49*, 5609–5614.

(14) Carrasco-Pancorbo, A.; Cerretani, L.; Bendini, A.; Segura-Carretero, A.; Lercker, G.; Fernández-Gutiérrez, A. Evaluation of the influence of thermal oxidation in the phenolic composition and in antioxidant activity of extra-virgin olive oils. *J. Agric. Food Chem.* **2007**, *55*, 4771–4780.

(15) Servili, M.; Baldioli, M.; Mariotti, F.; Montedoro, G. F. Phenolic composition of olive fruit and virgin olive oil: distribution in the constituents parts of fruit and evolution during the oil mechanical extraction process. *Acta Hortic.* **1999**, *474*, 609–613.

(16) Montedoro, G.; Servili, M.; Baldioli, M.; Selvaggini, R.; Miniati, E.; Macchioni, A. Simple and hydrolyzable compounds in virgin olive oil. 3. Spectroscopic characterizations of the secoiridoid derivatives. *J. Agric. Food Chem.* **1993**, *41*, 2228–2234.

(17) Christophoridou, S.; Dais, P.; Tseng, L. I.-H.; Spraul, M. Separation and identification of phenolic compounds in olive oil by coupling high-performance liquid chromatography with postcolumn solid-phase extraction to nuclear magnetic resonance spectroscopy (LC-SPE-NMR). *J. Agric. Food Chem.* **2005**, *53*, 4667–4679.

(18) Cortesi, N.; Azzolini, M.; Rovellini, P.; Fedeli, E. Minor polar components of virgin olive oils: a hypothetical structure by LC-MS. *Riv. Ital. Sostanze Grasse* **1995**, *72*, 241−251 (English abstract available).

(19) Angerosa, F.; d'Alessandro, N.; Corana, F.; Mellerio, G. Characterization of phenolic and secoiridoid aglycons present in virgin olive oil by gas chromatography-chemical ionization mass spectrometry. *J. Chromatogr., A* **1996**, *736*, 195–203.

(20) Boselli, E.; Di Lecce, G.; Minardi, M.; Pacetti, D.; Frega, N. G. Mass spectrometry in the analysis of polar minor components in virgin olive oil. *Riv. Ital. Sostanze Grasse* **2007**, *84*, 3−14 (English abstract available).

(21) Bonoli-Carbognin, M.; Cerretani, L.; Bendini, A.; Almajano, M. P.; Gordon, M. H. Bovine serum albumin produces a synergistic increase in the antioxidant activity of virgin olive oil phenolic compounds in oil-in-water emulsions. *J. Agric. Food Chem.* **2008**, *56*, 7076–7081.

(22) Bendini, A.; Cerretani, L.; Vecchi, S.; Carrasco-Pancorbo, A.; Lercker, G. Protective effects of extra virgin olive oil phenolics on oxidative stability in the presence or absence of copper ions. *J. Agric. Food Chem.* **2006**, *54*, 4880–4887.

(23) Lerma-García, M. J.; Simó-Alfonso, E. F.; Bendini, A.; Cerretani, L. Metal oxide semiconductor sensors for monitoring of oxidative status evolution and sensory analysis of virgin olive oils with different phenolic content. *Food Chem.* **2009**, *117*, 608–614.

(24) European Community, Commission Regulation 1989/2003 of 6 November 2003 amending Regulation No. 2568/91 on the characteristics of olive oil and olive-residue oil and on the relevant methods of analysis. *Off. J. Eur. Communities* **2003**, *L295*, 57−77.

(25) Aparicio, R.; Roda, L.; Albi, M. A.; Gutiérrez, F. Effect of various compounds on virgin olive oil stability measured by rancimat. *J. Agric. Food Chem.* **1999**, *47*, 4150–4155.

(26) Baldioli, M.; Servili, M.; Perretti, G.; Montedoro, G. F. Antioxidant activity of tocopherols and phenolic compounds of virgin olive oil. *J. Am. Oil Chem. Soc.* **1996**, *73*, 1589–1593.

(27) Bandarraa, N. M.; Campos, R. M.; Batista, I.; Nunes, M. L.; Empis, J. M. Antioxidant synergy of α-tocopherol and phospholipids. *J. Am. Oil Chem. Soc.* **1999**, *76*, 905–913.

(28) Di Lecce, G.; Bendini, A.; Cerretani, L.; Bonoli-Carbognin, M.; Lercker, G. Shelf stability of extra virgin olive oil under domestic conditions. *Ind. Aliment.−Italy* **2006**, *461*, 873–880.

(29) Cerretani, L.; Bendini, A.; Rodriguez-Estrada, M. T.; Vittadini, E.; Chiavaro, E. Microwave heating of different commercial categories of olive oil: Part I. Effect on chemical oxidative stability indices and phenolic compounds. *Food Chem.* **2009**, *115*, 1381–1388.

Received April 23, 2009. Revised manuscript received July 10, 2009. Accepted July 27, 2009. Project CTQ2007-61445 (MEC and FEDER funds) is acknowledged. M.J.L.-G. thanks the Generalitat Valenciana for an FPI grant for Ph.D. studies and for a grant to study in a foreign institution.

ANEXO XVII

Anal Bioanal Chem (2009) 395:1543–1550
DOI 10.1007/s00216-009-3129-6

ORIGINAL PAPER

Evaluation of the oxidative status of virgin olive oils with different phenolic content by direct infusion atmospheric pressure chemical ionization mass spectrometry

M. J. Lerma-García · J. M. Herrero-Martínez · E. F. Simó-Alfonso · G. Lercker · L. Cerretani

Received: 7 July 2009 / Revised: 29 August 2009 / Accepted: 31 August 2009 / Published online: 17 September 2009

Abstract Atmospheric pressure chemical ionization mass spectrometry was used to predict the oxidative status of virgin olive oils (VOO) during their storage. VOO samples, with and without phenolic compounds, were stored in the dark at 60 °C up to 7 weeks. The VOO samples were diluted in an alkaline propanol/methanol mixture and directly infused into an ion-trap mass spectrometer. The abundances of the $[M-H]^-$ peaks of free fatty acids, oxidized fatty acids, tocopherols and phenolic compounds, jointly with their oxidized forms, were measured and used as predictors. Two linear discriminant analysis (LDA) models were constructed in order to classify samples according to their oxidative levels. The first model was constructed using both VOO samples (with and without phenols), considering as predictors only fatty acids and their oxidized products. The second LDA model was constructed with the VOO sample with phenolic compounds considering as predictors all the peaks measured. In both models, the samples divided in the eight different storage times were correctly classified (100%) by leave-one-out cross-validation with an excellent resolution among all the category pairs (for the first model Wilks' lambda, λ_w=0.229 and for the second λ_w=0.928). This method is a very fast tool for on-line monitoring of VOO oxidation status.

M. J. Lerma-García · J. M. Herrero-Martínez · E. F. Simó-Alfonso (✉)
Departamento de Química Analítica, Universidad de Valencia, C. Doctor Moliner 50, 46100 Burjassot, Valencia, Spain
e-mail: ernesto.simo@uv.es

G. Lercker · L. Cerretani (✉)
Dipartimento di Scienze degli Alimenti, Università di Bologna, P. zza Goidanich 60, 47521 Cesena, FC, Italy
e-mail: lorenzo.cerretani@unibo.it

Keywords Direct infusion · Linear discriminant analysis · Lipid oxidation · Mass spectrometry · Oxidative status

Introduction

Autoxidation and photosensitized oxidation of lipids occurs by the interaction of the fatty acids of the triacylglycerols with triplet oxygen and singlet oxygen, respectively. However, because the activation energy of this reaction is high, the initiation of lipid oxidation is due mostly to the decomposition of hydroperoxides catalyzed by the presence of traces of transition metals or by exposure to light, being accelerated by an increase of temperature [1]. The unstable hydroperoxides decompose due to diverse factors, such as their quantitative presence, the interaction with free fatty acids [2], the unsaturation degree [3–5], and the storage conditions, producing a range of volatile and non volatile products. These products, mainly the aldehydes, are the major cause of the sensory perception of the rancid defect in edible oils [6]. Therefore, in the course of the autoxidation reaction a series of compounds are formed in edible oils, whereas minor components are degraded, causing rancidity and off-flavors, loss of nutritional value and finally consumer rejection for higher appreciated product (such as extra virgin olive oils, also called EVOO). This is evident from the fact that for several decades the participation of reactive oxygen species and/or free radicals in neurodegeneration has been suggested for each disease, whereas more recently, the participation of apoptosis has also received considerable attention [7, 8]. EVOO is particularly appreciated for its high stability with respect to other vegetable oils, due to their high content in monounsaturated fatty acids and to the presence of phenolic compounds [3]. Oil oxidation transforms essential fatty

Table 1 Chemical parameters of EV1 and EV2 samples at storage time zero

Parameter	EV1	EV2
Free acidity (%)	0.24[a]	0.18[a]
k_{232}	2.23[a]	2.45[a]
k_{270}	0.19[a]	0.16[a]
OSI time (h)	33.65[a]	10.80[b]
Myristic acid (%)	0.01[a]	0.01[a]
Palmitic acid (%)	13.07[a]	13.10[a]
Palmitoleic acid (%)	0.60[a]	0.60[a]
Stearic acid (%)	2.46[a]	2.46[a]
Oleic acid (%)	72.88[a]	72.83[a]
Linoleic acid (%)	9.26[a]	9.28[a]
Linolenic acid (%)	0.41[a]	0.41[a]

Means with different superscript letters for the same raw are significantly different (Tukey's HSD test, $p<0.05$)

acids and produces different types of compounds, such as volatile compounds, oxidized polymers, and molecules that have a similar parent structure with respect to the starting molecules (i.e., oxidized fatty acids called also OFAs) [1]. It should be noted that all these different compounds produced during oxidation represent secondary oxidation products, while the formation of oxidation products during oxidation reactions depend on the fatty acid composition of oils and the oxidation conditions [4, 5]. Different approaches have been attempted to find a reliable oxidation index that, combined with evaluation of primary oxidation products, would provide a realistic idea about the oxidation status of the fatty matrix [9]. The indices of secondary oxidation more widely applied to fat and vegetable oils are *p*-anisidine value, thiobarbituric acid reactive substances [10], content of hexanal or nonanal or their ratio [10, 11], measurement of total polar compounds [12, 13] and more recently OFA content determined by HPLC [14]. Other indices that consider the phenol content obtained by rapid electrochemical methods [15, 16] have been also used. During the last few years, direct infusion mass spectrometry (DIMS) methods combined with statistical analysis have been widely applied in the olive oil sector due to the ability of these techniques to fast acquire mass spectra and abundance of target compounds [17–20].

In this work, an atmospheric pressure chemical ionization (APCI)-DIMS method, jointly with the application of linear discriminant analysis (LDA), is used to evaluate different oxidative status of virgin olive oils (VOOs). In particular, eight levels of oxidized oils with and without phenolic compounds were used to construct LDA models. These models were based on the abundances of the $[M-H]^-$ peaks of free fatty acids, OFAs, tocopherols, and phenolic compounds, jointly with their oxidized forms.

Experimental

Reagents

The following reagents were used: sodium hydroxide (NaOH), sodium chloride (NaCl), potassium hydroxide (Carlo Erba, Milan, Italy), *n*-hexane, methanol (MeOH), diethyl ether (Sigma-Aldrich, St. Louis, MO, USA), *n*-propanol (PrOH; Scharlau, Barcelona, Spain), ammonia (NH_3, Panreac, Barcelona, Spain), hydrochloric acid (HCl), anhydrous sodium sulfate, ethanol, phenolphthalein, and iso-octane (Fluka, Buchs, Switzerland).

Instruments

Fatty acid (FA) composition of samples was established by capillary GC employing a fused silica capillary column BPX70 (50 m×0.22 mm i.d, 0.25 μm F.T) from SGE Forte (Palo Alto, CA, USA) that was fitted on a Clarus 500 gas chromatograph from Perkin-Elmer (Waltham, MA, USA) equipped with a flame ionization detector (FID).

The oxidative stability of samples was evaluated by the oxidized stability index (OSI), using an eight-channel oxidative stability instrument (Omnion, Decatur, IL, USA).

DIMS was performed on an HP 1100 series ion-trap mass spectrometer provided with an APCI ion source (Agilent Technologies, Waldbronn, Germany). A syringe pump (kdScientific, Holliston, MA, USA) was used to infuse the samples at 0.3 mL h^{-1} (5 μL min^{-1}) through a 50-μm i.d. PEEK tube. The MS working conditions, adapted from Lerma-García et al. [18], were: nebulizer gas pressure, 25 psi; drying gas flow, 5 L min^{-1} at 200 °C;

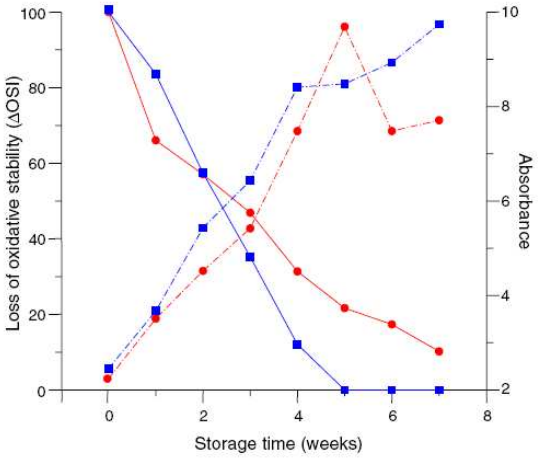

Fig. 1 Changes in oxidized stability index (*continuous line*) and in the conjugated diene contents (*dotted line*) of the EV1 (*filled circle*) and EV2 (*filled square*) samples during storage at 60 °C

Table 2 $[M-H]^-$ peaks of the selected fatty acids and antioxidant compounds

Peak no.	Compound (acronym)	$[M-H]^-$
Fatty acids		
1	Myristic acid (C14:0)	227
2	Palmitoleic acid (C16:1)	253
3	Palmitic acid (C16:0)	255
4	Linolenic acid (C18:3)	277
5	Linoleic acid (C18:2)	279
6	Oleic acid (C18:1)	281
7	Stearic acid (C18:0)	283
Oxidized fatty acids		
8	Keto-linolenic acid	291
9	Keto-linoleic acid	293
10	Hydroxy-linoleic acid	295
11	Keto-oleic acid	295
12	Hydroxy-oleic acid	297
Phenolic and tocopherol compounds		
13	Tyrosol (TY)	137
14	Hydroxytyrosol (HYTY)	153
15	Dialdehydic form of elenolic acid (DEA)	183
16	Elenolic acid (EA)	241
17	Apigenin (API)	269
18	Luteolin (LUT)	285
19	Decarboxymethyl ligstroside aglycone (DLA)	303
20	Decarboxymethyl oleuropein aglycone (DOA)	319
21	Ligstroside aglycone (LA)	361
22	Oleuropein aglycone (OA)	377
23	1-Acetoxypinoresinol (AcPIN)	415
24	α-Tocopherol	429
Oxidized phenols		
25	Oxidized form of DEA (OxDEA)	199
26	Oxidized form of EA (OxEA)	257
27	Oxidized form of DLA (OxDLA)	319
28	Oxidized form of DOA (OxDOA)	335
29	Oxidized form of LA (OxLA)	377
30	Oxidized form of OA (OxOA)	393

vaporizer temperature, 400 °C; capillary voltage, 2.6 kV; voltages of skimmers 1 and 2, −41.5 V and −7.6 V, respectively. Nitrogen was used as nebulizer and drying gas (Gaslab NG LCMS 20 generator, Equcien, Madrid, Spain). The mass spectrometer was scanned within the *m/z* 100-800 range in the negative-ion mode. The ion-trap target mass was set at *m/z* 281 ($[M-H]^-$ peak of oleic acid). Maximum loading of the ion trap was 3×10^4 counts, and maximum collection time was 300 ms. In all cases, data were averaged for 1 min.

Sample preparation and oxidation process

An EVOO sample from the olive fruit variety Brugnola produced at San Marino (picked on October 03, 2008) was used for the oxidative status evaluation. The olives were processed using an Oliomio 150 extraction machine (Tem, Tavernelle Val di Pesa, Florence, Italy) in order to obtain an EVOO. For evaluation of EVOO oxidation, the oil sample was divided in two aliquots: the oil without treatment (EV1) and the same oil without phenols (EV2). Phenolic compounds were removed from the oil according to the procedure described by Bonoli-Carbognin et al. [21]. Briefly, 35 g oil were washed with several aliquots of 0.5 M NaOH (4×15 mL). To eliminate the aqueous phase, the mixture was centrifuged (1,000×*g*, 5 min) after each washing. Combined olive oil fractions were then washed with 0.5 M HCl (2×10 mL) and saturated NaCl solution (5×10 mL), centrifuged at 1,000×*g* for 5 min, dried with anhydrous sodium sulfate and finally filtered under vacuum. Dried olive oil free of phenolic compounds (EV2) was

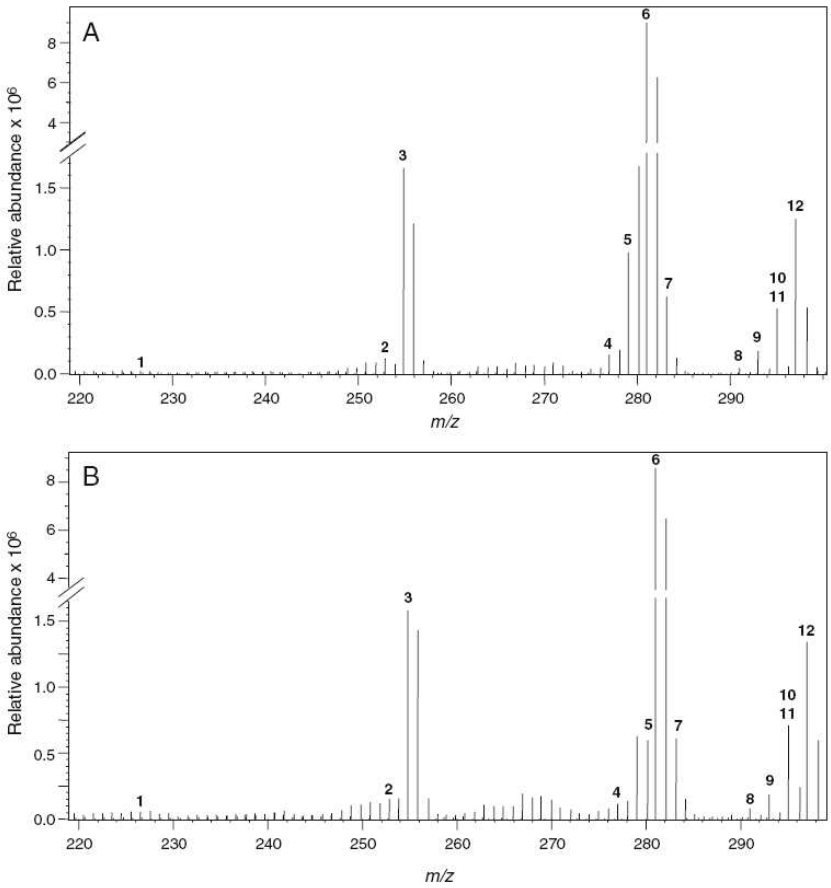

Fig. 2 MS spectra showing the peak profiles of fatty acid and their oxidized forms for the EV1 at storage times t_0 (**a**) and t_3 (**b**). The $[M-H]^-$ peaks are labeled as indicated in Table 2

obtained. Both samples, EV1 and EV2, were divided in eight aliquots each, stored in glass bottles, and kept in the dark at 60 °C up to 7 weeks. An aliquot of 250 mL of each sample was removed every week from the oven and stored at −20 °C (samples t_0–t_7). When all samples were collected, triplicate analyses on both EV1 and EV2 samples at each storage time were carried out for each analytical determination (except for the DIMS, in which four replicates were performed).

Qualitative parameters

The chemical parameters measured were: free acidity (free fatty acid content of the oil expressed as the percentage of oleic acid) and UV absorbance at 232 and 270 nm (k_{232}, k_{270}, which provide a measurement of the state of oxidation of the oils). These parameters were obtained as reported in the Regulation of the European Commission [22]. On the other hand, FA composition (expressed as percentage of methyl esters) was determined according to Bendini et al. [23] by GC-FID after alkaline treatment. Three replicates were prepared and analyzed for each sample.

Oxidative stability

A stream of purified air (120 mL min^{-1} air flow rate) was passed through 5 g oil sample and the effluent air for the oil sample was then bubbled through a vessel containing deionized water. The effluent air contains especially volatile organic acids as formic acid and other volatile compounds formed during thermal oxidation of the oil, which increased the conductivity of the water. The temperature at which this test was carried out was 110 °C. The OSI (or OSI time) was expressed in h and hundredth of h and corresponds to the end of lag period of the graph conductivity/time.

DIMS procedure

For DIMS, samples were 1:4 (*v*/*v*) diluted with an 85:15 PrOH/MeOH (*v*/*v*) mixture containing 40 mM NH_3 and

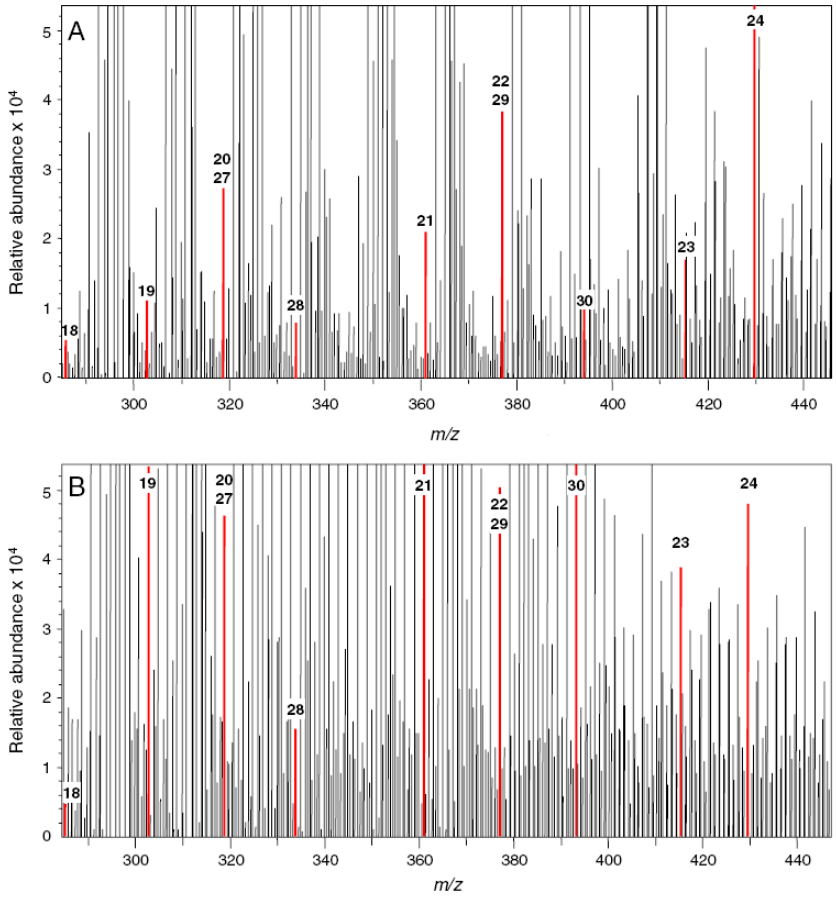

Fig. 3 MS spectra showing the peak profiles of tocopherol, phenolic, compounds and their oxidized forms for the EV1 at storage times t_0 (**a**) and t_3 (**b**). The $[M-H]^-$ peaks are labeled as indicated in Table 2

directly infused in the mass spectrometer. This mixture was also used to rinse and clean the capillary between successive infusions. Rinsing for 5 min was enough to achieve a satisfactory reduction of the background noise and reproducible oil profiles.

Data treatment and statistical analysis

The abundances of the $[M-H]^-$ peaks of free fatty acids, OFAs, tocopherols and phenolic compounds, jointly with their oxidized forms, were measured in 4 replicates for each VOO sample. These abundances were used as variables for LDA models, which were constructed using the SPSS software (v. 12.0.1, SPSS Inc., Chicago, IL, USA). LDA, a supervised classificatory technique, is widely recognized as an excellent tool to obtain vectors showing the maximal resolution between a set of previously defined categories. In LDA, vectors minimizing the Wilks' lambda, λ_w, are obtained [24]. This parameter is calculated as the sum of squares of the distances between points belonging to the same category divided by the total sum of squares. Values of λ_w approaching zero are obtained with well resolved categories, whereas overlapped categories made λ_w to approach one. Up to N–1 discriminant vectors are constructed by LDA, being N the lowest value for either the number of predictors or the number of categories. The selection of the predictors to be included in the LDA models was performed using the SPSS stepwise algorithm. According to this algorithm, a predictor is selected when the reduction of λ_w produced after its inclusion in the model exceeds F_{in}, the entrance threshold of a test of comparison of variances or F-test. However, the entrance of a new predictor modifies the significance of those predictors which are already present in the model. For this reason, after the inclusion of a new predictor, a rejection threshold, F_{out}, is used to decide if one of the other predictors should be removed from the model. The process terminates when there are no predictors entering or being eliminated from the model. The probability values of F_{in} and F_{out}, 0.05 and 0.10, respectively, were firstly adopted.

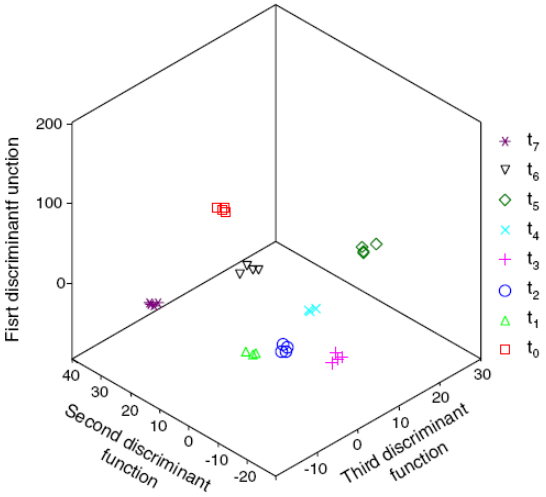

Fig. 4 Score plot on an oblique plane of the 3-D space defined by the three first discriminant functions of the LDA model constructed with the EV1 samples

SPSS was also used to perform one-way-analysis of variance and Tukey's honest significant difference (HSD) test at a 95% confidence level ($p<0.05$) to identify differences in the EV1 and EV2 samples at storage time zero.

Results and discussion

Evaluation of EVOO qualitative parameters during the accelerated oxidation process

The qualitative parameters and chemical composition of the EV1 and EV2 samples at t_0 are reported in Table 1. The free acidity percentage and the UV absorbance values of EV1 and EV2 were not statistically different. These values were below the limits set by the EC Regulation for EVOO [22]. The fatty acid composition of EV1 and EV2 samples at t_0 is also reported in Table 1. Their composition neither was statistically different. These data demonstrated that the phenol-removing procedure did not affect this fraction. On the other hand and as observed in Table 1, oxidative stability measured by OSI was affected by phenol removal. In fact, EV2 showed a reduction of a third part of OSI time (from 33.7 to 10.8 h).

Changes in the oxidative status of EV1 and EV2 during storage are represented in Fig. 1 as conjugated dienes (k_{232}) and OSI time. Both samples at t_1 showed values that exceeded the legal limit (3.51 and 3.67 for EV1 and EV2, respectively), reaching values of 8 and 10 for EV1 and EV2, respectively, after 7 weeks of storage. Similar trends were also found by Bendini et al. under comparable experimental conditions [23]. Regarding OSI time trend during sample storage (see Fig. 1), EV2 shown at t_0 an OSI value circa 10 h that could be principally related to the fatty acid composition of the oil, as phenolic fraction has been removed. Both EV1 and EV2 samples showed a significant decrease of OSI time, being faster for EV2 (in fact after 4 weeks was 100% reduced), confirming the role of phenolic fraction to the oxidative stability of EV1.

DIMS analysis, selection, and normalization of the variables

Several researches recently published have shown that several markers can be used to monitor the oxidation status of VOOs [14, 15, 23, 25–27]. In particular, OFA compounds have been used to evaluate the oxidative status of VOOs in several areas of applied research [14, 15, 23, 25], as well as for the determination of lipid extracts from other matrices, such as spaghetti pasta [26]. At the same time, the oxidized

Table 3 Predictors selected and corresponding standardized coefficients of the LDA model constructed with the EV1 samples to predict the oxidative status

Predictors[a]	f_1	f_2	f_3	f_4	f_5	f_6	f_7
227/277	−0.17	−0.45	−0.64	1.48	1.19	0.64	0.61
227/303	5.81	0.24	0.20	0.03	0.01	−0.35	0.06
255/279	9.83	1.70	2.87	2.25	1.79	0.80	−0.96
255/281	−4.33	1.60	−0.98	−1.96	−0.58	−0.36	0.83
255/361	−0.97	−3.79	−0.10	0.33	−0.20	−0.80	−2.27
277/283	4.65	1.00	−1.09	1.26	1.35	−0.96	−0.14
277/183	−5.48	−1.48	−0.52	0.35	−0.85	2.21	0.76
279/281	5.62	2.82	2.25	0.46	0.72	0.40	−1.72
281/361	4.94	3.66	0.40	−0.62	0.63	0.23	2.13
283/183	8.30	1.51	−0.05	0.22	0.96	−1.71	−0.87
269/257	−0.29	−2.13	−0.07	0.21	0.73	−0.01	0.68
377/335	−0.38	0.32	0.20	0.47	−1.04	0.01	0.20
199/393	−1.89	0.04	−0.09	0.16	0.17	0.27	0.74

[a] m/z values of the ratios of abundances of peak pairs

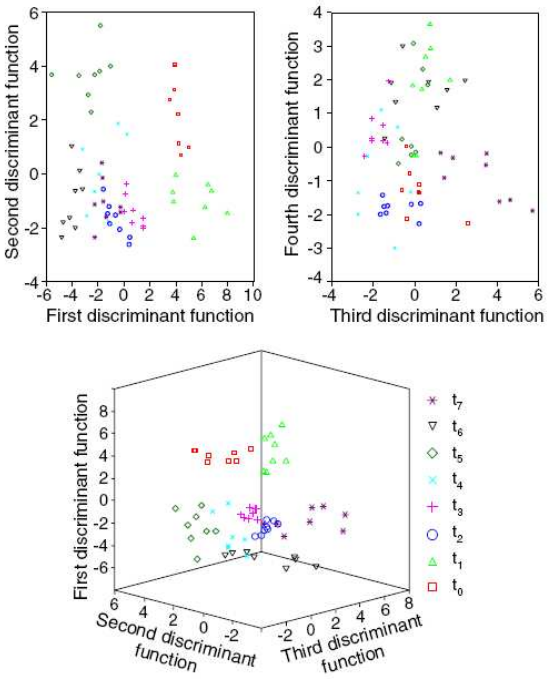

Fig. 5 Score plots on the planes of the first and second (**a**), and third and fourth discriminant functions (**b**), and on an oblique plane of the 3-D space defined by the three first discriminant functions (**c**) of the LDA model constructed with the EV1 and EV2 samples

forms of phenolic compounds have been identified as markers of the oxidation level of VOOs, being HPLC-MSD methods proposed for their analysis [25, 27]. Taking into account these considerations, free fatty acids, OFAs, phenols and their oxidized forms, jointly with α-tocopherol, have been selected as target compounds for this research. These 30 selected compounds and the *m/z* values of their corresponding $[M-H]^-$ peaks are indicated in Table 2. Owing to the coincidence of the *m/z* values of three peak pairs (hydroxy-linoleic acid/keto-oleic acid, DOA/OxDLA and OA/OxLA), these peaks were jointly measured; then, a total of 27 peaks were obtained to be used as predictors.

The MS spectra showing the peak profiles of the fatty acid and OFAs of EV1 at t_0 and t_3 are shown in Fig. 2. Several differences were observed for the OFAs (peaks 8–12), whose peak intensities increased from t_0 to t_3. This trend was also observed in the other storage times.

Figure 3 shows the MS spectra of the peak profiles of α-tocopherol, phenolic compounds and their oxidized forms (only those whose *m/z* range was between 280 and 450) for the EV1 at t_0 and t_3. As observed, several compounds (peaks 19 and 21) increased due to the transformation of *ortho*-diphenolic forms to mono oxydrilic forms. On the other hand, a decrease in α-tocopherol (peak 24) is noticeable while the oxidized forms of phenolic compounds (peaks 28 and 30) and the pairs 20/27 and 21/29 increased. For both pairs, the increase is probably due to the contribution of the oxidized forms 27 and 29. These trends are in agreement with previous works [23, 26].

In order to reduce the variability associated with the infusion in the mass spectrometer, and consequently minimize the influence of sources of variance non-associated to the origin and history of the oils, normalized ion abundances were employed for data analysis. For this purpose, and for each spectrum, the ion abundance of each peak was divided by each one of the abundances of the other 26 peaks; in this way, and taking into account that each pair of peaks should be considered only once, (27×26)/2=351 non-redundant peak ratios were obtained.

Construction of data matrices and LDA models

Using the normalized variables, LDA models capable of classifying the oil samples according to their oxidative status were performed. Two matrices were constructed. The first one was composed by EV1 samples (32 injections) and the 351 predictors. The second one comprised EV1 and EV2 samples (64 injections) and 66 predictors (which correspond to the α-tocopherol, fatty acid, and OFA peaks). In this case, only these predictors were selected due to the preliminary treatment carried out to EV2 samples, which had removed phenols and consequently their oxidized forms were not present in MS spectra. A response column,

Table 4 Predictors selected and corresponding standardized coefficients of the LDA model constructed with the EV1 and EV2 samples to predict the oxidative status

Predictors[a]	f_1	f_2	f_3	f_4	f_5	f_6	f_7
255/277	−0.36	−0.33	0.54	1.85	−0.91	0.83	−0.35
255/281	−0.11	−0.34	0.99	1.97	0.84	−1.34	0.55
255/291	−1.17	3.02	−2.94	−8.05	−2.68	−1.73	0.41
277/279	−0.96	−0.02	1.57	0.01	0.85	1.85	0.78
281/283	1.71	−0.18	1.81	2.76	1.26	0.10	0.37
283/291	0.81	−1.90	3.10	7.22	2.96	1.20	−0.17
443/277	−1.38	0.69	0.27	−1.37	3.45	1.23	1.30
443/279	2.91	0.19	−0.22	0.90	−3.26	−1.60	−2.49

[a] *m/z* values of the ratios of abundances of peak pairs

containing the eight storage times was added to both matrices.

Firstly, an LDA model was constructed using the matrix that contained EV1 samples. An excellent resolution between the eight categories was achieved (Fig. 4, λ_w= 0.229). The variables selected by the SPSS stepwise algorithm, and the corresponding standardized coefficients of the model, showing the predictors with large discriminant capabilities, are given in Table 3.

On the hand, another LDA model was constructed using the matrix that contained EV1 and EV2 samples. The eight categories were also very well resolved (λ_w=0.928). Taking into account that a large number of categories were simultaneously distinguished, this λ_w value was optimal. As observed in Fig. 5, part A, along the first discriminant function, f_1, the t_0 and t_1 appeared resolve from the other six categories, while t_0 and t_5 appeared resolved along f_2. As observed in Fig. 5, part B, f_3 was able to resolve t_7, while f_4 resolved the pair t_1/t_6 from the other categories. Finally, Fig. 5, part C, shows a score plot from an oblique perspective of the 3-D space defined by the three first discriminant functions. When this 3-D figure was rotated, the separation between all the different categories was clearly evidenced. Due to the fact that a large number of categories (seven) were included, it is logical that it was difficult to appreciate the separation between the categories when represented in a plane. The variables selected and the corresponding standardized coefficients of the model are given in Table 4.

For both LDA models, and using leave-one-out cross-validation, all the points of the respective matrices were correctly classified.

Conclusions

The use of DIMS to predict the oxidative status of VOO during storage has been demonstrated. For this purpose, the use of LDA models constructed using the intensity ratios of peak pairs as predictors is recommended. The MS intensities of the free fatty acids, OFAs, phenols, and their oxidation products can be measured after a simple dilution of the oil samples with a miscible alkaline solvent mixture. In this way, the conventional laborious extraction protocols commonly reported for phenolic compounds are avoided, being only necessary to rinse the spectrometer for 5 min between successive infusions to achieve low backgrounds and reproducible oil profiles. Thus, an extremely quick and simple procedure, which can be easily automated and used in other kind of matrices, has been described.

Acknowledgments Project CTQ2007-61445 (MEC of Spain and FEDER funds). M.J. Lerma-García thanks the Generalitat Valenciana for an FPI grant for PhD studies. L. Cerretani also thanks the University of Valencia for a contract.

References

1. Choe E, Min DB (2006) Compr Rev Food Sci F 5:169–186
2. Frega N, Mozzon M, Lercker G (1999) J Am Oil Chem Soc 76:325–329
3. Bendini A, Cerretani L, Carrasco-Pancorbo A, Gómez-Caravaca AM, Segura-Carretero A, Fernández-Gutiérrez A, Lercker G (2007) Molecules 12:1679–1719
4. Al-Ismail K, Caboni MF, Rodríguez-Estrada MT, Lercker G (1999) Grasas Aceites 50:448–453
5. Al-Ismail K, Caboni MF, Lercker G (1998) Riv Ital Sost Grasse 75:175–180
6. Lerma-García MJ, Simó-Alfonso EF, Bendini A, Cerretani L (2009) Food Chem 117:608–614
7. Fiskum G, Starkov A, Polster BM, Chinopoulos C (2003) Ann NY Acad Sci 991:111–119
8. Heidenreich KA (2003) Ann NY Acad Sci 991:237–250
9. Farhoosh R, Pazhouhanmehr S (2009) Food Chem 114:1002–1006
10. Frankel EN (1998) Lipid oxidation. Oily, Dundee (UK)
11. Vichi S, Pizzale L, Conte LS, Buxaderas S, López-Tamames E (2003) J Agr Food Chem 51:6564–6571
12. Melton SL, Jafra S, Sykes D, Trigiano MK (1994) J Am Oil Chem Soc 71:1301–1308
13. Caponio F, Pasqualone A, Gomes T (2002) Eur Food Res Technol 215:114–117
14. Rovellini P, Cortesi N, Fedeli E (1998) Riv Ital Sost Grasse 75:57–70
15. Del Carlo M, Sacchetti G, Di Mattia C, Compagnone D, Mastrocola D, Liberatore L, Cichelli A (2004) J Agric Food Chem 52:4072–4079
16. Carrasco-Pancorbo A, Cerretani L, Bendini A, Segura-Carretero A, Del Carlo M, Gallina-Toschi T, Lercker G, Compagnone D, Fernández-Gutiérrez A (2005) J Agric Food Chem 53:8918–8925
17. Lerma-García MJ, Herrero-Martínez JM, Ramis-Ramos G, Simó-Alfonso EF (2008) Food Chem 107:1307–1313
18. Lerma-García MJ, Herrero-Martínez JM, Ramis-Ramos G, Simó-Alfonso EF (2008) Food Chem 108:1142–1148
19. Lerma-García MJ, Ramis-Ramos G, Herrero-Martínez JM, Simó-Alfonso EF (2008) Rapid Commun Mass Spectrom 22:973–978
20. Lerma-García MJ, Ramis-Ramos G, Herrero-Martínez JM, Simó-Alfonso EF (2007) Rapid Commun Mass Spectrom 21:3751–3755
21. Bonoli-Carbognin M, Cerretani L, Bendini A, Almajano MP, Gordon MH (2008) J Agric Food Chem 56:7076–7081
22. European Community, Commission Regulation 1989/2003 of 6 November 2003 amending Regulation No. 2568/91 (2003) Off J Eur Commun L295:57-77
23. Bendini A, Cerretani L, Vecchi S, Carrasco-Pancorbo A, Lercker G (2006) J Agric Food Chem 54:4880–4887
24. Vandeginste BGM, Massart DL, Buydens LMC, De Jong S, Lewi PJ, Smeyers-Verbeke J (1998) Data handling in science and technology part B. Elsevier, Amsterdam
25. Armaforte E, Mancebo-Campos V, Bendini A, Salvador MD, Fregapane G, Cerretani L (2007) J Sep Sci 30:2401–2406
26. Verardo V, Ferioli F, Riciputi Y, Infelice G, Marconi E, Caboni MF (2009) Food Chem 114:472–477
27. Lerma-García MJ, Simó-Alfonso EF, Chiavaro E, Bendini A, Lercker G, Cerretani L (2009) J Agric Food Chem. doi:10.1021/jf901346n in press

ANEXO XVIII

Food Chemistry 117 (2009) 608–614

Contents lists available at ScienceDirect

Food Chemistry

journal homepage: www.elsevier.com/locate/foodchem

Metal oxide semiconductor sensors for monitoring of oxidative status evolution and sensory analysis of virgin olive oils with different phenolic content

M.J. Lerma-García [a,*], E.F. Simó-Alfonso [a], A. Bendini [b], L. Cerretani [b,*]

[a] Departamento de Química Analítica, Universidad de Valencia, C. Doctor Moliner 50, E-46100 Burjassot, Valencia, Spain
[b] Dipartimento di Scienze degli Alimenti, Università di Bologna, P. zza Goidanich 60, I-47023 Cesena (FC), Italy

ARTICLE INFO

Article history:
Received 8 January 2009
Received in revised form 19 February 2009
Accepted 15 April 2009

Keywords:
Electronic nose
Oxidative stability
Phenols
Sensory analysis
Storage
Virgin olive oil

ABSTRACT

An electronic nose based on an array of six metal oxide semiconductor sensors was used to monitor the oxidative status of virgin olive oils (VOO) during storage. VOO samples, with and without phenolic compounds, were stored at 60 °C for 7 weeks. Once a week, absorbance at 232 and 270 nm, oxidized stability index, electronic nose, and sensory analysis were evaluated. Linear discriminant analysis models were constructed in order to classify samples according to oxidative levels. Based on these models, VOO samples with and without phenolic compounds at different storage times, divided in eight categories, were correctly classified also achieving a good correlation for sensory analysis. The method is a fast and economical tool for on-line monitoring of VOO oxidation status.

1. Introduction

Among edible oils, virgin olive oil (VOO) is a basic component of the Mediterranean diet and has several characteristics that render it unique (Bendini et al., 2007a). The importance of VOO is mainly attributed to its high oxidative stability and its characteristic sensory and nutritional properties (Aparicio, Roda, Albi, & Gutiérrez, 1999; Bendini et al., 2007a; Cerretani, Salvador, Bendini, & Fregapane, 2008). The high oxidative stability of VOO with respect to other vegetable oils is mainly due to its fatty acid composition, and in particular to the high monounsaturated-to-polyunsaturated ratio and the presence of minor compounds, that play a major role in preventing oxidation. However, in spite of its high stability, VOO is also susceptible to suffer oxidative processes such as enzymatic oxidation (which occurs when the oil is in the fruit and during the technological extraction process), photo-oxidation (which occurs when the oil is exposed to light) and auto-oxidation (mainly produced during processing and storage when the oil is in contact with oxygen) (Bendini, Cerretani, Salvador, Fregapane, & Lercker, submitted for publication; Frankel, 1985). In these latter cases, the presence of antioxidant compounds can modify the oxidation process. A classification of the antioxidants based on their mechanism of action includes primary antioxidants, synergistic, and secondary antioxidants (Rajalakhmi & Narasimham, 1996). Phenolic compounds are one of the major groups in the polar fraction and act as primary antioxidants (AxH) to inhibit oxidation in VOO. These compounds act as chain breakers by donating a radical hydrogen to the alkylperoxyl radicals (ROO·) formed during the initiation step of lipid oxidation, and subsequently form a radical (Ax·) that is stabilized by resonance forms during the reaction (Carrasco-Pancorbo et al., 2005):

$$ROO^{\cdot} + AxH \rightarrow ROOH + Ax^{\cdot}$$

The polar extracts of VOO contain phenolic compounds that belong to different classes comprising phenolic acids, phenyl ethyl alcohols, hydroxy-isochromans, flavonoids, lignans, and secoiridoids. The secoiridoid family is characteristic of Oleaceae plants, being the main compounds of the phenolic fraction of VOO (Bendini et al., 2007a). The shelf-life of VOO is longer than other vegetable oils, mainly due to the presence of phenolic molecules possessing a catechol group, such as hydroxytyrosol and its secoiridoid derivatives. Three different assays (antiradical test, electrochemical method and a forced oxidation model system) have been used to establish the antioxidant activity of these phenolic compounds (Carrasco-Pancorbo et al., 2005).

VOO is also a unique, edible vegetable oil with characteristic sensory properties. The sensory attributes of VOO mainly depend on the content of minor components such as phenolics and volatile compounds. The individual components contribute to different sensory perceptions (Cerretani et al., 2008). Approximately 180

* Corresponding authors. Tel.: +34 96 354 4334; fax: +34 96 354 4436 (M.J. Lerma-García), tel.: +39 0547338121; fax: +39 0547382348 (L. Cerretani).
E-mail addresses: m.jesus.lerma@uv.es (M.J. Lerma-García), lorenzo.cerretani@unibo.it (L. Cerretani).

0308-8146/$ - see front matter © 2009 Elsevier Ltd. All rights reserved.
doi:10.1016/j.foodchem.2009.04.052

compounds belonging to several chemical classes such as aldehydes, alcohols, esters, ketones, acids, ethers, hydrocarbons and terpens have been separated from the volatile fractions of VOO (Angerosa et al., 2004). The oxidation process leads to the production of several products of varying volatility. These compounds, mainly saturated and unsaturated aldehydes generated by autoxidation, are the major cause of the sensory perception of the rancid defect in vegetable oils (Vichi, Pizzale, Conte, Buxaderas, & López-Tamames, 2003). Concerning gustatory perceptions, it is well established that phenolic compounds are responsible for bitterness (Beltrán, Ruano, Jiménez, Uceda, & Aguilera, 2007; Cerretani et al., 2008; Esti, Contini, Moneta, & Sinesio, 2009; Gutierrez-González, Albi, Palma, Rios, & Olias, 1989; Gutierrez-Rosales, Rios, & Gomez-Rey, 2003) and pungency in VOO (Andrewes, Busch, De Joode, Groenewegen, & Alexandre, 2003; Cerretani et al., 2008; Esti et al., 2009; Tovar, Motilva, & Romero, 2001). In particular, Andrewes et al. (2003) found that decarboxymethyl-ligstroside aglycon, also called oleocanthal (Beauchamp et al., 2005), is the major phenolic molecule responsible for the burning pungent sensation of VOO. Recently, Beauchamp et al. (2005) found that oleocanthal inhibits enzymes related to inflammation and also shows ibuprofen-like activity. Moreover, the phenolic content has been associated with protection against several chronic and degenerative diseases (Menendez et al., 2007).

For commercial classification of VOO, the European Union Commission has provided 26 chemical–physical and organoleptic parameters (EC Reg. 1989/03; EC Reg. 640/08; EEC Reg. 2568/91). The latter are important for quality analysis in order to identify sensory defects (mainly winey, fusty, mouldy, muddy, and rancid) present in VOO. Among these defects, only rancidity is linked with aging of VOO.

The official and/or routine chemical and sensory methods used for these determinations are expensive, time-consuming, labor intensive, and require large amounts of solvent and reagents (Bendini et al., 2007c). The use of spectroscopic techniques together with multivariate analysis (Bendini et al., 2007b,c; Maggio et al., 2009; Sinelli, Cosio, Gigliotti, & Casiraghi, 2007) can minimize these disadvantages and offer potentially rapid methods that can screen large numbers of samples. More recently, metal oxide semiconductor (MOS) sensors have been shown to be valid instruments that are applicable in many fields of food control; these sensors have a low cost and can work on-line without sample pretreatment (Escuderos, Uceda, Sánchez, & Jiménez, 2007; Esposto et al., 2009). Regarding control of aroma in VOO, electronic noses have been used to detect a variety of sensory defects (Aparicio, Rocha, Delgadillo, & Morales, 2000; Camurati, Tagliabue, Bresciani, Sberveglieri, & Zaganelli, 2006; García-González & Aparicio, 2002; García-González & Aparicio, 2003) and to authenticate VOOs according to varietal or geographical origin of olives (Tena, Lazzez, Aparicio-Ruiz, & García-González, 2007). In this regard, the oxidation level of VOO has been recently studied (Buratti, Benedetti, & Cosio, 2005; Cosio, Ballabio, Benedetti, & Gigliotti, 2007).

To date, only limited research has been carried out using MOS sensors coupled with linear discriminant analysis (LDA) to detect the oxidation level of VOO (Cosio et al., 2007). In this study, only three oxidation levels were identified.

The aim of the present investigation was to establish a non-destructive method based on MOS sensors, in combination with LDA, for the classification of the oxidative level of VOO. The application of this system allowed the classification of VOOs with and without phenolic compounds sampled at different storage times in eight oxidation levels. This approach is a fast and economical tool for on-line monitoring of the oxidation status of VOO.

2. Materials and methods

2.1. Reagents and sample preparation

The following reagents were used: sodium hydroxide (NaOH), sodium chloride (NaCl), potassium hydroxide (Carlo Erba, Milan, Italy), hexane, methanol, diethyl ether (Sigma–Aldrich, St. Louis, MO, USA), chloroform, acetonitrile, hydrochloric acid (HCl), anhydrous sodium sulfate, formic acid, ethanol, phenolphthalein, sodium thiosulfate (Merck, Darmstadt, Germany), iso-octane, potassium iodide, 3,4-dihydroxy phenyl acetic acid (3,4-DHPAA) and acetic acid (3, and acetic acid (Fluka, Buchs, Switzerland).

An extra-virgin olive oil (EVOO) sample from the olive fruit variety Brugnola produced at San Marino (picked on October 03, 2008) was used. The olives were processed using an Oliomio 150 extraction machine (Tem, Tavernelle Val di Pesa, Florence, Italy) in order to obtain EVOO. For evaluation of EVOO oxidation, the oil sample was divided in two aliquots: EVOO and EVOO without phenols (EVOOP). Phenolic compounds were removed from EVOO according to the procedure described by Bonoli-Carbognin, Cerretani, Bendini, Almajano, and Gordon (2008). Briefly, 35 g EVOO were washed with several aliquots of 0.5 M NaOH (4×15 mL). To eliminate the aqueous phase, the mixture was centrifuged (1000*g*, 5 min) after each washing. Combined olive oil fractions were then washed with 0.5 M HCl (2×10 mL) and saturated NaCl solution (5×10 mL), centrifuged at 1000*g* for 5 min, dried with anhydrous sodium sulfate and finally filtered under vacuum. Dried olive oil free of phenolic compounds (EVOOP) was obtained.

According to Bendini, Cerretani, Vecchi, Carrasco-Pancorbo, and Lercker (2006) and Bonoli-Carbognin et al. (2008), both samples, EVOO and EVOOP, were divided in eight aliquots each, stored in glass bottles and kept in the dark at 60 °C for 7 weeks. Every week an aliquot of each sample was analyzed for diene and triene, oxidized stability index, electronic nose, and sensory analysis.

Moreover, an additional 25 VOO samples were used to evaluate the model. To assure the robustness of the model, samples from different geographical origins and genetic varieties, collected during different years, were also analyzed.

2.2. Instrumentation

2.2.1. MOS sensor array

An electronic olfactory system (EOS 507, Sacmi Imola S.C., Imola, Bologna, Italy) composed of a measuring chamber with six MOS sensors and a personal computer was used for the acquisition and analysis of the data generated by the EOS 507. The sensors used were: sensor 1 (SnO_2), sensor 2 ($SnO_2 + SiO_2$), sensor 3, 4 and 5 (catalyzed SnO_2 with three different metals) and sensor 6 (WO_3). During the analysis, sensors were maintained at a temperature range of 350–450 °C. The EOS 507 was controlled by an integrated PDA equipped with proprietary software, and was connected to an automatic sampling apparatus (Model HT500H) which had a carousel of 10 sites for loading samples. Samples were kept at controlled temperature (37 °C) and placed in a chamber provided by a system that removes humidity from the surrounding environment.

2.2.2. Experimental procedure

After samples were removed from the oven, 15 g were placed in 100 mL Pyrex vials equipped with a pierceable silicon/Teflon cap. Samples were incubated at 37 °C for 7 min before injection. The oil headspace, sampled with an automatic syringe, was then pumped over the sensor surfaces for 2 min during which the sensor signals were recorded. The sensors were then exposed to filtered air at a constant flow rate of 50 sccm (standard cubic cm per min) to obtain the baseline. After this, another 7 min period was

then applied to restore the original MOS conditions. Ambient air filtered with activated silica and charcoal was used as a reference gas during the recovery phase of the measurement cycle. The previous conditions ensured that the baseline reading had indeed been recovered before the next analysis was performed.

The experimental conditions adapted from Camurati et al. (2006) were used, and each sample was evaluated in duplicate.

2.2.3. Oxidized stability instrument

An eight-channel oxidative stability instrument (OSI) (Omnion, Decatur, IL, USA) was used. The instrument was set at 110 °C with an air flow rate of 120 mL min^{-1}. The OSI index was determined twice for each sample and the mean value was expressed as OSI time in hours.

2.3. Qualitative parameters

The chemical parameters measured were: acidity, which is indicative of the free fatty acid content of the oil expressed as the percentage of oleic acid; peroxide value (PV), which is a measure of the amount of hydroperoxides expressed as meq O_2 kg^{-1}; UV absorbance at 232 and 270 nm (k_{232}, k_{270}), which provide a measurement of the state of oxidation of the oils and fatty acid (FA) composition, expressed as percentage of saturated, monounsaturated, and polyunsaturated FAs (as methyl esters). The ratio of oleic/linoleic acids was also calculated. All chemical analyses were performed according to the official methods of the European Commission (EEC Reg. 2568/91). The content in total phenols expressed as mg of 3,4-DHPAA kg^{-1} oil was measured, and the extraction procedure, high performance liquid chromatography (HPLC) with diode array detector (DAD) analysis and quantification were adapted from Carrasco-Pancorbo et al. (2007). The oxidative stability index of the samples was also monitored according to Bendini et al. (2007a).

2.4. Sensory analysis

Sensory analysis was performed according to the European normative reported in Annex XII of EEC Reg. 2568/91. Ten trained assessors working as a professional panel from the Dipartimento di Scienze degli Alimenti (panel recognized by Italian Ministry-Mipaaf on 20 July 2006) used a scorecard to provide a quantitative-descriptive analysis (Cerretani, Biasini, Bonoli-Carbognin, & Bendini, 2007) of orthonasal perceptions. A set of positive (green or ripe fruity and other pleasant attributes such as leaf, grass, artichoke, tomato, almond, apple, others) and negative (winey-vinegary, fusty, mouldy, muddy, rancid, others) sensory attributes were evaluated. Oil samples were graded for each positive and negative attribute using a numerical scale from 0 to 5 related to the perception of flavor stimuli, according to the judgement of assessors. The median, mean, and robust standard deviation (EC Reg. 640/08) were calculated for each attribute. If the value of the robust standard deviation was higher than 20%, the analysis was repeated. All samples were subjected to a panel test.

2.5. Data treatment and statistical analysis

The data from the electronic nose was extracted and analyzed with the statistical package "Nose Pattern Editor" (Sacmi Imola S.C.). A feature extraction algorithm called "classical feature" was applied to the data before other statistical treatments. The response extracted by each sensor was defined by:

$$X = R/R_0$$

where R_0 was the initial resistance of the sensor balanced in the air, R was the resistance of a sensor in the presence of the volatile compounds emitted from the VOO headspace (which decreased respect to R_0), and X was the response of each sensor recorded. This algorithm defined several conditions for evaluation of R_0 and R reported in the software package.

Successive statistical analyses were performed using SPSS (v. 11.0, Statistical Package for the Social Sciences, Chicago, IL, USA).

3. Results and discussion

3.1. Evaluation of VOOs during storage

The chemical composition and oxidative parameters of the EVOO and EVOOP from the Brugnola variety are reported in Table 1. The free acidity percentage of EVOO and EVOOP ranged from 0.24% to 0.18%, while the PV varied from 11.96 to 12.44 meq O_2 kg^{-1} oil (Table 1). These values (free acidity and PV) were below the limits set by the EC Regulation for extra-VOO (EC Reg. 1989/03).

The main groups of FA of samples at storage time zero (t_0) are reported in Table 1. EVOO and EVOOP showed very similar values in terms of FA composition, which demonstrate that the phenol-removing procedure does not affect this fraction. The oils were characterized by high values in terms of MUFA and the oleic/linoleic acid ratio, confirming the contribution of FA composition of these oils towards oxidative stability (Aparicio et al., 1999). On the contrary, a significant variation in total tocopherols was observed, and EVOOP showed a slight decrease with respect to EVOO.

EVOO and EVOOP were also analyzed by HPLC-DAD to quantify individual phenols. Considering the sum of all identified and quantified phenolic compounds, their total concentration in EVOO was high with a value of 162 mg DHPAA kg^{-1} oil. The stripping of phenolic compounds from the oil by alkaline washing reduced the concentration of these minor compounds to a very low level; in fact, the decrease was higher than 99.5% (Table 1). A similar effect has been previously observed by Bonoli-Carbognin et al. (2008). The oxidative status of oils was assessed by OSI time values, which underlined that phenols have a major contribution to the oxidative stability of VOO (Aparicio et al., 1999). In fact, as shown in Table 1, EVOOP showed a 73.4% reduction in terms of oxidative stability compared to EVOO.

The changes in the oxidative status of EVOO and EVOOP stored at 60 °C are shown in Fig. 1 as conjugated dienes (A) and trienes (B). The two samples at t_0 showed k_{232} and k_{270} values that were below the limits established by the EC Regulation for extra-VOO category (EC Reg. 1989/03), which corresponded to 2.50 and 0.22, respectively. However, after 1 week of storage (t_1), EVOO and EVOOP exceeded the limit for k_{232}, reaching values of 9 and

Table 1
Chemical parameters of EVOO and EVOOP samples at storage time zero.

Parameter	EVOO	EVOOP
Acidity (%)	0.24	0.18
PV (meq O_2 kg^{-1})	11.96	12.44
C18:1/C18:2[a]	7.87	7.85
MUFA[b] (%)	73.80	73.75
PUFA[c] (%)	9.67	9.68
SFA[d] (%)	16.53	16.57
k_{232}	2.23	2.45
k_{270}	0.19	0.16
Tocopherol (mg kg^{-1})	172.46	120.17
Total phenol (mg 3,4-DHPAA kg^{-1})	162.22	0.69
OSI time (h)	33.65	10.80

[a] Ratio oleic acid/linoleic acid.
[b] Monounsaturated fatty acids.
[c] Polyunsaturated fatty acids.
[d] Saturated fatty acids.

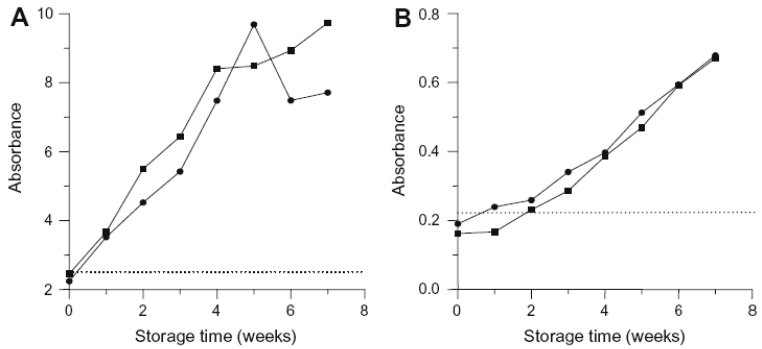

Fig. 1. Changes in conjugated diene at 232 nm (A) and triene at 270 nm (B) contents of the extra-VOO (●) and EVOOP (■) samples during storage at 60 °C. The horizontal line indicated the legal limit established by the EC Regulation for extra-VOO category.

7 for EVOOP and EVOO, respectively, after 7 weeks (t_7) of storage (Fig. 1). Concerning k_{270}, after 1 week of storage (t_1) only EVOO exceeded the EC limit, but 7 days later EVOOP also surpassed the legal value. k_{270} showed a similar trend respect to k_{232} and after 7 weeks (t_7) of storage final values of 0.7 for both types of samples were seen (Fig. 1). Similar trends were also found by Bendini et al. under comparable experimental conditions (Bendini et al., 2006).

Starting from t_0 to the end of the storage time (t_7), both EVOO and EVOOP samples showed a substantial decrease in terms of OSI time that was more evident for EVOO, also if this oil was characterized by a higher OSI time at t_0 (Fig. 2). This difference in terms of oxidative stability between EVOO and EVOOP, especially at the beginning of storage time, could be explained by the different amounts of phenolic compounds. For EVOOP, the OSI value at t_0 close to 10 h could only be attributed to the high oleic acid content, the low amounts of polyunsaturated FA, and thus to the high oleic/linoleic acid ratio.

3.2. Construction of the data matrices and LDA models

LDA, a supervised classificatory technique, is widely recognized as an excellent tool to obtain vectors showing the maximal resolution between a set of previously defined categories. In LDA, vectors minimizing the Wilks' lambda, λ_w, are obtained (Vandeginste et al., 1998). This parameter is calculated as the sum of squares of the distances between points belonging to the same category divided by the total sum of squares. Values of λ_w approaching zero are obtained with well resolved categories, whereas overlapped categories approach a λ_w of one. Up to N-1 discriminant vectors are constructed by LDA, and N has the lowest value for either the number of predictors or the number of categories.

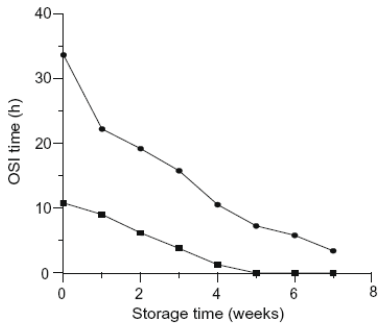

Fig. 2. Oxidized stability index of EVOO (●) and EVOOP (■) samples.

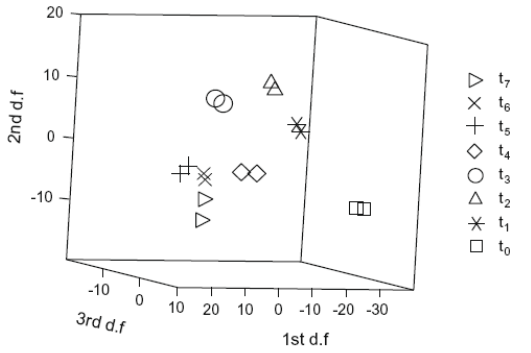

Fig. 3. Score plot on an oblique plane of the 3-D space defined by the three first discriminant functions of the LDA model constructed with EVOO samples. d.f., discriminant function.

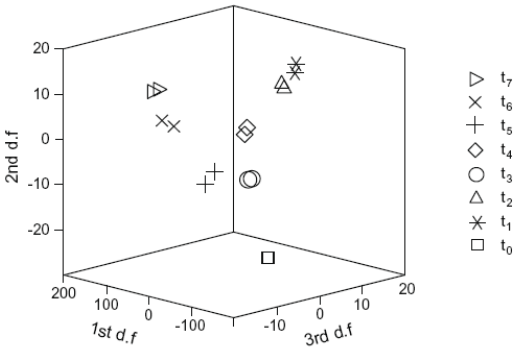

Fig. 4. Score plot on an oblique plane of the 3-D space defined by the three first discriminant functions of the LDA model constructed with EVOOP samples. See Fig. 3 for additional comments.

Table 2
Predictors selected and corresponding standardized coefficients of the three LDA models constructed to predict the storage time.

Predictor	EVOO				EVOOP				EVOO and EVOOP			
	f_1	f_2	f_3	f_4	f_1	f_2	f_3	f_4	f_1	f_2	f_3	f_4
Sensor 1	1.75	0.50	−1.46	3.58	−2.36	1.99	0.50	−2.58	−2.83	−4.84	−2.15	4.06
Sensor 2	−1.01	−0.00	1.27	1.47	−14.51	0.74	−1.62	0.03	−5.80	−0.90	−1.31	0.33
Sensor 3	0.53	−0.56	2.90	−3.62	–	–	–	–	–	–	–	–
Sensor 4	−1.22	1.06	−2.39	−1.30	10.73	−2.30	2.35	0.03	4.50	0.96	2.77	−0.36
Sensor 5	–	–	–	–	6.40	−0.12	−0.30	2.93	4.16	5.45	1.01	−3.25

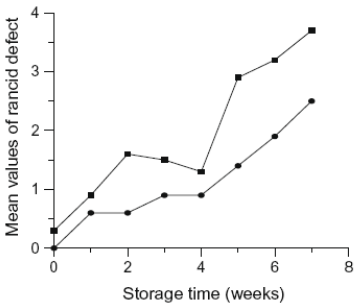

Fig. 5. Evolution of the rancid defect expressed as the mean of the sensory analysis values as a function of storage time for EVOO (●) and EVOOP (■) samples.

Using the 6 MOS sensors as predictors, LDA models capable of classifying the oil samples according to storage time were constructed. Three matrices containing the six predictors were constructed: one containing EVOO samples (8×2 replicates), another containing EVOOP samples (8×2 replicates), and the third containing both types of samples (16×2 replicates). A response column containing the eight categories corresponding to the different storage times was added to the matrices. To construct the LDA models, the SPSS stepwise algorithm was used. According to this algorithm, a predictor is selected when the reduction of λ_w produced after its inclusion in the model exceeds F_{in}, the entrance threshold of a test of comparison of variances or F-test. However, the entrance of a new predictor modifies the significance of those predictors which are already present in the model. For this reason, after the inclusion of a new predictor, a rejection threshold, F_{out}, is used to decide if one of the other predictors should be removed from the model. The process terminates when there are no predictors entering or being eliminated from the model. Probability values of F_{in} and F_{out}, 0.05 and 0.10, respectively, were adopted.

First, an LDA model was constructed using the matrix containing the EVOO samples, and excellent resolution between the category pairs was obtained (Fig. 3, $\lambda_w = 0.049$). This value was very low taking into account that a large number of categories were simultaneously distinguished. Next, another LDA model was constructed using the matrix constructed with the EVOOP samples. With this model, resolution between the category pairs was also excellent (Fig. 4, $\lambda_w = 0.068$). Finally, another LDA model was constructed using all the samples, and good resolution between all the category pairs was achieved ($\lambda_w = 0.892$). In this case, for the same category, two different groups were observed, one for EVOO and the other for EVOOP samples (data not shown). This dispersion within the same category could explain the high λ_w value achieved. With this LDA model, it is possible to conclude that electronic nose data discriminated between samples with and without phenolic compounds. The variables selected by the SPSS stepwise algorithm, and the corresponding standardized coefficients of the three

Table 3
Median values for the sensory attributes and predicted category (t_x) for the 25 samples used to evaluate the LDA model.

Sample	Fruity (type)	Other pleasant attributes	Defects	Predicted category
N1	3 (Green)	2 (Grass, tomato)	0	t_0
N2	2 (Green)	2 (Grass, artichoke, almond)	0	t_0
N3	2 (Green)	2 (Grass, artichoke)	0	t_0
N4	2 (Green)	2 (Leaf, almond)	0	t_0
N5	2 (Green)	2 (Leaf, grass, tomato, almond)	0	t_0
N6	3 (Green)	2 (Grass, artichoke, tomato)	0	t_0
N7	3 (Green)	3 (Grass, artichoke, tomato)	0	t_0
N8	3 (Green)	2 (Grass, artichoke, tomato)	0	t_0
N9	2 (Ripe)	2 (Others)	0	t_0
N10	2 (Ripe)	2 (Tomato)	0	t_0
N11	1 (Ripe)	0	1.5 (Fusty)	t_1
N12	1 (Ripe)	0	1 (Winey)	t_1
N13	1 (Ripe)	0	2 (Rancid)	t_1
N14	1 (Ripe)	0	5 (3 of Muddy, 2 of rancid)	t_2
N15	1 (Ripe)	0	2 (Rancid)	t_1
N16[a]	0	0	2 (Winey)	t_0
N17[a]	0	0	3 (Winey)	t_0
N18[a]	0	0	3 (Rancid)	t_3
N19[a]	0	0	5 (Rancid)	t_7
N20[a]	0	0	1 (Fusty)	t_1
N21[a]	0	0	3 (Fusty)	t_3
N22[a]	0	0	1 (Muddy)	t_1
N23[a]	0	0	2 (Muddy)	t_1
N24[a]	0	0	1 (Mouldy)	t_1
N25[a]	0	0	2 (Mouldy)	t_1

[a] Official defects provided by International Oil Council (IOC).

models, showing the predictors with large discriminant capabilities, are shown in Table 2. As can be deduced, the LDA model constructed with the EVOO samples was the only one which uses sensor 4 as a predictor. For this reason, this sensor was surmised to have a response due to volatile compounds formed after oxidation in the presence of phenolic compounds. For the three models, and using the leave-one-out validation, all points were correctly classified (the degree of classification is 100%).

3.3. Sensory analysis and evaluation of the LDA model

EVOO and EVOOP samples were evaluated by the panel of testers. Only the EVOO sample at t_0 was characterized by a green fruity and leaf and grass attributes, while all other samples had a ripe fruity and any pleasant attributes. Only the EVOO sample at t_1 showed a winey defect, probably masked at t_0 by the green fruity aspect, while rancidity was the only defect noted in all samples during the 7 week period. The evolution of the rancid defect is shown in Fig. 5 (mean values were used instead of median to better demonstrate inter-sample variations). As can be observed, rancidity was more pronounced for the EVOOP samples, which could be indirectly attributed to the absence of phenolic compounds. Therefore, the model clearly responded to the rancid defect.

An additional 25 VOOs were also subjected to the panel test assessment, being also used to evaluate the model in order to verify if they were well assigned according to sensory data. The most important sensory attributes of these samples and the predicted category for the model are shown in Table 3. As is evident, the model distinguished all the samples without defects from the others, assigning them to the t_0 category. Moreover, Table 3 shows that the model was able to correctly identify 13 defective samples, with the exception of N16 and N17, which were characterized by a winey defect and fruity absence. In particular, the model responded linearly for the four samples characterized by the rancid defect, quite well for N11, N20, and N21, which presented different intensities of fusty, but less for oils with other defects (mouldy, muddy).

It is interesting to note that slight differences were observed for the real defected samples (from N13 to N15) and those provided by IOC to recognize the rancid defect (N18 and N19). This could be linked to the differences in total volatile compounds between the profile of VOO and the rancid standard (Aparicio et al., 2000). In this respect, the near total absence of volatile components responsible for pleasant fruity note (from the LOX pathway) and the high presence of several saturated and unsaturated aldehydes in the IOC samples could have influenced the MOS response.

4. Conclusions

The possibility of classifying VOOs according to their oxidative level by using MOS sensor data has been demonstrated. In fact, for samples with and without phenols (EVOO and EVOOP) characterized by different storage times under forced oxidation (7 weeks at 60 °C), excellent resolution was achieved by LDA which divided oils into eight categories. Moreover, good correlation was obtained between the model and sensory analysis. In particular, the model distinguished all VOOs without defects from the others, and responded linearly for the four samples characterized by a rancid defect. The method is a fast and economical tool for on-line monitoring of VOO oxidation status, and could be also used to study the oxidative level of other vegetable oils during processing (i.e. refining steps) and distribution phases in addition to industrial uses (i.e. frying).

Acknowledgements

The authors gratefully acknowledge Sacmi Imola S.C. who kindly allowed us to use the MOS system (EOS 507), and Ibanez Riccò for technical assistance. Project CTQ2007-61445 (MEC and FEDER funds) are acknowledged. MJL-G thanks the Generalitat Valenciana for an FPI grant for PhD studies and for a grant to study in a foreign institution.

References

Andrewes, P., Busch, J. L. H. C., De Joode, T., Groenewegen, A., & Alexandre, H. (2003). Sensory properties of virgin olive oil polyphenols: Identification of deacetoxy-ligstroside aglycon as a key contributor to pungency. *Journal of Agricultural and Food Chemistry, 51*, 1415–1420.

Angerosa, F., Servili, M., Selvaggini, R., Taticchi, A., Esposto, S., & Montedoro, G. F. (2004). Volatile compounds in virgin olive oil: Occurrence and their relationship with the quality. *Journal of Chromatography A, 1054*, 17–31.

Aparicio, R., Rocha, S. M., Delgadillo, I., & Morales, M. T. (2000). Detection of rancid defect in virgin olive oil by the electronic nose. *Journal of Agricultural and Food Chemistry, 48*, 853–860.

Aparicio, R., Roda, L., Albi, M. A., & Gutiérrez, F. (1999). Effect of various compounds on virgin olive oil stability measured by rancimat. *Journal of Agricultural and Food Chemistry, 47*(10), 4150–4155.

Beauchamp, G. K., Keast, R. S. J., Morel, D., Lin, J., Pika, J., Han, Q., et al. (2005). Phytochemistry – Ibuprofen-like activity in extra-virgin olive oil. *Nature, 437*, 45–46.

Beltrán, G., Ruano, M. T., Jiménez, A., Uceda, M., & Aguilera, M. P. (2007). Evaluation of virgin olive oil bitterness by total phenol content analysis. *European Journal of Lipid Science and Technology, 109*, 193–197.

Bendini, A., Cerretani, L., Carrasco-Pancorbo, A., Gómez-Caravaca, A. M., Segura-Carretero, A., Fernández-Gutiérrez, A., et al. (2007a). Phenolic molecules in virgin olive oils: A survey of their sensory properties, health effects, antioxidant activity and analytical methods. An overview of the last decade. *Molecules, 12*, 1679–1719.

Bendini, A., Cerretani, L., Di Virgilio, F., Belloni, P., Bonoli-Carbognin, M., & Lercker, G. (2007b). Preliminary evaluation of the application of the FTIR spectroscopy to control the geographic origin and quality of virgin olive oils. *Journal of Food Quality, 30*, 424–437.

Bendini, A., Cerretani, L., Di Virgilio, F., Belloni, P., Lercker, G., & Gallina Toschi, T. (2007c). In-process monitoring in industrial olive mill by means of near infrared spectroscopy (FT-NIR). *European Journal of Lipid Science and Technology, 109*, 498–504.

Bendini, A., Cerretani, L., Vecchi, S., Carrasco-Pancorbo, A., & Lercker, G. (2006). Protective effects of extra-virgin olive oil phenolics on oxidative stability in the presence or absence of copper ions. *Journal of Agricultural and Food Chemistry, 54*, 4880–4887.

Bendini, A., Cerretani, L., Salvador, M. D., Fregapane, G., & Lercker, G. (submitted for publication). Stability of virgin olive oil sensory quality during storage: An overview. *Italian Journal of Food Science*.

Bonoli-Carbognin, M., Cerretani, L., Bendini, A., Almajano, M. P., & Gordon, M. H. (2008). Bovine serum albumin produces a synergistic increase in the antioxidant activity of virgin olive oil phenolic compounds in oil-in-water emulsions. *Journal of Agricultural and Food Chemistry, 56*, 7076–7081.

Buratti, S., Benedetti, S., & Cosio, M. S. (2005). An electronic nose to evaluate olive oil oxidation during storage. *Italian Journal of Food Science, 2*(17), 203–210.

Camurati, F., Tagliabue, S., Bresciani, A., Sberveglieri, G., & Zaganelli, P. (2006). Sensory analysis of virgin olive oil by means of organoleptic evaluation and electronic olfactory system. *Rivista Italiana Delle Sostanze Grasse, 83*(5), 205–211.

Carrasco-Pancorbo, A., Cerretani, L., Bendini, A., Segura-Carretero, A., Del Carlo, M., Gallina-Toschi, T., et al. (2005). Evaluation of the antioxidant capacity of individual phenolic compounds in virgin olive oil. *Journal of Agricultural and Food Chemistry, 53*, 8918–8925.

Carrasco-Pancorbo, A., Cerretani, L., Bendini, A., Segura-Carretero, A., Lercker, G., & Fernández-Gutiérrez, A. (2007). Evaluation of the influence of thermal oxidation in the phenolic composition and in antioxidant activity of extra-virgin olive oils. *Journal of Agriculture and Food Chemistry, 55*, 4771–4780.

Cerretani, L., Biasini, G., Bonoli-Carbognin, M., & Bendini, A. (2007). Harmony of virgin olive oil and food pairing: A methodological proposal. *Journal of Sensory Studies, 22*, 403–416.

Cerretani, L., Salvador, M. D., Bendini, A., & Fregapane, G. (2008). Relationship between sensory evaluation performed by Italian and Spanish official panels and volatile and phenolic profiles of virgin olive oils. *Chemosensory Perception, 1*, 258–267.

Cosio, M. S., Ballabio, D., Benedetti, S., & Gigliotti, C. (2007). Evaluation of different storage conditions of extra-virgin olive oils with an innovative recognition tool built by means of electronic nose and electronic tongue. *Food Chemistry, 101*, 485–491.

Escuderos, M. E., Uceda, M., Sánchez, S., & Jiménez, A. (2007). Instrumental technique evolution for olive oil sensory analysis. *European Journal of Lipid Science and Technology, 109*, 536–546.

Esposto, S., Montedoro, G. F., Selvaggini, R., Riccò, I., Taticchi, A., Urbani, S., et al. (2009). Monitoring of virgin olive oil volatile compounds evolution during olive malaxation by an array of metal oxide sensors. *Food Chemistry, 113*, 345–350.

Esti, M., Contini, M., Moneta, E., & Sinesio, F. (2009). Phenolic compounds and temporal perception of bitterness and pungency in extra-virgin olive oils: Changes occurring throughout storage. *Food Chemistry, 113*, 1095–1100.

European Community, Commission Regulation (1991). No. 2568/91 of 11 July 1991 on the characteristics of olive oil and olive pomace oil and on the relevant methods of analysis. *Official Journal of European Communities, L248*, 1–83.

European Community, Commission Regulation (2003). No. 1989/2003 of 6 November 2003 amending Regulation No. 2568/91 on the characteristics of olive oil and olive pomace oil and on the relevant methods of analysis. *Official Journal of European Communities, L295*(5), 7–77.

European Community, Commission Regulation (2008). No. 640/2008 of 4 July 2008 amending Regulation No. 2568/91/EEC. *Official Journal of the European Communities, L178*, 11–16.

Frankel, E. N. (1985). Chemistry of autoxidation: Mechanism, products and flavor significance. In D. B. Min & T. H. Smouse (Eds.), *Flavor chemistry of fats and oils* (pp. 1–37). Champaign, IL (USA): AOCS Press.

García-González, D. L., & Aparicio, R. (2002). Detection of vinegary defect in virgin olive oils by metal oxide sensors. *Journal of Agricultural and Food Chemistry, 50*, 1809–1814.

García-González, D. L., & Aparicio, R. (2003). Virgin olive oil quality classification combining neural network and MOS sensors. *Journal of Agricultural and Food Chemistry, 51*, 3515–3519.

Gutierrez-González, F., Albi, M. A., Palma, R., Rios, J. J., & Olias, J. M. (1989). Bitter taste of virgin olive oil: Correlation of sensory evaluation and instrumental HPLC analysis. *Journal of Food Science, 54*, 68–70.

Gutierrez-Rosales, F., Rios, J. J., & Gomez-Rey, M. A. L. (2003). Main polyphenols in the bitter taste of virgin olive oil. Structural confirmation by on-line high-performance liquid chromatography electrospray ionization mass spectrometry. *Journal of Agricultural and Food Chemistry, 51*, 6021–6025.

Maggio, R. M., Kaufman, T. S., Del Carlo, M., Cerretani, L., Bendini, A., Cichelli, A., et al. (2009). Monitoring of fatty acid composition in virgin olive oil by Fourier transformed infrared spectroscopy coupled with partial least squares. *Food Chemistry, 114*, 1549–1554.

Menendez, J. A., Vazquez-Martin, A., Colomer, R., Brunet, J., Carrasco-Pancorbo, A., Garcia-Villalba, R., et al. (2007). Olive oil's bitter principle reverses acquired autoresistance to trastuzumab (Herceptin™) in HER2-overexpressing breast cancer cells. *BMC Cancer, 7* [art. no. 80].

Rajalakhmi, D., & Narasimham, S. (1996). In D. L. Madhavi, S. S. Deshpande, & D. K. Salunkhe (Eds.), *Food antioxidants*. New York: Marcel Dekker. p. 65.

Sinelli, N., Cosio, M. S., Gigliotti, C., & Casiraghi, E. (2007). Preliminary study on application of mid infrared spectroscopy for the evaluation of the virgin olive oil "freshness". *Analytica Chimica Acta, 598*, 128–134.

Tena, N., Lazzez, A., Aparicio-Ruiz, R., & García-González, D. L. (2007). Volatile compounds characterizing Tunisian Chemlali and Chétoui virgin olive oils. *Journal of Agricultural and Food Chemistry, 55*, 7852–7858.

Tovar, M. J., Motilva, M. J., & Romero, M. P. (2001). Changes in the phenolic composition of virgin olive oil from young trees (*Olea europaea* L. Cv. *Arbequina*) grown under linear irrigation strategies. *Journal of Agricultural and Food Chemistry, 49*, 5502–5508.

Vandeginste, B. G. M., Massart, D. L., Buydens, L. M. C., De Jong, S., Lewi, P. J., & Smeyers-Verbeke, J. (1998). *Data handling in science and technology Part B*. Amsterdam: Elsevier Science. p. 237.

Vichi, S., Pizzale, L., Conte, L. S., Buxaderas, S., & López-Tamames, E. (2003). Solid-phase microextraction in the analysis of virgin olive oil volatile fraction: Modifications induced by oxidation and suitable markers of oxidative status. *Journal of Agricultural and Food Chemistry, 51*, 6564–6571.

ANEXO XIX

JOURNAL OF AGRICULTURAL AND FOOD CHEMISTRY
ARTICLE

J. Agric. Food Chem. **2009,** *57,* 9365–9369 **9365**
DOI:10.1021/jf901763n

Rapid Evaluation of Oxidized Fatty Acid Concentration in Virgin Olive Oils Using Metal Oxide Semiconductor Sensors and Multiple Linear Regression

María Jesús Lerma-García,*,† Ernesto F. Simó-Alfonso,† Alessandra Bendini,§ and Lorenzo Cerretani*,§

†Departamento de Química Analítica, Universidad de Valencia, C. Doctor Moliner 50, E-46100 Burjassot, Valencia, Spain, and §Dipartimento di Scienze degli Alimenti, Università di Bologna, Piazza Goidanich 60, I-47521 Cesena (FC), Italy

This works aims to set up a rapid and nondestructive method to evaluate the advanced oxidation of virgin olive oils (VOOs). An electronic nose based on an array of six metal oxide semiconductor sensors was used, jointly with multiple linear regression (MLR), to predict the oxidized fatty acid (OFA) concentration in VOO samples characterized by different oxidative status. An MLR model constructed using five predictors was able to predict OFA concentration with an average validation error of 9%.

KEYWORDS: Electronic nose; multiple linear regression; oxidative status; oxidized fatty acids; virgin olive oil

INTRODUCTION

Differently from other foods, oils and fats do not suffer microbiological problems during storage but suffer principally the oxidation process. The oxidation process is normally divided into three phases: primary phase (slow increase of oxidation); secondary phase (rapid propagation of oxidation), and termination phase. Each oxidation phase is characterized by the production of specific oxidized products (*1*, *2*), such as volatile compounds, oxidized polymers, and molecules that have a similar parent structure with respect to the starting molecules [i.e., oxidized fatty acids (OFA)] (*3*).

Virgin olive oils (VOOs) are characterized by a high oxidative stability with respect to other edible oils in terms of their fatty acid composition (a high oleic acid concentration) and antioxidant content (*4*). The formation of oxidation products during oxidation reactions depends on the fatty acid composition of oils and on antioxidant (phenolic compounds, tocopherols, carotenoids) and pro-oxidant factors (i.e., the presence of oxygen and metals, temperature, and light) (*5*, *6*).

The evaluation of secondary oxidation products represents a critical point to evaluate the storage status of fatty substances (*5*). The difficulty in determining these compounds is due to the fact that each fatty acid produces first hydroperoxides, followed by the production of different classes of compounds such as alcohols, ketones, and epoxides in various isomeric forms.

Several approaches have been attempted to find a reliable oxidation index that, combined with evaluation of primary oxidation products, would provide a realistic idea about the oxidation status of the fatty matrix (*7*). The secondary oxidation indices more widely applied to fat and vegetable oils are the *p*-anisidine value and thiobarbituric acid reactive substances as well as the content of hexanal or nonanal or their ratio (*8*, *9*). Among the chemical methods, the measurements of total polar compounds and polymerized triglycerides (in particular in oils subjected to heating) are the most common methods used (*10*) for the assessment of oil quality. In fact, the oxidized triglyceride and their polymers are good indicators of the oxidative level of oils and fats due to their high stability and low volatility. Nowadays, the official method used to measure the oxidation index entails gravimetric analysis of the polar products according to ISO 8420 (*11*).

An alternative method to analyze secondary oxidation products has been proposed by Rovellini, Cortesi, and Fedeli (*12*). This method evaluates the oxidation status of VOOs using RP-HPLC analysis of OFAs and permits reliable quantification thanks to the use of two reference standards. The method has been used to evaluate the oxidative status of VOOs in various areas of applied research (*2*, *13*, *14*).

This HPLC method (*12*, *14*) allows the identification and quantification of the main OFAs (hydroxy, keto, epoxy, and epidioxy) after a simple derivatization step with sodium benzyl oxide of the triglycerides. As these latter compounds are more stable than peroxides, OFAs seem to be a good index of oxidative changes in lipids. The disadvantages of this method include the long sample preparation time and the long HPLC analysis time (approximately 80 min). For this reason, other techniques that minimize these disadvantages and offer potentially rapid methods that can screen large numbers of samples are needed.

Metal oxide semiconductor (MOS) sensors have been shown to be valid instruments that are applicable in many fields of food control; these sensors have a low cost and can work online without sample pretreatment (*15*, *16*). Electronic noses have been used to detect a variety of sensory defects in VOOs (*17*−*21*) and

*Corresponding authors [(M.J.L.-G.) telephone +34963544334, fax +34963544436, e-mail m.jesus.lerma@uv.es; (L.C.) telephone +390547338121, fax +390547382348, e-mail lorenzo.cerretani@unibo.it].

Published on Web 10/06/2009

to authenticate them according to the varietal or geographical origin of olives (*22*). In this regard, the oxidation level of VOO has been recently studied (*21*, *23*, *24*). As far as we are aware, no research has been carried out using MOS sensors coupled with multiple linear regression (MLR) to predict OFA concentration in VOOs.

In this work, an electronic nose based on an array of six MOS was used jointly with the application of MLR models to predict OFA concentration in VOOs characterized by different oxidative status. For this purpose, sensor signals were used as predictors.

MATERIALS AND METHODS

Reagents and Samples. The following reagents and standards were used: tricaproin, triheptadecanoin, sodium benzyl oxide in benzyl alcohol, *n*-hexane, 2-propanol, acetone (Sigma-Aldrich, St. Louis, MO), acetonitrile (ACN), anhydrous sodium sulfate (Merck, Darmstadt, Germany), and acetic acid (Fluka, Buchs, Switzerland).

A series of 72 VOOs were sampled from different Italian regions (Abruzzo, Emilia-Romagna, Puglia, Sicilia, and Toscana) during the harvest seasons 2006−2007, 2007−2008, and 2008−2009. All samples were analyzed between November 2008 and January 2009. The oils differed in terms of olive cultivar, degree of ripening, area of growth, production system (type, productive capacity, and manufacturer), and storage time.

Instrumentation and Working Conditions. An electronic olfactory system (EOS 507, Sacmi Imola S.C., Imola, Bologna, Italy) composed of a measuring chamber with six metal oxide sensors and a personal computer was used for the acquisition and analysis of the data generated by the EOS 507. The sensors used were as follows: sensor 1 (SnO_2); sensor 2 ($SnO_2 + SiO_2$); sensors 3, 4, and 5 (catalyzed SnO_2 with three different metals); and sensor 6 (WO_3). During the analysis, sensors were maintained at a temperature range of 350−450 °C. The EOS 507 was controlled by an integrated personal digital assistant equipped with proprietary software and was connected to an automatic sampling apparatus (model HT500H), which had a carousel of 10 sites for loading samples. Samples were kept at controlled temperature (37 °C) and placed in a chamber provided by a system that removes humidity from the surrounding environment.

OFA determination was performed using an 1100 series liquid chromatograph (Agilent Technologies, Palo Alto, CA) provided with a binary pump delivery system, a degasser, an autosampler, and a diode array UV−Vis detector (DAD). The liquid chromatograph was also coupled (in series with the DAD) to an atmospheric pressure chemical ionization source from an HP 1100 series quadrupole mass analyzer (MS) (Agilent). OFA separation was carried out with a Luna C18 column (5 μm, 250 × 4.6 mm i.d., Phenomenex, Torrance, CA). Mobile phases were prepared by mixing ACN (A) and water (B) in gradient mode. The gradient elution was performed as follows: from 0 to 50 min, the A percentage was increased from 60 to 100%; an isocratic elution at 100% A was carried out from 50 to 70 min; an additional minute was used to decrease the A percentage from 100 to 60%; then, 60% A was maintained an additional 14 min to equilibrate the column. UV−Vis detection was performed at 255 ± 10 nm (reference 500 ± 50 nm). In all cases, 20 μL was injected at a flow rate of 1 mL min^{-1}. These conditions were adapted from the NGD C-88 official method published by Norme Grassi e Derivati (*25*). The MS working conditions were as follows: nebulizer gas pressure, 50 psi; drying gas flow, 9 L min^{-1} at 350 °C; vaporizer temperature, 300 °C; capillary voltage, 3 kV; corona current, 4 μA; and fragmentor voltage, 60 V. The mass spectrometer was scanned within the m/z 300−500 range in the positive-ion mode.

MOS Sensor Array Procedure. For each sample, 15 g was placed in a 100 mL Pyrex vial equipped with a pierceable silicon/Teflon cap. **Figure 1** represents the response of the six sensors for one of the samples employed in this study. For each sensor, the signal is divided in four parts: (A) conditioning phase (25 min period employed to obtain a constant baseline), (B) before injection phase (in which samples were incubated at 37 °C for 7 min before injection), (C) measurement cycle (in which the oil headspace, sampled with an automatic syringe, was then pumped over the sensor surfaces for 2 min during which the sensor signals were recorded; in this phase sensors were exposed to filtered air at a constant flow rate of 50 sccm (standard cubic cm per min) to obtain the baseline), and (D) recovery phase (another 7 min period applied to restore the original MOS conditions). Ambient air filtered with activated silica and charcoal was used as a reference gas during the recovery phase of the measurement cycle. The previous conditions ensured that the baseline reading had indeed been recovered before the next analysis was performed.

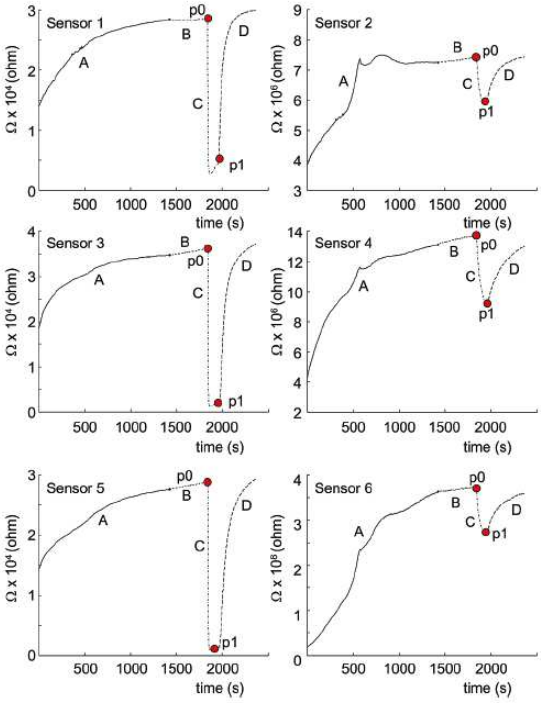

Figure 1. Plots representing the electrical resistance (Ω) of each MOS sensor during VOO evaluation: (A) conditioning phase; (B) before injection phase; (C) measurement cycle; (D) recovery phase.

The experimental conditions adapted from Camurati et al. (*18*) were used, and each sample was evaluated in duplicate.

Determination of OFAs. OFAs were prepared according to the literature (*14*, *25*), and analyzed by HPLC-DAD (*25*) and HPLC-MS after transesterification with 1.0 M sodium benzyl oxide in benzyl alcohol. Tricaproin and triheptadecanoin were used as internal standards (results are reported in percentages as g of total OFA expressed as benzyl heptadecanoate per 100 g of oil, whereas benzyl caproate was used as a control for the derivatization reaction).

Data Treatment and Construction of MLR Matrices. The data from the electronic nose were extracted and analyzed with the statistical package "Nose Pattern Editor" (Sacmi Imola S.C.). A feature extraction algorithm called "classical feature" was applied to the data before other statistical treatments. The response extracted by each sensor was defined by

$$X = p_1/p_0$$

where p_0 was the initial resistance of the sensor balanced in the air (see **Figure 1**), p_1 was the resistance (see **Figure 1**) of a sensor in the presence of the volatile compounds emitted from the VOO headspace (which decreased respect to p_0), and X was the response of each sensor recorded.

For MLR studies, calibration and external validation sets were constructed. The calibration matrix contained 60 objects (which were randomly selected), which corresponded to the average of the duplicates for each sample. The signal of the 6 sensors, which were used as predictors, was also added to this matrix. The external validation matrix was constructed with the remaining 12 objects also corresponding to the average of the duplicates of the samples. Also in this case, the signal of the 6 sensors was added to this matrix. A response column, containing the OFA concentration (obtained by HPLC), was then added to these matrices. Statistical analyses were performed using SPSS (v. 11.5, Statistical Package for the Social Sciences, Chicago, IL).

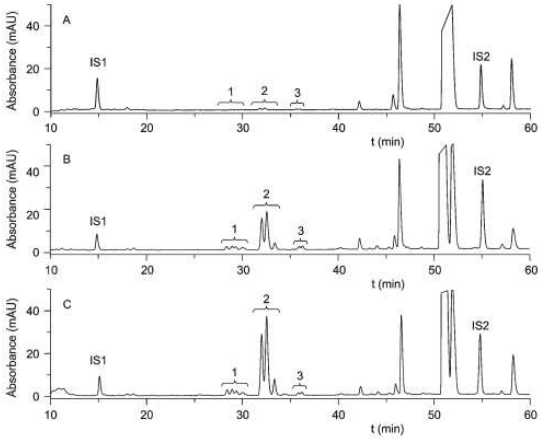

Figure 2. OFA HPLC traces of VOOs at (**A**) 2 weeks, (**B**) 16 months, and (**C**) 34 months after oil production. Detection was performed at 255 nm. Peak identification (as benzyl ester derivatives): 1, group of isomeric forms of ketolinolenic acid; 2, group of isomeric forms of ketolinoleic acid; 3, group of isomeric forms of keto-oleic acid. IS1 and IS2 are benzyl caproate and benzyl heptadecanoate, respectively.

RESULTS AND DISCUSSION

OFA Content in VOO Samples. The HPLC chromatograms in **Figure 2** show that the differences in OFA content (low, medium, and high) of three VOO samples are related to storage time (2 weeks, 16 months, and 34 months after oil production, which correspond to parts **A**, **B**, and **C**, respectively). On the basis of the study of MS spectra, three groups of OFAs were identified (see **Figure 2**): 1, for isomeric forms of ketolinolenic acid (m/z 383); 2, for isomeric forms of ketolinoleic acid (m/z 385); and 3, for isomeric forms of keto-oleic acid (m/z 387). All m/z values corresponded to the $[M + H]^+$ ions.

The OFA content was evaluated for the 72 VOO samples and was found to have a wide range, which varied from 0.3 to 6.5%. This can be attributed to the fact that the oil samples came from different harvest seasons and were analyzed at times ranging from 1 week to 36 months after production. Rovellini et al. (*14*) analyzed several VOOs and found that OFA percentages from 2 to 4% are typical for extra virgin olive oils stored from 2 to 18 months at room temperature, whereas oil samples characterized by a total OFA of >4% must be considered as "expired".

Taking into account the differences observed in OFA values, samples were grouped in four groups (**Figure 3**) on the basis of the OFA values (OFA < 1.0% for **Figure 3A**; 1.0% ≤ OFA < 2.5% for **Figure 3B**; 2.5% ≤ OFA < 4% for **Figure 3C**; and OFA ≥ 4% for **Figure 3D**). The 72 VOOs were subdivided as follows: a first group (G1, n = 23) with a mean of 0.6%; a second group (G2, n = 15) with a mean of 1.8%; a third group (G3, n = 23) with a mean of 3.0%; and a fourth group (G4, n = 11) with a mean of 5.3%. All of the samples produced within 1 month before analysis belonged to G1 with a very narrow range of OFA values (from 0.3 to 0.8%). In contrast, group G4 showed higher percentages and a wider range of variability (from 4.2 to 6.5%). These data confirm that it is possible to evaluate the freshness of VOOs with a simple OFA assay, thereby reducing the number of analyses (i.e., peroxide values or k_{232} for primary oxidation products and *p*-anisidine value or volatile content for secondary oxidation products).

Construction of MLR Models. The SPSS stepwise algorithm of the SPSS was used to select the variables to be included in the

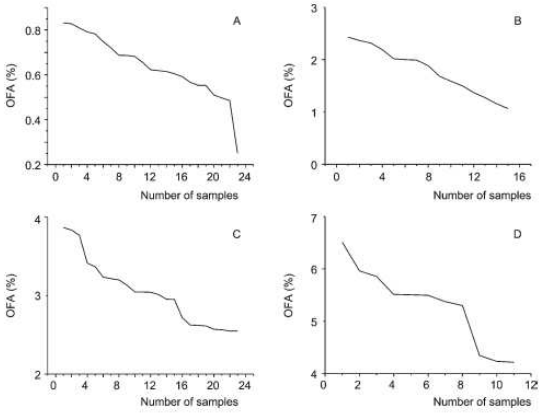

Figure 3. Plots representing the OFA values of the 72 VOOs employed in this study: (**A**) OFA < 1.0%; (**B**) 1.0% ≤ OFA < 2.5%; (**C**) 2.5% ≤ OFA < 4%; (**D**) OFA ≥ 4%. The first group (n = 23) shows a mean of 0.6%; the second group (n = 15), a mean of 1.8%; the third group (n = 23), a mean of 3.0%, and the fourth group (n = 11), a mean of 5.3%.

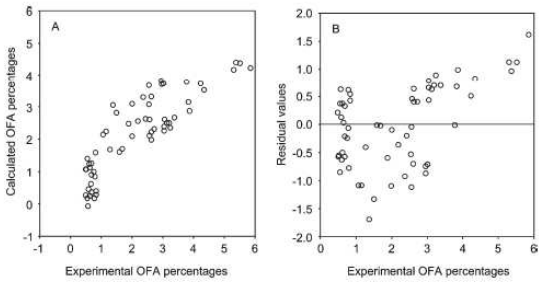

Figure 4. (**A**) Correlation plot of the calculated versus the experimental OFA percentages. (**B**) Plot of the residual values versus the experimental OFA percentages.

MLR models. For this purpose, the default probability values of F_{in} and F_{out}, 0.05 and 0.10, respectively, were adopted. Using the calibration matrix, two MLR models were constructed, both with and without the inclusion of an independent term (constant). The model including the constant gave lower linearity than the model without the constant (regression coefficient, r, of 0.961). For this reason, further studies were performed without the inclusion of the constant. The correlation plot of the calculated versus the experimental OFA percentages is shown in **Figure 4A**. When leave-one-out validation was applied, the average prediction error (calculated as the sum of the absolute differences between expected and calculated OFA concentrations divided by the number of predictions) was 30%. To obtain information regarding the fit of the model, residual values and/or the relative errors were examined. For this purpose, a plot representing the residual values against the experimental OFA percentages (**Figure 4B**) was obtained. A dependence of the residuals on the experimental values was observed and, therefore, heteroscedasticity (nonconstant variance) of the data. For this reason, the following variable transformations (*26*) were applied to the experimental OFA percentages: natural logarithm and square and cube roots. Homoscedasticity in the data distribution was obtained when the cube root transformation was used (see **Figure 5B**). Comparison of this plot with that in **Figure 4B** shows that homoscedasticity of the data

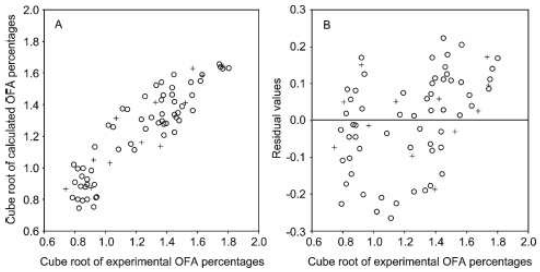

Figure 5. (**A**) Correlation plot of the calculated versus the experimental OFA percentages obtained after cube root transformation. (**B**) Plot of the residual values versus the experimental OFA percentages obtained after cube root transformation. For both **A** and **B**, samples are marked as calibration (○) and validation (+).

Table 1. Predictors Selected and Their Corresponding Nonstandardized Coefficients and Confidence Limits for the MLR Model Constructed with the Cube Root Transformation

predictor	coeff	confidence limits[a]
sensor 2	3.18	2.42, 3.94
sensor 3	10.12	7.67, 12.57
sensor 4	−8.61	−10.63, −6.58
sensor 5	−7.98	−10.12, −5.84
sensor 6	6.16	4.63, 7.69

[a] For a 95% confidence interval.

was observed. Using cube root transformation, an r of 0.995 was obtained with a squared correlation coefficient of 0.989. The correlation plot of the calculated versus the experimental OFA percentages obtained using the cube root transformation is shown in **Figure 5A**. The predictors selected for this model and their corresponding nonstandardized coefficients and confidence limits are detailed in **Table 1**. According to this table, the sensors selected corresponded to sensors 2−6, which corresponded to $SnO_2 + SiO_2$, SnO_2 catalyzed with three different metals, and WO_3. When leave-one-out validation was applied, the average prediction error was 8%. When the model was applied to the validation set, a good prediction capability was observed (see **Figure 4A**), the average validation error being 9%.

Thus, the possibility of estimating the oxidative status of VOO using OFA concentration as reference by means of electronic nose data has been demonstrated. After a cube root transformation of the experimental OFA percentages, an MLR model constructed using five predictors was able to predict OFA concentration with an average error of 9%. This method is useful, particularly considering the accordance with HPLC, the rapidity of analysis, and the lack of solvent consumption. This latter point should be taken into account considering the real problem of ACN shortage, which is the most widely solvent used in HPLC analysis.

ACKNOWLEDGMENT

We gratefully acknowledge Sacmi Imola S.C., who kindly allowed us to use the MOS 340 system (EOS 507), and Ibanez Riccò for technical assistance.

LITERATURE CITED

(1) Toschi, T. G.; Costa, A.; Lercker, G. Gas chromatographic study on high-temperature thermal degradation products of methyl linoleate hydroperoxides. *J. Am. Oil Chem. Soc.* **1997**, 74, 387–391.

(2) Bendini, A.; Cerretani, L.; Vecchi, S.; Carrasco-Pancorbo, A.; Lercker, G. Protective effects of extra virgin olive oil phenolics on oxidative stability in the presence or absence of copper ions. *J. Agric. Food Chem.* **2006**, 54, 4880–4887.

(3) Choe, E.; Min, D. B. Mechanisms and factors for edible oil oxidation. *Compr. Rev. Food Sci. Food Saf.* **2006**, 5, 169–186.

(4) Bendini, A.; Cerretani, L.; Carrasco-Pancorbo, A.; Gómez-Caravaca, A. M.; Segura-Carretero, A.; Fernández-Gutiérrez, A.; Lercker, G. Phenolic molecules in virgin olive oils: a survey of their sensory properties, health effects, antioxidant activity and analytical methods. An overview of the last decade. *Molecules* **2007**, 12, 1679–1719.

(5) Al-Ismail, K.; Caboni, M. F.; Lercker, G. The influence of oxygen availability on the extent of oxidation of some lipid model system. *Riv. Ital. Sostanze Grasse* **1998**, 75, 175–180.

(6) Al-Ismail, K.; Caboni, M. F.; Rodríguez-Estrada, M. T.; Lercker, G. The influence of oxygen content on the extent of oxidation of model systems of mixtures of methyl oleate and methyl linoleate at different ratios. *Grasas Aceites* **1999**, 50, 448–453.

(7) Farhoosh, R.; Pazhouhanmehr, S. Relative contribution of compositional parameters to the primary and secondary oxidation of canola oil. *Food Chem.* **2009**, 114, 1002–1006.

(8) Frankel, E. N. Chemistry of autoxidation: mechanism, products and flavor significance. In *Flavor Chemistry of Fats and Oils*; Min, D. B., Smouse, T. H., Eds.; AOCS Press: Champaign, IL, 1998; pp 1−37.

(9) Vichi, S.; Pizzale, L.; Conte, L. S.; Buxaderas, S.; López-Tamames, E. Solid-phase microextraction in the analysis of virgin olive oil volatile fraction: Modifications induced by oxidation and suitable markers of oxidative status. *J. Agric. Food Chem.* **2003**, 51, 6564–6571.

(10) Melton, S. L.; Jafra, S.; Sykes, D.; Trigiano, M. K. Review of stability measurements for frying oils and frying food flavour. *J. Am. Oil Chem. Soc.* **1994**, 71, 1301–1308.

(11) ISO, International Organization for Standardization. *Animal and vegetable fats and oils—determination of content of polar compounds* (ISO 8420:2002); pp 1−18.

(12) Rovellini, P.; Cortesi, N.; Fedeli, E. Oxidative profile and chemical structure of oxidation products of triglycerides by HPLC-ES-MS. *Riv. Ital. Sostanze Grasse* **1998**, 75, 57–70.

(13) Armaforte, E.; Mancebo-Campos, V.; Bendini, A.; Salvador, M. D.; Fregapane, G.; Cerretani, L. Retention effects of oxidized polyphenols during analytical extraction of phenolic compounds of virgin olive oil. *J. Sep. Sci.* **2007**, 30, 2401–2406.

(14) Rovellini, P.; Cortesi, N. Oxidative status of extra virgin olive oils: HPLC evaluation. *Ital. J. Food Sci.* **2004**, 16, 333–342.

(15) Escuderos, M. E.; Uceda, M.; Sánchez, S.; Jiménez, A. Instrumental technique evolution for olive oil sensory analysis. *Eur. J. Lipid Sci. Technol.* **2007**, 109, 536–546.

(16) Esposto, S.; Montedoro, G. F.; Selvaggini, R.; Riccò, I.; Taticchi, A.; Urbani, S.; Servili, M. Monitoring of virgin olive oil volatile compounds evolution during olive malaxation by an array of metal oxide sensors. *Food Chem.* **2009**, 113, 345–350.

(17) Aparicio, R.; Rocha, S. M.; Delgadillo, I.; Morales, M. T. Detection of rancid defect in virgin olive oil by the electronic nose. *J. Agric. Food Chem.* **2000**, 48, 853–860.

(18) Camurati, F.; Tagliabue, S.; Bresciani, A.; Sberveglieri, G.; Zaganelli, P. Sensory analysis of virgin olive oil by means of organoleptic evaluation and electronic olfactory system. *Riv. Ital. Sostanze Grasse* **2006**, 83, 205–211.

(19) García-González, D. L.; Aparicio, R. Detection of vinegary defect in virgin olive oils by metal oxide sensors. *J. Agric. Food Chem.* **2002**, 50, 1809–1814.

(20) García-González, D. L.; Aparicio, R. Virgin olive oil quality classification combining neural network and MOS sensors. *J. Agric. Food Chem.* **2003**, 51, 3515–3519.

(21) Lerma-García, M. J.; Simó-Alfonso, E. F.; Bendini, A.; Cerretani, L. Metal oxide semiconductor sensors for monitoring of oxidative status evolution and sensory analysis of virgin olive oils with different phenolic content. *Food Chem.* **2009**, *117*, 608−614.

(22) Tena, N.; Lazzez, A.; Aparicio-Ruiz, R.; García-González, D. L. Volatile compounds characterizing Tunisian Chemlali and Chétoui virgin olive oils. *J. Agric. Food Chem.* **2007**, 55, 7852–7858.
(23) Buratti, S.; Benedetti, S.; Cosio, M. S. An electronic nose to evaluate olive oil oxidation during storage. *Ital. J. Food Sci.* **2005**, 2, 203–210.
(24) Cosio, M. S.; Ballabio, D.; Benedetti, S.; Gigliotti, C. Evaluation of different storage conditions of extra virgin olive oils with an innovative recognition tool built by means of electronic nose and electronic tongue. *Food Chem.* **2007**, 101, 485–491.
(25) Norme Grassi e Derivati (NGD). Stazione Sperimentali degli Oli e dei Grassi, Milano, Italy, Method NGD C-88, **2007**.
(26) Vandeginste, B. G. M.; Massart, D. L.; Buydens, L. M. C.; De Jong, S.; Lewi, P. J.; Smeyers-Verbeke, J. *Data Handling in Science and Technology Part B*; Elsevier Science: Amsterdam, The Netherlands, 1998.

Received May 25, 2009. Revised manuscript received August 3, 2009. Accepted September 22, 2009. Project CTQ2007-61445 (MEC and FEDER funds) is acknowledged. M.J.L.-G. thanks the Generalitat Valenciana for an FPI grant for Ph.D. studies and for a grant to study in a foreign institution.